4

Gulf of Cadiz Expedition
Contribution Number 4

XCP Data from the Gulf of Cadiz Expedition:
R/V *Oceanus* Cruise 202

by
Maureen A. Kennelly
Mark D. Prater
John H. Dunlap
Eric L. Kunze
Thomas B. Sanford

Technical Report
APL-UW TR 8925
November 1989

Contract N00014-87-K-0004

Gulf of Cadiz Expedition
Contribution Number 4

XCP Data from the Gulf of Cadiz Expedition: R/V *Oceanus* Cruise 202

by
Maureen A. Kennelly
Mark D. Prater
John H. Dunlap
Eric L. Kunze
Thomas B. Sanford

Technical Report
APL-UW TR 8925
November 1989

Applied Physics Laboratory University of Washington
Seattle, Washington 98105-6698

Contract N00014-87-K-0004

Acknowledgments

This work was funded by the Office of Naval Research under Contract N00014-87-K-0004. The new coefficients for XCP processing were determined by Michael Horgan.

ABSTRACT

Velocity and temperature profiles from expendable current profilers (XCPs) were obtained during the Gulf of Cadiz Expedition, 4–28 September 1988, from R/V *Oceanus*. This report describes the instrumentation used, discusses data acquisition and processing methods, and presents the resulting velocity and temperature profiles.

TABLE OF CONTENTS

LIST OF FIGURES

LIST OF TABLES

1. INTRODUCTION

This report is the reference volume and data summary for expendable current profiler (XCP) data obtained during the Gulf of Cadiz Expedition, R/V *Oceanus* Cruise 202, 4–28 September 1988.

The objectives of this expedition were to observe the vortices shed in the wake of Ampere Seamount, to survey eddies (Meddies) formed by the Mediterranean outflow near Cape St. Vincent, Portugal, and to study the structure and dynamics of the outflow plume west of the Strait of Gibraltar. The cruise consisted of two legs: our leg 1, from 4–19 September 1988, corresponded to Leg IV of *Oceanus* voyage 202 and our leg 2, from 21–28 September 1988, corresponded to Leg V. In addition to XCP drops, XBTs, XSVs, and XDPs were deployed and CTD stations were taken during the cruise. During the Ampere Seamount component of the expedition, a radar transponder was moored, and four drifting buoys were tracked. The Gulf of Cadiz Expedition is described in detail by Kennelly et al. (1989a). The CTD data are presented by Kennelly et al. (1989b), the XBT and XSV data by Kennelly et al. (1989c), and the XDP data by Lynch and Lueck (1989).

The operational areas for the expedition included Ampere Seamount, the area around Cape St. Vincent, Portugal, and the Gulf of Cadiz west of the Strait of Gibraltar (Figure 1). The sampling pattern executed in the Meddy survey region, approximately delineated by the box in Figure 1, is shown in Figure 2.

The XCP drop locations are shown in Figures 3 through 9. XCP survey 1 (XCPs 2401–2428) was a cross pattern in the shear region between the eastward flow on the north flank of Ampere Seamount and a stagnation point to the southeast; the site was at 255° and 3 n.mi. from the radar transponder mooring, in the near wake of the seamount. Its location relative to the other stations is shown in Figure 3; individual XCP deployments are shown in Figure 4. The second XCP survey was centered 8 n.mi. east of the seamount (Figures 3 and 5). This time the section lines were twice as long to provide information on larger scales.

XCPs were deployed near Cape St. Vincent, Portugal, along lines 2–8 and line 17 of the Meddy survey pattern (Figure 2). The drop numbers and locations are shown in Figure 6.

After the Meddy survey pattern was completed and the data were reviewed, we studied a Meddy that had been identified near the site of CTD 25 (36°10.15′N, 9°02.1′W). The Meddy was found about 10 n.mi. southwest of the CTD 25 site, and a star pattern was executed to survey it with XCPs, XBTs, and XSVs. The XCP drops are shown in Figure 7.

XCPs 2521–2584 were dropped during the outflow component of the expedition. Drops 2521–2536 were at nine sites selected to study the temporal and spatial variability of the Mediterranean outflow (Figure 8). Sections A–I (XCPs 2537–2584) were then completed to characterize the outflow (Figure 9).

The positions and times of the XCP drops are listed in Appendix A.

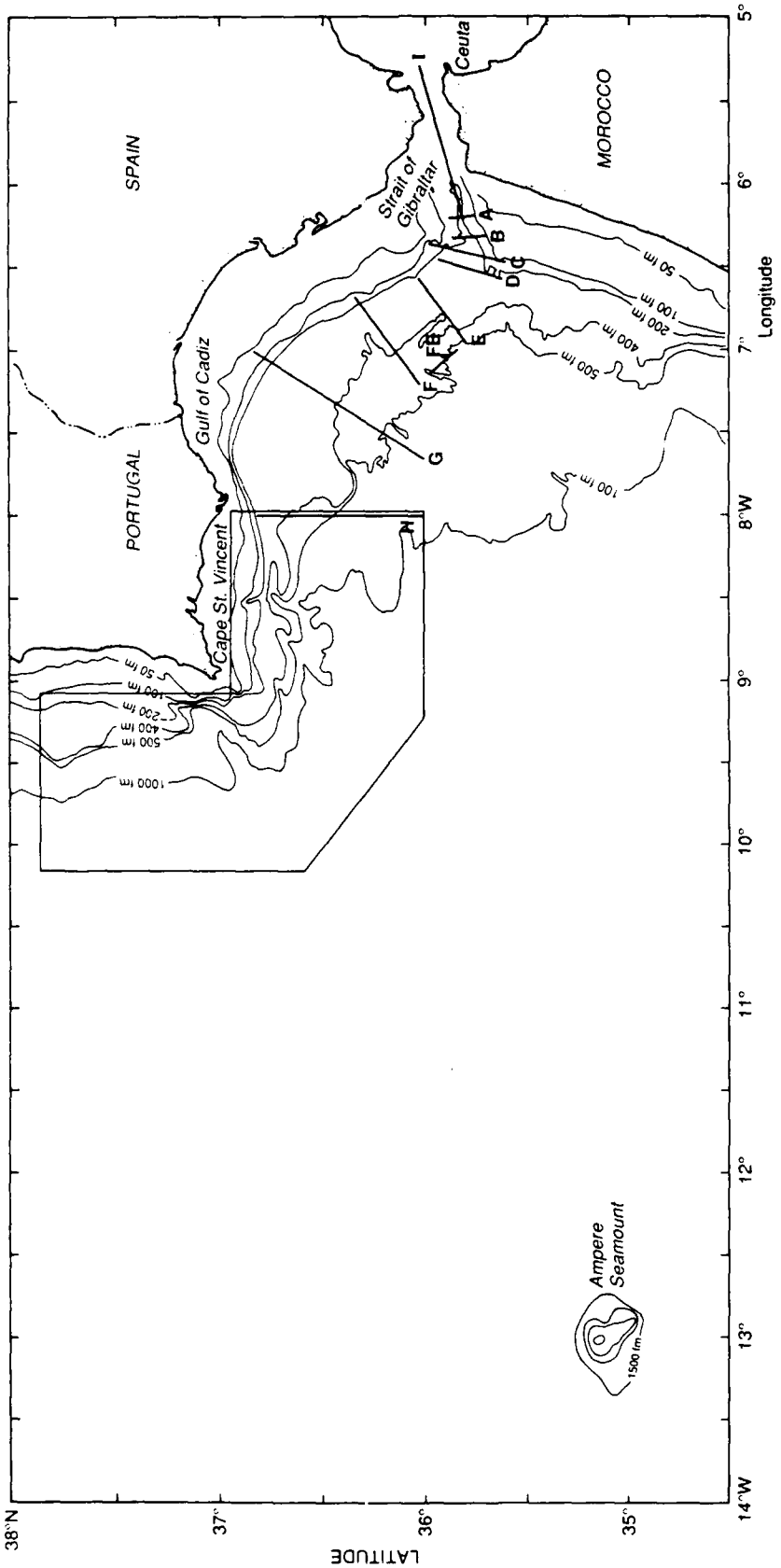

Figure 1. Operational areas for the Gulf of Cadiz Expedition. The areas included Ampere Seamount, the Cape St. Vincent region (boxed), and the continental slope west of the Strait of Gibraltar (sections A–I).

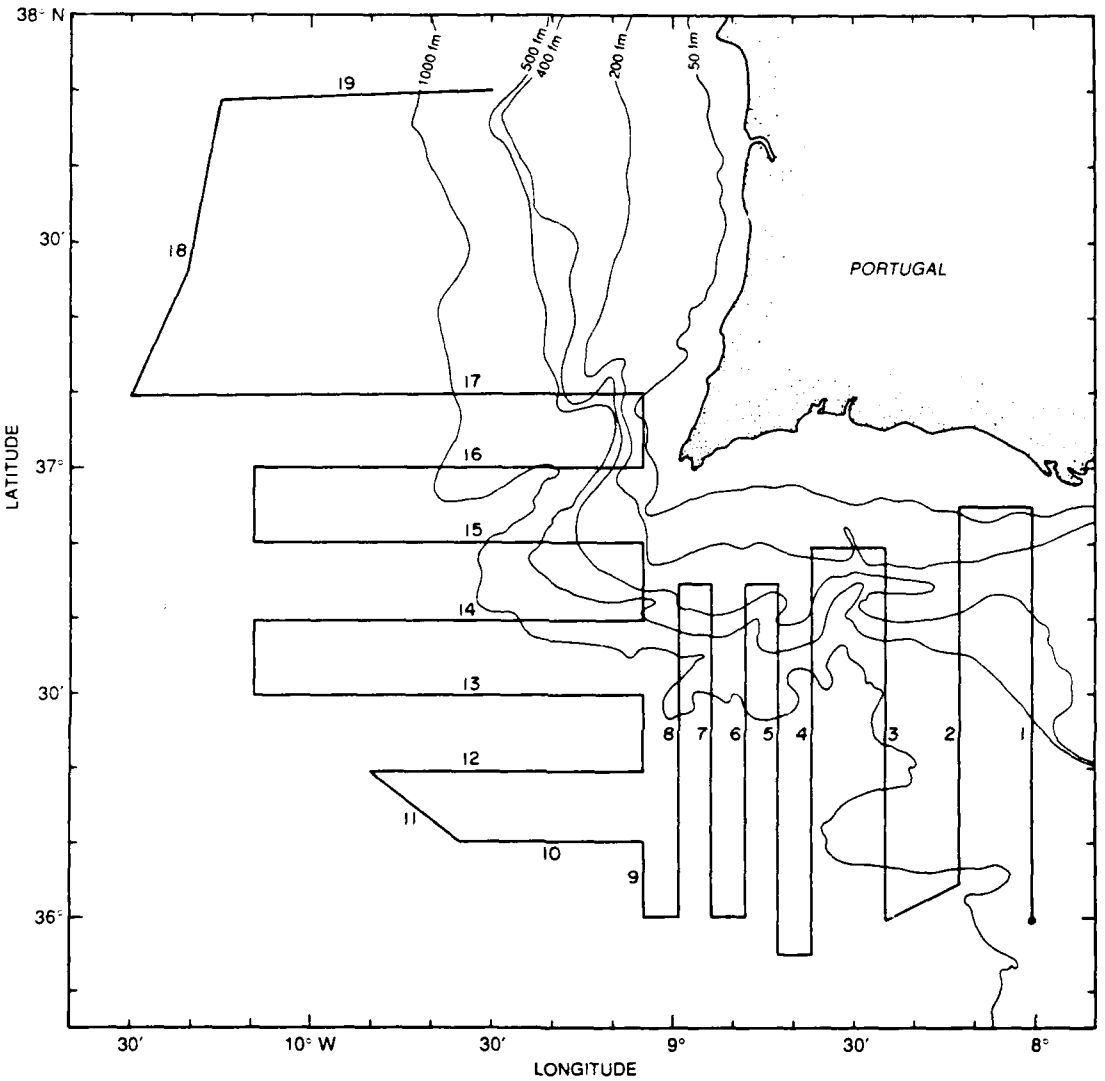

Figure 2. Survey pattern for Meddy component of the Gulf of Cadiz Expedition.

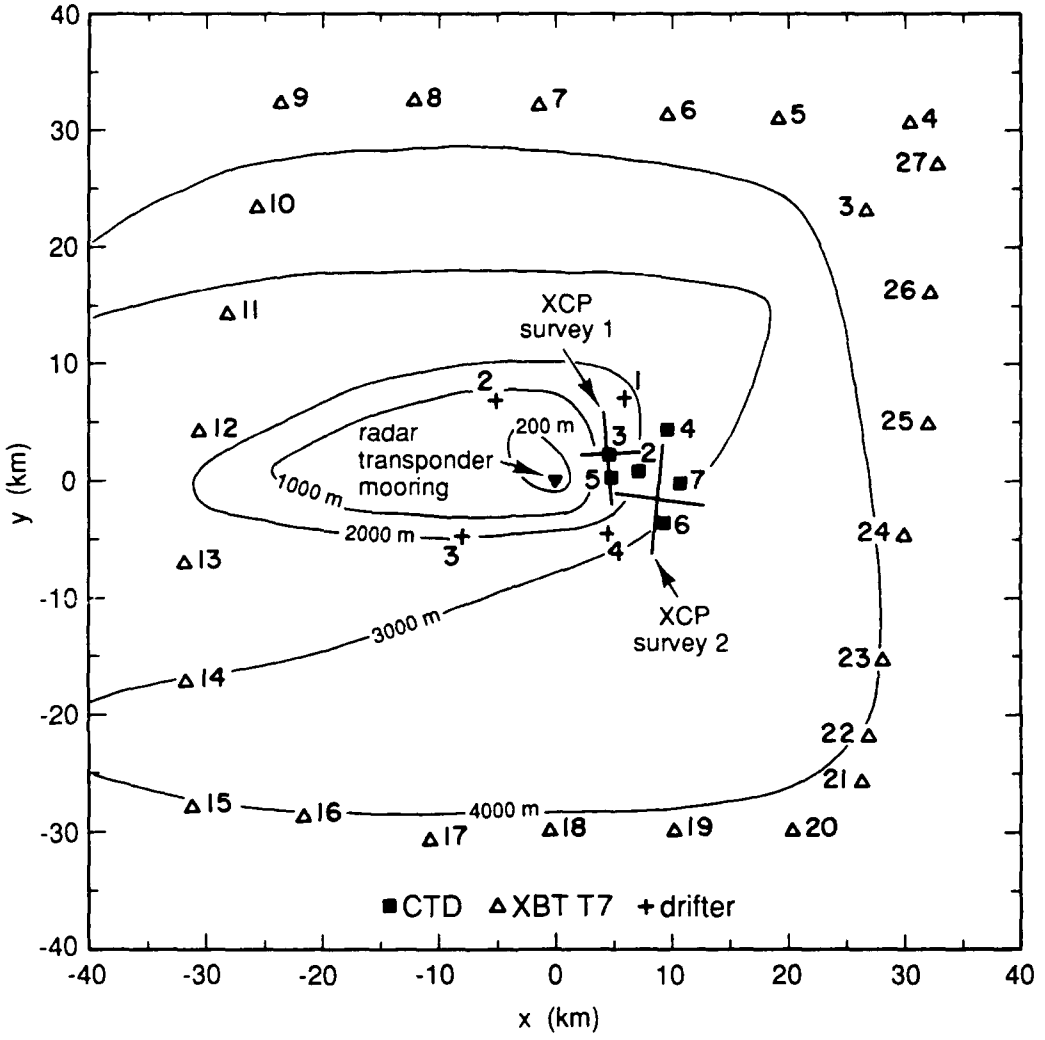

Figure 3. Locations of XBT drops, CTD stations, XCP survey patterns, and initial drifter deployments during the Ampere Seamount component. Crude topography is also shown.

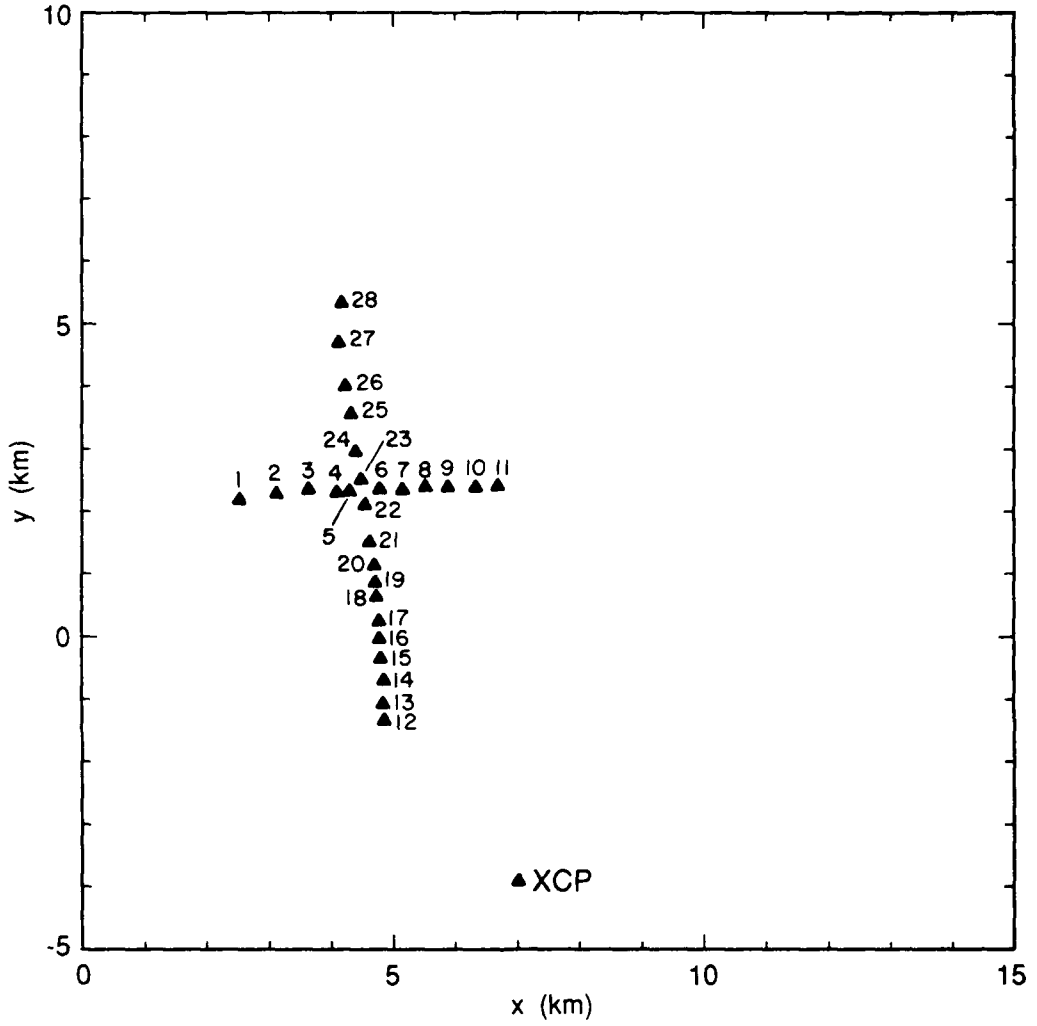

Figure 4. XCP survey 1, drop locations. Drop numbers have been shortened for plotting. Actual drop numbers are 2401 to 2428.

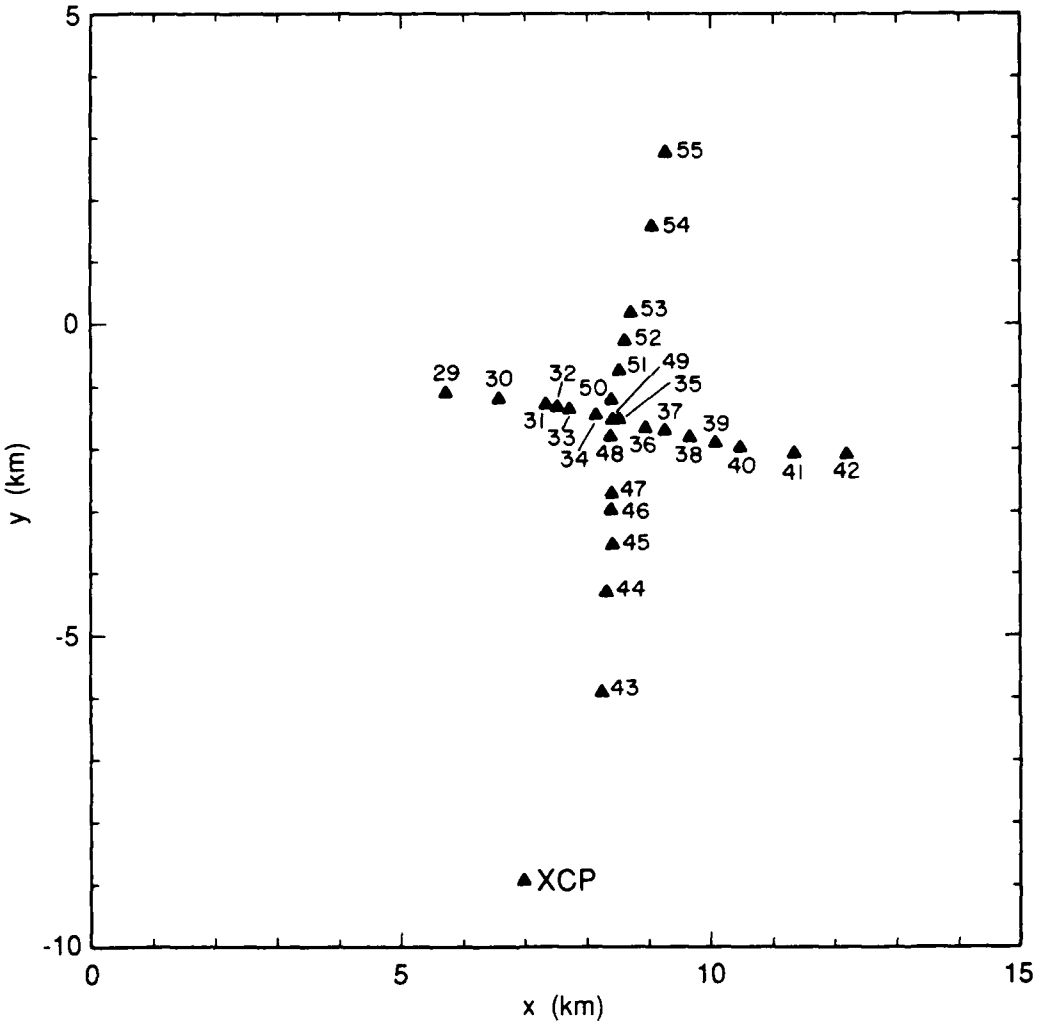

Figure 5. XCP survey 2, drop locations. Drop numbers have been shortened for plotting. Actual drop numbers are 2429 to 2455.

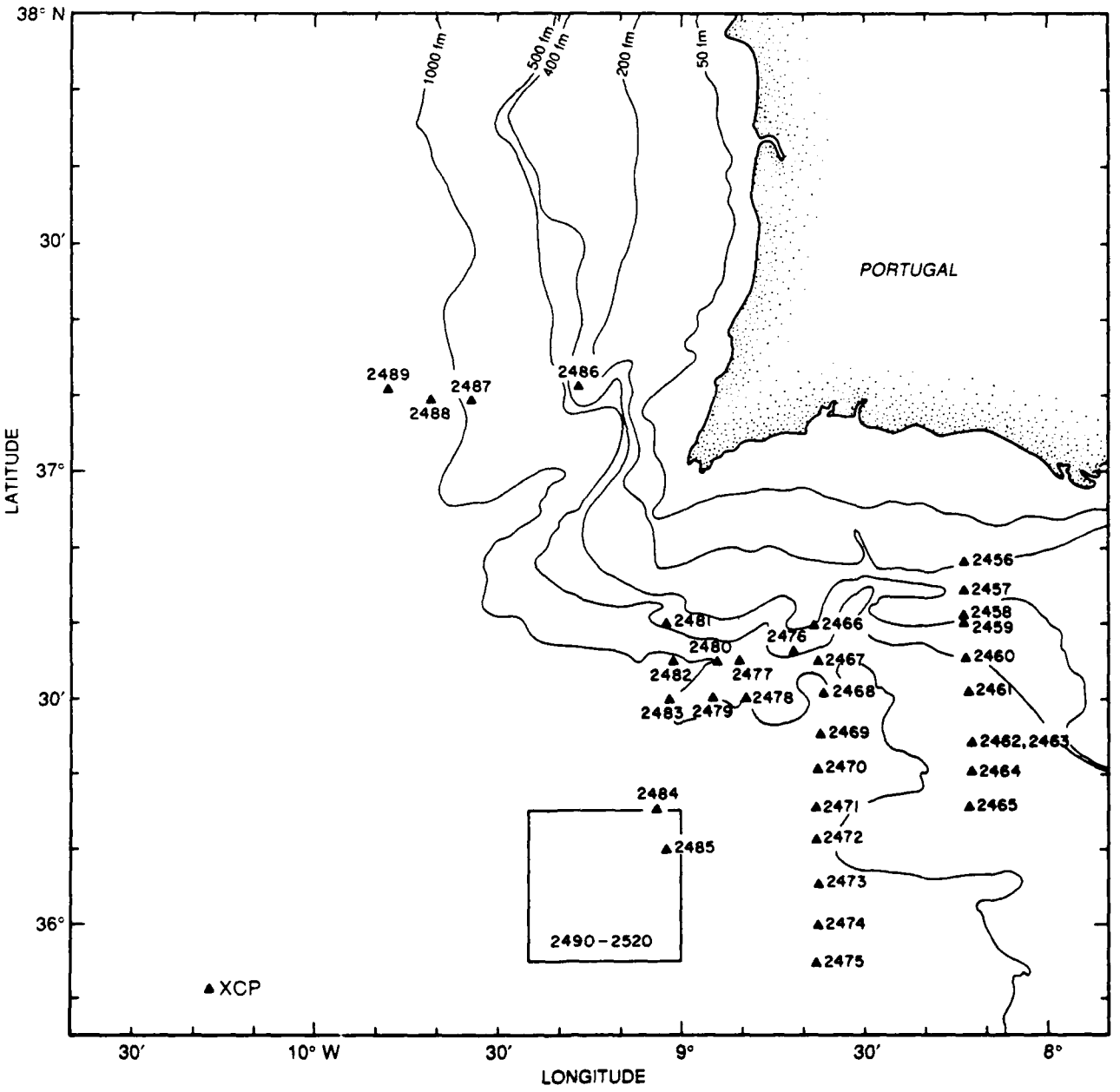

Figure 6. Locations of XCP drops during Meddy component. Drops during survey of Meddy (2490-2520, boxed area) are shown in detail in Figure 7.

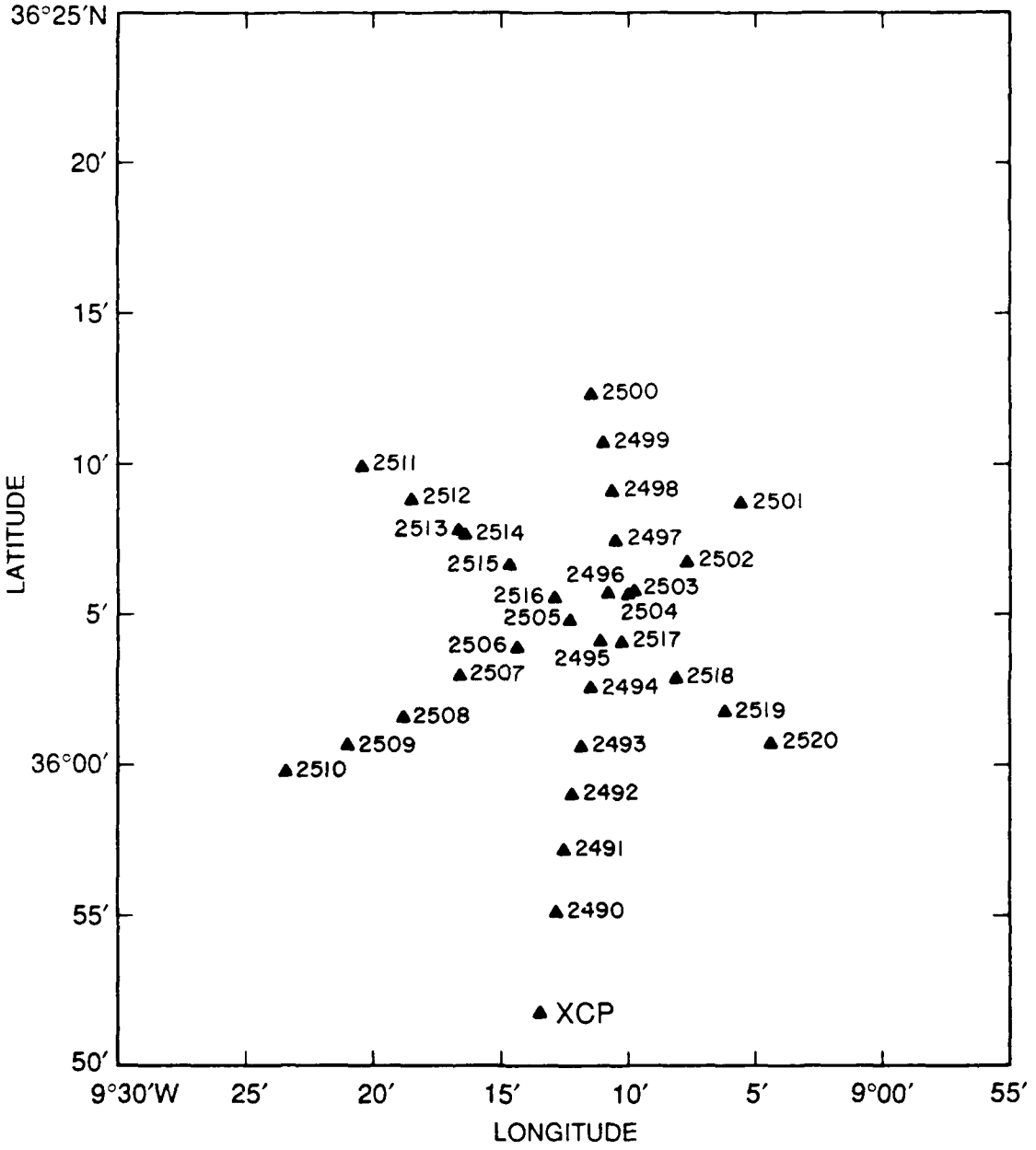

Figure 7. Locations of XCP drops in Meddy.

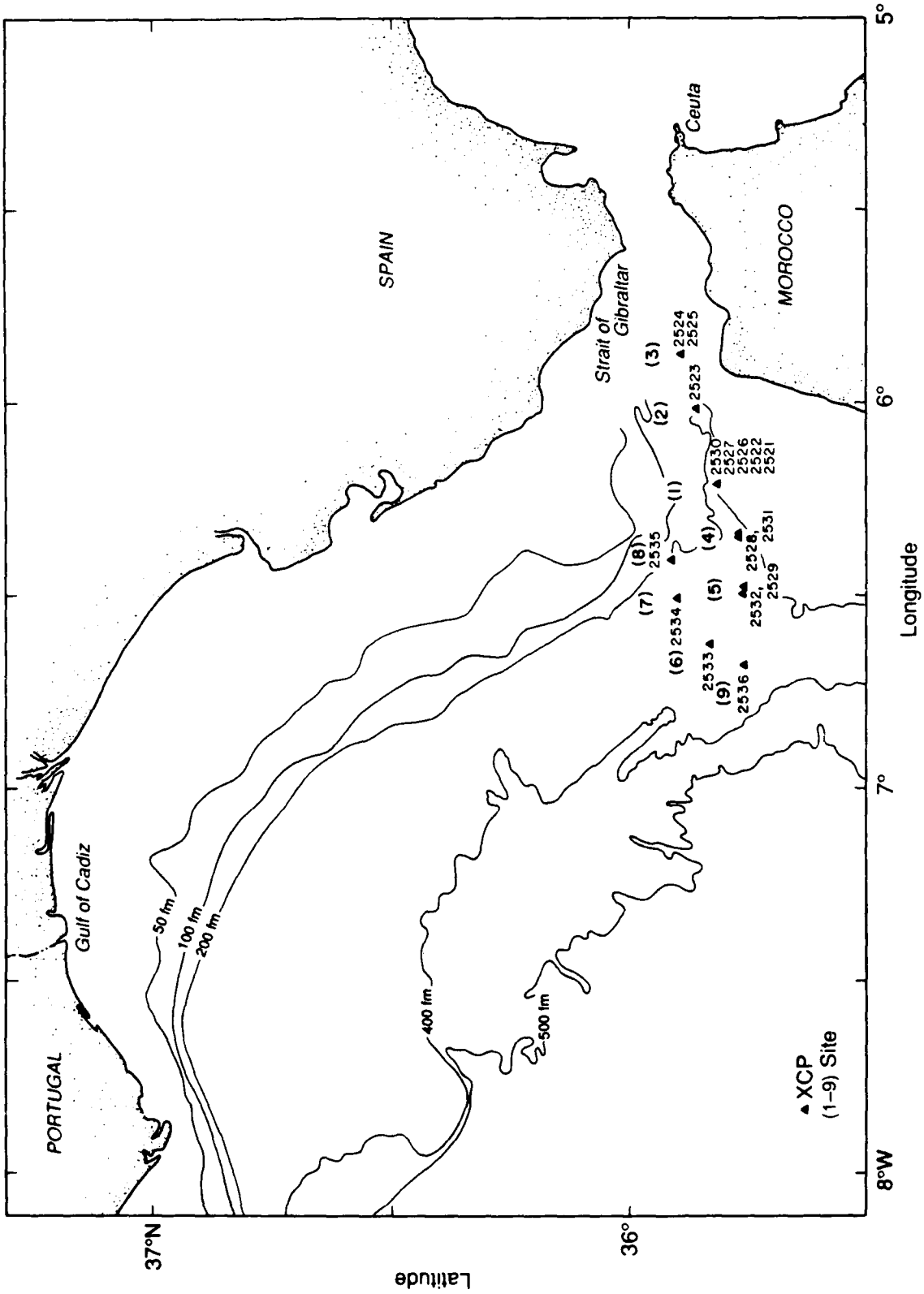

Figure 8. Locations of XCP drops, sites 1–9. Site numbers are in parentheses.

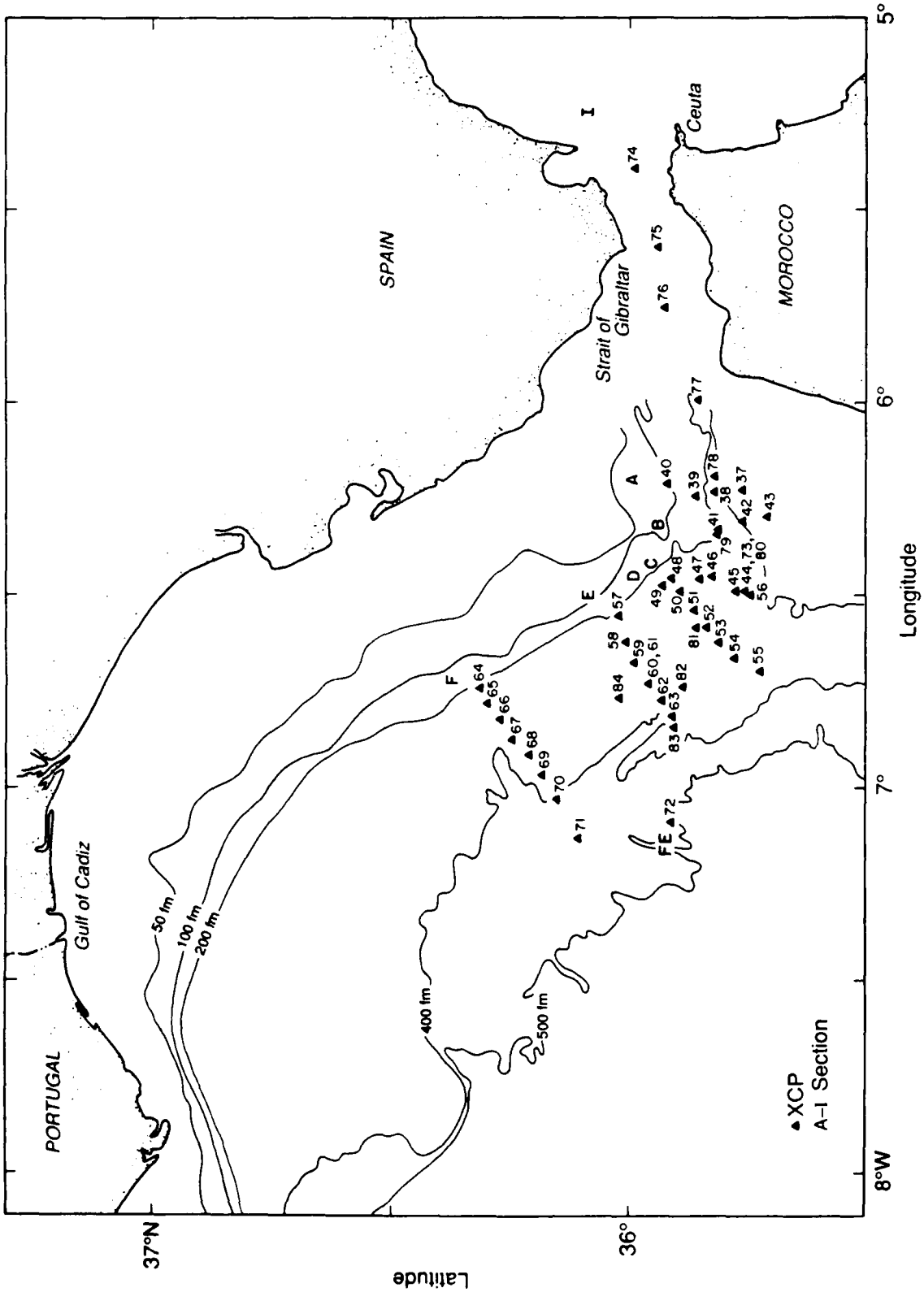

Figure 9. Locations of XCP drops, sections A–I. Drop numbers have been shortened for plotting. Actual numbers are 2537–2584.

2. INSTRUMENTATION

To obtain profiles of relative velocity and temperature, four channels (10, 12, 14, and 16) of Sippican Inc. Mod 7 XCPs were used during the cruise. In all, 184 XCPs were launched. The channel-10 XCPs were specially manufactured for this expedition. Appendix A gives the drop particulars.

Three aluminum antennas (Cushcraft, four-element Yagi) were mounted on the *Oceanus* for XCP reception. The antennas were located facing aft on the main mast, facing starboard on the main mast, and facing forward on the catwalk between the stacks. All antennas were mounted with the elements vertical for vertical polarization. All the elements were on one side of the aluminum mounting pipe in the direction of the antenna's directivity. RG-8 cable connected the antennas to the Mk-10 XCP signal processors.

Before deployment, each probe was tested for radio operation, probe operation (shown by the presence of the three audio frequencies), and compass-channel response to a moving magnet. The squib wires coming out of the base of the electronics housing were also examined. Only one XCP failed the pre-launch check for radio operation and was not deployed.

Of the 184 XCPs deployed, 46 were on channel 10, 46 on channel 12, 45 on channel 14, and 47 on channel 16. The channel-16 probes had the poorest record with 11 failures, followed by channel 12 with 7 failures, channel 10 with 4 failures, and channel 14 with 2 failures. Two failure modes were channel specific: the wire broke early on two channel-10 probes and the compass coil area was half its expected value on two channel-14 probes. The other problems, excluding drops for which there were no good data at all, were electrode reversals, bad temperature data, and noisy data. The overall success rate for the XCPs was 87%, or 160 good drops.

3. DATA ACQUISITION

XCP, XBT, and XSV data were acquired with a Hewlett Packard HP9020 computer using an integrated acquisition program written in HP-Basic that allowed real-time processing and display of the data. In this report only the XCP part of the acquisition system will be discussed. Kennelly et al. (1989c) discuss the XBT and XSV portions of the acquisition system. Data from up to three probes could be acquired and displayed simultaneously (with three co-running "partition" programs controlled by a fourth "master" program). As the data were acquired, the complete raw data stream was saved on an HP9144 magnetic cartridge tape drive connected to the HP9020. Raw data from the XCPs were stored along with a time stamp, an indication of the probe type, and the program partition that acquired the data. Processed XCP data were archived on floppy disk.

A schematic of the acquisition system is shown in Figure 10. There were four Sippican-manufactured Mk-10 XCP signal processors, one for each of the four channels (10, 12, 14, and 16) of XCPs deployed. Table 1 lists the serial numbers of the Mk-10s used. Only three Mk-10s could be connected (via GPIB cables) to the three available I/O ports on the computer at one time. Therefore the channel-10 Mk-10 and the channel-12 Mk-10 were alternately attached to partition 1. The channel-14 Mk-10 was always attached to partition 2, and the channel-16 Mk-10 to partition 3.

Data were also stored on VHS audio/video magnetic tape. One backup system was dedicated to the XCP data. The backup system consisted of a VCR, a Sony model PCM-F1 digital audio processor (PCM stands for pulse code modulation), and a power adapter. The frequency-modulated data from XCP channels 14 and 16 were stored directly on the audio tracks of the VHS tape. XCP data from channels 10 and 12 passed through the digital audio processor for storage on the video tracks.

Table 1. Mk-10 XCP receiver configuration during R/V Oceanus *Cruise 202.*

Channel	Serial #	Local ID
10	844003	AMP
12	852601	EM2
14	844001	EM1
16	845104	Niiler

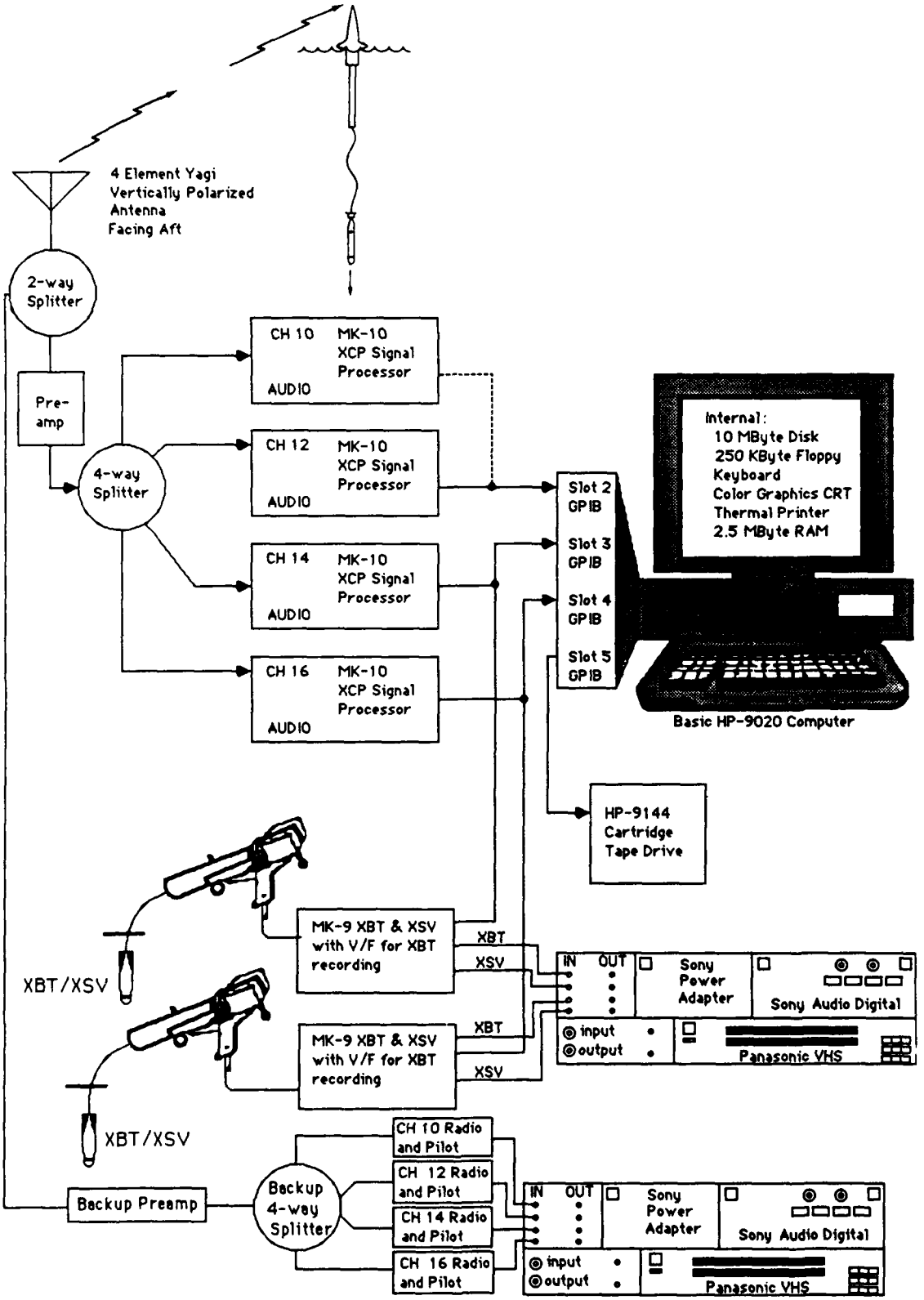

Figure 10. Configuration of XCP/XBT/XSV acquisition system.

4. AT-SEA DATA PROCESSING

The acquisition program provided a printout of the isotherm depths as the probe was falling. Waterfall plots of the temperature profiles overlaid on computer-generated isotherm sections could be produced while the acquisition program was paused. The profiles were inadvertently processed using the fall-rate coefficients for XCP Mod 6 (see Table 4 on p. 26 for values). Later checks, however, showed these values produced profiles that corresponded better to near-simultaneous CTD profiles than the coefficients published for the Mod 7. Temperature was computed using Sippican's method (a fifth-order polynomial going directly from frequency to temperature) with the coefficients listed in Table 2. Section 5.2.4 describes the XCP temperature processing in more detail.

Horizontal and vertical components of the earth's magnetic field ($F_h = 0.270$, $F_z = -0.327$) representative of the Gulf of Cadiz region were used for all at-sea processing. The values of constants C_1 and C_2 were 0.97 and -0.02, respectively. The processed data were averaged over 22 points (~5 m) in 11 point (~2.5 m) steps for displaying the temperature and velocity profiles on the HP9020 screen as the probe fell and for storing on floppy disk. To obtain a hard copy of an individual XCP profile (temperature and velocity), the floppy disk with the processed XCP data was removed from the HP9020 running HP-Basic (the acquisition computer) and transferred to an HP9020 running UNIX. A UNIX decoding program written by John Dunlap was run on the data, and a profile was generated.

Table 2. Temperature coefficients used in at-sea data processing.

Coefficient	Value
Tcal0	−99.0687286644
Tcal1	1.13422688945
Tcal2	$-6.54532084971 \times 10^{-3}$
Tcal3	$2.13113005561 \times 10^{-5}$
Tcal4	$-3.48347929616 \times 10^{-8}$
Tcal5	$2.33466947038 \times 10^{-11}$

5. POST-CRUISE DATA PROCESSING

5.1 Calibrations

In order to combine the XCP data and the CTD data for contouring and for computing heat and salt fluxes, the XCP depth and temperature values need to be calibrated against a standard. The data collected during the Gulf of Cadiz experiment presented the opportunity to verify the depth estimates of the XCPs by comparing the high-wavenumber structure of their temperature signals with those obtained by a Sea-Bird CTD unit. This process also allowed us to estimate the random errors and the systematic offsets in both depth and temperature. This section summarizes the computational procedure used in these calibrations and presents the results.

Because the CTD's vertical reference is pressure and the XCP's reference is depth, a conversion is needed before any calibration can be done. We chose to convert the CTD pressure to depth. Saunders and Fofonoff (1976) present a conversion method that consists of integrating the hydrostatic equation downward from the sea surface while accounting for the horizontal and vertical variations in the earth's gravitational field. Their method is given by

$$z = \frac{-\int_o^p \frac{dp}{\rho}}{g_o + \frac{1}{2}\gamma p},$$

where z is the depth in meters (positive upward from the surface), p is the pressure in decibars, ρ is the *in situ* density of seawater, g_o is the surface value of gravity which is a function of latitude, and γ is the vertical increase in gravity with depth, taken to be 2.226×10^{-6} m s^{-2} per meter. The variation of gravity with latitude is given by

$$g_o(\phi) = 9.780318\,(1 + 5.3024 \times 10^{-3}\sin^2\phi - 5.9 \times 10^{-6}\sin^2 2\phi)\ \text{m s}^{-2},$$

where ϕ is latitude. At a latitude of 36°N, $g_o = 9.81075$ m s^{-2}.

For this analysis, the CTD pressure data collected on the cruise were averaged into 10-dbar bins, and the vertical integration was performed for each cast. At each bin level,

a ratio was formed between the computed depth (in meters) and the measured pressure (in decibars). The resulting ratio-pressure curves from all the casts were combined at each bin level to give a curve for the average ratio. An approximation to the average-ratio curve is given by

$$\text{ratio}(p) = -0.9927 + 2.55 \times 10^{-6} p - 0.0073 \exp(-p/50) .$$

Figure 11 shows the average ratio curve (steppy) and the approximate curve (smooth). The depth is found by multiplying the pressure by the ratio appropriate for that pressure. Thus when the pressure is 1000 dbar, the corresponding depth is 1000×-0.9901, or -990.1 m. The maximum error in depth caused by using the approximate curve instead of the computed one for any particular CTD cast is about 0.5 m.

Software was then developed to map XCP depth to CTD depth, assuming the instruments passed through similar ocean features on their descent. The mapping was obtained by matching features of the XCP temperature profile to their counterparts in the CTD profile. The result was a table of depth offsets as a function of XCP depth for each XCP/CTD pair. To make this pattern matching more robust, the profiles were filtered to remove very-high-wavenumber noise and low-wavenumber features. The vertical scales of the remaining features were between 10 and 100 m. At each depth interval of the XCP drop, the XCP profile was shifted with respect to the CTD profile until the correlation of the two profiles over a 100-m range was maximized. The depth offset at the maximum correlation was the amount that the XCP depth was in error, and was considered the optimal offset at that depth. Rather than shifting the XCP profile one depth increment at a time and recomputing the correlation for every offset possible, a "golden section search" (Press et al., 1986) was performed to find the maximum correlation. This method assumes that the correlation is a smoothly varying function of offset, with a global maximum at the optimal offset. The optimized search procedure gave results comparable to the point-by-point search and ran 5 to 10 times faster. The maximum correlation achieved and the corresponding depth offset were recorded, as well as the temperature difference in the nonfiltered signals at the optimal offset.

An XCP/CTD pair was considered acceptable for analysis if the XCP was dropped within 1 hour and 1 n.mi. (2 km) of the CTD cast. These spatial and temporal constraints may appear harsh, especially compared with a previous error analysis by Heinmiller et al.

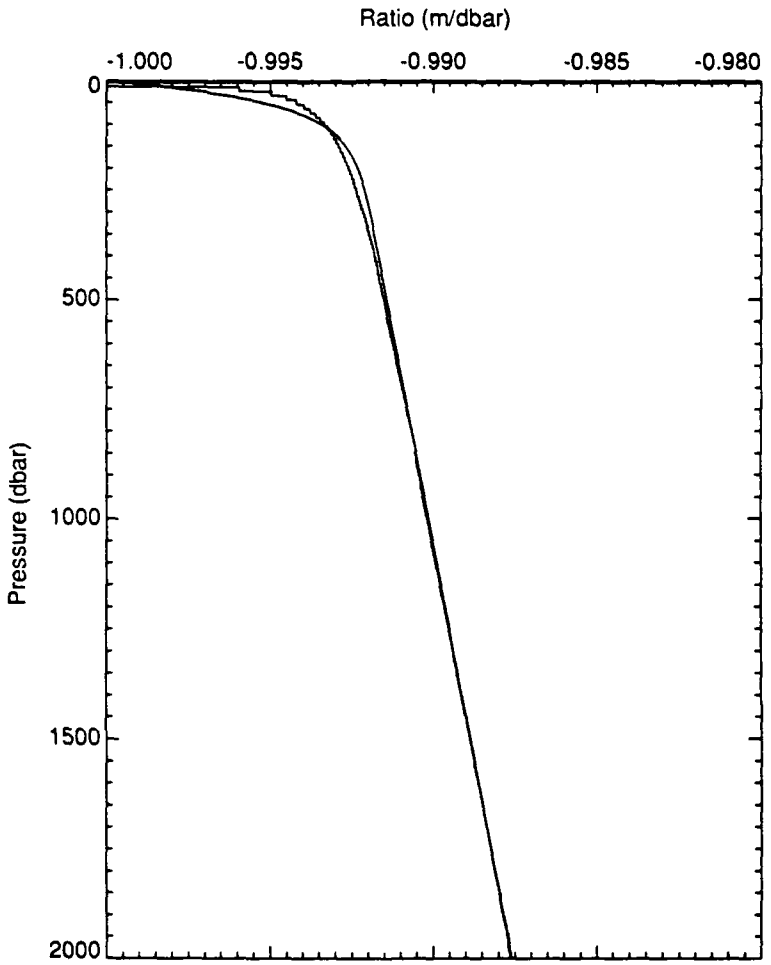

Figure 11. Relation between pressure and depth derived from the vertical integration of CTD data.

(1983) which used XBT/CTD pairs 15 to 50 km apart; because of the complex structure and interleaving of the Mediterranean outflow in the Gulf of Cadiz, however, small differences in time or position severely degraded the temperature correlations. Table 3 lists the 65 CTD/XCP (Mod 7) drop pairs accepted for processing. The times (in GMT) and locations given in Table 3 for the CTD casts are for the bottom of the cast. The depths were taken from the underway log, where the values recorded were read off the ship's depth recorder. The CTD data were processed as described by Kennelly et al. (1989b), whereas the at-sea processing described in Section 4 was used for the XCPs. Figure 12 is an example of the program output for an XCP/CTD pair.

After a depth-offset record was obtained for all the XCP/CTD pairs, a second program was used to compute the mean and rms error of the depth offset and the temperature difference. During most drops, the maximum correlation was below 0.9 at some depth bins, lowering the confidence that a good estimate of the depth offset and temperature difference was obtained at those bins. To keep these values from being included in the average and contributing to the rms error value, the depth offset and temperature difference were not included in the subsequent calculation if the maximum correlation obtained for a depth bin was below 0.9. When this minimum correlation criterion was imposed, the number of accepted values at a depth bin was much smaller than the number of drop pairs. Figure 13 gives the depth offsets found from this analysis, as well as the number of drop pairs contributing to each depth bin. The depth offset varies from 0 at the surface to nearly 30 m by the end of the drop, near −1700 m.

The next step was to find XCP depth coefficients that would minimize the depth offsets. For the XCP, the depth of the probe is estimated as a quadratic function of the fall time, such that

$$-z = \mathrm{pcal0} + (\mathrm{pcal1} \times t) + (\mathrm{pcal2} \times t^2)\,, \qquad (1)$$

where z is the depth in meters (positive upward) and t is the elapsed time of fall in seconds. The coefficients (pcals) of the quadratic polynomial are empirically determined. Because the computed depth-offset curve was very erratic, a hand-drawn estimate was made through the data and digitized at 50 m intervals. The XCP depth equation was then inverted, allowing us to solve for time given depth, such that

$$t = \frac{-\mathrm{pcal1} + \sqrt{(\mathrm{pcal1})^2 - 4\,\mathrm{pcal2}\,(\mathrm{pcal0} + z)}}{2\,\mathrm{pcal2}}\,.$$

Table 3. XCP/CTD Pairs Used for Depth and Temperature Comparisons

XCP #	CTD #	Date	Time	Latitude (N)	Longitude (W)	Depth (m)
	010	09/11/88	23:43	36 35.28	8 38.17	1250
2467		09/12/88	00:21	36 34.63	8 37.70	1325
	011	09/12/88	01:23	36 30.24	8 37.01	2385
2468		09/12/88	02:05	36 30.31	8 36.85	2420
	012	09/12/88	03:13	36 24.82	8 36.94	2610
2469		09/12/88	03:50	36 24.95	8 37.34	2575
	013	09/12/88	05:00	36 20.32	8 37.87	2680
2470		09/12/88	05:38	36 20.27	8 37.80	2700
	014	09/12/88	07:20	36 15.56	8 39.65	2160
2471		09/12/88	07:48	36 15.30	8 38.02	2100
	015	09/12/88	08:56	36 10.76	8 37.98	2110
2472		09/12/88	09:32	36 10.96	8 38.03	2090
	016	09/12/88	10:45	36 05.38	8 37.47	2930
2473		09/12/88	11:41	36 05.12	8 37.54	2950
	017	09/12/88	12:47	36 00.06	8 37.55	3100
2474		09/12/88	13:33	35 59.61	8 37.64	3050
	018	09/12/88	14:44	35 54.41	8 37.66	2900
2475		09/12/88	15:37	35 54.60	8 37.96	2875
	020	09/13/88	10:38	36 40.02	9 02.46	760
2481		09/13/88	11:04	36 39.60	9 02.56	840
	021	09/13/88	12:07	36 35.16	9 01.31	2015
2482		09/13/88	12:46	36 34.59	9 01.51	2020
	022	09/13/88	13:57	36 29.90	9 01.80	1860
2483		09/13/88	14:37	36 29.50	9 02.09	1750
	024	09/13/88	17:29	36 15.13	9 03.52	3260
2484		09/13/88	18:36	36 15.05	9 04.17	3300
	025	09/13/88	19:45	36 09.97	9 02.51	3365
2485		09/13/88	20:27	36 09.66	9 02.50	3400
	028	09/15/88	11:59	37 10.84	9 15.60	655
2486		09/15/88	12:20	37 11.01	9 16.99	400
	030	09/15/88	15:11	37 09.80	9 34.50	1700
2487		09/15/88	15:44	37 09.14	9 34.49	1750
	031	09/15/88	16:56	37 08.96	9 40.40	2275
2488		09/15/88	17:34	37 09.25	9 41.09	2300
	032	09/15/88	19:12	37 10.47	9 47.12	2850
2489		09/15/88	20:05	37 10.65	9 48.16	3190
	052	09/21/88	17:04	35 53.13	5 52.59	460
2525		09/21/88	17:10	35 53.26	5 52.44	425
	053	09/21/88	19:08	35 48.97	6 13.10	420
2527		09/21/88	19:36	35 49.02	6 12.94	425
	054	09/21/88	22:01	35 46.03	6 20.65	
2528		09/21/88	22:22	35 46.10	6 20.82	435
	055	09/22/88	01:49	35 45.24	6 28.47	
2529		09/22/88	02:10	35 45.39	6 28.57	475
	057	09/22/88	05:40	35 45.89	6 20.08	395
2531		09/22/88	05:56	35 46.04	6 20.39	412

Table 3 (continued).

XCP #	CTD #	Date	Time	Latitude (N)	Longitude (W)	Depth (m)
	058	09/22/88	07:08	35 45.55	6 28.92	
2532		09/22/88	07:40	35 45.49	6 29.68	
	059	09/22/88	08:48	35 49.52	6 37.25	
2533		09/22/88	09:08	35 49.74	6 37.46	555
	060	09/22/88	10:15	35 53.97	6 30.61	457
2534		09/22/88	10:36	35 53.82	6 30.43	
	061	09/22/88	11:36	35 54.98	6 24.67	
2535		09/22/88	12:04	35 54.44	6 24.44	360
	062	09/22/88	14:02	35 45.15	6 40.60	
2536		09/22/88	14:18	35 45.34	6 40.74	700
	063	09/22/88	17:25	35 45.67	6 13.34	280
2537		09/22/88	17:34	35 45.68	6 13.47	260
	064	09/22/88	18:15	35 49.13	6 13.76	425
2538		09/22/88	18:25	35 49.21	6 13.77	420
	065	09/22/88	19:07	35 51.77	6 14.25	341
2539		09/22/88	19:20	35 51.57	6 14.42	335
	066	09/22/88	20:05	35 55.20	6 12.13	
2540		09/22/88	20:16	35 55.14	6 12.53	
	069	09/22/88	22:46	35 48.73	6 19.98	361
2541		09/22/88	22:58	35 48.76	6 19.80	
	070	09/22/88	23:45	35 45.73	6 18.66	
2542		09/23/88	00:05	35 45.58	6 18.34	390
	071	09/23/88	00:40	35 42.96	6 17.74	
2543		09/23/88	00:56	35 42.62	6 17.59	275
	075	09/23/88	04:36	35 45.16	6 29.17	
2544		09/23/88	04:45	35 45.04	6 29.51	490
	076	09/23/88	05:41	35 46.68	6 28.98	435
2545		09/23/88	05:55	35 46.49	6 29.28	430
	077	09/23/88	06:44	35 49.73	6 26.84	
2546		09/23/88	06:55	35 49.51	6 27.00	
	078	09/23/88	08:00	35 51.35	6 27.07	
2547		09/23/88	08:12	35 51.04	6 27.35	460
	079	09/23/88	09:06	35 54.95	6 27.01	415
2548		09/23/88	09:18	35 54.59	6 27.22	415
	081	09/23/88	11:26	35 56.05	6 28.58	425
2549		09/23/88	11:50	35 55.65	6 28.43	420
	082	09/23/88	12:27	35 53.90	6 29.07	427
2550		09/23/88	12:45	35 53.47	6 29.27	430
	083	09/23/88	13:21	35 52.05	6 31.99	520
2551		09/23/88	13:39	35 51.72	6 32.25	520
	084	09/23/88	14:14	35 50.45	6 34.62	528
2552		09/23/88	14:31	35 50.22	6 34.89	530
	085	09/23/88	15:37	35 48.74	6 36.92	540
2553		09/23/88	15:56	35 48.67	6 37.25	540

Table 3 (continued).

XCP #	CTD #	Date	Time	Latitude (N)	Longitude (W)	Depth (m)
	086	09/23/88	16:47	35 46.70	6 39.28	602
2554		09/23/88	17:07	35 46.65	6 39.67	620
	087	09/23/88	17:50	35 43.72	6 41.42	610
2555		09/23/88	18:11	35 43.45	6 41.76	610
	091	09/23/88	22:13	35 44.87	6 29.41	525
2556		09/23/88	22:29	35 44.64	6 29.83	480
	092	09/24/88	01:08	36 01.62	6 33.60	
2557		09/24/88	01:43	36 01.24	6 33.09	380
	093	09/24/88	02:34	36 00.52	6 36.99	510
2558		09/24/88	02:57	36 00.41	6 37.19	
	094	09/24/88	03:46	35 59.25	6 40.26	
2559		09/24/88	04:06	35 59.33	6 40.43	
	096	09/24/88	05:51	35 55.50	6 46.00	680
2562		09/24/88	06:32	35 55.77	6 46.26	710
	097	09/24/88	07:24	35 54.34	6 48.72	
2563		09/24/88	07:47	35 54.53	6 48.71	775
	102	09/24/88	17:49	36 18.89	6 43.92	
2564		09/24/88	18:01	36 18.66	6 44.25	400
	103	09/24/88	18:36	36 17.87	6 46.56	575
2565		09/24/88	19:55	36 16.25	6 49.04	580
	104	09/24/88	19:43	36 16.20	6 49.02	680
2566		09/24/88	20:03	36 16.15	6 49.13	672
	105	09/24/88	20:44	36 14.79	6 52.19	700
2567		09/24/88	21:03	36 14.66	6 52.38	700
	107	09/24/88	22:50	36 10.82	6 57.52	737
2569		09/24/88	23:23	36 10.88	6 57.91	740
	108	09/25/88	00:38	36 09.22	7 01.04	725
2570		09/25/88	01:08	36 09.11	7 01.68	
	110	09/25/88	03:00	36 06.40	7 07.57	760
2571		09/25/88	03:25	36 06.42	7 07.74	760
	137	09/26/88	21:25	35 54.84	7 05.72	940
2572		09/26/88	21:45	35 54.63	7 05.19	940
	140	09/27/88	09:53	35 59.28	5 22.40	905
2574		09/27/88	10:24	35 59.17	5 23.50	900
	142	09/27/88	12:29	35 56.34	5 35.03	
2575		09/27/88	12:46	35 56.25	5 35.68	450
	146	09/27/88	17:08	35 50.96	6 00.04	354
2577		09/27/88	17:24	35 51.21	5 59.46	350
	148	09/27/88	19:39	35 49.11	6 11.81	435
2578		09/27/88	19:56	35 49.11	6 11.34	405

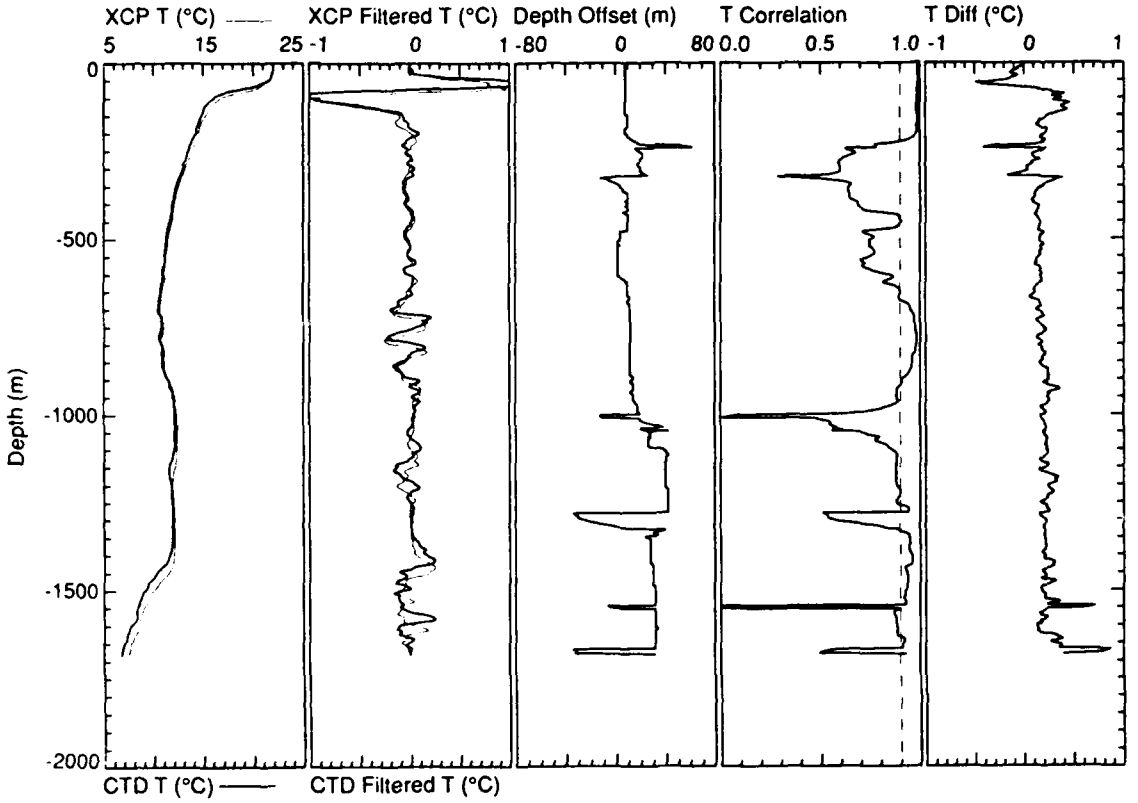

Figure 12. Output of program matching an XCP/CTD pair. The dashed line in the "T Correlation" panel marks the 0.9 correlation criterion.

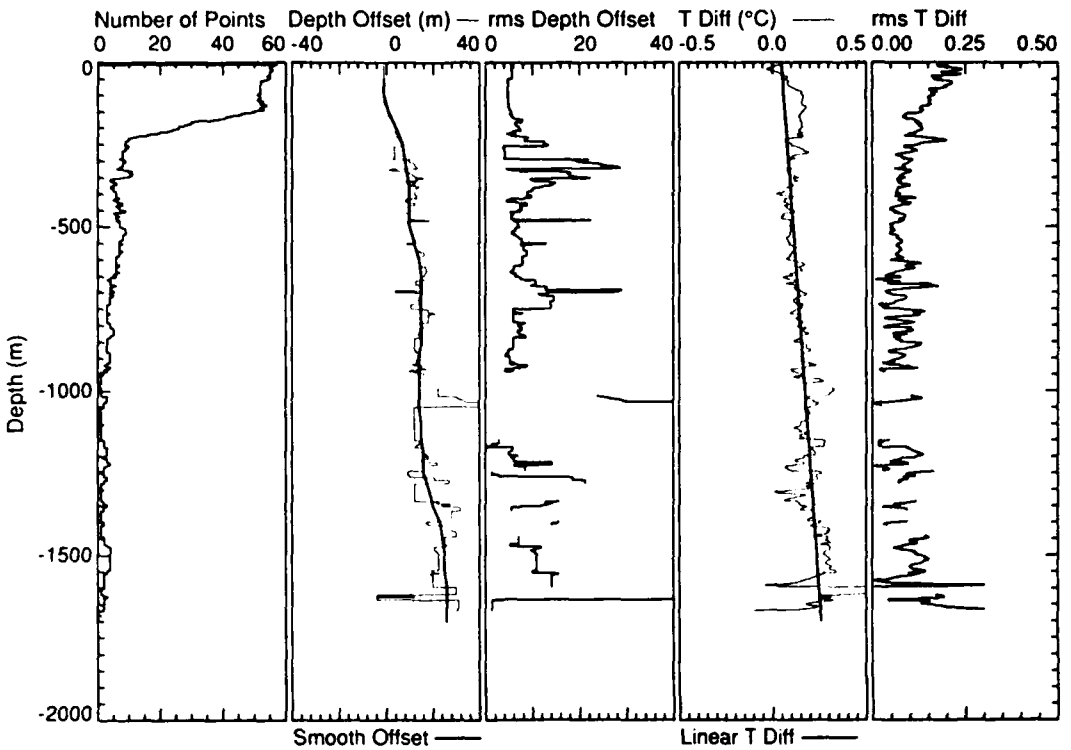

Figure 13. Combined result of matching program for all XCP/CTD pairs. Here "rms" refers to the rms error at each depth bin.

Although the XCP probes employed during the Gulf of Cadiz cruise were Mod 7s, Mod 6 depth coefficients were used for the at-sea processing (see Section 4.1). Mod 6 coefficients were thus used in the inverted depth equation. Times of fall were computed for depths at 50 m intervals. The depth offset was then added to these depths, creating a new depth-versus-time curve. The curve was fitted with a second-order polynomial such that depth was a quadratic function of time, and thus new depth coefficients were obtained. These depth coefficients are given in Table 4 along with those for the Mod 6 and the Mod 7 probes.

Figure 14 shows the difference in computed XCP depth as a function of fall time when using the polynomial expression with the Mod 7 coefficients and with the Mod 6 coefficients. The top dark line is the Mod 7 depth difference relative to the Mod 6 depth, which is the dark line centered at zero deviation. The shaded areas on the figure are the $\pm 2\%$ error given by Sippican Inc. as the depth accuracy of the two probes. The dashed line is the depth deviation when using the coefficients determined from the Cadiz cruise analysis. The XCP probes dropped during the Gulf of Cadiz cruise fell almost 0.2 m s^{-1} faster than indicated by the Mod 7 coefficients, and 0.08 m s^{-1} slower than indicated by the Mod 6 coefficients. The rms variation in the depth offset (Figure 13) is about 10 m.

The temperature offset (Figure 13) increases linearly, with the XCPs being 0.05°C warmer at the surface and 0.25°C warmer at the bottom of the drop (1700 m). A linear correction to the XCP temperatures was found such that

$$T' = T + \mathrm{tcor0} + (\mathrm{tcor1} \times z) ,$$

where T' is the corrected temperature, T is the temperature computed using Dunlap's method described in Section 5.2.4, z is the depth in meters (positive upward), and the tcor coefficients are -0.05°C and 1.25×10^{-6} °C m^{-1} respectively. The rms temperature variation is 0.1°C. It is unknown at this time whether the trend is due to a pressure effect on the thermistor and circuitry or to a temperature effect (e.g., self-heating) on the circuitry.

Table 4. XCP depth coefficients.

Coefficient	Mod 7	Mod 6	Cadiz Cruise Analysis
pcal0	4.875	3.1	4.0
pcal1	4.276	4.544	4.461
pcal2	−0.00063	−0.0006749	−0.000635

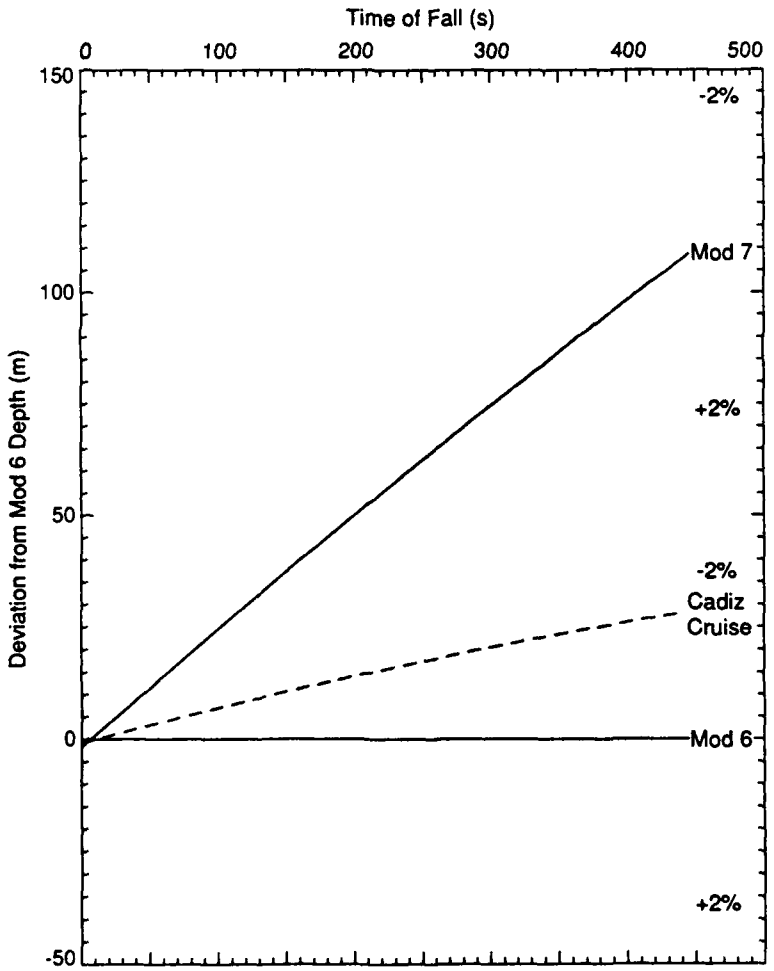

Figure 14. Differences in probe depth as computed from XCP coefficients. All differences are referenced to the depth computed using the coefficients for Mod 6. The shaded area is the ±2% range given by Sippican Inc. as the accuracy of the computed depth.

Further work is needed to determine whether the depth and temperature corrections are characteristic of the warm saline waters of the Mediterranean outflow or can be used regardless of location. Additional comparisons of XCP/CTD pairs from cruises where the temperature and salinity structure is substantially different than in the Gulf of Cadiz would be helpful.

5.2 XCP Processing Programs

Following the Gulf of Cadiz Expedition, a new set of XCP processing programs was written by John Dunlap. This set implements the functions of the old XCP processing program outlined by Sanford et al. (1982) but using a number of simpler programs. The old program performed so many functions that it was difficult to maintain. Since then, many variants of the XCP processing program have emerged to do different things, and no one version has existed for the general user. The new group of programs modularizes the processing and attempts to split it into functional groups. Modules are easier to understand and modify, encouraging clearer processing development in the future.

XCP processing is routinely done on an HP9050 computer. The processing sequence can be broken down into steps as follows: set up a database of information specific to each drop (such as time of drop, location, F_h and F_z), split the XCP data archived on the 9144 tapes by the Basic acquisition program (see Section 3) into a separate file for each drop, convert the 16-bit integer data into 32-bit floating point values, add the time-base information, determine the exact turn numbers where the drop started and stopped and add this information to the database, do the baseline corrections, produce profiles of the east and north velocity components and temperature as a function of depth and pressure, grid the data, and finally produce a standard plot. This sequence is actually done in two groupings. Both groupings start with the raw data, which are the individual drop files. This method is employed for efficient computer storage of the data, and therefore intermediate outputs are not kept. Grouping one takes the raw data to the turn number stage of processing. Grouping two starts with the raw data, repeats the steps in grouping one with the exception of the turn step, and outputs gridded data. The XCP overview section of the programmer's manual outlines the general processing sequence in more detail (Appendix B). The UNIX commands and programs necessary to process the Cadiz cruise data are summarized below.

```
awk -f mag.in.awk prpos.out |
geomag |
awk -f mag.out.awk |
hdrmerge dropdatafile

awk -f extras.awk prpos.out |
hdrmerge dropdatafile

cadiztape -p channel < 9144.tapefile |
xcpsplit debug channel outtype filenamefile rawdirectory

xcpfloat < rawdirectory/drop |
xcpaddt xcpaddt.p |
xcpturn xcpturn.p dropdatafile

xcpfloat < rawdirectory/drop |
xcpaddt xcpaddt.p |
xcpblf xcpblf.p |
xcppro xcppro.p dropdatafile |
xcpgrid xcpgrid.p > griddirectory/drop

xcpplot griddirectory/drop | hpp7
```

A database, *dropdatafile*, was developed to contain the processing parameters known to change from drop to drop. This database is an ASCII file, so it can be easily modified by hand with an editing program. Editing is needed when it is not possible to obtain correct values automatically (the start and stop turn numbers, for example, may be hard to determine for some drops for various reasons). Various programs modify and add to the database such items as the geomagnetic field, the start and stop turn numbers, etc.

The components of the earth's magnetic field (F_h and F_z) at each XCP drop site are obtained by running the program *geomag* using times and positions from the underway log. Program *geomag* was obtained from the National Geophysical Data Center and replaces the program PADOC used by Sanford et al. (1982). Program *geomag* calculates

the value of the seven magnetic field parameters for a specified date and location from a set of Schmidt quasi-normalized spherical harmonic coefficients read from an input model file. The model used for the Cadiz data was the International Geomagnetic Reference Field (IGRF85) model. The *awk* program is a UNIX command. In this application, *awk* uses *mag.in.awk* to reformat the log file into the format required by *geomag*. The *awk* program is run again with *mag.out.awk* on the output of *geomag* to format the results correctly for inclusion in the *dropdatafile* database. Program *hdrmerge* adds new entries or replaces previous entries in the database. Appendix C gives the programmer's manual entry for *hdrmerge*. The *mag.in.awk* and *mag.out.awk* programs used for the Cadiz data are listed in Appendix B. In addition, extra parameters (such as XCP serial number and launch time) can be added to *dropdatafile* (Appendix B).

For the Cadiz cruise, the continuous stream of XCP, XBT, and XSV data was recorded on HP9144 tape. Program *cadiztape* was written to separate out just the XCP data. The output of *cadiztape* is piped to *xcpsplit*, which is used to divide the raw XCP data from the HP-9020 Basic acquisition program files into separate files, one per drop. The programmer's manual entry for *xcpsplit* is shown in Appendix D.

Program *xcpfloat* converts the 16-bit integer data from *xcpsplit* into 32-bit floating point values to make a standard format file. The programmer's manual entry for *xcpfloat* is given in Appendix E.

Program *xcpturn* is used to find the turn numbers where the drop starts and ends. It examines the record of the rotation frequency during a drop to determine when the probe was released from the surface and when the drop terminated at the bottom. The turn number at half the average rotation frequency soon after the probe has spun up and the turn number for the last turn with good data are added to the *dropdatafile* database for later use by the program *xcppro*. The programmer's manual entry for *xcpturn* is given in Appendix F.

Programs *xcpaddt*, *xcpblf*, and *xcppro* actually perform the processing. The purpose of *xcpaddt* is to develop a good time base for the data samples from the Mk-10 so that correct depths can be assigned to the data. This is needed to estimate shear correctly as well as to compare XCP profiles with other measurements or other XCP profiles. The

programmer's manual entry for *xcpaddt* is given in Appendix G. Program *xcpblf* corrects the in-phase and quadrature data from the Mk-10 by estimating and removing the contributions from a slowly changing baseline or average frequency of the signals. In addition, the data from the Mk-10 are converted to frequencies. The programmer's manual entry for *xcpblf* is listed in Appendix H. Program *xcppro* accepts the corrected in-phase and quadrature carrier frequencies as well as the XCP probe rotation frequency. All frequencies are assumed to be the estimated probe frequencies with units of hertz. The standard input is typically produced by *xcpblf*. Program *xcppro* produces profiles of east and north velocity components and temperature as a function of depth and pressure on standard output. Program *xcppro* implements the part of the processing that is specific to the probe. It executes Eqs. 23 through 30 of Sanford et al. (1982). The programmer's manual entry for *xcppro* is shown in Appendix I. The output of *xcppro* is suitable for input to *xcpgrid*, which averages the data onto a uniformly sampled depth grid and can optionally produce vertical gradients of velocity and temperature. The programmer's manual entry for *xcpgrid* is given in Appendix J. Program *xcpplot* displays data from *xcpgrid* using standard scales on an HP-7550 pen plotter. The programmer's manual entry for *xcpplot* is shown in Appendix K.

5.2.1 New coefficients for XCP processing

New coefficients were determined for the XCP system gains and phases by Michael Horgan (Horgan et al., 1989) for use in the XCP processing programs. Horgan's phase and gain work was prompted by his examination of slow-fall AXCP profiles obtained during the Ocean Storms Experiment. Confirmation of his work was needed for the fast-fall XCPs (i.e., the type used during the Cadiz cruise) before the new coefficients would be considered valid for incorporation into the Cadiz data processing sequence. John Dunlap examined Horgan's findings for the 14–18 Hz rotation rate, fast-fall range. The results of Dunlap's work are summarized below. The gains and phases are computed as $a_0 + a_1 f + a_2 f^2$. The coefficients are listed in Table 5. The a's at the end of the coefficient names denote amplitude; the p's denote phase. Sanford et al. (1982) describe the meaning of each of the coefficient names.

These new polynomial coefficients describe the measured gains and phases as a function of rotation frequency for the entire XCP system from electrode and coil inputs

to the digital output of the Mk-10s. The original coefficients modeled only the analog section of the probe from the inputs to points just before the voltage-to-frequency (V/F) converters and only the phase dependence on rotation frequency.

Table 5. Horgan's new polynomial coefficients of gain and phase.

	a_0	a_1	a_2
G_{efa}	23866.12044581	107.99111272898	–0.905827321
G_{cca}	1809.877761	–1.25653911	0.18856556
G_{cora}	898.89564739	0.453188608	0.0717425016
G_{efp}	–138.158938796	9.759010754	–0.180878978
G_{ccp}	29.826971133	10.265226263	–0.176531452
G_{corp}	56.552652832	7.783581145	–0.112472607
G_{evfa}	494.66025		
G_{evfp}	0		
G_{cvfa}	500		
G_{cvfp}	0		

To test the gain and phase coefficients, a short Fortran program (see Appendix L) was written to estimate the amplitudes and phases of the frequency-modulation signals obtained from several Mk-10 XCP processors during controlled tests with a single pair of XCP circuit boards. Comparisons between the model estimates and the recorded data are shown in Table 6 for a 16-Hz rotation rate and several test signal configurations.

The first lines under each test result show measured data from various receivers and RF channels. The measured data are followed by their average and standard deviation. These are followed by the values predicted using Horgan's new coefficients and then the values using the original coefficients. After each prediction, the differences from the averages of the measured values are shown. The column labeled "Freq." is the rotation frequency. The columns labeled "F_{efa}" and "F_{cca}" are the amplitude of the frequency deviation for the electric field and compass coil channels, respectively. That labeled $F_{efp}-F_{ccp}$ is the phase difference between the same frequency deviations.

The type 1 tests were run with known electric field (EF) and compass coil (CC) signals and with equal phase angle at the probe inputs. The type 2 tests were the same except that the EF input was set to zero. (The CC signal was not set to zero; if it were, the Mk-10 would not function.) Each test was run with several different Mk-10 units and at two signal levels. The amplitude and phase estimates using the new (Horgan) coefficients are nearly always closer to the measurements than the estimates made using the original coefficients. The only exception occurs for F_{efa} during test type 1 with V_{in} set to 0.492 V peak to peak (p-p). (See "Horgan Diff" vs "Orig Diff" rows in column "F_{efa}" in Table 6.)

It may be that the 0.848 V (p-p) input caused the frequency deviations of the EF channel to exceed the linear range of the Mk-10. The frequency deviation for this test is about 320 Hz whereas the Mk-10 specification indicates the maximum deviation should be less than 250 Hz. In this case, the $F_{efp}-F_{ccp}$ phase difference measured at the Mk-10 output is about 1.2° smaller than predicted.

We are concerned that the phase difference depends on amplitude. At a rotation frequency of 16 Hz, the phase difference $F_{efp}-F_{ccp}$ changes more than 2° as the input amplitude is changed from 0.5 to 1.4 V (p-p). To verify that this is caused by the Mk-10 and not some other part of the circuit, a special setup was used in which the output of the CC V/F converter was wired to the input of the EF V/F converter so that the EF frequency was exactly half the CC frequency. The normal EF signal input to the EF V/F converter was disconnected.

Dunlap tried to determine if the phase shift could be explained by constant offsets in the in-phase (I) and quadrature (Q) outputs of the Mk-10, but the data do not fit a simple model. The Cartesian coordinates of the F_{efa}, F_{efp}, F_{cca}, and F_{ccp} values output by the previous XCP processing program, *xpro* 3, are F_{efx}, F_{efy}, F_{ccx}, and F_{ccy}. Four linear fits of these Cartesian coordinates were determined from the amplitudes and phases of the two Mk-10 channels as a function of the three input voltages, 0.495, 0.848, and 1.392 V (p-p). These coordinates are listed in Table 7. The column labeled V_{in} is the peak-to-peak voltage input to the probe. The one labeled Dev is the deviation from the fit. The fits showed standard deviations from 2 to 11 Hz. The polynomial is defined as $a_0 + a_1 V$. The zero offsets were from 5 to 27 Hz. We hoped to find constant values for

Table 6. Comparison of measured data and new and original coefficients.

Test Type	V_{in} (V p-p)	Freq. (Hz)	Receiver Channel	F_{efa} (Hz)	F_{cca} (Hz)	$F_{efp}-F_{ccp}$ (deg)
1	0.848	16.0	NII-16	319.6	214.7	1.9
			EM2-12	319.4	214.5	1.6
			EM2-14	318.7	214.3	1.8
			Average	319.2	214.5	1.8
			Std dev	0.5	0.2	0.2
			Horgan	319.6	214.5	3.0
			Diff	0.4	0.0	1.2
			Orig	318.0	211.6	5.8
			Diff	−1.2	−2.9	4.0
2	0.848	16.1	NII-16	106.2	213.9	3.6
			NII-16	106.7	213.9	3.6
			Average	106.5	213.9	3.6
			Std dev	0.4	0.0	0.0
			Horgan	106.8	214.6	3.4
			Diff	0.3	0.7	−0.2
			Orig	106.0	211.6	5.5
			Diff	−0.5	−2.3	1.9
1	0.492	16.1	NII-16	182.6	125.1	2.9
			AMP	174.1	124.8	3.0
			Average	178.4	125.0	3.0
			Std dev	6.0	0.2	0.1
			Horgan	185.5	124.5	3.0
			Diff	7.1	−0.5	0.1
			Orig	184.5	122.8	5.8
			Diff	6.1	−2.2	2.9
2	0.492	16.1	NII-16	65.4	125.2	3.5
			AMP	61.9	124.9	3.4
			Average	63.7	125.1	3.4
			Std dev	2.5	0.2	0.1
			Horgan	62.0	124.5	3.4
			Diff	−1.7	−0.6	−0.1
			Orig	61.5	122.8	5.5
			Diff	−2.2	−2.3	2.0

a_0, indicating an offset, but this is not the case. The I and Q results from the 0.848 V (p-p) input are not in line with others. In addition the frequency deviation using the 1.392 V (p-p) input may exceed the range of the phase-locked loops in the Mk-10.

This problem should be investigated further, since it indicates nonlinear behavior in the Mk-10. A 2° phase error causes an error of about 1 cm s^{-1} in the east component if the coil injection compensates for 80% of the fall rate and an error of 5 cm s^{-1} with no compensation.

We concluded that the new coefficients were much more accurate than the original ones for predicting the Mk-10 receiver output and thus should provide better estimates of the probe inputs during actual drops. The new coefficients were used in the XCP processing for the Cadiz cruise; however, they were determined only for one set of XCP boards and may be different for other boards.

Table 7. Linear fits of Mk-10 estimates versus input voltage.

V_{in} (V p-p)	F_{efx} (Hz)	Dev (Hz)	Std Dev (Hz)	a_0 (Hz)	a_1 (Hz V^{-1})
0.495	47.2	2.6	5.4	−4.9	99.9
0.848	75.5	−4.3			
1.392	135.9	1.7			
V_{in} (V p-p)	F_{efy} (Hz)	Dev (Hz)	Std Dev (Hz)	a_0 (Hz)	a_1 (Hz V^{-1})
0.495	−33.4	−1.4	2.9	4.9	−74.6
0.848	−56.0	2.3			
1.392	−99.8	−0.9			
V_{in} (V p-p)	F_{ccx} (Hz)	Dev (Hz)	Std Dev ((Hz)	a_0 (Hz)	a_1 (Hz V^{-1})
0.495	101.6	2.5	5.0	5.4	189.4
0.848	161.9	−4.1			
1.392	270.6	1.6			
V_{in} (V p-p)	F_{ccy} (Hz)	Dev (Hz)	Std Dev (Hz)	a_0 (Hz)	a_1 (Hz V^{-1})
0.495	−57.5	−5.9	11.9	27.5	−159.8
0.848	−98.4	9.7			
1.392	−198.8	−3.8			

5.2.2 A_{mean}

The area (in square centimeters) times the number of turns of the compass coil is called A_{mean}. In old XCP processing programs, it was actually computed as the average value of the area; now it is entered as a constant. Previous work shows that a value of 695 cm^2 is appropriate for Mod 6 probes. Michael Horgan initially used this figure in calculations for Ocean Storms AXCPs, Mod 7's, but later determined an A_{mean} of 667 cm^2 for those probes. We used Horgan's value for the Gulf of Cadiz data set. Subsequent analysis revealed that the average area for all Gulf of Cadiz XCPs deeper than 1000 m was 662.3 cm^2 with a standard deviation of 8.2 cm^2. Because 667 cm^2 is within one standard deviation of the Gulf of Cadiz average area, no change in value was considered necessary. A change of 1 cm^2 in area represents a change of 0.0027 m s^{-1} in the v component. Many of the XCPs that went deeper than 1000 m hit the seafloor and may be subject to local magnetic effects.

5.2.3 New C_2 for XCPs

Michael Horgan also determined a new value for C_2, which is a scale factor depending on the shape of the XCP and is used by the processing program *xcppro*. Because the A_{mean} (695) and fall rate he used are not appropriate for the Cadiz data set, John Dunlap converted Horgan's C_2 value to one suitable for the A_{mean} and fall-rate values determined (Section 5.1) for Mod 7 probes.

For C_2, Horgan used the north component of velocity, v, determined near the fall-rate transition depth for 17 Ocean Storms slow-fall AXCP drops (Horgan et al., 1989). It was assumed that the difference in v near the transition between the slow- and fast-fall sections of the drop, when averaged over many drops, should be zero. The apparent average difference was forced to zero by adjusting C_2. In some cases, if a profile had approximately the same shear above and below the speed transition depth, an offset was determined that caused the profile to have no discontinuity.

Using an A_{mean} value of 695 cm^2 and the Sippican Mod 6 depth coefficients, Horgan obtained a value of -0.0127 for C_2.

The fall rate in the upper (slow) section of the slow-fall drops is determined from the elapsed time and the calibration of the pressure-sensitive device used to release the drogue and blades from the slow-fall XCP.

Let v_w refer to the second term for v as described in Eq. 30 by Sanford et al. (1982). That term contains the north velocity component sensitivity to C_2, W, and $\overline{A}$, where $\overline{A}$ is the average area per drop.

$$v_w = W \frac{F_h(1+C_2)}{F_z(1+C_1)} \frac{A}{\overline{A}} .$$

The fall rate, W, is the derivative of Eq. 1 (p. 19) with respect to time, or

$$-W = -\frac{dz}{dt} = \text{pcal1} + (2 \times \text{pcal0} \times t) = [\text{pcal1}^2 - 4\ \text{pcal0}\ (\text{pcal2} + z)]^{-1/2} .$$

Note that both z and W are less than zero, since the vertical coordinate axis is positive upward with the origin at the surface and the XCP falls downward below the surface.

The values for the Mod 7 fast-fall depth coefficients have been determined in various ways. Until the Gulf of Cadiz experiment, we used the Mod 7 values published by Sippican. We are not certain how they were determined, but they seem to be in error by about 4% when XCP temperature fluctuations are compared with nearly simultaneous XBT and CTD data obtained during the Cadiz cruise. In June 1989, new coefficients were computed for the Mod 7 probes using the Cadiz data (Section 5.1). The new coefficients are close to the Mod 6 coefficients. Table 4 lists the three sets of coefficients, and Table 8 gives the value for W at $z = -200$ m (the average depth of the speed transition in the slow-fall probes) for the three sets.

The average area per drop, $\overline{A}$, is no longer used. Instead, an average value, A_{mean}, is computed for many drops and inserted as a fixed parameter in the processing. For Mod 6 probes, this value is 695 cm^2. It appears to be 667 cm^2 for the Mod 7 probes deployed during Ocean Storms.

Table 8. Fall rates at 200 m depth.

Coefficient	Fall Rate
Mod 6	−4.485
Sippican Mod 7	−4.218
Cadiz Cruise Analysis	−4.405

In order to use the results of Horgan's C_2 adjustment with the correct A_{mean} and W values, it is assumed that v_w should remain constant and C_2 should be adjusted to offset the effects of changes in A_{mean} and W. The primed terms in the following equation indicate use of the new values:

$$C'_2 = (1 + C_2) \frac{A'_{mean}}{A_{mean}} \frac{W}{W'} - 1 .$$

Using Horgan's value for C_2, we obtain the following value for the new C'_2:

$$C'_2 = (1 - 0.0127) \frac{667}{695} \frac{-4.485}{-4.405} - 1 = -0.035 .$$

The new value of -0.035 for C_2 is somewhat different from the historical value of -0.02. The sensitivity of v_w to C_2 is about 0.9 m s^{-1}, so the difference in v is about 1.4 cm s^{-1}.

It is not known if this new value departs too much from the historical value determined from a prolate spheroidal model of the body (Sanford et al., 1982). A number of pitfalls are present. The value for C_2 may depend on fall speed if the amount of entrained water changes with fall speed. C_1, the electric potential amplification factor due to body shape, might change when the drogue and blade assembly of the slow-fall XCP is jettisoned. The 17 profiles used by Horgan may actually have an average mean shear across the fall-speed transition depth of 200 m. Nonetheless, the new C_2 value of -0.035 was used for the Cadiz cruise XCP processing.

5.2.4 XCP temperature processing

John Dunlap developed a simple method of using probe calibrations in our XCP temperature processing. Coefficients for a model of frequency versus thermistor resistance in the probe circuit were derived from the XCP calibration values supplied by Sippican. Coefficients for a model of temperature versus resistance were derived from the Sippican thermistor specification. Dunlap's equation based on the model has been incorporated into the new XCP processing programs and is described here.

The Mod 7 XCP temperature circuit frequency was modeled as

$$F_t = 1/[a \times C \times (R_s + R_t)] ,$$

where $a = 4.4$, C is the value of the timing capacitor, R_t is the thermistor resistance, and R_s is the value of a resistor in series with the thermistor. Sippican supplies a calibration for each XCP which gives two frequencies, F_{t1} and F_{t2}, when two different resistors, R_{t1} and R_{t2}, are attached to the XCP in place of the thermistor. This is done on the unpotted circuit board before installation in an XCP. Resistors R_{t1} and R_{t2} are 16329 Ω and 4024 Ω, respectively, which corresponds to the Sippican thermistor specifications at 0 and 30°C.

These calibration frequencies and resistances can be used to determine R_s and C in the foregoing equation as follows.

$$R_s = \frac{F_{t1} R_{t1} - F_{t2} R_{t2}}{F_{t2} - F_{t1}}$$

$$C = \frac{1}{a\, F_{t1} (R_s + R_{t1})} .$$

Early probes used a timing capacitor with a tolerance of 10% and a potentiometer which was adjusted to give $F_t = 381$ Hz when $R_t = 7855$ Ω (the resistance specified for 15°C). It was realized that this procedure did not make the transfer function of all the probes equal.

Sometime after April 1984, the potentiometer was replaced with a fixed 1% resistor (R_s) of 17400 Ω, and a parallel combination of three capacitors was used to obtain C in order to have F_t close to 381 Hz with $R_t = 7855$ Ω (see Sippican Memorandum OM-7438, 1984). This was done to make the variability from probe to probe less than 0.2°C overall, including the thermistor variability which is approximately 0.1°C.

Old probes had nominal component values of $R_s = 14238$ Ω and $C = 0.027$ μF, whereas in new probes $R_s = 17400$ Ω and $C = 0.02362$ μF. Note that any error in the model coefficient a is lumped in with C.

The calibration values for probe 1531 are $F_{t1} = 286.2$ Hz and $F_{t2} = 449.8$ Hz. These values give $R_s = 17502$ Ω and $C = 0.0235$ μF.

This circuit model can be used to process data from Mod 6 probes as well. In fact, the old Mod 6 method differs only in detail. Nominal calibration values for Mod 6 probes are $F_{t1} = 263.9$ Hz and $F_{t2} = 475.3$ Hz. The probes seldom deviate from those values more than 0.2 Hz, and thus individual temperature calibrations are not used.

It will probably not be necessary to use individual temperature calibrations with newer Mod 7 probes. They should be within 0.2° of each other (neglecting self-heating problems).

The model of temperature T given thermistor resistance R_t is

$$T = 1/\{c0 + [c1 \times \ln(R_t)] + [c2 \times \ln(R_t)^2] + [c3 \times \ln(R_t)^3]\} - 273.15 .$$

To obtain the coefficients $c0, \ldots, c3$, the Sippican XBT thermistor specification for resistance R_t versus temperature T was used as data for a polynomial least-squares fit to

$$y = c0 + (c1 \times x) + (c2 \times x^2) + (c3 \times x^3) ,$$

where

$$y = 1/(T + 273.15)$$

$$x = \ln(R_t) .$$

The maximum deviation from the fit when using data from −2 to 35.55°C was 0.01°C except at 35.00°C and 35.55°C, where the points deviated by more than three standard deviations. When those two points were removed from the fitting, the following coefficients were obtained:

$$c0 = 1.73323450654\, e \times 10^{-3}$$
$$c1 = 8.755085297563\, e \times 10^{-5}$$
$$c2 = 1.640669605119\, e \times 10^{-5}$$
$$c3 = -5.098817533782\, e \times 10^{-7}$$

The standard deviation of the residuals from −2°C to 34°C is 0.004°C. This is much better than the 0.2°C given in the XCP temperature specification.

Sippican Memorandum OM-7438 (1984) has coefficients for a fifth-order polynomial (listed in Table 2) going directly from frequency to temperature for a nominal probe ($R_s = 17400\ \Omega$ and $C = 0.02362\ \mu$F).

$$T = c0 + (c1 \times F_t) + (c2 \times F_t^2) + (c3 \times F_t^3) + (c4 \times F_t^4) + (c5 \times F_t^5) .$$

The residuals have a standard deviation of 0.010°C when using the thermistor specifications for −2° to 34°C. Examination of the residuals indicates that the fit used to obtain these coefficients included the faulty points at 35.00°C and 35.55°C and that the standard deviation would probably decrease if those two values were removed during fitting.

Dunlap's method fit the data better than Sippican's, although both fit much better than needed and Sippican's method can be improved by removing the 35.00°C and 35.55°C points. Dunlap's method offers a much simpler solution for the model coefficients. Sippican's method offers somewhat speedier computation once the coefficients are obtained. Dunlap's method was used in processing the Cadiz data.

5.2.5 Validation of new processing

After the post-cruise processing was completed, the calibrations outlined in Section 5.1 were repeated to verify the depth and temperature corrections. Figure 15 shows the results of the calibration verification. Because the vertical reference of the post-cruise processed XCP data is pressure, the CTD pressures were not converted to depth for the analysis. When the temperature correction and the new depth coefficients presented in Section 5.1 are used, the resulting pressure (shown in Figure 15 in decibars) and temperature offsets are both well centered around zero.

5.3 Final XCP Processing

Parameter files are used to input variable values to the XCP processing programs. Because these values can change, we have included the parameter file listings used for the Cadiz processing in Appendix M. This was done primarily so that a record of the values can be easily viewed (values are stored in the header information of the individual XCP computer files). The parameter files are listed with the name of the file followed by its contents. The parameter file usage can be found by reviewing the XCP processing program overview in Appendix B and the appropriate program documentation (Appendices B–K). Some of the important developments in the XCP processing are as follows:

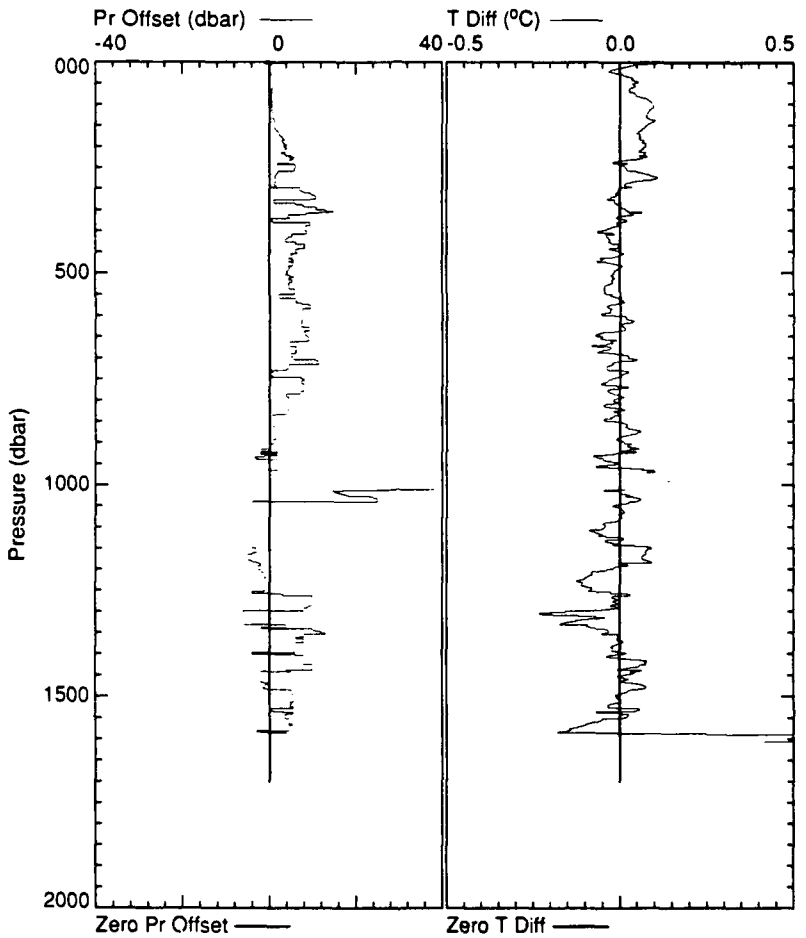

Figure 15. Pressure offsets and temperature differences computed for XCP/CTD pairs when using the Cadiz post-cruise XCP Mod 7 depth coefficients and temperature corrections.

Horgan's new coefficients were used (Section 5.2.1 and probe.p in Appendix M); new fall-rate coefficients were determined for this data set and implemented in the processing program, and depths were converted to pressures (Section 5.1 and pcal.p in Appendix M); a linear temperature correction was applied to the XCP temperature values (Section 5.1 and tcal.p in Appendix M); the data were averaged over 6 dbar and output every 2 dbar (*xcpgrid.p* in Appendix M).

5.4 XCP Offsets

To quantify XCP variability from probe to probe, an investigation was made of subsets of the Cadiz XCP data set. Our assumption was that over small distances oceanic features should be similar and thus the XCP profiles should be similar. Major deviations or offsets would then be due to instrument variability. The Ampere Seamount surveys and the Meddy star pattern are particularly good subsets for looking at this issue.

To study the probe-to-probe variability, we first made waterfall plots of temperature, area, and the u and v velocity components. The data shown in these plots were based on the standard processing discussed earlier in this report. Successive profiles were shifted for easy viewing. In each waterfall plot, the first XCP was plotted to scale, and each successive drop was shifted 2°C in temperature, 40 cm^2 in area, and 0.2 m s^{-1} for u and v.

During the Ampere Seamount survey, profiles were dropped every 5 min while steaming at 3 kn (Figures 4 and 5); during the Meddy pattern, drops were made every 20 min at 5 kn (Figure 7).

One method of determining instrument variability is to find a homogeneous vertical interval with, if possible, low shear in the profiles and to compute the means over that interval. An alternative method is to average over a larger interval of the water column (excluding the surface), for example, 500 to 1500 dbar. If the probes were launched in similar oceanic conditions, the interval's mean velocity would be expected to be a constant from probe to probe or, if not constant, to vary slowly because of evolving features in the ocean. The reason for plotting area is that trends in this variable will indicate local effects, such as magnetic disturbances near the seafloor. If such trends appear, those profiles should not be included in the analysis.

Let the vertical mean of an individual profile of an ensemble be denoted as

$$\bar{u}_i = \bar{U} + \varepsilon_i^O + \varepsilon_i^I ,$$

where $\bar{U}$ is the ensemble mean,

$$\bar{U} = \frac{1}{N} \sum \bar{u}_i ,$$

and ε_i^O and ε_i^I are the noise and errors in the estimate of the vertical mean due to, respectively, the ocean and the instrument. The variance of the vertical mean over the ensemble is

$$\sigma_{\bar{U}}^2 = \frac{1}{N-1}\sum (\bar{u}_i - \bar{U})^2 .$$

Substituting for $\bar{u}_i$ yields

$$\sigma_{\bar{U}}^2 = \frac{1}{N-1}\sum (\bar{U} + \varepsilon_i^O + \varepsilon_i^I - \bar{U})^2$$

$$= \frac{1}{N-1}\sum (\varepsilon_i^{O\,2} + 2\varepsilon_i^O\varepsilon_i^I + \varepsilon_i^{I\,2}) .$$

The variance of the vertical mean contributed by oceanic variability is defined as

$$\sigma_{\bar{u}}^2 = \frac{1}{N-1}\sum \varepsilon_i^{O\,2} .$$

According to Lumley and Tennekes (1972), the uncertainty in the vertical mean is related to the variance of the velocity over the interval P (both P = 500–1500 dbar and P = 600–1100 dbar were used in the following sections), divided by $P/2p$, the number of independent observations in the interval, where p is the ensemble average integral length scale determined from an ensemble average autocorrelation function.

$$\sigma_{\bar{u}}^2 = \frac{1}{N-1}\sum \varepsilon_i^{O\,2} = \sigma_u^2 \frac{p}{P} .$$

The variance due to probe-to-probe or instrumental variability is

$$\sigma_I^2 = \frac{1}{N-1}\sum \varepsilon_i^{I\,2} .$$

If the ocean and instrument errors and noise are assumed to be uncorrelated,

$$\frac{1}{N-1}\sum 2\varepsilon_i^O\varepsilon_i^I = 0 .$$

Thus the variance of the vertical means over a set of profiles is given as the sum of the contributions from oceanic processes and instrument noise.

$$\sigma_{\bar{U}}^2 = \sigma_{\bar{u}}^2 + \sigma_I^2$$

or

$$\sigma_I = \sqrt{\sigma_{\bar{U}}^2 - \sigma_{\bar{u}}^2 \, 2 \, \frac{p}{P}} \, . \tag{2}$$

5.4.1 XCP survey 1, leg 1 (XCPs 2401–2411)

The waterfall plots of temperature versus pressure for XCP drops 2401–2411 are shown in Figure 16. The temperature data for XCPs 2401 and 2402 were of poor quality and have not been included in the plots. (The temperatures for those drops are shown on the individual plots in Appendix N). Plots of area are shown for the entire leg in Figure 17. XCP 2401 was not used for determining the means because of the trend in the area (probably caused by magnetic anomalies due to the seamount). The u and v velocity components tracked nicely, especially the feature at 800 dbar (Figures 18 and 19). Note, however, the gap between drops 2404 and 2405 and the proximity of drops 2408 and 2409 in the u profiles. The coil was reversed on XCP 2410. Post-cruise programs enabled the data to be processed, but it appears they were not entirely correct (as seen in the large offset in the waterfall plots for the v component, Figure 19). Therefore drop 2410 was also not used in determining the XCP offsets.

It was hard to pick a level with small shear for both velocity components. The upper 100 dbar should be discounted because of surface wave effects. Two intervals were tried. First we averaged over 500 to 1500 dbar. Then, based on the temperature plot (Figure 16), the 600 to 1100 dbar level was chosen for averaging because it seemed fairly isothermal from profile to profile. For the 600 to 1100 dbar interval, the u component had more variability than the v.

The vertical means ($\bar{u}_i$ and $\bar{v}_i$) and rms (σ_{u_i} and σ_{v_i}) were found for the velocity components for each profile between 500 and 1500 dbar and 600 and 1100 dbar (Table 9). The plot of $\bar{u}_i$ and $\bar{v}_i$ for the 500 to 1500 dbar interval is shown in Figure 20a and that for the 600 to 1100 dbar interval in Figure 20b. The $\bar{v}_i$ values are more uniform than the $\bar{u}_i$ over both intervals. XCP 2407, however, is an outlier. It was thought that the large deviation in 2407 might be due to a random variation in fall rate. When 2407 was

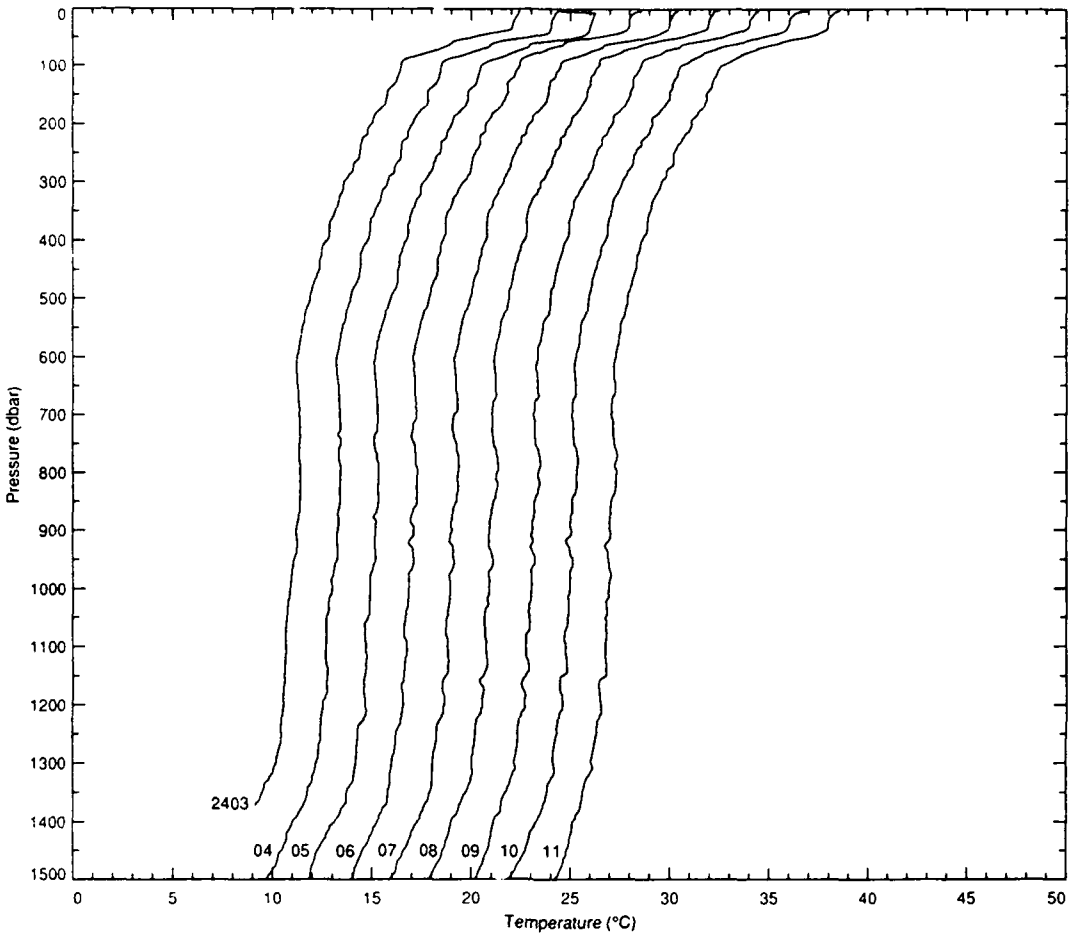

Figure 16. Plot of temperature (°C) versus pressure measured by XCPs during leg 1 of first Ampere Seamount survey.

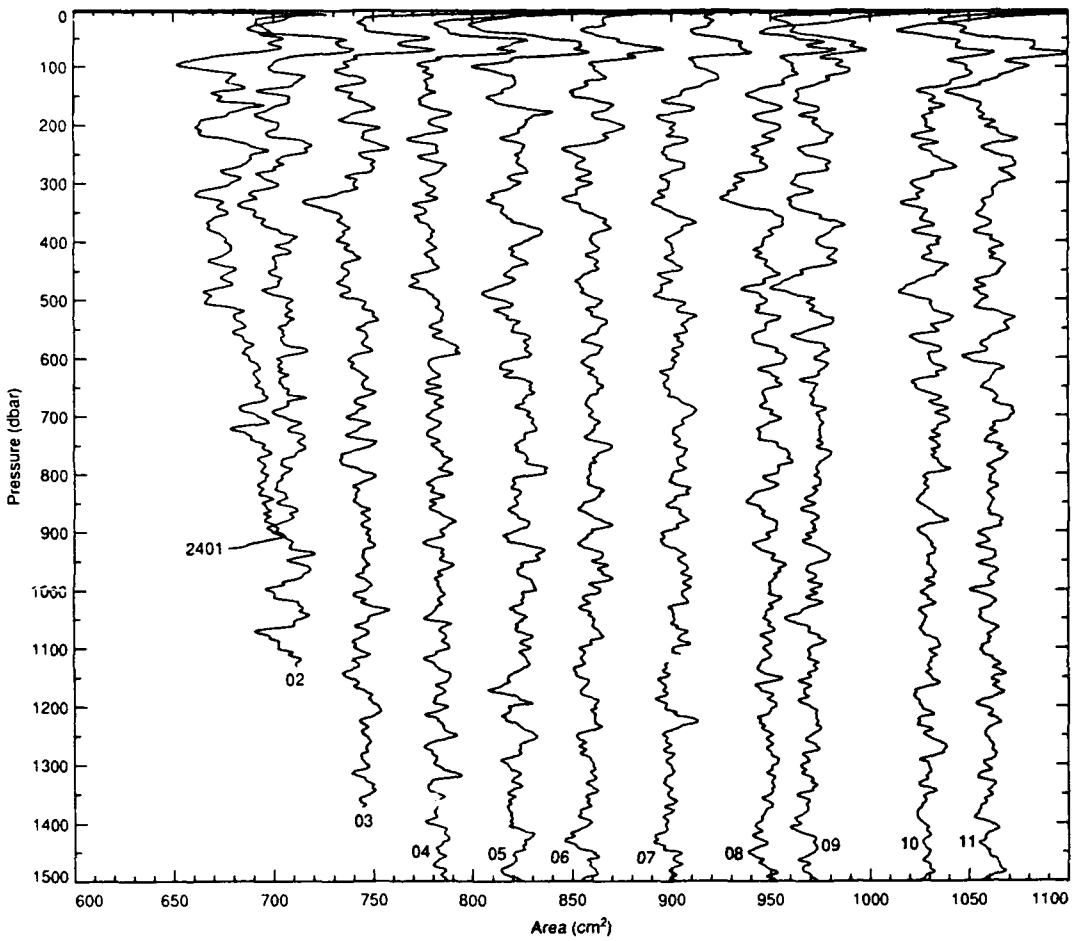

Figure 17. Plot of area (cm^2) versus pressure measured by XCPs during leg 1 of first Ampere Seamount survey.

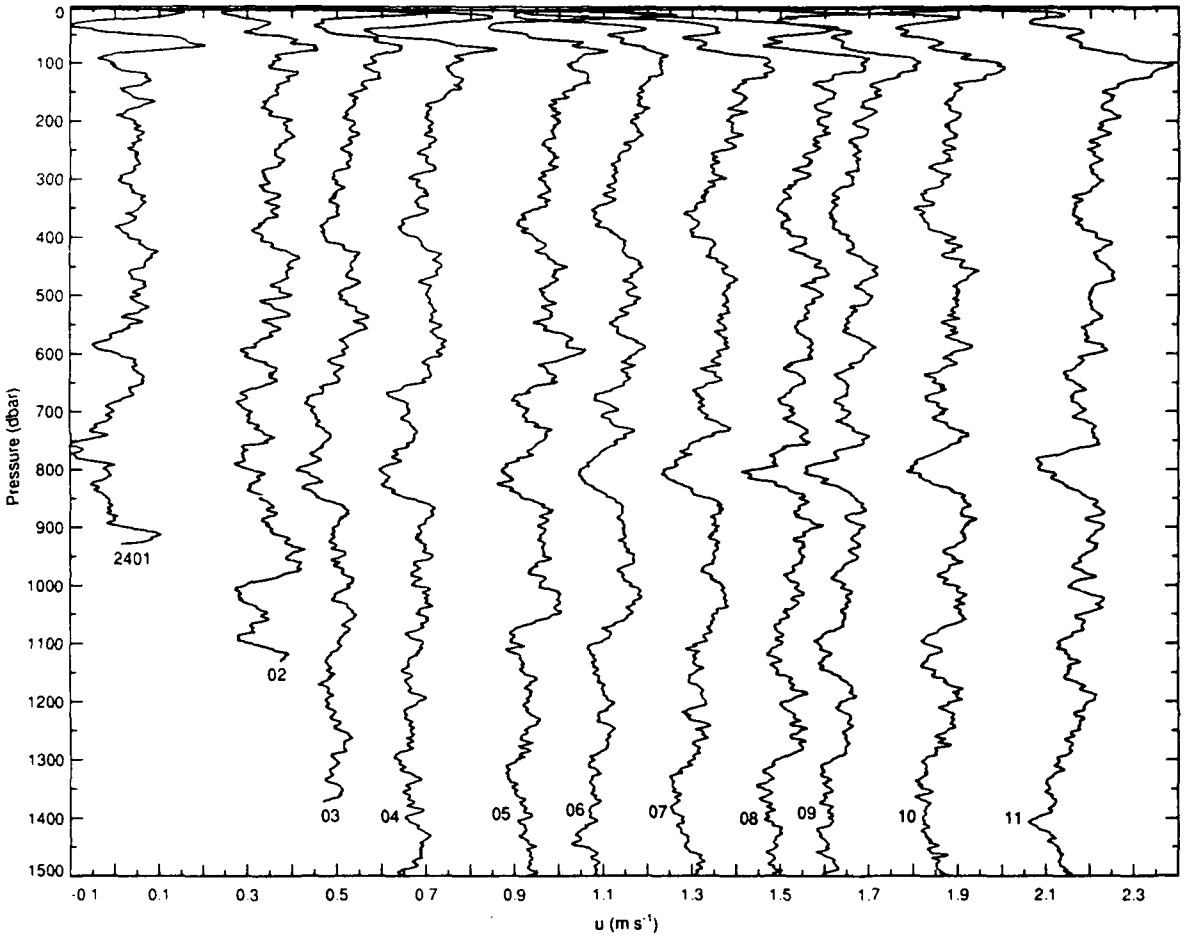

Figure 18. Plot of u velocity (m s^{-1}) versus pressure measured by XCPs during leg 1 of first Ampere Seamount survey.

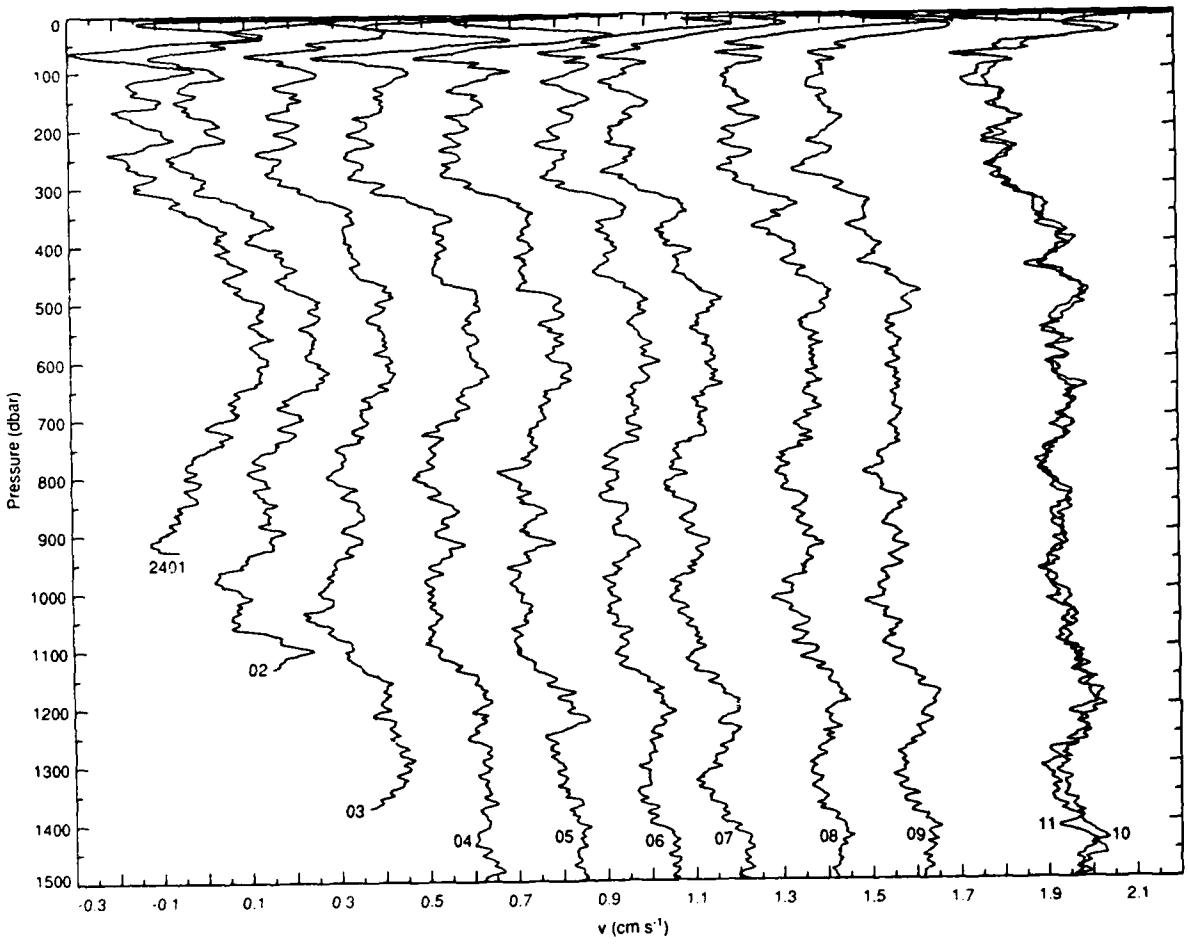

Figure 19. Plot of v velocity (m s^{-1}) versus pressure measured by XCPs during leg 1 of first Ampere Seamount survey.

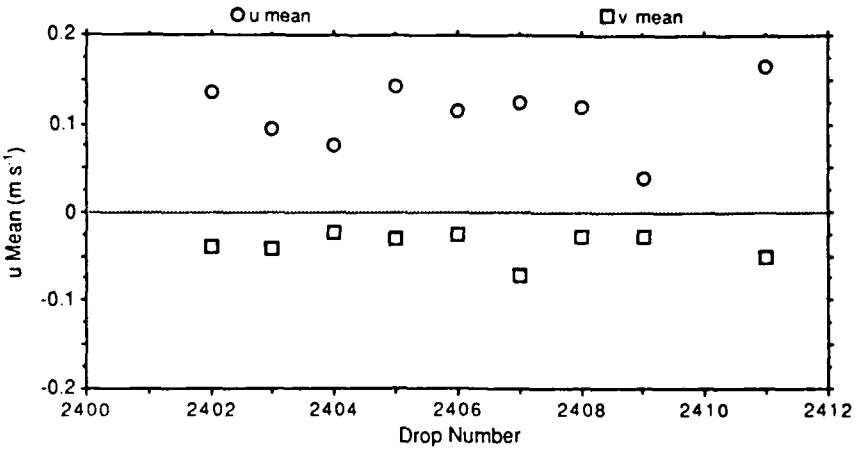

Figure 20a. Plots of $\overline{u}_i$ and $\overline{v}_i$ for the interval 500 to 1500 dbar for leg 1 XCP drops of first Ampere Seamount survey.

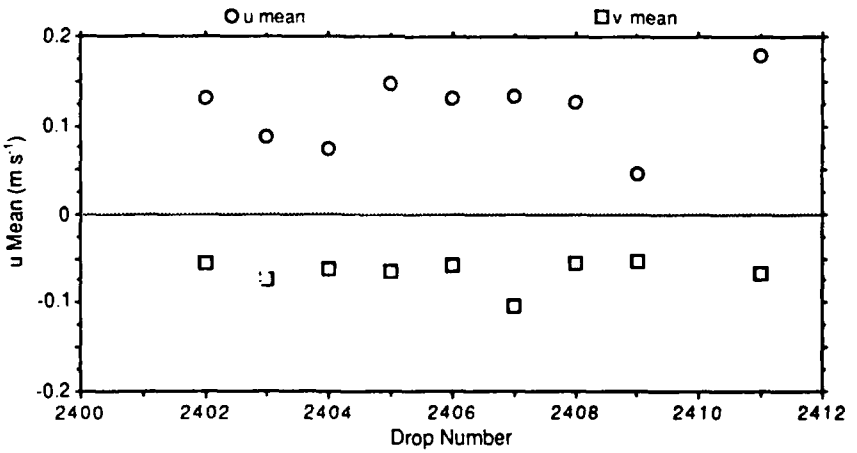

Figure 20b. Plots of $\overline{u}_i$ and $\overline{v}_i$ for the interval 600 to 1100 dbar for leg 1 XCP drops of the first Ampere Seamount survey.

Table 9. Mean velocities for Ampere Seamount, survey 1, leg 1.

Interval: 500 to 1500 dbar

Drop	$\bar{u}_i$ (m s^{-1})	σ_{u_i} (m s^{-1})	$\bar{v}_i$ (m s^{-1})	σ_{v_i} (m s^{-1})
2402	0.1355180	0.0373045	−0.0379905	0.0668154
2403	0.0950679	0.0302631	−0.0412865	0.0565167
2404	0.0760176	0.0297996	−0.0238456	0.0505072
2405	0.1417320	0.0368229	−0.0299658	0.0487937
2406	0.1143570	0.0381170	−0.0262929	0.0439085
2407	0.1231460	0.0372407	−0.0713292	0.0474129
2408	0.1184120	0.0339236	−0.0276000	0.0378288
2409	0.0387295	0.0325608	−0.0276737	0.0364952
2411	0.1660300	0.0400320	−0.0498906	0.0316086
$\bar{U}$	0.1121122			
$\sigma_{\bar{U}}$	0.0378766			
σ_u		0.0351182		
$\bar{V}$			−0.0373194	
$\sigma_{\bar{V}}$			0.0153118	
σ_v				0.046541

Interval: 600 to 1100 dbar

Drop	$\bar{u}_i$ (m s^{-1})	σ_{u_i} (m s^{-1})	$\bar{v}_i$ (m s^{-1})	σ_{v_i} (m s^{-1})
2402	0.1310270	0.0380485	−0.0554317	0.0624655
2403	0.0875540	0.0317969	−0.0746622	0.0468059
2404	0.0733940	0.0323923	−0.0621857	0.0388957
2405	0.1474890	0.0374331	−0.0637873	0.0361658
2406	0.1302380	0.0343837	−0.0571617	0.0292473
2407	0.1341120	0.0343984	−0.1030310	0.0313965
2408	0.1256500	0.0311744	−0.0544721	0.0267606
2409	0.0459406	0.0306386	−0.0524057	0.0209593
2411	0.1783190	0.0356370	−0.0655996	0.0225697
$\bar{U}$	0.1170804			
$\sigma_{\bar{U}}$	0.0406927			
σ_u		0.0339892		
$\bar{V}$			−0.0654152	
$\sigma_{\bar{V}}$			0.0156938	
σ_v				0.0350296

plotted with the preceding and following drops (Figures 21a and 21b), however, this did not appear to be the case. When the data were plotted with the mean removed, they were more uniformly spaced (Figures 22 through 25). The plots for the two averaging intervals were nearly identical. Using Eq. 2, we calculated the quantity σ_I from the data in Table 9 for the 500 to 1500 dbar interval. Autocorrelation functions for u and v were determined for each of the XCPs. An ensemble average autocorrelation function was constructed from the individual autocorrelation functions. The ensemble average integral length scale was then computed from the average autocorrelation function. It was determined that $p = 35$ dbar for u and $p = 65$ dbar for v. For u, σ_I is 0.0367193. For v, it is 0.0 (i.e., there is no instrument noise) to within the limit of the data set. That σ_I is not 0.0 for u may be due to a phase shift variability from probe to probe in the electronics.

5.4.2 XCP survey 2, leg 2 (XCPs 2443–2455)

The waterfall plots of temperature versus pressure for XCPs 2443–2455 are shown in Figure 26. XCP 2446 was bad and no data are shown for this drop. Drops 2443 and 2449 have also been omitted because the temperature data were of poor quality. Area is shown for the entire leg in Figure 27. XCP 2445 exhibits a slight trend in area below 800 dbar and XCP 2448 is noiser than the others, but both were included in the analysis. The u and v velocity components (Figures 28 and 29) track nicely on this leg also. However, large gaps and closely spaced profiles can again be seen in both figures. Note, for example, the large gap between drops 2444 and 2445 in both Figure 28 (u component) and Figure 29 (v component) and the proximity of drops 2451 and 2452 in Figure 29.

It appeared that there was little difference in using the two averaging intervals (Section 5.4.1). Therefore we worked only with the larger interval, 500 to 1500 dbar. The vertical means ($\overline{u}_i$ and $\overline{v}_i$) and rms (σ_{u_i} and σ_{v_i}) were found for the velocity components for each profile (Table 10). The plot of $\overline{u}_i$ and $\overline{v}_i$ for the 500 to 1500 dbar interval is shown in Figure 30. The data plotted with the mean removed are again more uniformly spaced (Figures 31 and 32). Using Eq. 2, we calculated the quantity σ_I from the data in Table 10. From the average autocorrelation function for these data, we found $p = 59$ dbar for u and $p = 110$ dbar for v. For the 500 to 1500 dbar interval, σ_I was 0.0448 for u and 0.02607 for v.

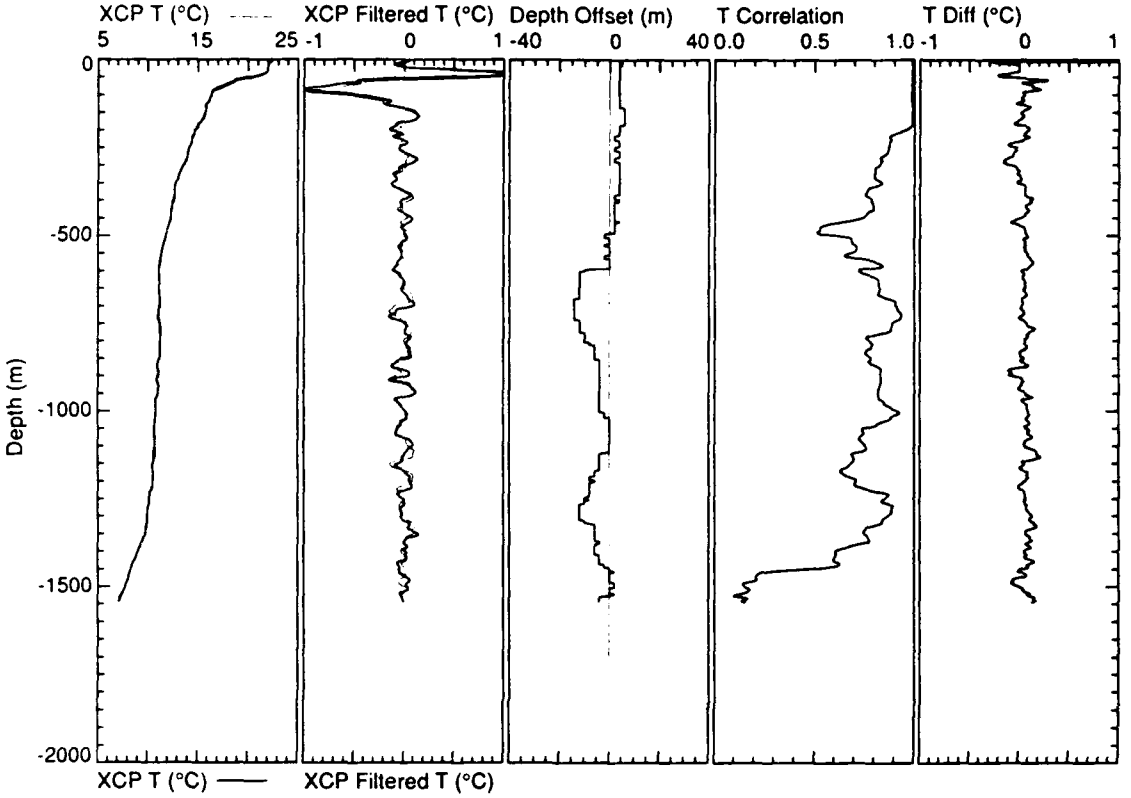

Figure 21a. Fall-rate analysis of XCP drop 2407 (light lines) referenced to drop 2406 (heavy lines). Maximum depth offset does not exceed 15 m.

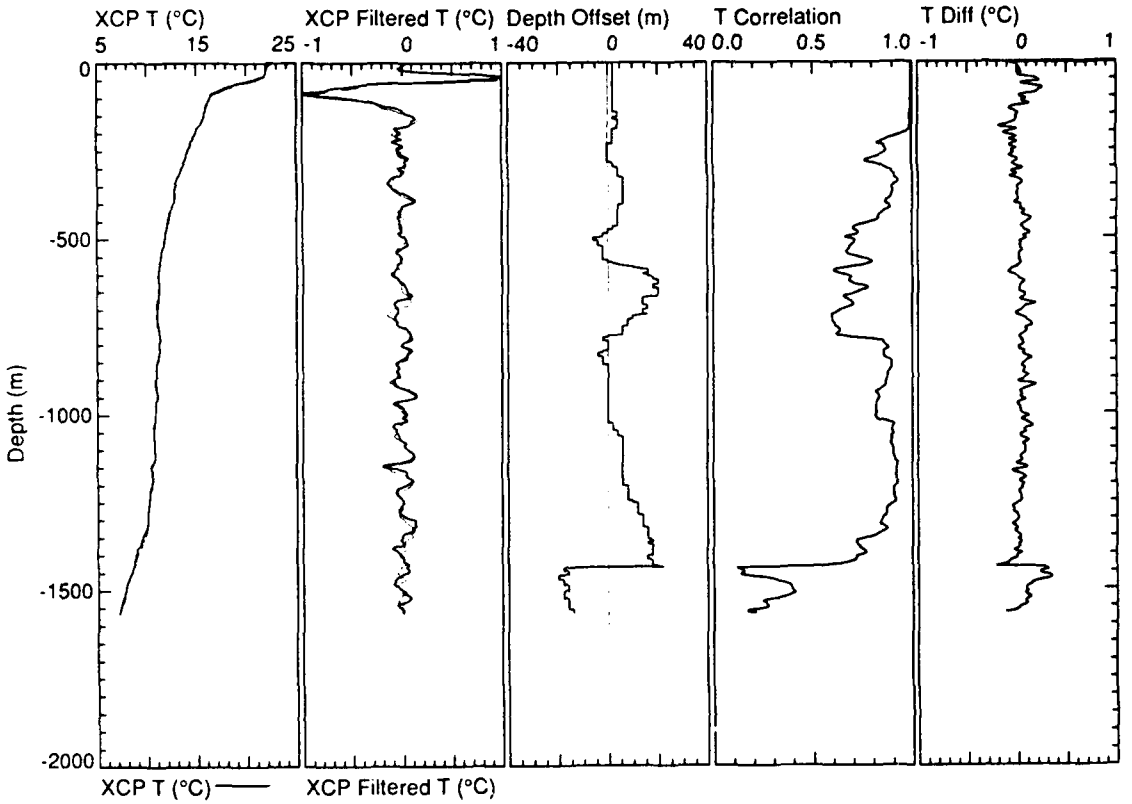

Figure 21b. Fall-rate analysis of XCP drop 2407 (light lines) referenced to drop 2408 (heavy lines). Maximum depth offset does not exceed 20 m.

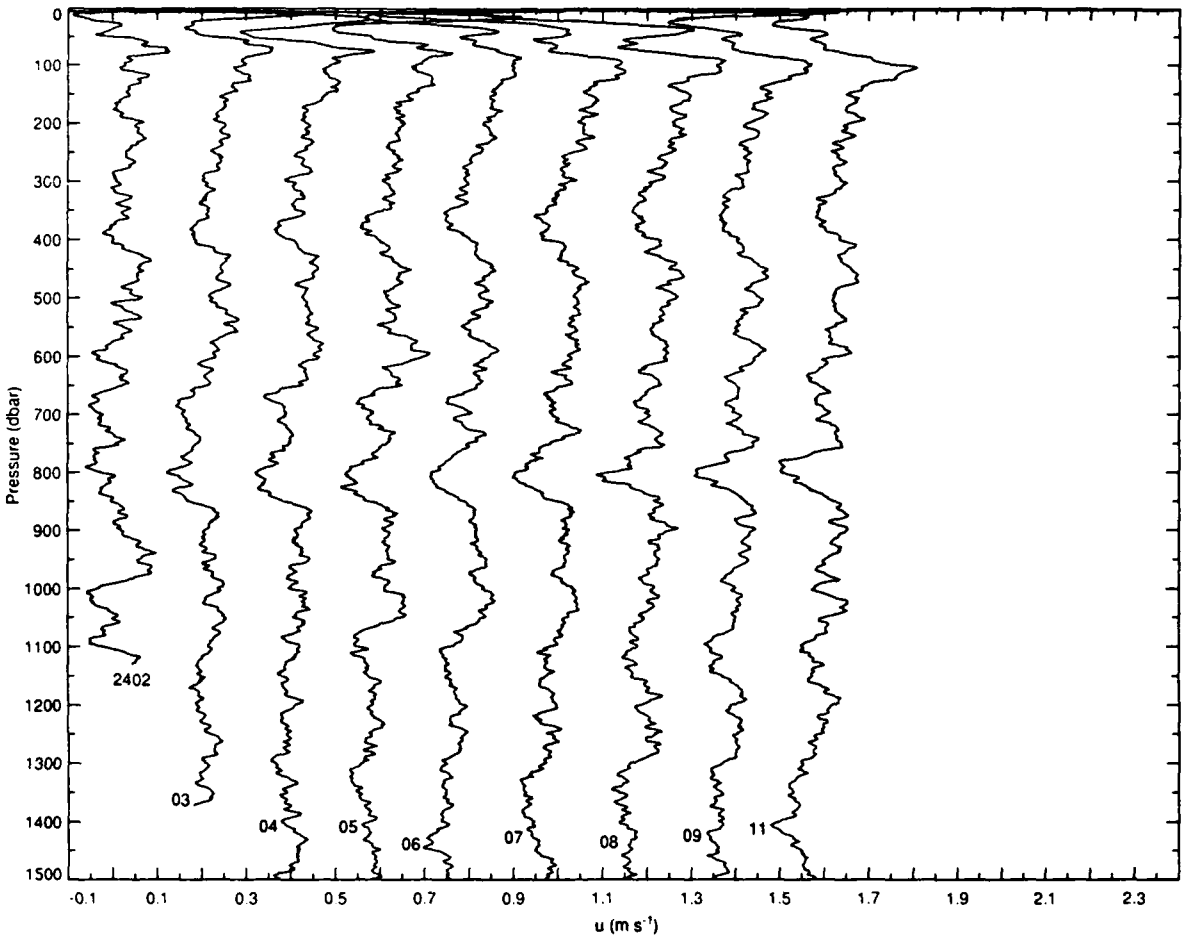

Figure 22. Plot of u velocity ($m\ s^{-1}$) versus pressure with mean from 500 to 1500 dbar removed from XCP data, leg 1 of first Ampere Seamount survey.

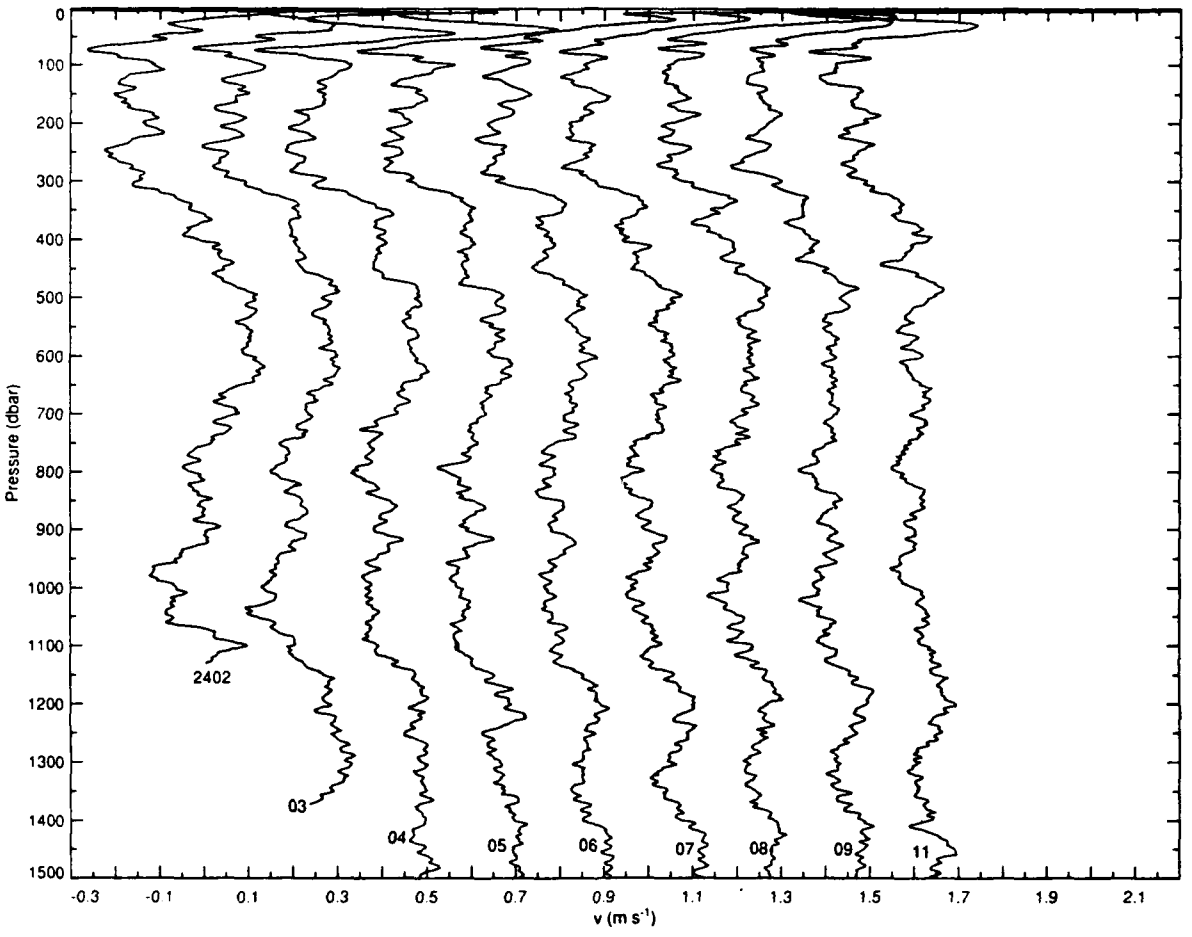

Figure 23. Plot of v velocity ($m\ s^{-1}$) versus pressure with mean from 500 to 1500 dbar removed from XCP data, leg 1 of first Ampere Seamount survey.

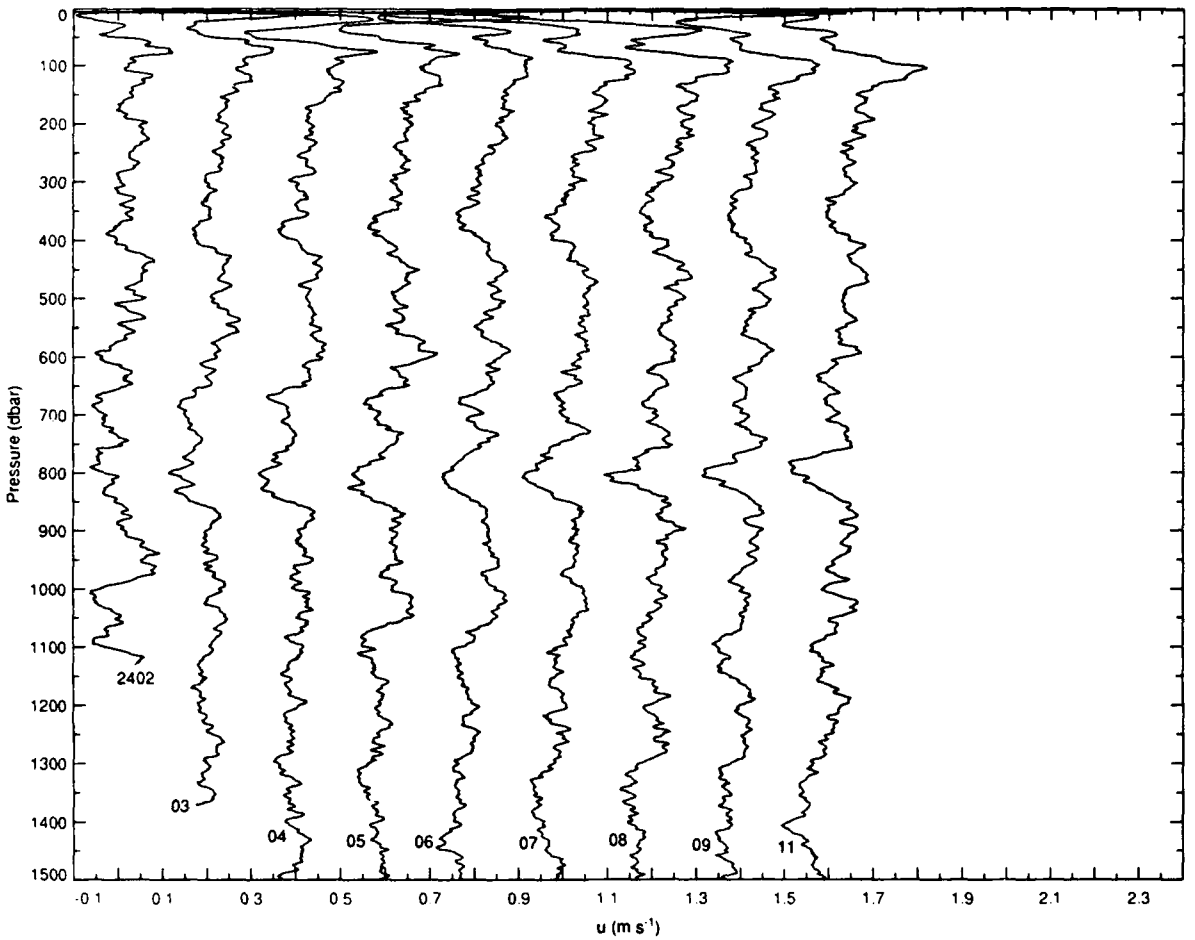

Figure 24. Plot of u velocity (m s^{-1}) versus pressure with mean from 600 to 1100 dbar removed from XCP data, leg 1 of first Ampere Seamount survey.

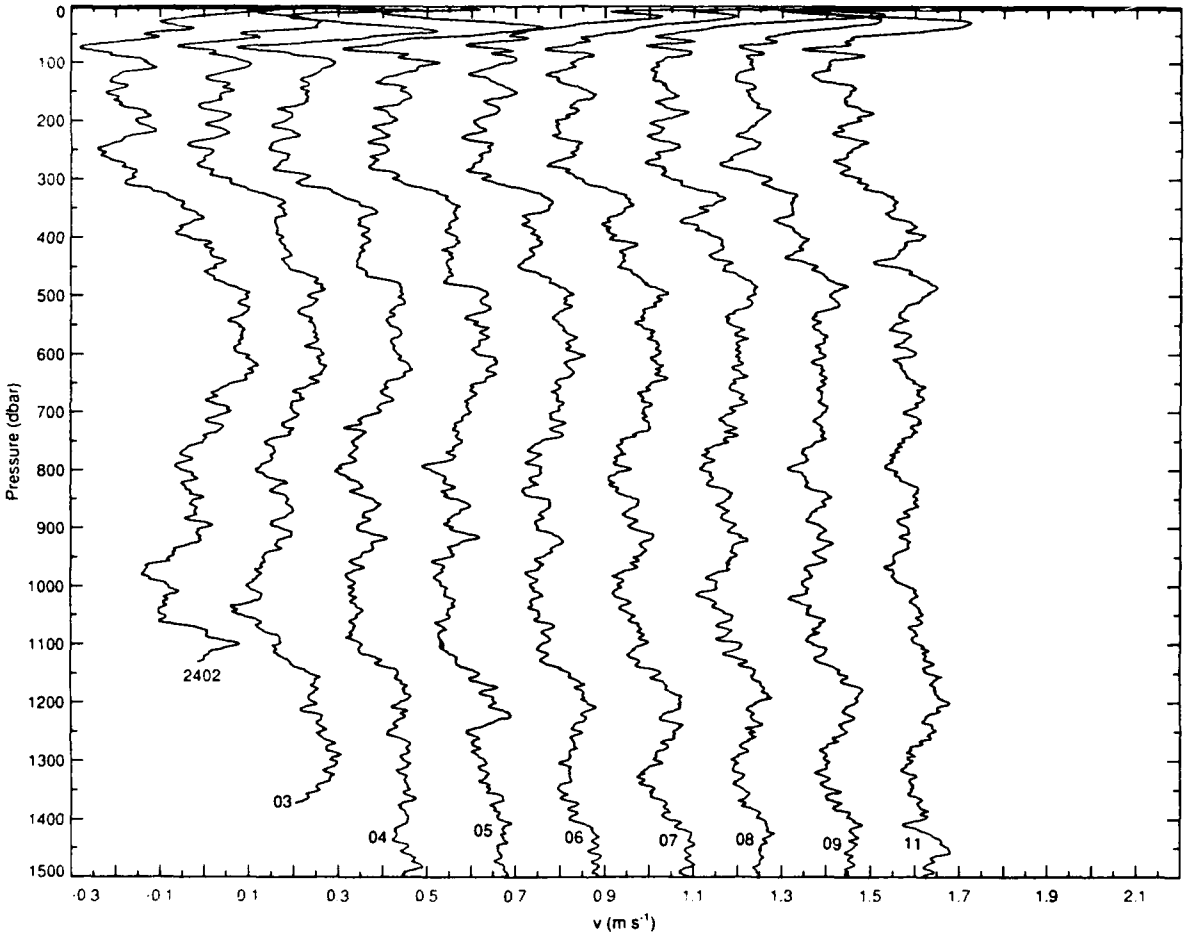

Figure 25. Plot of v velocity ($m\ s^{-1}$) versus pressure with mean from 600 to 1100 dbar removed from XCP data, leg 1 of first Ampere Seamount survey.

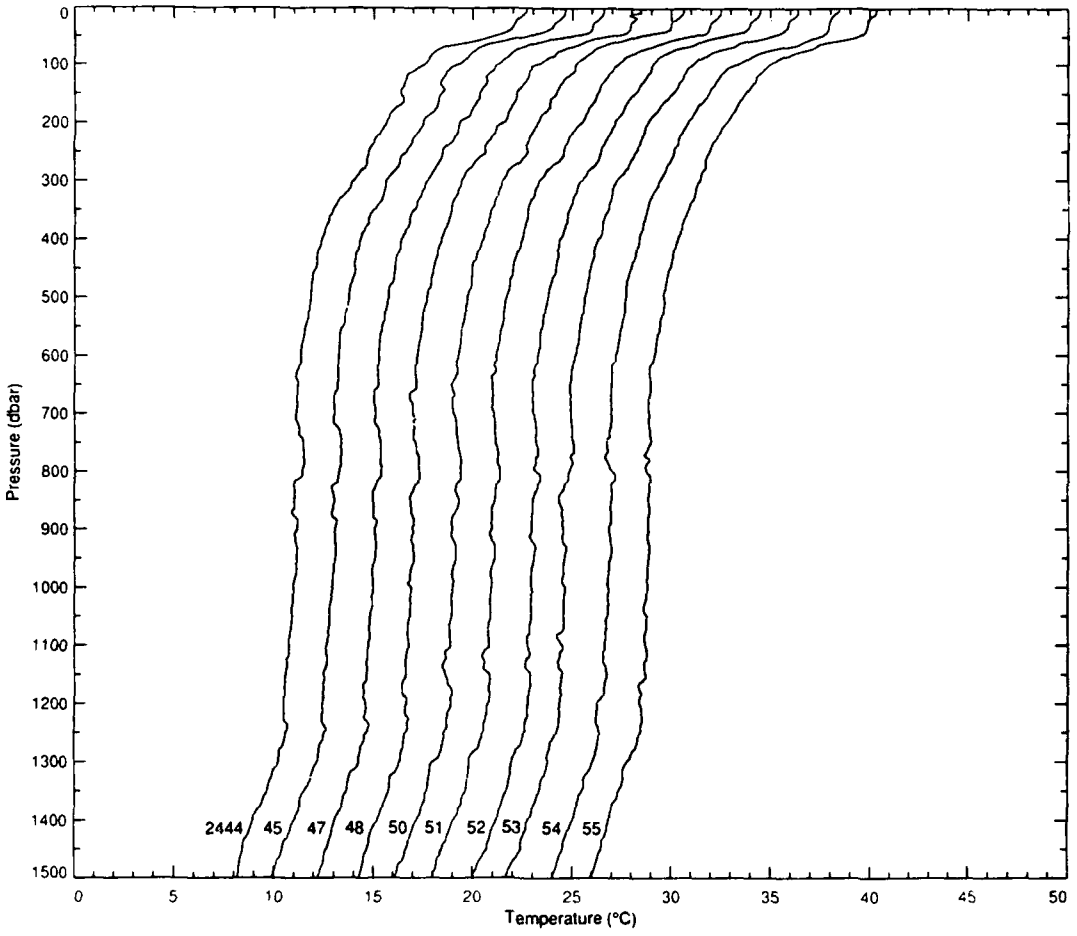

Figure 26. Plot of temperature (°C) versus pressure measured by XCPs during leg 2 of second Ampere Seamount survey.

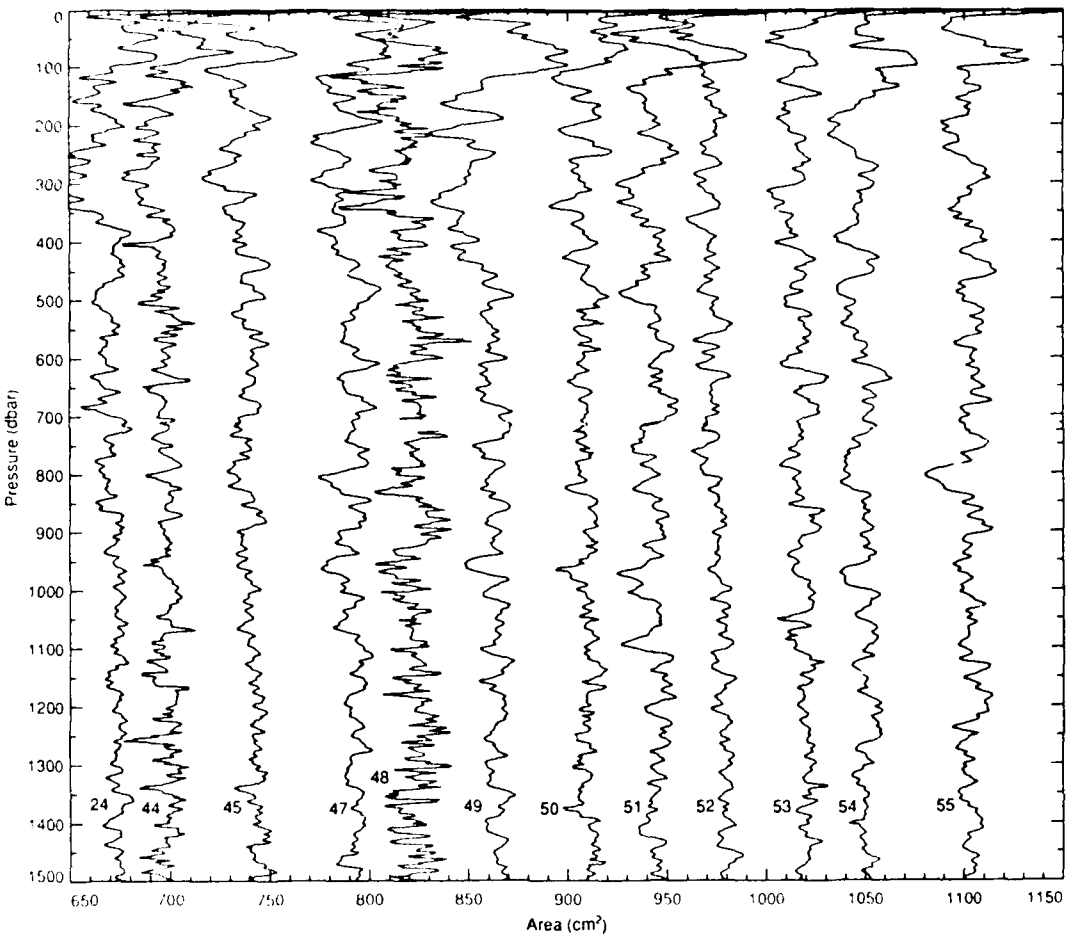

Figure 27. Plot of area (cm^2) versus pressure measured by XCPs during leg 2 of second Ampere Seamount survey.

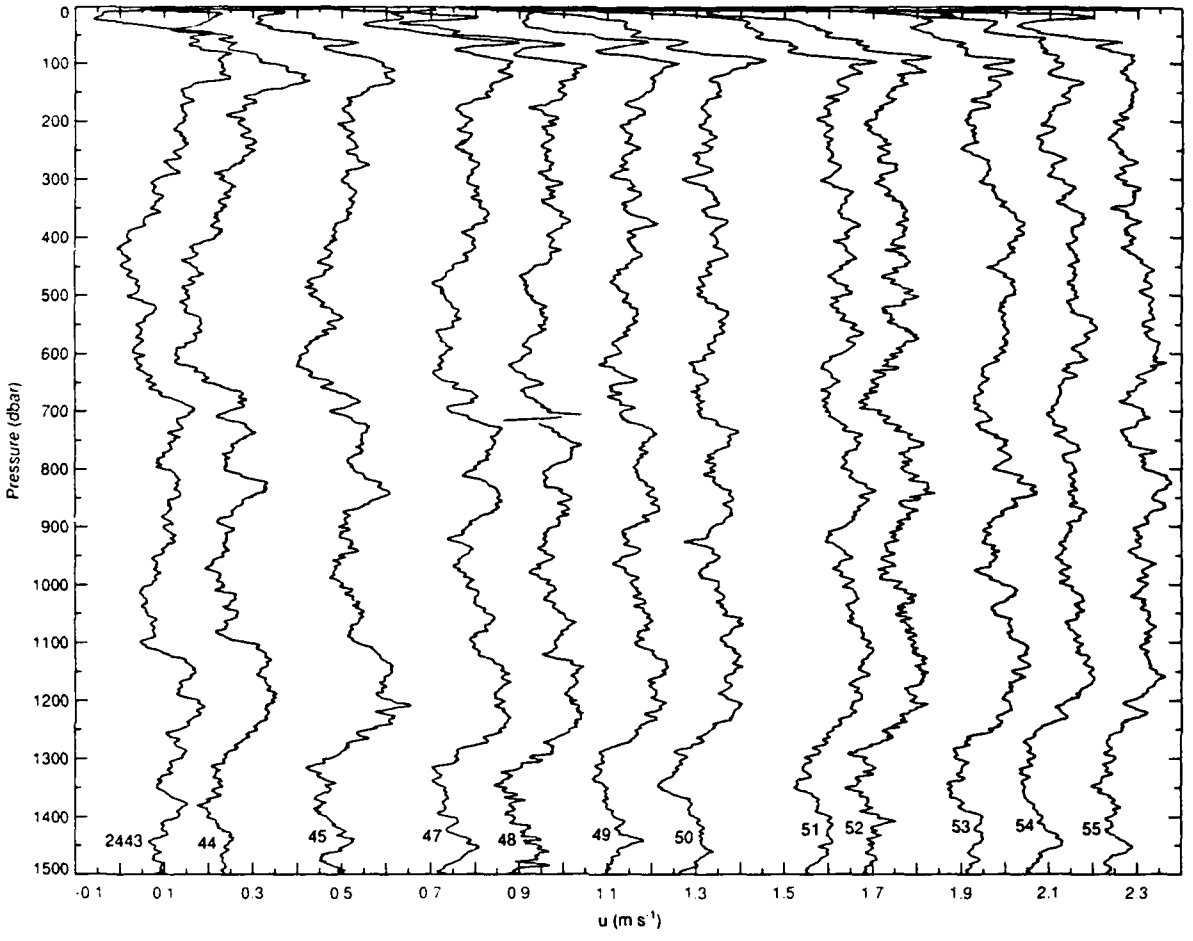

Figure 28. Plot of u velocity (m s^{-1}) versus pressure measured by XCPs during leg 2 of second Ampere Seamount survey.

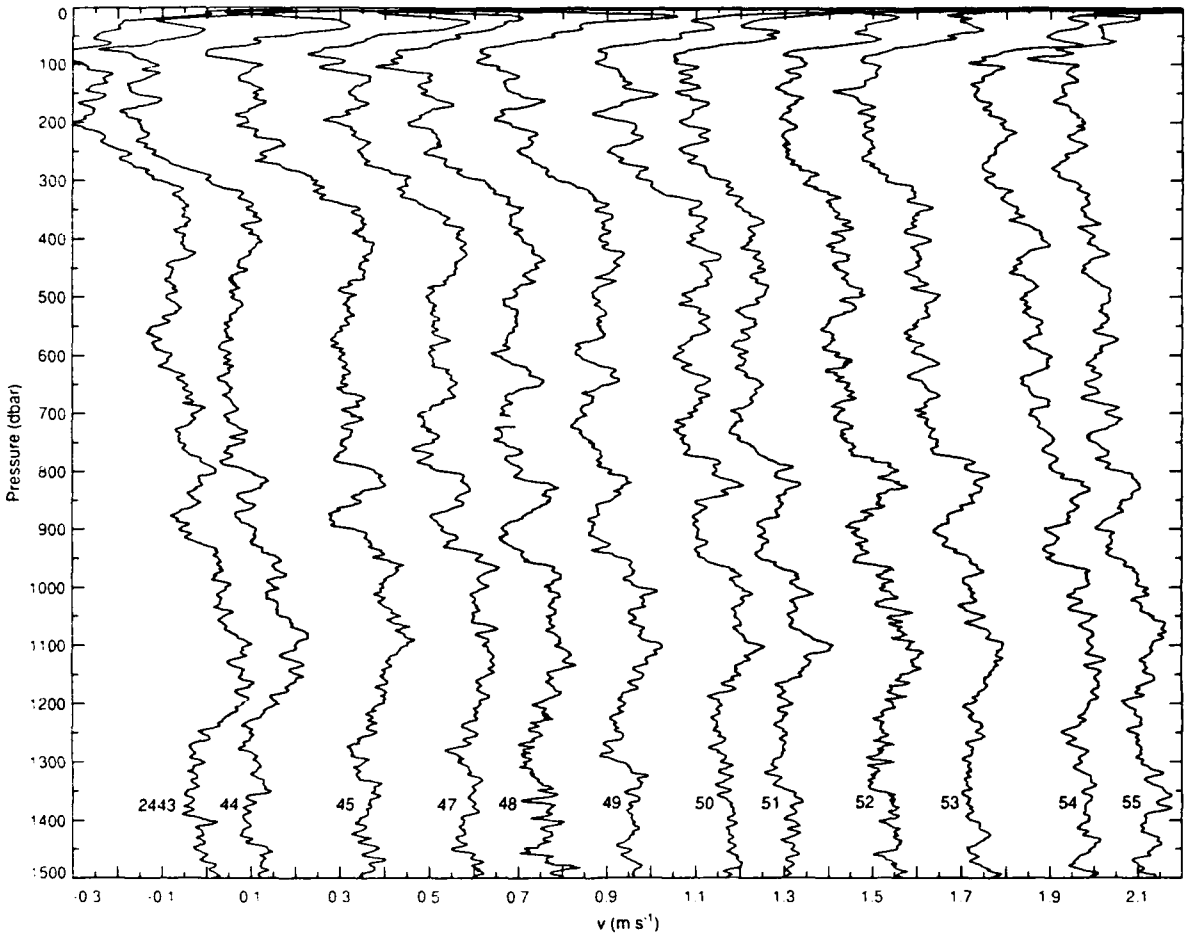

Figure 29. Plot of v velocity (m s^{-1}) versus pressure measured by XCPs during leg 2 of second Ampere Seamount survey.

Table 10. Mean velocities for Ampere Seamount, survey 2, leg 2.

	Interval: 500 to 1500 dbar			
Drop	$\bar{u}_i$ (m s^{-1})	σ_{u_i} (m s^{-1})	$\bar{v}_i$ (m s^{-1})	σ_{v_i} (m s^{-1})
2443	0.1017730	0.0373257	−0.0099698	0.0539021
2444	0.0455992	0.0527067	−0.0905654	0.0501054
2445	0.1135490	0.0537793	−0.0410891	0.0438220
2447	0.1888840	0.0481854	−0.0291658	0.0470357
2448	0.1603580	0.0470038	−0.0658104	0.0519545
2449	0.1555320	0.0402809	−0.0761876	0.0476847
2450	0.1347750	0.0408426	−0.0527266	0.0456861
2451	0.2272660	0.0406902	−0.1188640	0.0506297
2452	0.1475430	0.0447361	−0.0954143	0.0563499
2453	0.1727880	0.0452642	−0.1017490	0.0560300
2454	0.1309910	0.0438273	−0.0585785	0.0521978
2455	0.0985547	0.0400542	−0.1215090	0.0517176
$\bar{U}$	0.1398011			
$\sigma_{\bar{U}}$	0.0473774			
σ_u		0.0445580		
$\bar{V}$			−0.0718025	
$\sigma_{\bar{V}}$			0.0352527	
σ_v				0.0505930

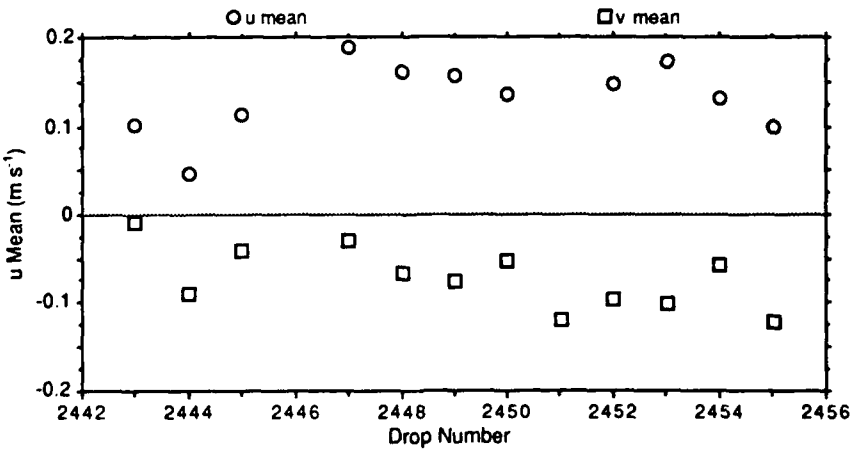

Figure 30. Plots of $\bar{u}_i$ and $\bar{v}_i$ for the interval 500 to 1500 dbar for leg 2 drops of second Ampere Seamount survey.

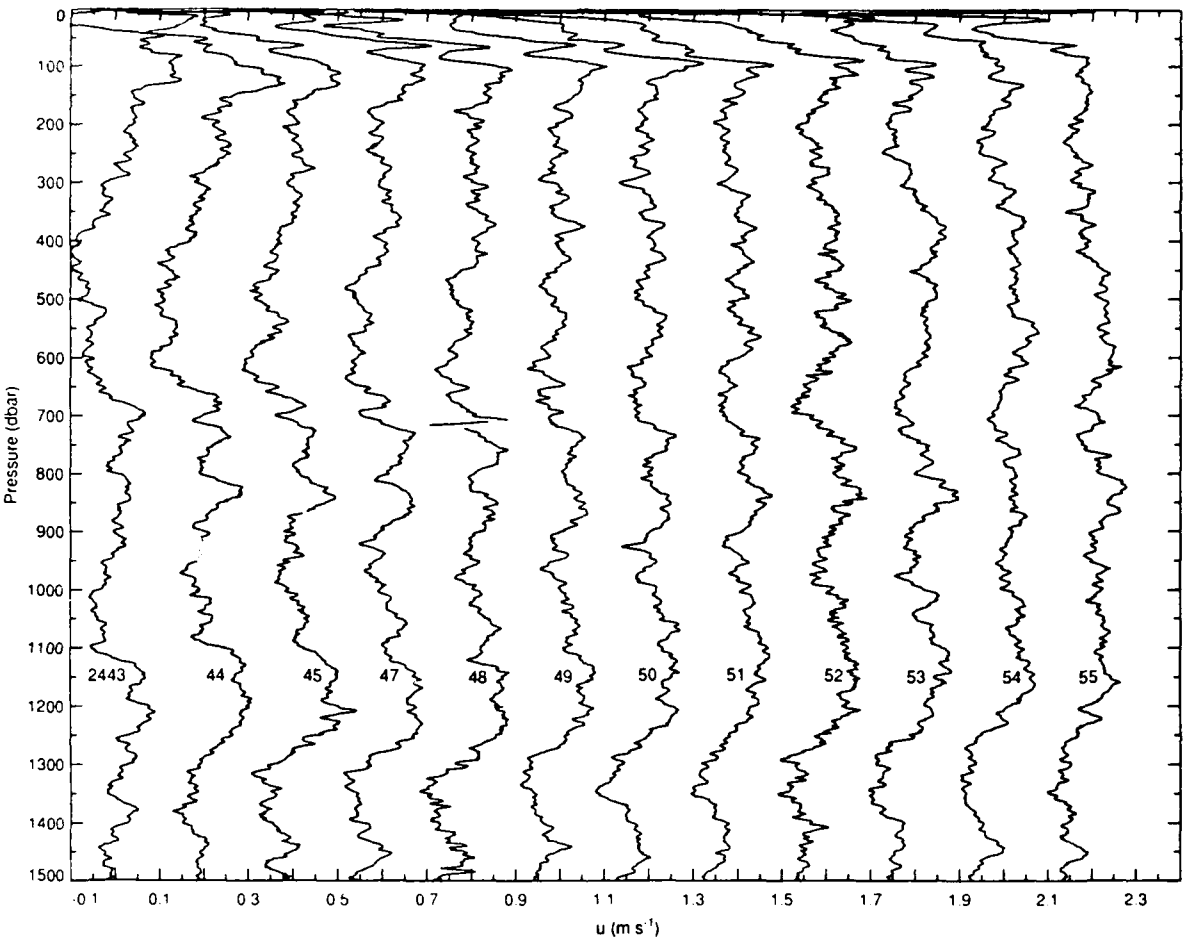

Figure 31. Plot of u velocity (m s^{-1}) versus pressure with mean from 500 to 1500 dbar removed from XCP data, leg 2 of second Ampere Seamount survey.

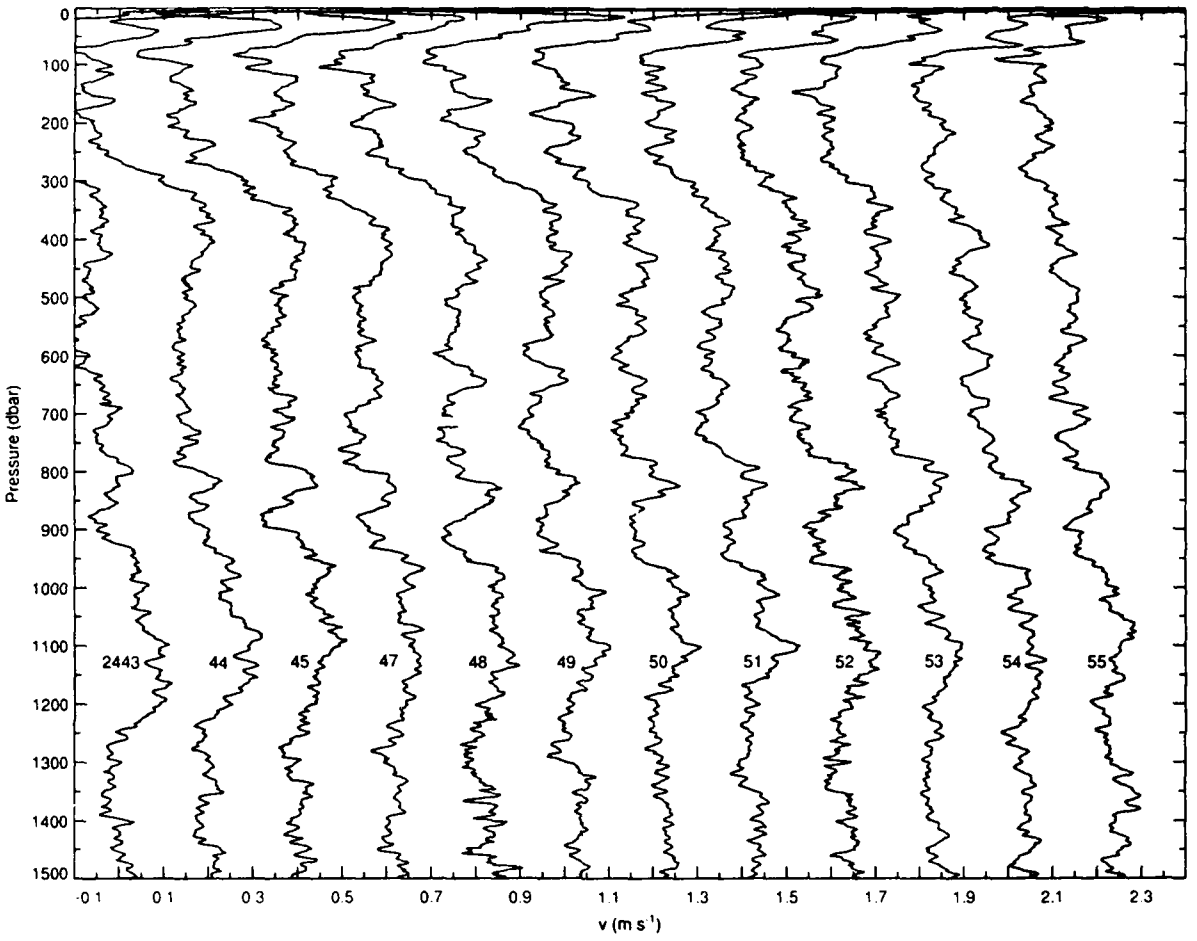

Figure 32. Plot of v velocity (m s^{-1}) versus pressure with mean from 500 to 1500 dbar removed from XCP data, leg 2 of second Ampere Seamount survey.

6. XCP DATA PRESENTATION

Profiles of relative velocity and temperature versus pressure are presented in Appendix N for the XCP data. The data have been averaged over 6 dbar and output every 2 dbar. Drops for which no data are presented are shown in Table 11. The drops listed are those for which no file was created with the acquisition system. It is assumed that these XCPs either failed to fall or that no data were transmitted. Problems such as electrode reversals and half compass coil areas have been corrected for in the new processing software, so profiles for these probes are included.

Two sets of scales have been used for the profiles shown in Appendix N. The profiles for the first leg of the cruise (2401–2520) are plotted on a 0 to 2000 dbar pressure scale with a velocity range of -0.5 m s^{-1} to 0.75 m s^{-1}. The profiles for the second leg (2522–2584) were all less than 1000 dbar and the velocities tended to be larger. These are plotted on a 0 to 1000 dbar pressure scale and with a -1.5 m s^{-1} to 1.0 m s^{-1} velocity range.

Table 11. XCP drops for which there is no velocity or temperature profile.

2431	*2513*
2446	*2521*
2462	*2524*
2480	*2526*
2503	*2560*

7. REFERENCES

Heinmiller, R.H., C.C. Ebbesmeyer, B.A. Taft, D.B. Olson, and O.P. Nikitin, 1983: Systematic errors in expendable bathythermograph (XBT) profiles. *Deep-Sea Res., 30,* 1185–1196.

Horgan, M.S., R.G. Drever, and M.A. Kennelly, 1989: XCP Phase and Gain Tests. APL-UW TR 8924, Applied Physics Laboratory, University of Washington, Seattle (in press).

Kennelly, M.A., J.H. Dunlap, T.B. Sanford, E.L. Kunze, M.D. Prater, and R.G. Drever, 1989a: The Gulf of Cadiz Expedition: R/V *Oceanus* Cruise 202. APL-UW TR 8914, Applied Physics Laboratory, University of Washington, Seattle, 115 pp.

Kennelly, M.A., T.B. Sanford, and T.W. Lehman, 1989b: CTD Data from the Gulf of Cadiz Expedition: R/V *Oceanus* Cruise 202. APL-UW TR8917, Applied Physics Laboratory, University of Washington, Seattle, 129 pp.

Kennelly, M.A., M.D. Prater, and T.B. Sanford, 1989c: XBT and XSV Data from the Gulf of Cadiz Expedition: R/V *Oceanus* Cruise 202. APL-UW TR8920, Applied Physics Laboratory, University of Washington, Seattle, 209 pp.

Lumley, J.L. and H. Tennekes, 1972: *A First Course in Turbulence.* MIT Press, Cambridge, Massachusetts, 300 pp.

Lynch, J. and R. Lueck, 1989: Expendable Dissipation Profiler (XDP) Data from the Mediterranean Out-Flow Experiment: R/V *Oceanus* Cruise 202 leg V. JHU-CBI TR89-01, The Johns Hopkins University Chesapeake Bay Institute, Baltimore, MD., 284 pp.

Press, W.H., B.P. Flannery, S.A. Teukolsky, and W.T. Vetterling, 1986: *Numerical Recipes.* Cambridge University Press, New York, 818 pp.

Sanford, T.B., R.G. Drever, J.H. Dunlap, and E.A. D'Asaro, 1982: Design, Operation and Performance of an Expendable Temperature and Velocity Profiler (XTVP). APL-UW 8110, Applied Physics Laboratory, University of Washington, Seattle, 164 pp.

Saunders, P. M., and N. P. Fofonoff, 1976: Conversion of pressure to depth in the ocean. *Deep-Sea Res., 23,* 109–111.

Sippican, Inc., 1984: Ocean Systems Inter-Office Memorandum OM-7438 to R. Lancaster from M. DeConto, Subject: XCP Temperature Circuit Revision, dtd 20 April 1984.

APPENDIX A

Oceanus **Cruise 202**
XCP Log

OC202 XCP Log

Drop #	Serial #	Channel #	Date	Time	Latitude	Longitude	Method	Comment
			Ampere Seamount Survey 1					
2401	88031	12	09/08/88	13:59	35 03.89	12 51.00	LC*	T poor
2402	88142	14	09/08/88	14:06	35 03.94	12 50.61	LC	T poor
2403	871084	16	09/08/88	14:12	35 03.98	12 50.28	LC	good
2404	88215	12	09/08/88	14:17	35 03.96	12 49.97	LC	good
2405	88159	14	09/08/88	14:19	35 03.97	12 49.84	LC	good
2406	8708290	16	09/08/88	14:25	35 03.98	12 49.52	LC	good
2407	88179	12	09/08/88	14:29	35 03.98	12 49.28	LC	good
2408	88153	14	09/08/88	14:34	35 04.00	12 49.03	LC	good
2409	88206	16	09/08/88	14:38	35 04.00	12 48.79	LC	good
2410	88038	12	09/08/88	14:43	35 04.00	12 48.50	LC	Note 1
2411	88141	14	09/08/88	14:47	35 04.00	12 48.26	LC	good
2412	871079	16	09/08/88	15:20	35 01.98	12 49.15	LC	good
2413	8708209	12	09/08/88	15:24	35 02.12	12 49.18	LC	good
2414	871027	14	09/08/88	15:29	35 02.33	12 49.21	LC	good
2415	8708289	16	09/08/88	15:33	35 02.52	12 49.27	LC	good
2416	88196	12	09/08/88	15:37	35 02.68	12 49.31	LC	good
2417	871047	14	09/08/88	15:41	35 02.84	12 49.34	LC	good
2418	87087	16	09/08/88	15:46	35 03.05	12 49.40	LC	good
2419	871044	12	09/08/88	15:49	35 03.17	12 49.43	LC	T bad
2420	871065	14	09/08/88	15:53	35 03.32	12 49.47	LC	good
2421	88187	16	09/08/88	15:58	35 03.52	12 49.55	LC	good
2422	88184	10	09/08/88	16:05	35 03.85	12 49.65	LC	good
2423	8710126	14	09/08/88	16:10	35 04.07	12 49.72	LC	good
2424	871068	16	09/08/88	16:15	35 04.31	12 49.82	LC	good
2425	88171	10	09/08/88	16:22	35 04.63	12 49.92	LC	good
2426	8710135	14	09/08/88	16:27	35 04.87	12 50.02	LC	good
2427	871093	16	09/08/88	16:35	35 05.25	12 50.15	LC	good
2428	88101	10	09/08/88	16:41	35 05.60	12 50.17	LC	good

Drop #	Serial #	Channel #	Date	Time	Latitude	Longitude	Method	Comment
			Ampere Seamount Survey 2					
2429	88174	10	09/09/88	14:00	35 02.10	12 48.60	LC	good
2430	88150	14	09/09/88	14:05	35 02.05	12 48.03	LC	good
2431	8710100	16	09/09/88	14:10	35 02.00	12 47.52	LC	bad
2432	88153	10	09/09/88	14:12	35 01.98	12 47.40	LC	good
2433	88178	14	09/09/88	14:15	35 01.96	12 47.27	LC	good
2434	8708292	16	09/09/88	14:21	35 01.91	12 46.98	LC	good
2435	88169	10	09/09/88	14:26	35 01.87	12 46.72	LC	good
2436	88207	14	09/09/88	14:31	35 01.80	12 46.42	LC	good
2437	871059	16	09/09/88	14:35	35 01.78	12 46.22	LC	good
2438	88162	10	09/09/88	14:40	35 01.72	12 45.94	LC	good
2439	88194	14	09/09/88	14:45	35 01.67	12 45.66	LC	good
2440	871057	16	09/09/88	14:50	35 01.63	12 45.39	LC	started late
2441	88160	10	09/09/88	14:58	35 01.58	12 44.81	LC	good
2442	88211	14	09/09/88	15:03	35 01.57	12 44.25	LC	good
2443	8710149	16	09/09/88	15:56	34 59.50	12 46.53	LC	T bad
2444	88188	12	09/09/88	16:04	35 00.38	12 46.62	LC	good
2445	88209	14	09/09/88	16:08	35 00.79	12 46.62	LC	good
2446	8710134	16	09/09/88	16:14	35 01.09	12 46.68	LC	bad
2447	88161	10	09/09/88	16:16	35 01.23	12 46.70	LC	good
2448	871089	14	09/09/88	16:24	35 01.72	12 46.79	LC	good
2449	870825	16	09/09/88	16:27	35 01.88	12 46.79	LC	T bad
2450	88177	10	09/09/88	16:30	35 02.05	12 46.83	LC	good
2451	8708286	14	09/09/88	16:35	35 02.30	12 46.79	LC	good
2452	8708281	16	09/09/88	16:40	35 02.56	12 46.77	LC	good
2453	88168	10	09/09/88	16:45	35 02.80	12 46.73	LC	good
2454	88208	16	09/09/88	16:54	35 03.55	12 46.63	LC	good
2455	88189	14	09/09/88	17:00	35 04.20	12 46.59	LC	good

Drop #	Serial #	Channel #	Date	Time	Latitude	Longitude	Method	Comment
			Cape St. Vincent Region					
			(line 2)					
2456	87085	12	09/11/88	09:24	36 47.82	8 13.71	LC	good
2457	88205	12	09/11/88	09:43	36 44.07	8 13.75	LC	Note 1
2458	870842	12	09/11/88	10:00	36 40.70	8 13.86	LC	noisy
2459	88155	10	09/11/88	10:05	36 39.70	8 13.86	LC	good
2460	8708170	12	09/11/88	10:30	36 35.10	8 13.54	LC	good
2461	8708197	12	09/11/88	10:58	36 30.57	8 13.01	LC	good
2462	88039	12	09/11/88	11:32	36 23.88	8 12.43	LC	bad
2463	88169A	10	09/11/88	11:32	36 23.88	8 12.43	LC	good
2464	871064	12	09/11/88	11:51	36 20.08	8 12.48	LC	good
2465	871061	12	09/11/88	12:20	36 15.36	8 12.88	LC	good
			(line 4)					
2466	871058	12	09/11/88	22:40	36 39.40	8 38.37	LC	good
2467	88142	10	09/12/88	00:21	36 34.63	8 37.70	LC	good
2468	88165	10	09/12/88	02:05	36 30.31	8 36.85	LC	good
2469	88175	10	09/12/88	03:50	36 24.95	8 37.34	LC	Note 2
2470	88170A	10	09/12/88	05:38	36 20.27	8 37.80	LC	good
2471	88161A	10	09/12/88	07:48	36 15.30	8 38.02	LC	good
2472	88150	10	09/12/88	09:32	36 10.96	8 38.03	LC	good
2473	88157	10	09/12/88	11:41	36 05.12	8 37.54	LC	good
2474	88163	10	09/12/88	13:33	35 59.61	8 37.64	LC	good
2475	88158	10	09/12/88	15:37	35 54.60	8 37.96	LC	good
			(line 5)					
2476	88176	10	09/12/88	20:07	36 36.07	8 41.75	LC	Note 2
			(line 6)					
2477	8708118	12	09/12/88	23:25	36 34.63	8 50.64	LC	good
2478	871026	12	09/13/88	00:01	36 29.70	8 49.52	LC	good
			(line 7)					
2479	870824	12	09/13/88	06:49	36 29.77	8 55.01	LC	good
2480	88035	16	09/13/88	07:22	36 34.51	8 54.27	LC	bad

Drop #	Serial #	Channel #	Date	Time	Latitude	Longitude	Method	Comment
			Cape St. Vincent Region					
			(line 8)					
2481	871048	16	09/13/88	11:04	36 39.60	9 02.56	LC	good
2482	871086	14	09/13/88	12:46	36 34.59	9 01.51	LC	good
2483	8710173	16	09/13/88	14:37	36 29.50	9 02.09	LC	good
2484	871088	16	09/13/88	18:36	36 15.05	9 04.17	LC	good
2485	88036	16	09/13/88	20:27	36 09.66	9 02.50	LC	Note 1
			(line 17)					
2486	8710133	16	09/15/88	12:20	37 11.01	9 16.99	LC	good
2487	8708282	16	09/15/88	15:44	37 09.14	9 34.49	LC	good
2488	870819	16	09/15/88	17:34	37 09.25	9 41.09	LC	good
2489	88034	16	09/15/88	20:05	37 10.65	9 48.16	LC	good
			Meddy Survey (leg 1)					
2490	8710122	16	09/17/88	21:07	35 55.05	9 12.79	LC	T bad
2491	871050	14	09/17/88	21:31	35 57.14	9 12.48	LC	Note 3
2492	871073	14	09/17/88	21:52	35 59.00	9 12.16	LC	good
2493	871094	14	09/17/88	22:10	36 00.58	9 11.82	LC	good
2494	88125	14	09/17/88	22:32	36 02.52	9 11.44	LC	good
2495	88166	14	09/17/88	22:50	36 04.11	9 11.09	LC	good
2496	88151A	14	09/17/88	23:08	36 05.69	9 10.77	LC	good
2497	88210	14	09/17/88	23:29	36 07.45	9 10.46	LC	good
2498	88154	14	09/17/88	23:48	36 09.09	9 10.60	LC	good
2499	871049	14	09/18/88	00:08	36 10.75	9 10.97	LC	Note 3
2500	88173	14	09/18/88	00:27	36 12.34	9 11.43	LC	good
			Meddy Survey (leg 2)					
2501	88181	10	09/18/88	02:49	36 08.71	9 05.54	LC	good
2502	88168	10	09/18/88	03:20	36 06.71	9 07.66	LC	good
2503	88170	10	09/18/88	03:40	36 05.75	9 09.74	LC	bad
2504	88145	10	09/18/88	03:42	36 05.66	9 09.99	LC	good
2505	88130	10	09/18/88	04:03	36 04.79	9 12.27	LC	good
2506	88183	10	09/18/88	04:23	36 03.88	9 14.35	LC	good
2507	88163	10	09/18/88	04:44	36 02.93	9 16.56	LC	good
2508	88108	10	09/18/88	05:34	36 01.56	9 18.80	LC	good
2509	88165	10	09/18/88	05:54	36 00.65	9 21.03	LC	good
2510	88157	10	09/18/88	06:16	35 59.73	9 23.46	LC	good

Drop #	Serial #	Channel #	Date	Time	Latitude	Longitude	Method	Comment
			Meddy Survey (leg 3)					
2511	870874	12	09/18/88	07:48	36 09.92	9 20.43	LC	good
2512	870884	12	09/18/88	08:08	36 08.82	9 18.53	LC	good
2513	870318	12	09/18/88	08:28	36 07.78	9 16.63	LC	bad
2514	870322	12	09/18/88	08:30	36 07.67	9 16.44	LC	T bad
2515	88180	12	09/18/88	08:50	36 06.61	9 14.63	LC	good
2516	870320	12	09/18/88	09:10	36 05.53	9 12.88	LC	good
2517	870841	12	09/18/88	09:40	36 04.04	9 10.25	LC	good
2518	88212	12	09/18/88	10:06	36 02.85	9 08.05	LC	good
2519	88169	12	09/18/88	10:30	36 01.73	9 06.14	LC	good
2520	870845	12	09/18/88	10:55	36 00.67	9 04.31	LC	good

Drop #	Serial #	Channel #	Date	Time	Latitude	Longitude	Method	Comment
			Outflow Component					
			(site 1)					
2521	8710128	16	09/21/88	13:33	35 48.46	6 12.18	LC	bad
2522	88202	14	09/21/88	13:58	35 49.14	6 12.64	LC	good
			(site 2)					
2523	871096	16	09/21/88	15:45	35 51.40	6 00.96	LC	good
			(site 3)					
2524	871062	16	09/21/88	17:06	35 53.18	5 52.54	LC	bad
2525	88143	10	09/21/88	17:10	35 53.26	5 52.44	LC	good
			(site 1)					
2526	871082	16	09/21/88	19:30	35 48.99	6 13.10	LC	bad
2527	870839	12	09/21/88	19:36	35 49.02	6 12.94	LC	good
			(site 4)					
2528	8710132	16	09/21/88	22:22	35 46.10	6 20.82	LC	good
			(site 5)					
2529	8710101	16	09/22/88	02:10	35 45.39	6 28.57	LC	good
			(site 1)					
2530	870403	16	09/22/88	04:41	35 48.71	6 12.34	LC	good
			(site 4)					
2531	871091	16	09/22/88	05:56	35 46.04	6 20.39	LC	good
			(site 5)					
2532	8708127	16	09/22/88	07:40	35 45.49	6 29.68	LC	good
			(site 6)					
2533	870316	12	09/22/88	09:08	35 49.74	6 37.46	LC	good

Drop #	Serial #	Channel #	Date	Time	Latitude	Longitude	Method	Comment
			Outflow Component					
			(site 7)					
2534	8710148	14	09/22/88	10:36	35 53.82	6 30.43	LC	good
			(site 8)					
2535	8708166	12	09/22/88	12:04	35 54.44	6 24.44	LC	good
			(site 9)					
2536	8708126	12	09/22/88	14:18	35 45.34	6 40.74	LC	good
			Section A					
2537	870846	12	09/22/88	17:34	35 45.68	6 13.47	LC	good
2538	88115	12	09/22/88	18:25	35 49.21	6 13.77	LC	good
2539	88158	14	09/22/88	19:20	35 51.57	6 14.42	LC	good
2540	871028	12	09/22/88	20:16	35 55.14	6 12.53	LC	good
			Section B					
2541	88170	12	09/22/88	22:58	35 48.76	6 19.80	LC	good
2542	871085	14	09/23/88	00:05	35 45.58	6 18.34	LC	good
2543	88195	14	09/23/88	00:56	35 42.62	6 17.59	LC	good
			Section C					
2544	870823	12	09/23/88	04:45	35 45.04	6 29.51	LC	good
2545	870331	12	09/23/88	05:55	35 46.49	6 29.28	LC	good
2546	8708125	12	09/23/88	06:55	35 49.51	6 27.00	LC	good
2547	8710129	14	09/23/88	08:12	35 51.04	6 27.35	LC	good
2548	88156	10	09/23/88	09:18	35 54.59	6 27.22	LC	good
			Section D					
2549	88148	10	09/23/88	11:50	35 55.65	6 28.43	LC	good
2550	88152	14	09/23/88	12:45	35 53.47	6 29.27	LC	good
2551	88122	10	09/23/88	13:39	35 51.72	6 32.25	LC	good
2552	88175	14	09/23/88	14:31	35 50.22	6 34.89	LC	good
2553	871045	14	09/23/88	15:56	35 48.67	6 37.25	LC	good
2554	88191	12	09/23/88	17:07	35 46.65	6 39.67	LC	good
2555	88144	10	09/23/88	18:11	35 43.45	6 41.76	LC	good

Drop #	Serial #	Channel #	Date	Time	Latitude	Longitude	Method	Comment
			(Station C4)					
2556	88146	10	09/23/88	22:29	35 44.64	6 29.83	LC	good
			Section E					
2557	8708280	14	09/24/88	01:43	36 01.24	6 33.09	LC	good
2558	88160	14	09/24/88	02:57	36 00.41	6 37.19	LC	good
2559	8708293	14	09/24/88	04:06	35 59.33	6 40.43	LC	good
2560	88159	10	09/24/88	05:14	35 57.60	6 43.59	LC	bad
2561	88216	16	09/24/88	05:21	35 57.53	6 43.86	LC	fair
2562	88032	16	09/24/88	06:32	35 55.77	6 46.26	LC	good
2563	88193	16	09/24/88	07:47	35 54.53	6 48.71	LC	good
			Section F					
2564	871081	14	09/24/88	18:01	36 18.66	6 44.25	LC	good
2565	88173	10	09/24/88	18:56	36 17.78	6 46.68	LC	good
2566	88167	10	09/24/88	20:03	36 16.15	6 49.13	LC	good
2567	88141	10	09/24/88	21:03	36 14.66	6 52.38	LC	good
2568	88143A	10	09/24/88	21:55	36 12.46	6 54.77	LC	good
2569	88167	10	09/24/88	23:23	36 10.88	6 57.91	LC	good
2570	88118	12	09/25/88	01:08	36 09.11	7 01.68	LC	good
2571	870872	12	09/25/88	03:25	36 06.42	7 07.74	LC	good
			Section FE					
2572	871041	16	09/26/88	21:45	35 54.63	7 05.19	LC	good
			(Station C4)					
2573	871095	16	09/27/88	02:09	35 45.85	6 29.08	LC	good
			Section I					
2574	871037	12	09/27/88	10:24	35 59.17	5 23.50	LC	good
2575	871074	14	09/27/88	12:46	35 56.25	5 35.68	LC	good
2576	871099	14	09/27/88	14:29	35 55.38	5 45.16	LC	fair
2577	88204	16	09/27/88	17:24	35 51.21	5 59.46	LC	good
2578	871060	16	09/27/88	19:56	35 49.11	6 11.34	LC	Note 1
			(Station B8)					
2579	871080	16	09/27/88	20:59	35 48.82	6 20.37	LC	good

Drop #	Serial #	Channel #	Date	Time	Latitude	Longitude	Method	Comment
			(Station C4)					
2580	871067	16	09/27/88	21:50	35 45.28	6 29.19	LC	good
			(Station D6)					
2581	8710136	16	09/27/88	22:38	35 51.50	6 34.95	LC	good
			(Extra station)					
2582	870317	12	09/27/88	23:22	35 53.18	6 44.10	LC	good
			(Station E6)					
2583	88197	14	09/27/88	23:56	35 54.35	6 50.43	LC	good
			(Extra station)					
2584	88149	10	09/28/88	00:47	36 01.12	6 45.91	LC	good

Notes:

1 coil reversed
2 wire broke early
3 1/2 compass coil area

LC* dead reckoned position based on LC derived positions for drops 2 and 3.

APPENDIX B

XCP Processing Program Overview

NAME

xcpover – overview of XCP processing

SYNOPSIS

awk -f mag.in.awk prpos.out | \
geomag | \
awk -f mag.out.awk | \
hdrmerge dropdatafile

awk -f extras.awk prpos.out | \
hdrmerge dropdatafile

cadiztape -p channel < kunzetapefile | \
xcpsplit debug channel outtype filenamefile rawdirectory

xcpsplit debug channel outtype filenamefile rawdirectory < dasarotapefile

xcpftoi [-dD] indir infile filenamefile outdir

xcpfloat < rawdirectory/drop | \
xcpaddt xcpaddt.p | \
xcpturn xcpturn.p dropdatafile

xcpfloat < rawdirectory/drop | \
xcpaddt xcpaddt.p | \
xcpblf xcpblf.p | \
xcppro xcppro.p dropdatafile | \
xcpgrid xcpgrid.p > griddirectory/drop

xcpplot griddirectory/drop | hpp7

DESCRIPTION

This set of programs implements the functions of old XCP processing programs *tapetogpl*, *xpro*, and *xgrid* using a number of simpler programs. XCP processing in *xpro* included so many functions that it was difficult to maintain. There were many variants to do different things and no one version existed for the general user. This group of programs modularizes the processing. An attempt was made to split the processing into functional groups. Hopefully modules are easier to understand and modify thus encouraging clearer processing development in the future.

The programs allocate main memory for the entire input file and output data so that multiple passes can be made on the data. This allows the programs to be written simply but does require more system resources. This should not be a great problem as the XCP files are not extremely large.

The data base of raw files is kept as small as possible by keeping it in 16 bit integers.

DROP DATA FILE

A small data base, *dropdatafile*, was developed for the processing parameters that are known to change from drop to drop. This data base is an ASCII file so that it can be easily modified by hand with an editing program. This is for the cases where it is not possible to obtain correct values automatically, e.g., the start and stop turn numbers may be hard to determine for some drops for various reasons. Various programs modify and add to the data base for items such as the geomagnetic field, start and stop turn numbers, etc.

GEOMAGNETIC FIELD

The earth's magnetic field at each XCP drop site is obtained from *geomag* by using times and positions from the log. *Awk* uses *mag.in.awk* to reformat the log file into the format required by *geomag*. *Awk* is run again with *mag.out.awk* on the output of geomag to format the results correctly for inclusion in the *dropdatafile* data base. *hdrmerge* actually adds new entries or replaces previous entries in the data base.

Here is *mag.in.awk* used for the Cadiz data:

```
BEGIN {
        FS = "\t"
        print "y"
        print "/usr/local/geomag/igrf"
        print "9"
}
$7 == "XCP" {
        drop = $8
        date = $1
        lat = $2
        lon = $4
        yr = substr(date,1,2)
        mo = substr(date,3,2)
        da = substr(date,5,2)
        latd = substr(lat,1,2)
        latm = substr(lat,4,5)
        lath = substr(lat,10,1)
        lond = substr(lon,1,3)
        lonm = substr(lon,5,5)
        lonh = substr(lon,11,1)
        printf "%-8s 19%02d %02d %02d %2d %05.2f %s %3d %05.2f %s\n",\
              drop,yr,mo,da,latd,latm,lath,lond,lonm,lonh
}
```

Here is the version of *mag.out.awk* used for the Cadiz data

```
# mag.out.awk
# modifies the "geomag" batch output for the XCP data base
# this output should be piped into "hdrmerge" to modify the data base.
# see "mag.in.awk" for the "geomag" input

BEGIN {
        line = 0;
}
        {
        line ++;
# skip first two lines of geomag output
        if(line<3)
              continue;
        drop = $1;
        yr = $2;
        mo = $3;
        da = $4;
        latd = $5;
        latm = $6;
        lath = $7;
        lond = $8;
        lonm = $9;
        lonh = $10;
        fh = $11;
        fh *= 1.0e-5;
        fz = $12;
```

```
        fz *= -1.0e-5;
        magvar = $13;
        printf "# %s_lat %2d %05.2f %s\n",drop,latd,latm,lath;
        printf "# %s_lon %2d %05.2f %s\n",drop,lond,lonm,lonh;
        printf "# %s_fh %5.3f\n",drop,fh;
        printf "# %s_fz %5.3f\n",drop,fz;
        if(magvar < 0)
              printf "# %s_magvar %6.1f W\n",drop,-magvar
        else
              printf "# %s_magvar %6.1f E\n",drop,magvar
}
```

EXTRA PARAMETERS IN DROP DATA FILE

Here is the version of *extras.awk* used for the Cadiz data. As many additional parameters as desired can be added in any manner for later use by later processing programs. The following two parameters are required by *xcppro* only to add them to the output file header. They are not used in any *xcppro* computations.

```
BEGIN {
      FS = "\t"
}
$7 == "XCP" {
      drop = $8
      printf "# %s_serialno %s\n",drop,$29
      printf "# %s_launchtime %s\n",drop,$1
}
```

XCPSPLIT

Xcpsplit is used to transfer the raw data from the HP-9020 Basic acquisition program files into separate files, one per drop. There is lots of extra rubbish in the raw files to be sure no data is thrown away during acquisition.

XCPFTOI

Data files from Eric D'Asaro's "tapetogpl" program are converted to the new 16 bit format by *xcpftoi*.

XCPFLOAT

Xcpfloat converts the 16 bit integer data from *xcpsplit* into 32 bit floating point values to make a standard GPL file. *Xcpfloat* can be run with the *-ms* option on the command line to make output suitable for input to Eric D'Asaro's "xpro3" or "xpro4" processing programs.

XCPTURN

Xcpturn is used to find the turn numbers where the drop starts and ends. These are added to the *dropdatafile* data base for later use by *xcppro* and possibly other programs in the future.

PROCESSING

Xcpaddt, *xcpblf* and *xcppro* actually perform the processing previously done in *xpro*. *Xcpgrid* averages the data onto a uniformly sampled depth grid.

DISPLAY

Xcpplot displays data from *xcpgrid* using standard scales on the HP-7550 pen plotter. This program is used

to make the books of standard plots. *Gpl(1)* can also be used for other more refined plotting.

CHECKING START AND STOP POINTS

The following C-shell command file will plot the output of *xcppro* near the beginning of a drop. This is useful to check that *xcpturn* found the correct points. The user may modify the *dropdatafile* by hand if these points seem incorrect.

```
# csh
@ ref = `grep $drop"_turnhalf" dropdatafile | awk '{ print $3 }'`
@ start = $ref - 50
@ stop = $ref + 50
xcpfloat < split/xcp$drop | \
xcpaddt xcpaddt.p | \
xcpblf xcpblf.p | \
xcppro xcppro.p dropdatafile | \
pick diag=0 tag=turn.$ref start=$start stop=$stop | \
gpw zoom.cf
```

By replacing *turnhalf* above with *turnstop* the end of the drop may be plotted.

SEE ALSO

awk(1), geomag(1), hdrmerge(1), cadiztape(1), xcpsplit(1), xcpftoi(1), xcpfloat(1), xcpaddt(1), xcpturn(1), xcpblf(1), xcppro(1), xcpgrid(1), xcpplot(1), pick(1)

BUGS

Slow fall probes are not handled presently.

Drever Receiver data is not handled presently.

AUTHOR

John Dunlap, Applied Physics Laboratory, University of Washington

APPENDIX C

hdrmerge Documentation

NAME

hdrmerge – add or replace data in headers of GPL files

SYNOPSIS

hdrmerge filename

DESCRIPTION

Hdrmerge modifies the GPL header in *filename* according to another GPL header from standard input. If a header label from standard input does not exist in *filename* it is added to *filename*. If a header label from standard input exists in *filename* its value in *filename* is changed to that from standard input.

If the header labels **n_values** and **nquan** exist in *filename* and their product is greater than zero then floating point binary data is assumed to follow the header in filename. This data is rewritten after the modfied header in *filename*.

FILES

/usr/local/bin/hdrmerge

SEE ALSO

xcpover(1)

DIAGNOSTICS

BUGS

AUTHOR

John Dunlap, Applied Physics Laboratory, University of Washington

APPENDIX D

xcpsplit Documentation

NAME

xcpsplit – Split raw XCP HP-9020 Basic acquisition files into separate drops

SYNOPSIS

xcpsplit debug channel outtype filenamefile directory

DESCRIPTION

xcpsplit separates XCP raw data into files, one per drop, suitable for the rest of the XCP processing programs. The raw files were written on HP-9144 cartridge tape for Ocean Storms and Cadiz data but can also be written on other media. When *xcpsplit* is run the files have been copied to disk. The files from Eric Kunze's version of the HP-9020 Basic acquisition program are piped through *cadiztape* before being processed by *xcpsplit*. This is to remove the XBT and XSV data which *xcpsplit* does not accept. For Eric D'Asaro's version *xcpsplit* accepts the original Basic file directly.

If *debug* is greater than zero various diagnostics are printed on stderr. The higher the value the more is printed.

Data is extracted from the tape from *channel* which corresponds to the partition number *XCP.READ* ran under in *MASTER.READ*.

If *outtype* is **short** then files with integer data are produced. This is the recommended usage in order to save space. *Xcpfloat* converts these files for use by the rest of the processing programs. When *outtype* is **float** then a true GPL file is produced which is the same as that produced by the output of *xcpfloat* above. Both *outtype* **short** and **float** files have the same GPL header except for the **data_type** entries for each variable.

The *filenamefile* is a file which provides the correspondence between the original Basic filenames and new filenames which are the drop number. If there is no entry in *filenamefile* the original Basic filename is used for output. An example of one line in the *filenamefile* for the Cadiz cruise using Eric Kunze's Basic acquisition program is:

```
# VF09112242_1 2466
```

An example for the Ocean Storms data using Eric D'Asaro's Basic acquisition program is:

```
# Oct23/1036_1 2201
```

Output files with names found in *filenamefile* are created in *directory*.

drop in the GPL header is set the same as the output file name. This drop number is used later in *xcppro* to look up values in the *dropdatafile*.

An example for splitting channel 1 of tape number 6 of the Cadiz data is:

```
cadiztape -p 1 < SEP11.tape6 | xcpsplit 0 1 short fn.cadiz splitdir
```

FILES

/usr/local/bin/xcpsplit
/usr/tmp/xtmp.xxxxx where xxxxx is the process id of the job.

SEE ALSO

xcpover(1), cadiztape(1)

DIAGNOSTICS

BUGS

AUTHOR

John Dunlap, Applied Physics Laboratory, University of Washington

APPENDIX E

xcpfloat Documentation

NAME

xcpfloat – converts xcpsplit output to GPL format

SYNOPSIS

xcpfloat

DESCRIPTION

Xcpfloat reads standard input and writes standard output. The input is assumed to come from *xcpsplit* output and the output is a GPL file. The data base is usually kept as *xcpsplit* output files which are 16 bit integers to conserve space. All the processing programs use floating point values in the files.

FILES

/usr/local/bin/xcpfloat

SEE ALSO

xcpover(1)

DIAGNOSTICS

BUGS

AUTHOR

John Dunlap, Applied Physics Laboratory, University of Washington

APPENDIX F

xcpturn Documentation

NAME

xcpturn – determine where XCP drop starts and stops turning

SYNOPSIS

xcpturn paramfile dropdatafile [infile]

DESCRIPTION

Xcpturn examines the rotation frequency record of a drop to determine when it was released from the surface and when the drop terminated at the bottom. The turn number at half the average rotation frequency soon after it has spun up as well as the turn number for the last turn with good data are added to the *dropdatafile* data base for later use by *xcppro(1)*.

Standard input is used for the input unless the input file, *infile* is specified.

paramfile contains some run time parameters in GPL header format as described below.

debug is set to 0 normally. For more diagnostic output increase the value.

timeused
should be set to **tmaster.**

rotfmin, rotfmax
are the minimum and maximum rotation frequencies allowed in the computations.

mavg, diffmax, nokneed
are used to determine the end of the drop. The drop is considered to stop at the last turn where the difference between its rotation frequency and the average for the previous **mavg** turns is more than **diffmax** for **nokneed** turns in a row.

The following is an example *paramfile*.

```
# debug 0
# timeused tmaster
# rotfmin 2
# rotfmax 20
# mavg 20
# diffmax 1
# nokneed 20
```

An example of the two records added to the *dropdatafile* for drop 2208 are:

```
# 2208_turnhalf 740
# 2208_turnstop 5947
```

FILES

/usr/local/bin/xcpturn

SEE ALSO

xcpover(1)

DIAGNOSTICS

BUGS

The start of the drop depends on the **downturn** value in the header of the input file. This is computed in *xcpaddt(1)*. The average from 30 to 50 turns past **downturn** is used to get the average rotation frequency near the beginning of the drop. This is not good practice – the code should be put all in this program. And the use of magic numbers is poor.

The end of drop algorithm works fairly well for the drops that hit the bottom but does not find the point where the wire starts to stretch just before breaking when the probe spool is exhausted. Thus there are usually three to ten turns of data near the end of a deep drop where the fall rate is not known and so the north

component of velocity is not computed correctly.

Slow fall probes are not handled yet.

AUTHOR

John Dunlap, Applied Physics Laboratory, University of Washington

APPENDIX G

xcpaddt Documentation

NAME

xcpaddt – computes the time base for XCP raw data

SYNOPSIS

xcpaddt paramfile [infile [outfile]]

DESCRIPTION

Xcpaddt reads standard input or *infile* and writes standard output or *outfile*. The *paramfile* contains several parameters needed. These are entered in the GPL header format.

The goal of this program is to develop a good time base for the data samples from the MK-10 receiver so that correct depths can be assigned to the data. This is needed to estimate shear correctly as well as to compare XCP profiles to other measurements or other XCP profiles. Three time bases are available as input: the incremental rotation period in the MK-10 "G" (good) packets, the "elapsed" time in the MK-10 "B" (bad) packets and the HP-9020 time stamp of the arrival of every 30th packet.

The code is modified to operate in the time domain from the depth algorithm written by Eric D'Asaro in his xpro4.c. This version may not operate entirely correctly as it has not been tested on drops with RF dropouts.

PARAMETERS

debug is set to zero normally. For more diagnostics increase its value.

tag if present is used to override the default tag of **xcpaddt.**

dtmin, dtmax
are the minimum and maximum allowed time difference between the sum of the rotation periods from "G" packets and the elapsed time from "B" packets.

dtbad is the average time assumed for a "B" packet when the above criteria fails. It has been empirically determined to be 0.118 s.

rotfmin, rotfmax
are the minimum and maximum values of rotation frequency considered in the *tfall* and *tquit* tests below.

tfall is the time required with all rotation frequencies between the above limits and with all "G" packets to determine the point the XCP starts to fall.

tquit is the duration of continuous bad packets or rotation frequencies continuously outside the above limits to determine when the XCP stops turning. It generally indicates a point for quitting which is significantly later than the drop actually stops turning. See xcpturn for a better method.

tquit determines *finishturn* and *finishtime* in the output header but these are not used in any later processing so *tquit* has no particular use.

tspinup is a time delay after the XCP started turning before the *tquit* criteria above is used.

rotferrmax
is the threshold value of the maximum value of the forward or backward first difference of rotation frequency above which the time base, *tsampf*, is corrected by linearly interpolating between points where the differences are less than *rotferrmax*.

The following is an example of a *paramfile*.

```
# debug          0
# tag        xcpaddt
# tfall            2
# tquit            0.5
# dtmin          .05
# dtmax          .2
# dtbad          .118
```

```
# rotfmin   8
# rotfmax   20
# rotferrmax      0.5
# tspinup   3.5
```

FILES

/usr/local/bin/xcpaddt

SEE ALSO

xcpover(1)

DIAGNOSTICS

BUGS

The Drever Receiver is not handled yet.

AUTHOR

John Dunlap, Applied Physics Laboratory, University of Washington

APPENDIX H

xcpblf **Documentation**

NAME

xcpblf – XCP baseline correction and conversion to frequencies

SYNOPSIS

xcpblf paramfile [infile [outfile]]

DESCRIPTION

Xcpblf corrects the in-phase and quadrature data from the XCP receiver by estimating and removing the contributions from a slowly changing base line or average frequency of the signals.

In addition the data from the receiver is converted to frequencies.

The *paramfile* has several parameters described below in GPL header format.

debug is set to 0 normally. Higher values produce more diagnostic output.

tag if present is used to override the default tag of **xcpblf.**

blctype is the baseline correction type. There are presently three options, **none, original, 2back.** The **none** option applies no corrections. The **original** option uses the method in the XTVP report, APL-UW 8110. The **2back** option solves the equations in the report assuming only a linear baseline model (E=0) and only using the present and previous rotation. This option allows one to calculate velocities on the last turn as the XCP hits the bottom.

s1, s2, s3

are the inverse of the multiplication ratios of the phase lock loops for the three channels, temperature, electric field and compass coil.

rotfmin, rotfmax

are the minimum and maximum rotation frequency used to determine if the data are reasonable. Rotation frequency data is set to a bad flag value if not in the above range.

An example of *paramfile* contents is below.

```
# debug     0
# tag       xcpblf
# blctype   2back
# s1        .005
# s2        .0125
# s3        .025
# rotfmin   1
# rotfmax   20
```

FILES

/usr/local/bin/xcpblf

SEE ALSO

DIAGNOSTICS

BUGS

AUTHOR

John Dunlap, Applied Physics Laboratory, University of Washington

APPENDIX I

xcppro Documentation

NAME

xcppro – XCP processing

SYNOPSIS

xcppro paramfile dropdatafile [infile [outfile]]

DESCRIPTION

xcppro accepts the corrected in-phase and quadrature carrier frequencies as well as XCP probe rotation frequency. All are assumed to be the estimated probe frequencies with units of hertz. The *infile* or standard input is typically produced by *xcpblf*. *xcppro* produces profiles of east and north velocity components and temperature as a function of depth and pressure on standard output or *outfile*. The output of *xcppro* is suitable for input to *xcpgria*.

paramfile has the processing parameters and other files of parameters to use. All the parameter files use the *mkhdr* format similar to the GPL header for the data files. If a parameter is present in more than one parameter file it's value is taken from the first parameter file. The parameter file on the command line is considered before the rest.

dropdatafile contains processing parameters specific to each drop such as the earth's magnetic field, position and start and stop points for processing. This data is maintained by other programs and *xcppro* reads from it. It is an ASCII file so any text editing program can be used to change values. See *xcpturn(1)* and *hdrmerge(1)*.

One *dropdatafile* is maintained for each cruise or group of drops. Each parameter is prefixed by the drop name. Usually the drop name is just the sequential number of the XCP launch.

xcppro implements the part of the processing that is specific to the probe. It executes equations (23) through (30) of the XCP report, APL-UW 8110.

There is no filtering option in *xcppro* as that is typically done in *xcpgrid*.

PARAMFILE CONTENTS

debug is set to 0 for no debugging messages on stderr. The higher it is set the more messages are printed.

paramfiles

specifies a list of additional parameter files to be used to supply the parameters to *xcppro*.

timeused

should be set to **tmaster.**

efccp0 efccp1

are the intercept and slope as a function of rotation frequency respectively of the differential phase between the electric field and compass coil channels of the digital receiver used. I have not set these to anything but zero.

amean is the area in cm^2 times the number of turns of the compass coil. In old programs it was actually computed as the average value of the area. Now it is entered as a constant. For Mod 6 probes a value of 695 seemed to be correct. The value 667 has been determined by Michael Horgan for the Ocean Storms AXCP probes. This may hold for all Mod 7 probes.

gcca gcora gefa

are the polynomial coefficients as a function of rotation frequency of the amplitudes of the gains of the compass coil, correction and electric field channels before the voltage to frequency (V/F) converters in the probe. Each set of coefficients is entered on one line. The zeroth order coefficient is first with the others following. There may be up to 6 coefficients for up to a 5th order polynomial.

For example if three coefficients are entered for **gcca,** *gcca0, gcca1, gcca2,* and the rotation frequency is *rotf* then the compass coil amplitude used in the calculations is *gcca0 + gcca1 * rotf + gcca2 * rotf*^2.

gccp gcorp gefp
are polynomial coefficients used to compute the phases of the probe channel gains as a function of rotation frequency in the same fashion as **gcca, gcora** and **gefa** above.

esep is the distance in cm between electrode ports. It is also the diameter of the probe.

c1 + 1.0 is the amplification factor of the electric potential sensed across the probe because the electric currents must go around the insulating body. The usual value used for **c1** for an XCP is 0.97. It depends on the shape of the body. For an infinite cylinder **c1** would be 1.0. See the EMVP report, WHOI-74-46, eqn. III-11.

c2 + 1.0 is the factor controlling the addition of vertical fall rate to the north component of velocity. Usually **c2** is assumed to be -0.02 for XCP probes. See the EMVP report, WHOI-74-46, eqn. III-11.

gevfa gevfp
are the amplitude and phase of the gain of the voltage to frequency converters for the electric field channel.

gcvfa gcvfp
are the amplitude and phase of the gain of the compass coil voltage to frequency converter.

depthcal
are the coefficients of the depth polynomial as a function of time: *depth = depthcal0 + depthcal1 * time + depthcal2 * time^2*. Note that the depthcal values should be entered to obtain a positive downward depth. The programs compute "z" which is positive upwards with the same absolute value as depth but opposite sign.

prconv are the four coefficients used to convert depth to pressure using the following formula: *pr = depth / (prconv0 + prconv1 * depth + prconv2 * exp(depth / prconv3))* Setting the coefficients to zero inhibits the conversion.

tcalfreq
are the two frequencies of the temperature carrier (Hz) with resistances **tcalres** below.

tcalres are the two resistances (ohms) of the XCP thermistor at 0 and 30 degrees C respectively.

tcal are the four coefficients of the standard polynomial of logarithms of resistance to compute temperature from resistance. These coefficients were found by fitting the published temperature and resistance tables in the specification of the XCP thermistors: *T = 273.15 + 1.0 / (tcal0 + tcal1*ln(R) + tcal2*ln(R)^2 + tcal3*ln(R)^3).*

tcor Specifies a linear correction as a function of depth to be added to temperature as computed above. *Correction = tcor0 + tcor1 * depth*

DROP DATA FILE CONTENTS

<drop>**_halfcoil**
is set to 1 to indicate that the processing should use half the usual amean in the tilt correction. If this parameter is not present in the *dropdatafile* it is assumed to be zero.

<drop>**_revcoil**
is set to 1 to indicate that the probe was wired with the coil reversed. If this parameter is not present in the *dropdatafile* it is assumed to be zero. Note that when the coil is reversed it actually appears to the processing as if the electrodes were reversed since the reference is the coil. It is thought that most of the wiring errors are actually coil wiring errors since those wires are easier to cross in the probe assembly.

<drop>**_fh** <drop>**_fz**
are the horizontal and vertical magnetic field at the drop site. The units are gauss which is 100,000 nT. The vertical magnetic field is negative in the northern (magnetic) hemisphere.

<drop>**_turnhalf**
is the turn number at which the probe comes to half its nominal rotation frequency. Depth is

computed according to time since the time at *turnhalf*.

<drop>**_turnstop**
is the last turn number with good rotation frequency. When a drop hits the bottom this turn is the last turn with good data. When the probe spool wire is exhausted the probe spin rate noticeably slows for the last 10 to 20 turns. This effect is also seen in the north velocity so the fall rate is probably changing. Presently the last 10 or 20 turns of deep drops are not processed correctly.

<drop>**_launchtime**
is the time the probe was released from the ship or aircraft. This time determines the position of launch which is assumed to be the same position of the drop. If there is significant wind this assumption will be incorrect.

<drop>**_serialno**
is the serial number of the probe.

<drop>**_magvar**
is the magnetic variation for use in coordinate rotation from the natural geomagnetic to geographic coordinates. No coordinate rotation is done in the standard processing: the U and V components are left in the magnetic coordinate system.

PARAMFILE EXAMPLES

The following is an example of parameter files used in testing with the Cadiz data. There is nothing magic about the file names or partioning of the data into the various files. It should be done to minimize the number of redundant entries.

The contents of xcppro.p are:

```
# debug           0
# paramfiles      deckbox.p probe.p depthcal.p tcal.p
# timeused  tmaster
```

The contents of deckbox.p are:

```
# efccp0    0.
# efccp1    0.
```

The contents of probe.p with Michael Horgan's new coefficients are:

```
# amean           667
# c1        .97
# c2        -.02
# esep            5.19
# gevfa           494.66025
# gevfp           0
# gcvfa           500
# gcvfp           0
# gefa      23866.12044581    107.99111272898   -0.905827321
# gcca      1809.877761 -1.25653911 0.18856556
# gcora     898.89564739      0.453188608 0.0717425016
# gefp      -138.158938796    9.759010754 -0.180878978
# gccp      29.826971133      10.265226263      -0.176531452
# gcorp     56.552652832      7.783581145 -0.112472607
```

The contents of depthcal.p with depth calibration and Cadiz pressure conversion follow. Mark Prater's recommendation is that the Mod 6 fall rates should be used for Cadiz processing of Mod 7 probes. This change was made when he recomputed the XCP/CTD pressure offsets after correctly converting the XCP

depths to pressures.

```
# depthcal          3.1    4.544 -0.0006749
# prconv     0.9927        -2.55e-06    0.0073        -50.0
```

The contents of tcal.p follow. The values shown for tcor are for the Cadiz cruise as determined by Mark Prater.

```
# tcalfreq          285.3 449.1
# tcalres           16329 4024
# tcal       1.73323e-3  8.75509e-5  .64067e-5    -5.09882e-7
# tcor       -0.05       -1.25e-04
```

DROP DATA FILE EXAMPLES

The items for drop 2466 in the *dropdata* file are as follows. Not all of these items are used in *xcppro* computations but they are all required to be present for inclusion in the output header.

```
# 2466_serialno 871058
# 2466_launchtime 880911-224000
# 2466_lat 36 39.40 N
# 2466_lon 8 38.37 W
# 2466_fh 0.268
# 2466_fz -0.330
# 2466_magvar 5.9 W
# 2466_turnhalf 739
# 2466_turnstop 3479
```

FILES

/usr/local/bin/xcppro

SEE ALSO

xcpover(1)

BUGS

Please report them.

AUTHOR

John Dunlap, Applied Physics Laboratory, University of Washington

APPENDIX J

xcpgrid Documentation

NAME

xcpgrid – put XCP data on uniformly spaced depth grid

SYNOPSIS

xcpgrid paramfile [infile [outfile]]

DESCRIPTION

Xcpgrid reads from standard input or *infile* if it is present. It writes standard output or *outfile* if it is present. Input data is assumed to be from *xcppro*.

The *paramfile* has some parameters used in the processing:

debug is set to 0 normally. Increasing amounts of diagnostic output is written to standard error as *debug* is increased.

shearout
is a flag controlling the output of the shear variables. If 1 they are and if 0 they are not.

auxout is a flag controlling the output of area, rotf, efbl and ccbl. If 1 they are and if 0 they are not.

z0 is the initial value of the depth grid.

dz is the interval of the depth grid.

dzbin is the averaging interval for each output grid point. Usually this is set to two times **dz.**

zvar is the depth variable name from *xcppro*. It can be set to **z, depth,** or **pr. z** is positive up while **depth** and **pr** (pressure) are positive down. **z** and **depth** have units of meters while **pr** has units of dbar.

binmin is the fraction of a bin which must be averaged to obtain the last data point.

tmin, tmax
are the minimum and maximum temperatures allowed to be included in the output bins.

umin, umax
are the minimum and maximum velocity components (u & v) allowed to be included in the output bins.

rotfmin, rotfmax
are the minimum and maximum rotation frequencies allowed for any data to be included in the output bins.

zfiltrotf is the recursive filtering distance for averaging the rotation frequency.

maxdevrotf
is maximum deviation of rotf from the average rotation frequency. If the deviation is greater than **maxdevrotf** then no data is used from this scan.

An example of a *paramfile* follows:

```
# debug      0
# shearout   1
# auxout     1
# z0         0
# dz         2
# dzbin            6
# zvar             pr
# binmin     0.75
# tmax             35.0
# tmin             -3.0
# umax             2.0
# umin             -2.0
# rotfmax    20.0
```

```
# rotfmin   8.0
# zfiltrotf 3.0
# maxdevrotf      2.0
```

FILES

/usr/local/bin/xcpgrid

SEE ALSO

xcpover(1)

DIAGNOSTICS

BUGS

AUTHOR

John Dunlap, Applied Physics Laboratory, University of Washington

APPENDIX K

xcpplot Documentation

NAME

xcpplot – standard plot for XCPs

SYNOPSIS

xcpplot [-d] [infile] | hpp7

DESCRIPTION

Xcpplot produces a standardized color plot of *xcpgrid(1)* output using the HP-7550 pen plotter. The dimensions are 10 inches high and 7 inches wide. The scales are 200 meters per inch for depth and 0.2 m/s per inch for velocity. Processing parameters which are specific to the drop are labeled on the plot. Others should be obtained from a listing of the parameter files for each program.

The **-d** option is used for debugging the program. *Infile* is the data file input. If *infile* is not present the input is taken from standard input. The standard output of *xcpplot* contains HP-GL plotter commands and is normally directed to the standard input of *hpp7*, the pen plotter spooler.

FILES

/usr/local/bin/xcpplot

SEE ALSO

xcpover(1)

AUTHOR

John Dunlap, Applied Physics Laboratory, University of Washington

APPENDIX L

Listing of FORTRAN Program Used to Estimate the Mk-10 Output for Comparison with Data from Various Measurements

```
$ALIAS getarg = 'Ftn_getarg'(%ref,%ref,%ref)
$ALIAS atoi = 'atoi'(%ref)
$ALIAS atof = 'atof'(%ref)

      integer getarg,atoi
      double precision atof
      character*20 str
      integer argnum,len,which,test,ret

      complex gef,gcor,gcc,gevf,gcvf
      complex fcc,fef

      do argnum = 0,6
            len = 20
            ret = getarg(argnum,str,len)
            if(ret .eq. -1) then
                  write(*,*)
     a  "usage: evalgph test which vpp freq1 freq2 dfreq"
                  write(*,*) "  which=1 for orig gains & phases"
                  write(*,*) "  which=2 for Mike Horgan Mar 89"
                  stop
            end if
            if(argnum .eq. 1) test = atoi (str)
            if(argnum .eq. 2) which = atoi (str)
            if(argnum .eq. 3) vpp = atof (str)
            if(argnum .eq. 4) freq1 = atof (str)
            if(argnum .eq. 5) freq2 = atof (str)
            if(argnum .eq. 6) dfreq = atof (str)
      end do

      vin = 0.5 * vpp

      pi = 3.14159265
      rad = pi/180.0
      deg = 1.0/rad

      if(which .eq. 2) then
            gevfa = 494.66025
            gevfp = 0
            gcvfa = 500
```

```
        gcvfp = 0

        gefa0 = 23866.12044581
        gefa1 = 107.99111272898
        gefa2 = -0.905827321

        gcca0 = 1809.877761
        gcca1 = -1.25653911
        gcca2 = 0.18856556

        gcora0 = 898.89564739
        gcora1 = 0.453188608
        gcora2 = 0.0717425016

        gefp0 = -138.158938796
        gefp1 = 9.759010754
        gefp2 = -0.180878978

        gccp0 = 29.826971133
        gccp1 = 10.265226263
        gccp2 = -0.176531452

        gcorp0 = 56.552652832
        gcorp1 = 7.783581145
        gcorp2 = -0.112472607
end if
if (which .eq. 1) then
        gevfa = 494.66025
        gevfp = 0
        gcvfa = 500
        gcvfp = 0

        gefa0 = 25260
        gefa1 = 0
        gefa2 = 0

        gcca0 = 1813
        gcca1 = 0
        gcca2 = 0

        gcora0 = 918
        gcora1 = 0
        gcora2 = 0
```

```
            gefp0 = 17.22857
            gefp1 = -.9371427
            gefp2 = .014285706

            gccp0 = 179.16568
            gccp1 = .158575
            gccp2 = -.007143

            gcorp0 = -159.30284
            gcorp1 = -1.414293
            gcorp2 = .0285716
        end if

        write(*,99) which,test,vpp
99      format("which=",i1," test=",i1," vpp=",f6.3)
        write(*,100)
100     format(" freq  fefa  fcca fefp-fccp")

        do freq=freq1,freq2,dfreq

        gefa = gefa0 + freq * ( gefa1 + freq * gefa2)
        gefp = gefp0 + freq * ( gefp1 + freq * gefp2)

        gcora = gcora0 + freq * ( gcora1 + freq * gcora2)
        gcorp = gcorp0 + freq * ( gcorp1 + freq * gcorp2)

        gcca = gcca0 + freq * ( gcca1 + freq * gcca2)
        gccp = gccp0 + freq * ( gccp1 + freq * gccp2)

        gef = cmplx(gefa*cos(gefp*rad),gefa*sin(gefp*rad))
        gcor = cmplx(gcora*cos(gcorp*rad),gcora*sin(gcorp*rad))
        gcc = cmplx(gcca*cos(gccp*rad),gcca*sin(gccp*rad))

        gevf = cmplx(gevfa*cos(gevfp*rad),gevfa*sin(gevfp*rad))
        gcvf = cmplx(gcvfa*cos(gcvfp*rad),gcvfa*sin(gcvfp*rad))

        attef = 40.02e-6
        attcc = 550.5e-6

        if(test .eq. 1) then
        fef = vin * attef * gef * gevf - vin * attcc * gcor * gevf
        fcc = -vin * attcc * gcc * gcvf
        end if

        if(test .eq. 2) then
```

```
        fef = -vin * attcc * gcor * gevf
        fcc = -vin * attcc * gcc * gcvf
        end if

        if(test .eq. 3) then
        fef = vin * gevf
        fcc = vin * gcvf
        end if

        if(test .eq. 4 .or. test .eq. 5) then
        fcc = vin * attcc * gcc * gcvf
        fef = 0.5 * fcc
        end if

        if(test .eq. 6) then
        fcc = vin * gcvf
        fef = 0.5 * fcc
        end if

        fefa = abs(fef)
        fefp = deg * atan2(imag(fef),real(fef))

        fcca = abs(fcc)
        fccp = deg * atan2(imag(fcc),real(fcc))

        write(*,101) freq,fefa,fcca,fefp-fccp
101     format(f5.1,f6.1,f6.1,f10.1)
        end do

        end
```

APPENDIX M

Parameter Files used in Cadiz XCP Processing

```
# debug          0
# mod            7
# slow_fall      0
# tag            xcpaddt

# tfall           2
# tquit          10.
# dtmin         .05
# dtmax         .2
# dtbad         .118

# rotfmin        8        /* use 2 for slow fall */
# rotfmax        20
# rotfbreak      10       /* used for slow falls */
# rotferrmax     0.5
# tspinup        3.5

# bad_flag       -1.e30
```

```
# debug         0
# diffmax       1
# timeused      tmaster
# nokneed       20
# rotfmin       2
# rotfmax       20
# mavg          20
```

```
# debug         0
# tag           xcpblf
# blctype       original

# s1            .005
# s2            .0125
# s3            .025

# rotfmin       1
# rotfmax       20
```

```
# debug          0
# tag            orig

# paramfiles     deckbox.p probe.p pcal.p tcal.p

# timeused       tmaster
```

```
/* deck box phase errors */

# efccp0        0.
# efccp1        0.
```

```
/* probe EM calibrations */

# amean          667
# gevfa          494.66025
# gevfp          0
# gcvfa          500
# gcvfp          0

# esep           5.19
# c1             .97
# c2             -0.0353  /* new c2 from modified fallrate - June 22, 1989 */

# gefa 23866.12044581 107.99111272898 -0.905827321
# gcca 1809.877761 -1.25653911 0.18856556
# gcora 898.89564739 0.453188608 0.0717425016

# gefp -138.158938796 9.759010754 -0.180878978
# gccp 29.826971133 10.265226263 -0.176531452
# gcorp 56.552652832 7.783581145 -0.112472607
```

```
/* -- depth coefficients derived from Cadiz data - June 22, 1989 -- */

# depthcal  4.0  4.461 -0.000635
# prconv    0.9927 -2.55e-06  0.0073  -50.
```

```
/* probe temp calibrations standard for mod 7 */

# tcalfreq      285.3   449.1
# tcalres       16329   4024
# tcal          1.73323e-3   8.75509e-5    1.64067e-5   -5.09882e-7
# tcor          -0.05   -1.25e-04
```

```
# debug          0
# shearout       1
# auxout         1

# z0             0       /* initial depth of sampling grid */
# dz             2.      /* output sampling grid in meters */
# dzbin          6.      /* bin size in meters */

# zvar           pr      /* depth variable name -- z or zs */
# binmin         0.75    /* fraction of a bin which can be included as
                                a data point on last point only */

# tmax           35.0    /* max temp allowed deg C */
# tmin           -3.0    /* min */
# umax            2.00   /* maximum u & v velocity allowed m/s */
# umin           -2.00   /* minimum */

# rotfmax        20.0    /* max rotf allowed -- used to screen all data */
# rotfmin        8.0     /* min */
# zfiltrotf      3.0     /* recursive filtering distance for rotfav */
# maxdevrotf     2.0     /* max deviation of rotf from rotfav allowed Hz */
```

APPENDIX N

Velocity and Temperature Profiles

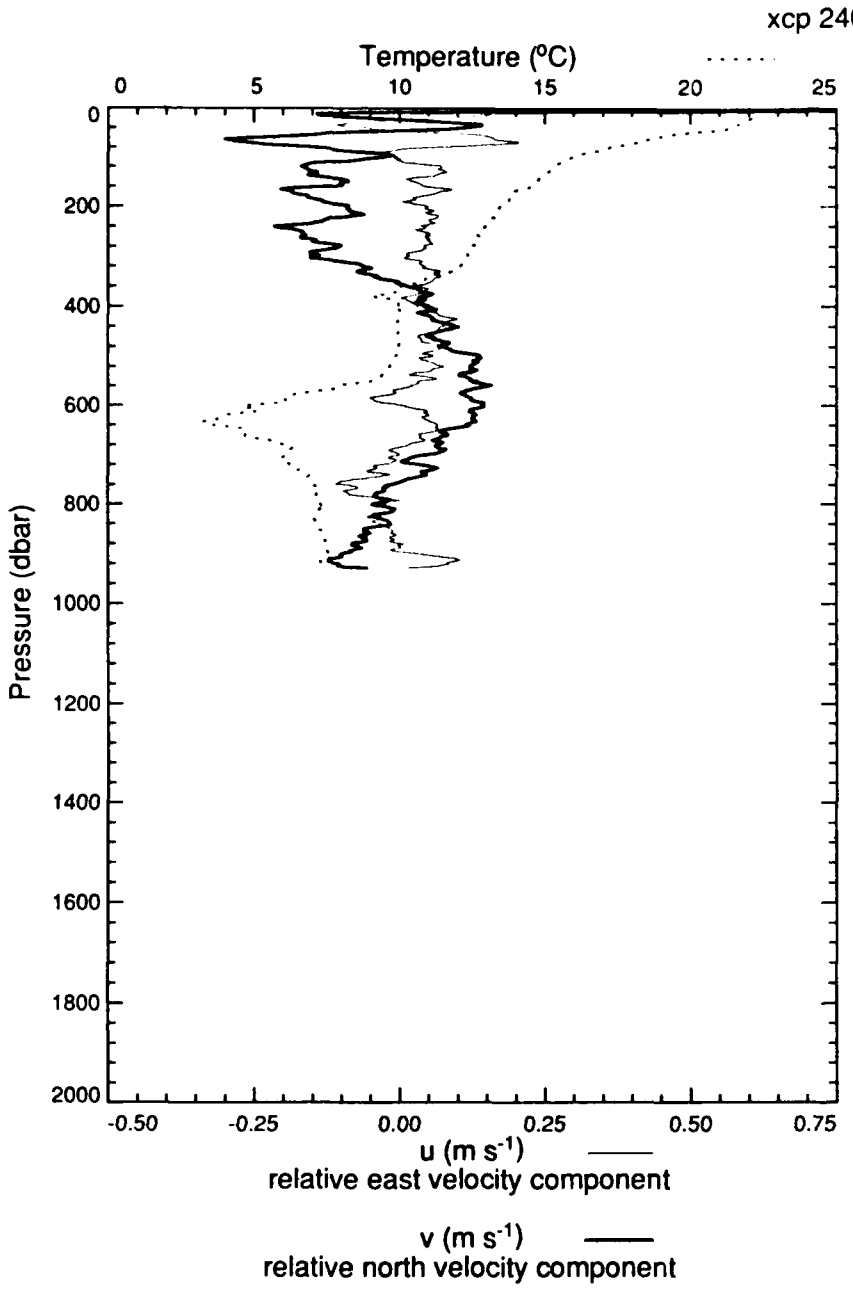
xcp 2401
Temperature (°C)
0
5
10
15
20
25
Pressure (dbar)
0
200
400
600
800
1000
1200
1400
1600
1800
2000
-0.50
-0.25
0.00
0.25
0.50
0.75
u (m s-1)
relative east velocity component
v (m s-1)
relative north velocity component

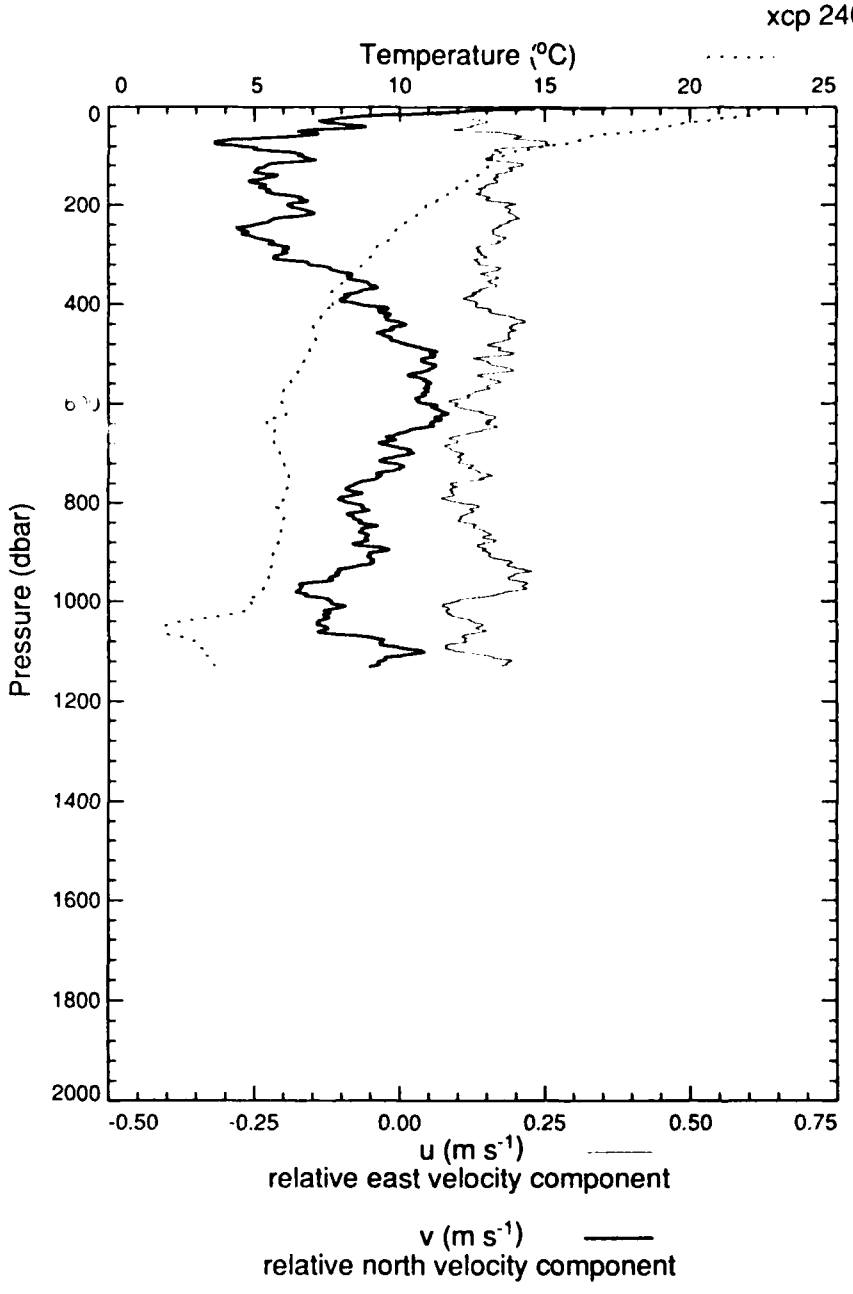
xcp 2402
Temperature (°C)
0
5
10
15
20
25
Pressure (dbar)
0
200
400
800
1000
1200
1400
1600
1800
2000
-0.50
-0.25
0.00
0.25
0.50
0.75
u (m s-1)
relative east velocity component
v (m s-1)
relative north velocity component

TR 8925 N1

N2 TR 8925

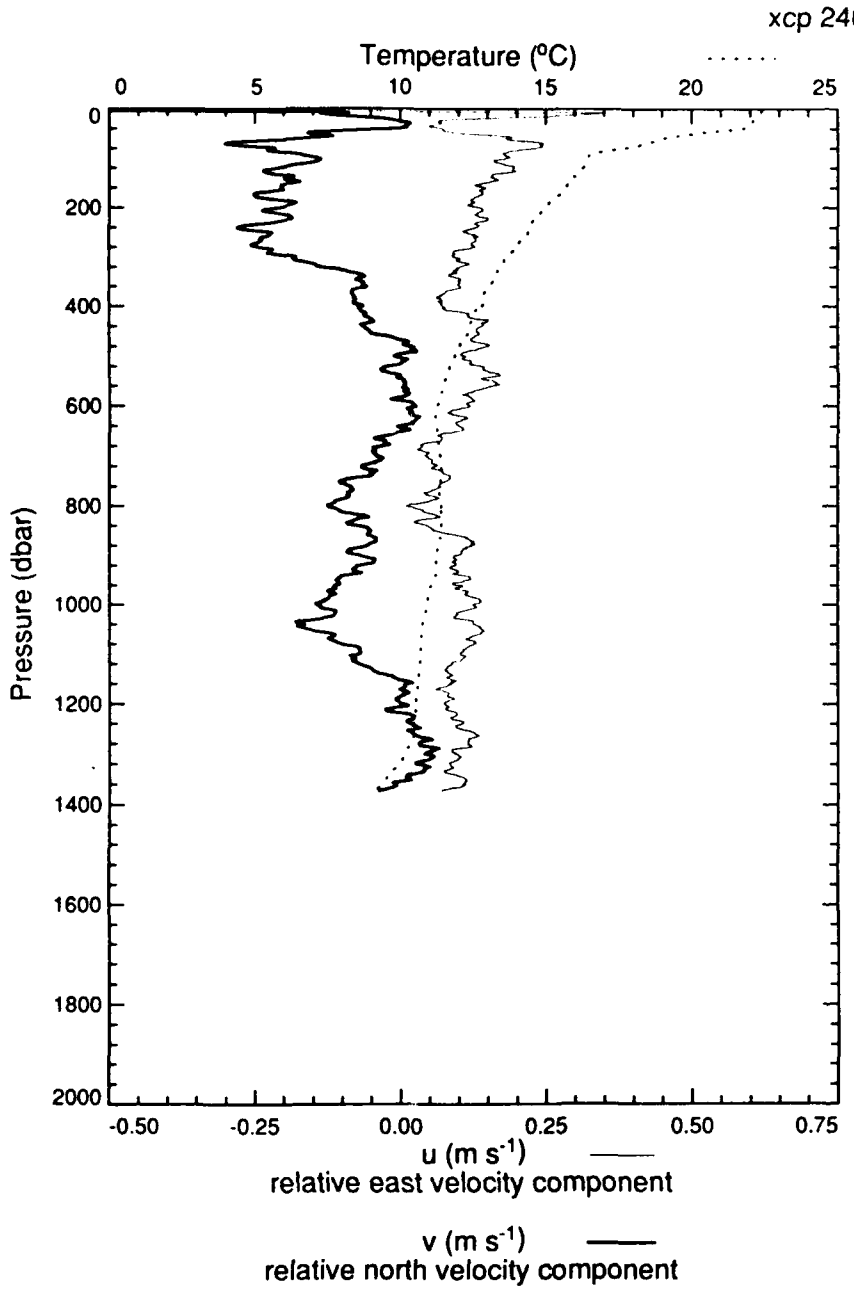
xcp 2403
Temperature (°C)
0
5
10
15
20
25
Pressure (dbar)
0
200
400
600
800
1000
1200
1400
1600
1800
2000
-0.50
-0.25
0.00
0.25
0.50
0.75
u (m s-1)
relative east velocity component
v (m s-1)
relative north velocity component

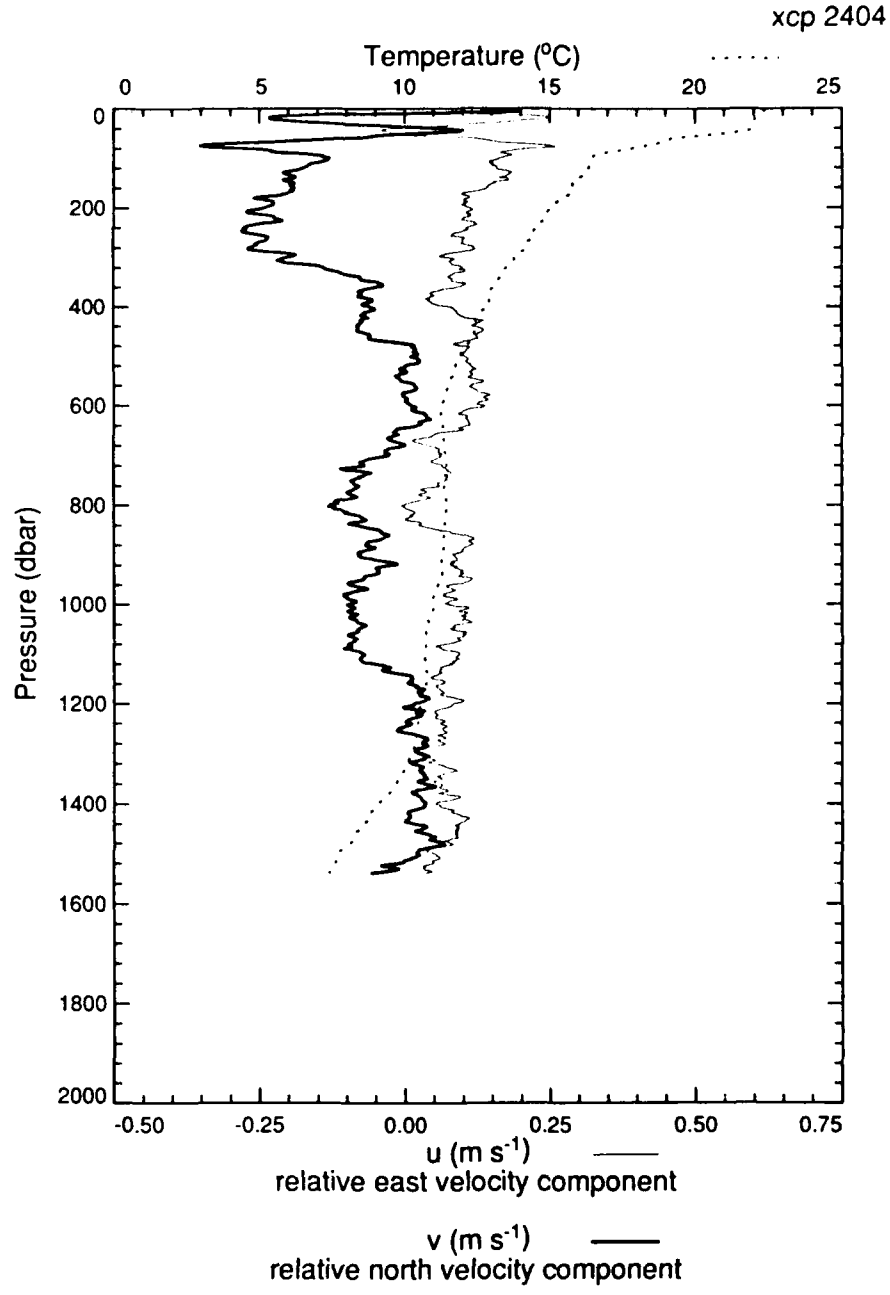
xcp 2404
Temperature (°C)
0
5
10
15
20
25
Pressure (dbar)
0
200
400
600
800
1000
1200
1400
1600
1800
2000
-0.50
-0.25
0.00
0.25
0.50
0.75
u (m s-1)
relative east velocity component
v (m s-1)
relative north velocity component

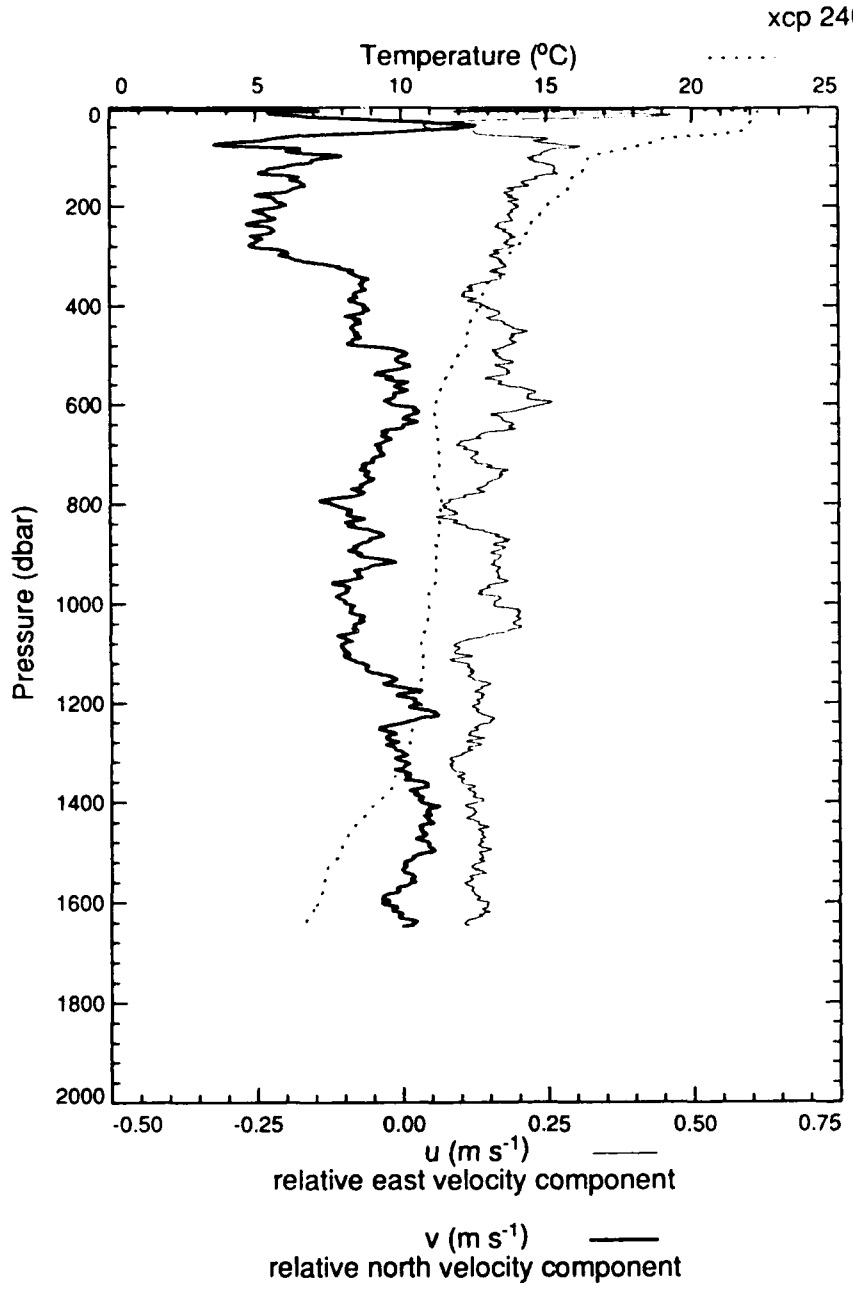
xcp 2405
Temperature (°C)
0
5
10
15
20
25
Pressure (dbar)
0
200
400
600
800
1000
1200
1400
1600
1800
2000
-0.50
-0.25
0.00
0.25
0.50
0.75
u (m s-1)
relative east velocity component
v (m s-1)
relative north velocity component

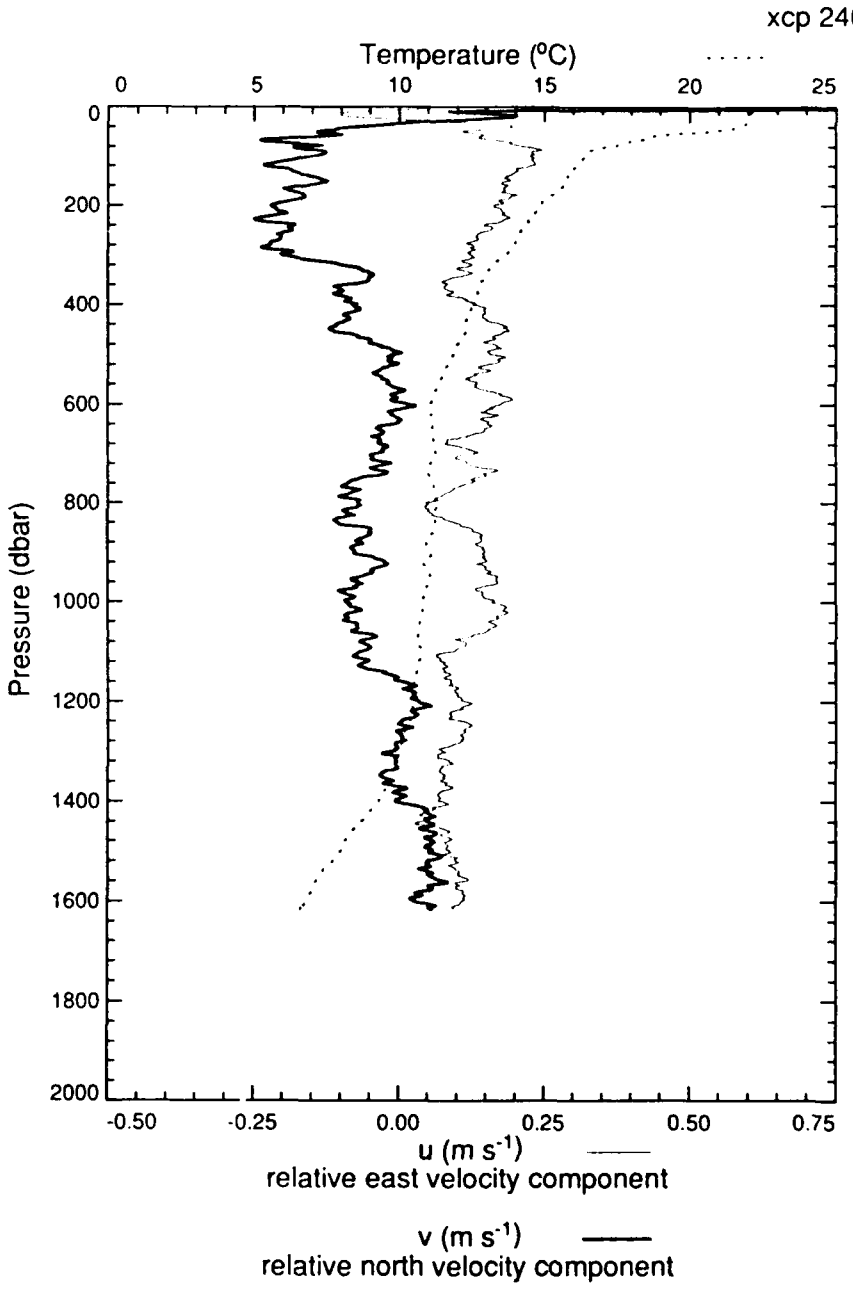
xcp 2406
Temperature (°C)
0
5
10
15
20
25
Pressure (dbar)
0
200
400
600
800
1000
1200
1400
1600
1800
2000
-0.50
-0.25
0.00
0.25
0.50
0.75
u (m s-1)
relative east velocity component
v (m s-1)
relative north velocity component

TR 8925 N3

N4 TR 8925

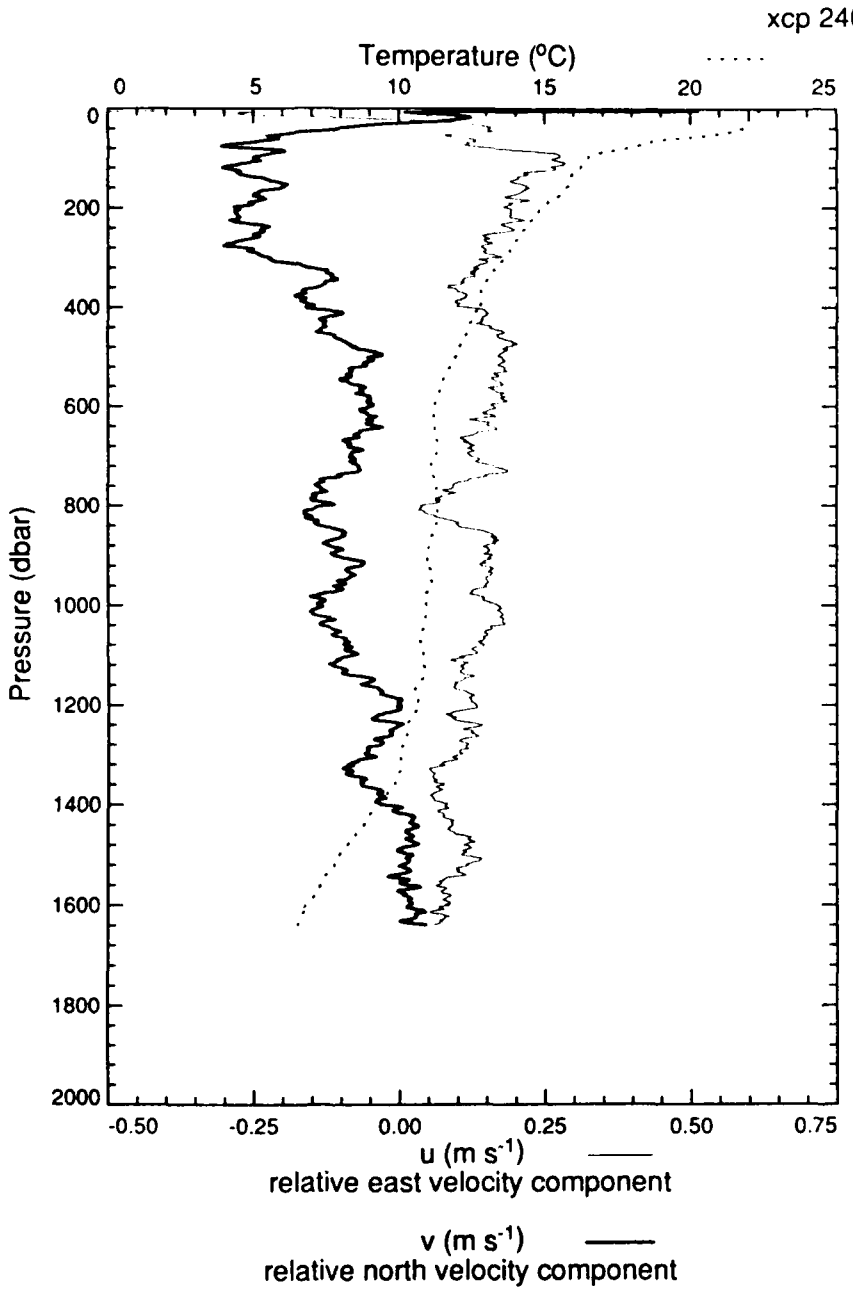
xcp 2407
Temperature (°C)
0
5
10
15
20
25
Pressure (dbar)
0
200
400
600
800
1000
1200
1400
1600
1800
2000
-0.50
-0.25
0.00
0.25
0.50
0.75
u (m s-1)
relative east velocity component
v (m s-1)
relative north velocity component

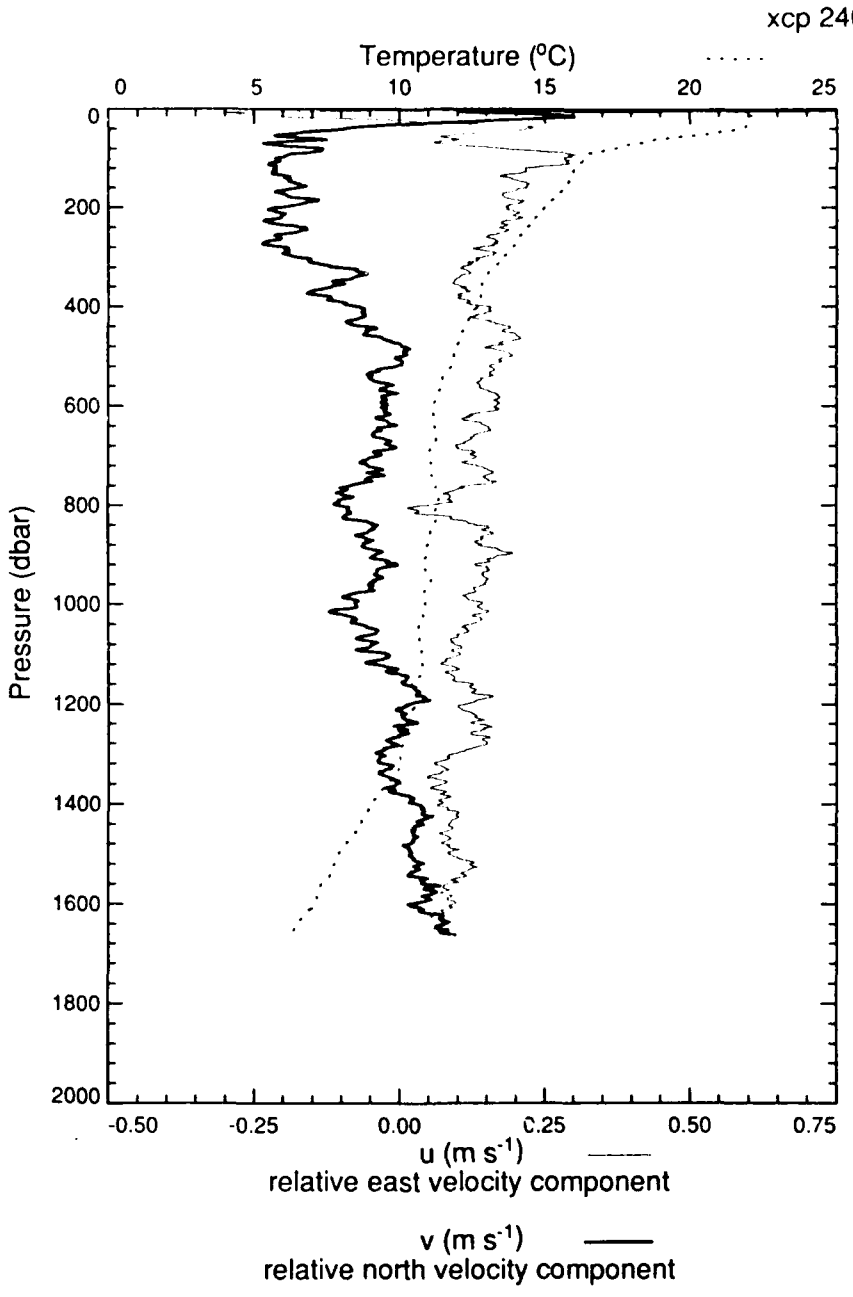
xcp 2408
Temperature (°C)
0
5
10
15
20
25
Pressure (dbar)
0
200
400
600
800
1000
1200
1400
1600
1800
2000
-0.50
-0.25
0.00
0.25
0.50
0.75
u (m s-1)
relative east velocity component
v (m s-1)
relative north velocity component

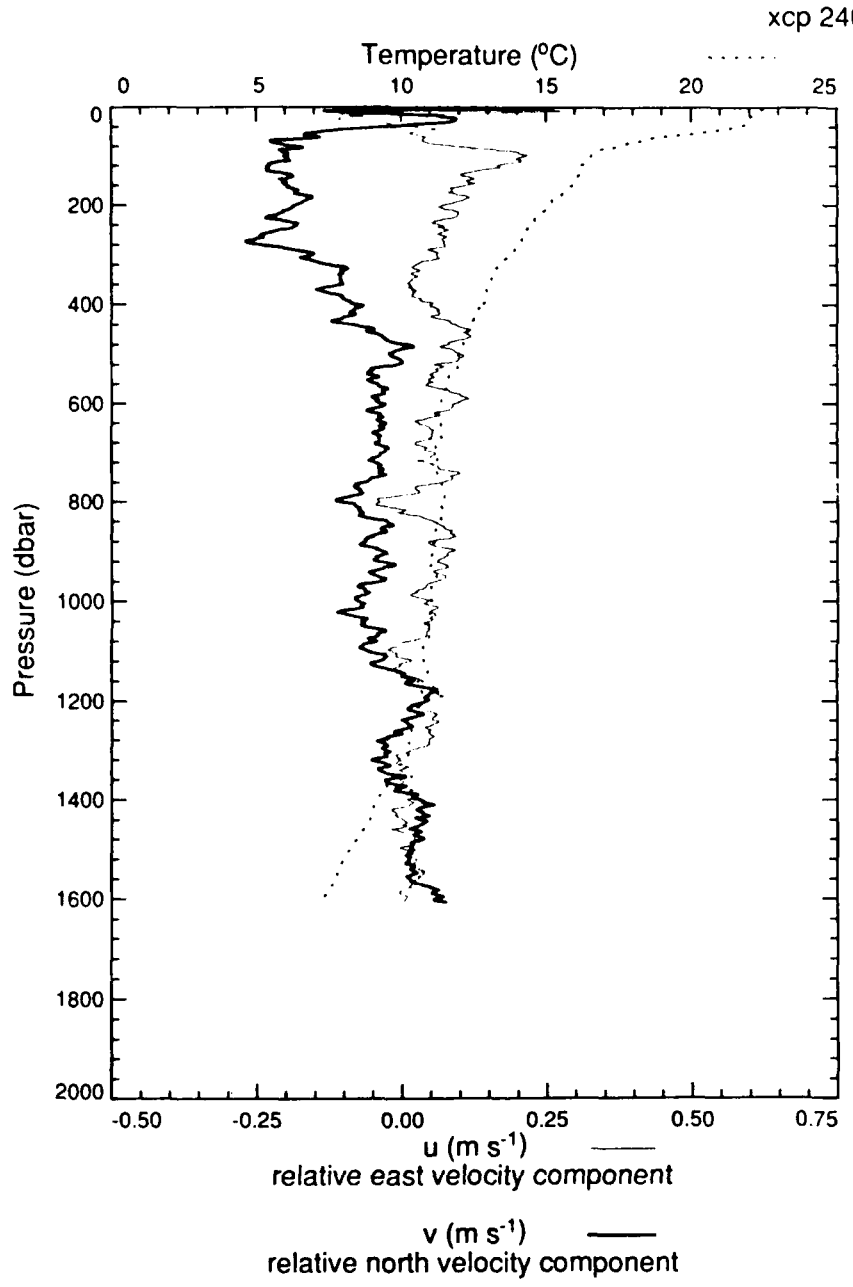
xcp 2409
Temperature (°C)
0
5
10
15
20
25
Pressure (dbar)
0
200
400
600
800
1000
1200
1400
1600
1800
2000
-0.50
-0.25
0.00
0.25
0.50
0.75
u (m s-1)
relative east velocity component
v (m s-1)
relative north velocity component

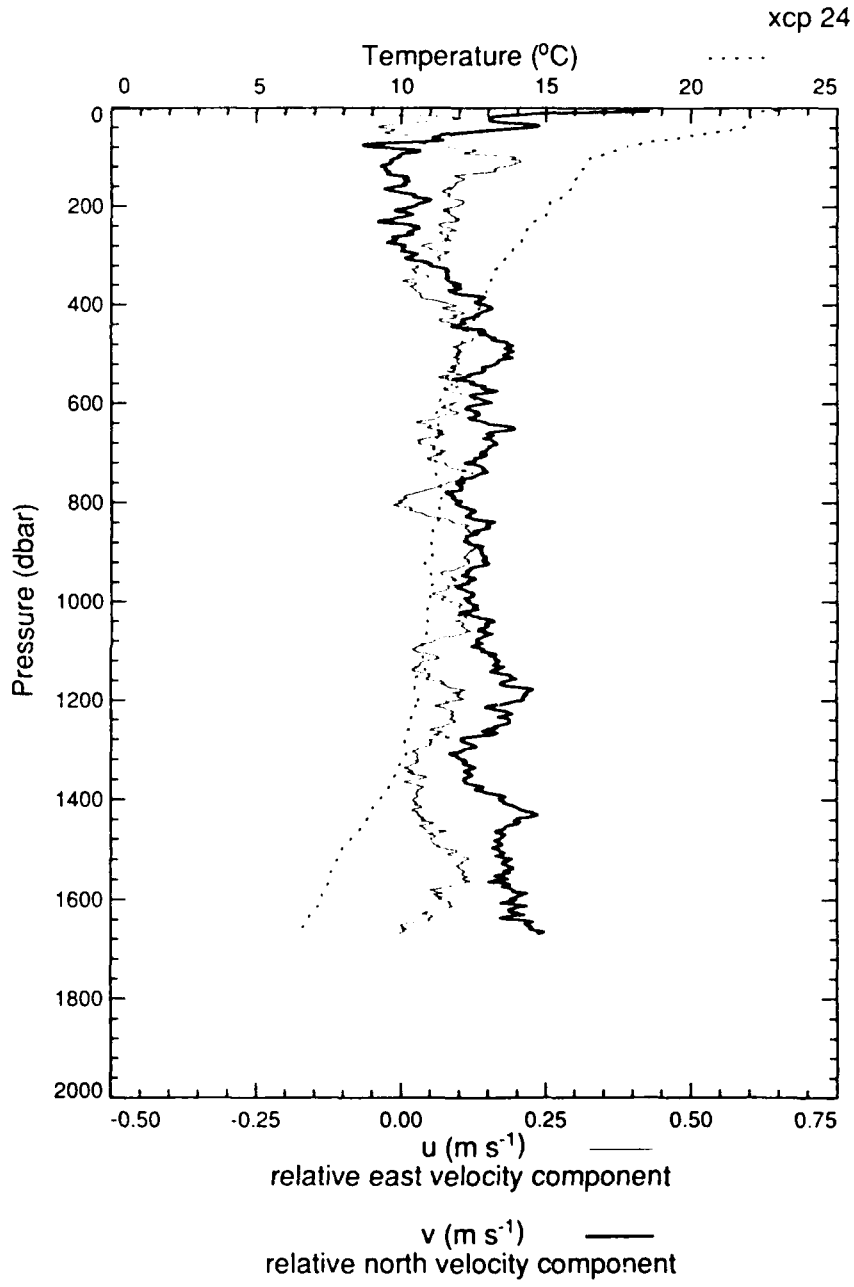
xcp 2410
Temperature (°C)
0
5
10
15
20
25
Pressure (dbar)
0
200
400
600
800
1000
1200
1400
1600
1800
2000
-0.50
-0.25
0.00
0.25
0.50
0.75
u (m s-1)
relative east velocity component
v (m s-1)
relative north velocity component

TR 8925 N5

N6 TR 8925

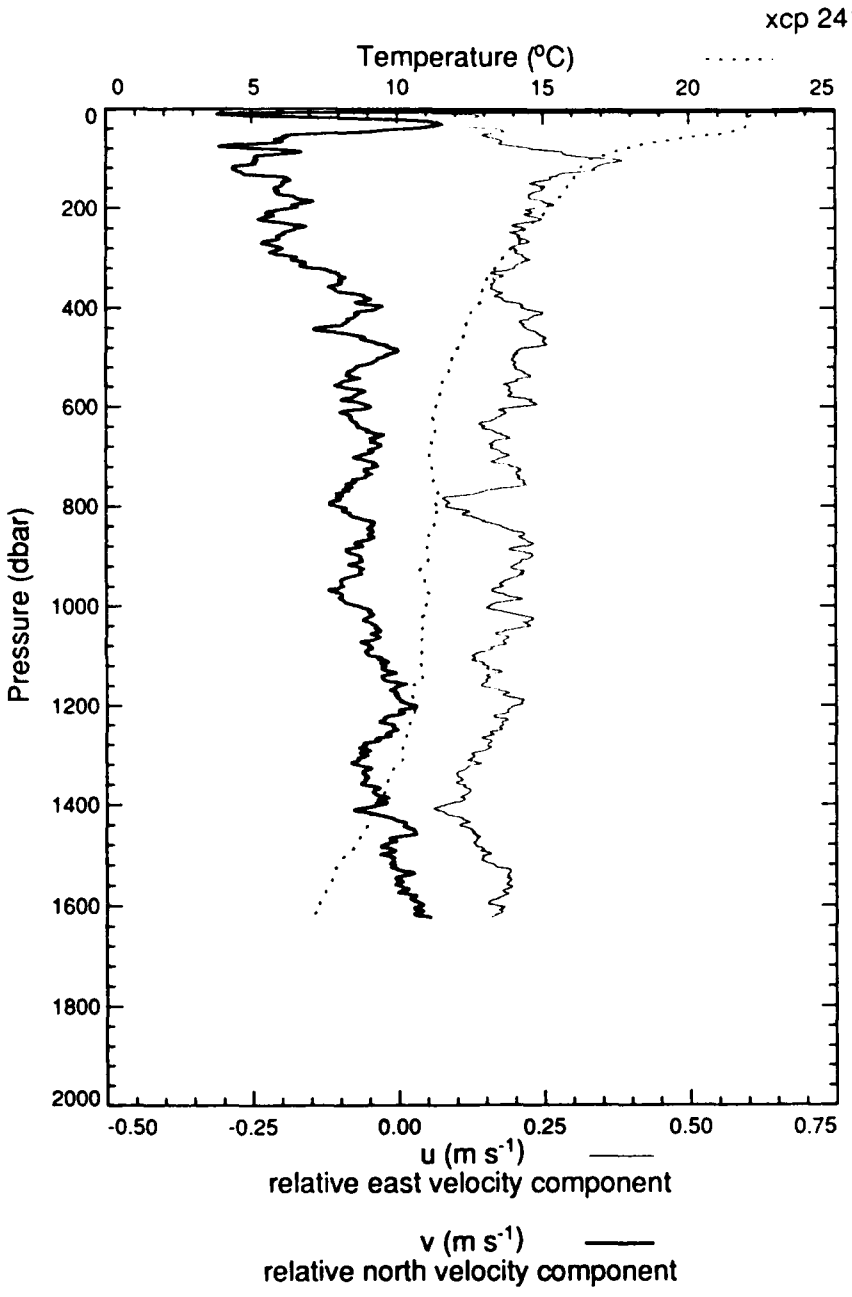
xcp 2411
Temperature (°C)
0
5
10
15
20
25
Pressure (dbar)
0
200
400
600
800
1000
1200
1400
1600
1800
2000
-0.50
-0.25
0.00
0.25
0.50
0.75
u (m s-1)
relative east velocity component
v (m s-1)
relative north velocity component

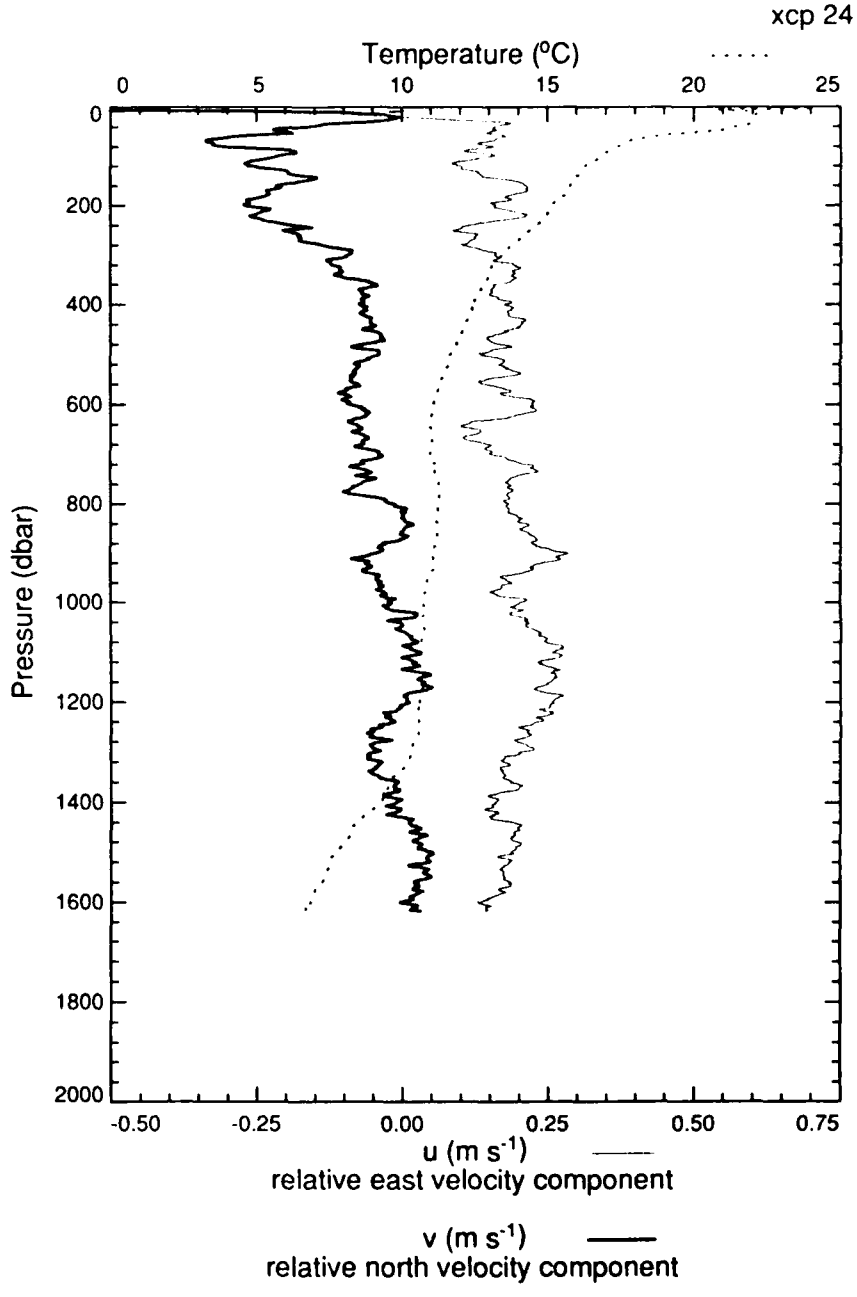
xcp 2412
Temperature (°C)
0
5
10
15
20
25
Pressure (dbar)
0
200
400
600
800
1000
1200
1400
1600
1800
2000
-0.50
-0.25
0.00
0.25
0.50
0.75
u (m s-1)
relative east velocity component
v (m s-1)
relative north velocity component

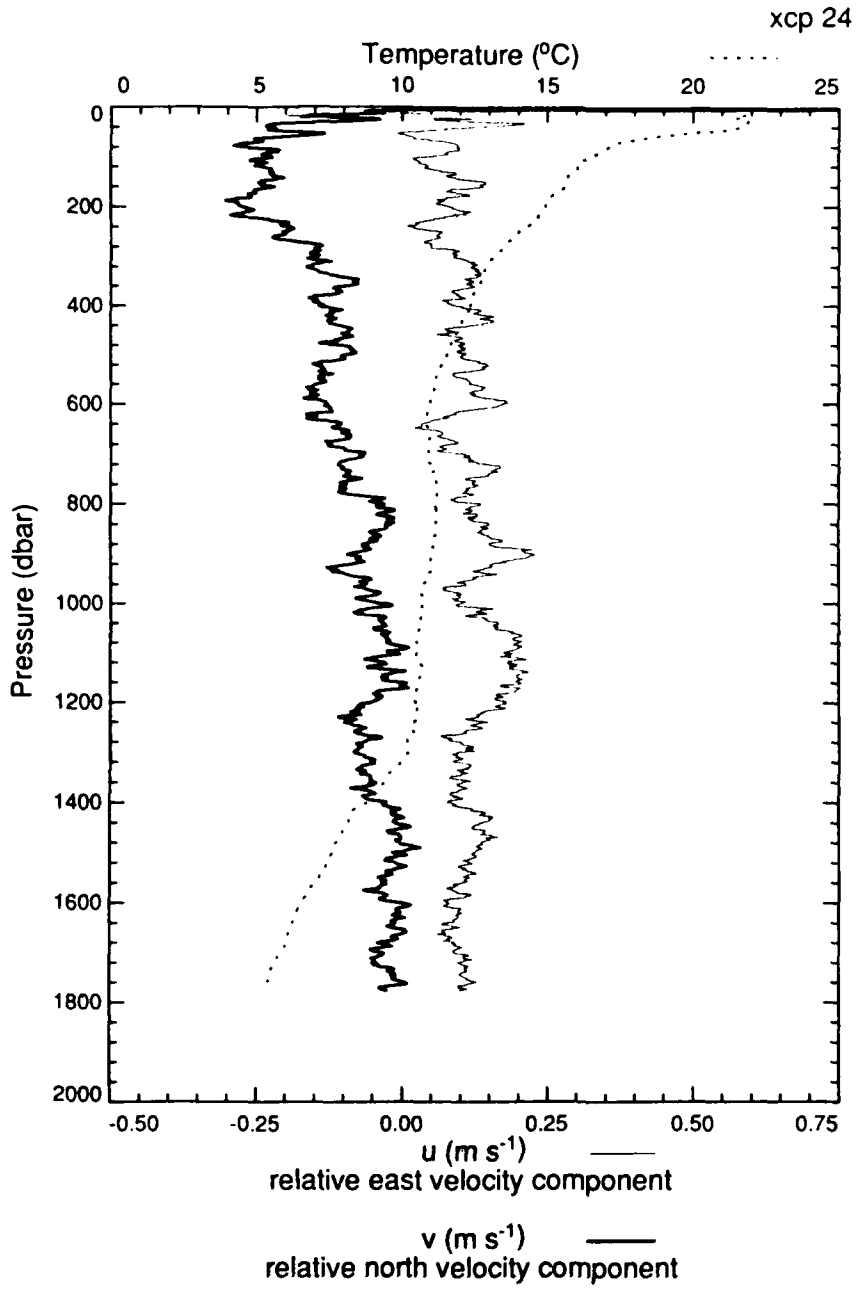
xcp 2413
Temperature (°C)
0
5
10
15
20
25
Pressure (dbar)
0
200
400
600
800
1000
1200
1400
1600
1800
2000
-0.50
-0.25
0.00
0.25
0.50
0.75
u (m s-1)
relative east velocity component
v (m s-1)
relative north velocity component

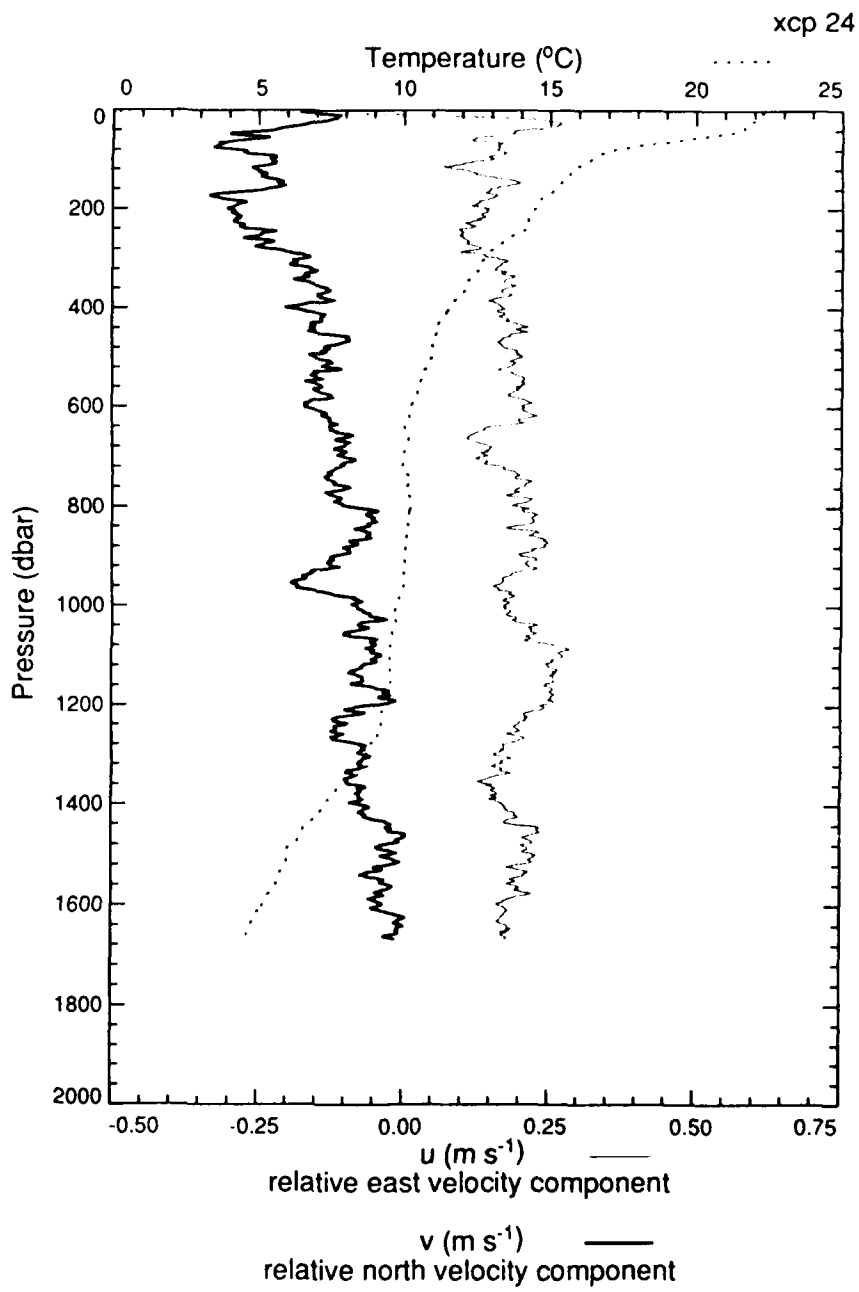
xcp 2414
Temperature (°C)
0
5
10
15
20
25
Pressure (dbar)
0
200
400
600
800
1000
1200
1400
1600
1800
2000
-0.50
-0.25
0.00
0.25
0.50
0.75
u (m s-1)
relative east velocity component
v (m s-1)
relative north velocity component

TR 8925 N7

N8 TR 8925

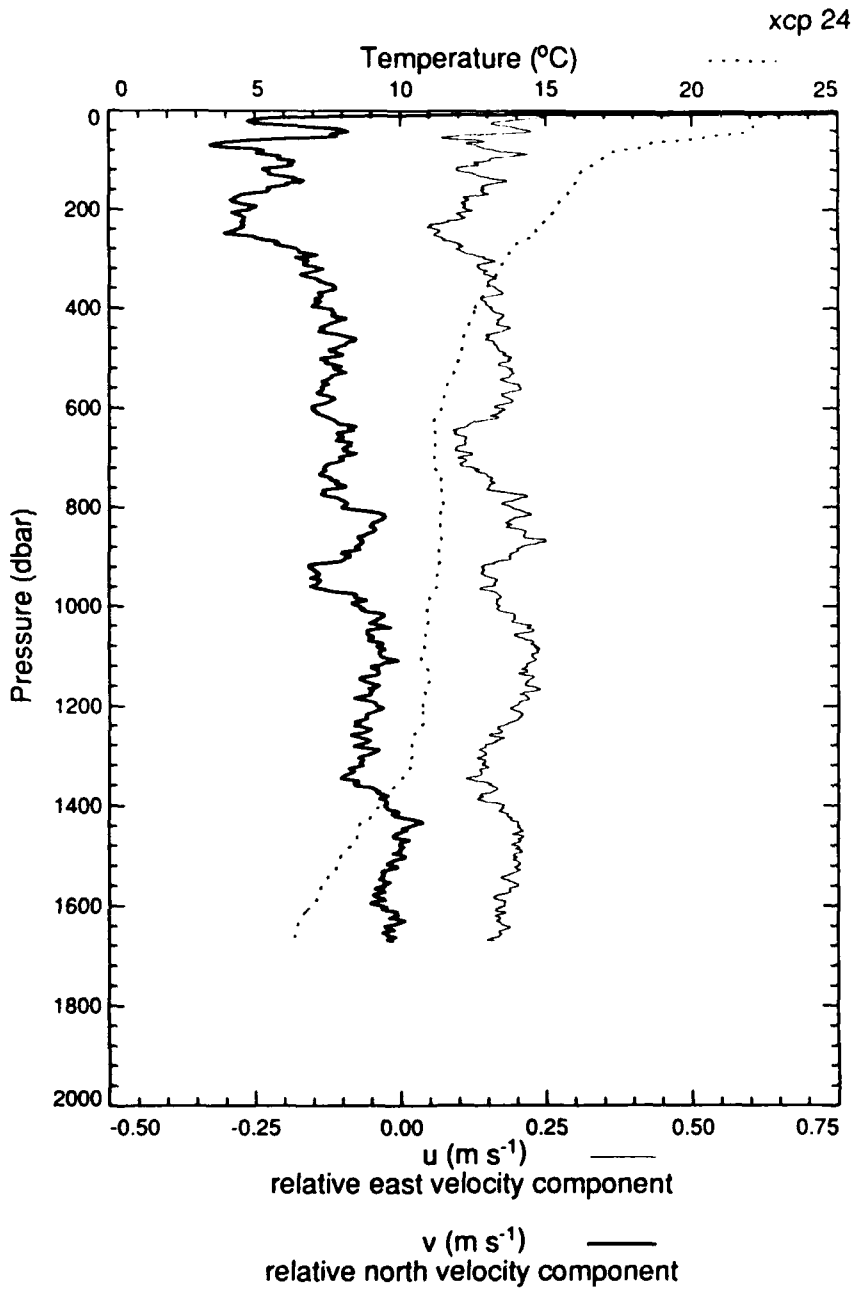
xcp 2415
Temperature (°C)
0
5
10
15
20
25
Pressure (dbar)
0
200
400
600
800
1000
1200
1400
1600
1800
2000
-0.50
-0.25
0.00
0.25
0.50
0.75
u (m s-1)
relative east velocity component
v (m s-1)
relative north velocity component

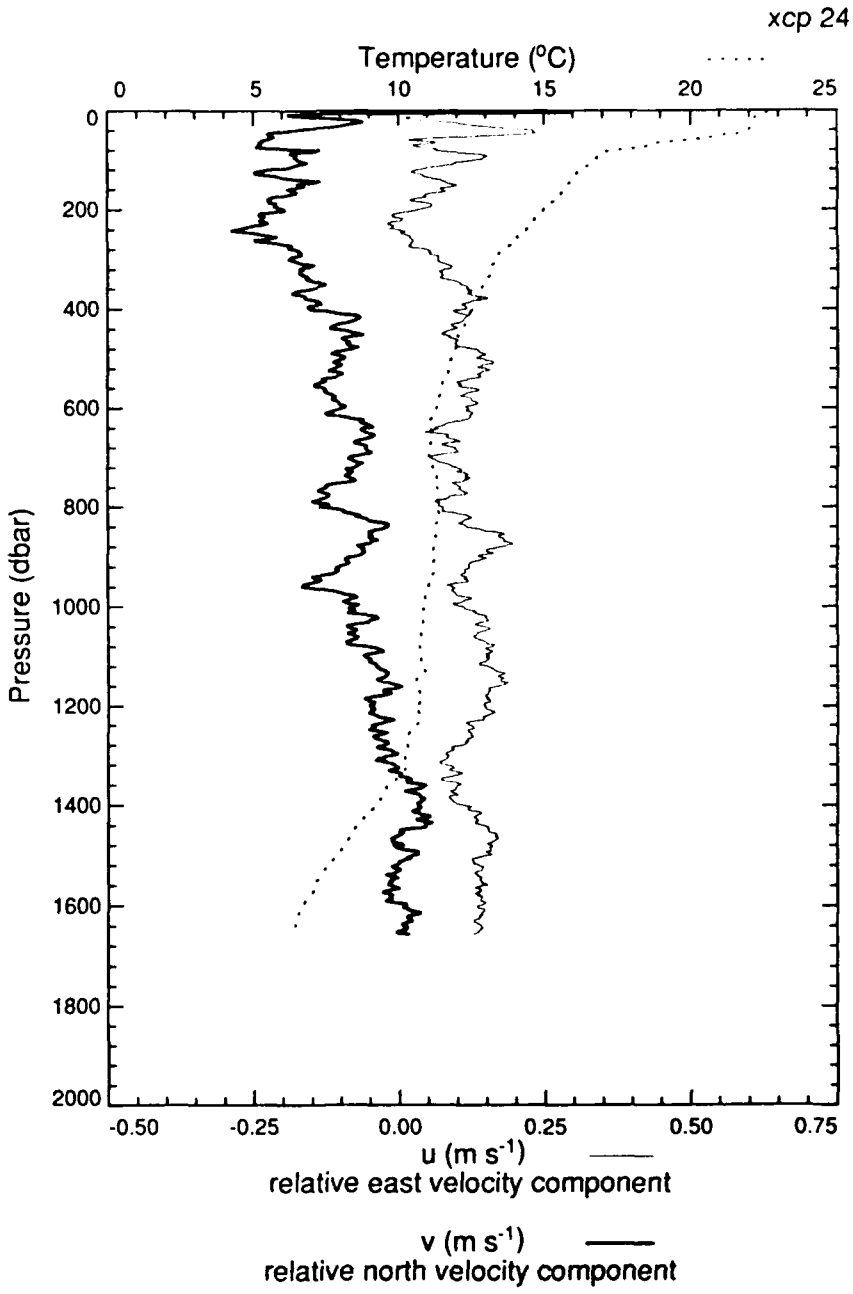
xcp 2416
Temperature (°C)
0
5
10
15
20
25
Pressure (dbar)
0
200
400
600
800
1000
1200
1400
1600
1800
2000
-0.50
-0.25
0.00
0.25
0.50
0.75
u (m s-1)
relative east velocity component
v (m s-1)
relative north velocity component

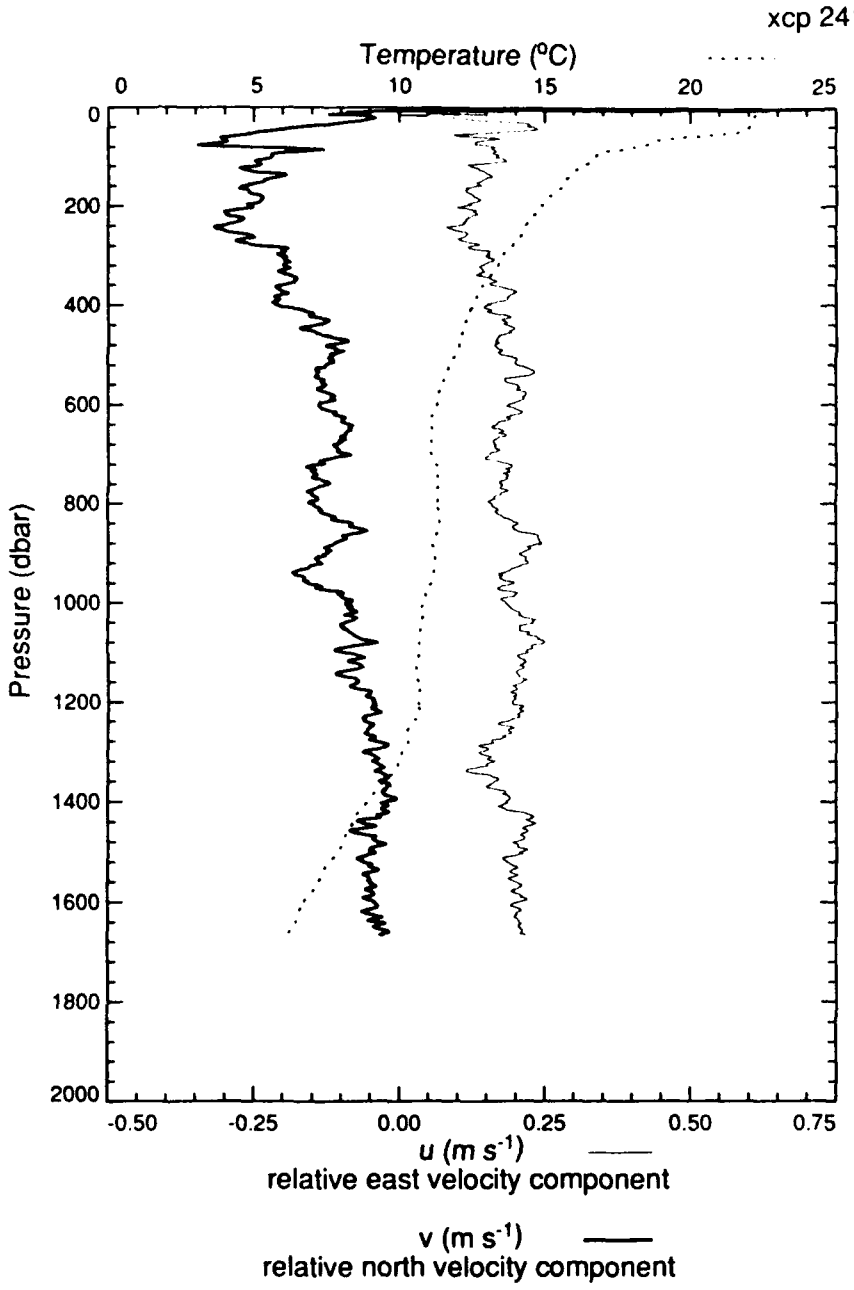
xcp 2417
Temperature (°C)
0
5
10
15
20
25
Pressure (dbar)
0
200
400
600
800
1000
1200
1400
1600
1800
2000
-0.50
-0.25
0.00
0.25
0.50
0.75
u (m s-1)
relative east velocity component
v (m s-1)
relative north velocity component

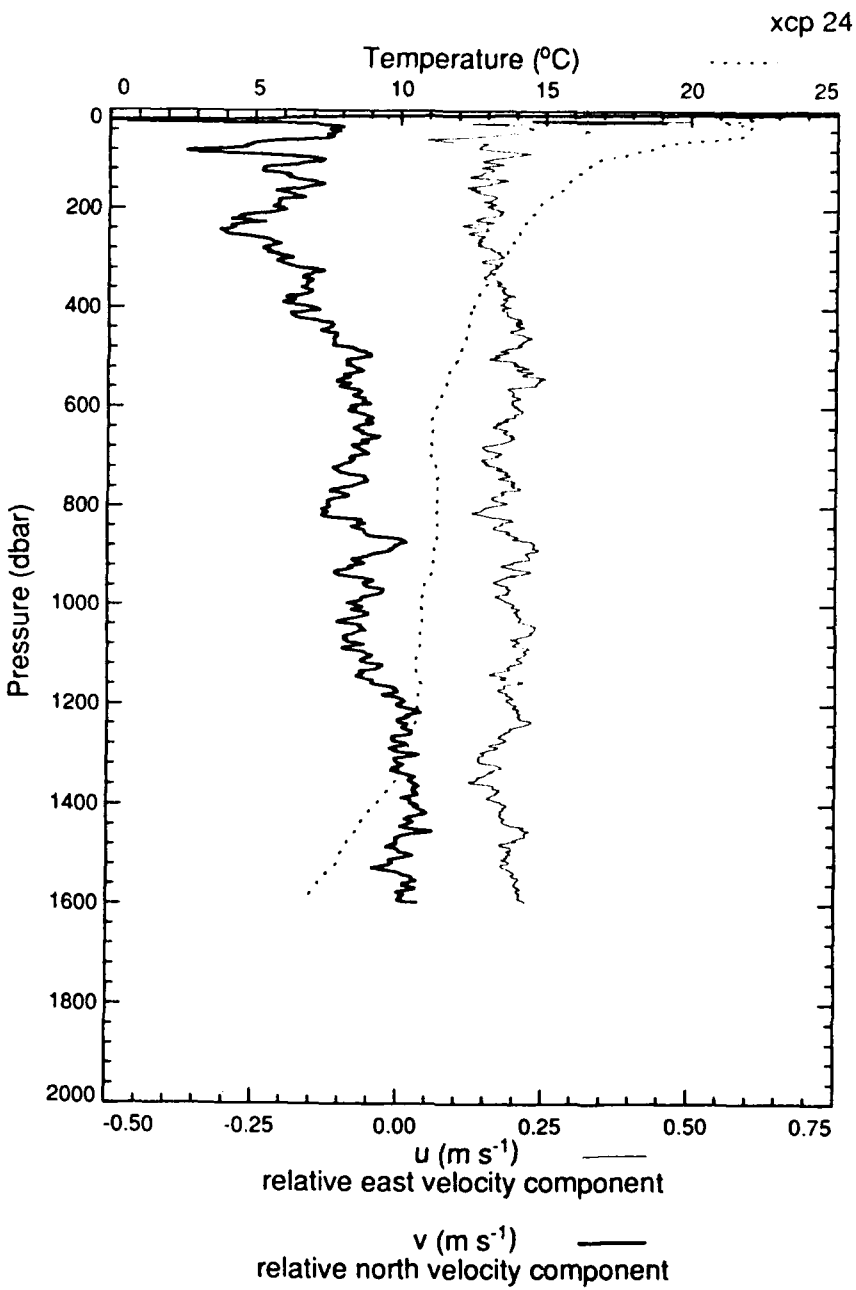
xcp 2418
Temperature (°C)
0
5
10
15
20
25
Pressure (dbar)
0
200
400
600
800
1000
1200
1400
1600
1800
2000
-0.50
-0.25
0.00
0.25
0.50
0.75
u (m s-1)
relative east velocity component
v (m s-1)
relative north velocity component

TR 8925 N9

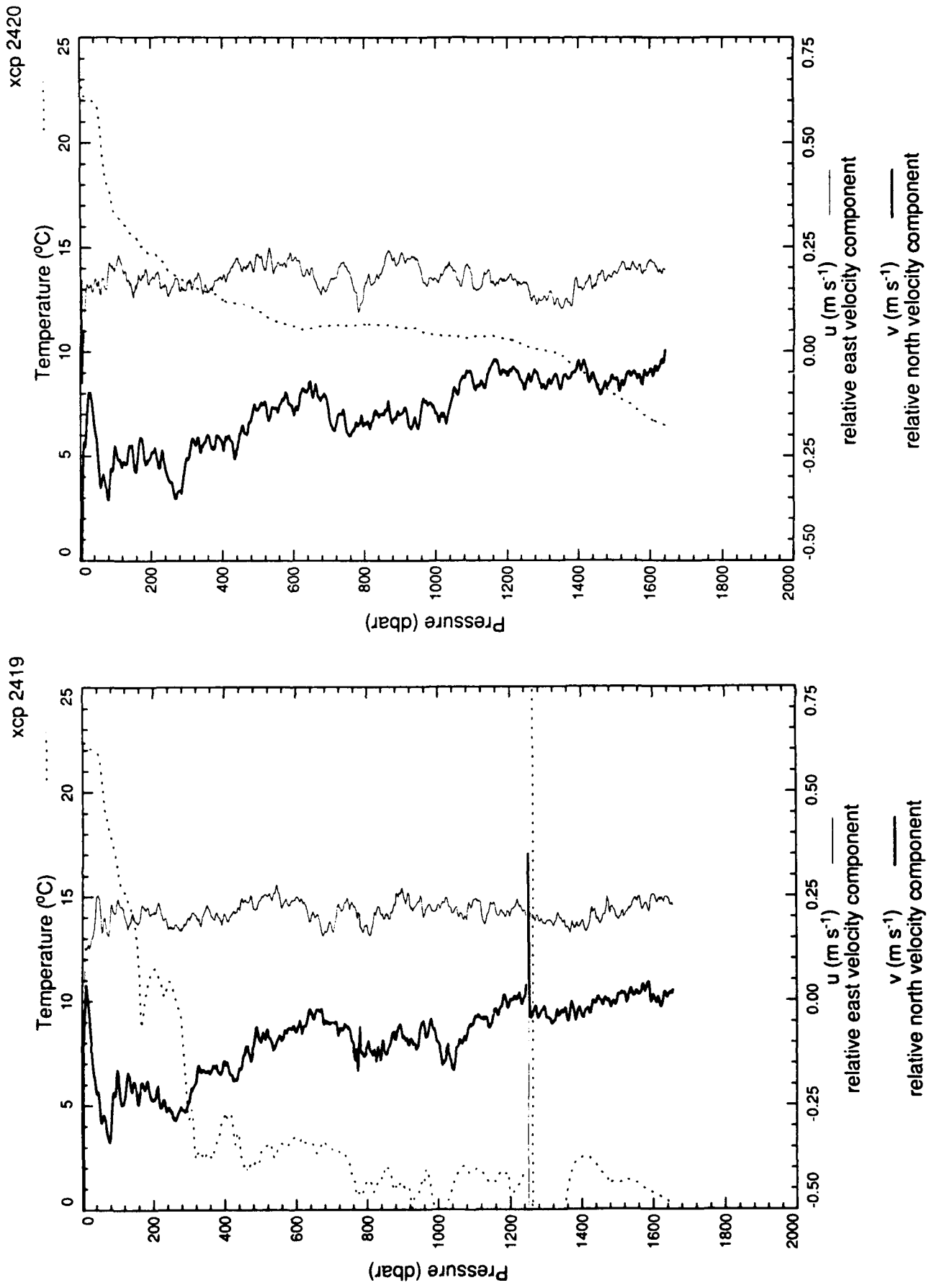
xcp 2420
Temperature (°C)
Pressure (dbar)
u (m s-1)
relative east velocity component
v (m s-1)
relative north velocity component
xcp 2419
Temperature (°C)
Pressure (dbar)
u (m s-1)
relative east velocity component
v (m s-1)
relative north velocity component

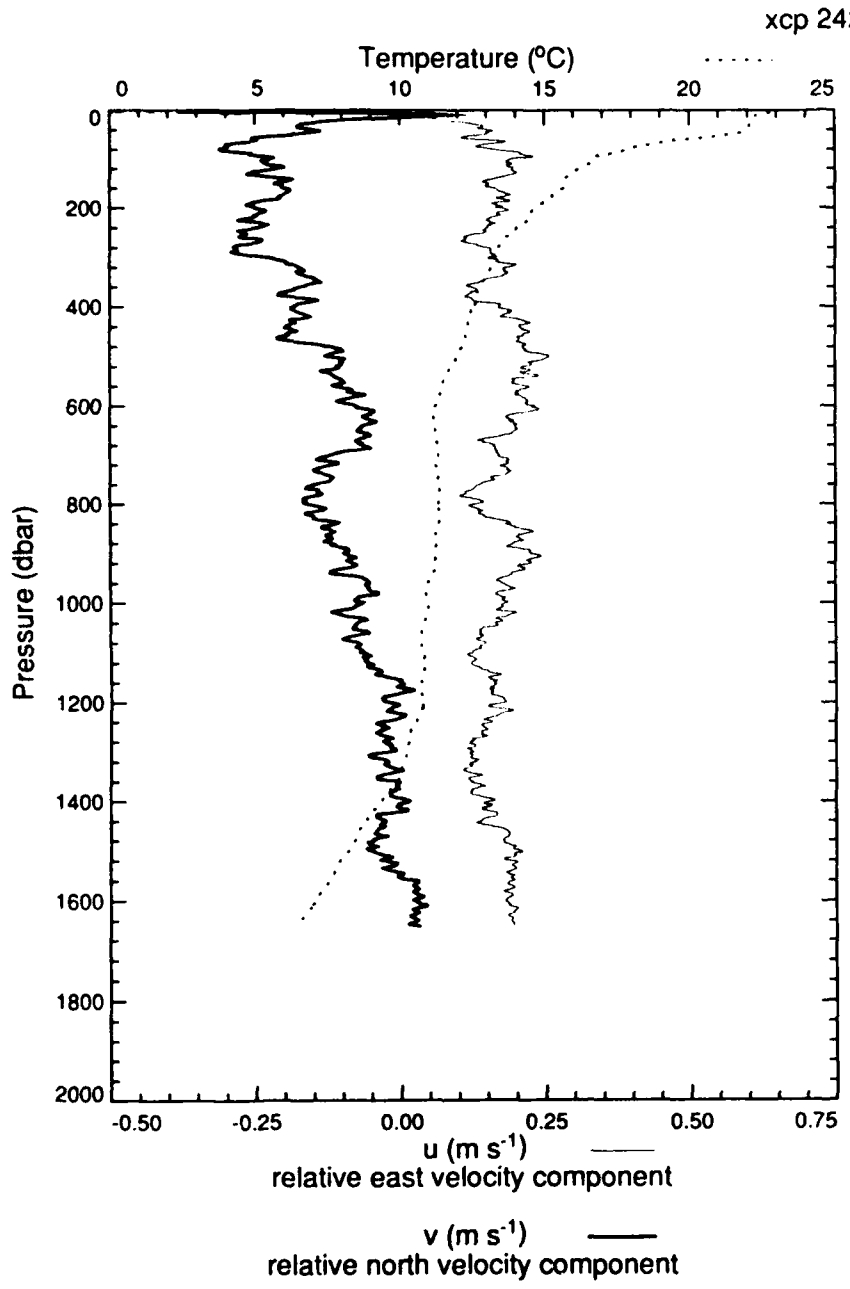
xcp 2421
Temperature (°C)
0
5
10
15
20
25
Pressure (dbar)
0
200
400
600
800
1000
1200
1400
1600
1800
2000
-0.50
-0.25
0.00
0.25
0.50
0.75
u (m s-1)
relative east velocity component
v (m s-1)
relative north velocity component

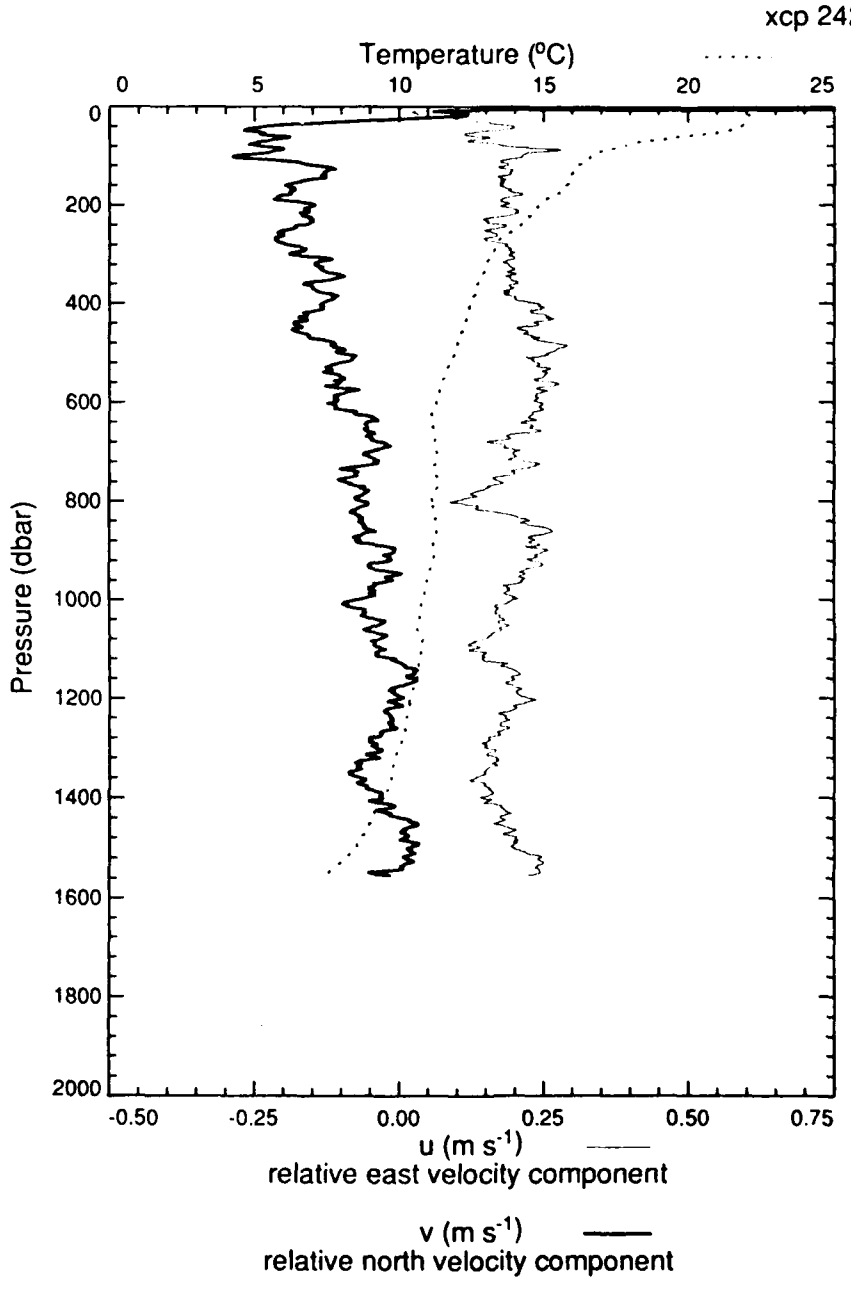
xcp 2422
Temperature (°C)
0
5
10
15
20
25
Pressure (dbar)
0
200
400
600
800
1000
1200
1400
1600
1800
2000
-0.50
-0.25
0.00
0.25
0.50
0.75
u (m s-1)
relative east velocity component
v (m s-1)
relative north velocity component

N12 TR 8925

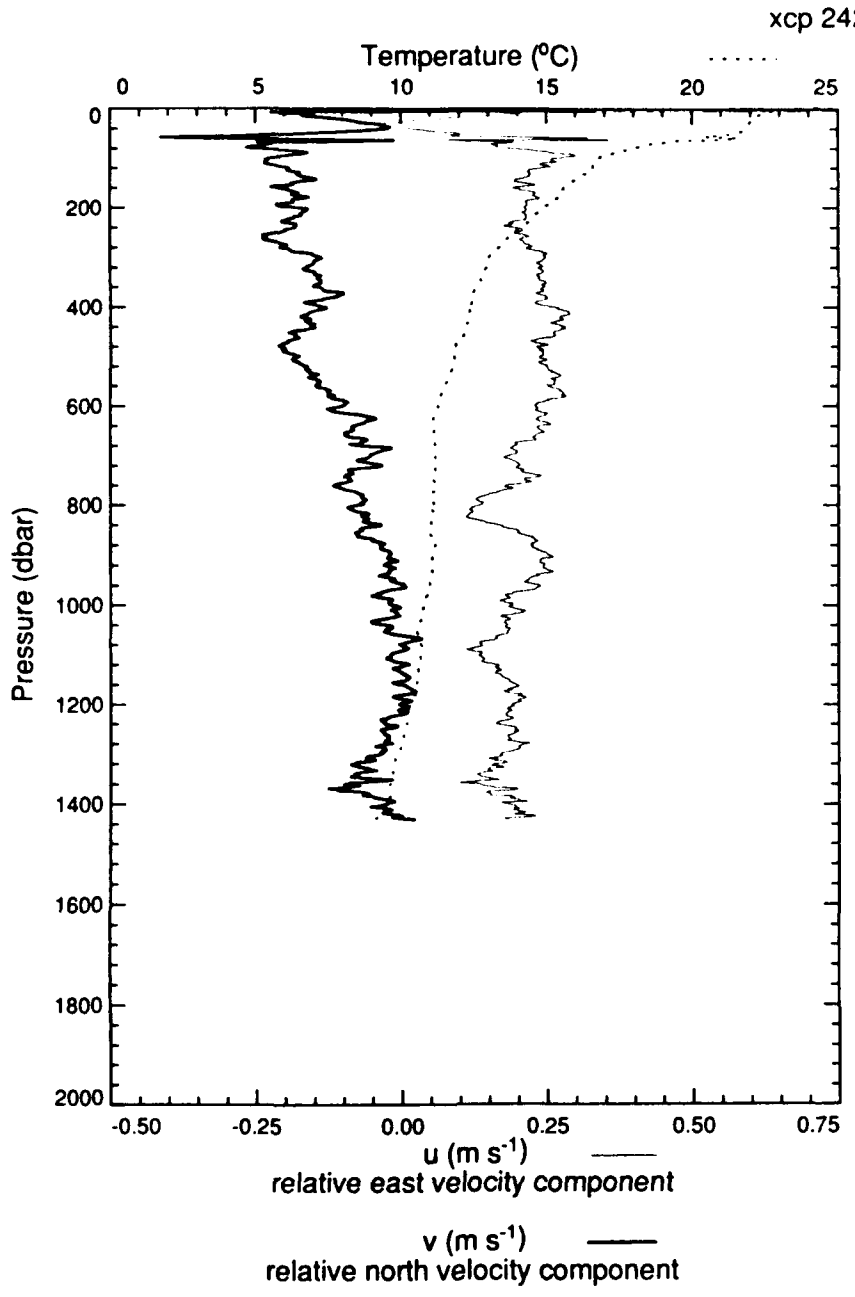
xcp 2423
Temperature (°C)
0
5
10
15
20
25
Pressure (dbar)
0
200
400
600
800
1000
1200
1400
1600
1800
2000
-0.50
-0.25
0.00
0.25
0.50
0.75
u (m s-1)
relative east velocity component
v (m s-1)
relative north velocity component

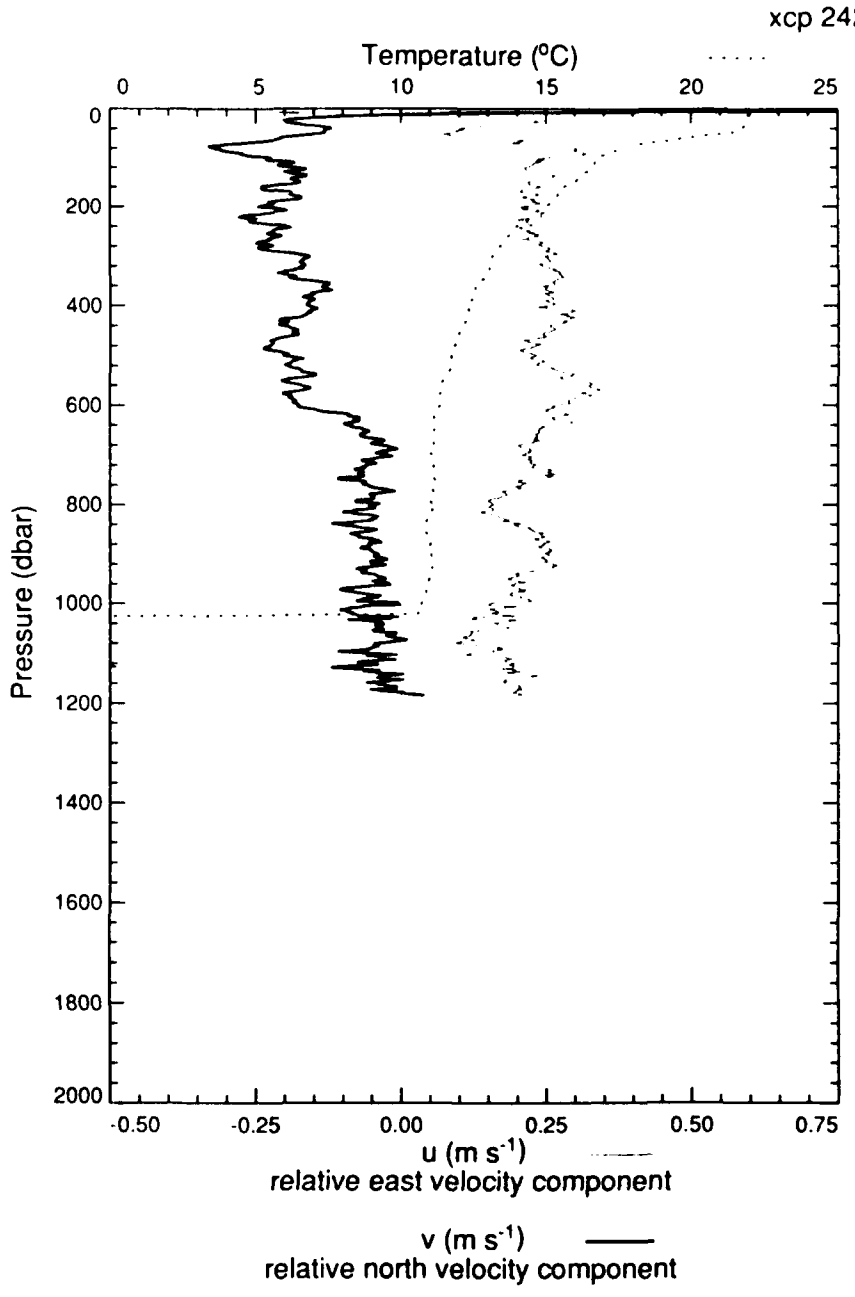
xcp 2424
Temperature (°C)
0
5
10
15
20
25
Pressure (dbar)
0
200
400
600
800
1000
1200
1400
1600
1800
2000
-0.50
-0.25
0.00
0.25
0.50
0.75
u (m s-1)
relative east velocity component
v (m s-1)
relative north velocity component

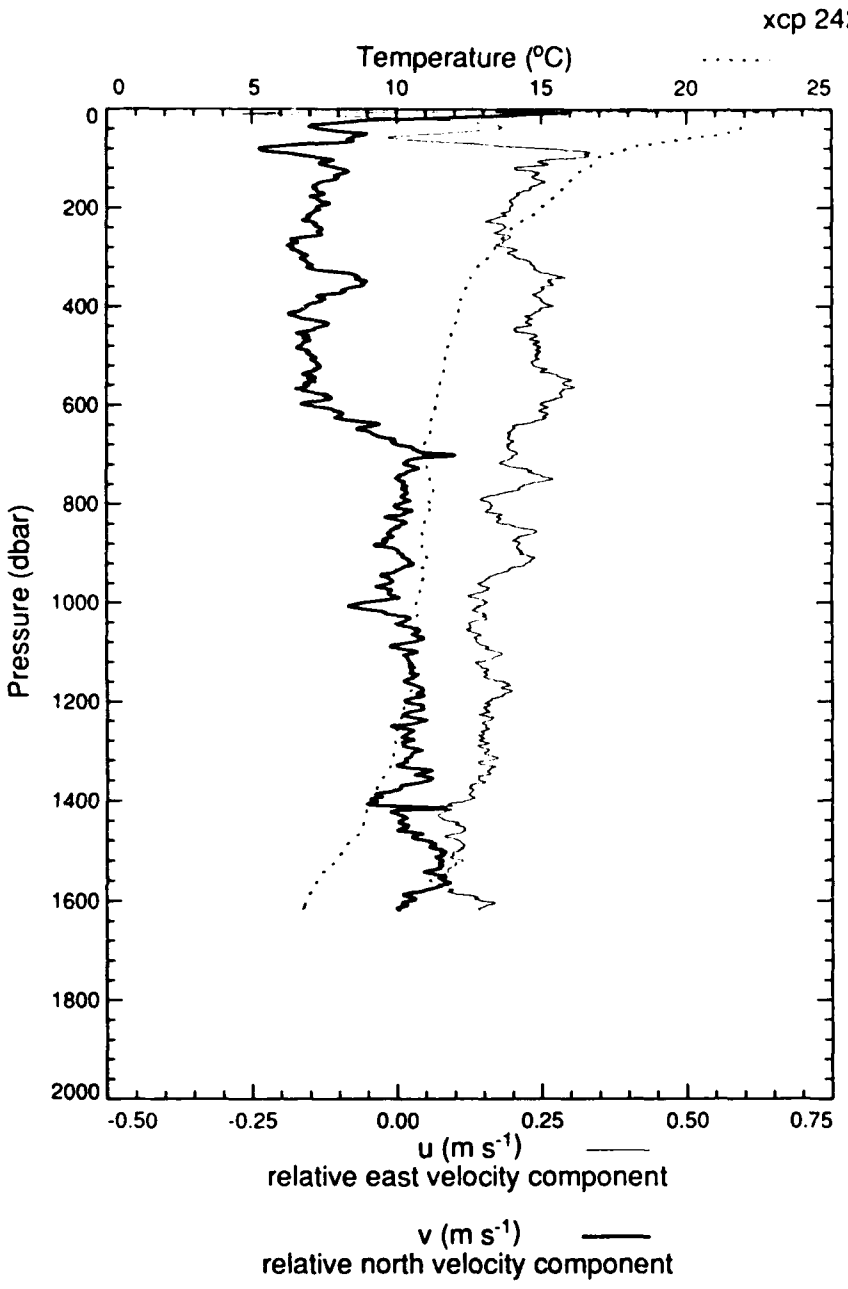
xcp 2425
Temperature (°C)
0
5
10
15
20
25
Pressure (dbar)
0
200
400
600
800
1000
1200
1400
1600
1800
2000
-0.50
-0.25
0.00
0.25
0.50
0.75
u (m s-1)
relative east velocity component
v (m s-1)
relative north velocity component

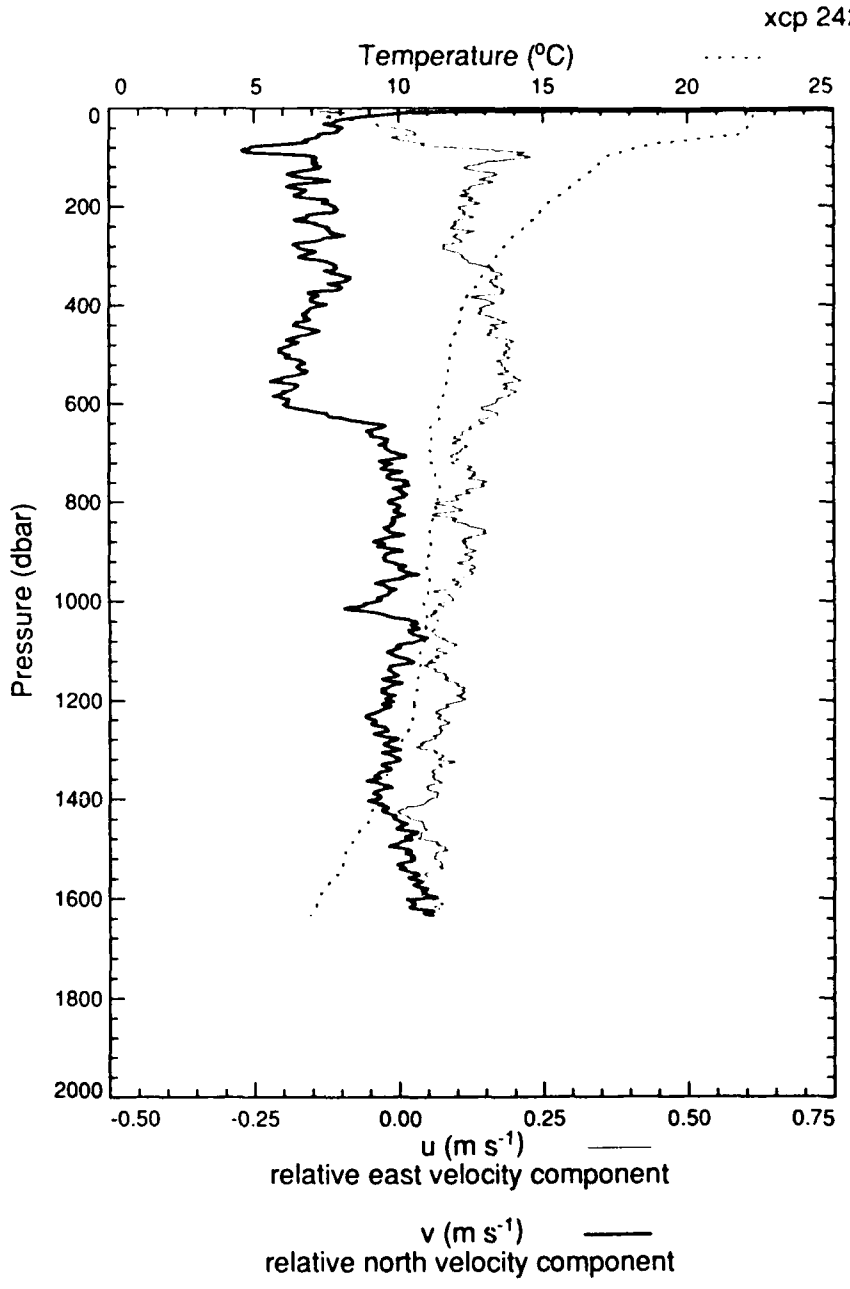
xcp 2426
Temperature (°C)
0
5
10
15
20
25
Pressure (dbar)
0
200
400
600
800
1000
1200
1400
1600
1800
2000
-0.50
-0.25
0.00
0.25
0.50
0.75
u (m s-1)
relative east velocity component
v (m s-1)
relative north velocity component

TR 8925 N13

N14 TR 8925

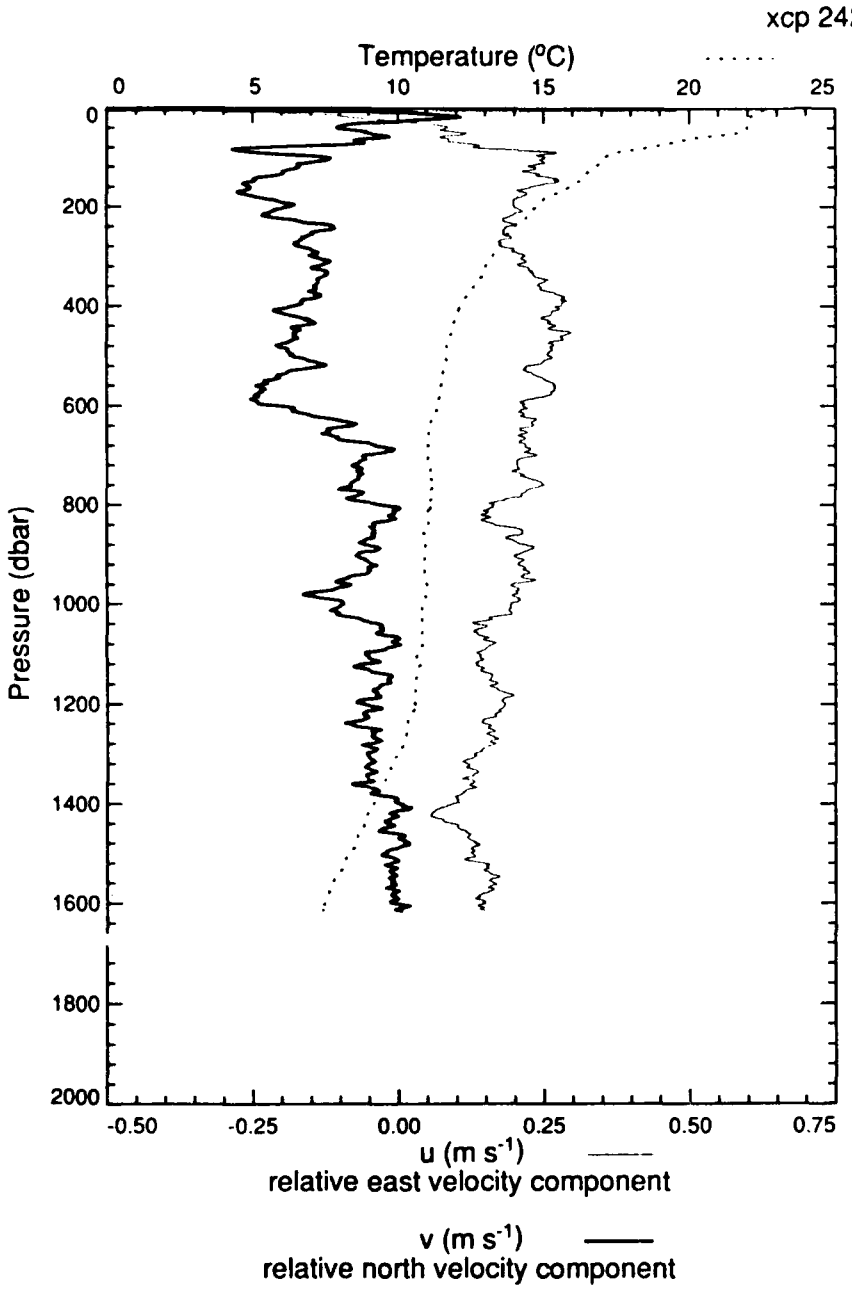
xcp 2427
Temperature (°C)
0
5
10
15
20
25
Pressure (dbar)
0
200
400
600
800
1000
1200
1400
1600
1800
2000
-0.50
-0.25
0.00
0.25
0.50
0.75
u (m s-1)
relative east velocity component
v (m s-1)
relative north velocity component

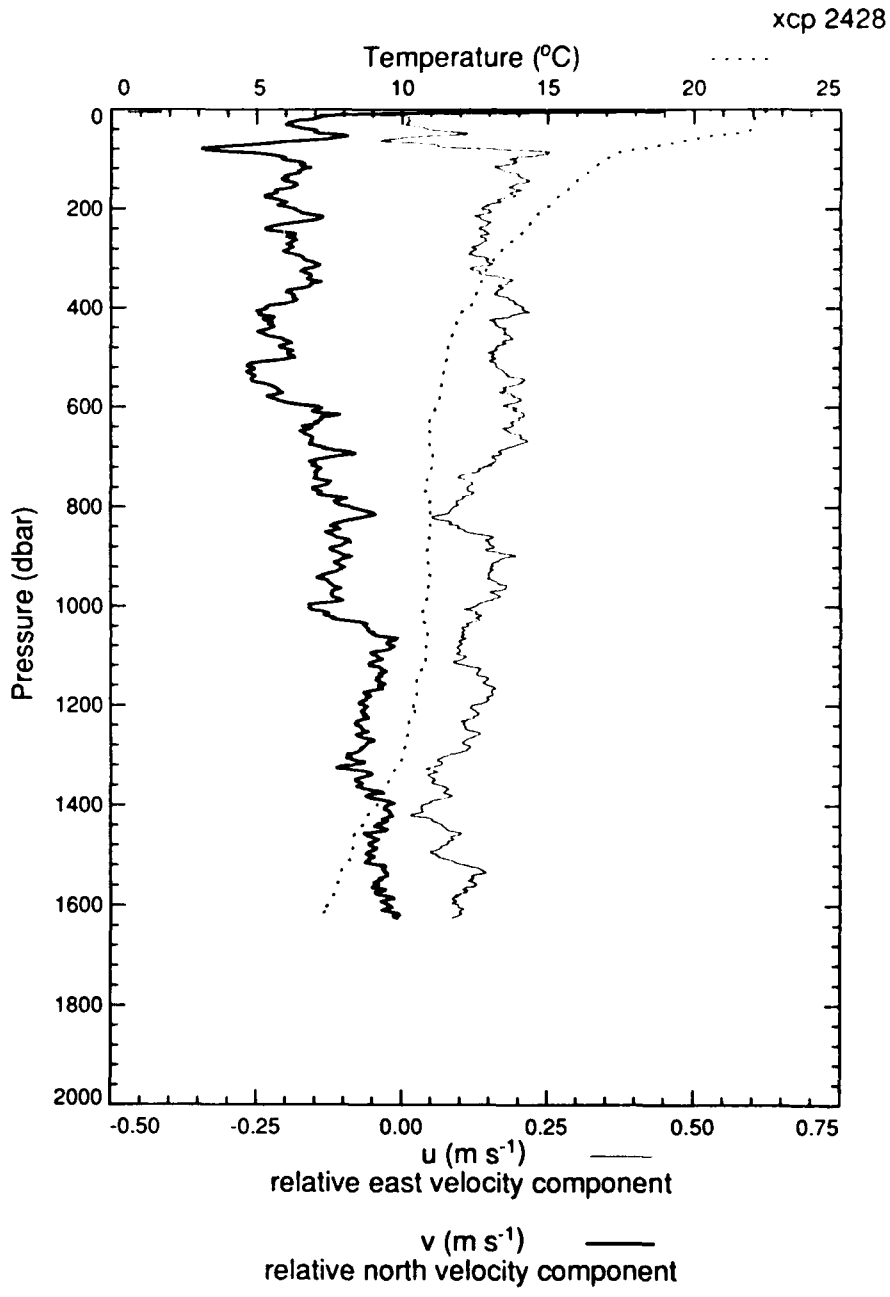
xcp 2428
Temperature (°C)
0
5
10
15
20
25
Pressure (dbar)
0
200
400
600
800
1000
1200
1400
1600
1800
2000
-0.50
-0.25
0.00
0.25
0.50
0.75
u (m s-1)
relative east velocity component
v (m s-1)
relative north velocity component

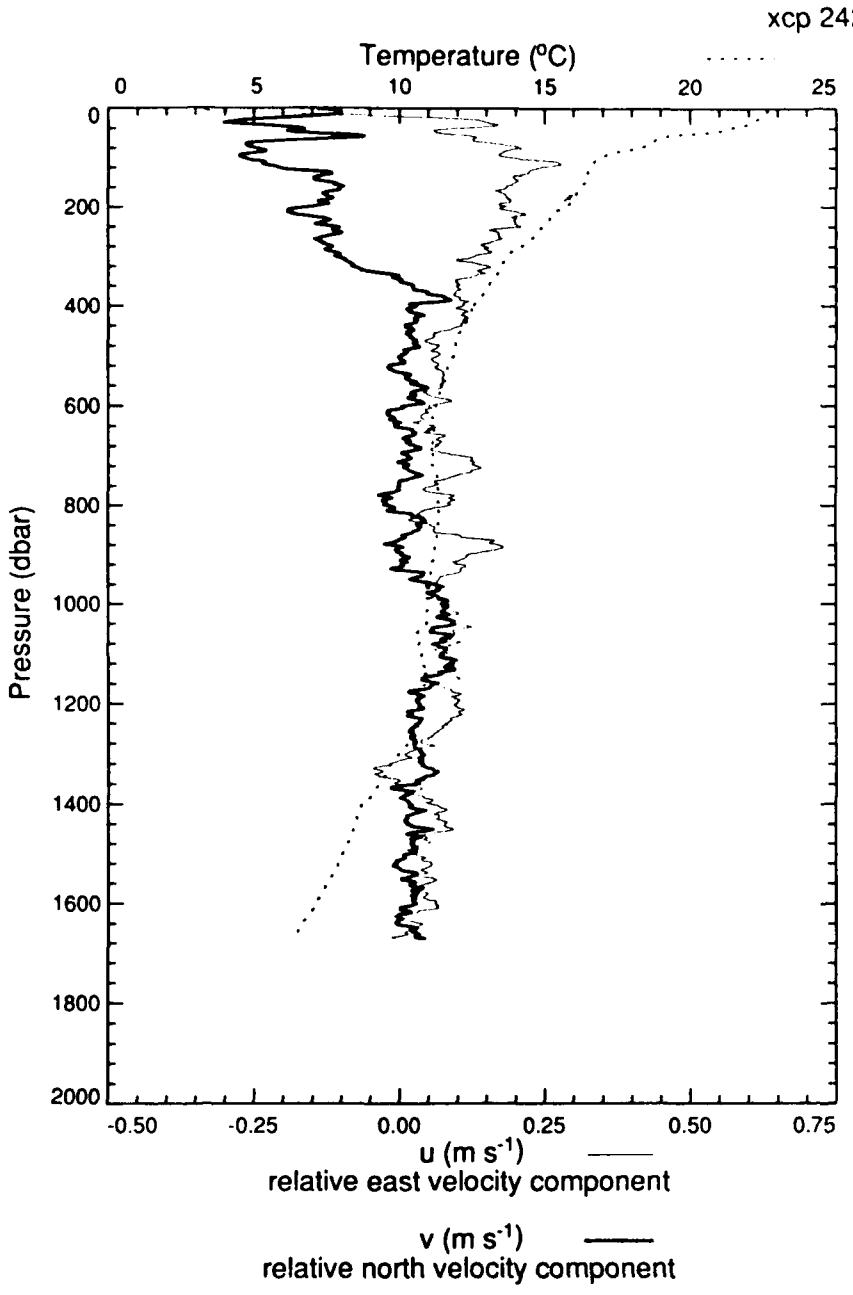
xcp 2429
Temperature (°C)
0
5
10
15
20
25
Pressure (dbar)
0
200
400
600
800
1000
1200
1400
1600
1800
2000
-0.50
-0.25
0.00
0.25
0.50
0.75
u (m s-1)
relative east velocity component
v (m s-1)
relative north velocity component

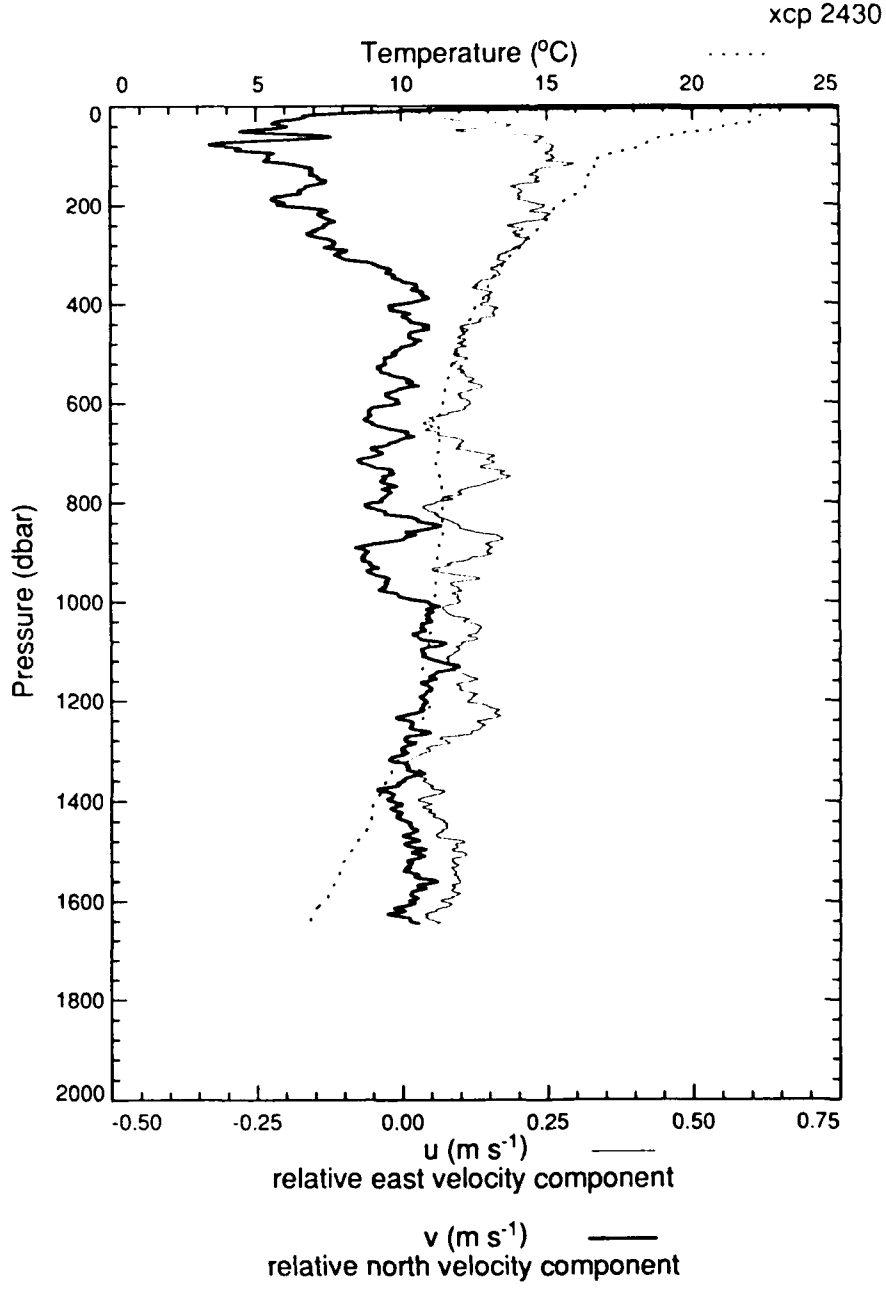
xcp 2430
Temperature (°C)
0
5
10
15
20
25
Pressure (dbar)
0
200
400
600
800
1000
1200
1400
1600
1800
2000
-0.50
-0.25
0.00
0.25
0.50
0.75
u (m s-1)
relative east velocity component
v (m s-1)
relative north velocity component

N16 TR 8925

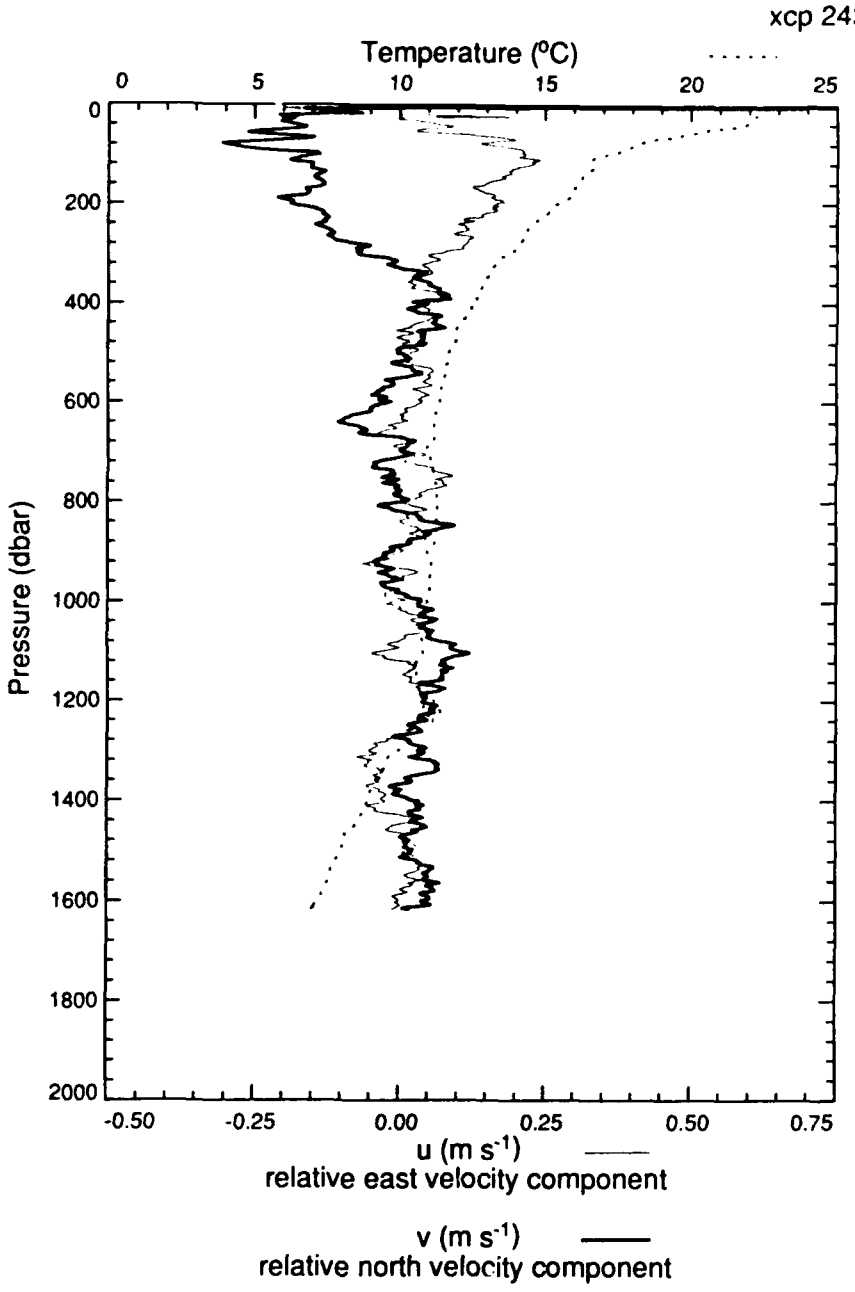
xcp 2432
Temperature (°C)
0
5
10
15
20
25
Pressure (dbar)
0
200
400
600
800
1000
1200
1400
1600
1800
2000
-0.50
-0.25
0.00
0.25
0.50
0.75
u (m s-1)
relative east velocity component
v (m s-1)
relative north velocity component

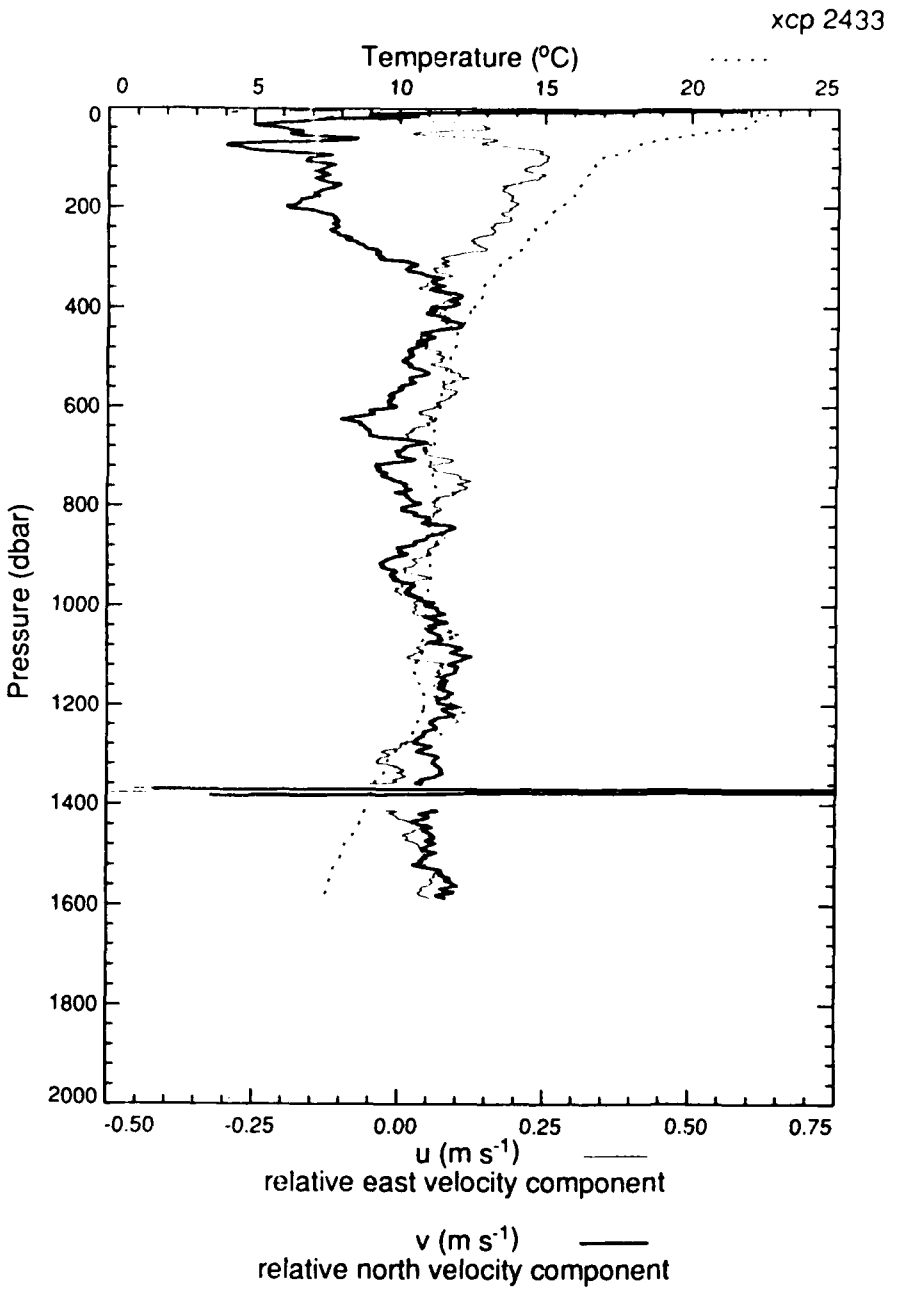
xcp 2433
Temperature (°C)
0
5
10
15
20
25
Pressure (dbar)
0
200
400
600
800
1000
1200
1400
1600
1800
2000
-0.50
-0.25
0.00
0.25
0.50
0.75
u (m s-1)
relative east velocity component
v (m s-1)
relative north velocity component

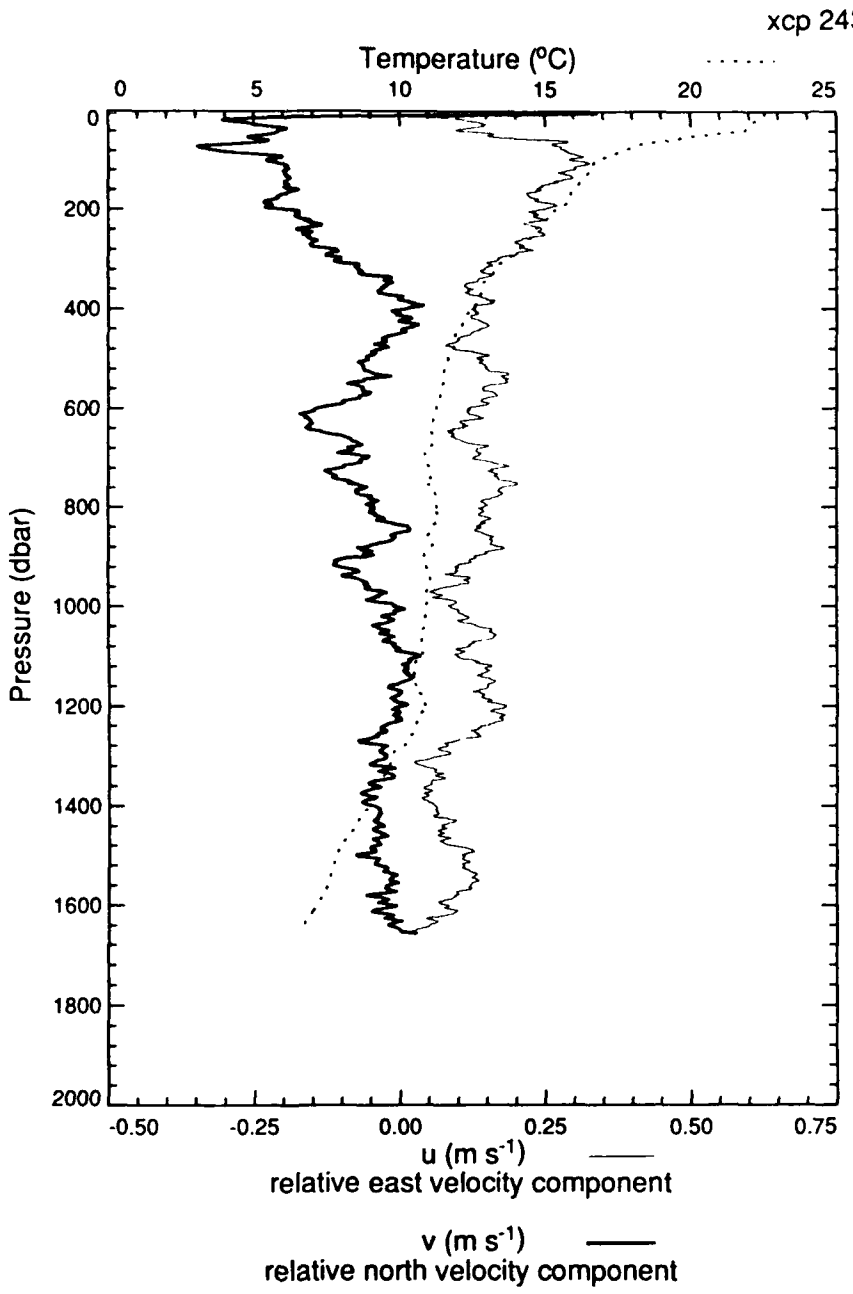
xcp 2434
Temperature (°C)
0
5
10
15
20
25
Pressure (dbar)
0
200
400
600
800
1000
1200
1400
1600
1800
2000
-0.50
-0.25
0.00
0.25
0.50
0.75
u (m s-1)
relative east velocity component
v (m s-1)
relative north velocity component

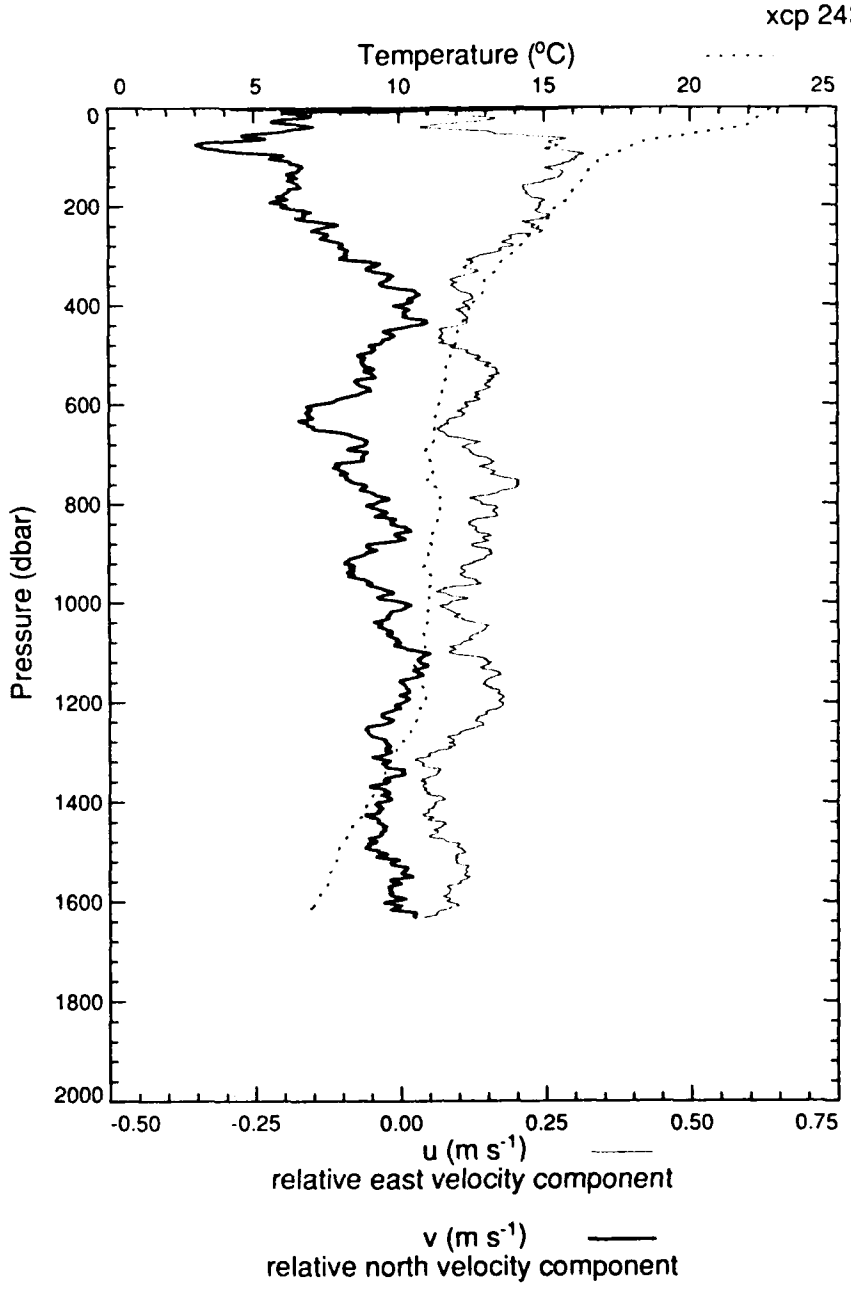
xcp 2435
Temperature (°C)
0
5
10
15
20
25
Pressure (dbar)
0
200
400
600
800
1000
1200
1400
1600
1800
2000
-0.50
-0.25
0.00
0.25
0.50
0.75
u (m s-1)
relative east velocity component
v (m s-1)
relative north velocity component

TR 8925 N17

N18 TR 8925

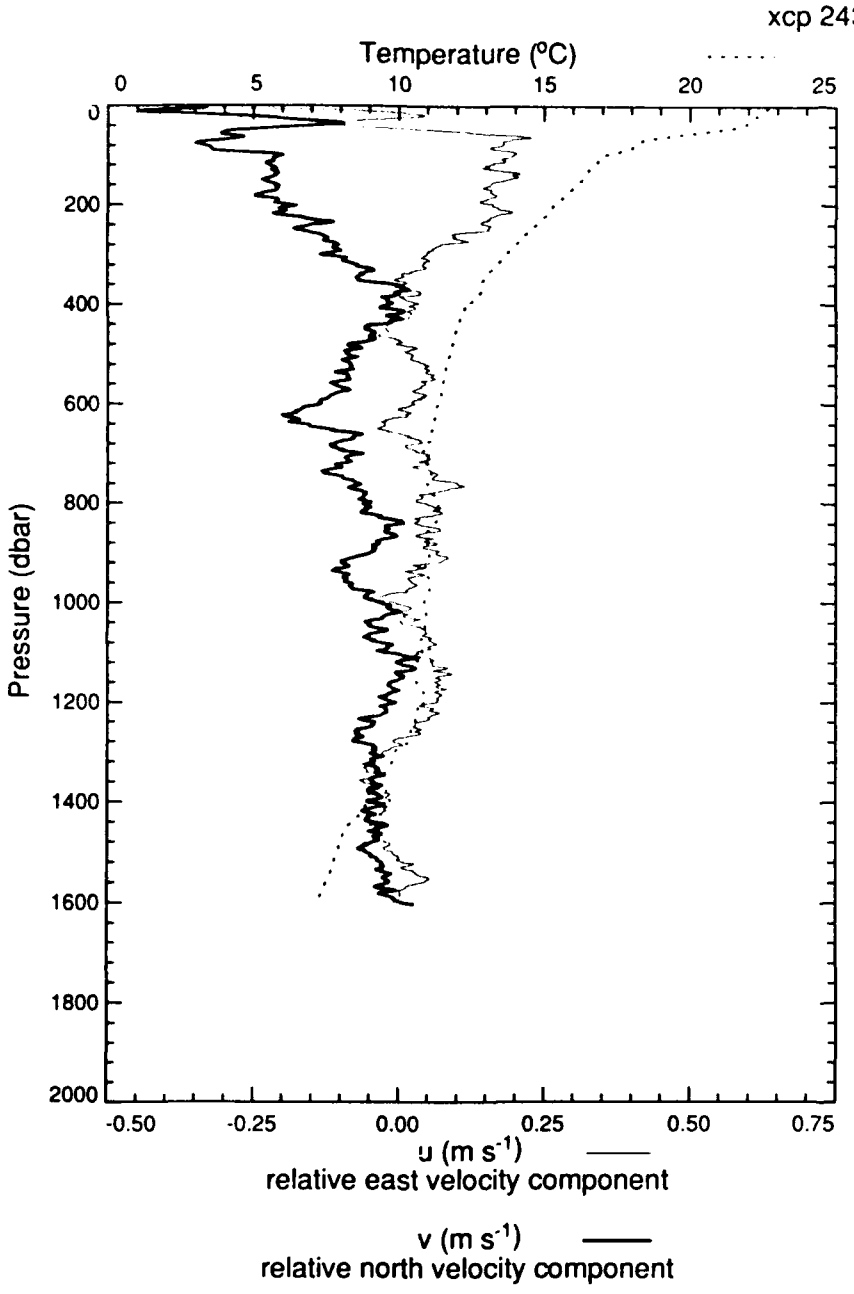
xcp 2436
Temperature (°C)
0
5
10
15
20
25
Pressure (dbar)
0
200
400
600
800
1000
1200
1400
1600
1800
2000
-0.50
-0.25
0.00
0.25
0.50
0.75
u (m s-1)
relative east velocity component
v (m s-1)
relative north velocity component

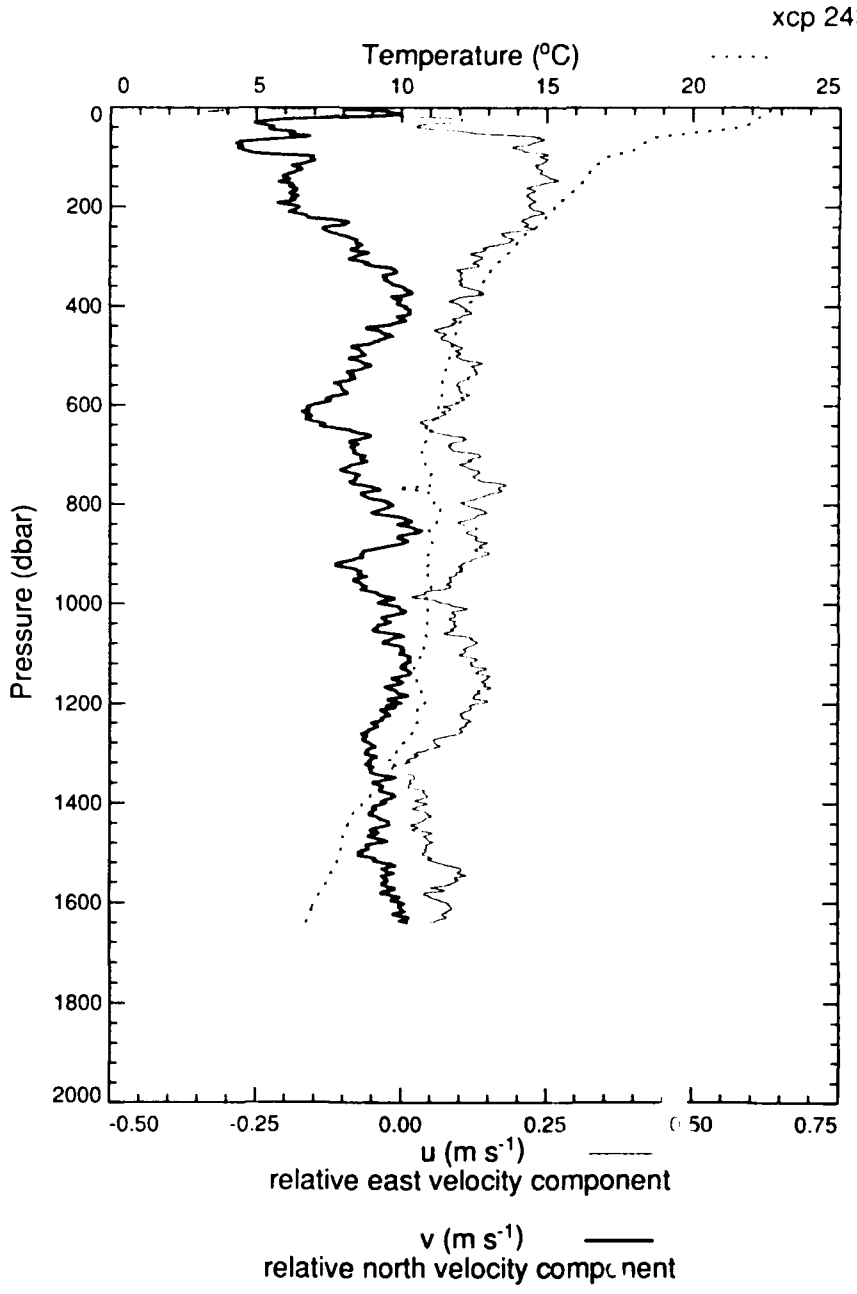
xcp 2437
Temperature (°C)
0
5
10
15
20
25
Pressure (dbar)
0
200
400
600
800
1000
1200
1400
1600
1800
2000
-0.50
-0.25
0.00
0.25
0.75
u (m s-1)
relative east velocity component
v (m s-1)
relative north velocity component

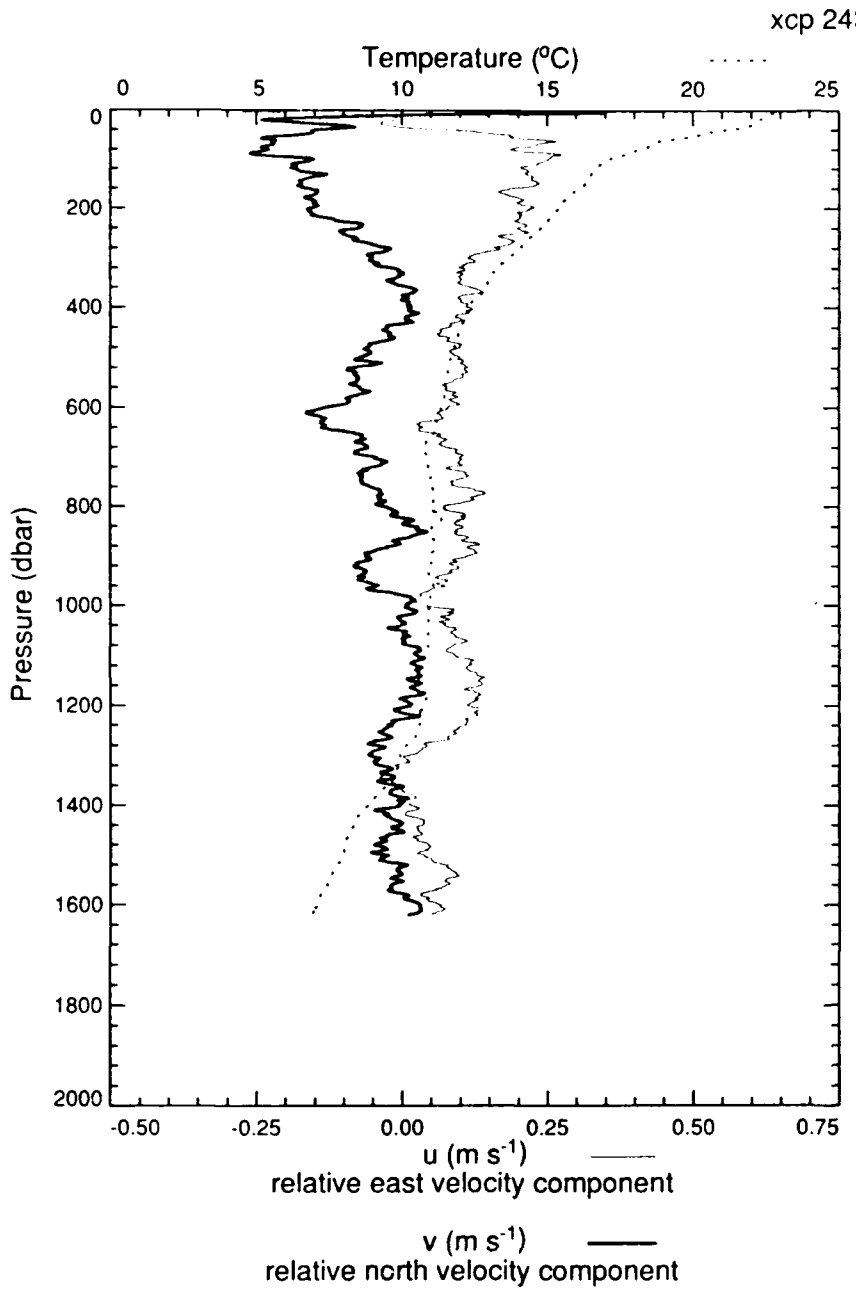
xcp 2438
Temperature (°C)
0
5
10
15
20
25
Pressure (dbar)
0
200
400
600
800
1000
1200
1400
1600
1800
2000
-0.50
-0.25
0.00
0.25
0.50
0.75
u (m s-1)
relative east velocity component
v (m s-1)
relative north velocity component

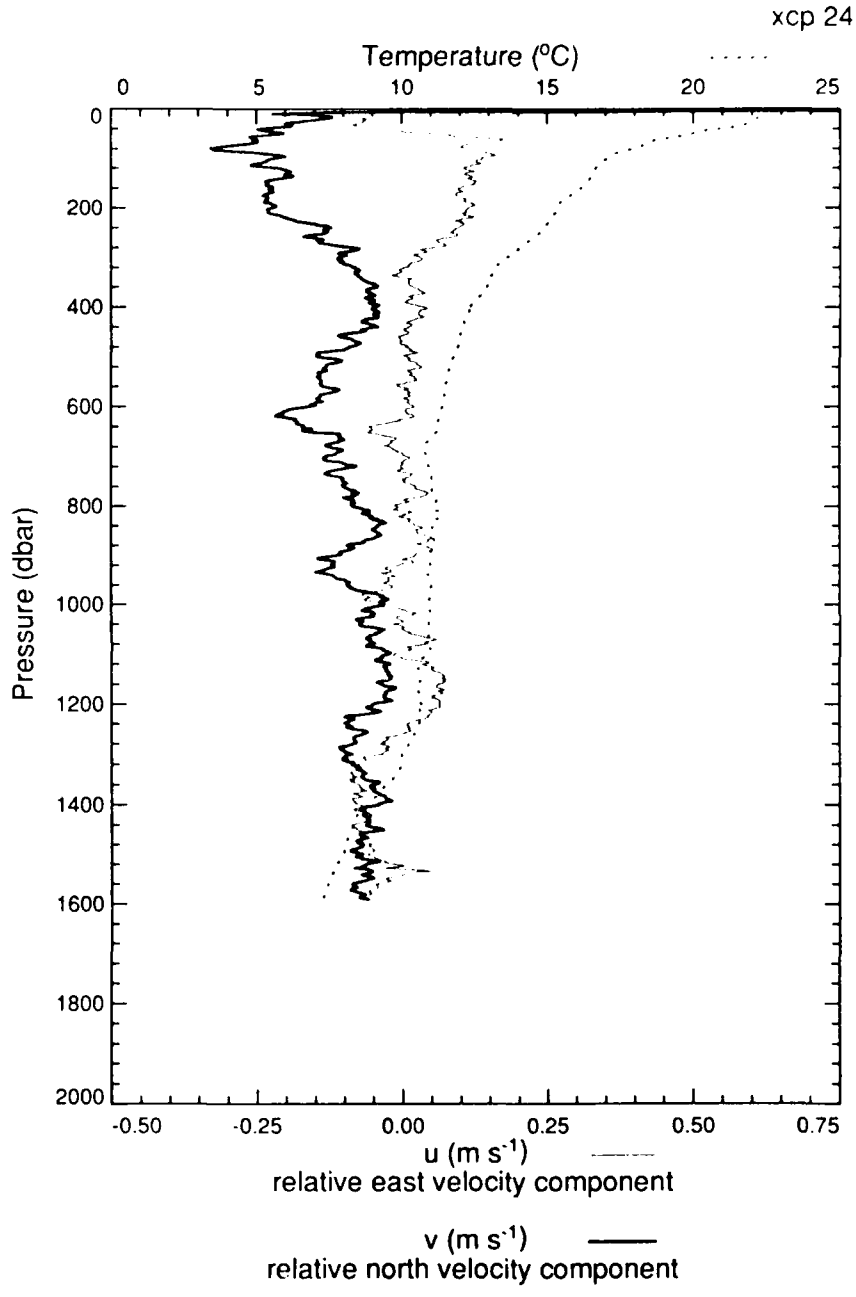
xcp 2439
Temperature (°C)
0
5
10
15
20
25
Pressure (dbar)
0
200
400
600
800
1000
1200
1400
1600
1800
2000
-0.50
-0.25
0.00
0.25
0.50
0.75
u (m s-1)
relative east velocity component
v (m s-1)
relative north velocity component

N20 TR 8925

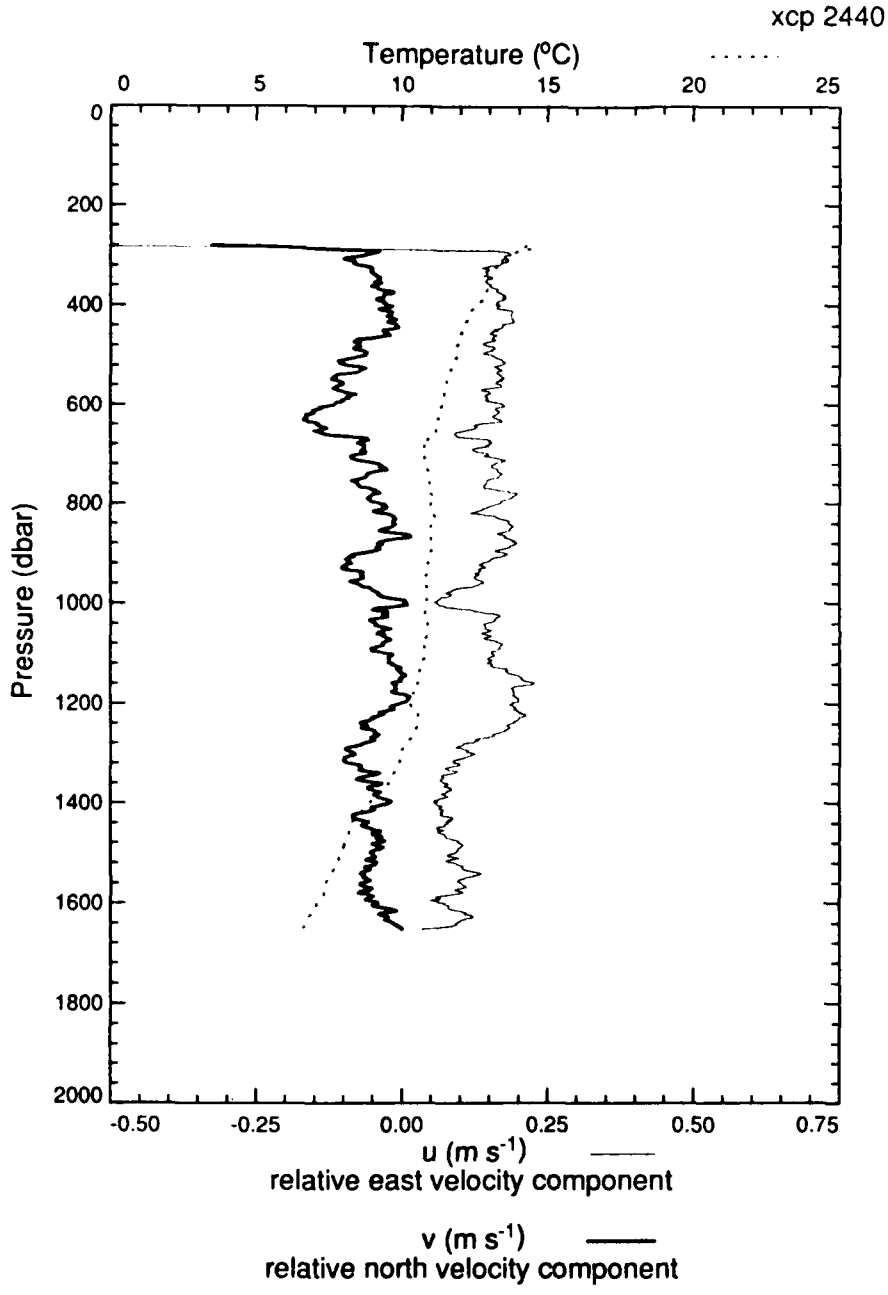
xcp 2440
Temperature (°C)
0
5
10
15
20
25
Pressure (dbar)
0
200
400
600
800
1000
1200
1400
1600
1800
2000
-0.50
-0.25
0.00
0.25
0.50
0.75
u (m s-1)
relative east velocity component
v (m s-1)
relative north velocity component

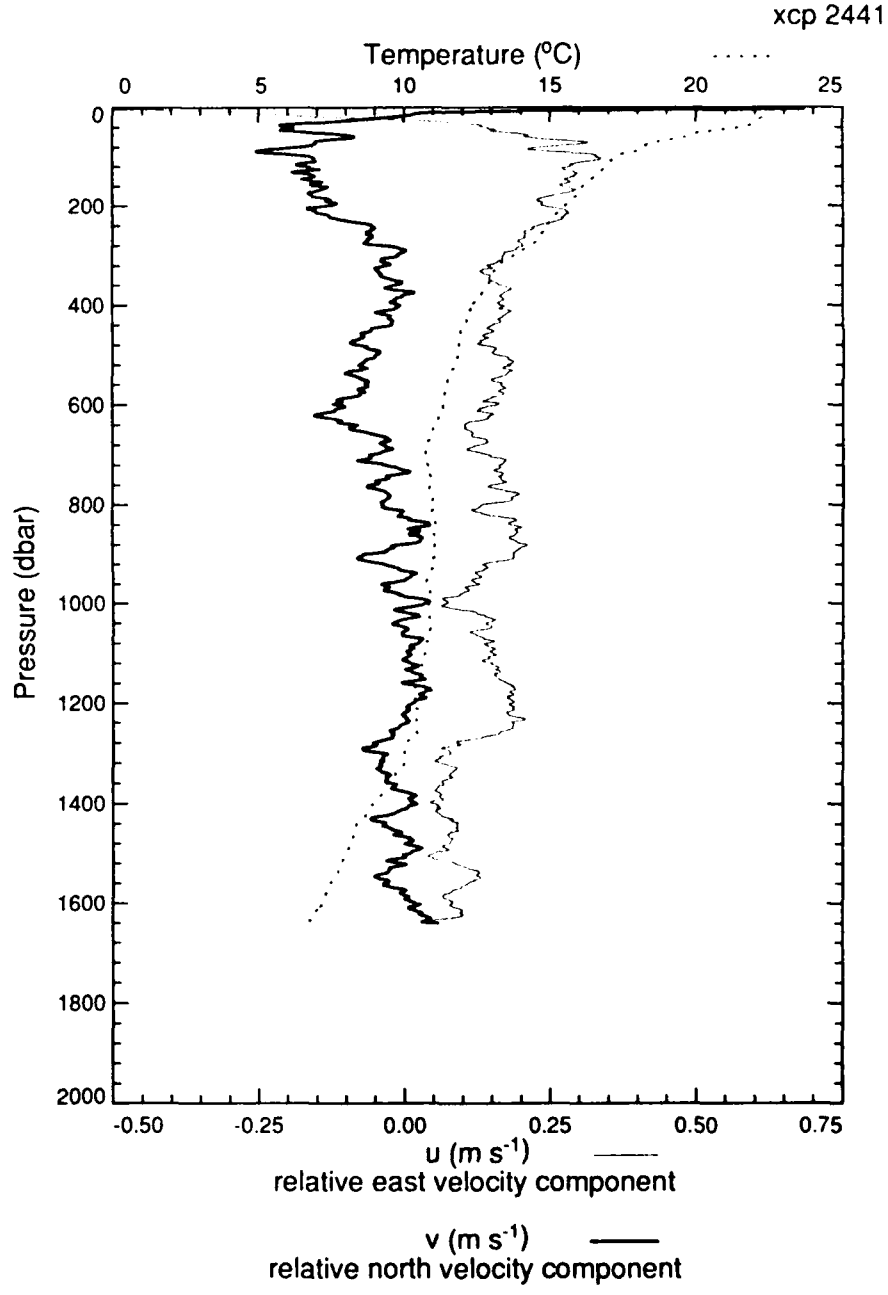
xcp 2441
Temperature (°C)
0
5
10
15
20
25
Pressure (dbar)
0
200
400
600
800
1000
1200
1400
1600
1800
2000
-0.50
-0.25
0.00
0.25
0.50
0.75
u (m s-1)
relative east velocity component
v (m s-1)
relative north velocity component

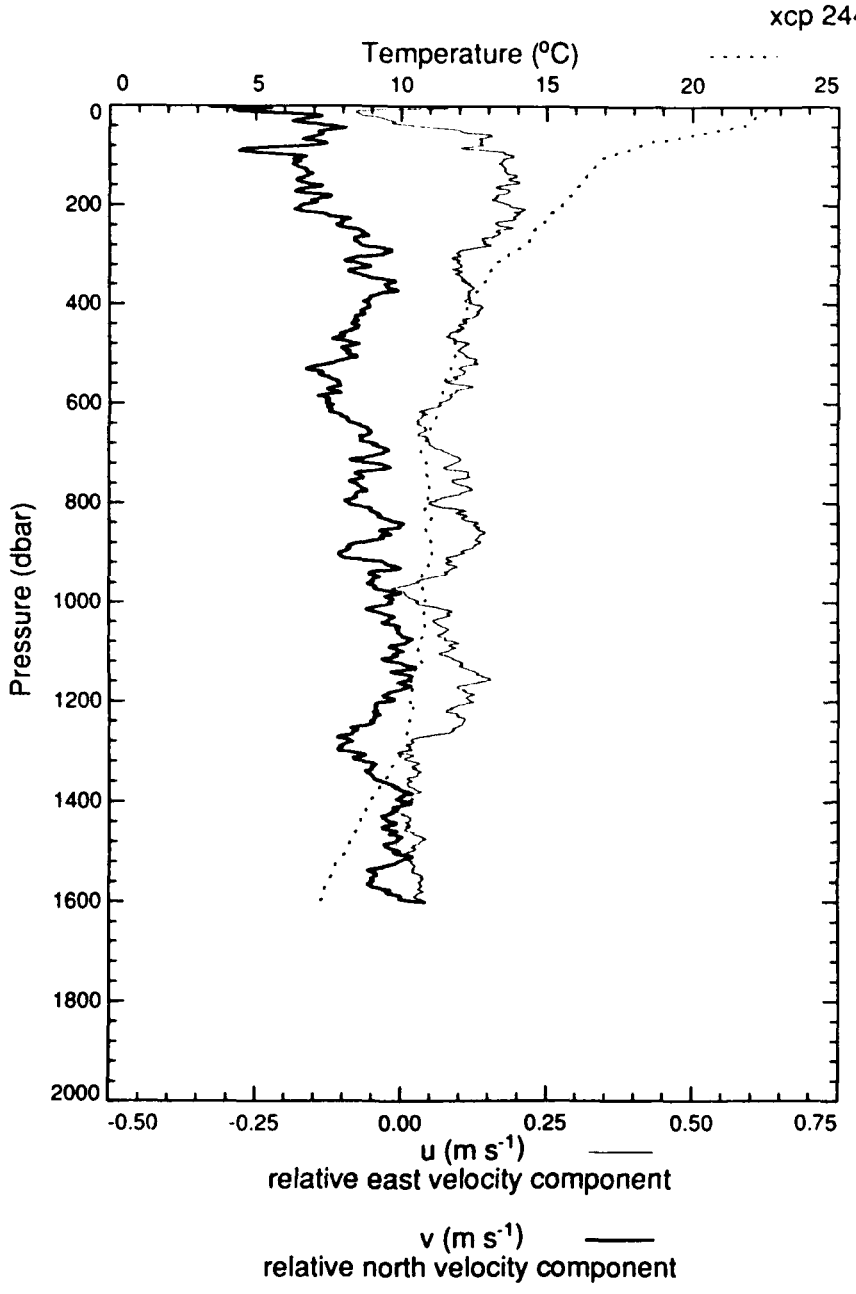
xcp 2442
Temperature (°C)
0
5
10
15
20
25
Pressure (dbar)
0
200
400
600
800
1000
1200
1400
1600
1800
2000
-0.50
-0.25
0.00
0.25
0.50
0.75
u (m s-1)
relative east velocity component
v (m s-1)
relative north velocity component

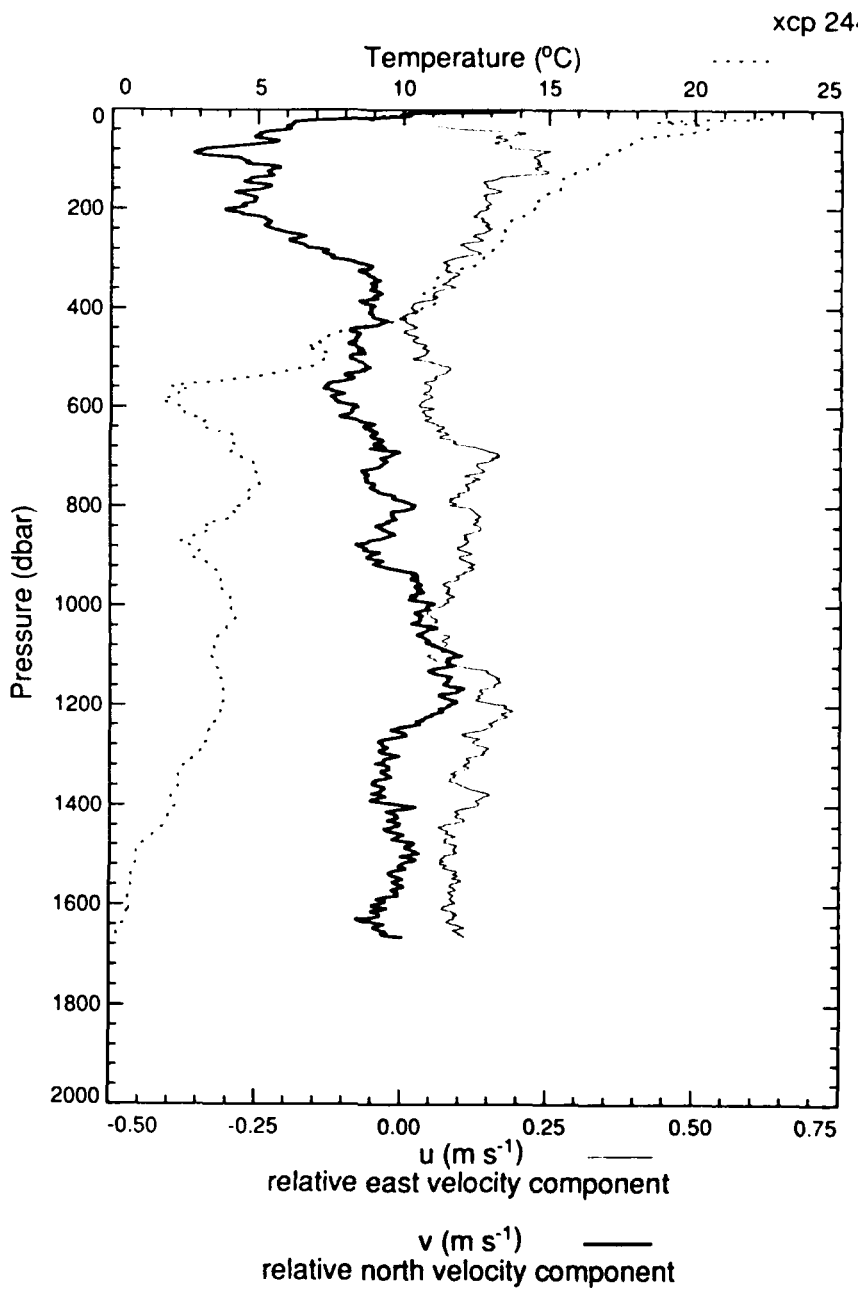
xcp 2443
Temperature (°C)
0
5
10
15
20
25
Pressure (dbar)
0
200
400
600
800
1000
1200
1400
1600
1800
2000
-0.50
-0.25
0.00
0.25
0.50
0.75
u (m s-1)
relative east velocity component
v (m s-1)
relative north velocity component

TR 8925 N21

N22 TR 8925

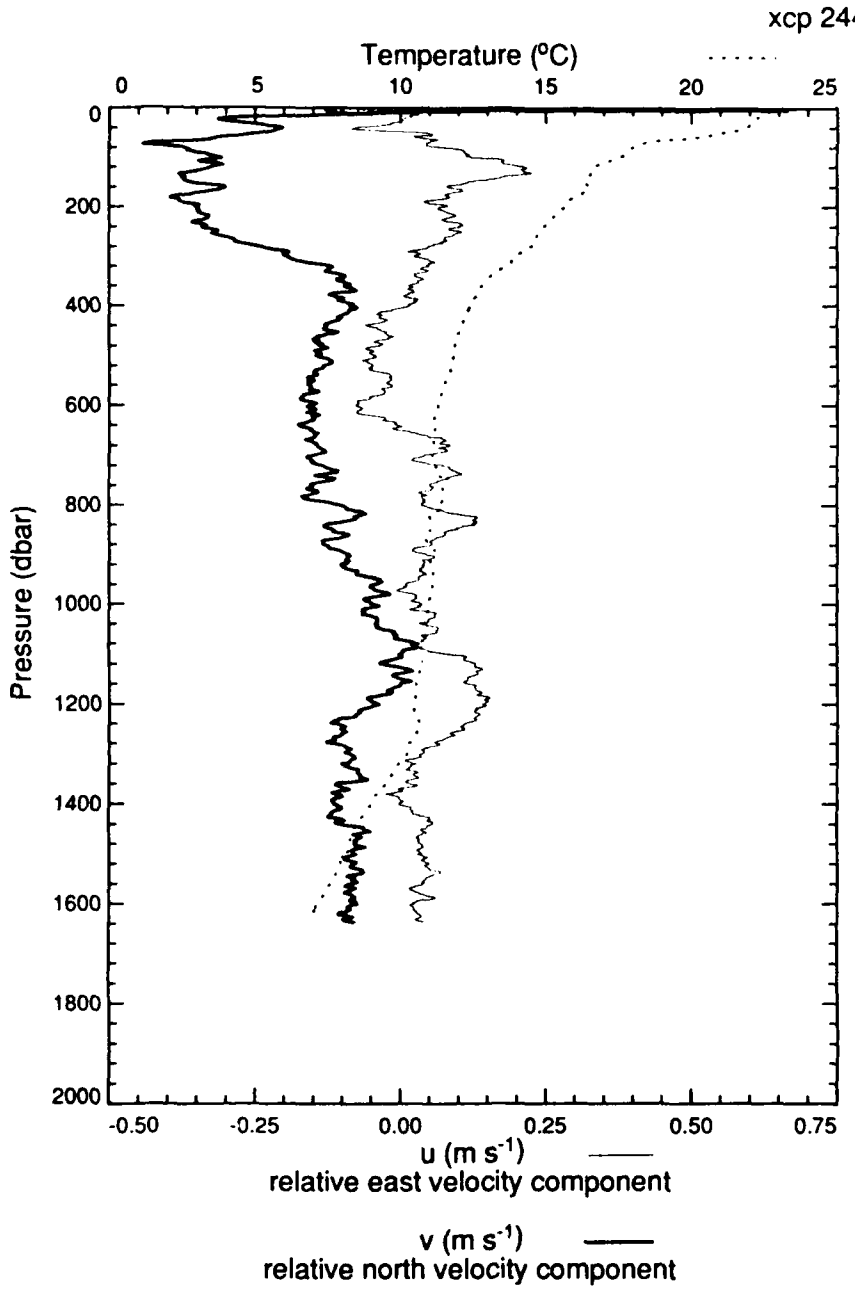
xcp 2444
Temperature (°C)
0
5
10
15
20
25
Pressure (dbar)
0
200
400
600
800
1000
1200
1400
1600
1800
2000
-0.50
-0.25
0.00
0.25
0.50
0.75
u (m s-1)
relative east velocity component
v (m s-1)
relative north velocity component

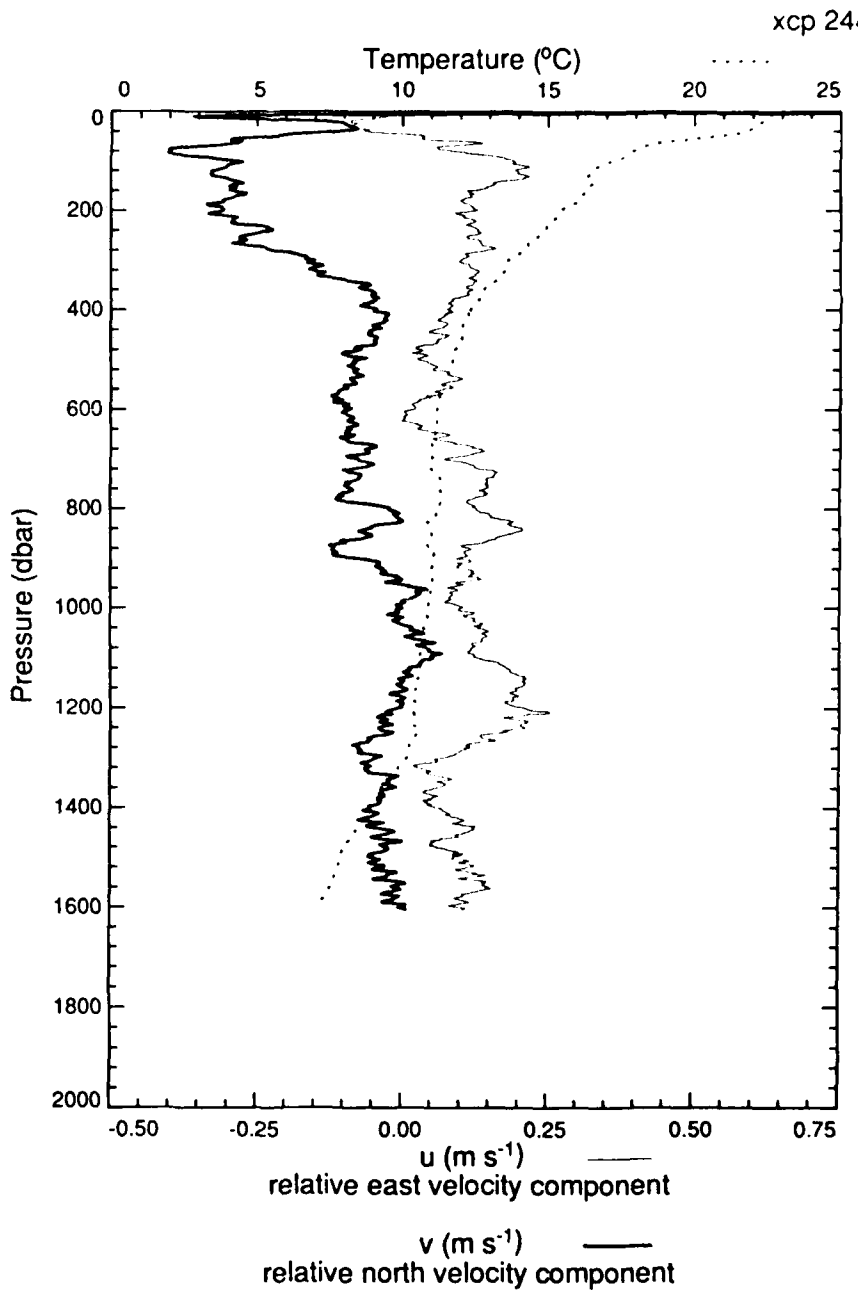
xcp 2445
Temperature (°C)
0
5
10
15
20
25
Pressure (dbar)
0
200
400
600
800
1000
1200
1400
1600
1800
2000
-0.50
-0.25
0.00
0.25
0.50
0.75
u (m s-1)
relative east velocity component
v (m s-1)
relative north velocity component

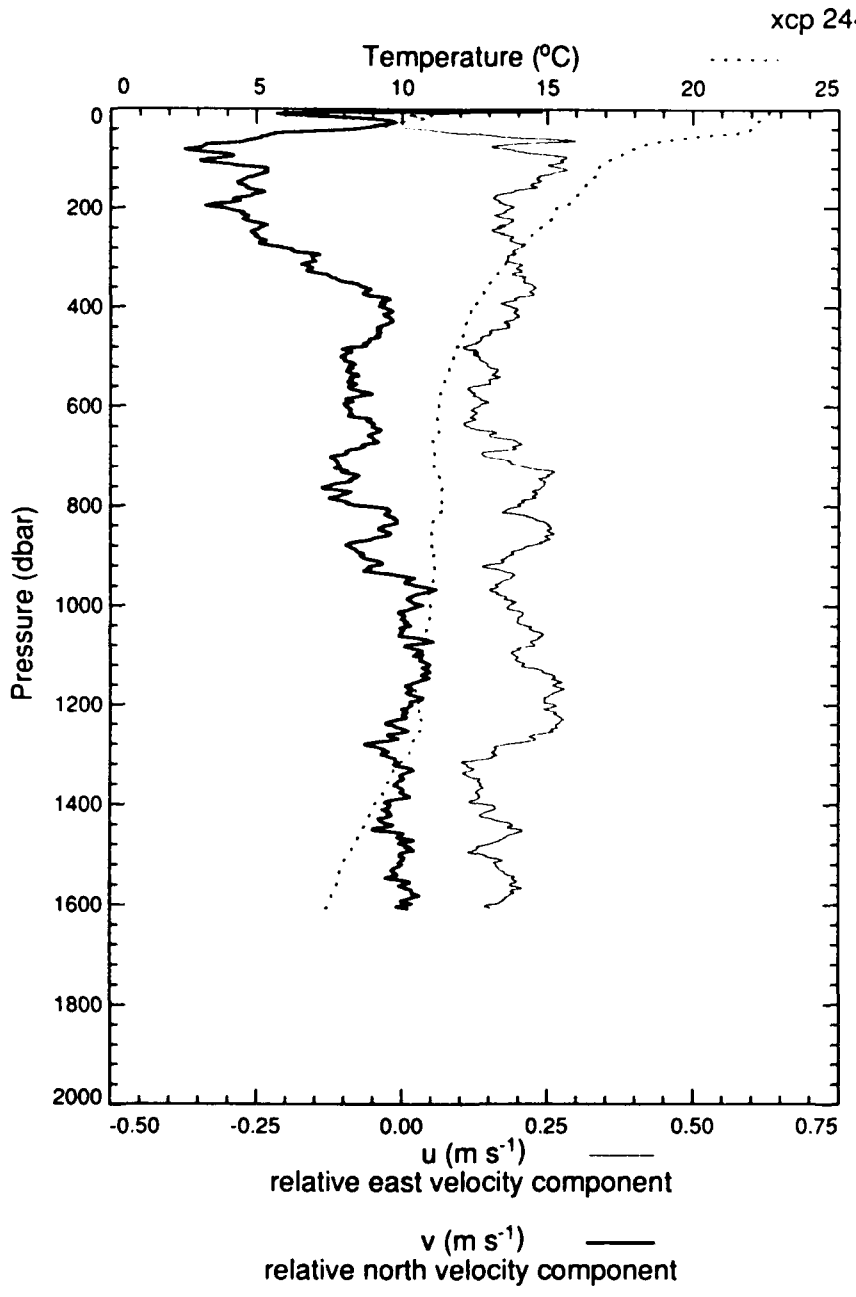
xcp 2447
Temperature (°C)
0
5
10
15
20
25
Pressure (dbar)
0
200
400
600
800
1000
1200
1400
1600
1800
2000
-0.50
-0.25
0.00
0.25
0.50
0.75
u (m s-1)
relative east velocity component
v (m s-1)
relative north velocity component

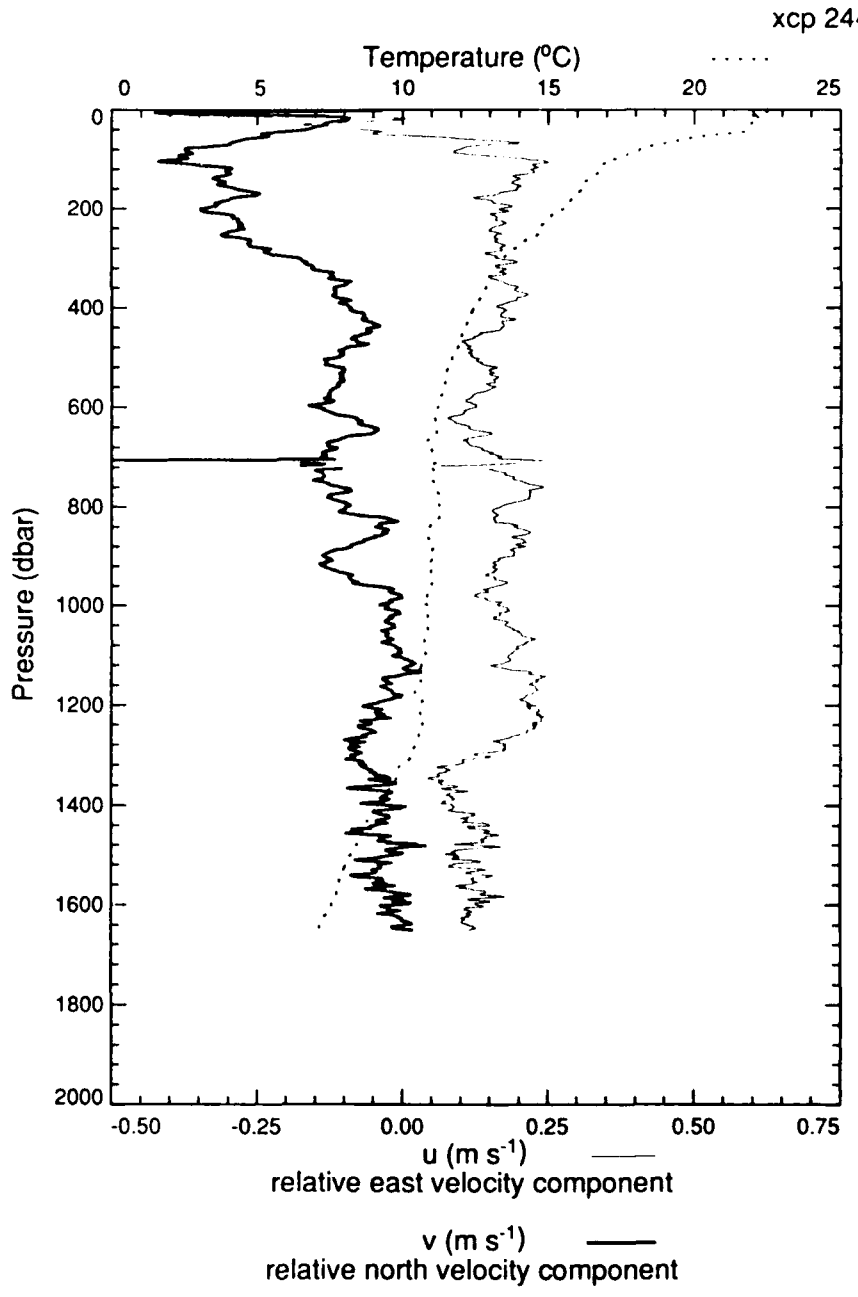
xcp 2448
Temperature (°C)
0
5
10
15
20
25
Pressure (dbar)
0
200
400
600
800
1000
1200
1400
1600
1800
2000
-0.50
-0.25
0.00
0.25
0.50
0.75
u (m s-1)
relative east velocity component
v (m s-1)
relative north velocity component

N24 TR 8925

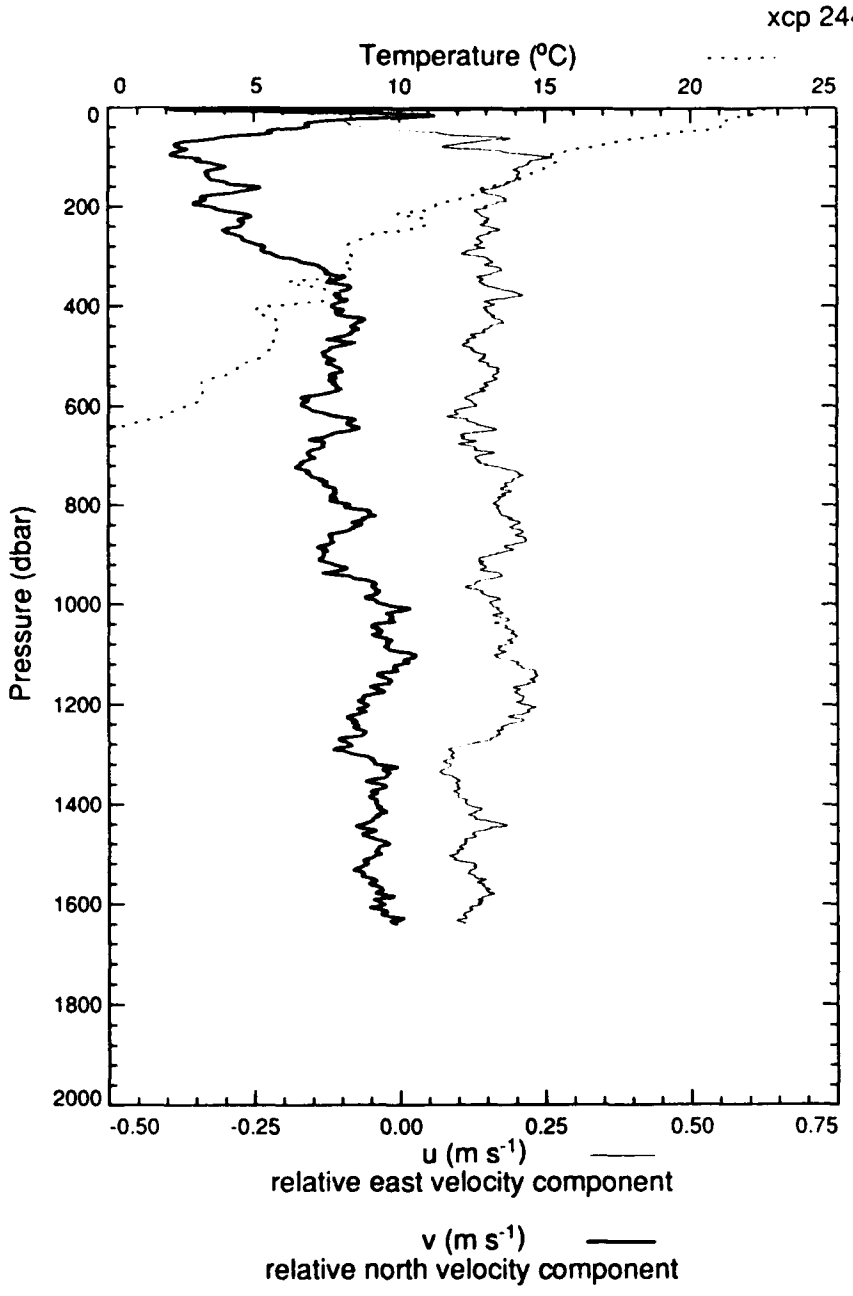
xcp 2449
Temperature (°C)
0
5
10
15
20
25
Pressure (dbar)
0
200
400
600
800
1000
1200
1400
1600
1800
2000
-0.50
-0.25
0.00
0.25
0.50
0.75
u (m s-1)
relative east velocity component
v (m s-1)
relative north velocity component

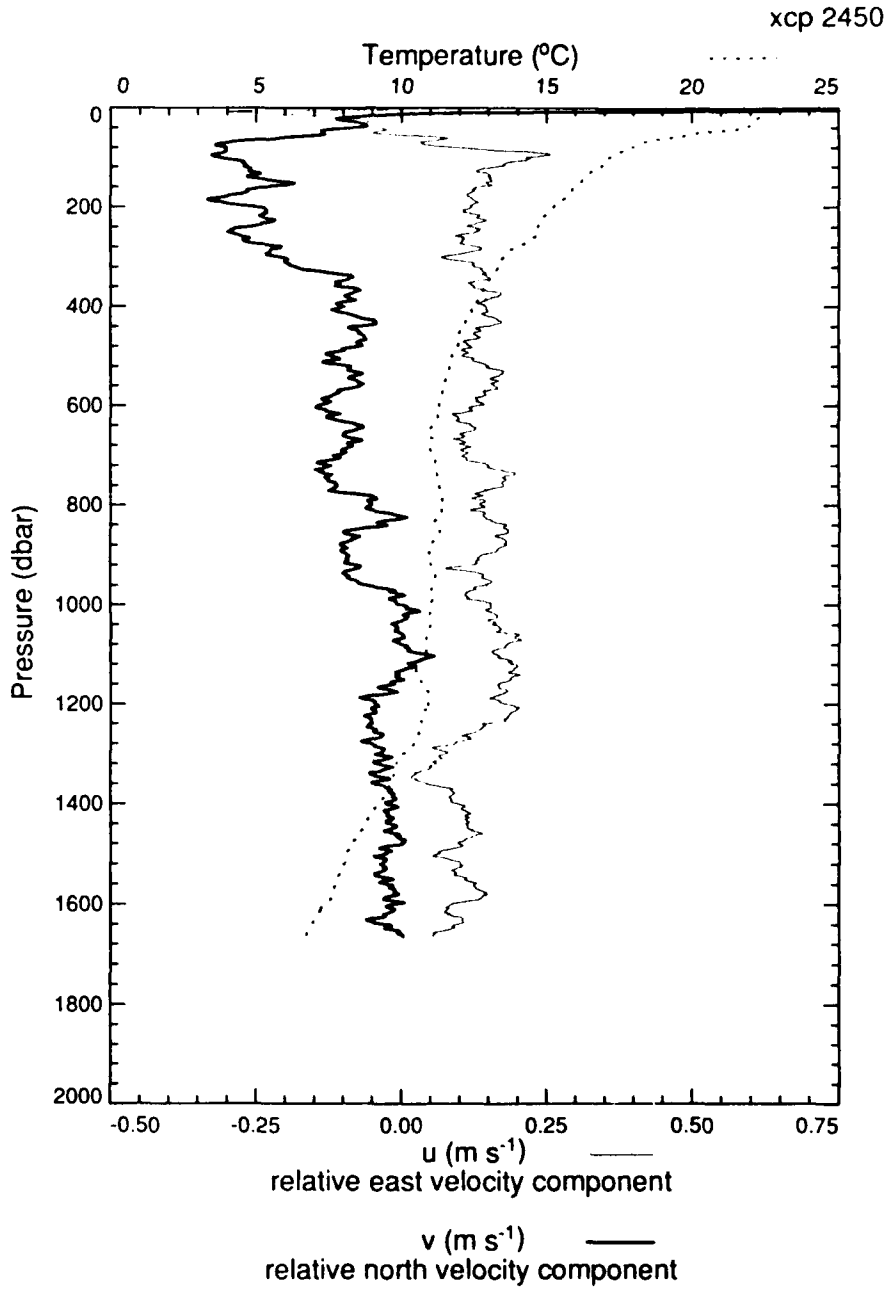
xcp 2450
Temperature (°C)
0
5
10
15
20
25
Pressure (dbar)
0
200
400
600
800
1000
1200
1400
1600
1800
2000
-0.50
-0.25
0.00
0.25
0.50
0.75
u (m s-1)
relative east velocity component
v (m s-1)
relative north velocity component

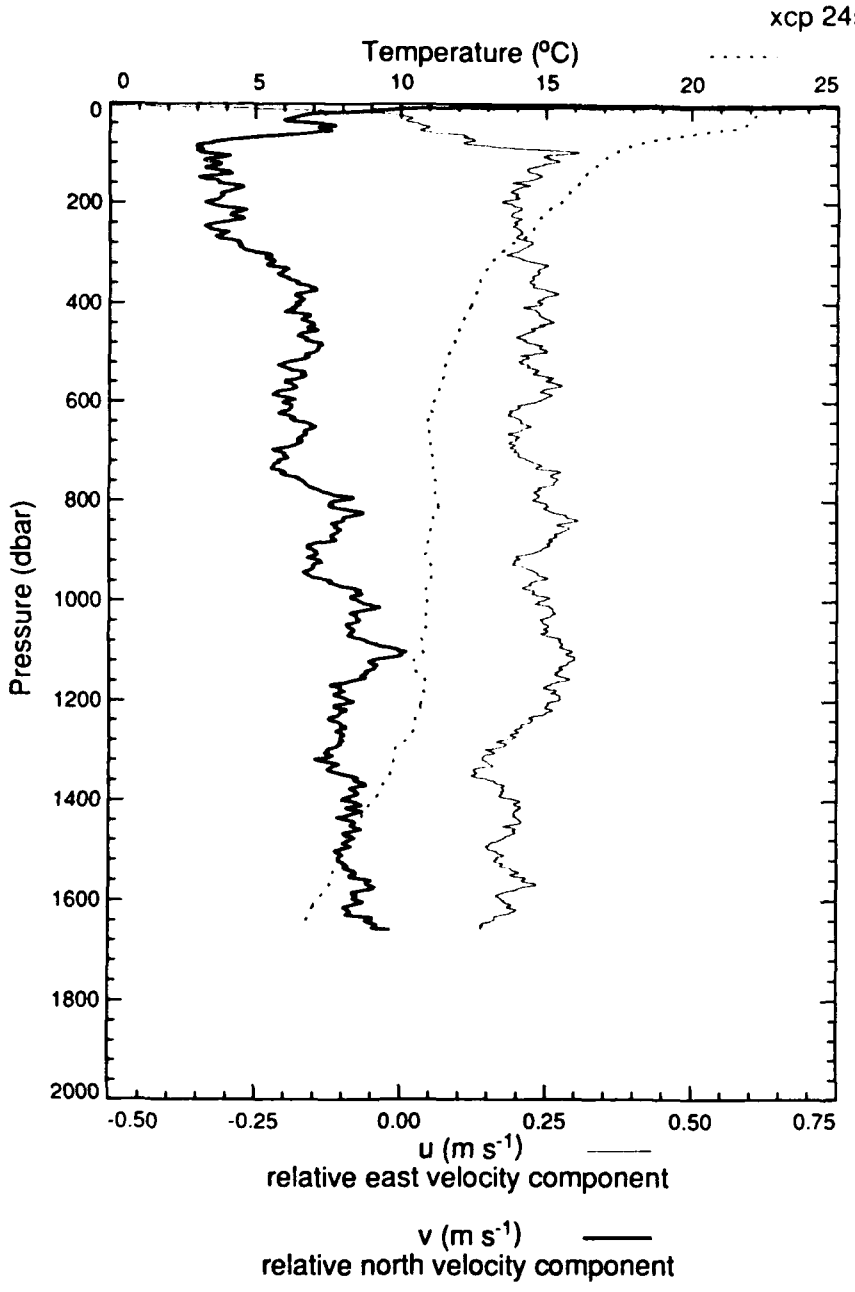
xcp 2451
Temperature (°C)
0
5
10
15
20
25
Pressure (dbar)
0
200
400
600
800
1000
1200
1400
1600
1800
2000
-0.50
-0.25
0.00
0.25
0.50
0.75
u (m s-1)
relative east velocity component
v (m s-1)
relative north velocity component

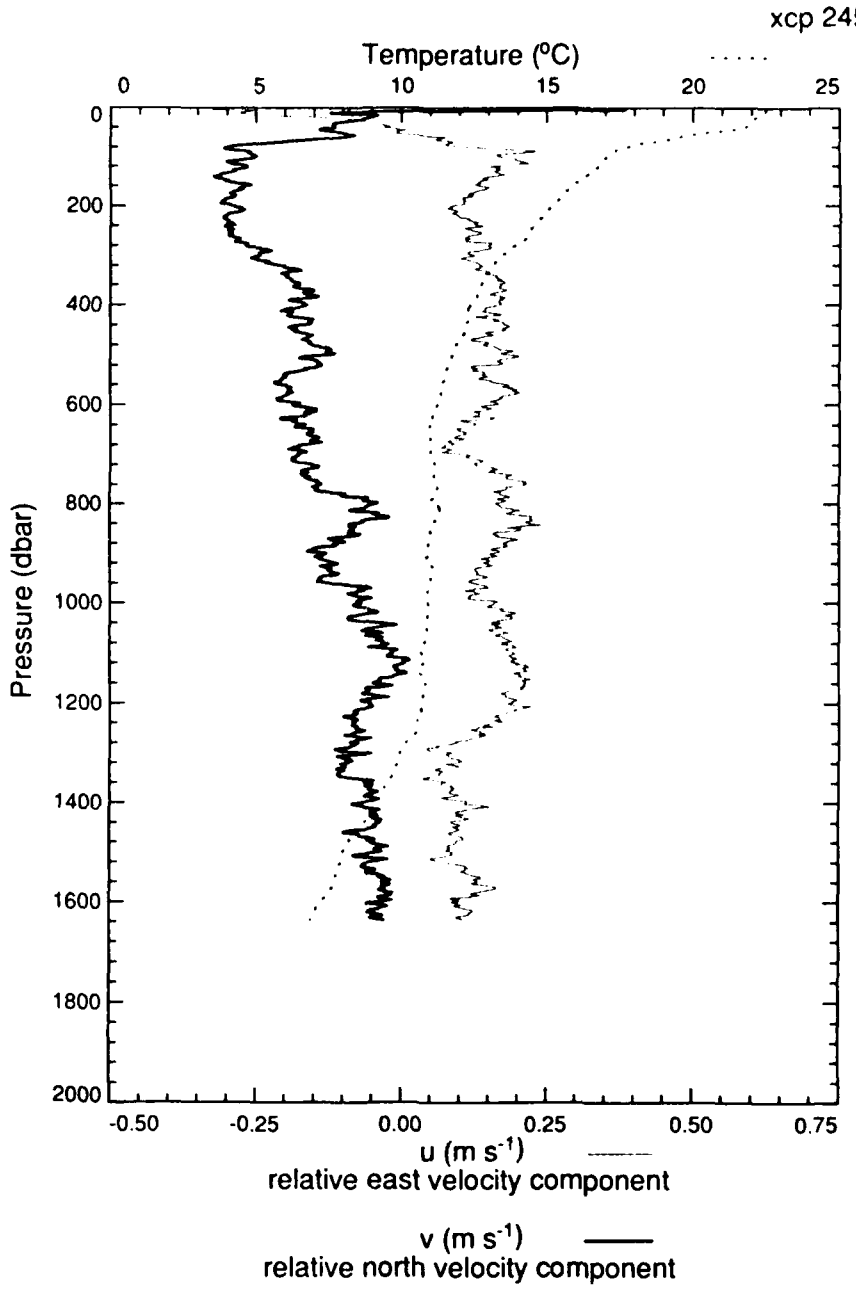
xcp 2452
Temperature (°C)
0
5
10
15
20
25
Pressure (dbar)
0
200
400
600
800
1000
1200
1400
1600
1800
2000
-0.50
-0.25
0.00
0.25
0.50
0.75
u (m s-1)
relative east velocity component
v (m s-1)
relative north velocity component

TR 8925 N25

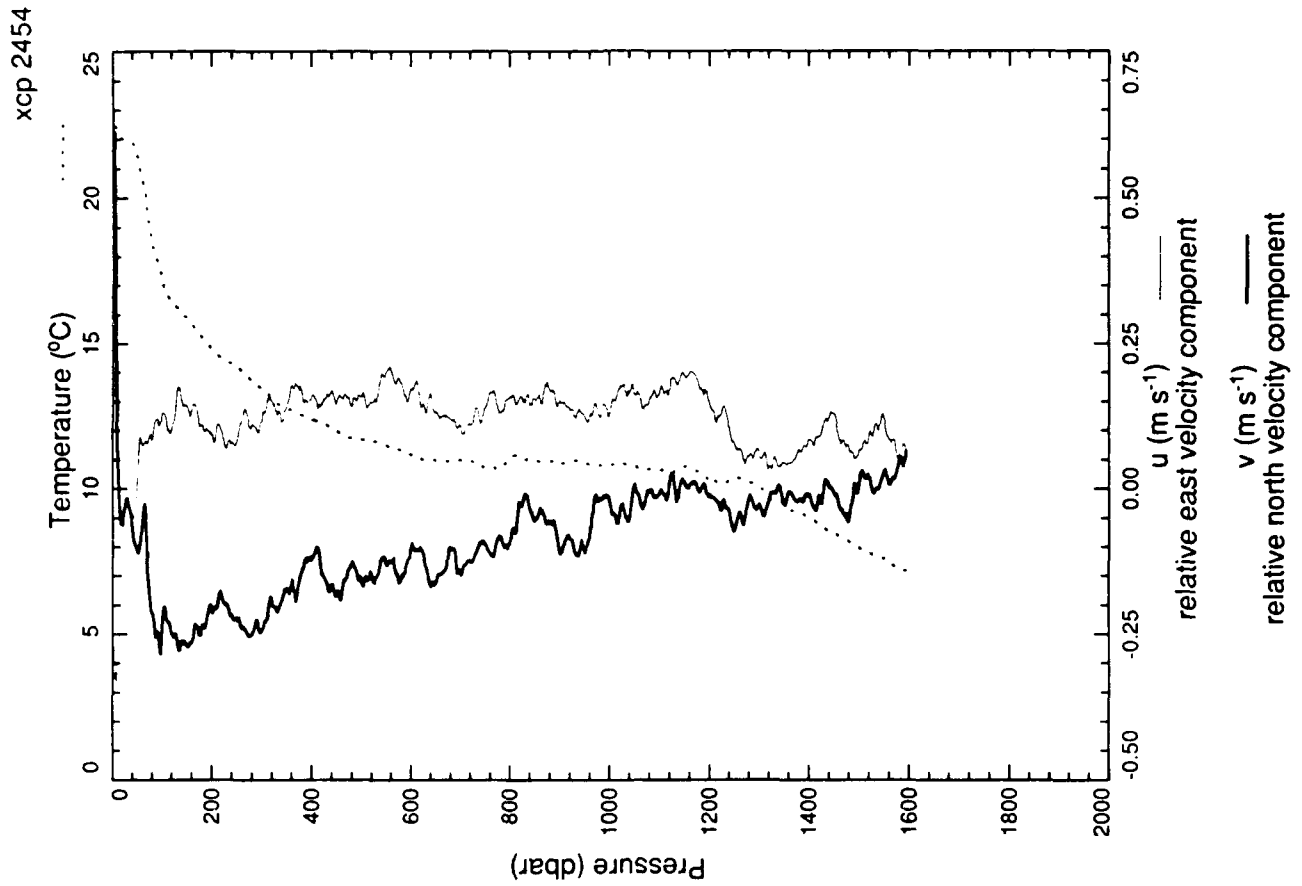
xcp 2454
Temperature (°C)
Pressure (dbar)
u (m s-1)
relative east velocity component
v (m s-1)
relative north velocity component

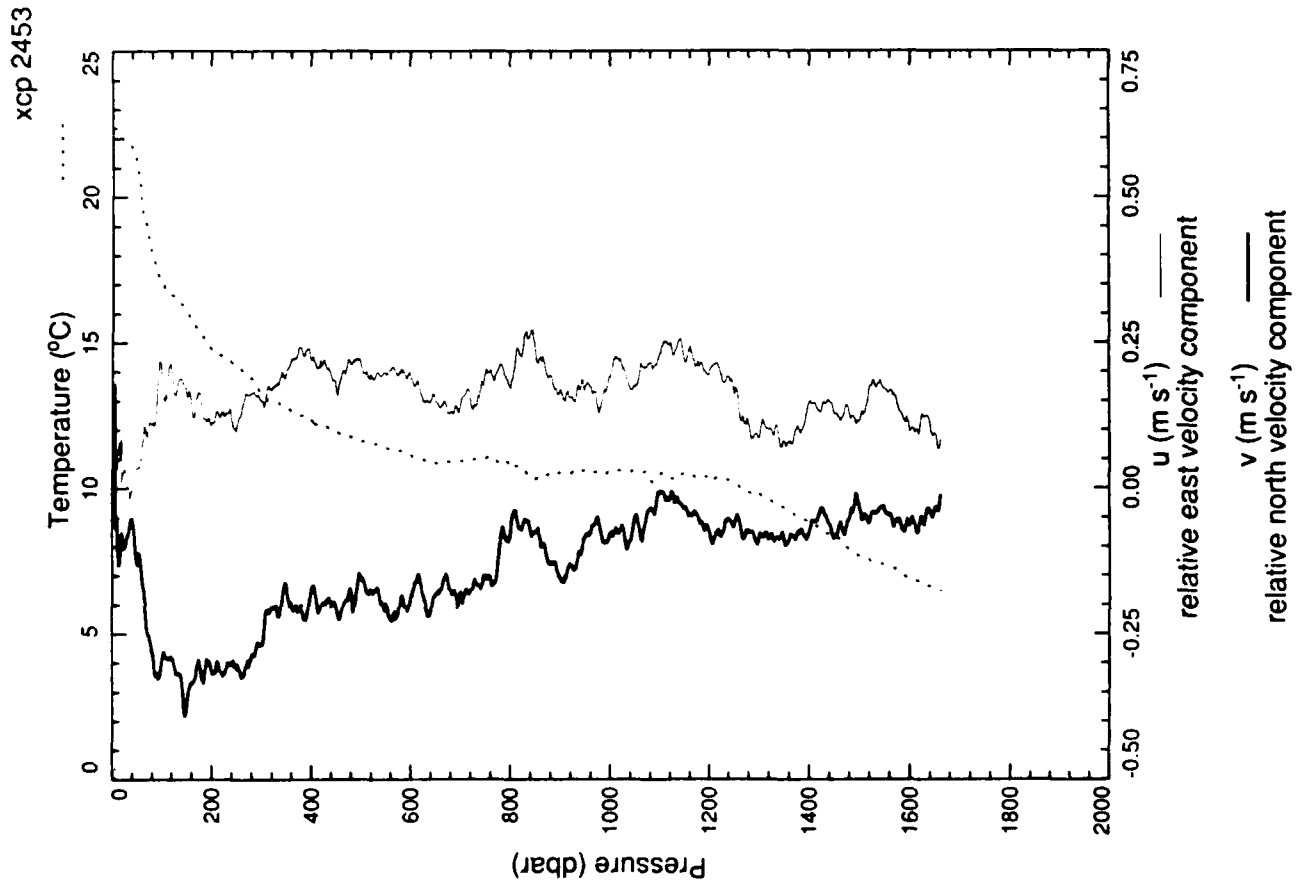
xcp 2453
Temperature (°C)
Pressure (dbar)
u (m s-1)
relative east velocity component
v (m s-1)
relative north velocity component

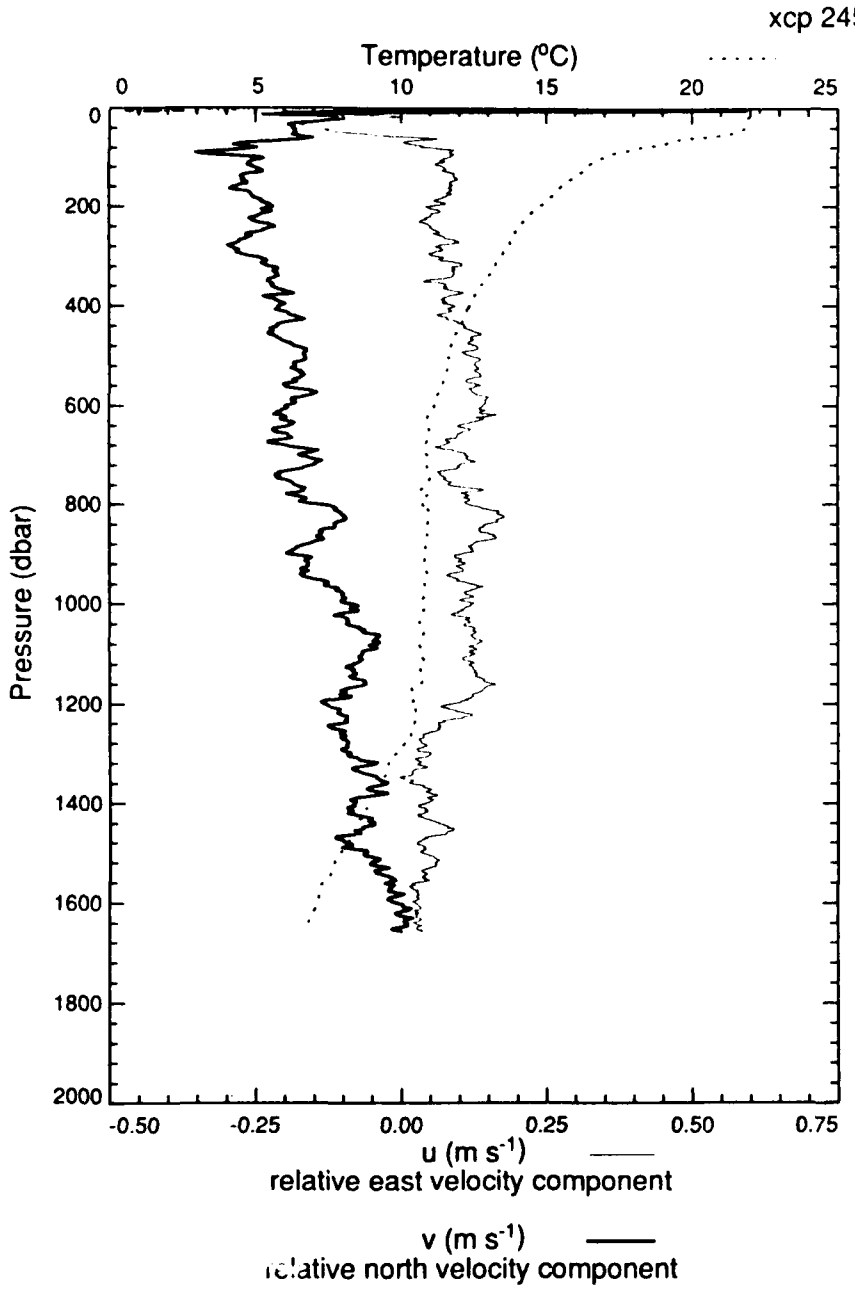
xcp 2455
Temperature (°C)
0
5
10
15
20
25
Pressure (dbar)
0
200
400
600
800
1000
1200
1400
1600
1800
2000
-0.50
-0.25
0.00
0.25
0.50
0.75
u (m s-1)
relative east velocity component
v (m s-1)
relative north velocity component

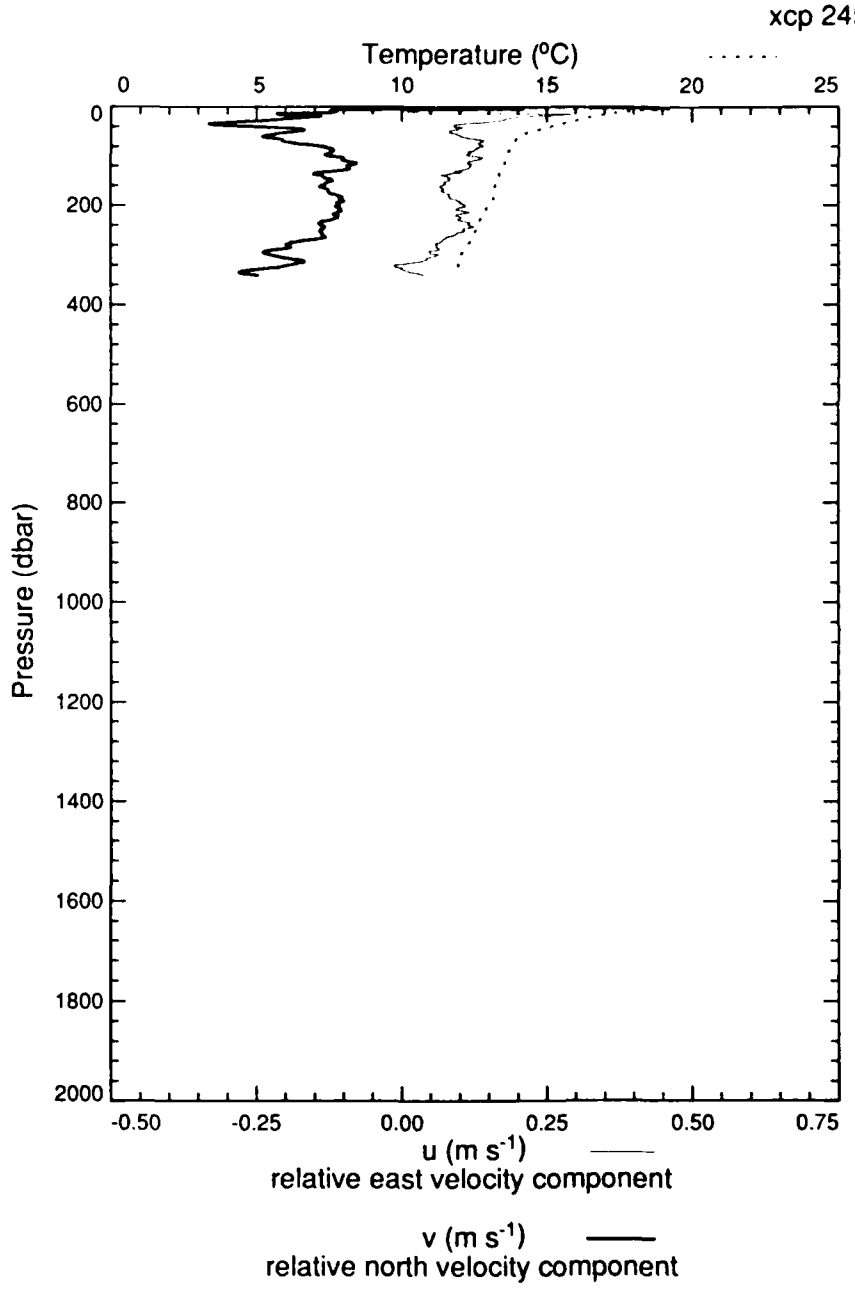
xcp 2456
Temperature (°C)
0
5
10
15
20
25
Pressure (dbar)
0
200
400
600
800
1000
1200
1400
1600
1800
2000
-0.50
-0.25
0.00
0.25
0.50
0.75
u (m s-1)
relative east velocity component
v (m s-1)
relative north velocity component

N28 TR 8925

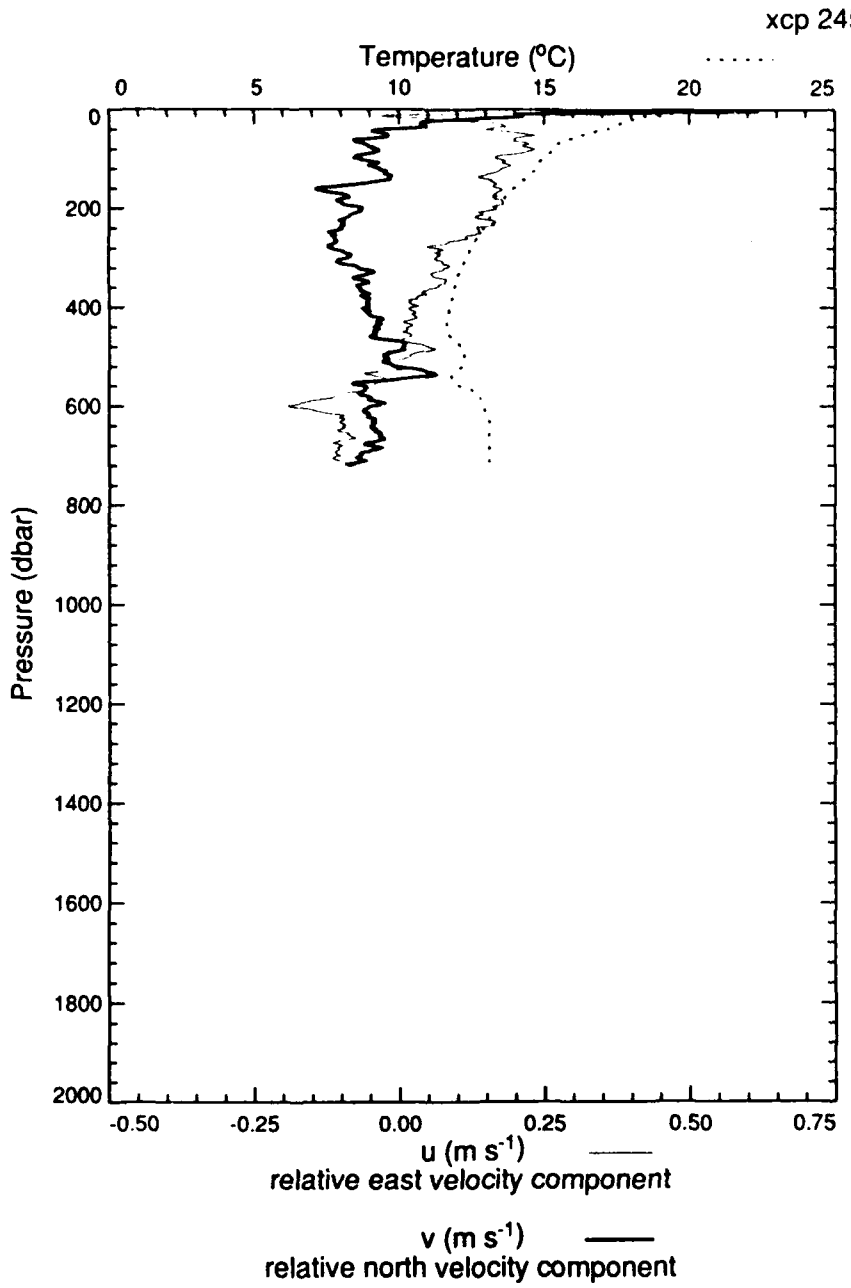
xcp 2457
Temperature (°C)
0
5
10
15
20
25
Pressure (dbar)
0
200
400
600
800
1000
1200
1400
1600
1800
2000
-0.50
-0.25
0.00
0.25
0.50
0.75
u (m s-1)
relative east velocity component
v (m s-1)
relative north velocity component

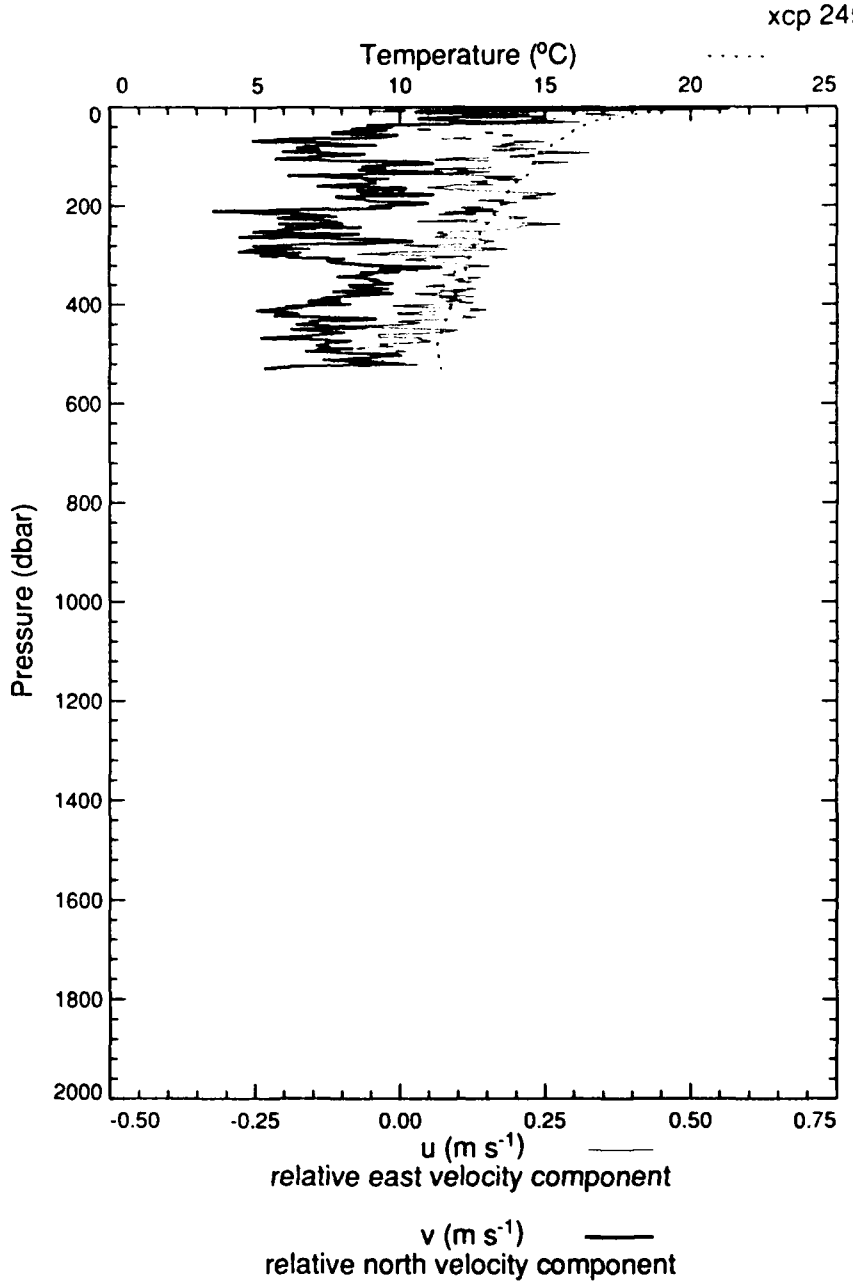
xcp 2458
Temperature (°C)
0
5
10
15
20
25
Pressure (dbar)
0
200
400
600
800
1000
1200
1400
1600
1800
2000
-0.50
-0.25
0.00
0.25
0.50
0.75
u (m s-1)
relative east velocity component
v (m s-1)
relative north velocity component

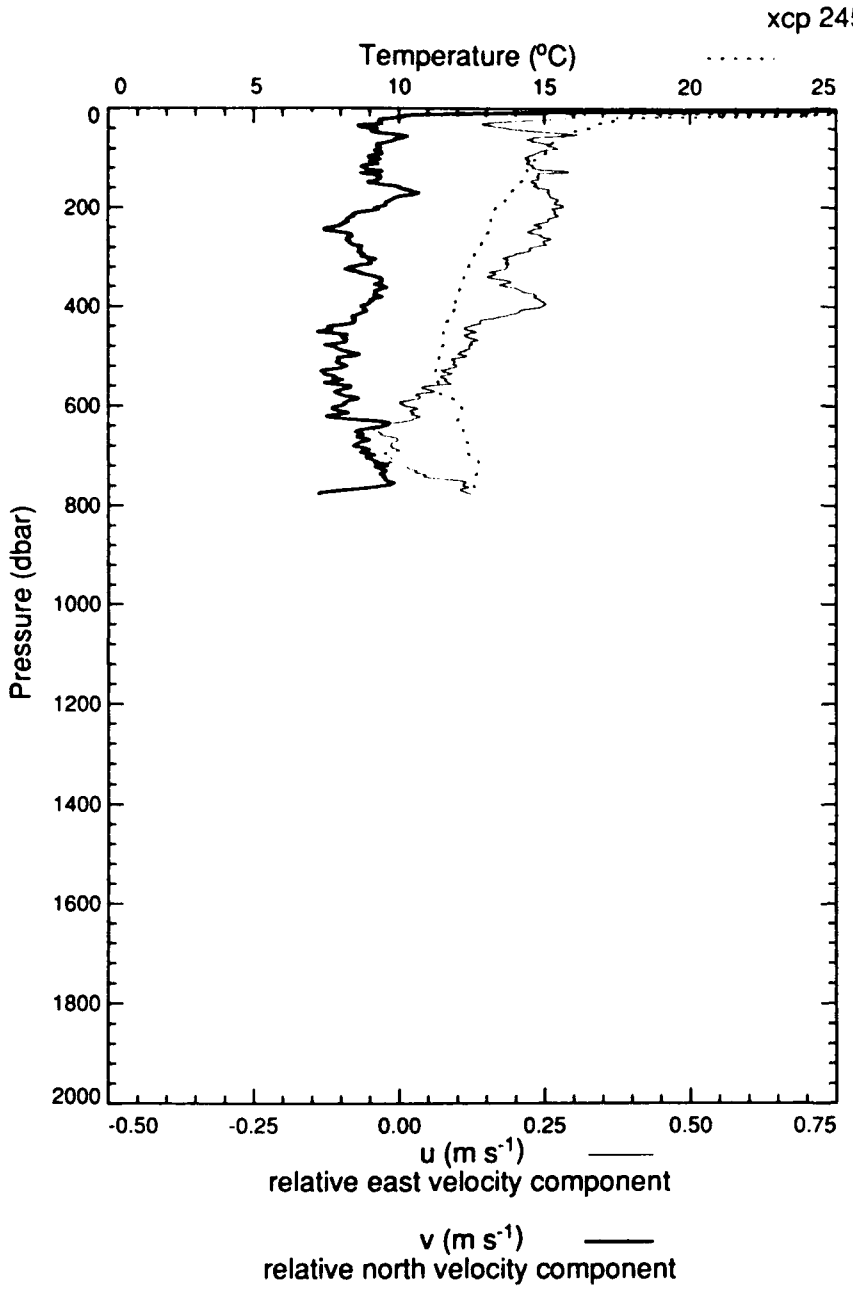
xcp 2459
Temperature (°C)
0
5
10
15
20
25
Pressure (dbar)
0
200
400
600
800
1000
1200
1400
1600
1800
2000
-0.50
-0.25
0.00
0.25
0.50
0.75
u (m s-1)
relative east velocity component
v (m s-1)
relative north velocity component

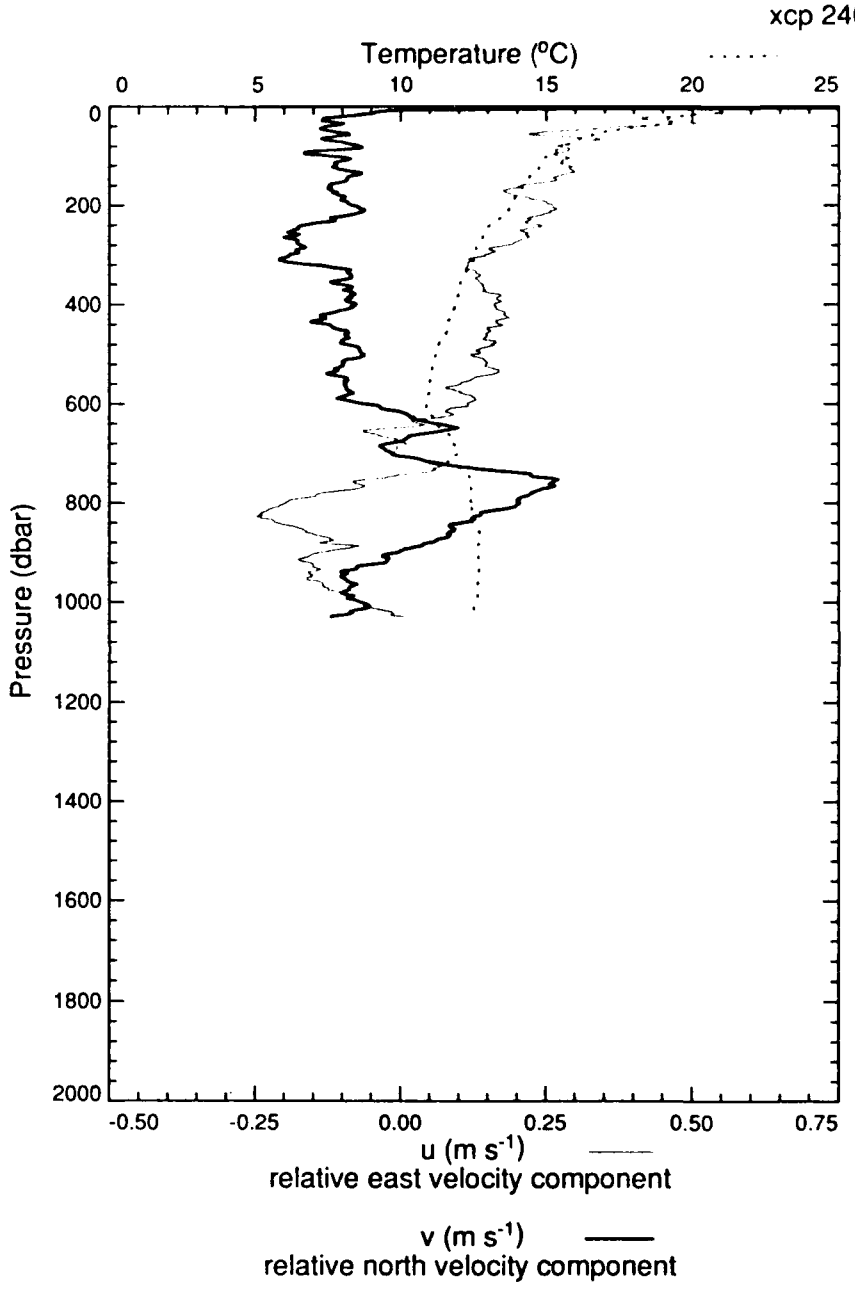
xcp 2460
Temperature (°C)
0
5
10
15
20
25
Pressure (dbar)
0
200
400
600
800
1000
1200
1400
1600
1800
2000
-0.50
-0.25
0.00
0.25
0.50
0.75
u (m s-1)
relative east velocity component
v (m s-1)
relative north velocity component

TR 8925 N29

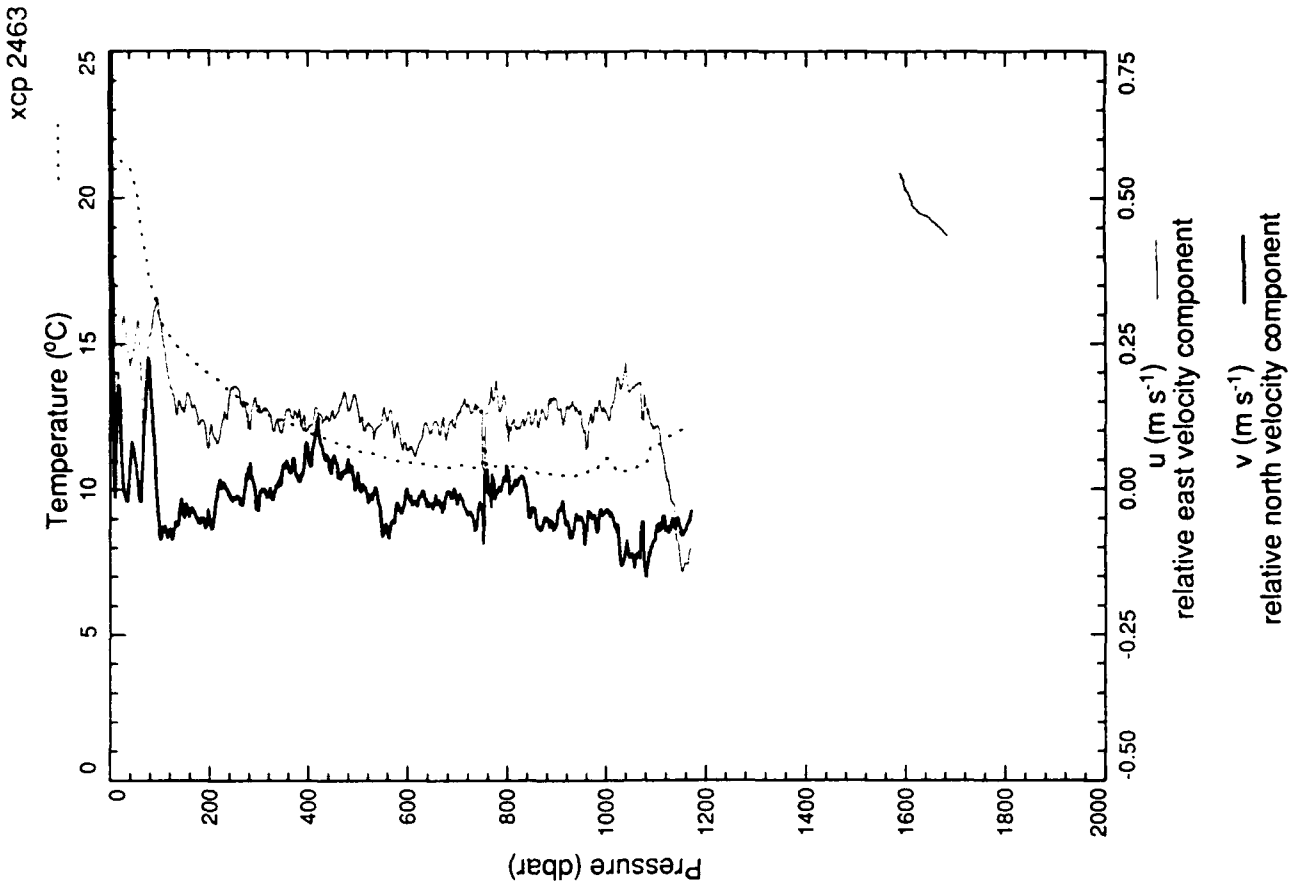
xcp 2463
Temperature (°C)
Pressure (dbar)
u (m s-1)
relative east velocity component
v (m s-1)
relative north velocity component

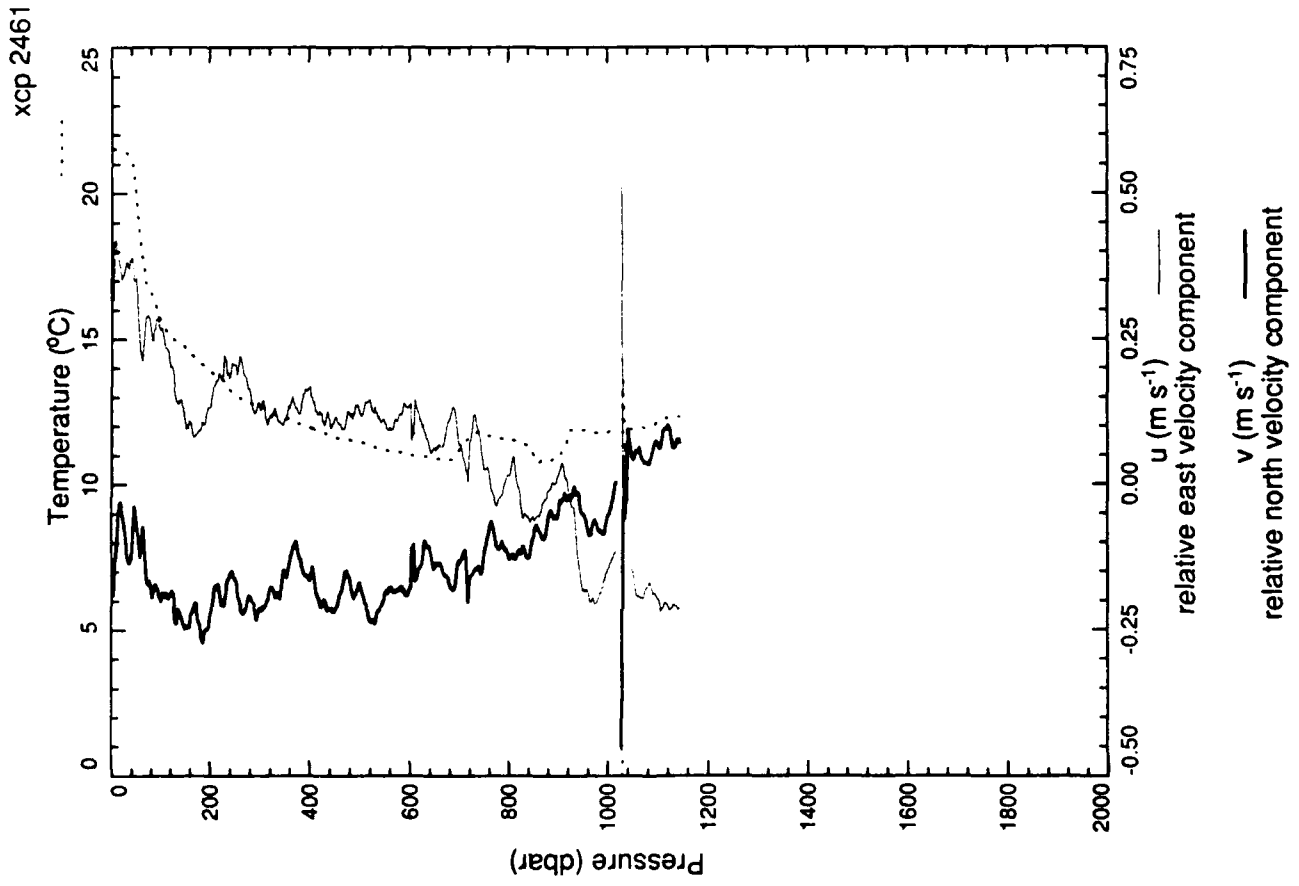
xcp 2461
Temperature (°C)
Pressure (dbar)
u (m s-1)
relative east velocity component
v (m s-1)
relative north velocity component

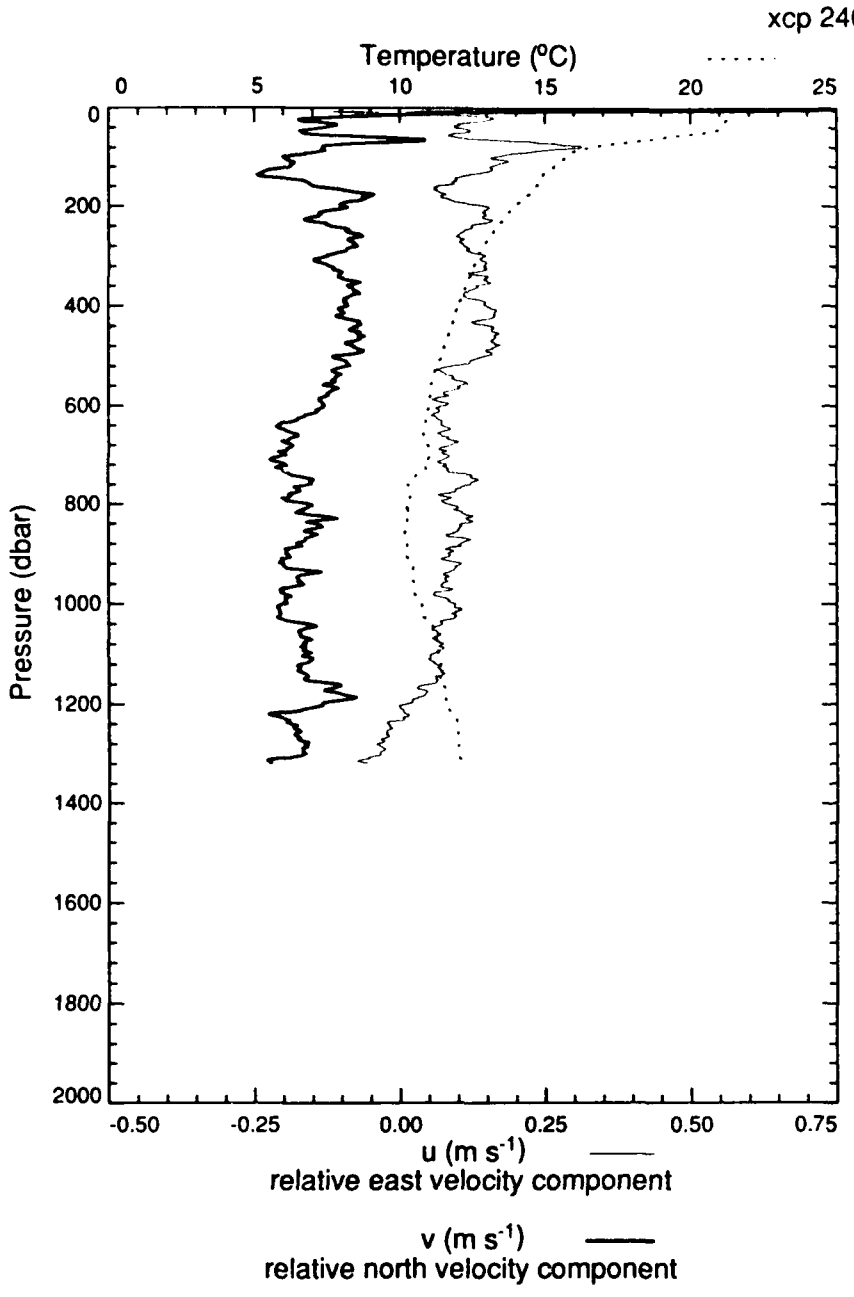
xcp 2464
Temperature (°C)
0
5
10
15
20
25
Pressure (dbar)
0
200
400
600
800
1000
1200
1400
1600
1800
2000
-0.50
-0.25
0.00
0.25
0.50
0.75
u (m s-1)
relative east velocity component
v (m s-1)
relative north velocity component

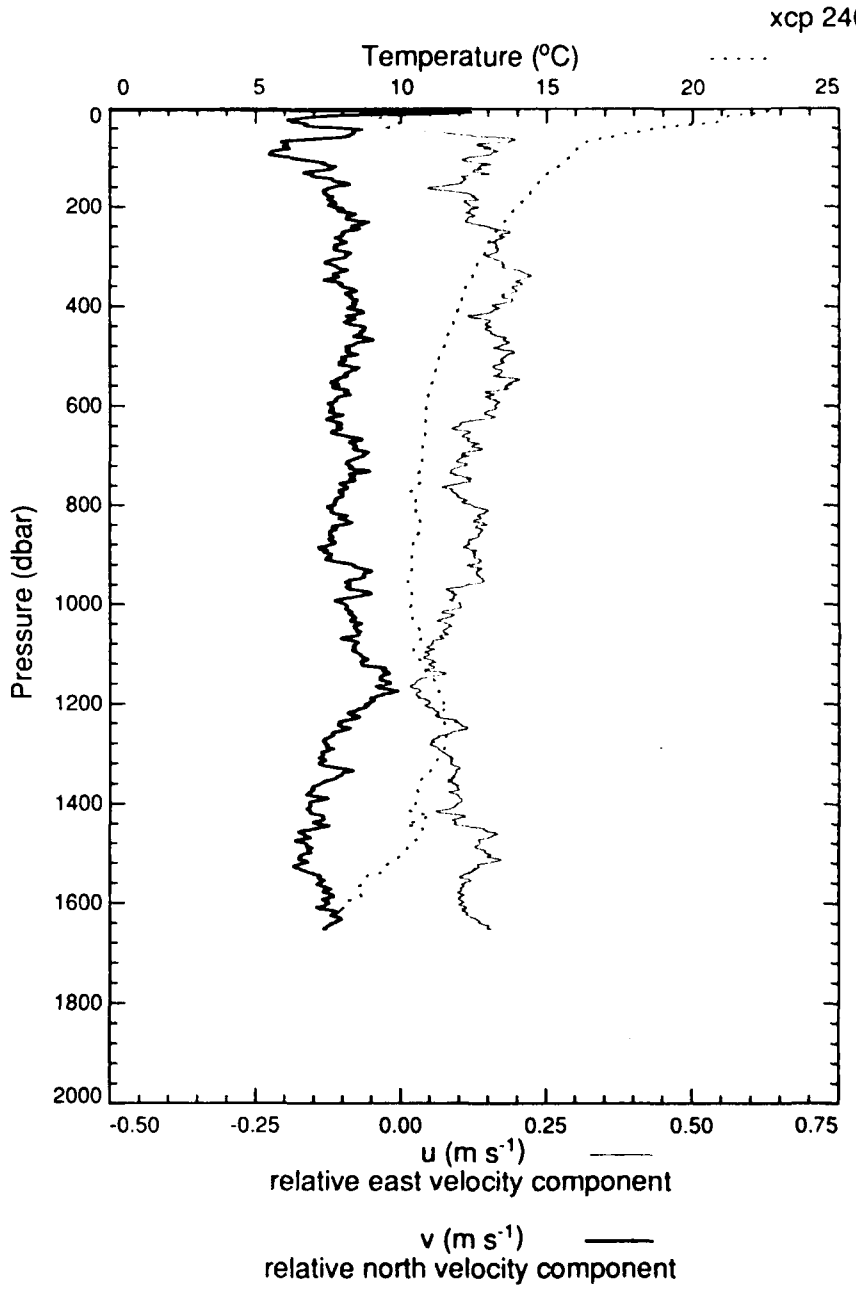
xcp 2465
Temperature (°C)
0
5
10
15
20
25
Pressure (dbar)
0
200
400
600
800
1000
1200
1400
1600
1800
2000
-0.50
-0.25
0.00
0.25
0.50
0.75
u (m s-1)
relative east velocity component
v (m s-1)
relative north velocity component

N32 TR 8925

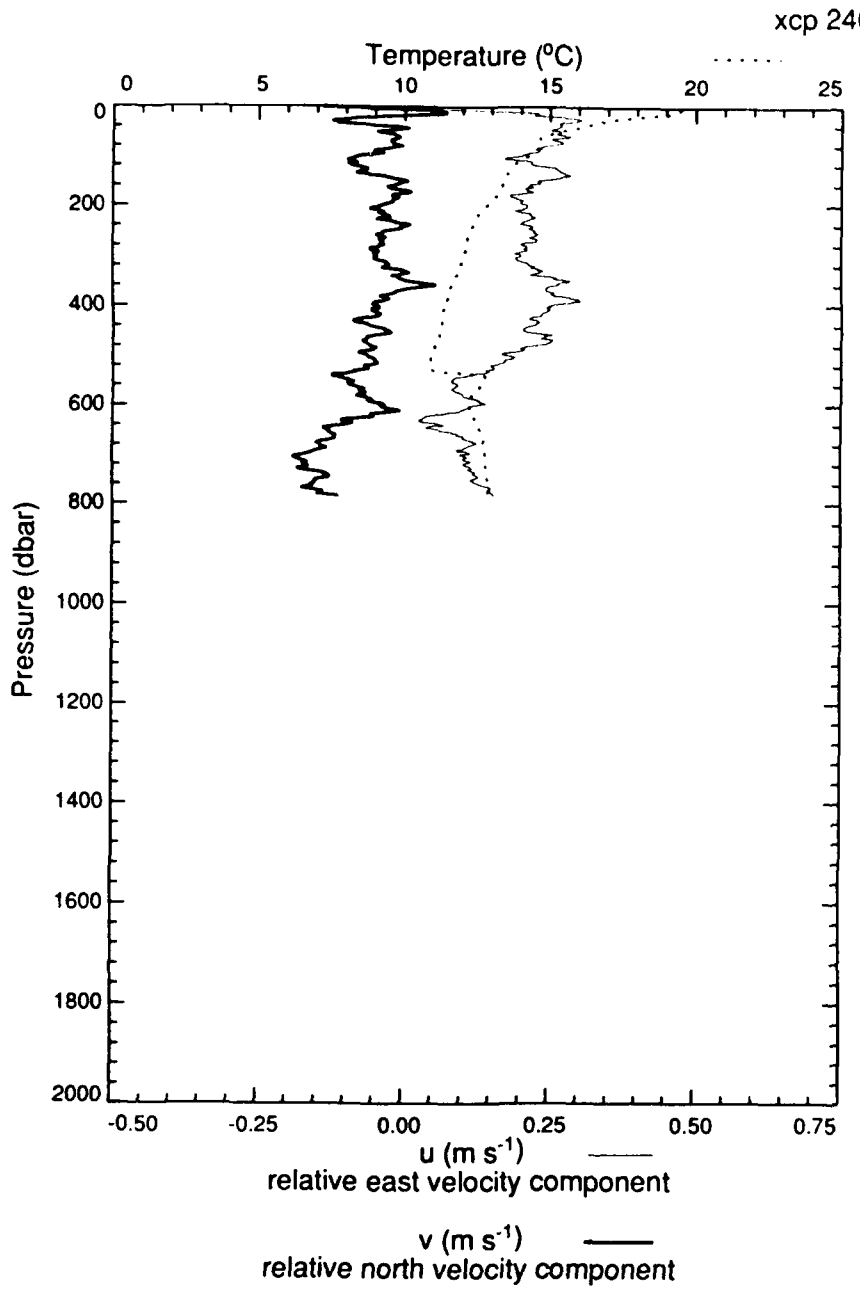
xcp 2466
Temperature (°C)
0
5
10
15
20
25
Pressure (dbar)
0
200
400
600
800
1000
1200
1400
1600
1800
2000
-0.50
-0.25
0.00
0.25
0.50
0.75
u (m s-1)
relative east velocity component
v (m s-1)
relative north velocity component

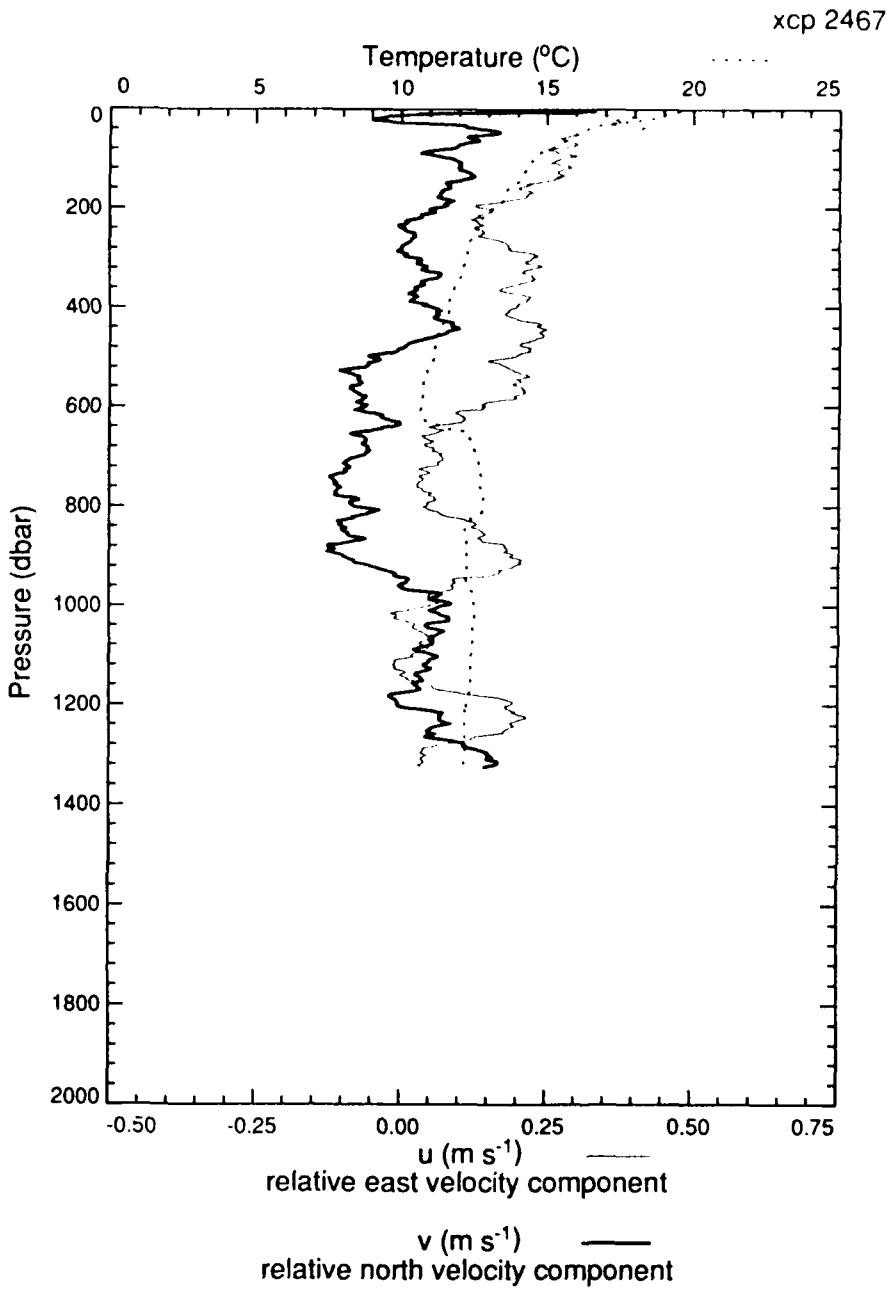
xcp 2467
Temperature (°C)
0
5
10
15
20
25
Pressure (dbar)
0
200
400
600
800
1000
1200
1400
1600
1800
2000
-0.50
-0.25
0.00
0.25
0.50
0.75
u (m s-1)
relative east velocity component
v (m s-1)
relative north velocity component

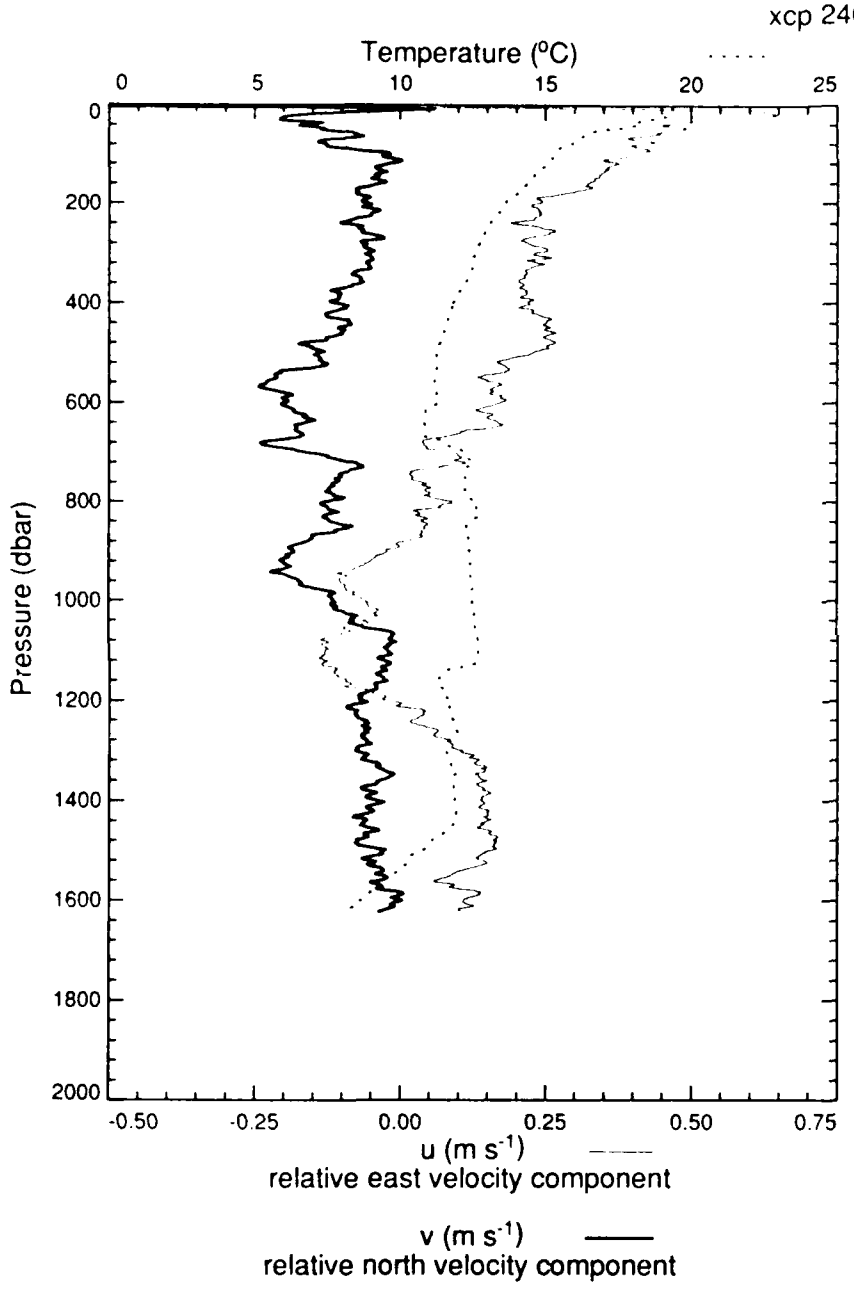
xcp 2468
Temperature (°C)
0
5
10
15
20
25
Pressure (dbar)
0
200
400
600
800
1000
1200
1400
1600
1800
2000
-0.50
-0.25
0.00
0.25
0.50
0.75
u (m s-1)
relative east velocity component
v (m s-1)
relative north velocity component

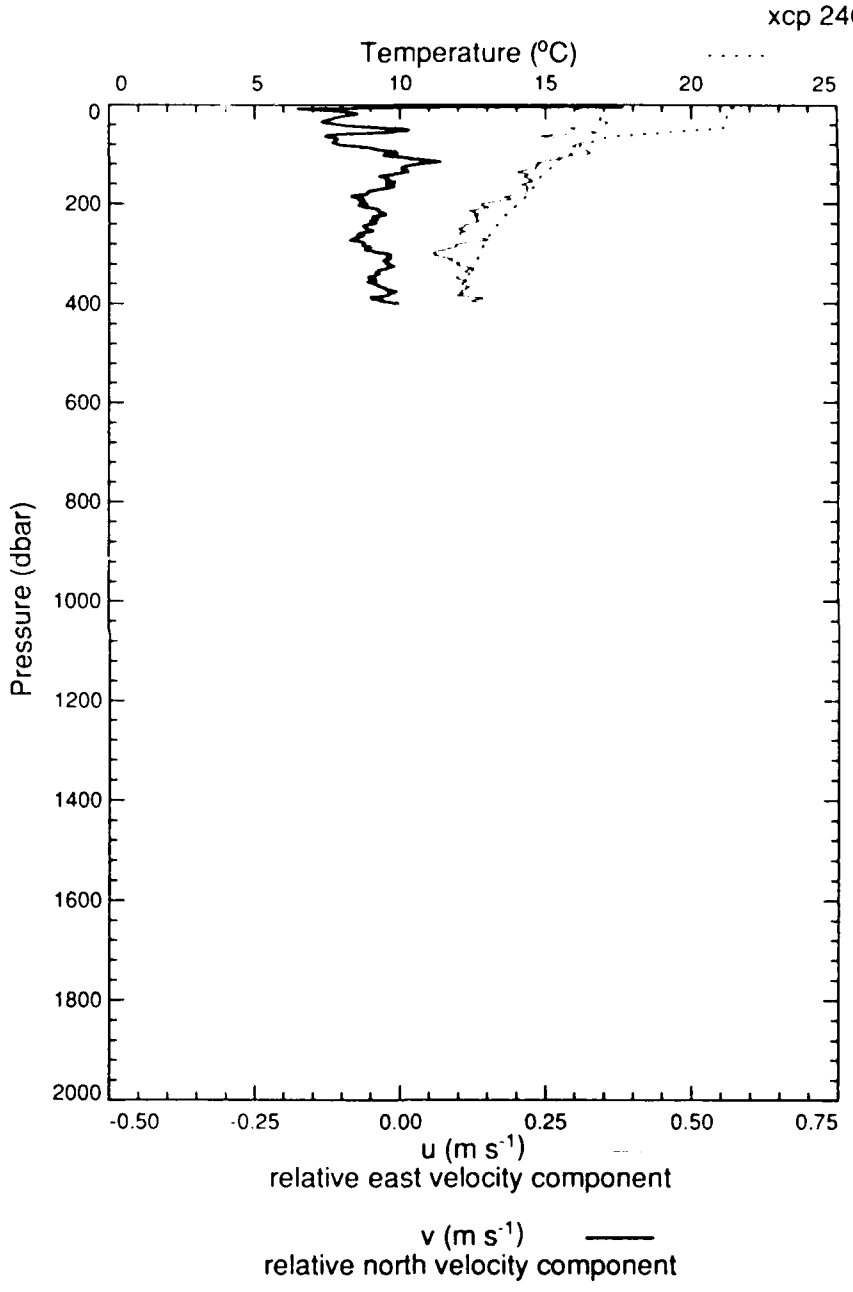
xcp 2469
Temperature (°C)
0
5
10
15
20
25
Pressure (dbar)
0
200
400
600
800
1000
1200
1400
1600
1800
2000
-0.50
-0.25
0.00
0.25
0.50
0.75
u (m s-1)
relative east velocity component
v (m s-1)
relative north velocity component

TR 8925 N33

N34 TR 8925

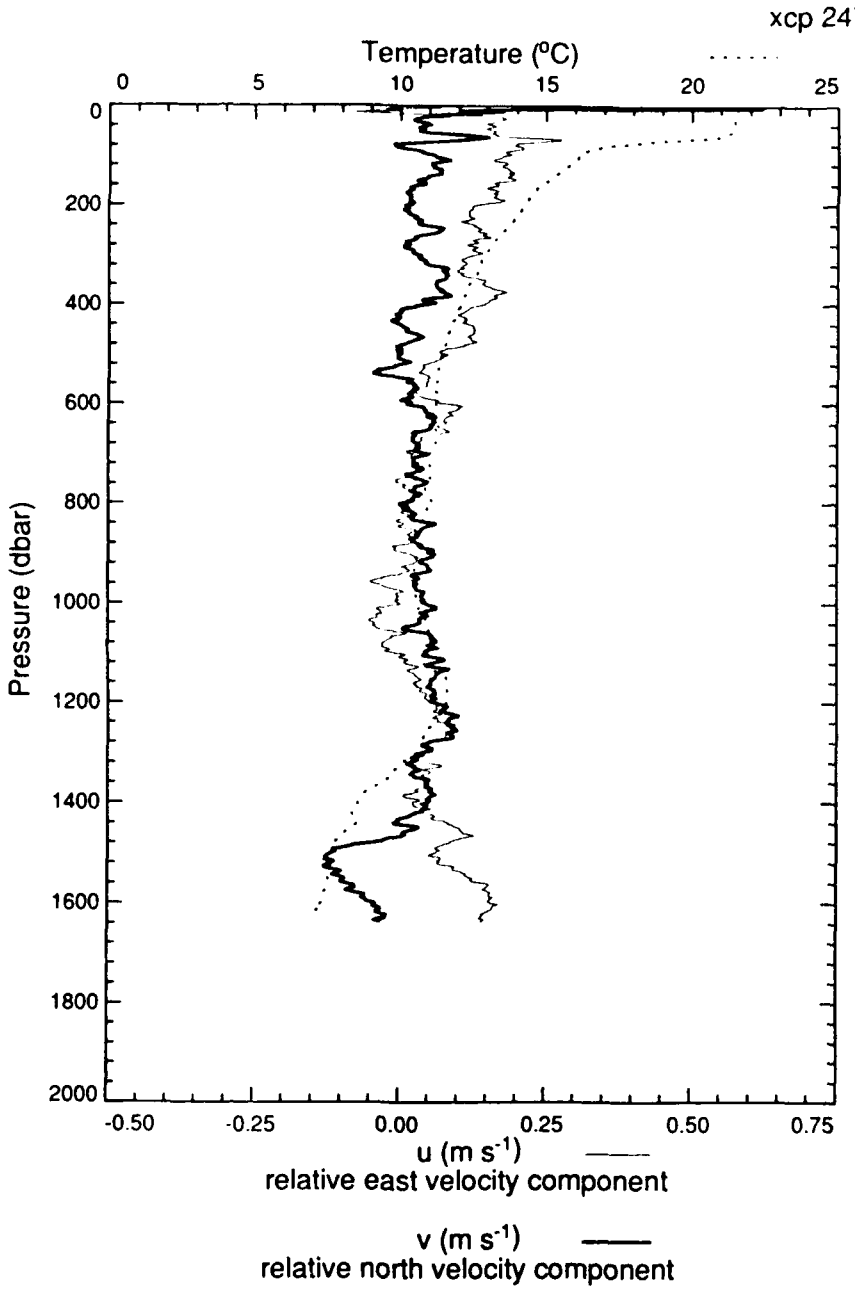
xcp 2470
Temperature (°C)
0
5
10
15
20
25
Pressure (dbar)
0
200
400
600
800
1000
1200
1400
1600
1800
2000
-0.50
-0.25
0.00
0.25
0.50
0.75
u (m s-1)
relative east velocity component
v (m s-1)
relative north velocity component

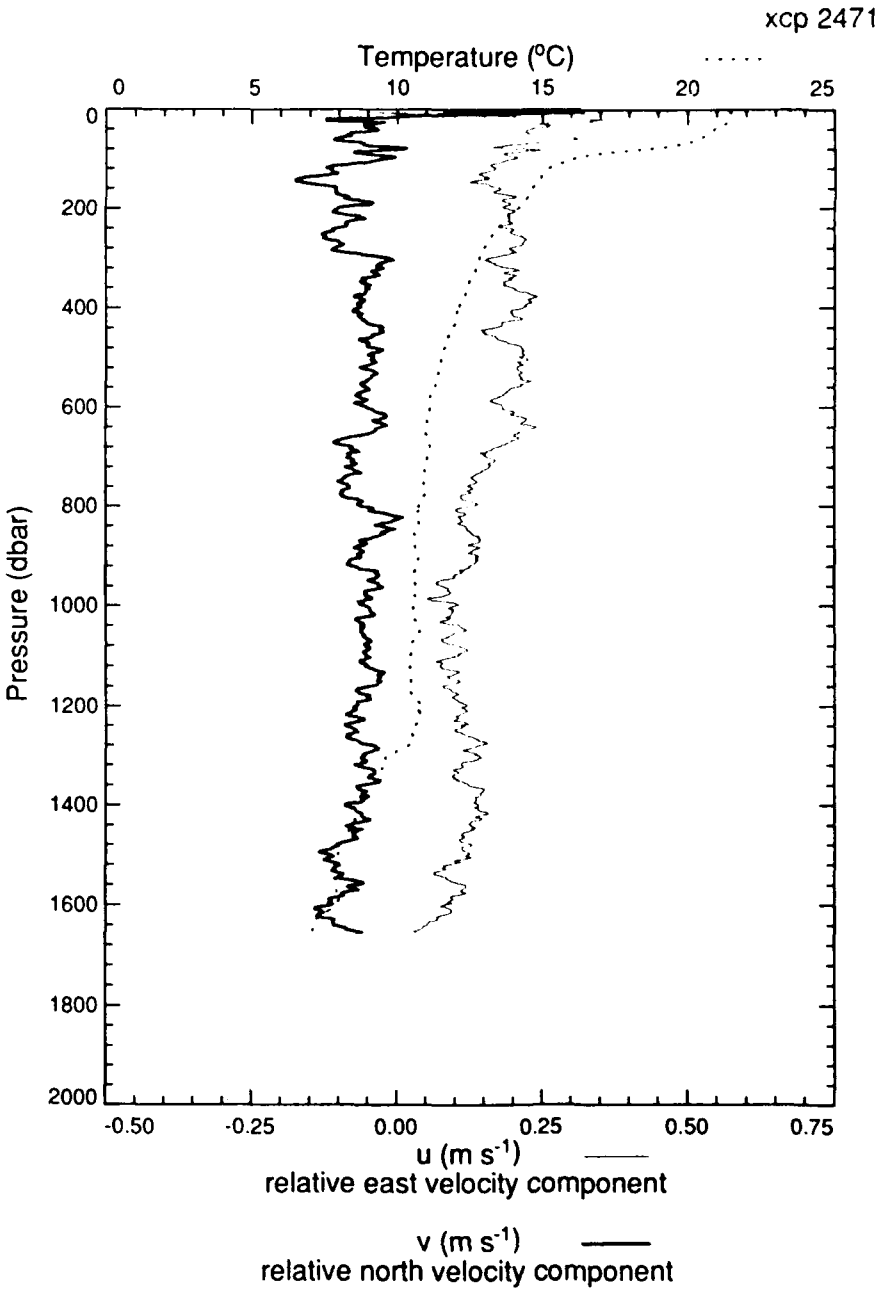
xcp 2471
Temperature (°C)
0
5
10
15
20
25
Pressure (dbar)
0
200
400
600
800
1000
1200
1400
1600
1800
2000
-0.50
-0.25
0.00
0.25
0.50
0.75
u (m s-1)
relative east velocity component
v (m s-1)
relative north velocity component

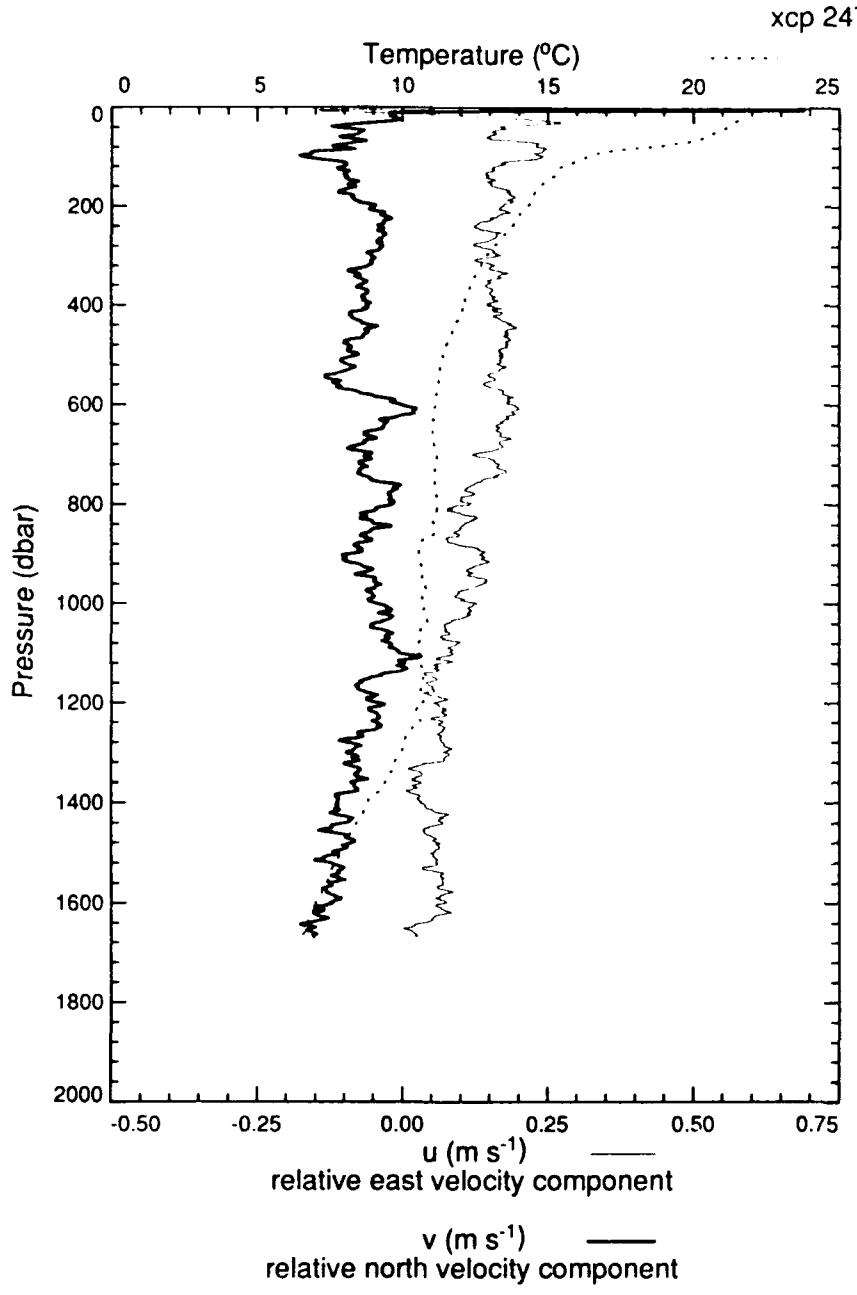
xcp 2472
Temperature (°C)
0
5
10
15
20
25
Pressure (dbar)
0
200
400
600
800
1000
1200
1400
1600
1800
2000
-0.50
-0.25
0.00
0.25
0.50
0.75
u (m s-1)
relative east velocity component
v (m s-1)
relative north velocity component

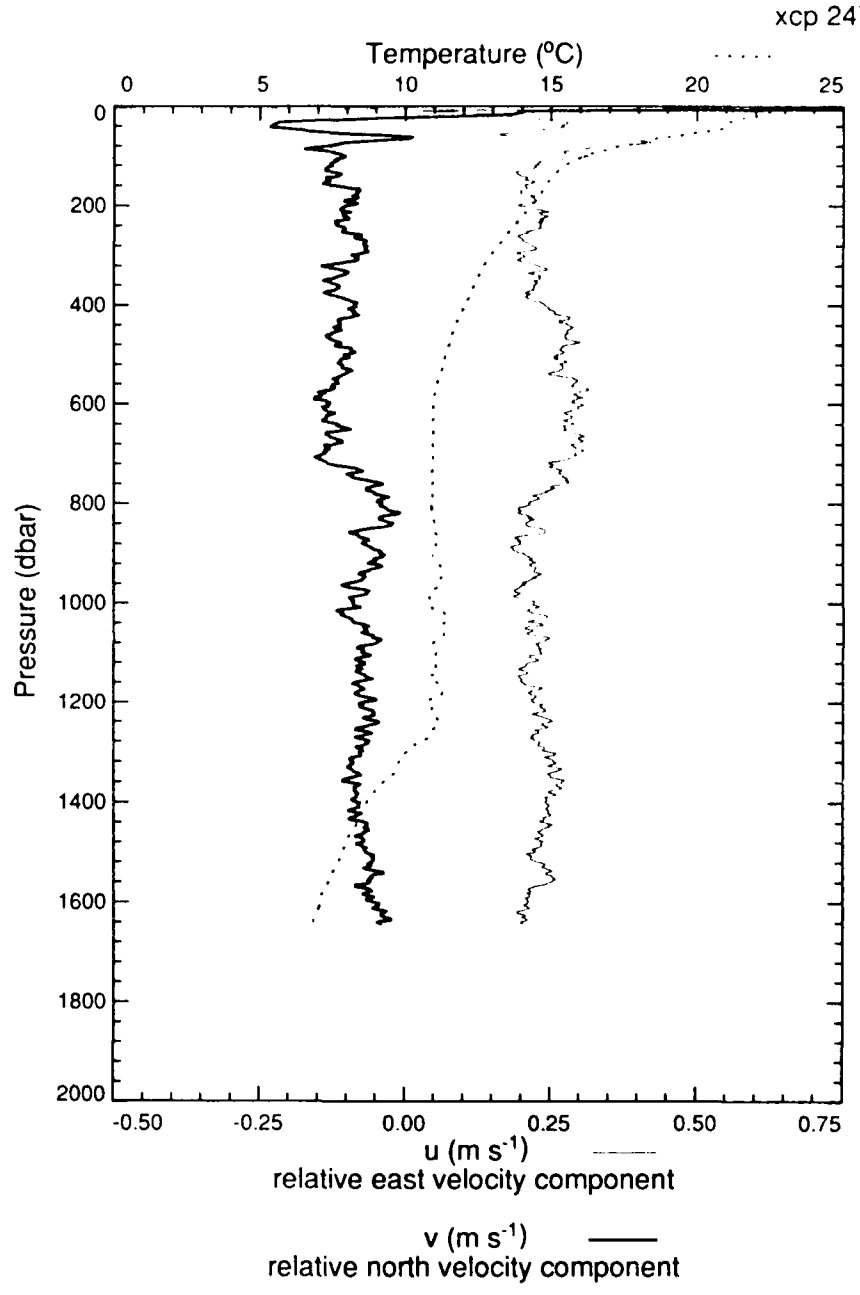
xcp 2473
Temperature (°C)
0
5
10
15
20
25
Pressure (dbar)
0
200
400
600
800
1000
1200
1400
1600
1800
2000
-0.50
-0.25
0.00
0.25
0.50
0.75
u (m s-1)
relative east velocity component
v (m s-1)
relative north velocity component

TR 8925 N35

N36 TR 8925

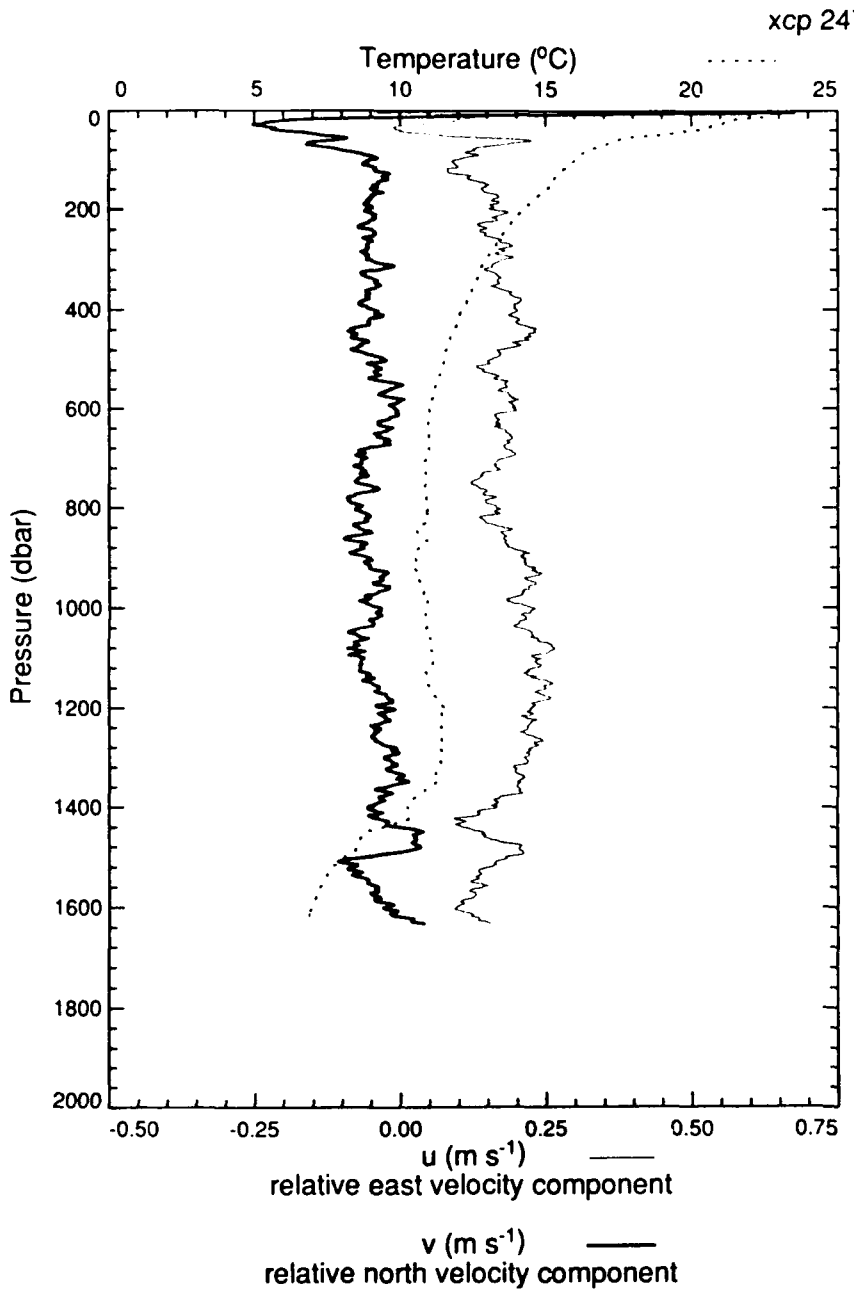
xcp 2474
Temperature (°C)
0
5
10
15
20
25
Pressure (dbar)
0
200
400
600
800
1000
1200
1400
1600
1800
2000
-0.50
-0.25
0.00
0.25
0.50
0.75
u (m s-1)
relative east velocity component
v (m s-1)
relative north velocity component

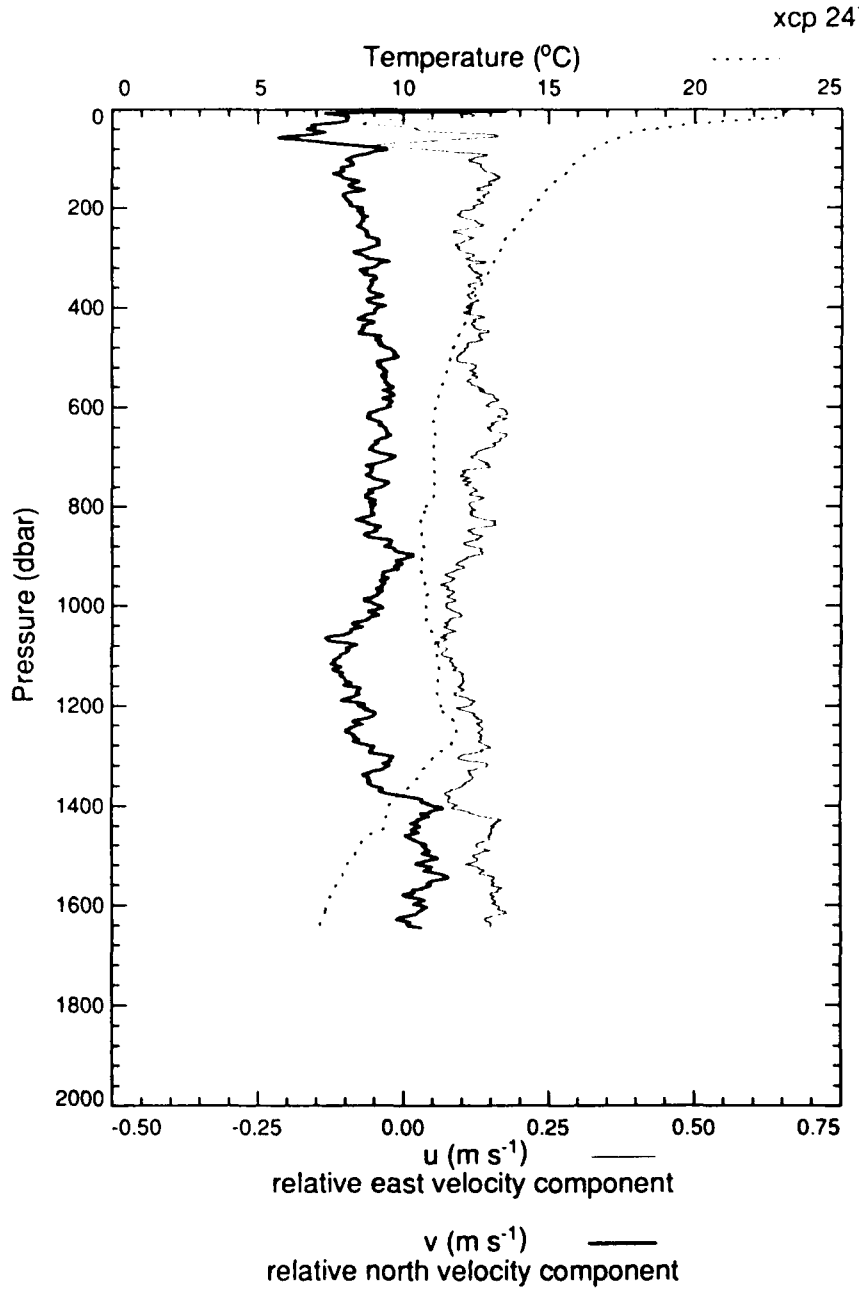
xcp 2475
Temperature (°C)
0
5
10
15
20
25
Pressure (dbar)
0
200
400
600
800
1000
1200
1400
1600
1800
2000
-0.50
-0.25
0.00
0.25
0.50
0.75
u (m s-1)
relative east velocity component
v (m s-1)
relative north velocity component

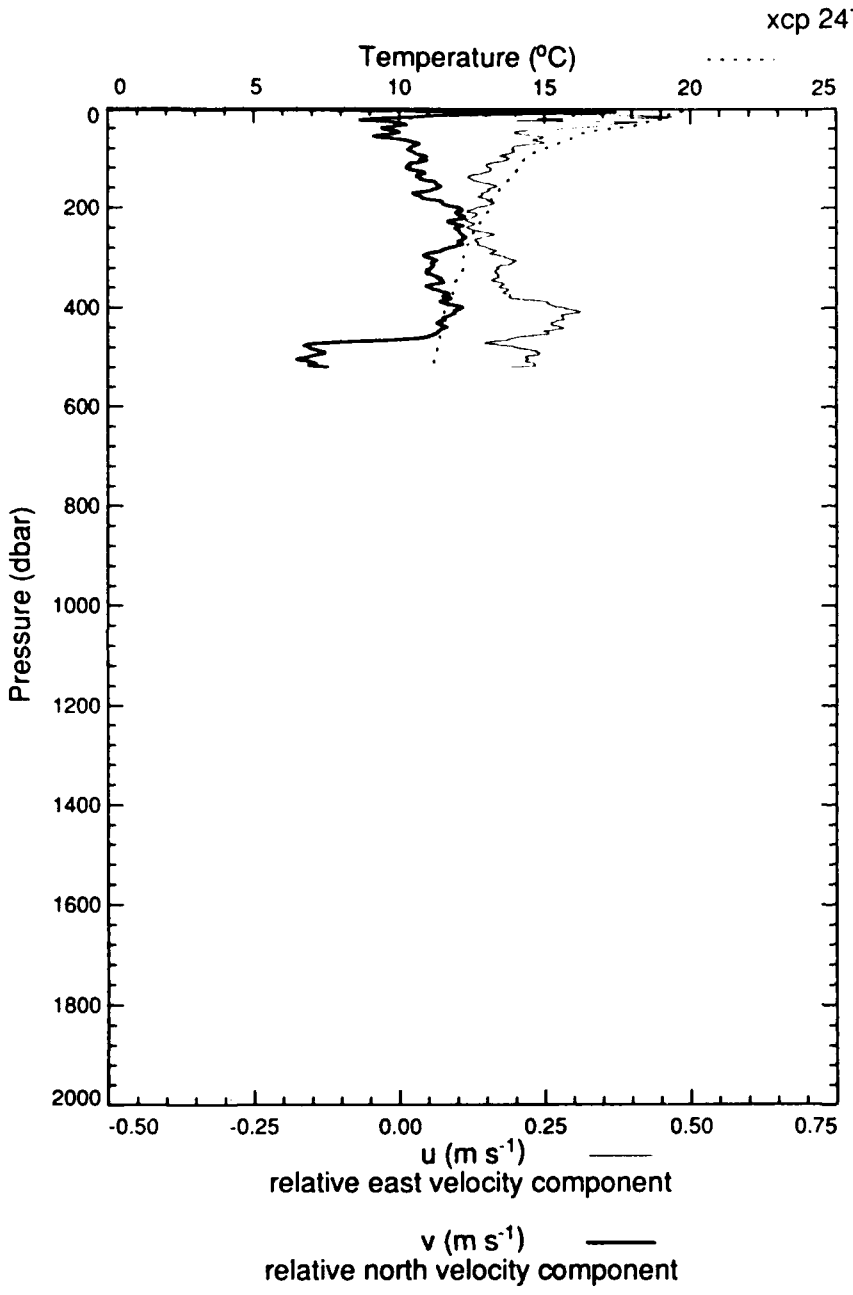
xcp 2476
Temperature (°C)
0
5
10
15
20
25
Pressure (dbar)
0
200
400
600
800
1000
1200
1400
1600
1800
2000
-0.50
-0.25
0.00
0.25
0.50
0.75
u (m s-1)
relative east velocity component
v (m s-1)
relative north velocity component

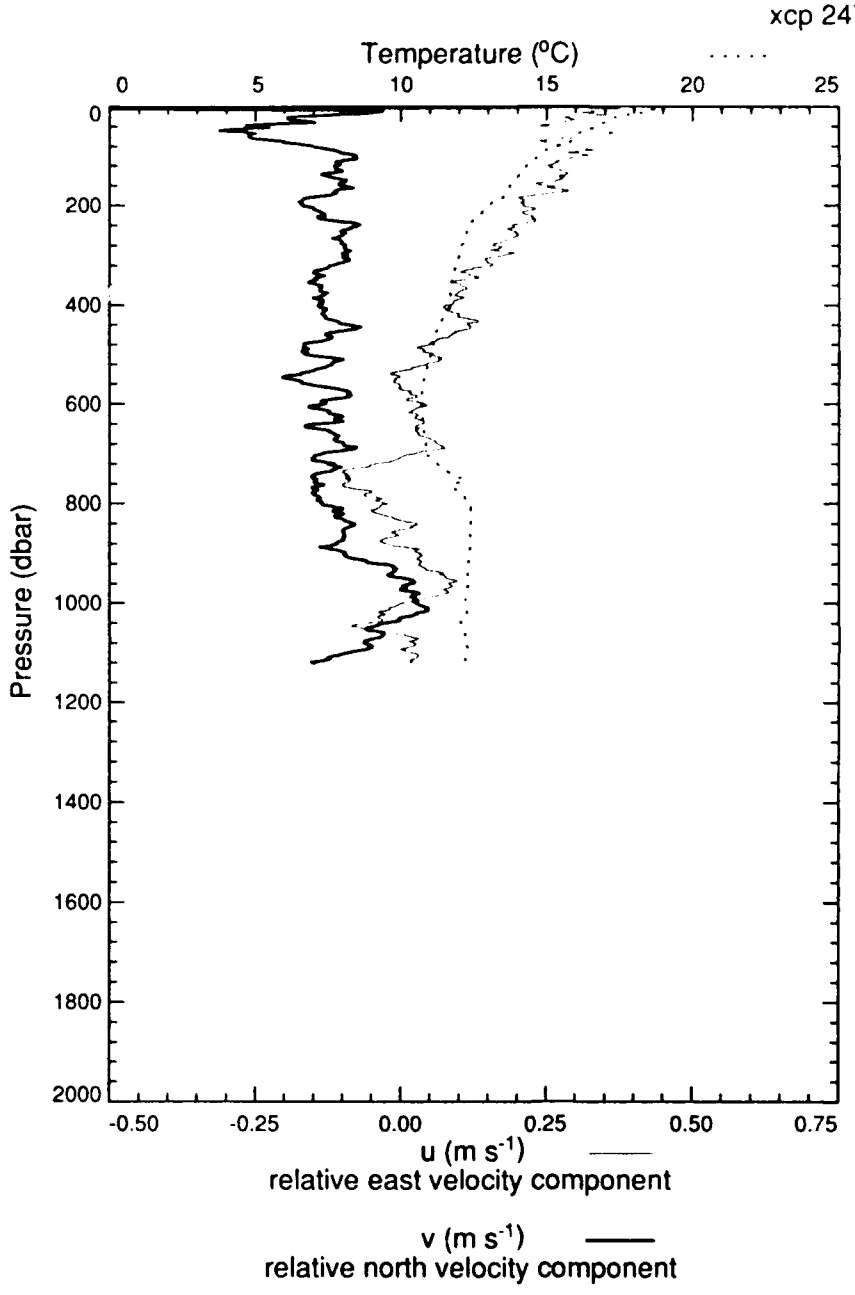
xcp 2477
Temperature (°C)
0
5
10
15
20
25
Pressure (dbar)
0
200
400
600
800
1000
1200
1400
1600
1800
2000
-0.50
-0.25
0.00
0.25
0.50
0.75
u (m s-1)
relative east velocity component
v (m s-1)
relative north velocity component

TR 8925 N37

N38 TR 8925

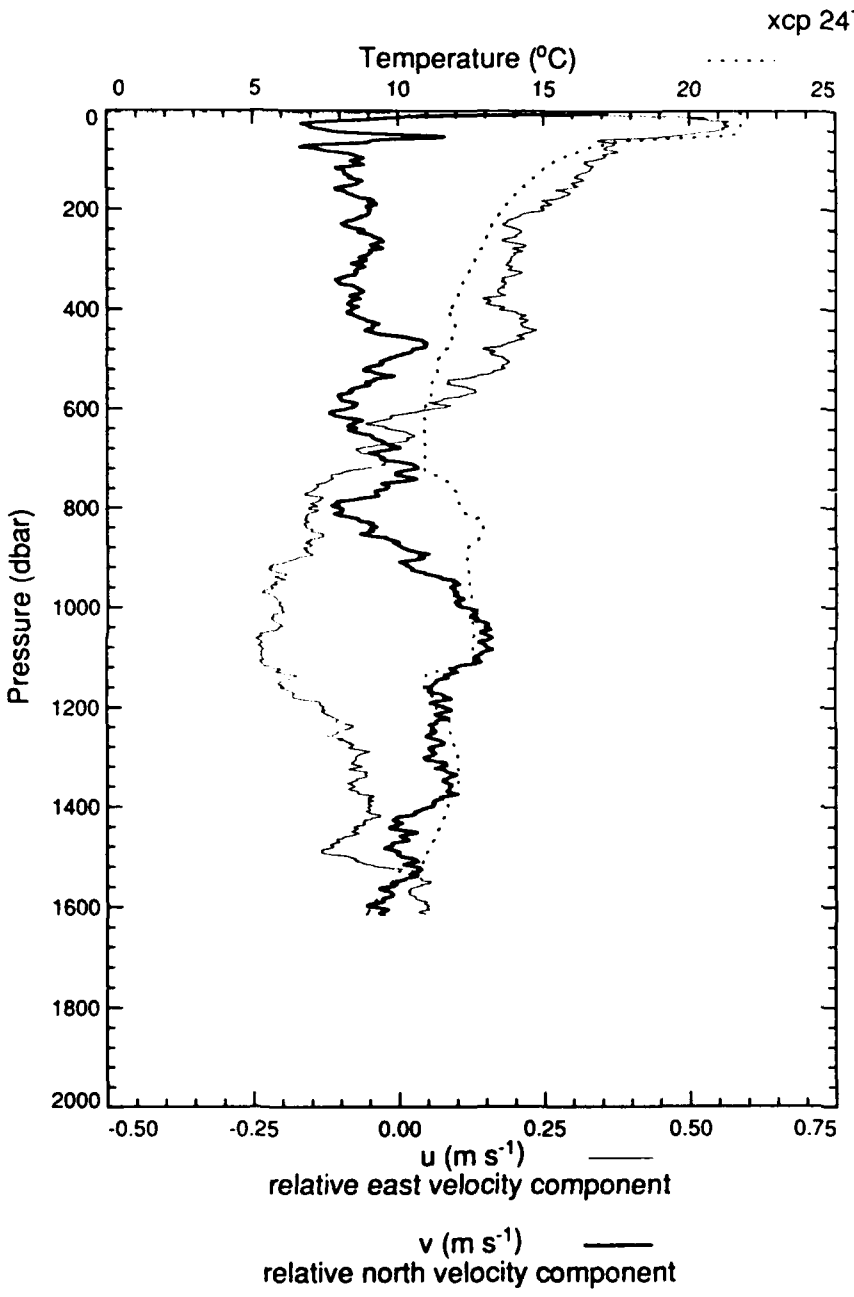
xcp 2478
Temperature (°C)
0
5
10
15
20
25
Pressure (dbar)
0
200
400
600
800
1000
1200
1400
1600
1800
2000
-0.50
-0.25
0.00
0.25
0.50
0.75
u (m s-1)
relative east velocity component
v (m s-1)
relative north velocity component

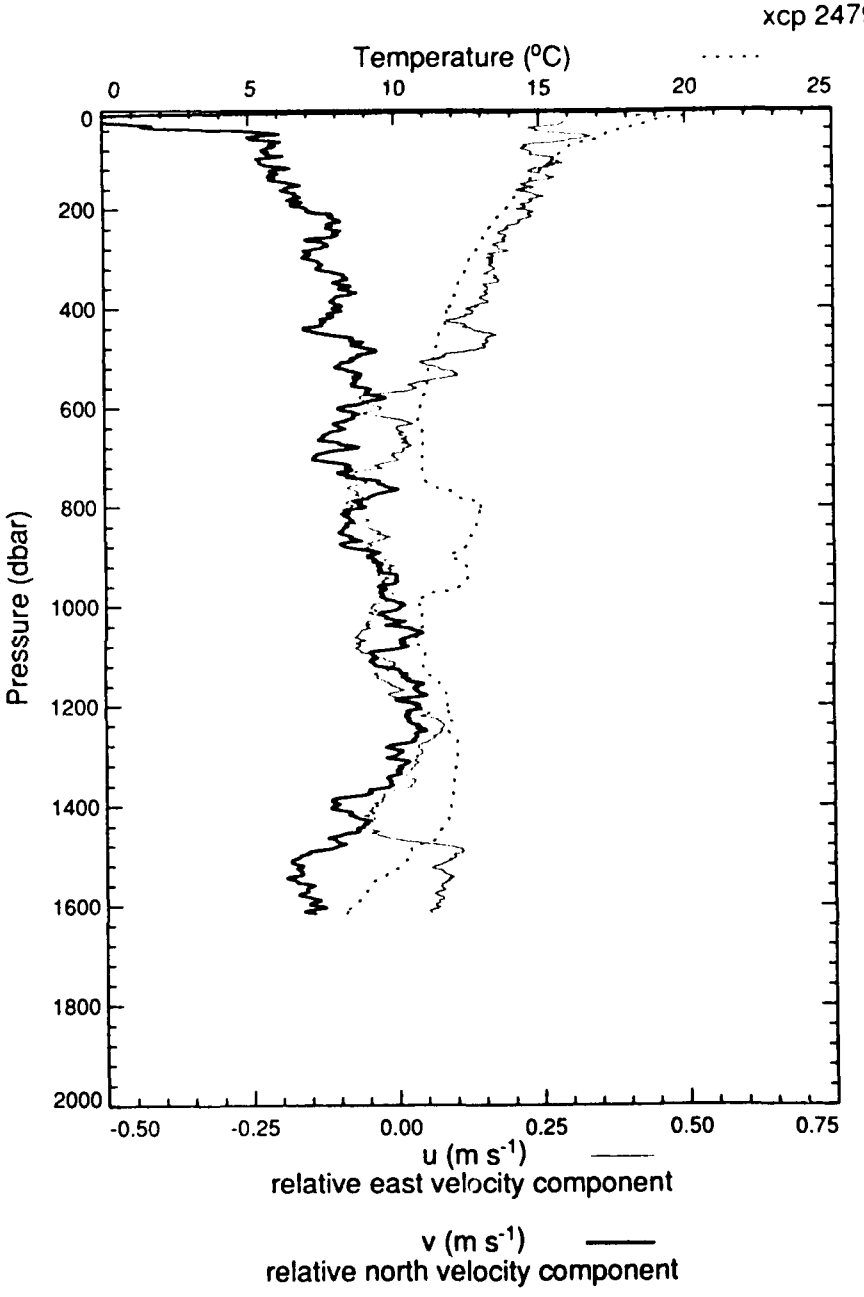
xcp 2479
Temperature (°C)
0
5
10
15
20
25
Pressure (dbar)
0
200
400
600
800
1000
1200
1400
1600
1800
2000
-0.50
-0.25
0.00
0.25
0.50
0.75
u (m s-1)
relative east velocity component
v (m s-1)
relative north velocity component

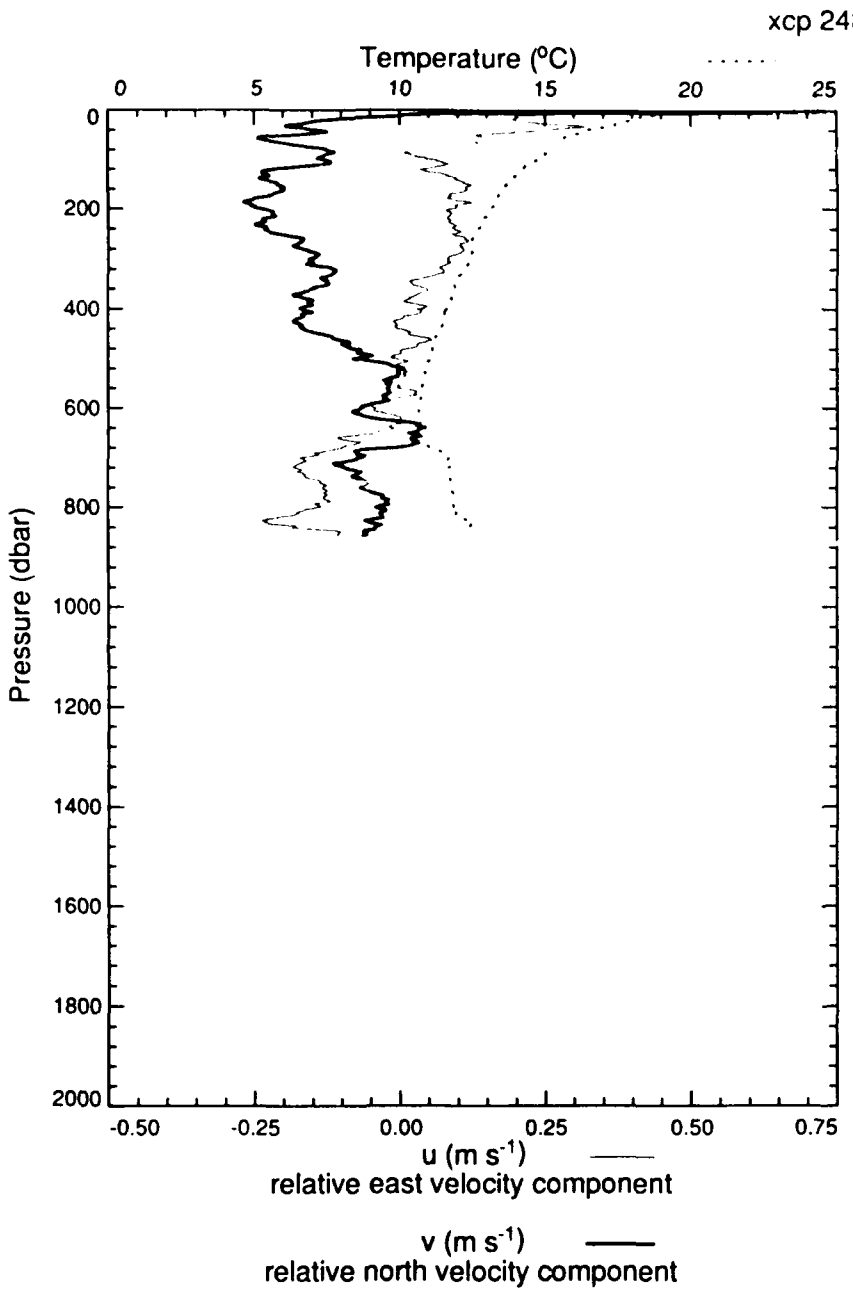
xcp 2481
Temperature (°C)
0
5
10
15
20
25
Pressure (dbar)
0
200
400
600
800
1000
1200
1400
1600
1800
2000
-0.50
-0.25
0.00
0.25
0.50
0.75
u (m s-1)
relative east velocity component
v (m s-1)
relative north velocity component

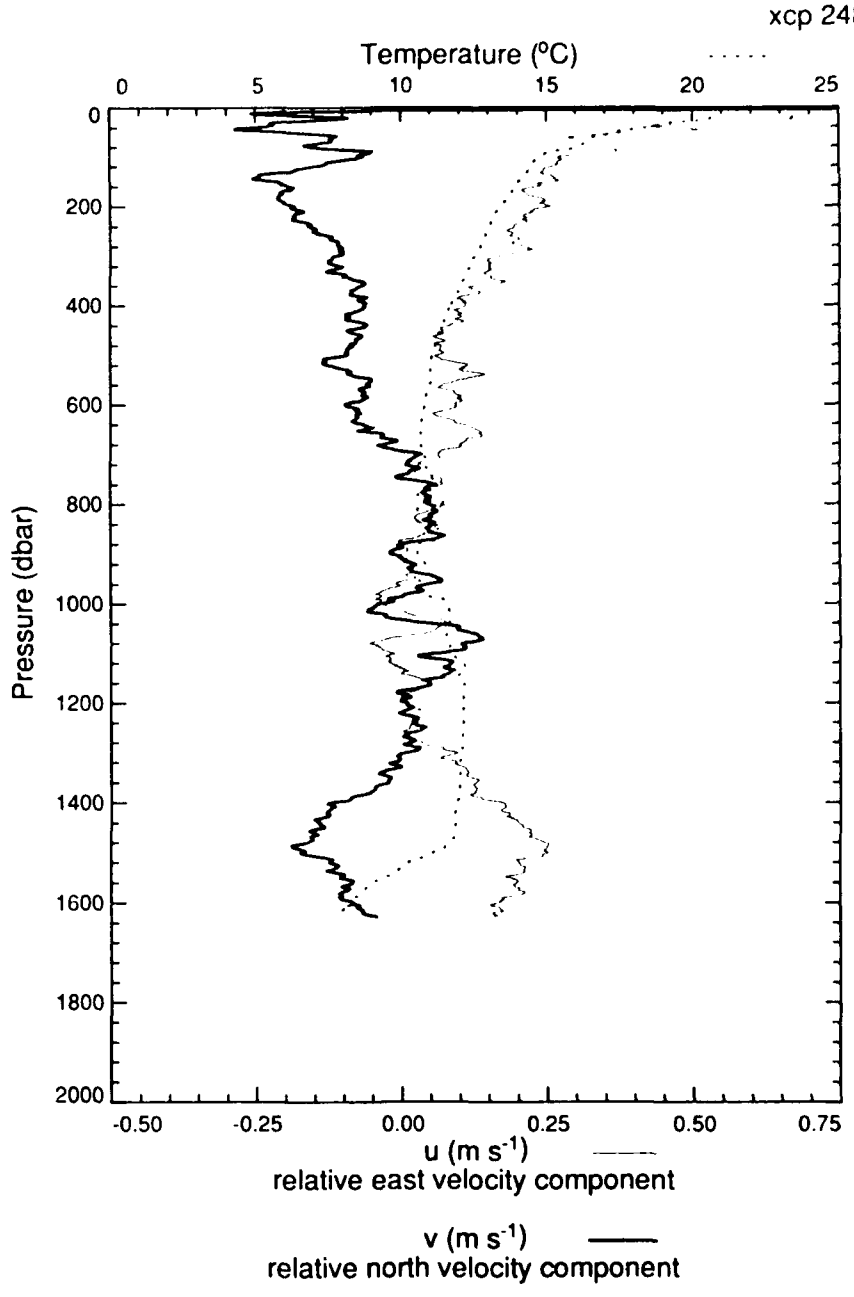
xcp 2482
Temperature (°C)
0
5
10
15
20
25
Pressure (dbar)
0
200
400
600
800
1000
1200
1400
1600
1800
2000
-0.50
-0.25
0.00
0.25
0.50
0.75
u (m s-1)
relative east velocity component
v (m s-1)
relative north velocity component

N40 TR 8925

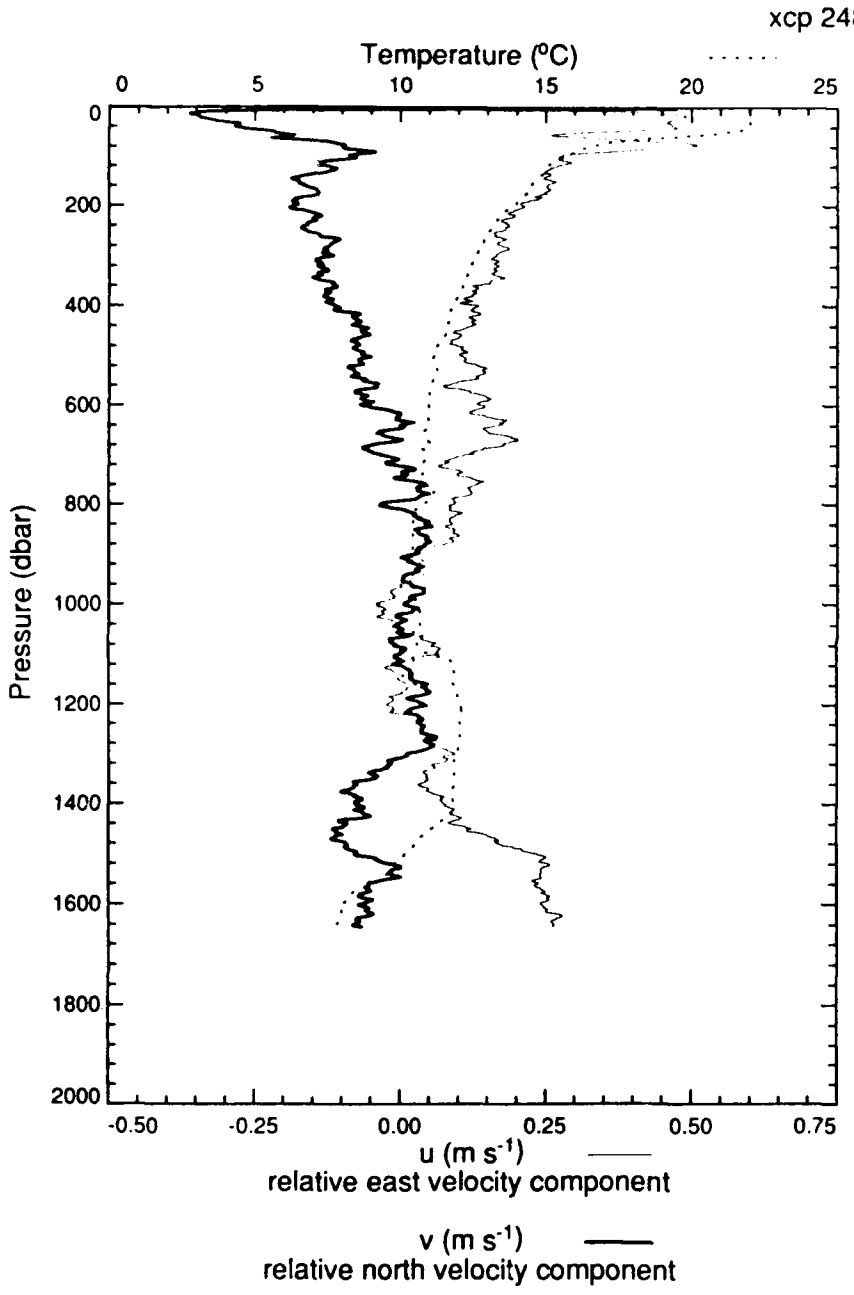
xcp 2483
Temperature (°C)
0
5
10
15
20
25
Pressure (dbar)
0
200
400
600
800
1000
1200
1400
1600
1800
2000
-0.50
-0.25
0.00
0.25
0.50
0.75
u (m s-1)
relative east velocity component
v (m s-1)
relative north velocity component

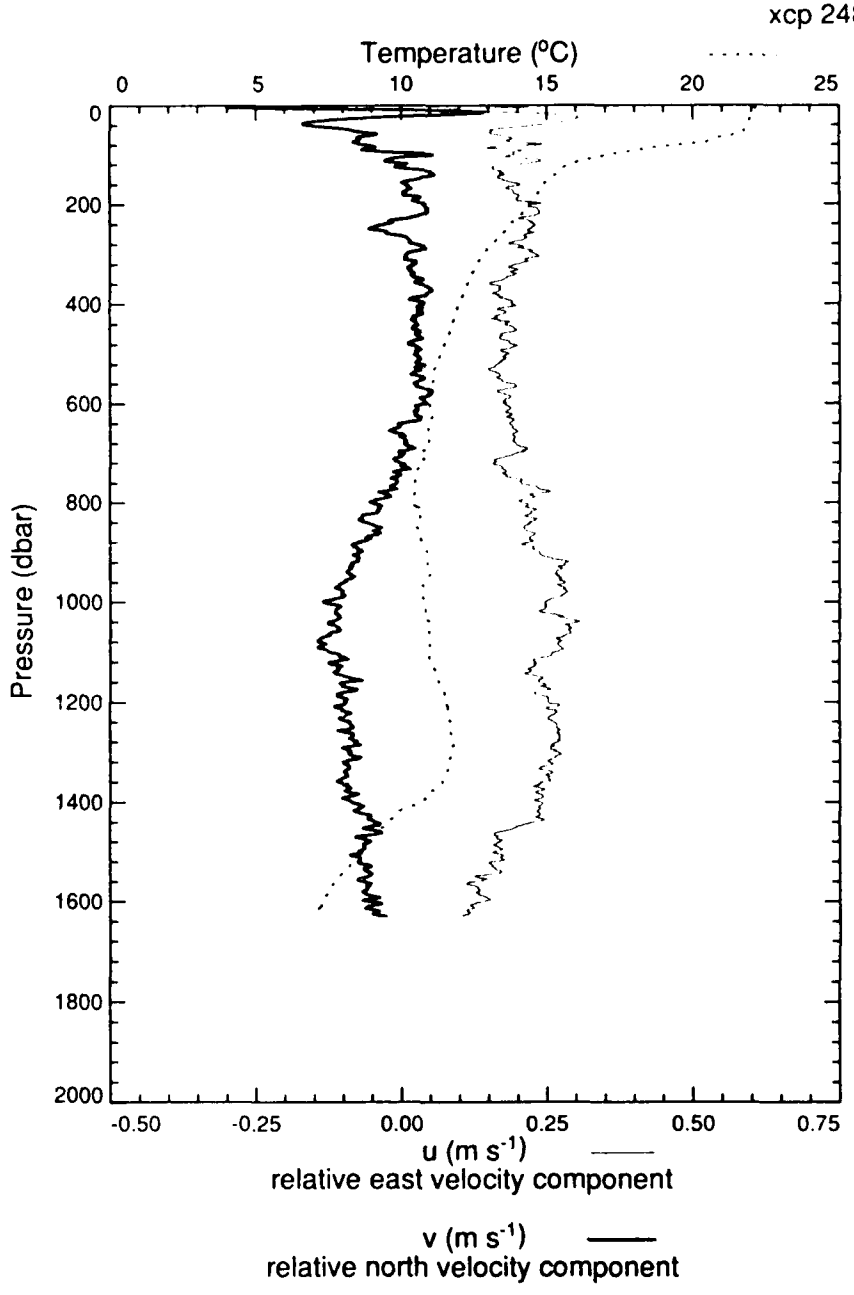
xcp 2484
Temperature (°C)
0
5
10
15
20
25
Pressure (dbar)
0
200
400
600
800
1000
1200
1400
1600
1800
2000
-0.50
-0.25
0.00
0.25
0.50
0.75
u (m s-1)
relative east velocity component
v (m s-1)
relative north velocity component

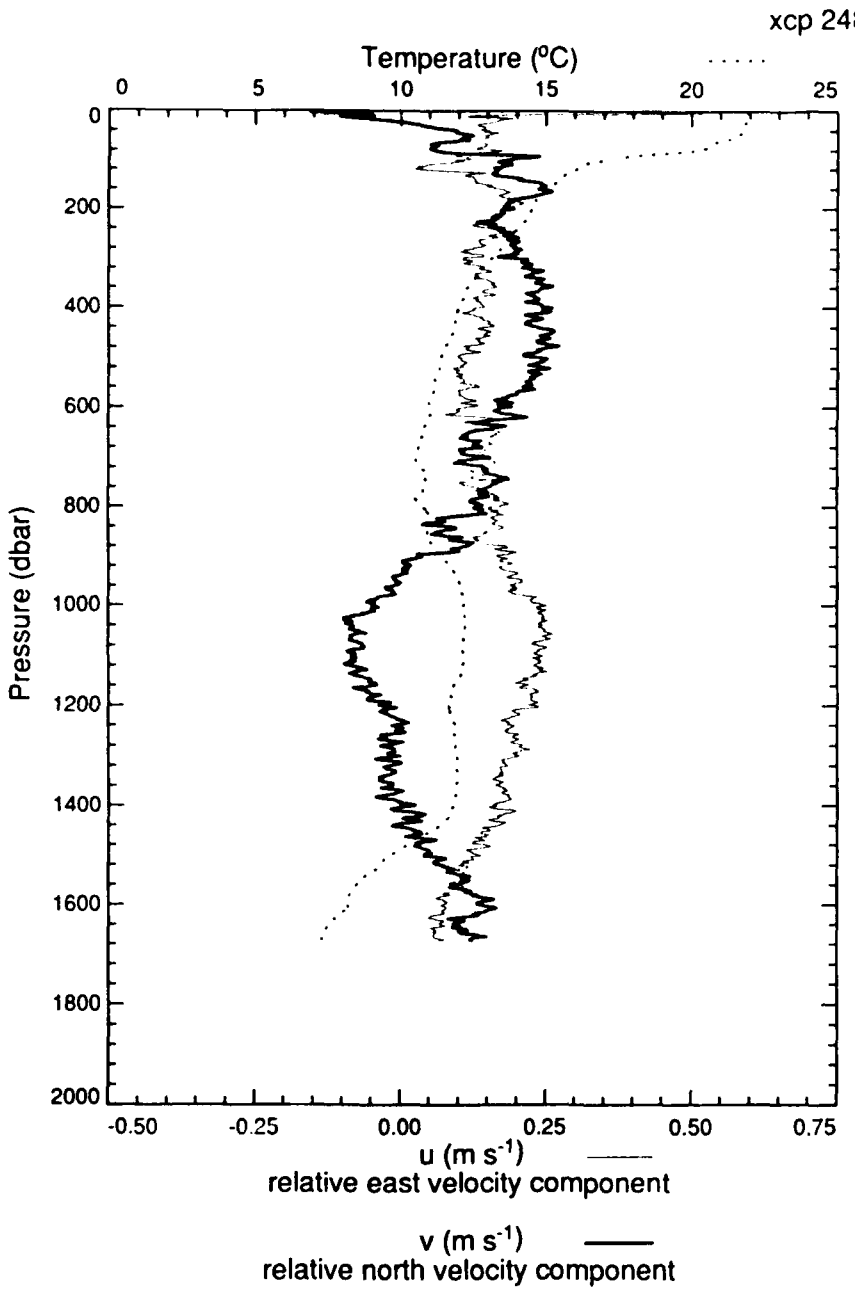
xcp 2485
Temperature (°C)
0
5
10
15
20
25
Pressure (dbar)
0
200
400
600
800
1000
1200
1400
1600
1800
2000
-0.50
-0.25
0.00
0.25
0.50
0.75
u (m s-1)
relative east velocity component
v (m s-1)
relative north velocity component

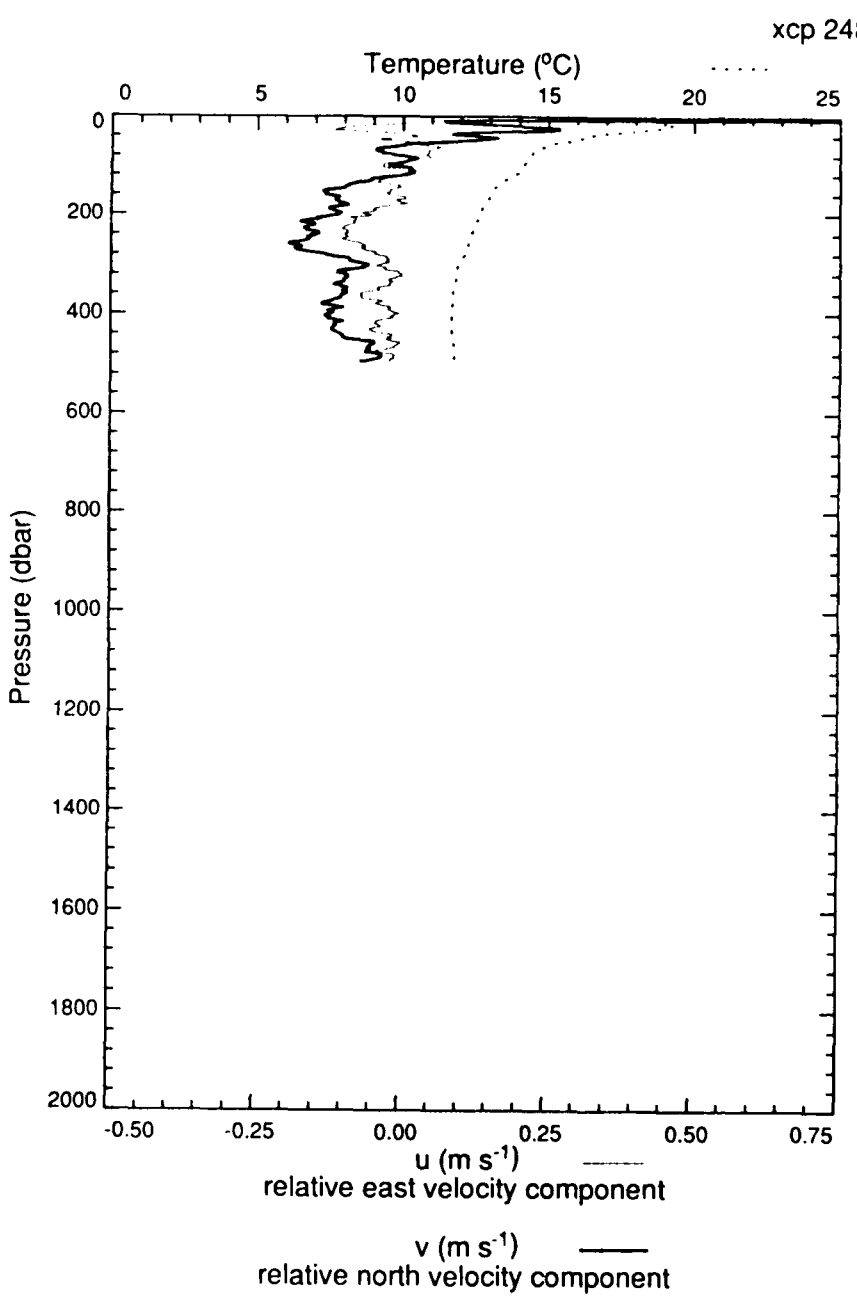
xcp 2486
Temperature (°C)
0
5
10
15
20
25
Pressure (dbar)
0
200
400
600
800
1000
1200
1400
1600
1800
2000
-0.50
-0.25
0.00
0.25
0.50
0.75
u (m s-1)
relative east velocity component
v (m s-1)
relative north velocity component

TR 8925 N41

N42 TR 8925

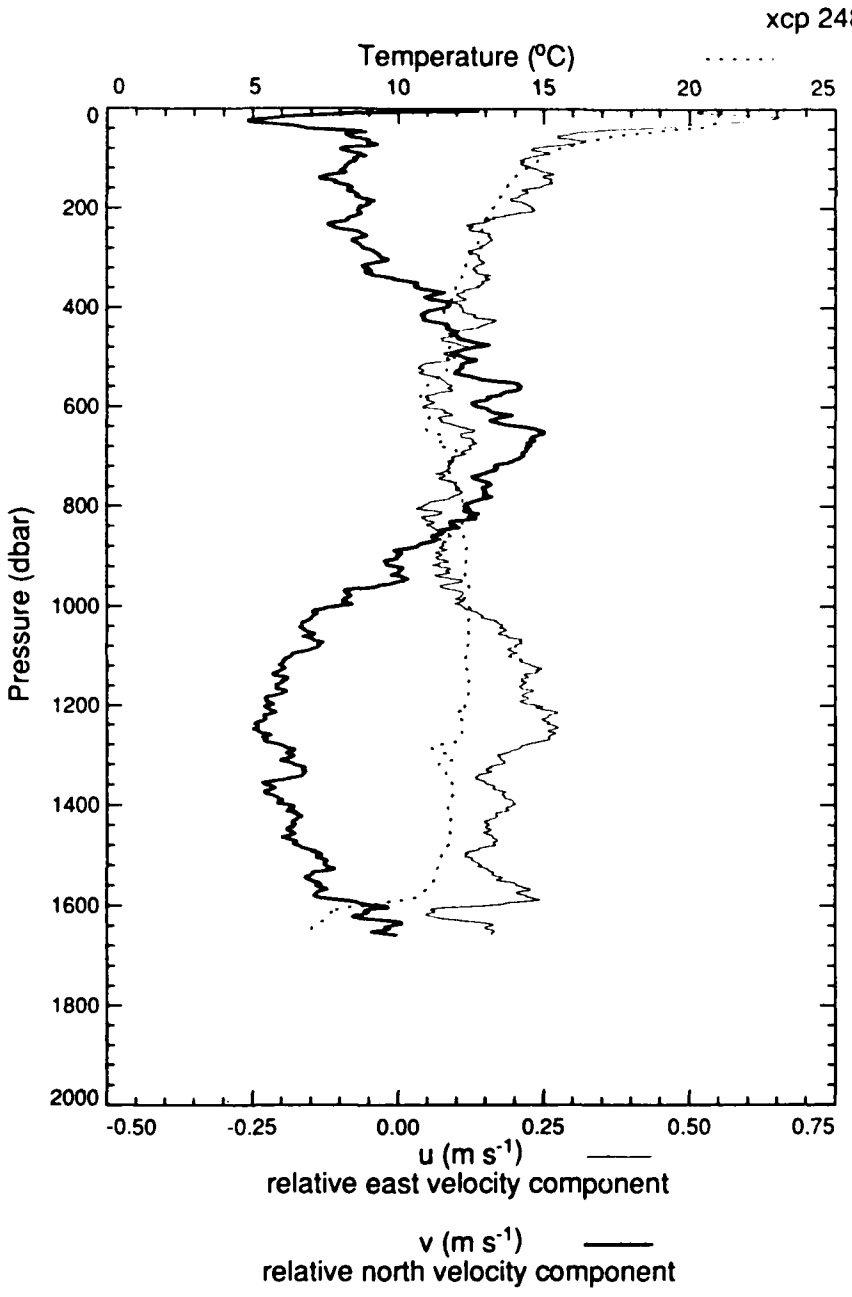
xcp 2487
Temperature (°C)
0
5
10
15
20
25
Pressure (dbar)
0
200
400
600
800
1000
1200
1400
1600
1800
2000
-0.50
-0.25
0.00
0.25
0.50
0.75
u (m s-1)
relative east velocity component
v (m s-1)
relative north velocity component

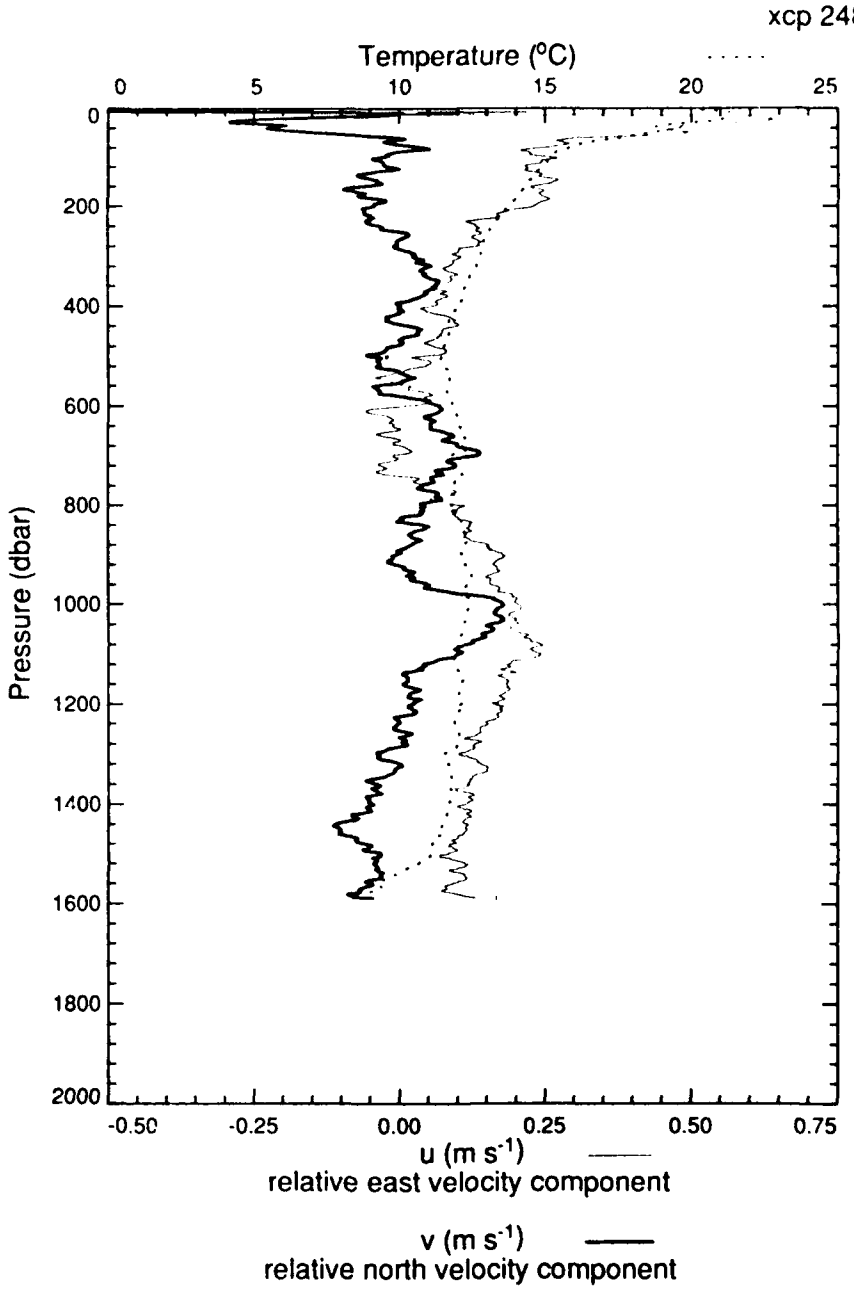
xcp 2488
Temperature (°C)
0
5
10
15
20
25
Pressure (dbar)
0
200
400
600
800
1000
1200
1400
1600
1800
2000
-0.50
-0.25
0.00
0.25
0.50
0.75
u (m s-1)
relative east velocity component
v (m s-1)
relative north velocity component

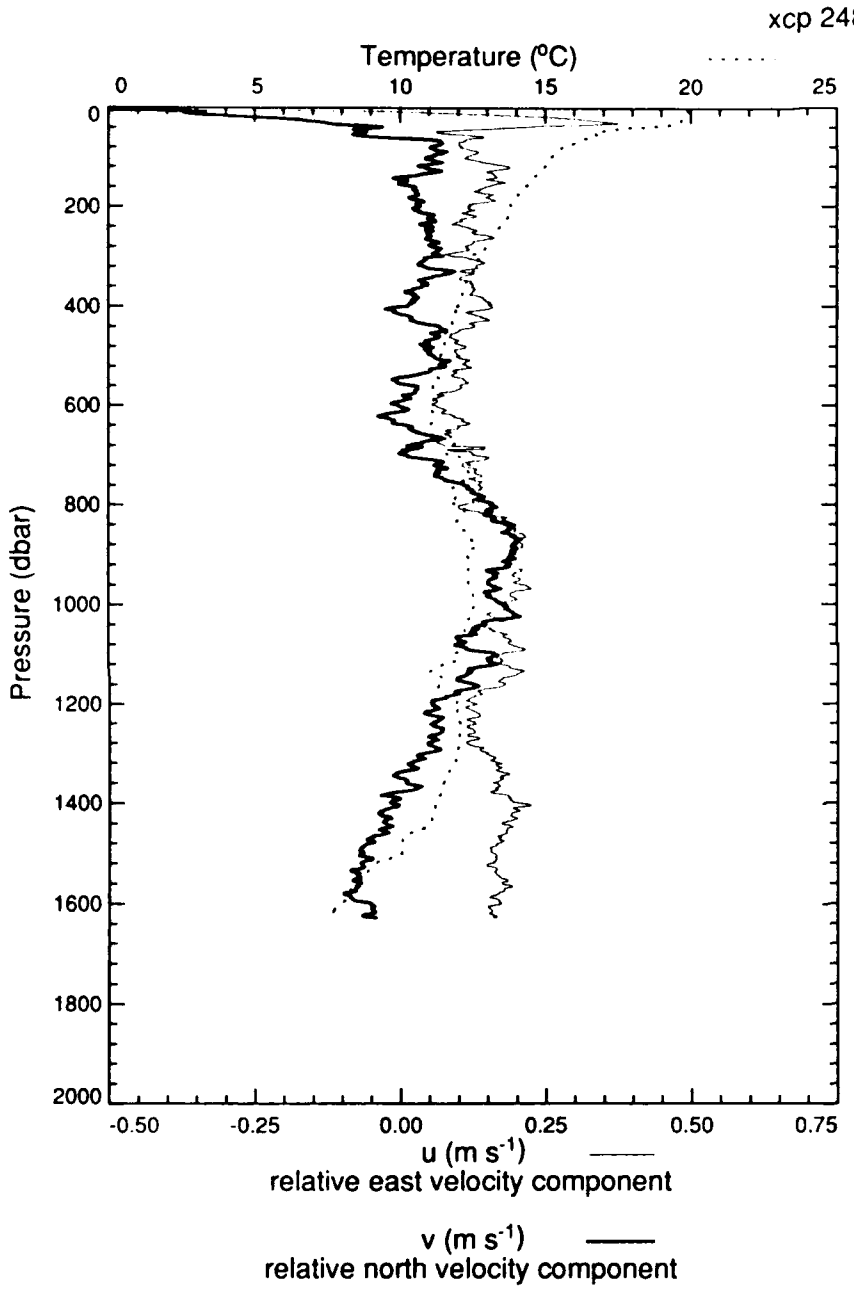
xcp 2489
Temperature (°C)
0
5
10
15
20
25
Pressure (dbar)
0
200
400
600
800
1000
1200
1400
1600
1800
2000
-0.50
-0.25
0.00
0.25
0.50
0.75
u (m s-1)
relative east velocity component
v (m s-1)
relative north velocity component

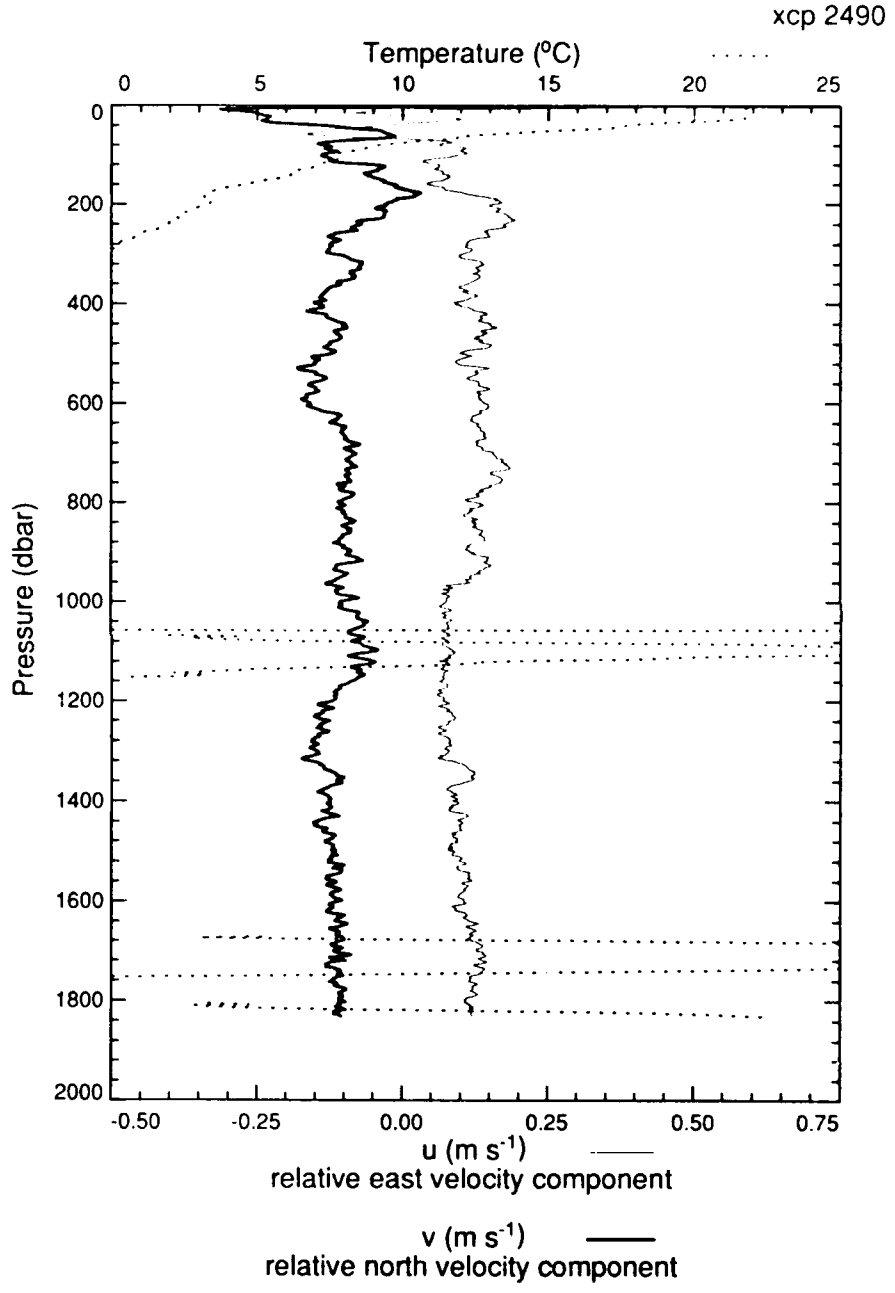
xcp 2490
Temperature (°C)
0
5
10
15
20
25
Pressure (dbar)
0
200
400
600
800
1000
1200
1400
1600
1800
2000
-0.50
-0.25
0.00
0.25
0.50
0.75
u (m s-1)
relative east velocity component
v (m s-1)
relative north velocity component

N44 TR 8925

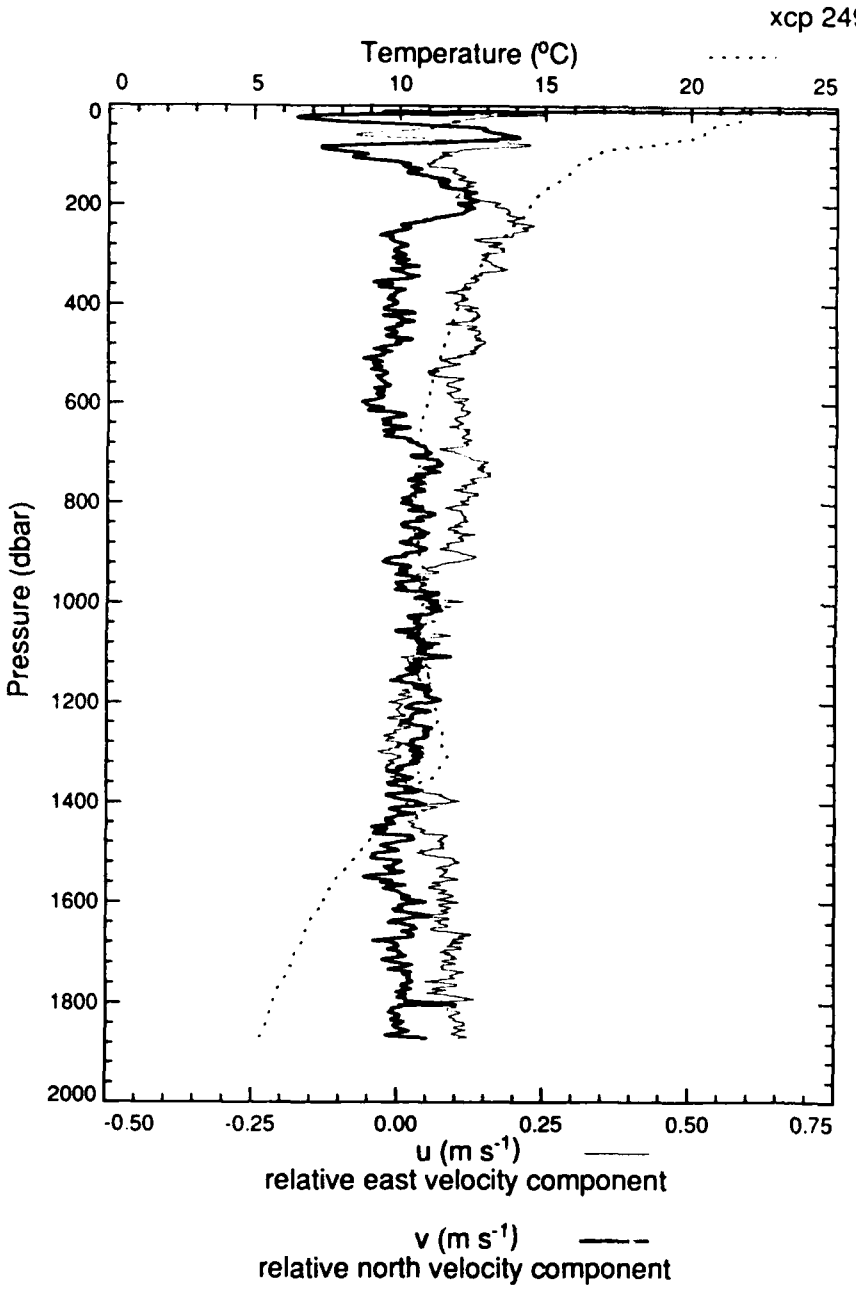
xcp 2491
Temperature (°C)
0
5
10
15
20
25
Pressure (dbar)
0
200
400
600
800
1000
1200
1400
1600
1800
2000
-0.50
-0.25
0.00
0.25
0.50
0.75
u (m s-1)
relative east velocity component
v (m s-1)
relative north velocity component

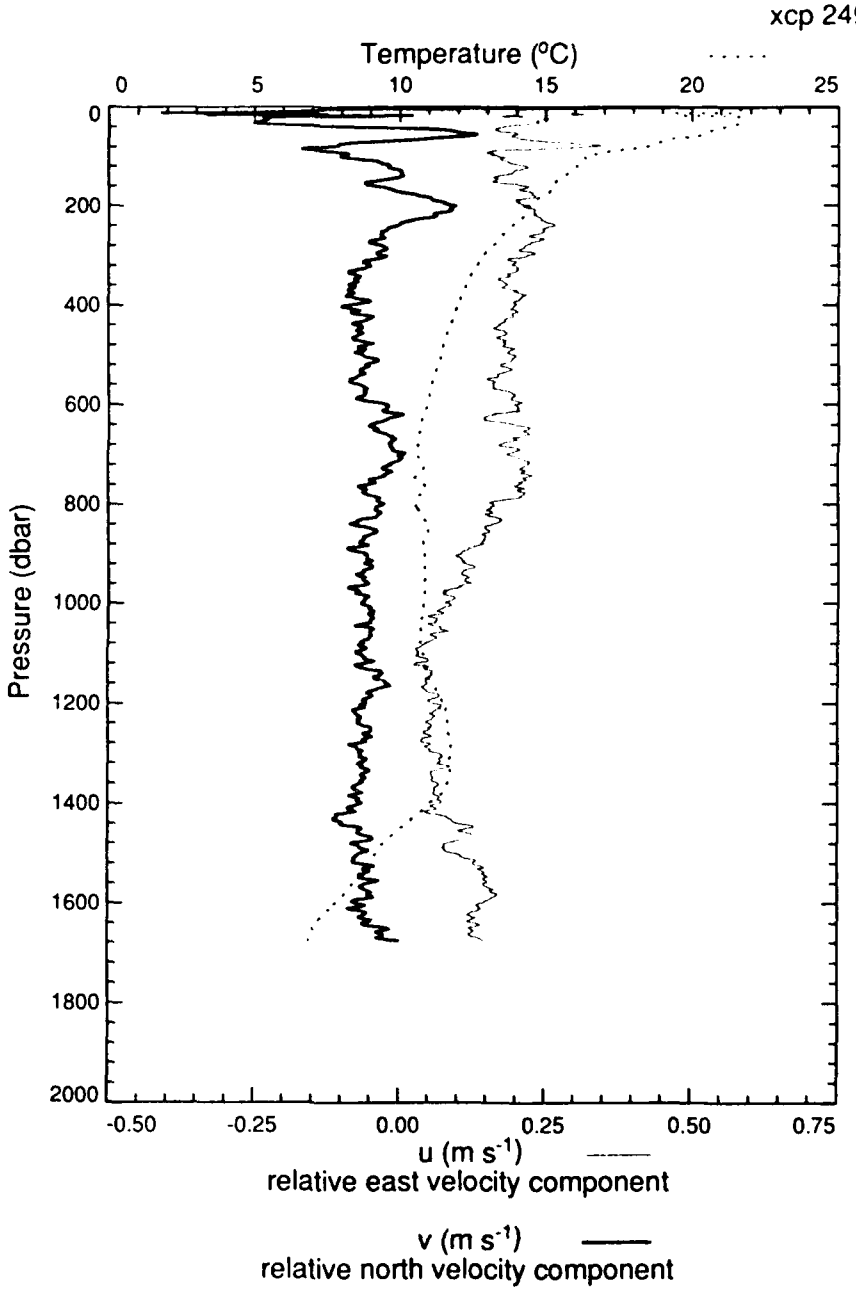
xcp 2492
Temperature (°C)
0
5
10
15
20
25
Pressure (dbar)
0
200
400
600
800
1000
1200
1400
1600
1800
2000
-0.50
-0.25
0.00
0.25
0.50
0.75
u (m s-1)
relative east velocity component
v (m s-1)
relative north velocity component

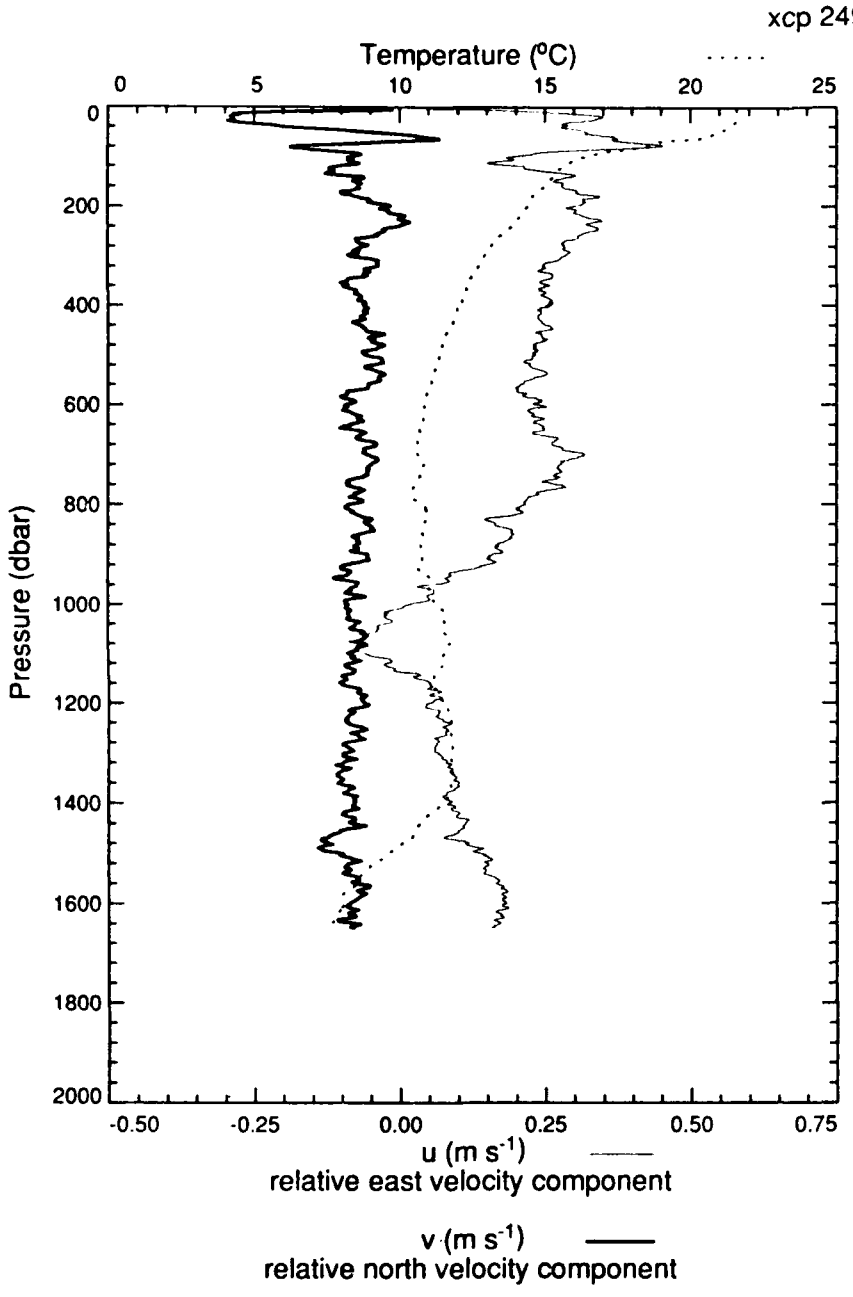
xcp 2493
Temperature (°C)
0
5
10
15
20
25
Pressure (dbar)
0
200
400
600
800
1000
1200
1400
1600
1800
2000
-0.50
-0.25
0.00
0.25
0.50
0.75
u (m s-1)
relative east velocity component
v (m s-1)
relative north velocity component

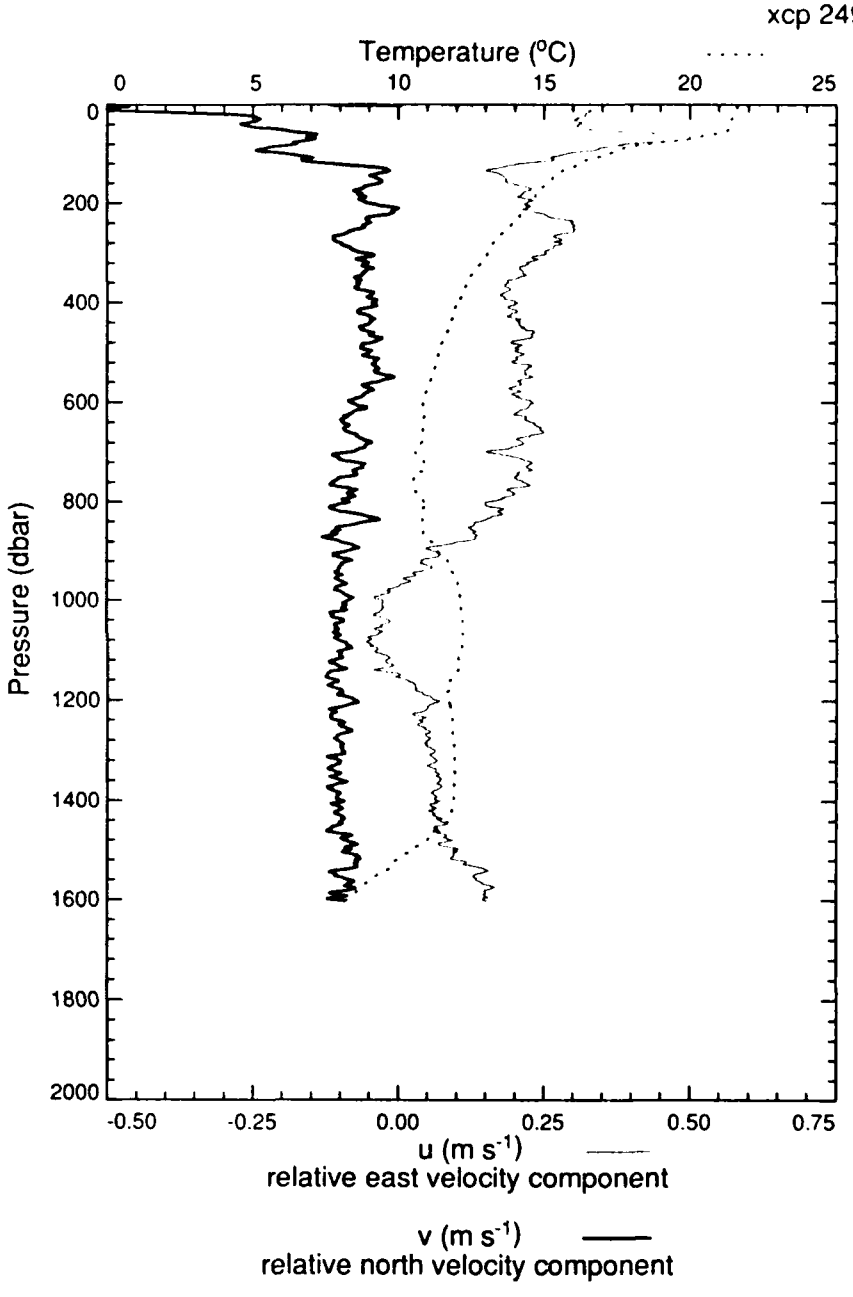
xcp 2494
Temperature (°C)
0
5
10
15
20
25
Pressure (dbar)
0
200
400
600
800
1000
1200
1400
1600
1800
2000
-0.50
-0.25
0.00
0.25
0.50
0.75
u (m s-1)
relative east velocity component
v (m s-1)
relative north velocity component

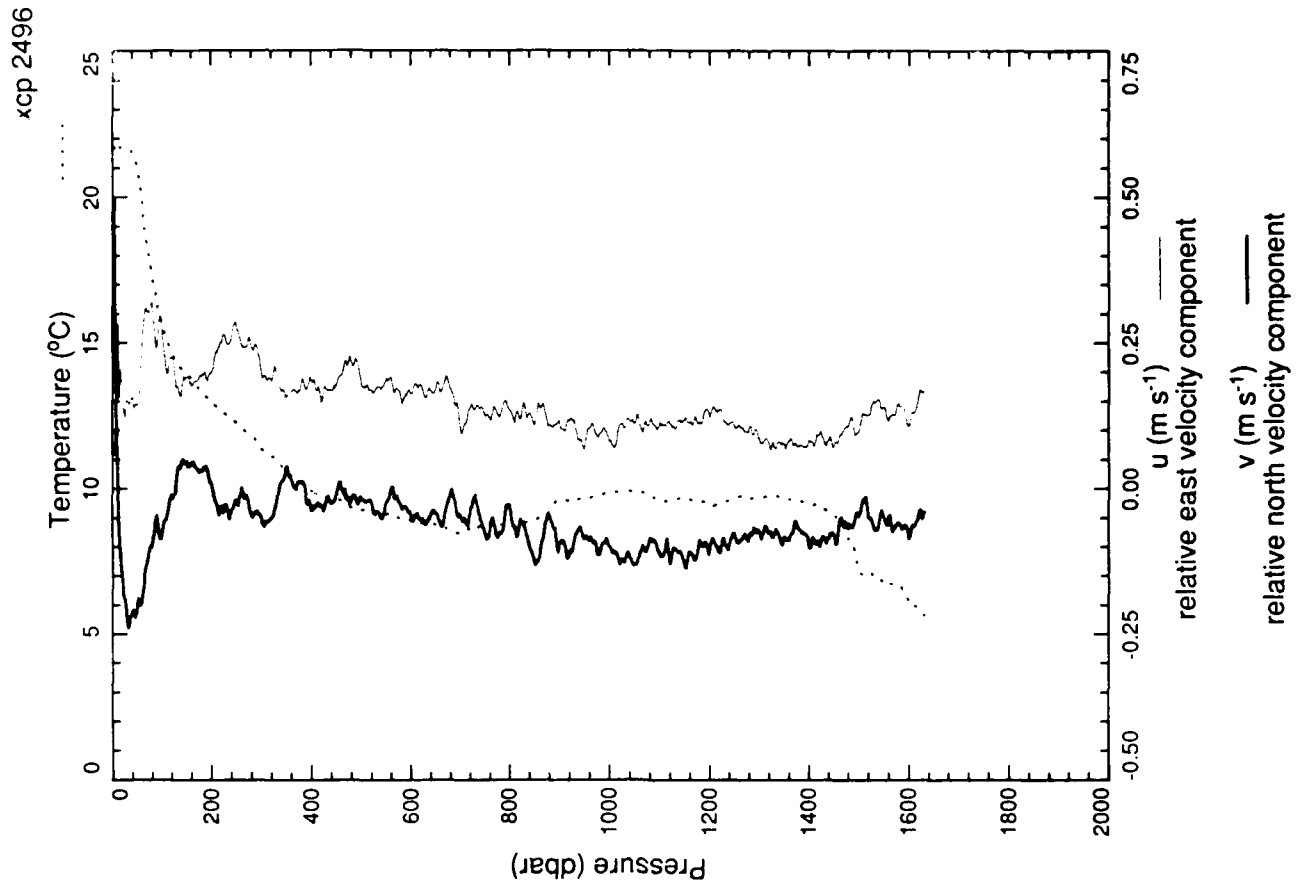
xcp 2496
Temperature (°C)
Pressure (dbar)
u (m s-1)
relative east velocity component
v (m s-1)
relative north velocity component

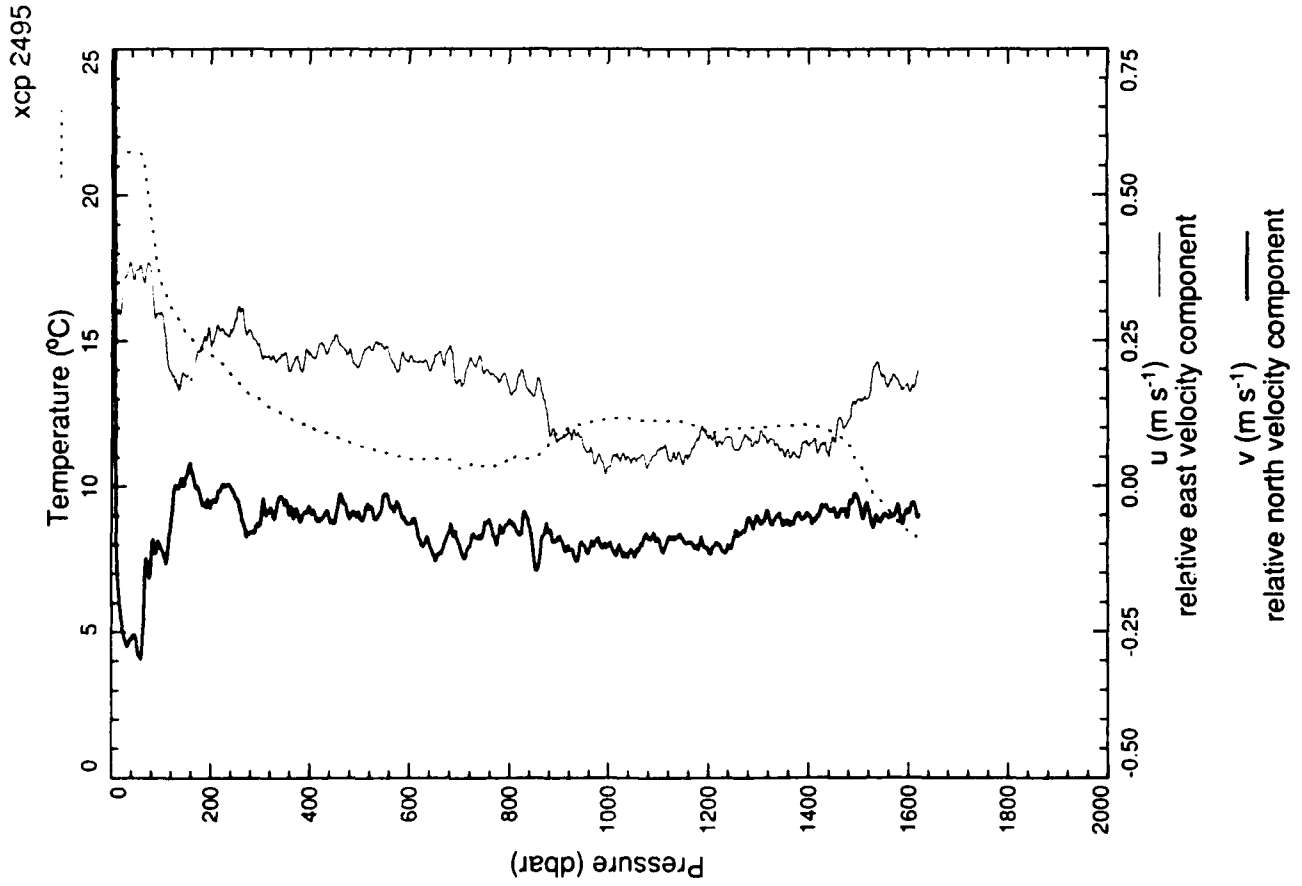
xcp 2495
Temperature (°C)
Pressure (dbar)
u (m s-1)
relative east velocity component
v (m s-1)
relative north velocity component

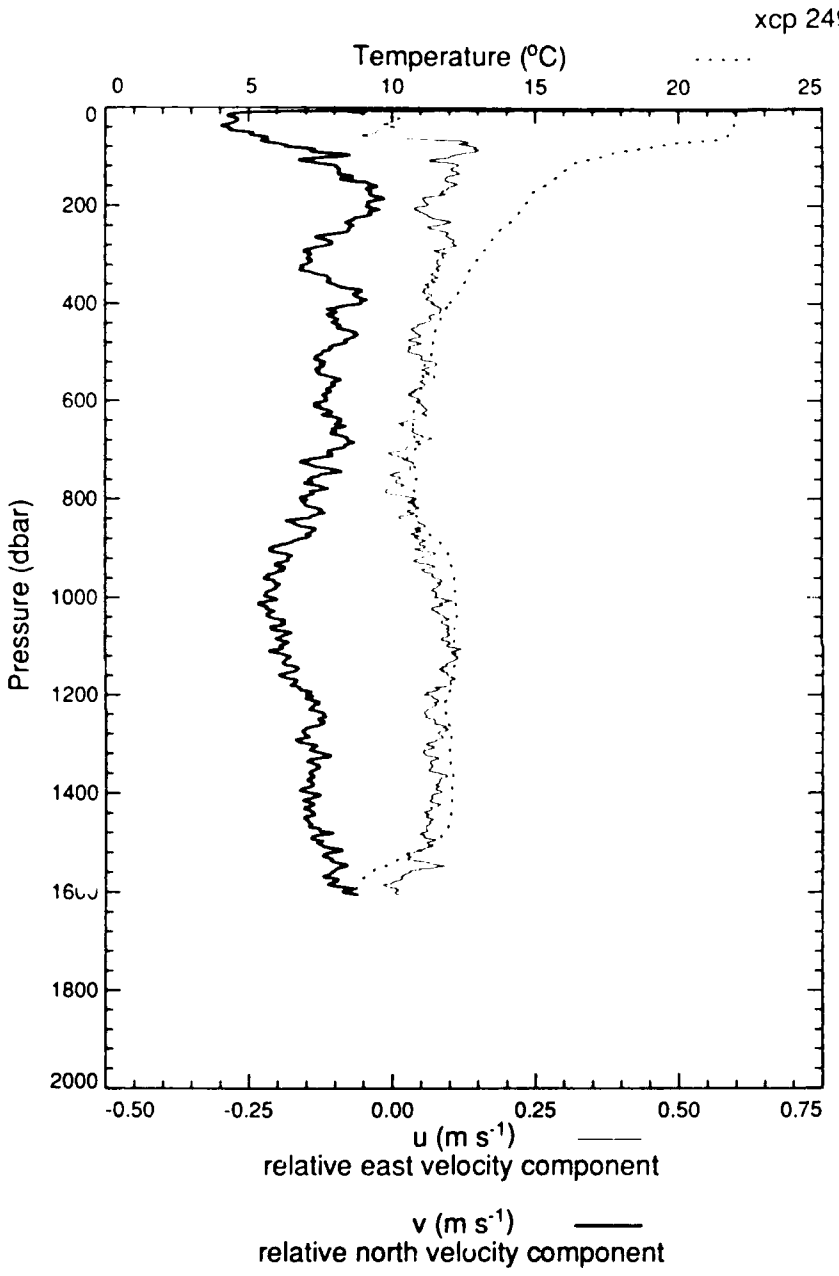
xcp 2497
Temperature (°C)
0
5
10
15
20
25
Pressure (dbar)
0
200
400
600
800
1000
1200
1400
1600
1800
2000
-0.50
-0.25
0.00
0.25
0.50
0.75
u (m s-1)
relative east velocity component
v (m s-1)
relative north velocity component

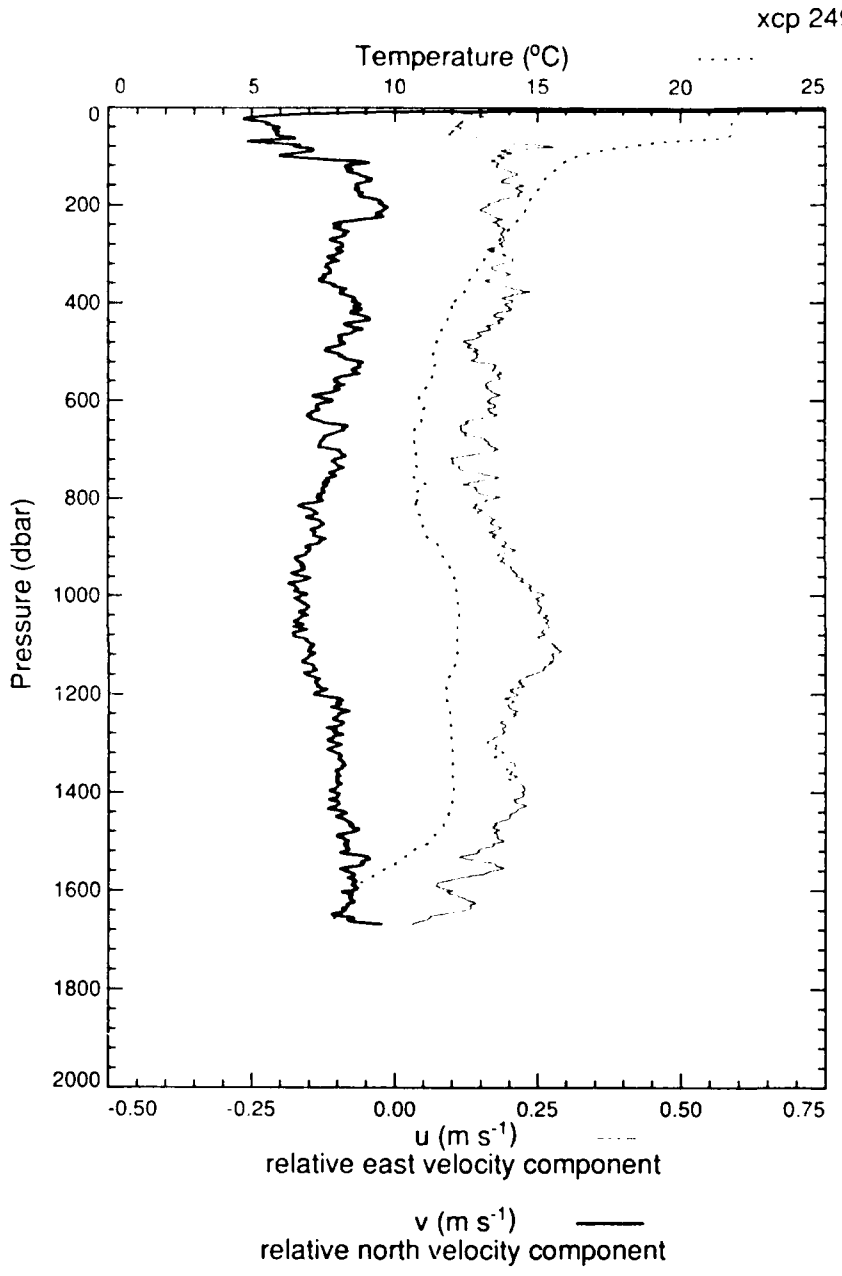
xcp 2498
Temperature (°C)
0
5
10
15
20
25
Pressure (dbar)
0
200
400
600
800
1000
1200
1400
1600
1800
2000
-0.50
-0.25
0.00
0.25
0.50
0.75
u (m s-1)
relative east velocity component
v (m s-1)
relative north velocity component

TR 8925 N47

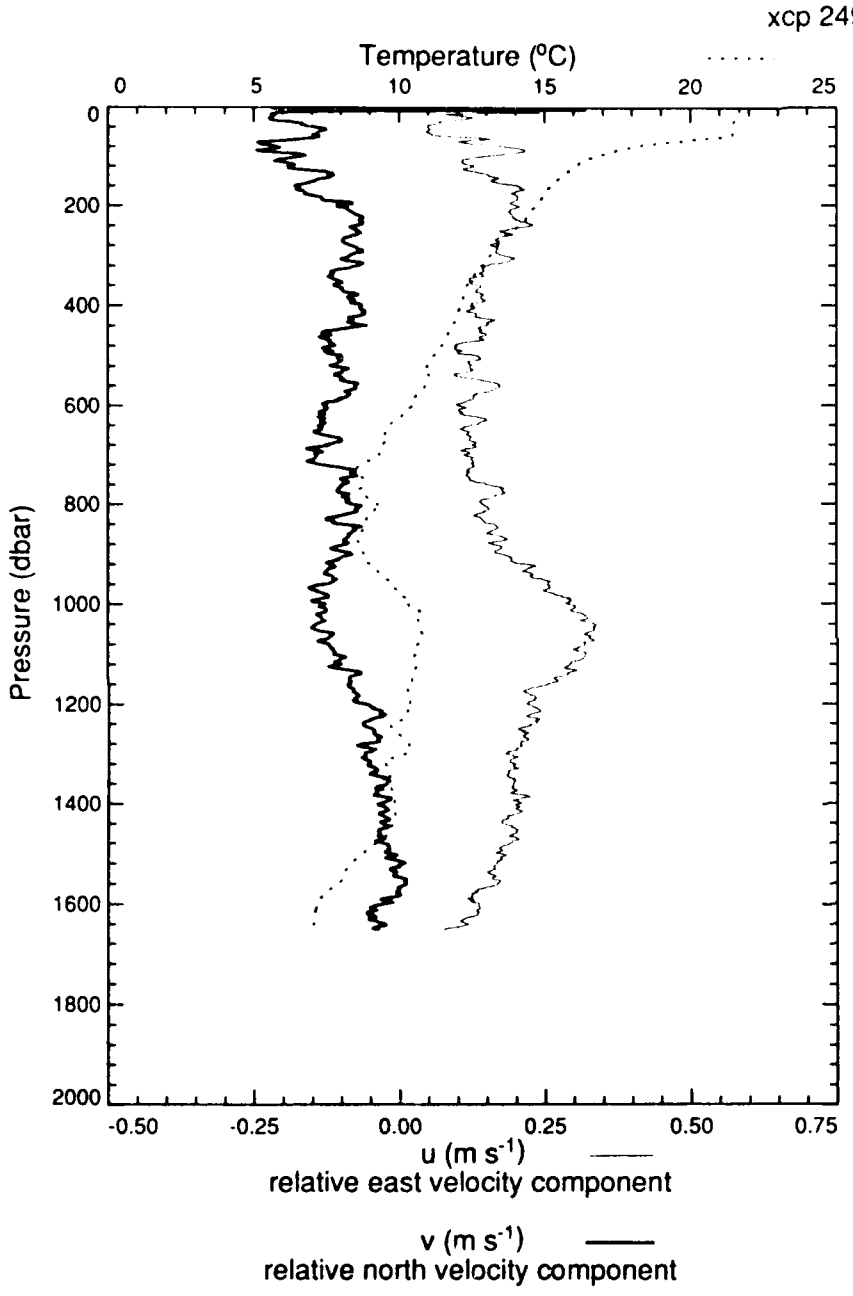
xcp 2499
Temperature (°C)
0
5
10
15
20
25
Pressure (dbar)
0
200
400
600
800
1000
1200
1400
1600
1800
2000
-0.50
-0.25
0.00
0.25
0.50
0.75
u (m s-1)
relative east velocity component
v (m s-1)
relative north velocity component

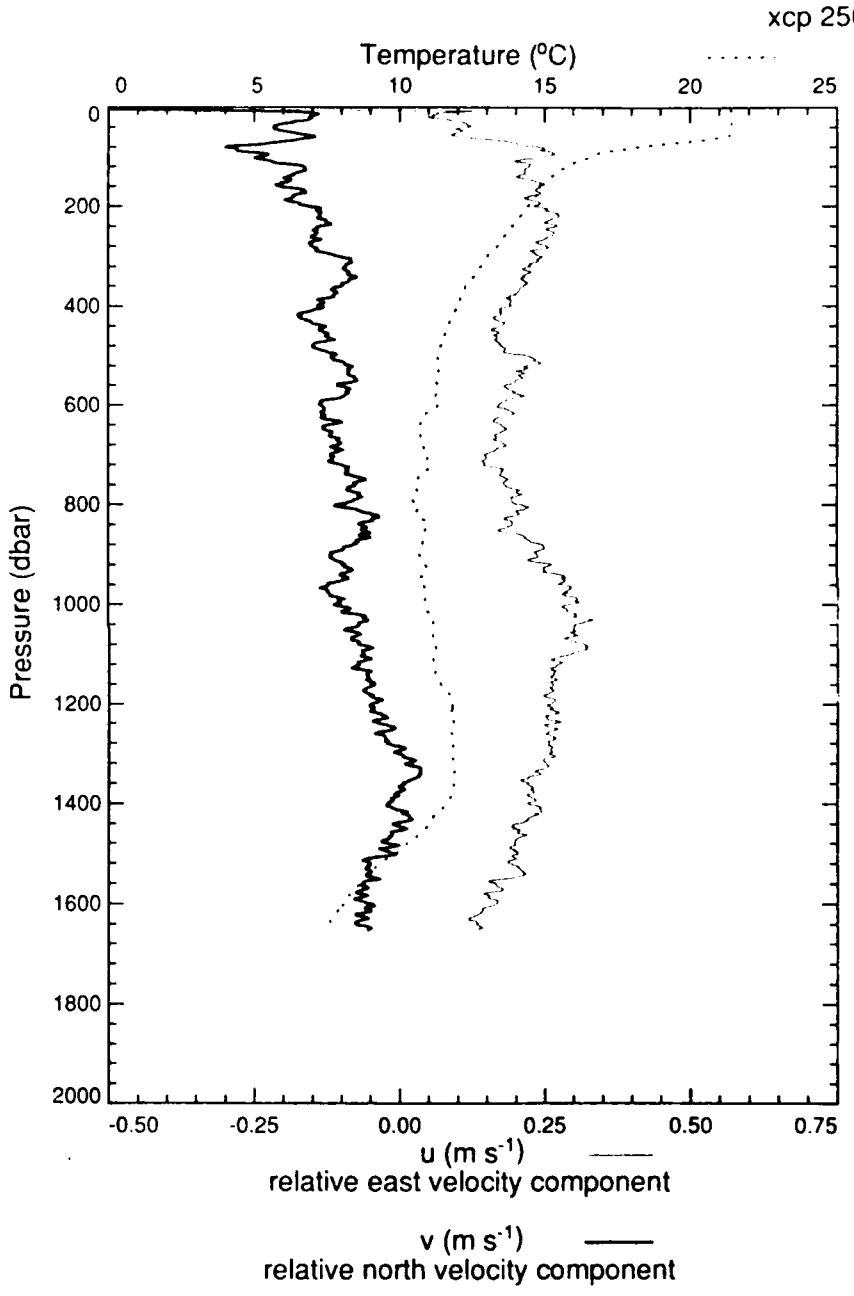
xcp 2500
Temperature (°C)
0
5
10
15
20
25
Pressure (dbar)
0
200
400
600
800
1000
1200
1400
1600
1800
2000
-0.50
-0.25
0.00
0.25
0.50
0.75
u (m s-1)
relative east velocity component
v (m s-1)
relative north velocity component

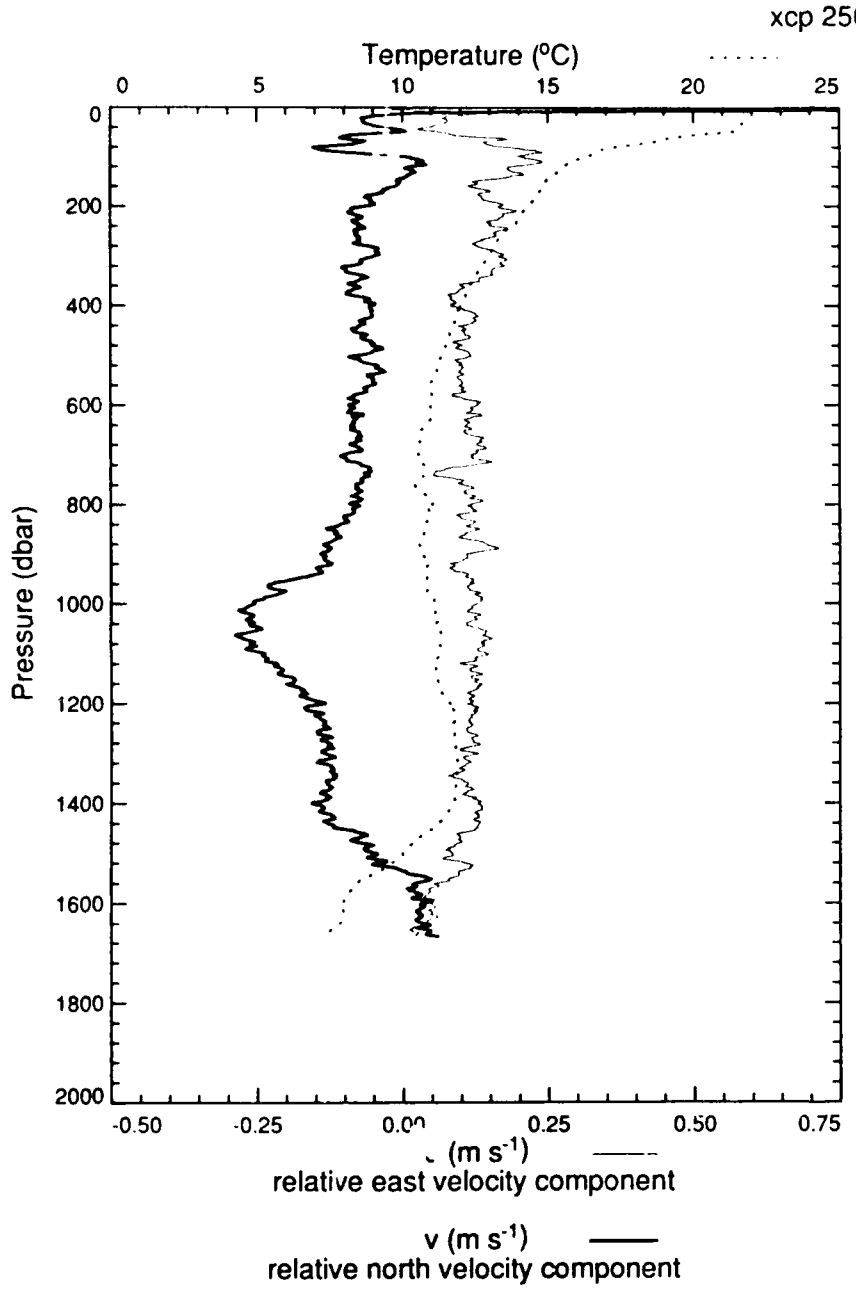
xcp 2501
Temperature (°C)
0
5
10
15
20
25
Pressure (dbar)
0
200
400
600
800
1000
1200
1400
1600
1800
2000
-0.50
-0.25
0.00
0.25
0.50
0.75
u (m s-1)
relative east velocity component
v (m s-1)
relative north velocity component

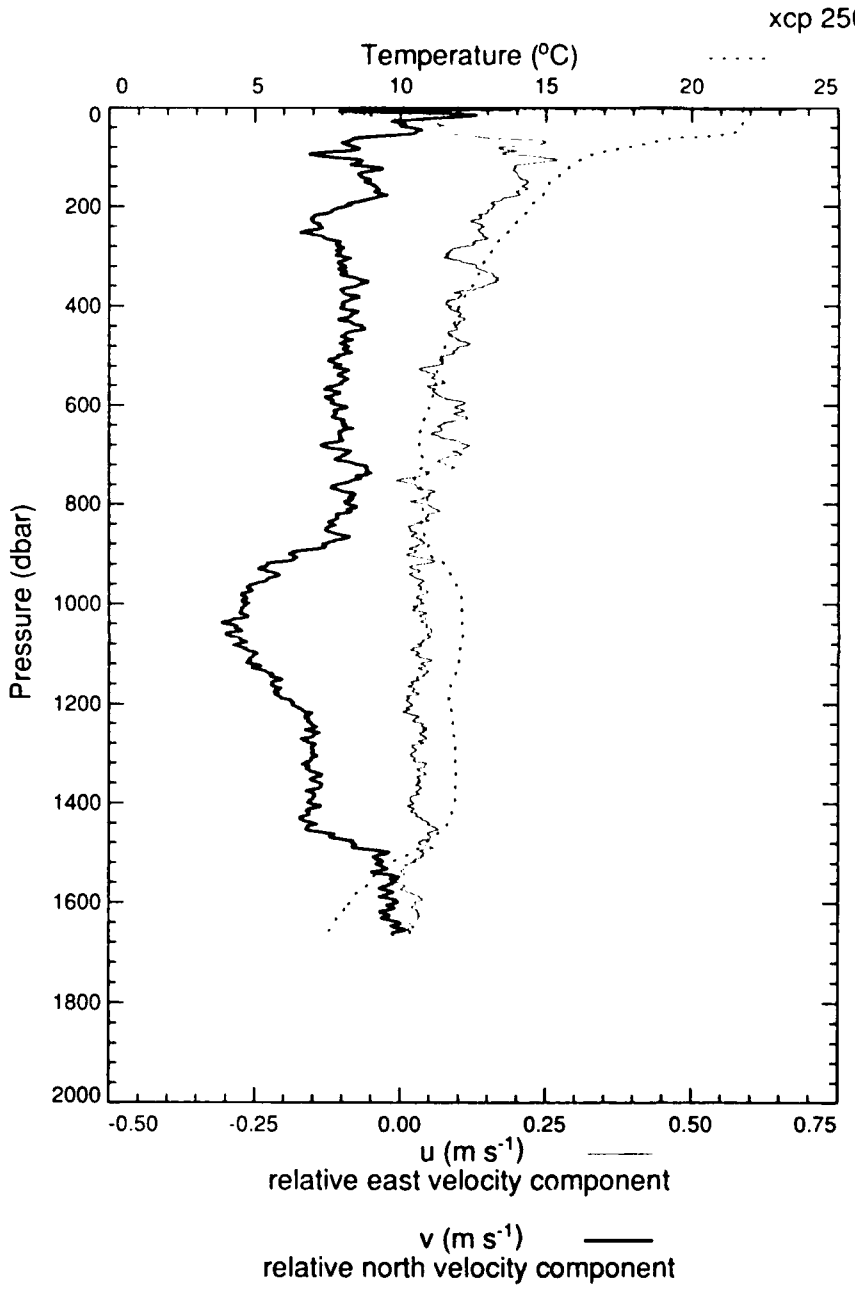
xcp 2502
Temperature (°C)
0
5
10
15
20
25
Pressure (dbar)
0
200
400
600
800
1000
1200
1400
1600
1800
2000
-0.50
-0.25
0.00
0.25
0.50
0.75
u (m s-1)
relative east velocity component
v (m s-1)
relative north velocity component

TR 8925 N49

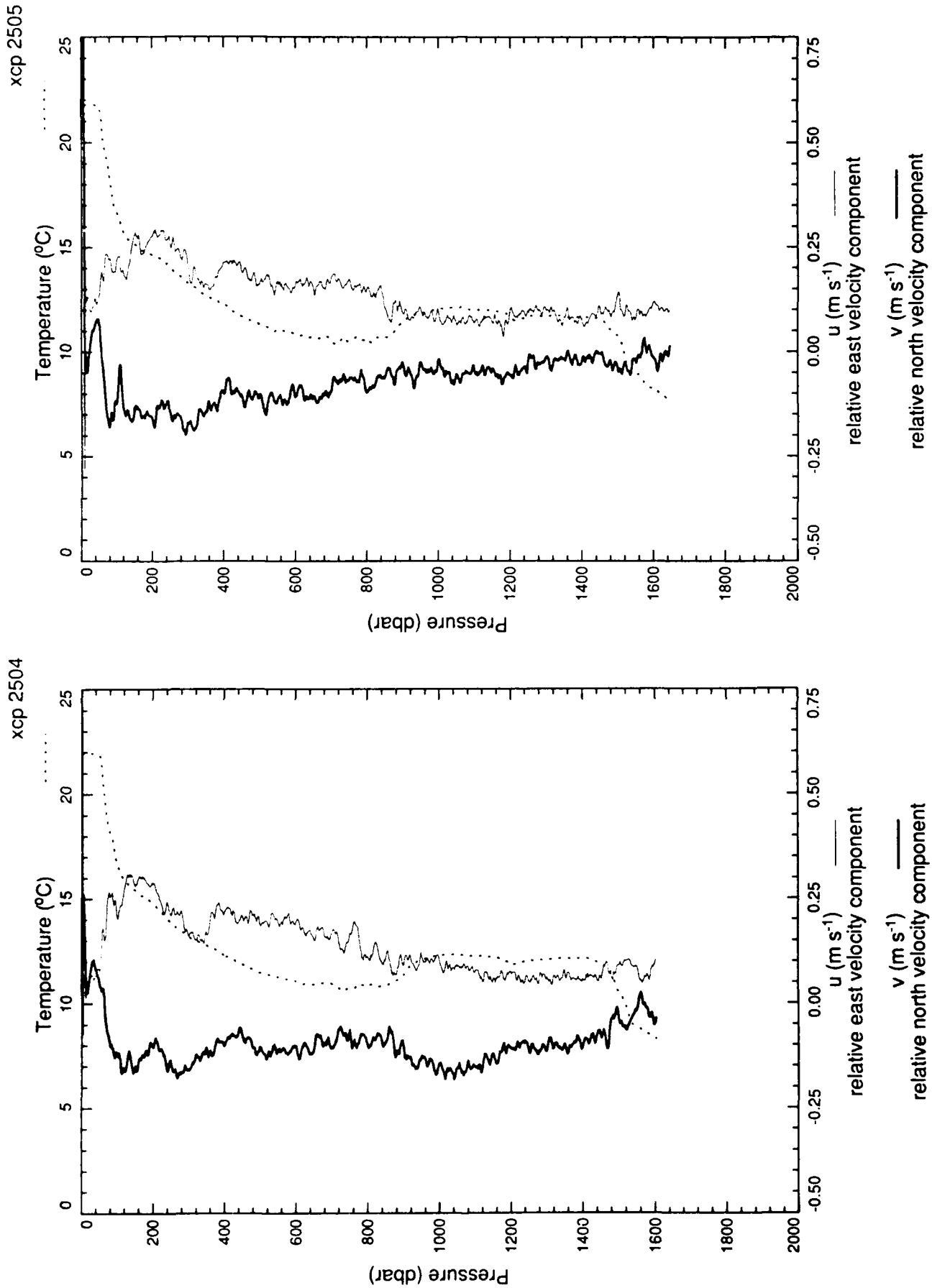
xcp 2505
Temperature (°C)
Pressure (dbar)
u (m s-1)
relative east velocity component
v (m s-1)
relative north velocity component
xcp 2504
Temperature (°C)
Pressure (dbar)
u (m s-1)
relative east velocity component
v (m s-1)
relative north velocity component

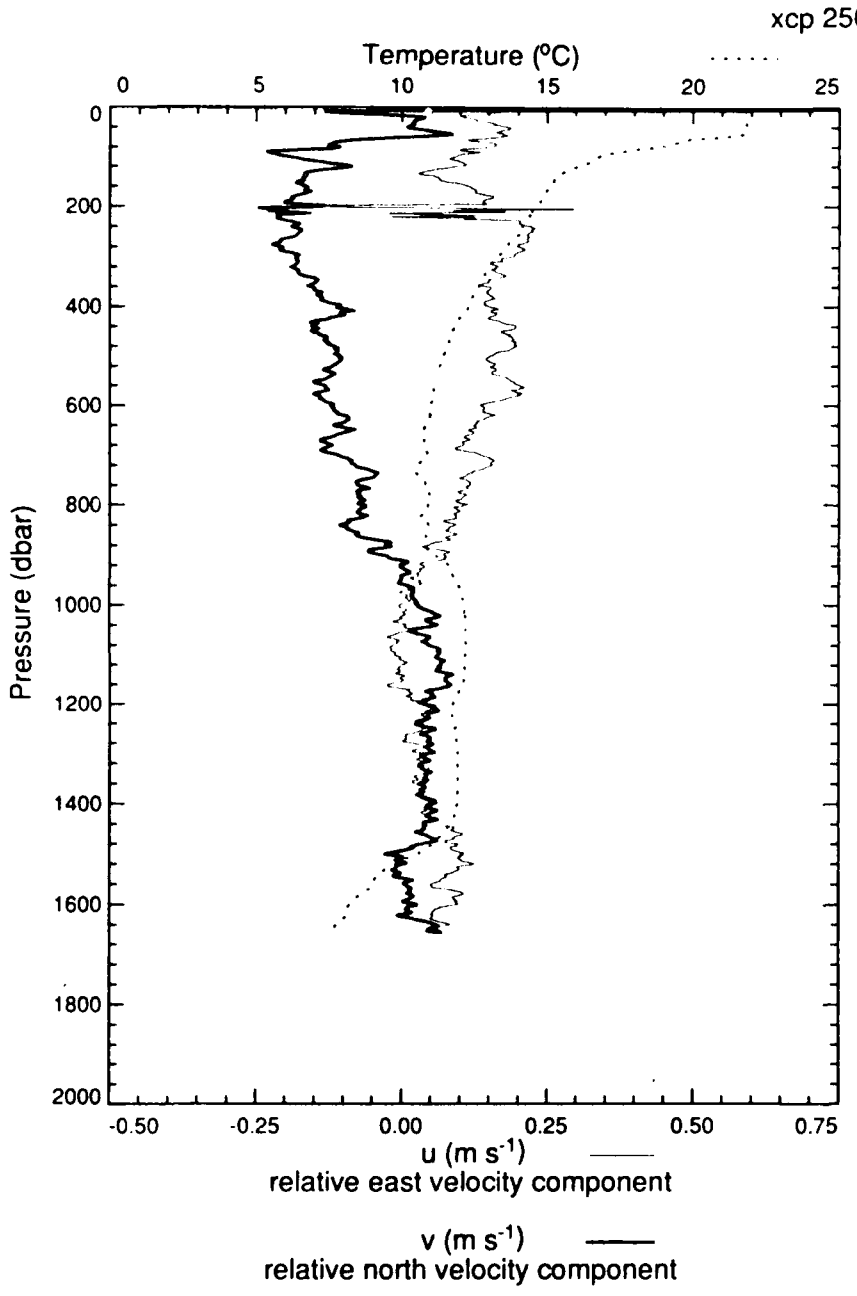
xcp 2506
Temperature (°C)
0
5
10
15
20
25
Pressure (dbar)
0
200
400
600
800
1000
1200
1400
1600
1800
2000
-0.50
-0.25
0.00
0.25
0.50
0.75
u (m s-1)
relative east velocity component
v (m s-1)
relative north velocity component

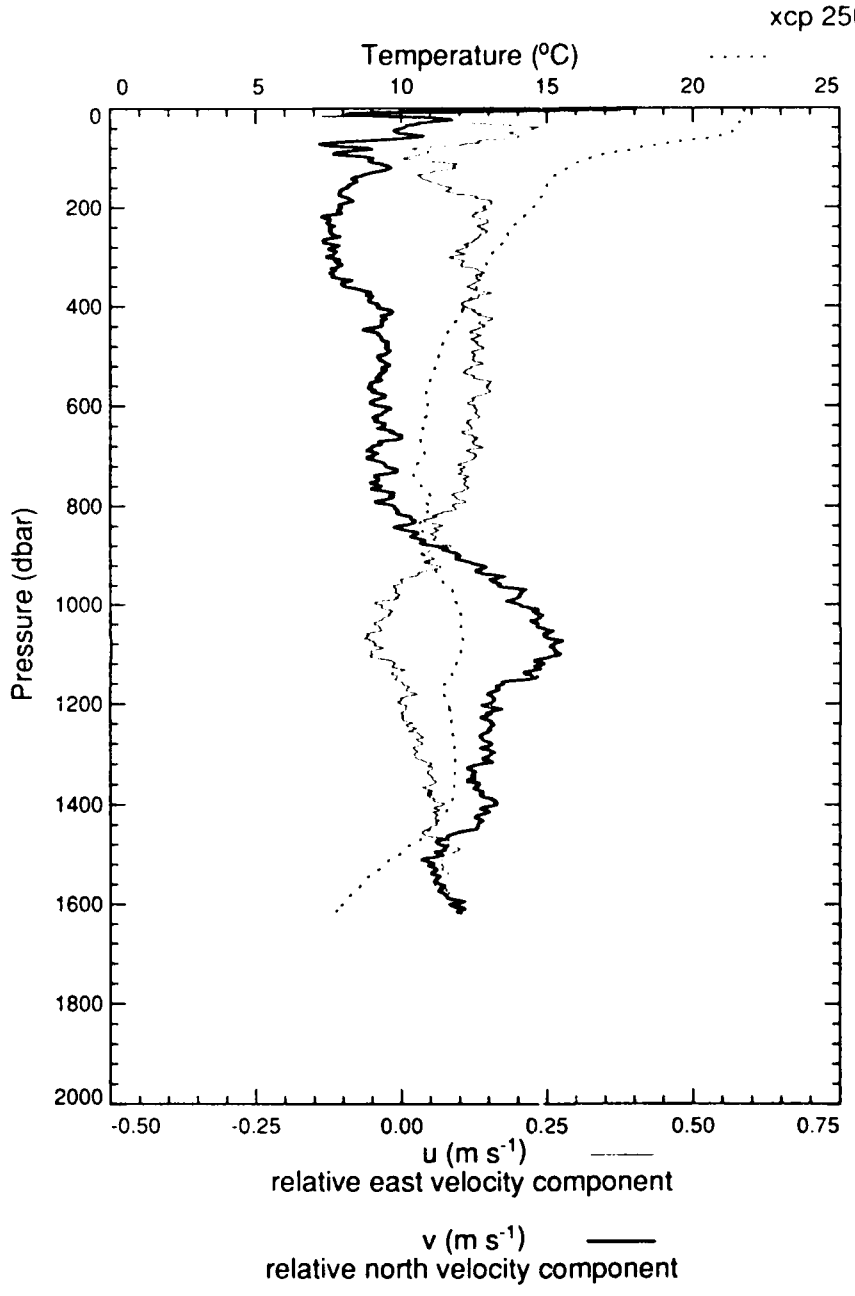
xcp 2507
Temperature (°C)
0
5
10
15
20
25
Pressure (dbar)
0
200
400
600
800
1000
1200
1400
1600
1800
2000
-0.50
-0.25
0.00
0.25
0.50
0.75
u (m s-1)
relative east velocity component
v (m s-1)
relative north velocity component

TR 8925 N51

N52 TR 8925

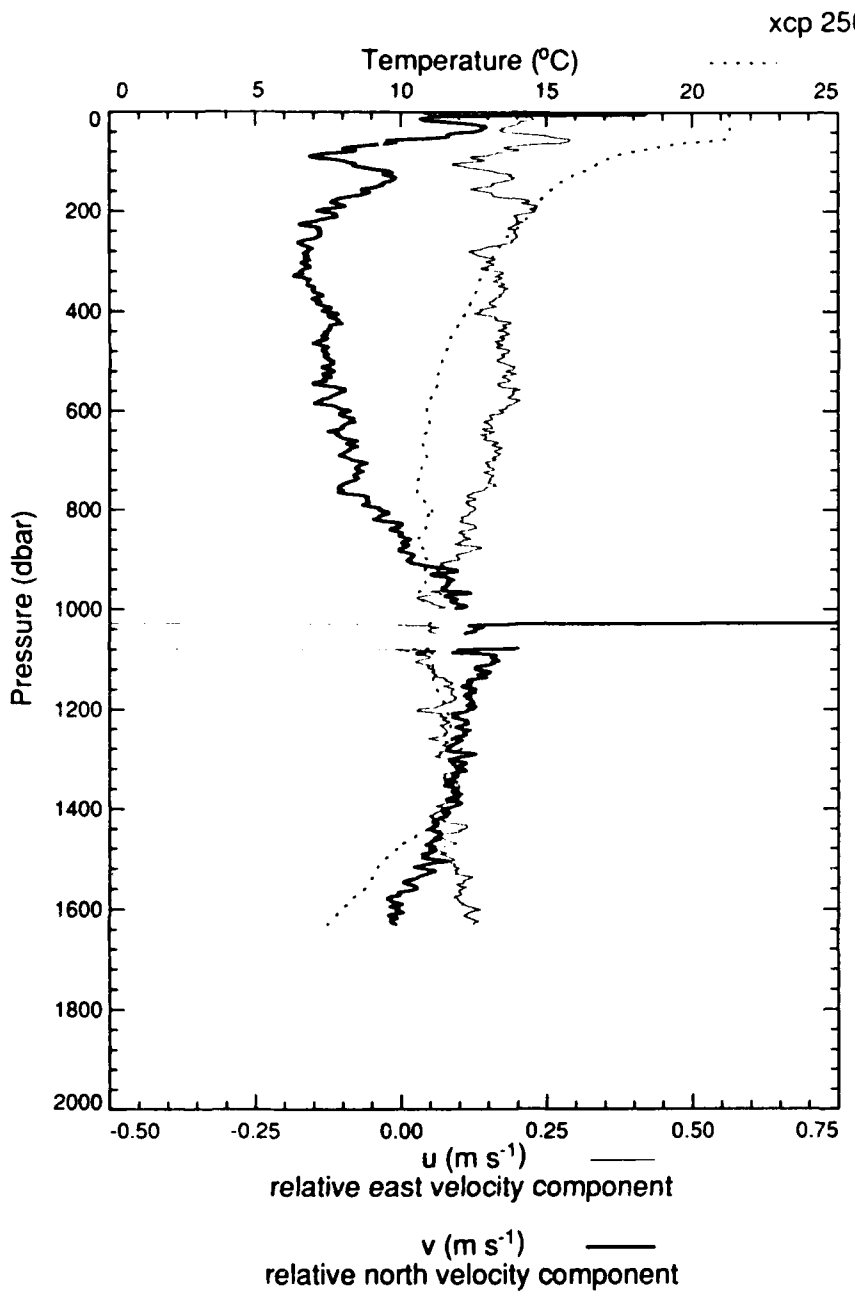
xcp 2508
Temperature (°C)
0
5
10
15
20
25
Pressure (dbar)
0
200
400
600
800
1000
1200
1400
1600
1800
2000
-0.50
-0.25
0.00
0.25
0.50
0.75
u (m s-1)
relative east velocity component
v (m s-1)
relative north velocity component

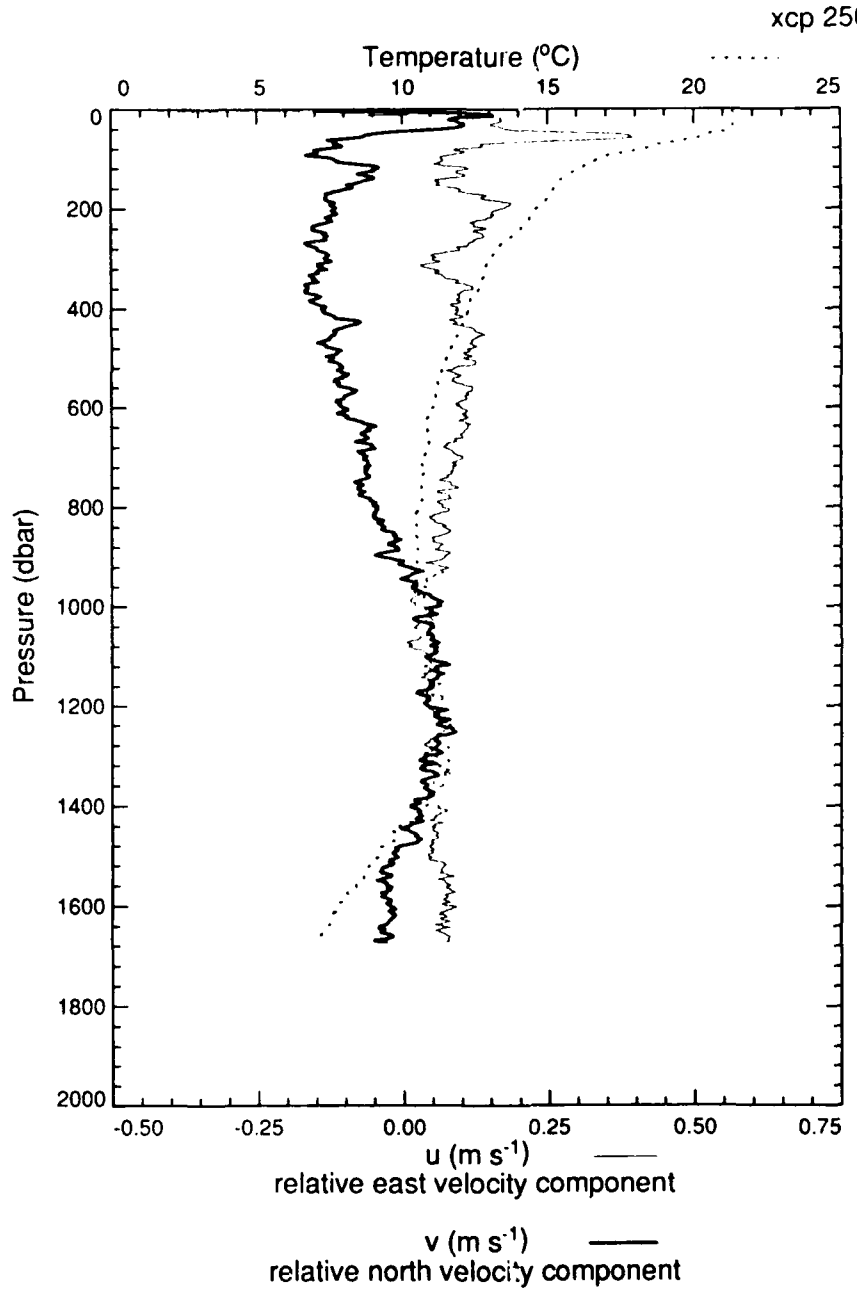
xcp 2509
Temperature (°C)
0
5
10
15
20
25
Pressure (dbar)
0
200
400
600
800
1000
1200
1400
1600
1800
2000
-0.50
-0.25
0.00
0.25
0.50
0.75
u (m s-1)
relative east velocity component
v (m s-1)
relative north velocity component

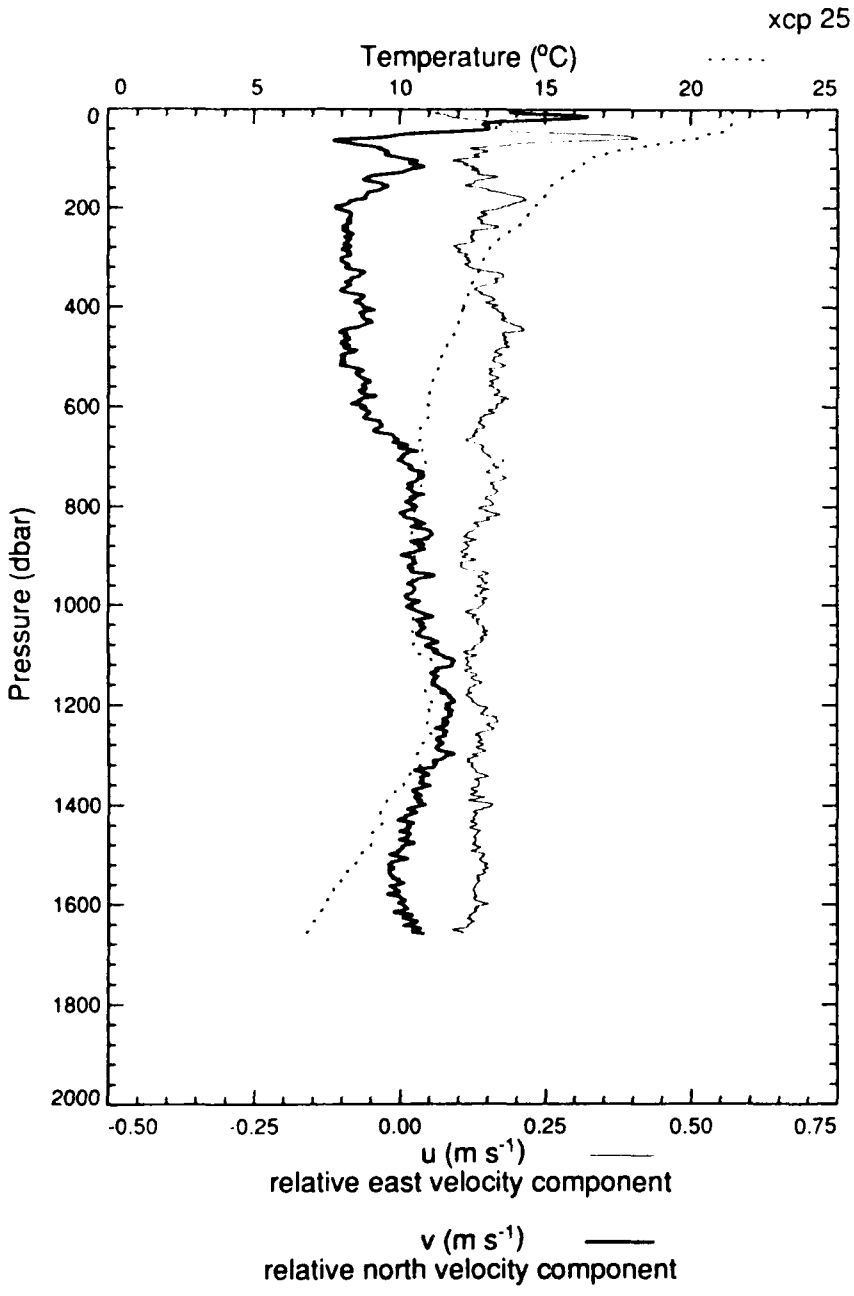
xcp 2510
Temperature (°C)
0
5
10
15
20
25
Pressure (dbar)
0
200
400
600
800
1000
1200
1400
1600
1800
2000
-0.50
-0.25
0.00
0.25
0.50
0.75
u (m s-1)
relative east velocity component
v (m s-1)
relative north velocity component

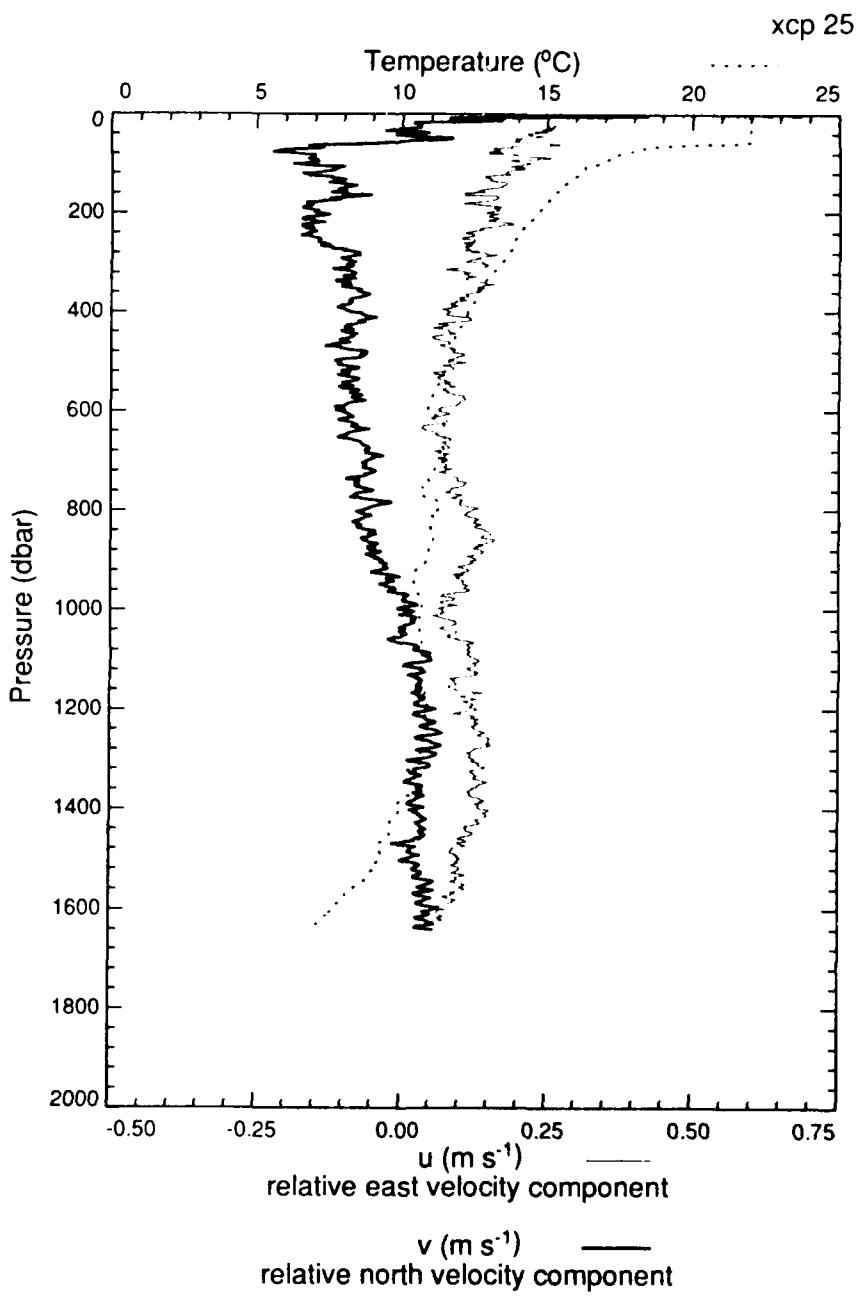
xcp 2511
Temperature (°C)
0
5
10
15
20
25
Pressure (dbar)
0
200
400
600
800
1000
1200
1400
1600
1800
2000
-0.50
-0.25
0.00
0.25
0.50
0.75
u (m s-1)
relative east velocity component
v (m s-1)
relative north velocity component

N54 TR 8925

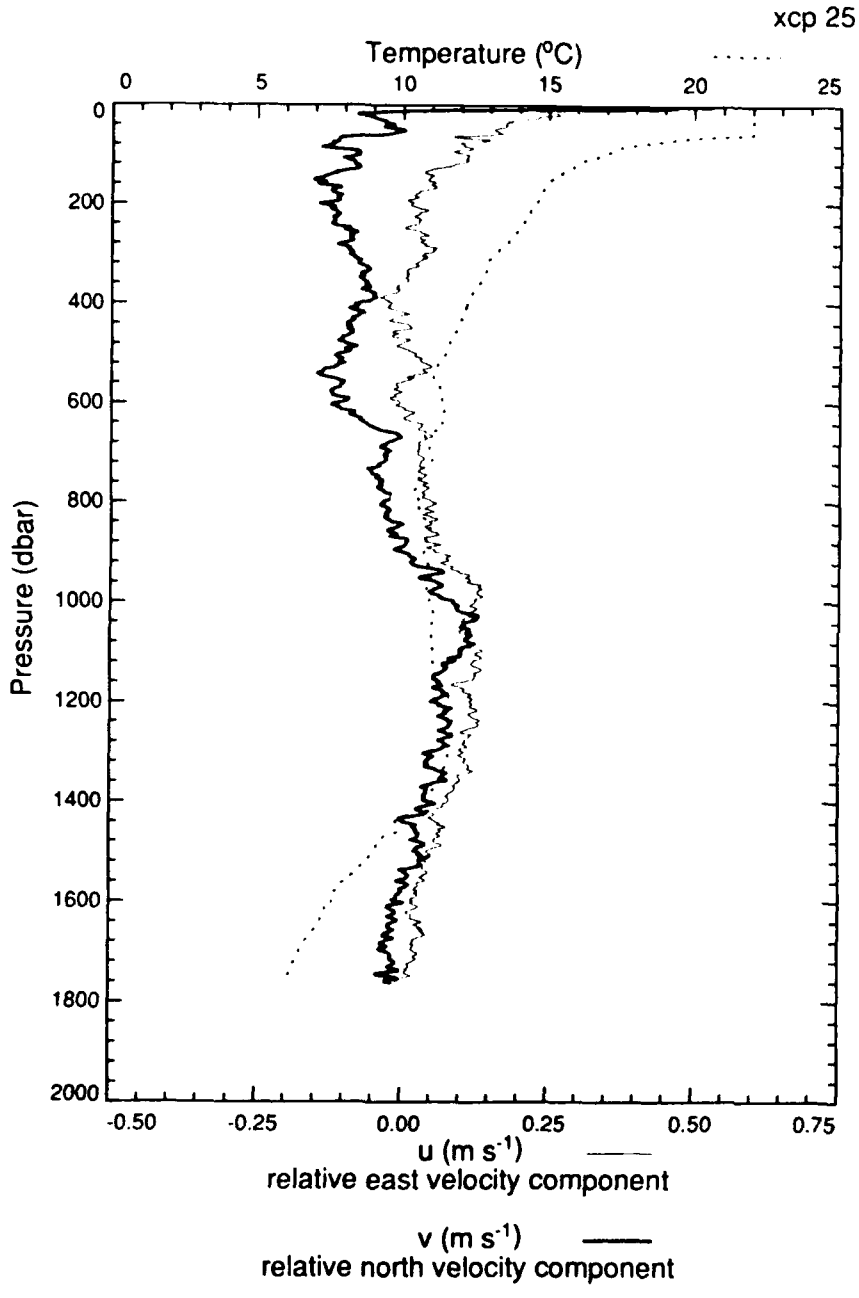
xcp 2512
Temperature (°C)
0
5
10
15
20
25
Pressure (dbar)
0
200
400
600
800
1000
1200
1400
1600
1800
2000
-0.50
-0.25
0.00
0.25
0.50
0.75
u (m s-1)
relative east velocity component
v (m s-1)
relative north velocity component

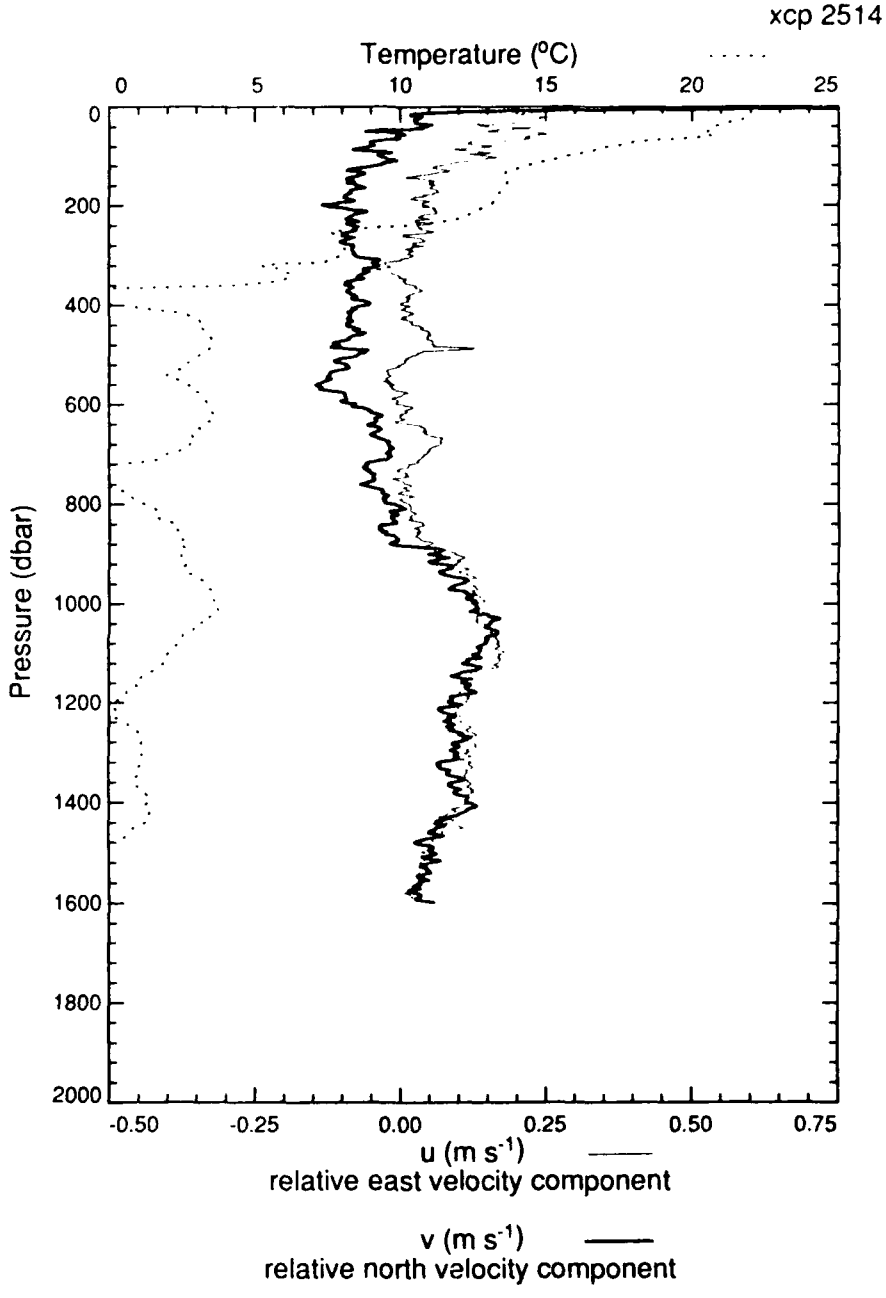
xcp 2514
Temperature (°C)
0
5
10
15
20
25
Pressure (dbar)
0
200
400
600
800
1000
1200
1400
1600
1800
2000
-0.50
-0.25
0.00
0.25
0.50
0.75
u (m s-1)
relative east velocity component
v (m s-1)
relative north velocity component

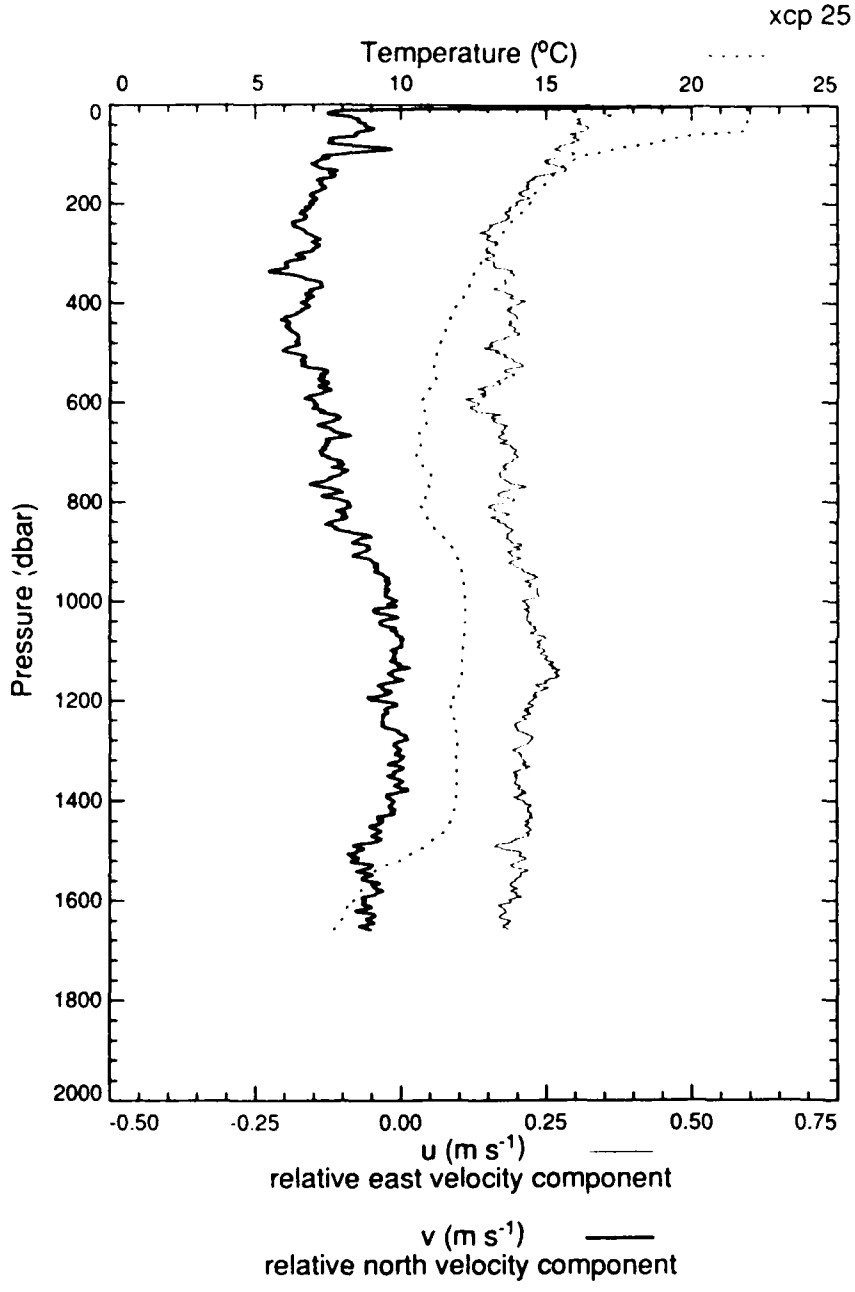
xcp 2515
Temperature (°C)
0
5
10
15
20
25
Pressure (dbar)
0
200
400
600
800
1000
1200
1400
1600
1800
2000
-0.50
-0.25
0.00
0.25
0.50
0.75
u (m s-1)
relative east velocity component
v (m s-1)
relative north velocity component

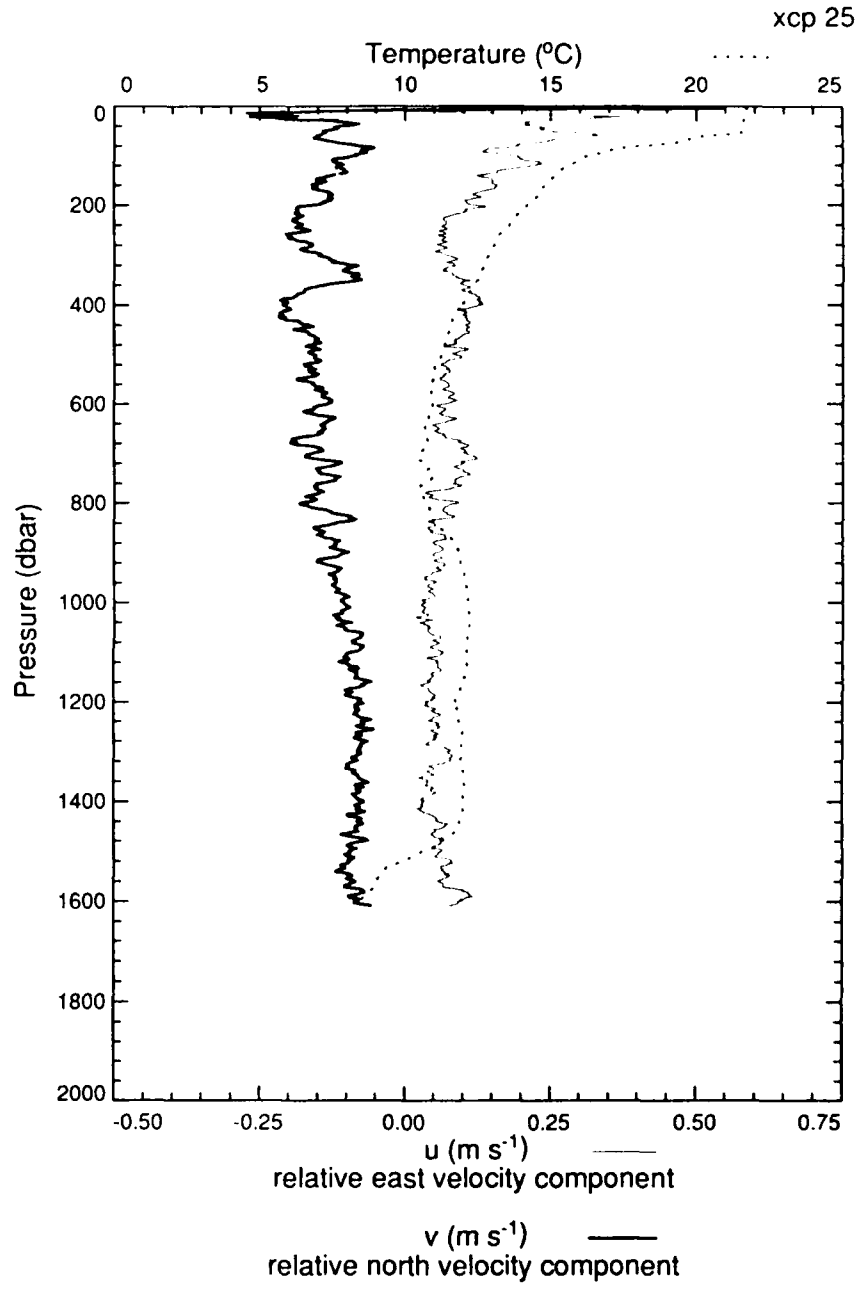
xcp 2516
Temperature (°C)
0
5
10
15
20
25
Pressure (dbar)
0
200
400
600
800
1000
1200
1400
1600
1800
2000
-0.50
-0.25
0.00
0.25
0.50
0.75
u (m s-1)
relative east velocity component
v (m s-1)
relative north velocity component

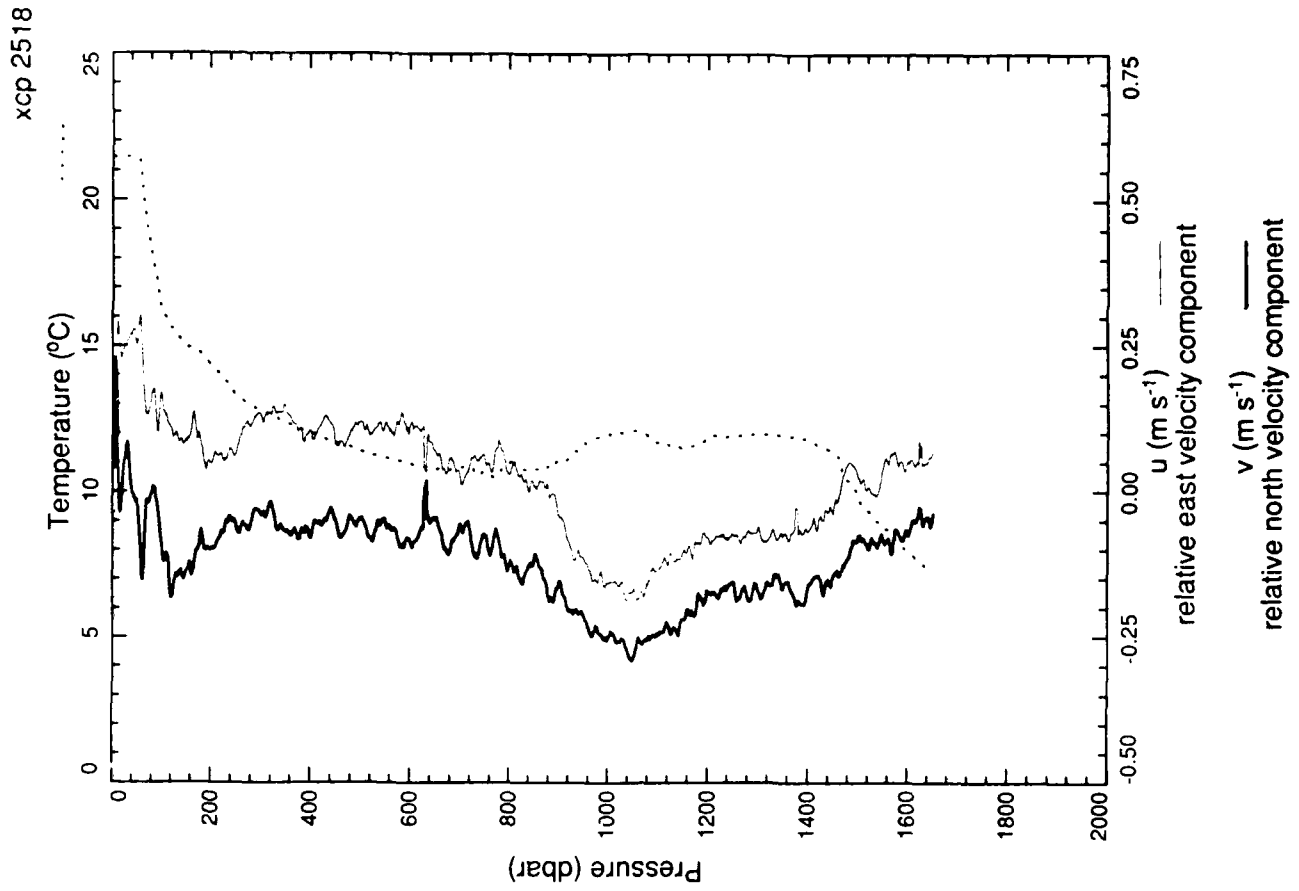
xcp 2518
Temperature (°C)
Pressure (dbar)
u (m s-1)
relative east velocity component
v (m s-1)
relative north velocity component

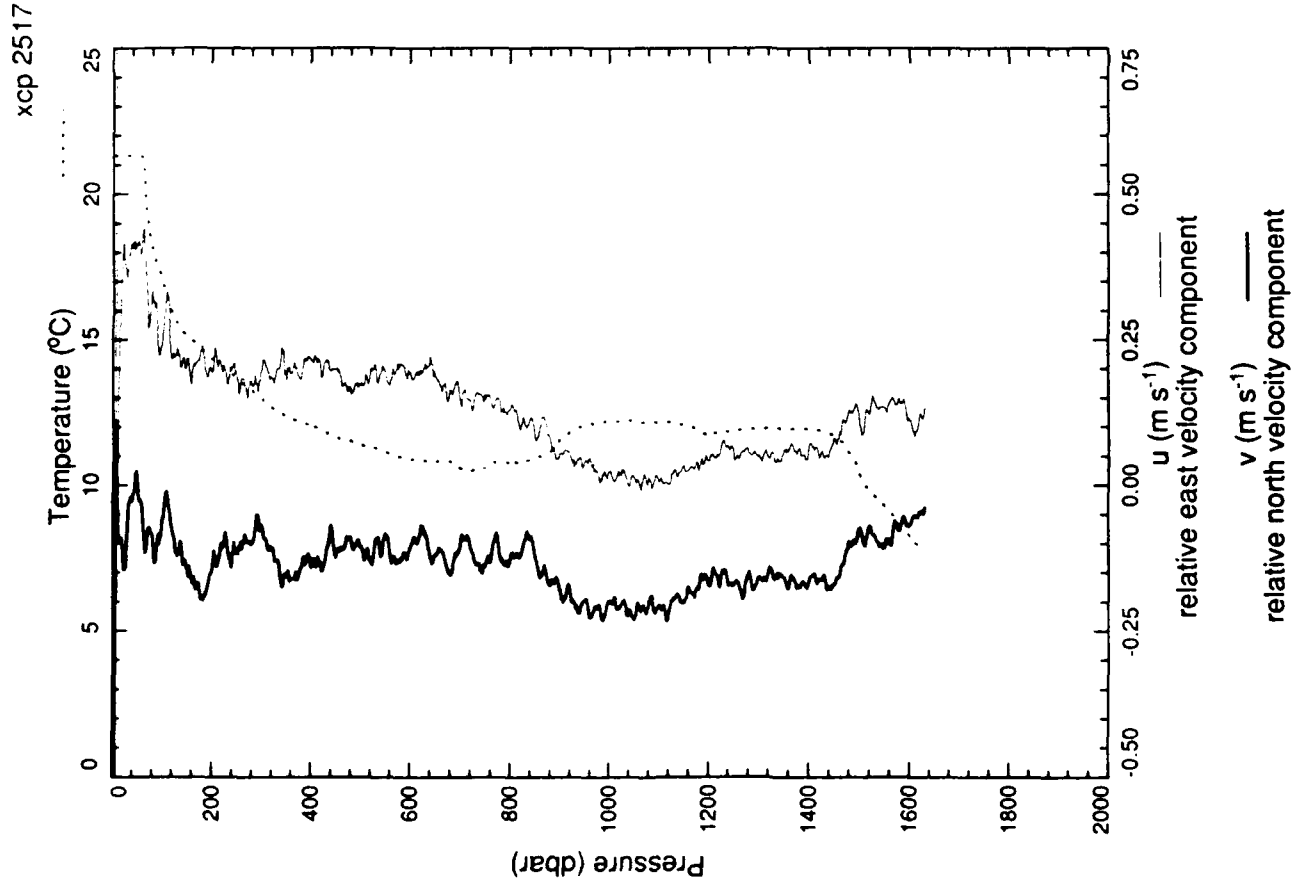
xcp 2517
Temperature (°C)
Pressure (dbar)
u (m s-1)
relative east velocity component
v (m s-1)
relative north velocity component

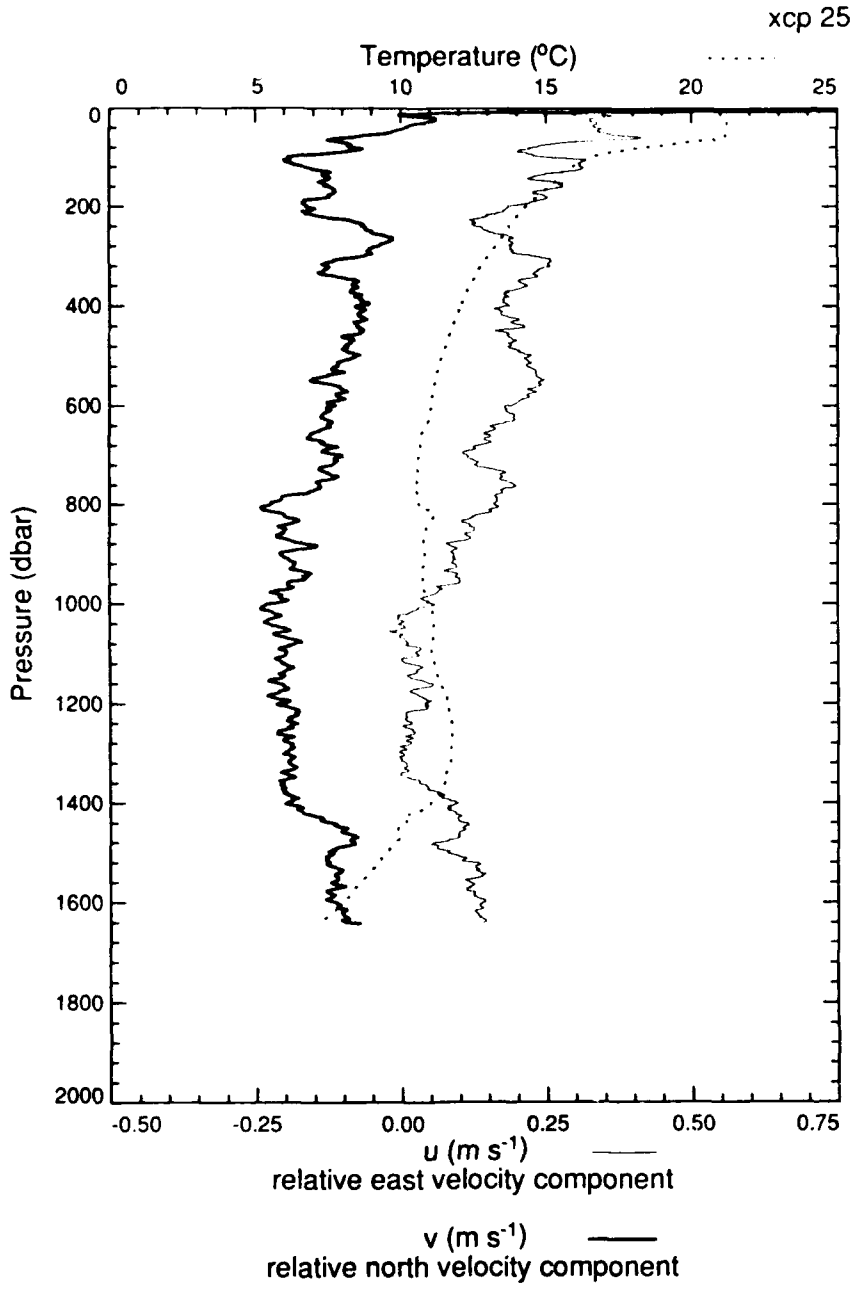
xcp 2519
Temperature (°C)
0
5
10
15
20
25
Pressure (dbar)
0
200
400
600
800
1000
1200
1400
1600
1800
2000
-0.50
-0.25
0.00
0.25
0.50
0.75
u (m s-1)
relative east velocity component
v (m s-1)
relative north velocity component

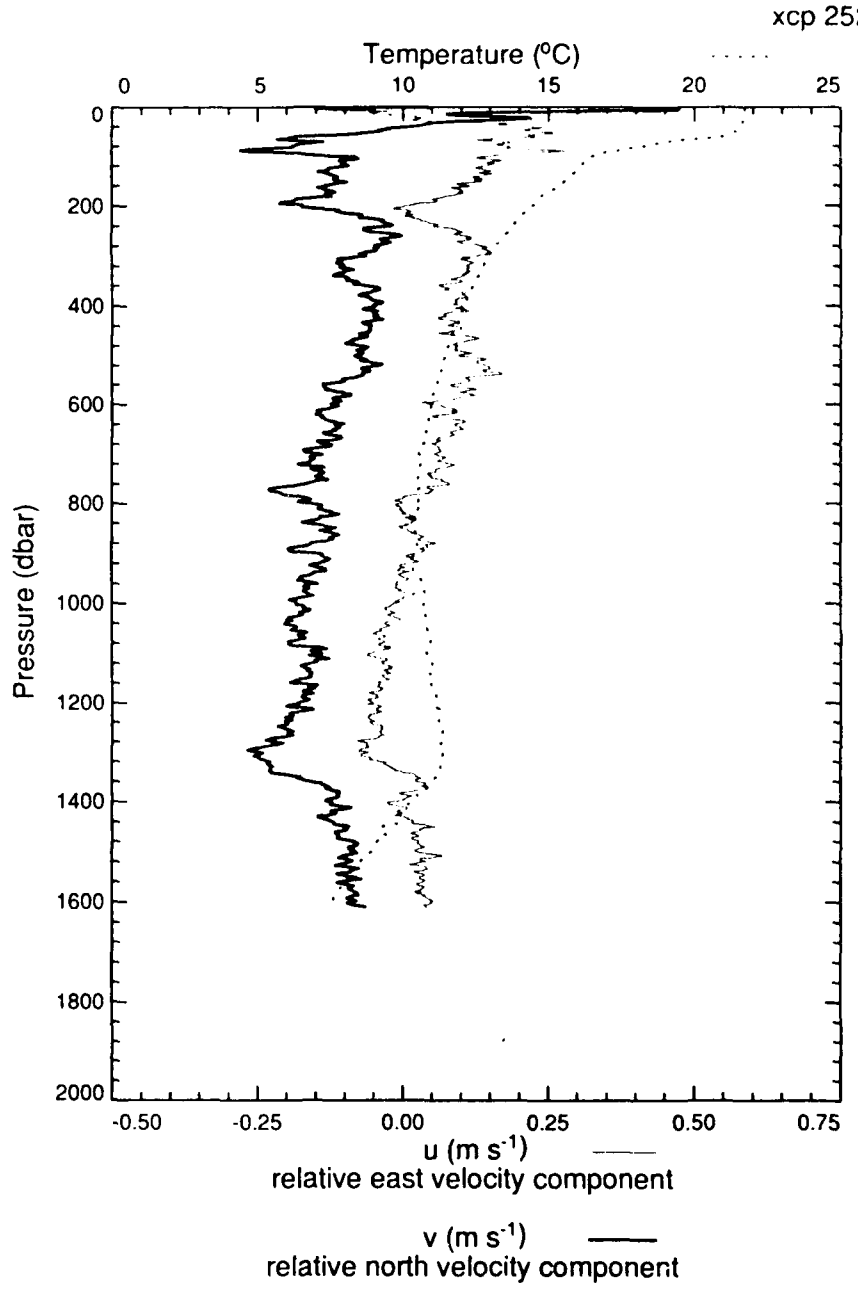
xcp 2520
Temperature (°C)
0
5
10
15
20
25
Pressure (dbar)
0
200
400
600
800
1000
1200
1400
1600
1800
2000
-0.50
-0.25
0.00
0.25
0.50
0.75
u (m s-1)
relative east velocity component
v (m s-1)
relative north velocity component

TR 8925 N57

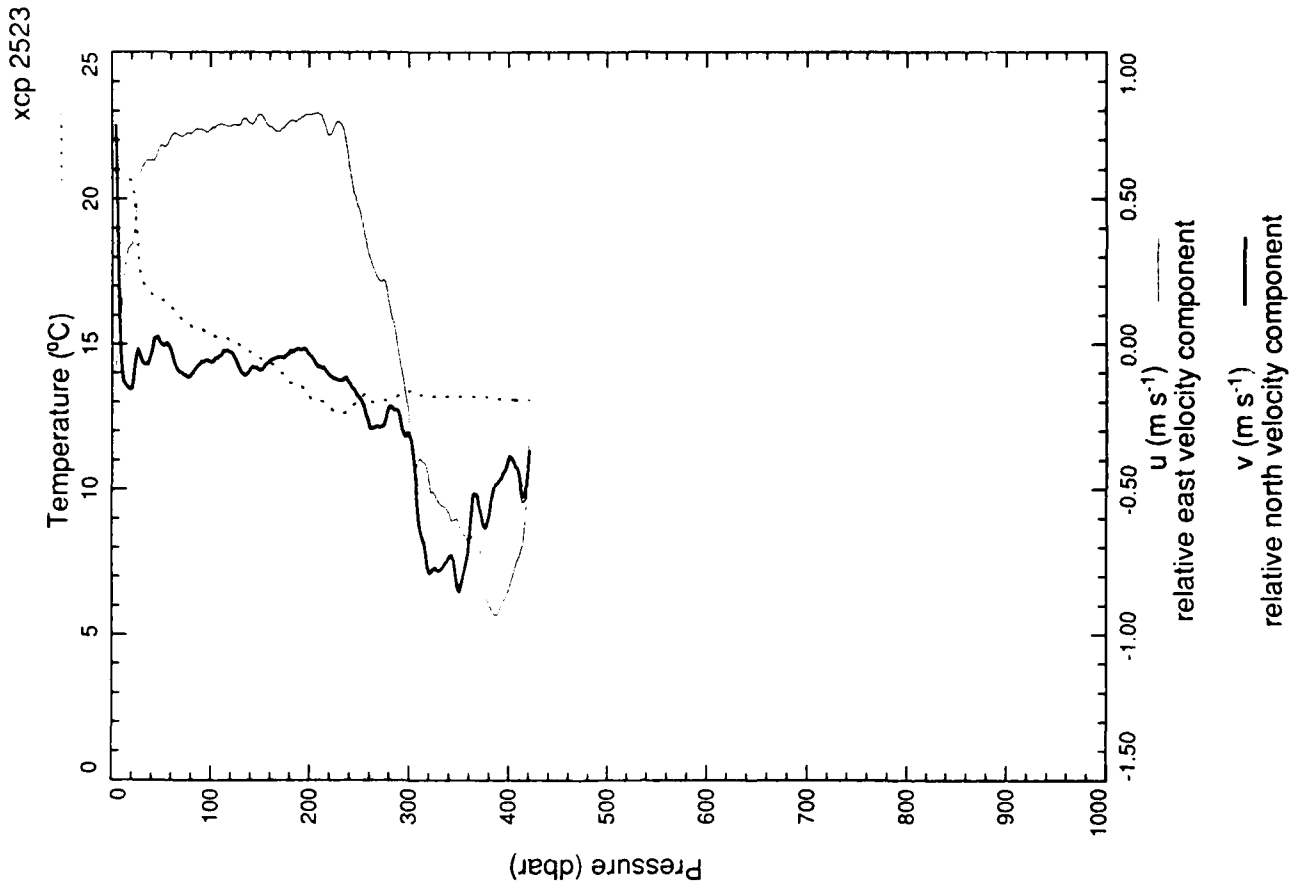
xcp 2523
Temperature (°C)
Pressure (dbar)
u (m s-1)
relative east velocity component
v (m s-1)
relative north velocity component

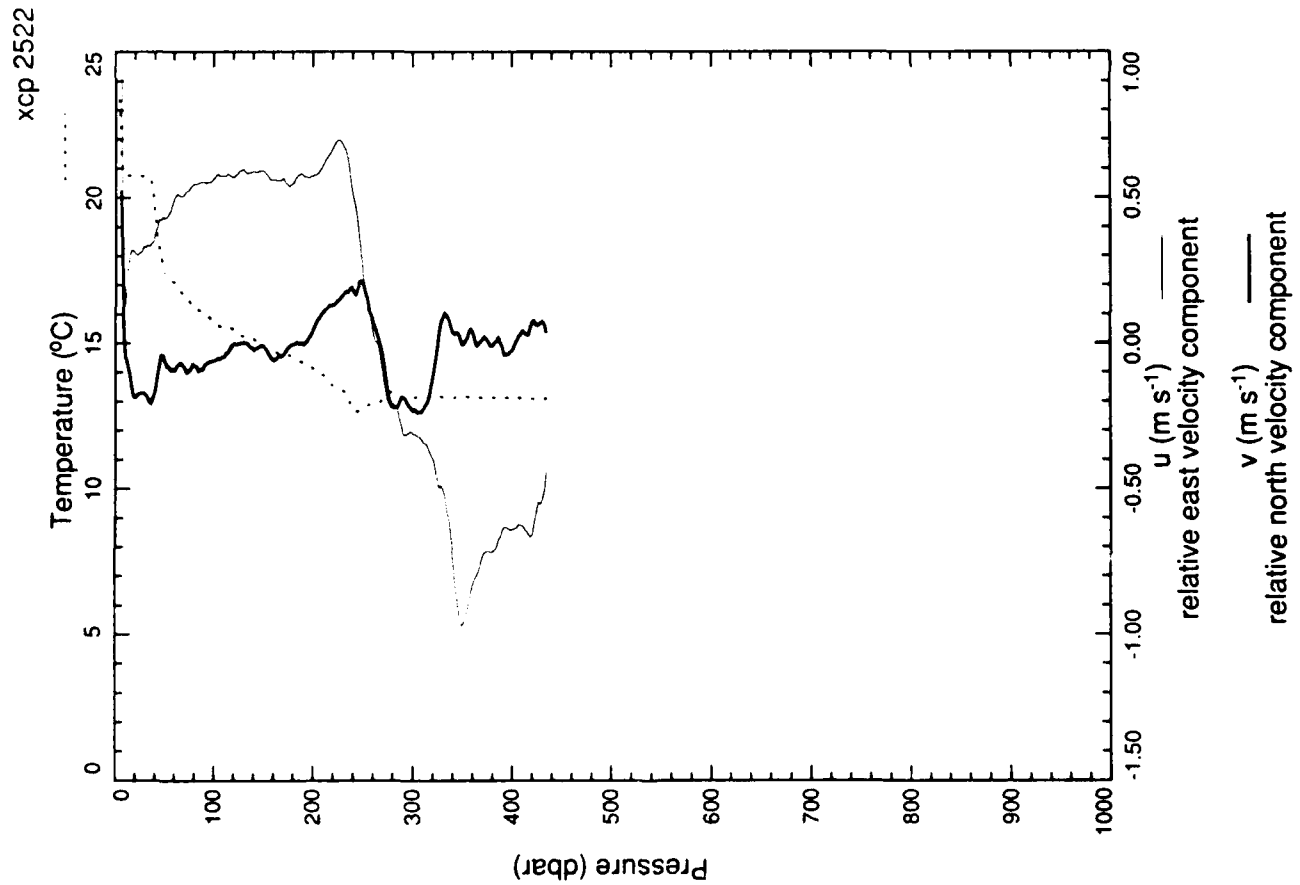
xcp 2522
Temperature (°C)
Pressure (dbar)
u (m s-1)
relative east velocity component
v (m s-1)
relative north velocity component

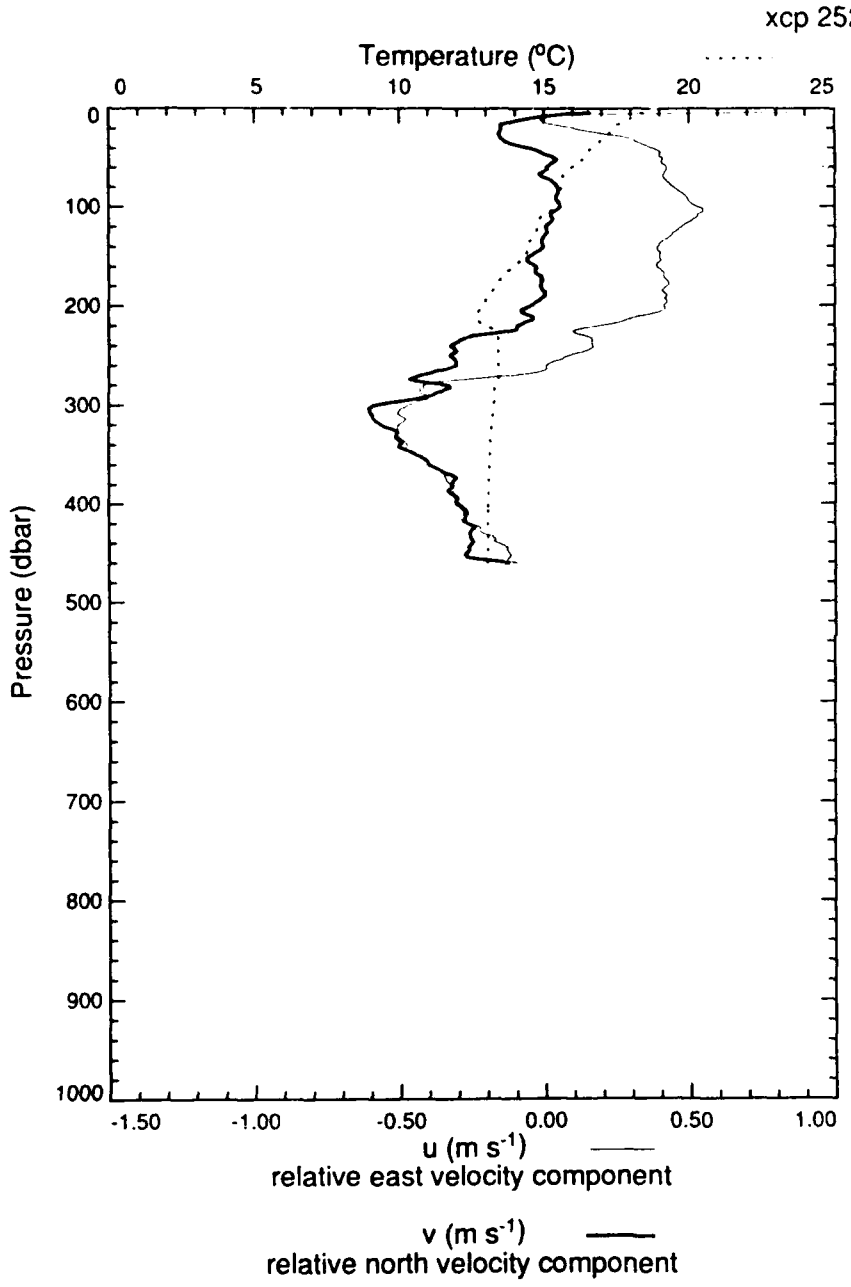
xcp 2525
Temperature (°C)
0
5
10
15
20
25
Pressure (dbar)
0
100
200
300
400
500
600
700
800
900
1000
-1.50
-1.00
-0.50
0.00
0.50
1.00
u (m s-1)
relative east velocity component
v (m s-1)
relative north velocity component

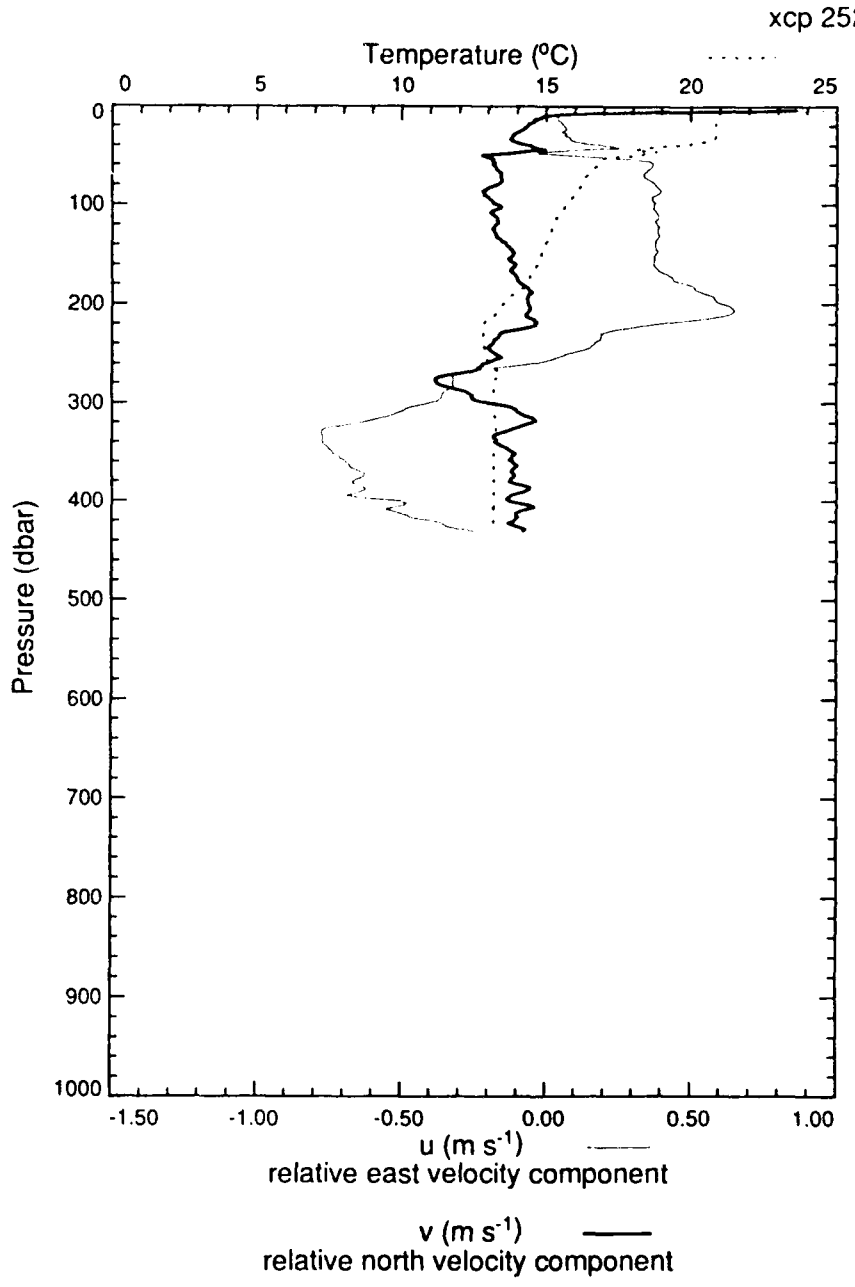
xcp 2527
Temperature (°C)
0
5
10
15
20
25
Pressure (dbar)
0
100
200
300
400
500
600
700
800
900
1000
-1.50
-1.00
-0.50
0.00
0.50
1.00
u (m s-1)
relative east velocity component
v (m s-1)
relative north velocity component

TR 8925 N59

N60 TR 8925

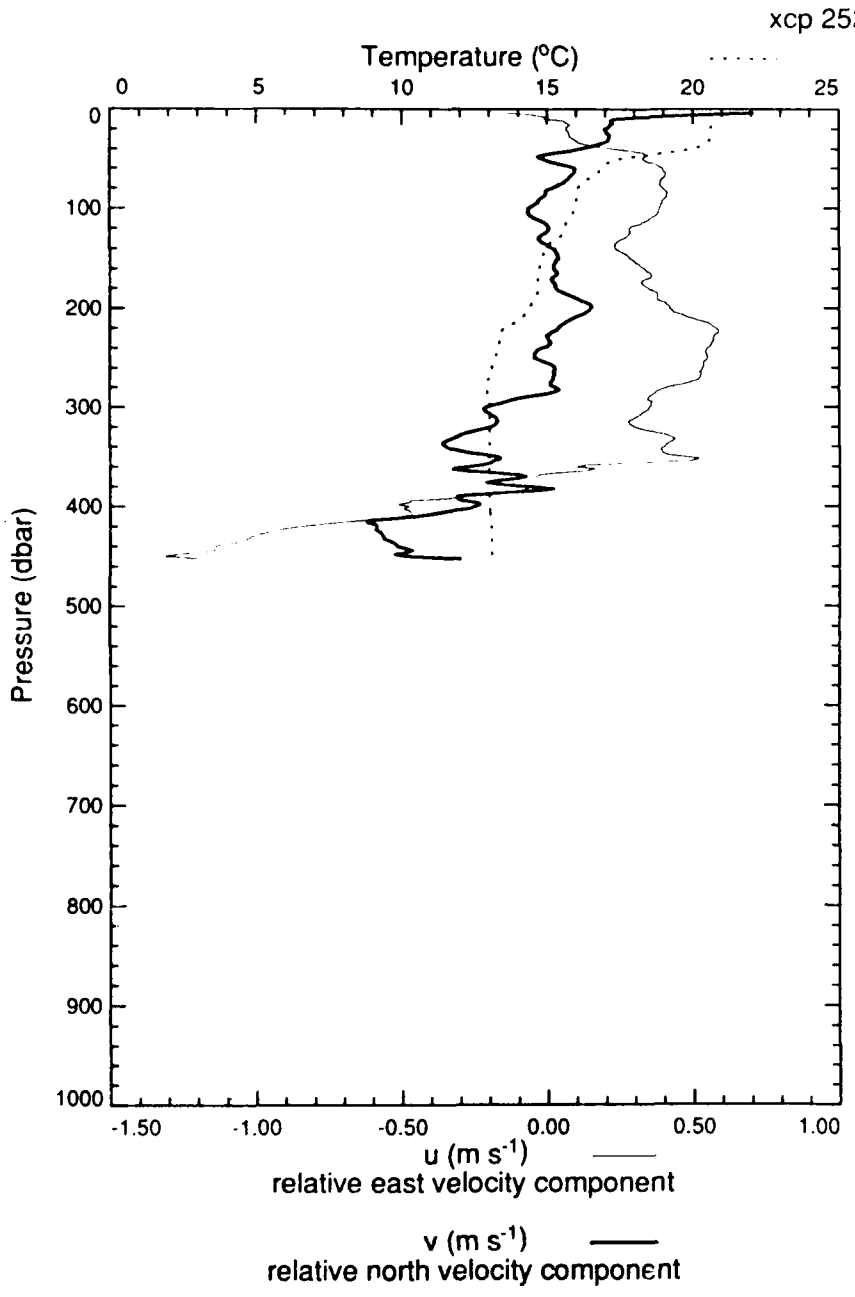
xcp 2528
Temperature (°C)
0
5
10
15
20
25
Pressure (dbar)
0
100
200
300
400
500
600
700
800
900
1000
-1.50
-1.00
-0.50
0.00
0.50
1.00
u (m s-1)
relative east velocity component
v (m s-1)
relative north velocity component

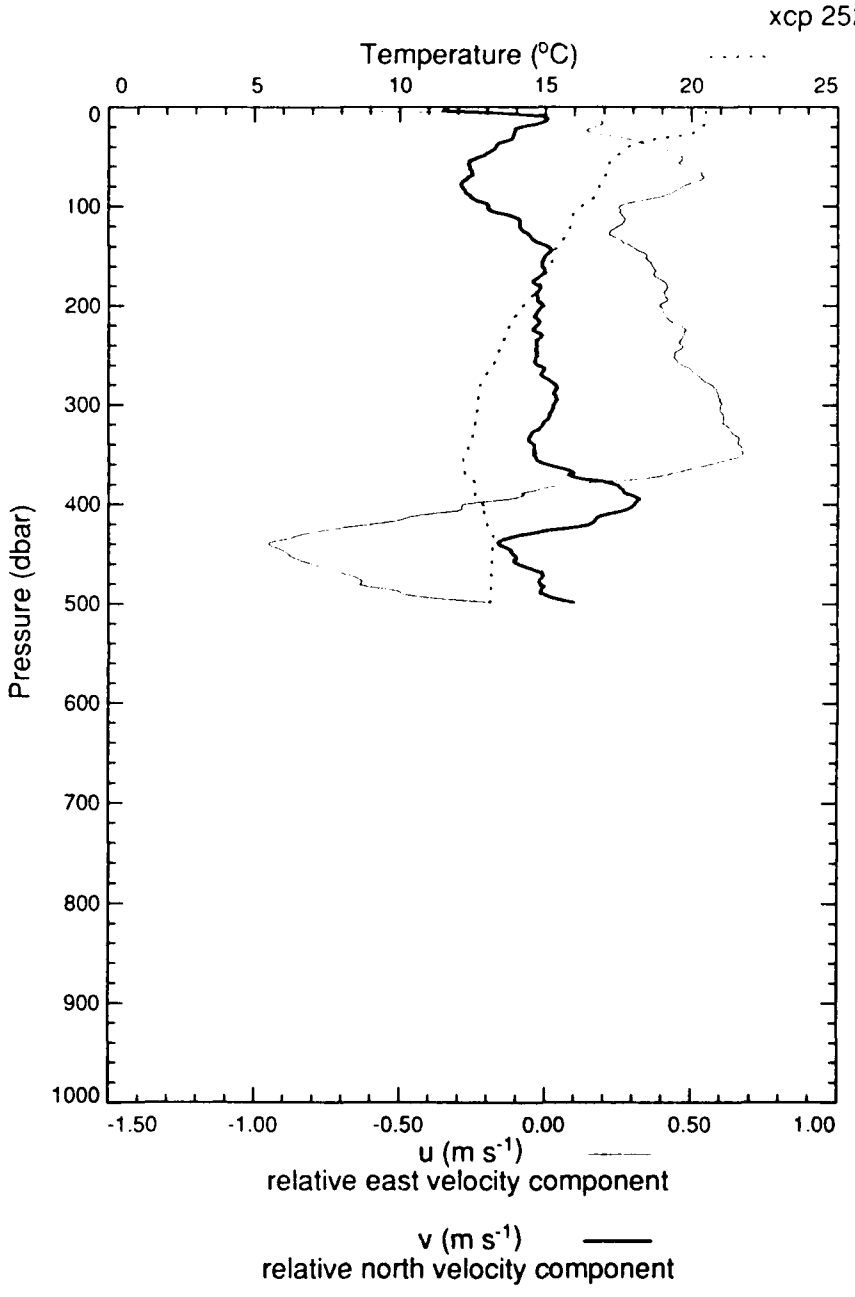
xcp 2529
Temperature (°C)
0
5
10
15
20
25
Pressure (dbar)
0
100
200
300
400
500
600
700
800
900
1000
-1.50
-1.00
-0.50
0.00
0.50
1.00
u (m s-1)
relative east velocity component
v (m s-1)
relative north velocity component

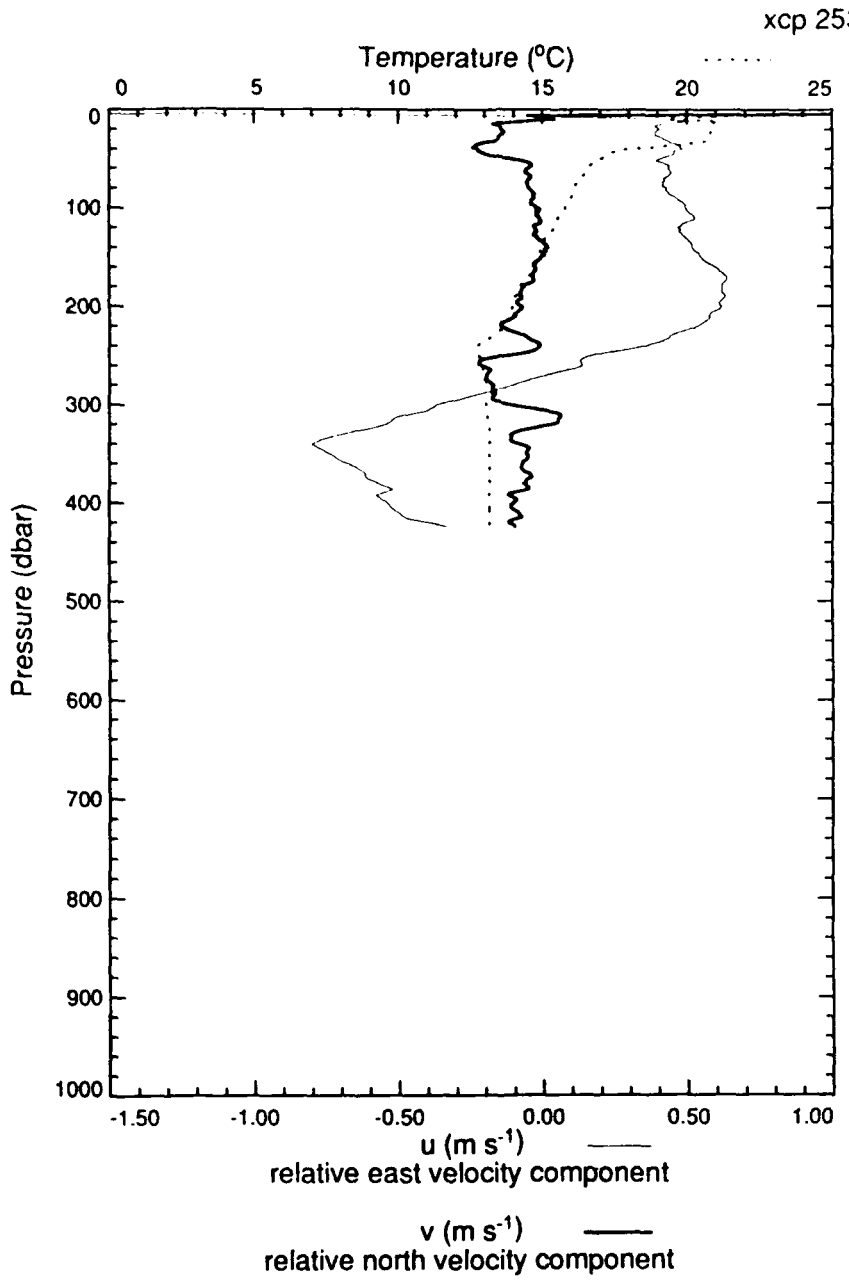
xcp 2530
Temperature (°C)
0
5
10
15
20
25
Pressure (dbar)
0
100
200
300
400
500
600
700
800
900
1000
-1.50
-1.00
-0.50
0.00
0.50
1.00
u (m s-1)
relative east velocity component
v (m s-1)
relative north velocity component

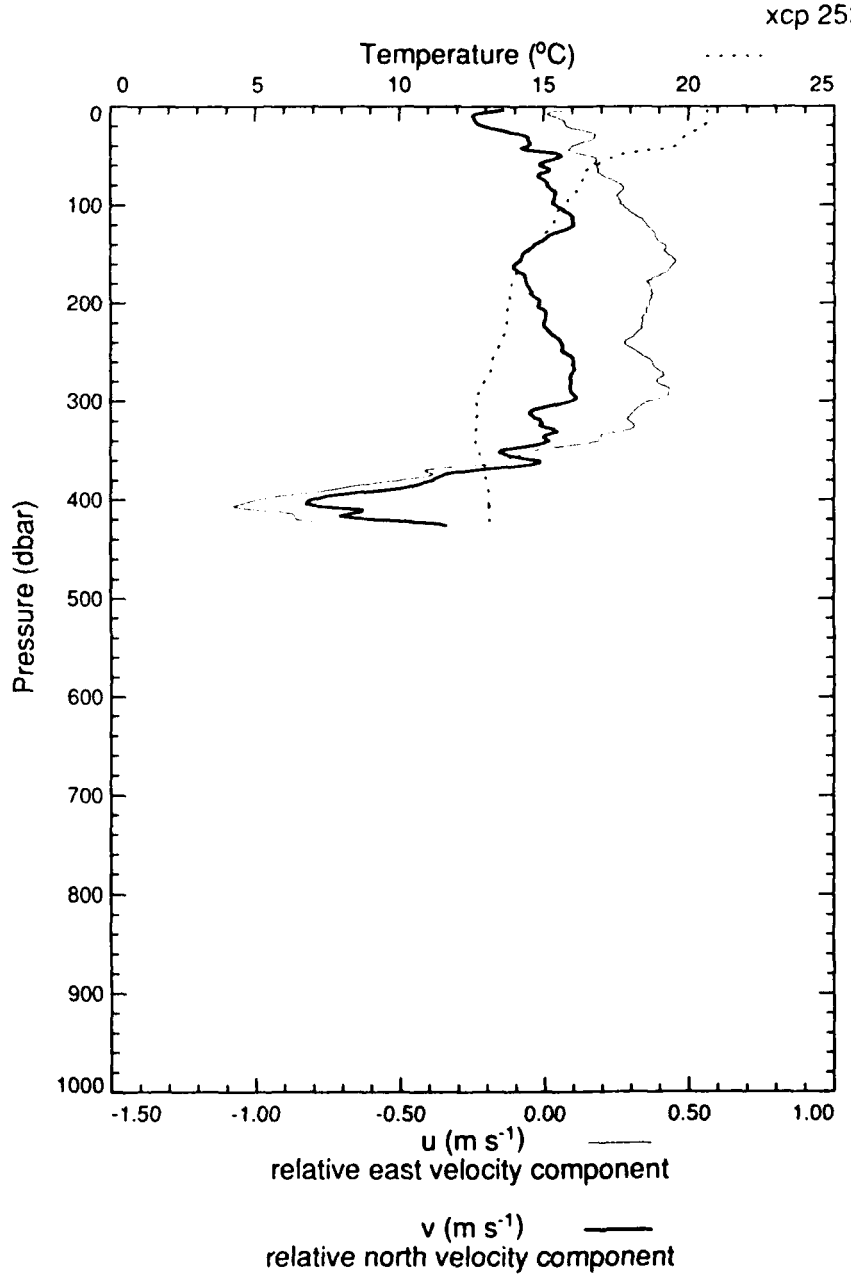
xcp 2531
Temperature (°C)
0
5
10
15
20
25
Pressure (dbar)
0
100
200
300
400
500
600
700
800
900
1000
-1.50
-1.00
-0.50
0.00
0.50
1.00
u (m s-1)
relative east velocity component
v (m s-1)
relative north velocity component

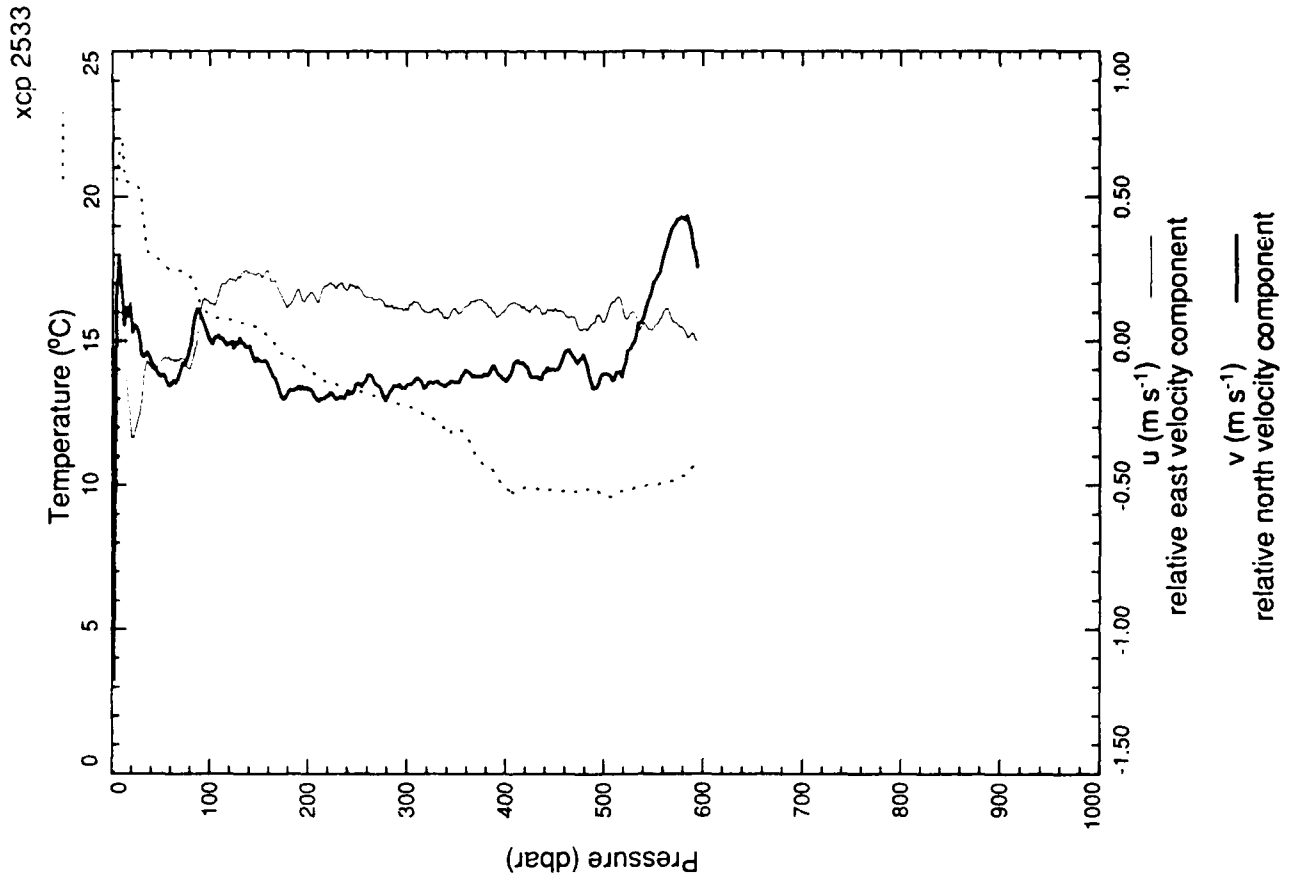
xcp 2533
Temperature (°C)
Pressure (dbar)
u (m s-1)
relative east velocity component
v (m s-1)
relative north velocity component

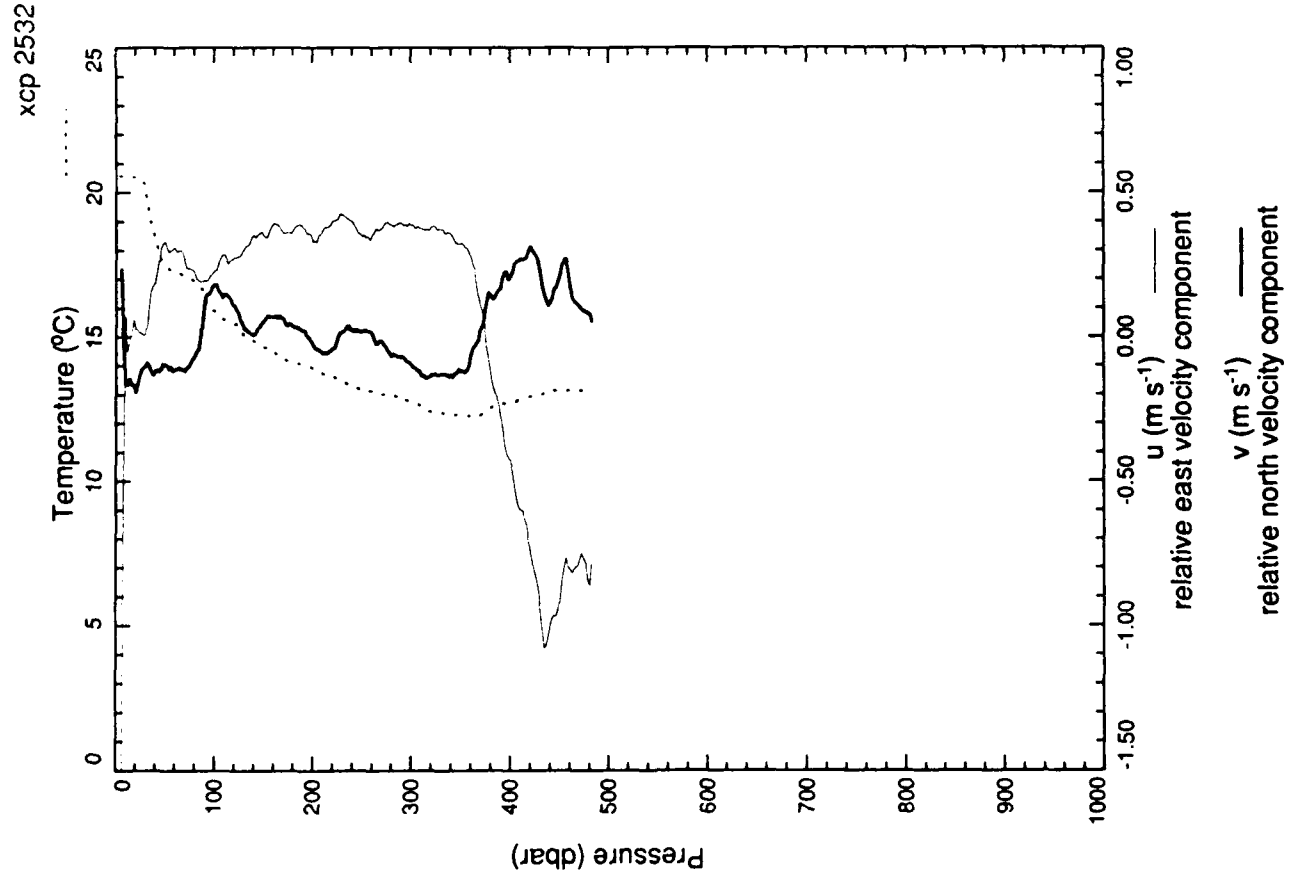
xcp 2532
Temperature (°C)
Pressure (dbar)
u (m s-1)
relative east velocity component
v (m s-1)
relative north velocity component

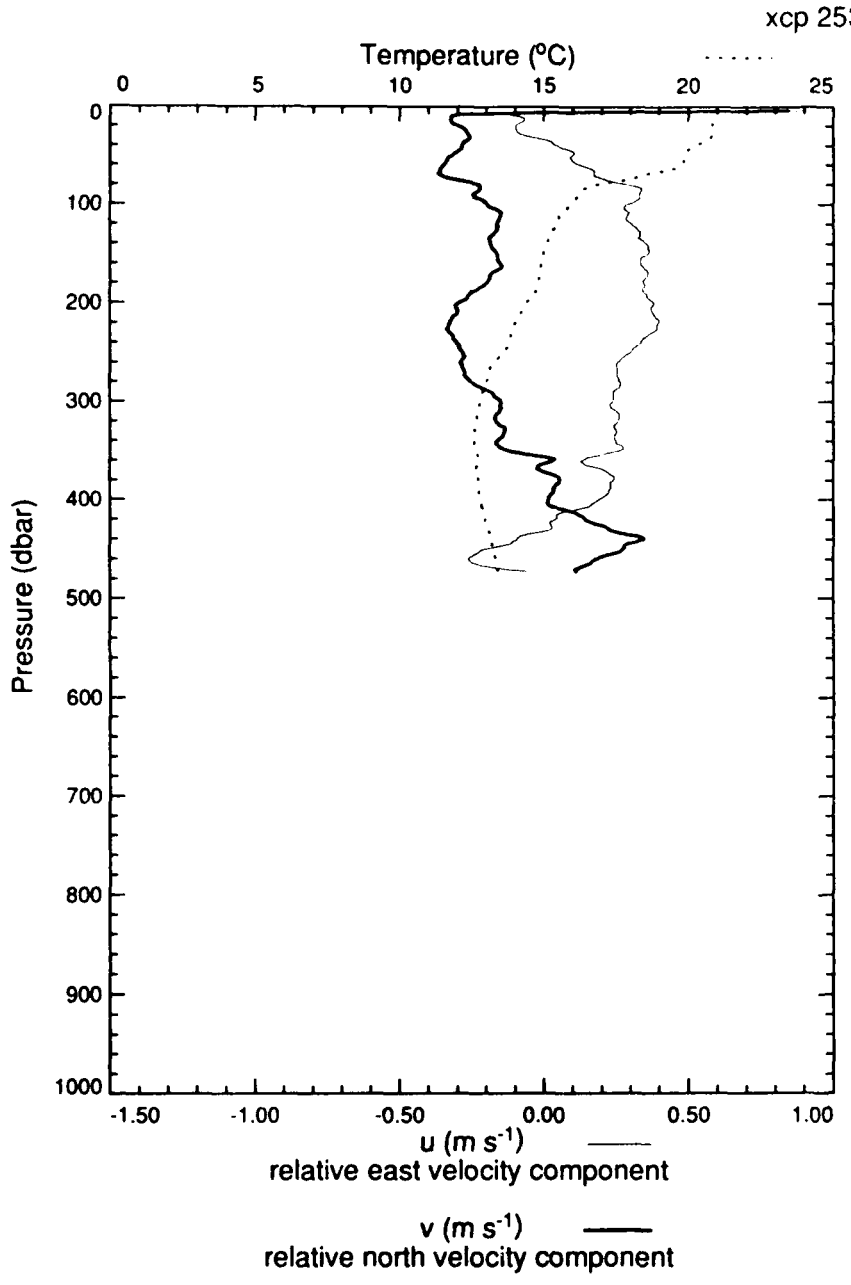
xcp 2534
Temperature (°C)
0
5
10
15
20
25
Pressure (dbar)
0
100
200
300
400
500
600
700
800
900
1000
-1.50
-1.00
-0.50
0.00
0.50
1.00
u (m s-1)
relative east velocity component
v (m s-1)
relative north velocity component

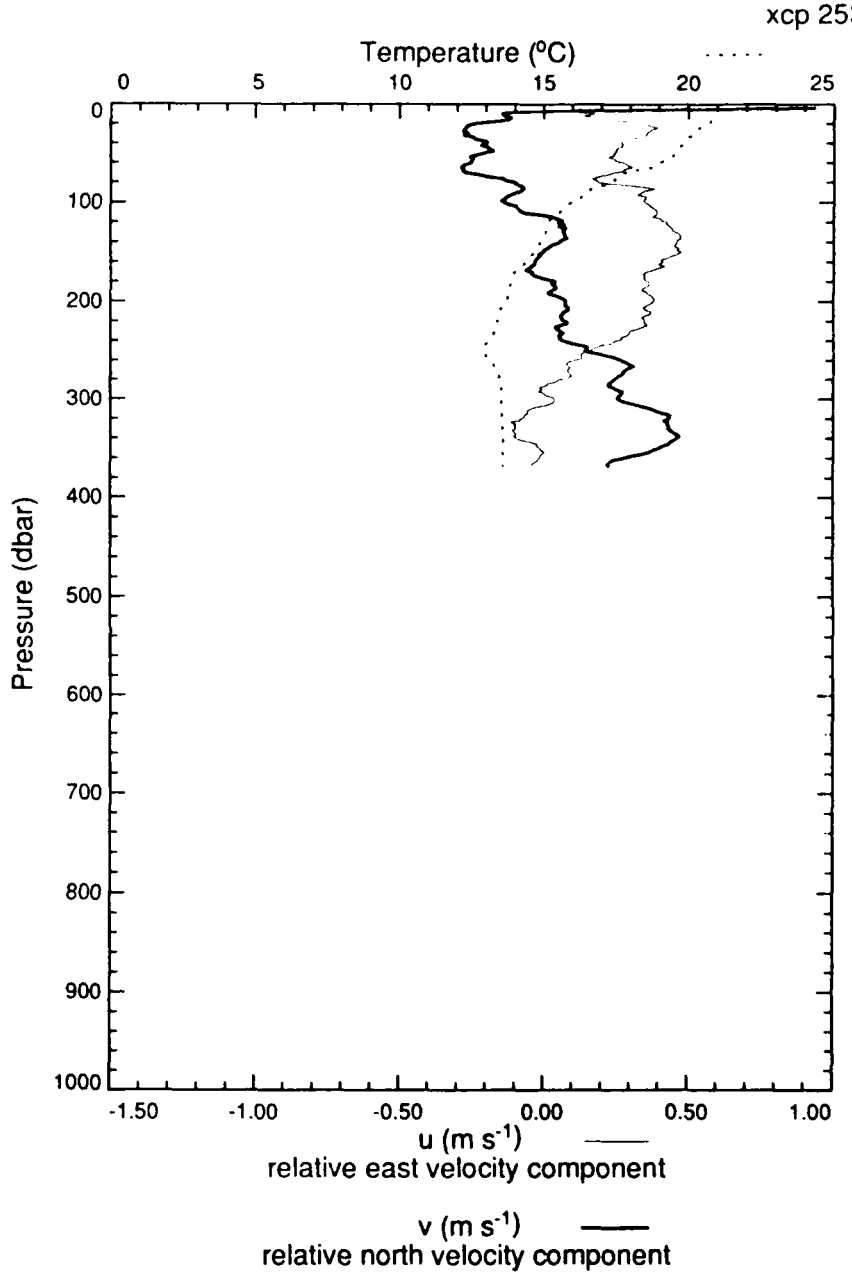
xcp 2535
Temperature (°C)
0
5
10
15
20
25
Pressure (dbar)
0
100
200
300
400
500
600
700
800
900
1000
-1.50
-1.00
-0.50
0.00
0.50
1.00
u (m s-1)
relative east velocity component
v (m s-1)
relative north velocity component

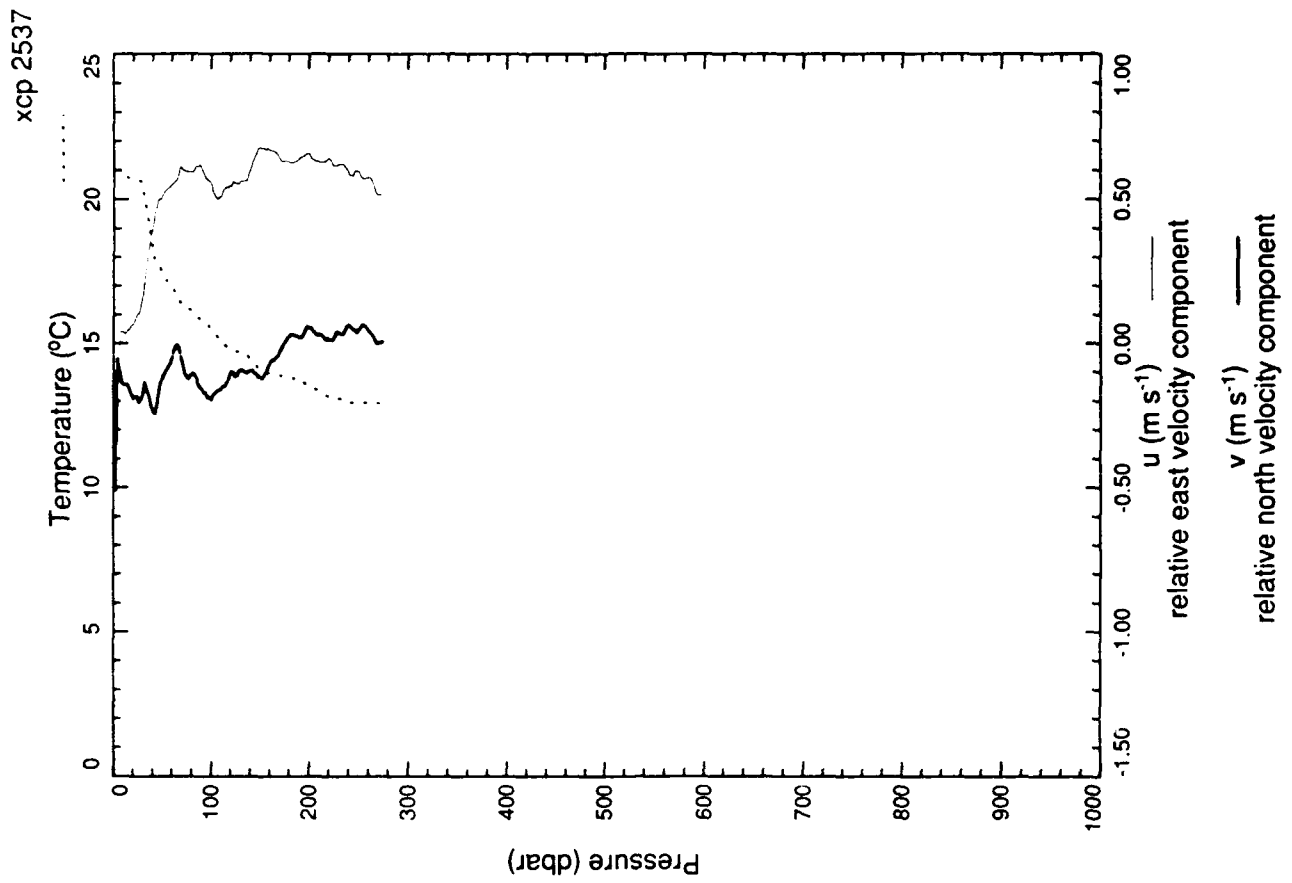
xcp 2537
Temperature (ºC)
Pressure (dbar)
u (m s-1)
relative east velocity component
v (m s-1)
relative north velocity component

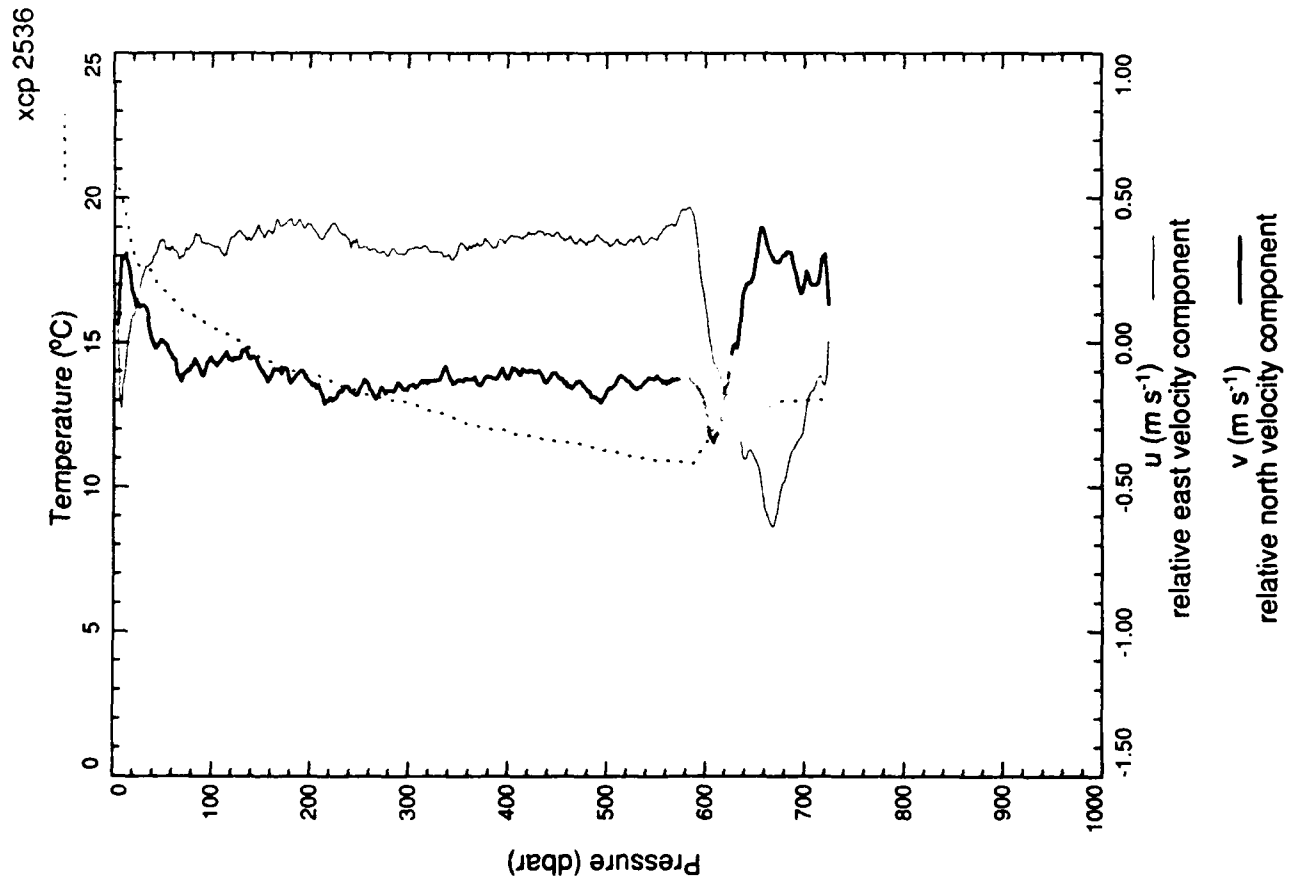
xcp 2536
Temperature (ºC)
Pressure (dbar)
u (m s-1)
relative east velocity component
v (m s-1)
relative north velocity component

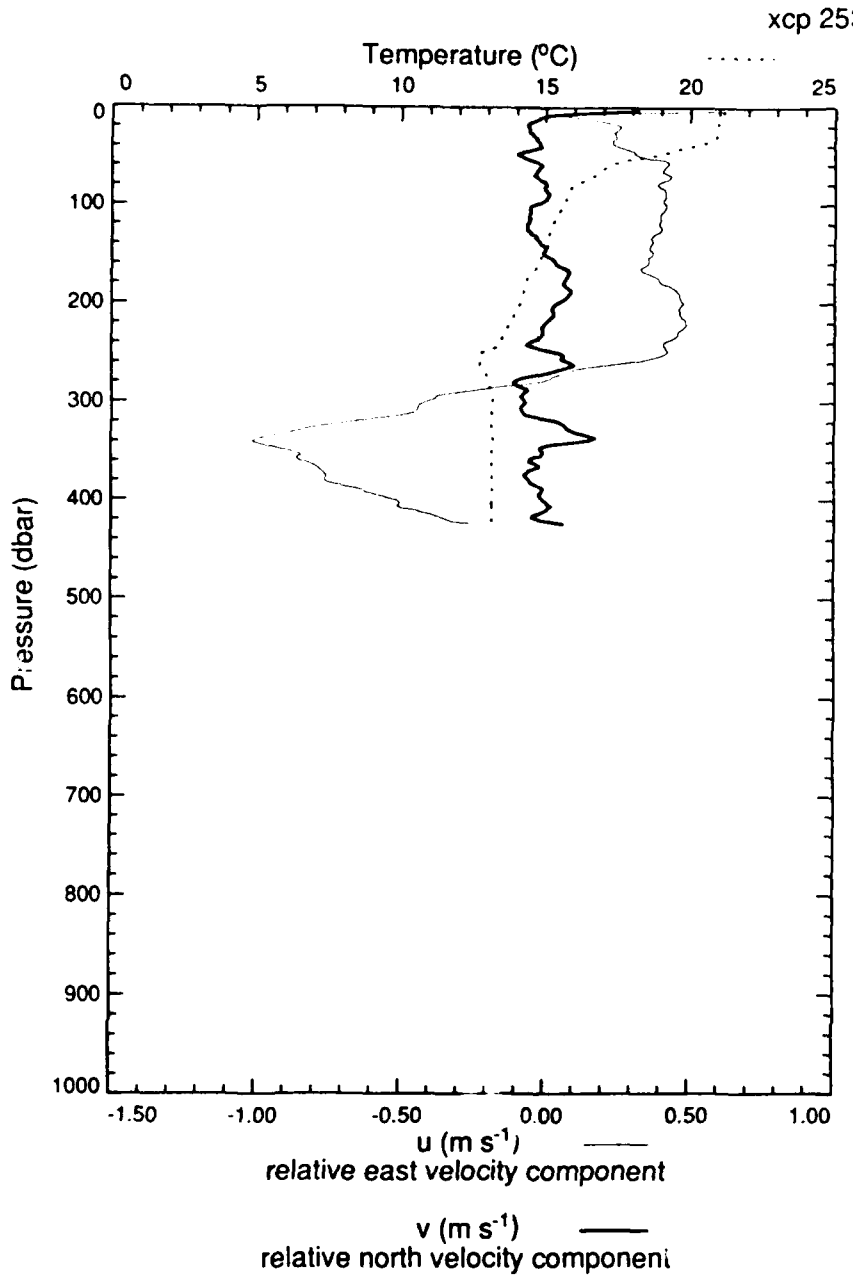
xcp 2538
Temperature (°C)
0
5
10
15
20
25
Pressure (dbar)
0
100
200
300
400
500
600
700
800
900
1000
-1.50
-1.00
-0.50
0.00
0.50
1.00
u (m s-1)
relative east velocity component
v (m s-1)
relative north velocity component

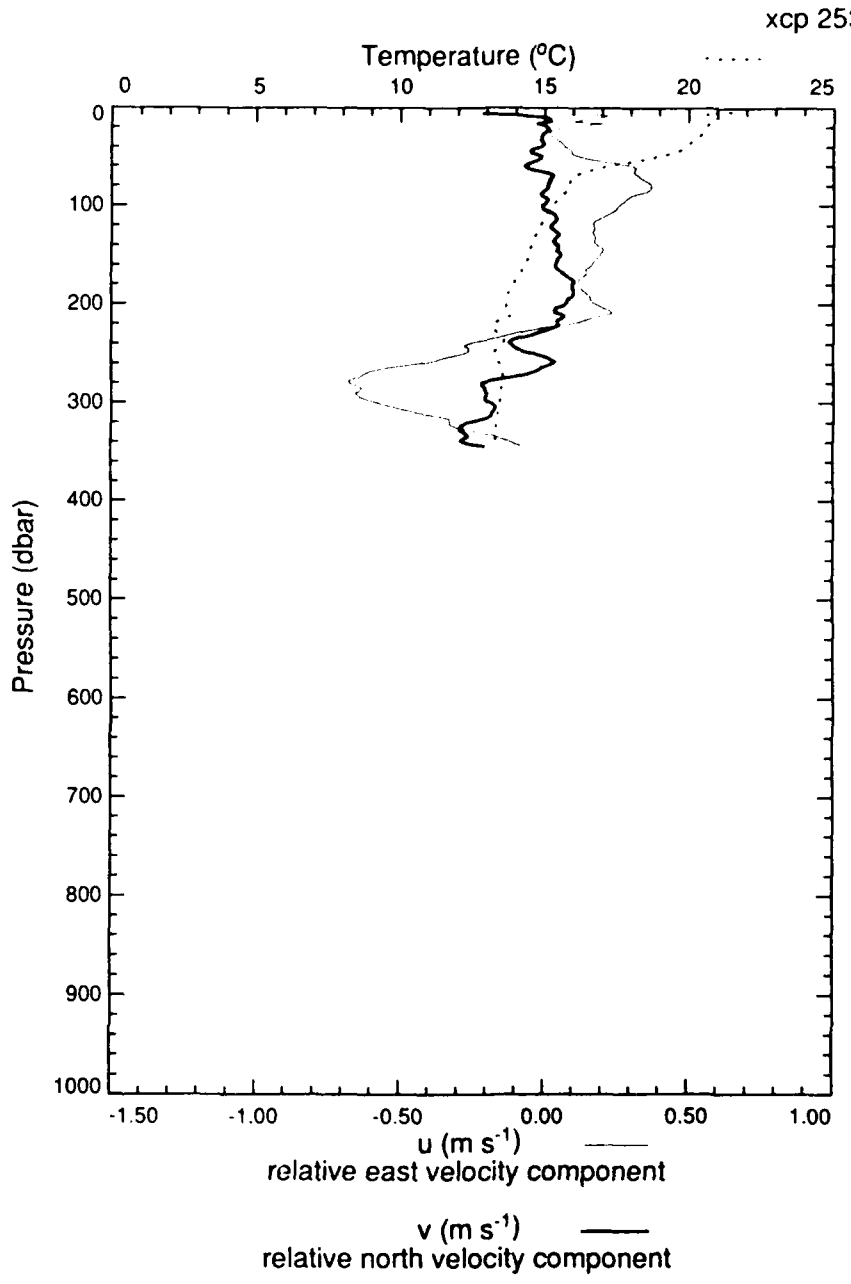
xcp 2539
Temperature (°C)
0
5
10
15
20
25
Pressure (dbar)
0
100
200
300
400
500
600
700
800
900
1000
-1.50
-1.00
-0.50
0.00
0.50
1.00
u (m s-1)
relative east velocity component
v (m s-1)
relative north velocity component

TR 8925 N65

N66 TR 8925

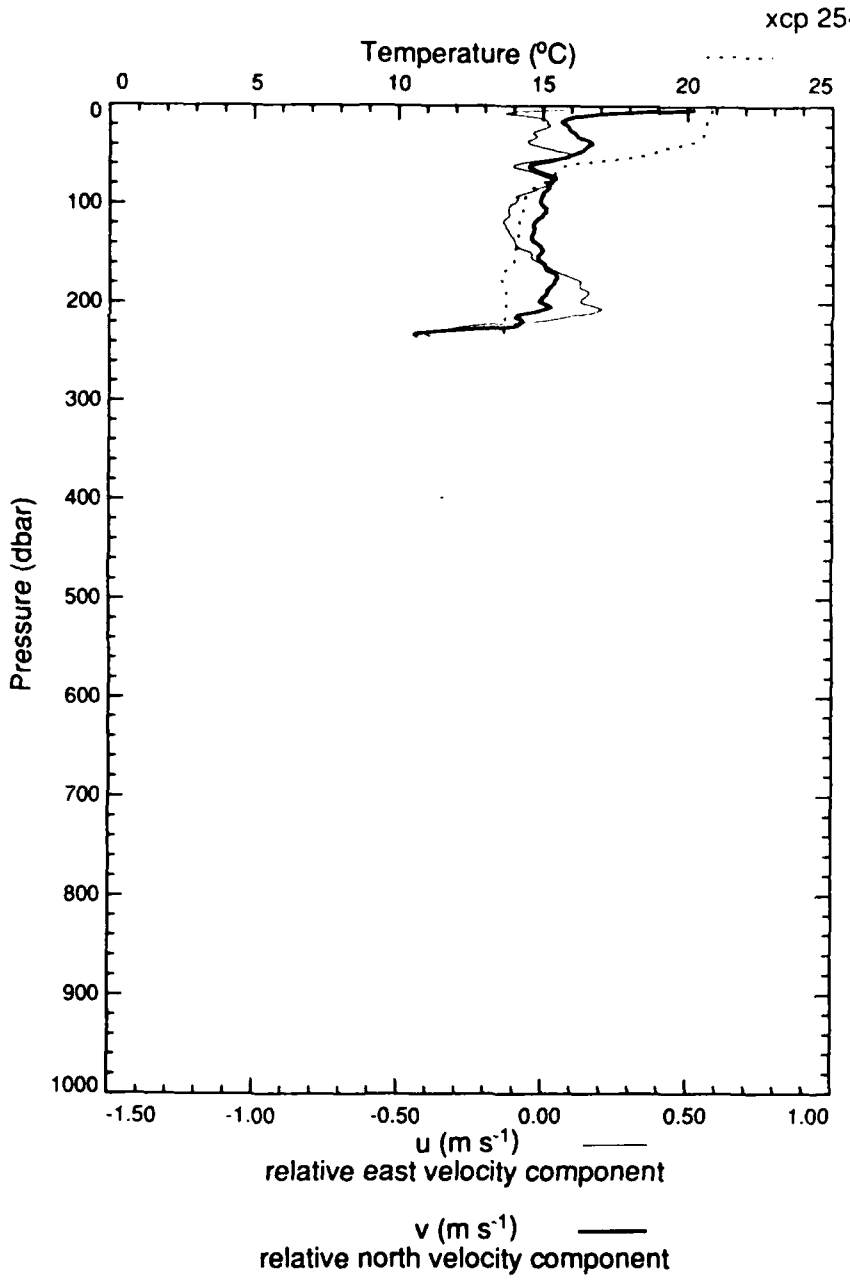
xcp 2540
Temperature (°C)
0
5
10
15
20
25
Pressure (dbar)
0
100
200
300
400
500
600
700
800
900
1000
-1.50
-1.00
-0.50
0.00
0.50
1.00
u (m s-1)
relative east velocity component
v (m s-1)
relative north velocity component

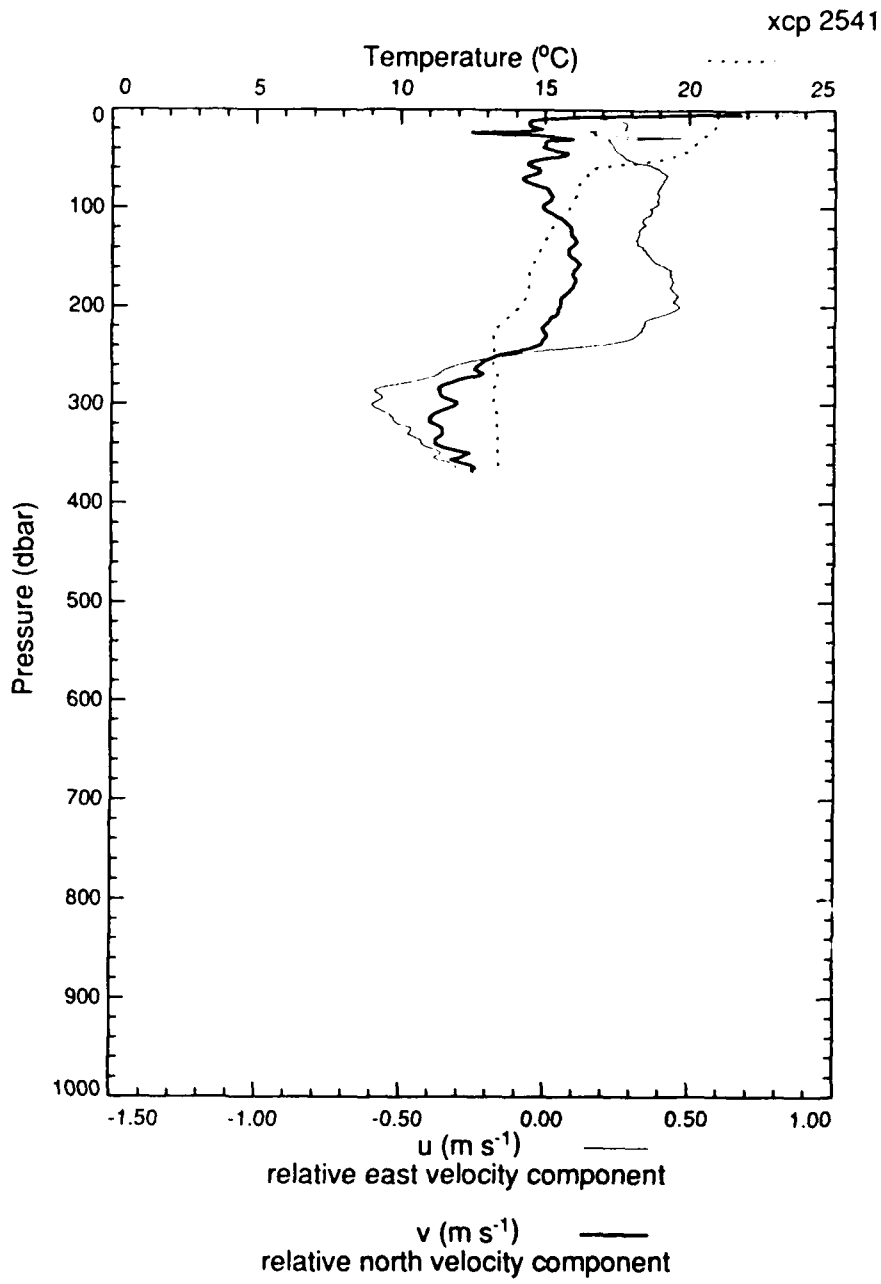
xcp 2541
Temperature (°C)
0
5
10
15
20
25
Pressure (dbar)
0
100
200
300
400
500
600
700
800
900
1000
-1.50
-1.00
-0.50
0.00
0.50
1.00
u (m s-1)
relative east velocity component
v (m s-1)
relative north velocity component

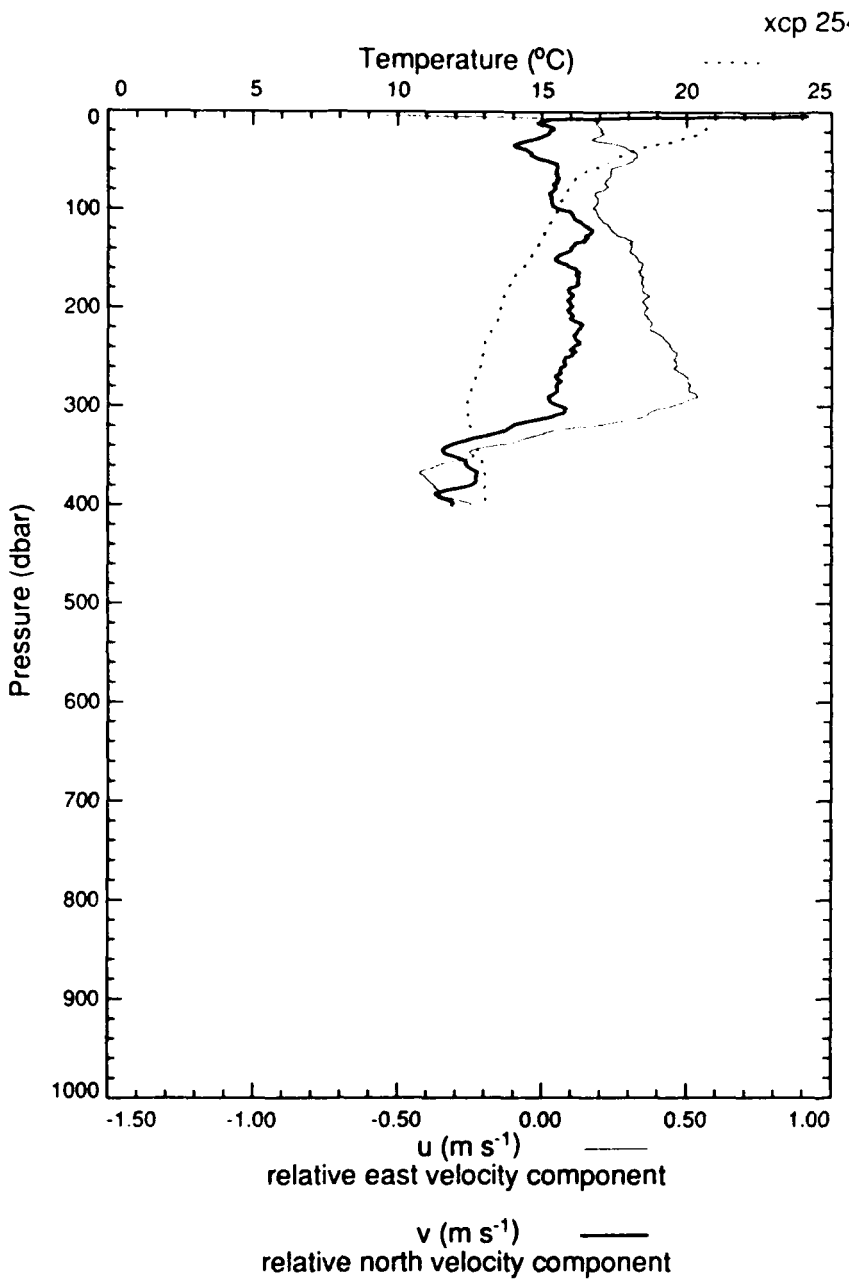
xcp 2542
Temperature (°C)
0
5
10
15
20
25
Pressure (dbar)
0
100
200
300
400
500
600
700
800
900
1000
-1.50
-1.00
-0.50
0.00
0.50
1.00
u (m s-1)
relative east velocity component
v (m s-1)
relative north velocity component

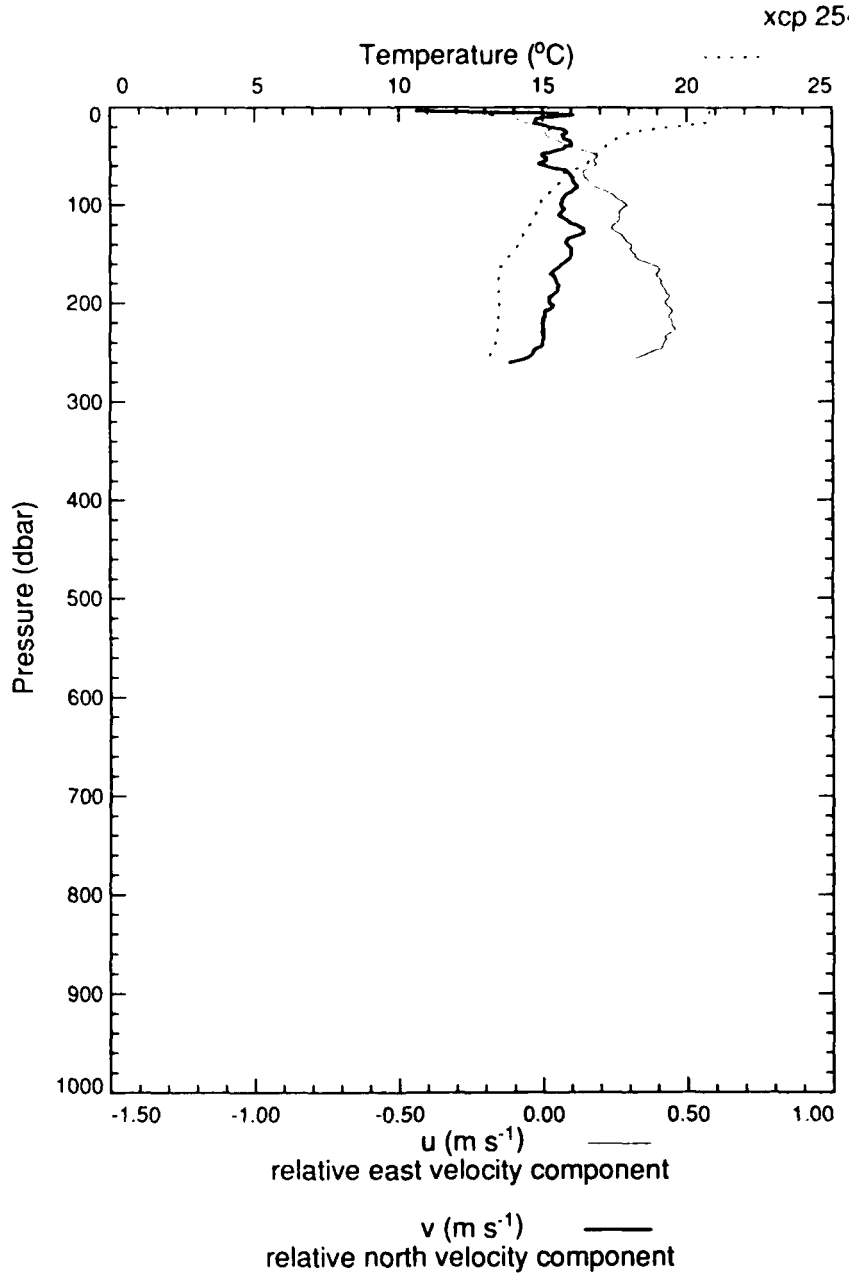
xcp 2543
Temperature (°C)
0
5
10
15
20
25
Pressure (dbar)
0
100
200
300
400
500
600
700
800
900
1000
-1.50
-1.00
-0.50
0.00
0.50
1.00
u (m s-1)
relative east velocity component
v (m s-1)
relative north velocity component

N68 TR 8925

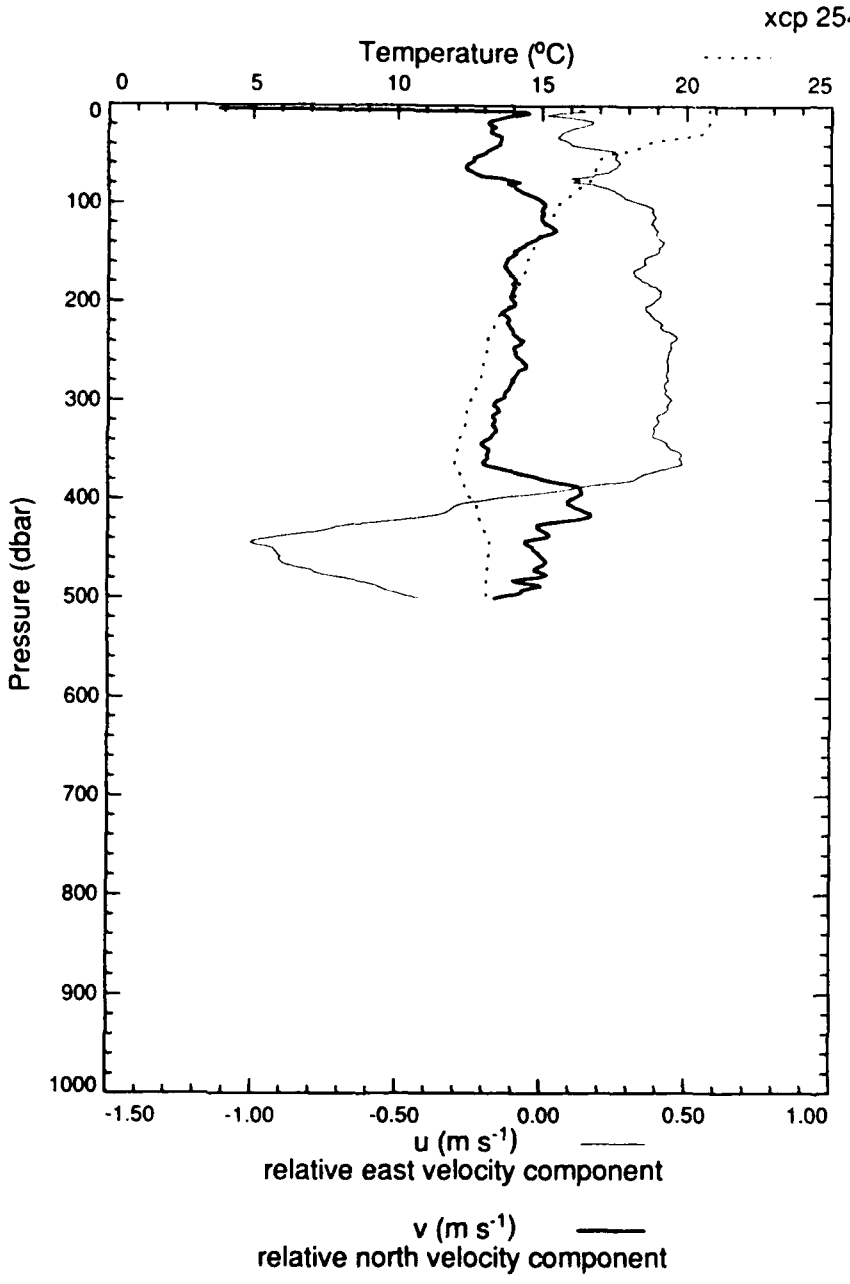
xcp 2544
Temperature (°C)
0
5
10
15
20
25
Pressure (dbar)
0
100
200
300
400
500
600
700
800
900
1000
-1.50
-1.00
-0.50
0.00
0.50
1.00
u (m s-1)
relative east velocity component
v (m s-1)
relative north velocity component

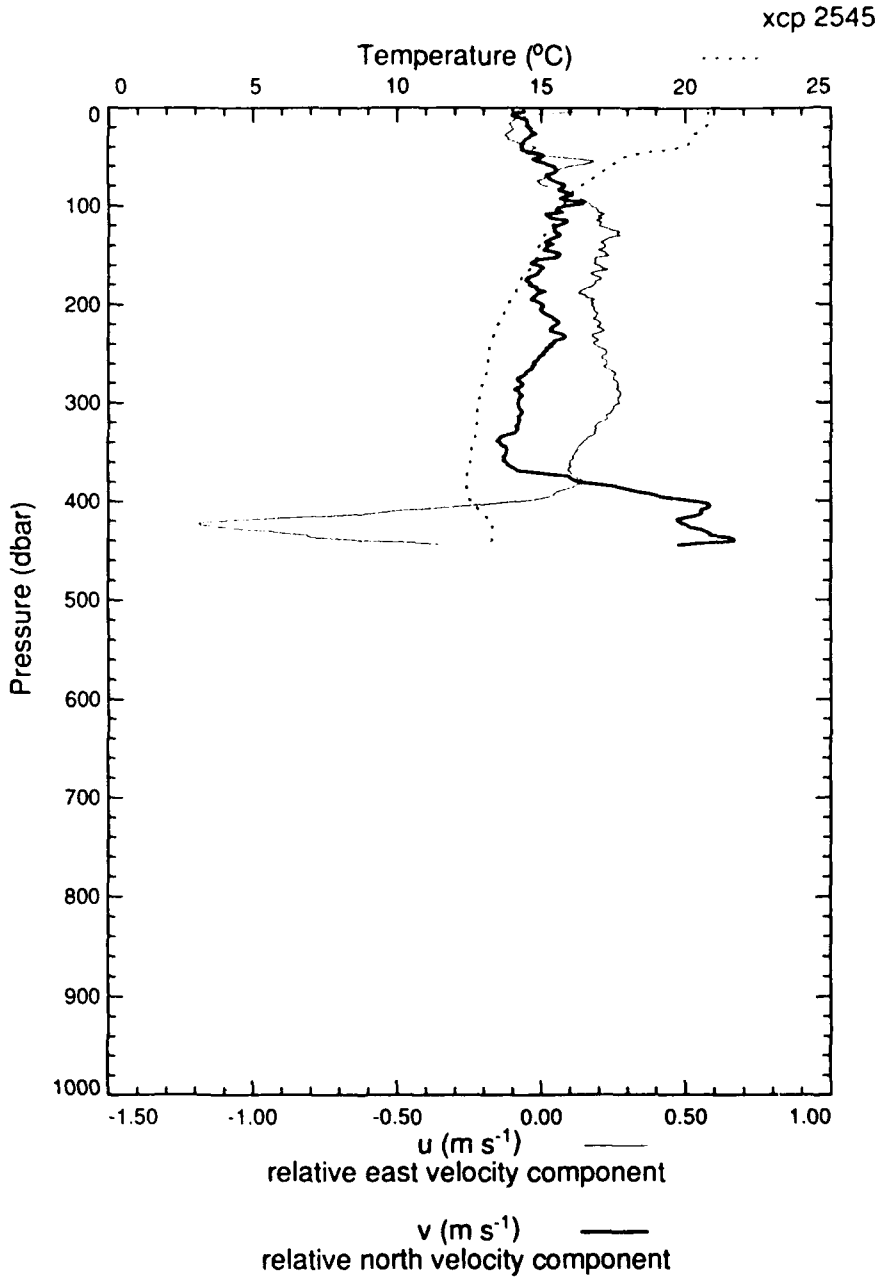
xcp 2545
Temperature (°C)
0
5
10
15
20
25
Pressure (dbar)
0
100
200
300
400
500
600
700
800
900
1000
-1.50
-1.00
-0.50
0.00
0.50
1.00
u (m s-1)
relative east velocity component
v (m s-1)
relative north velocity component

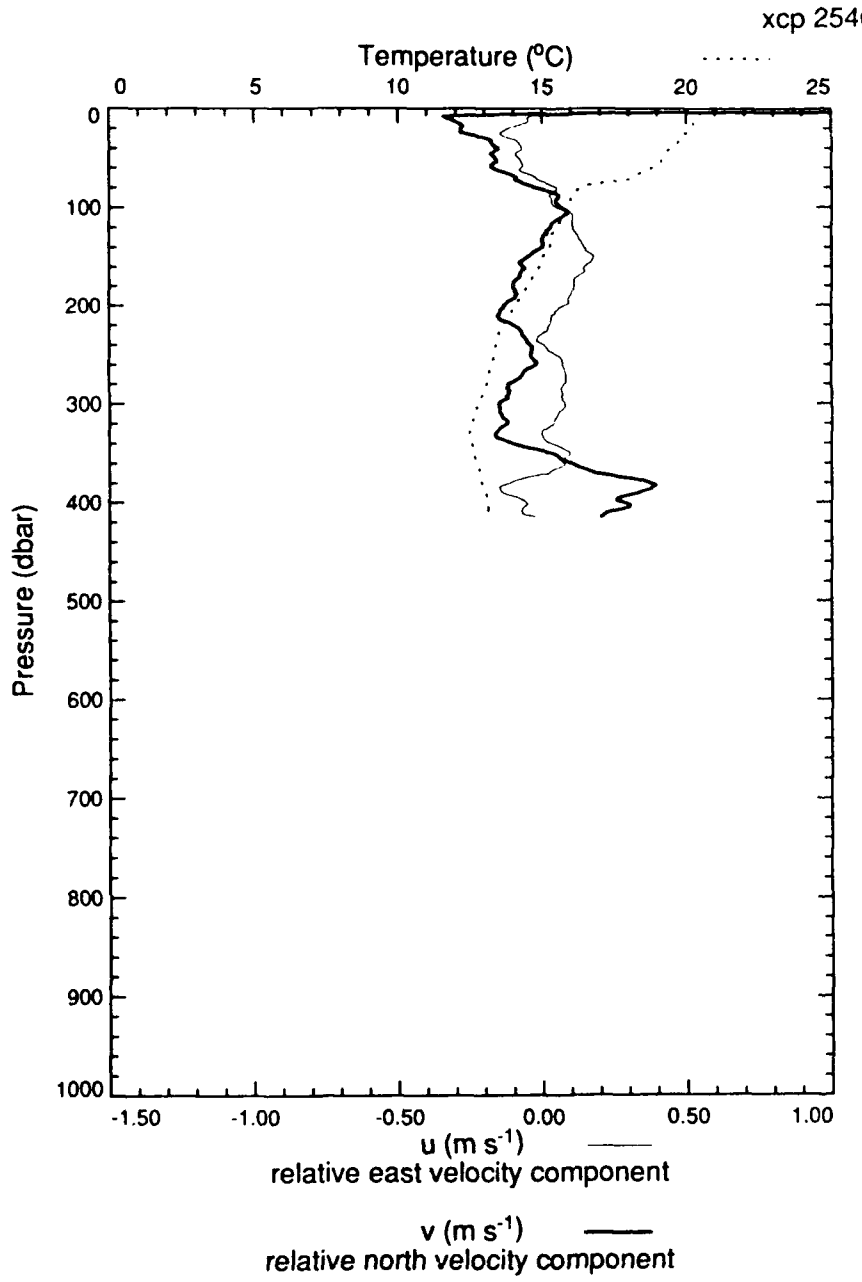
xcp 2546
Temperature (°C)
0
5
10
15
20
25
Pressure (dbar)
0
100
200
300
400
500
600
700
800
900
1000
-1.50
-1.00
-0.50
0.00
0.50
1.00
u (m s-1)
relative east velocity component
v (m s-1)
relative north velocity component

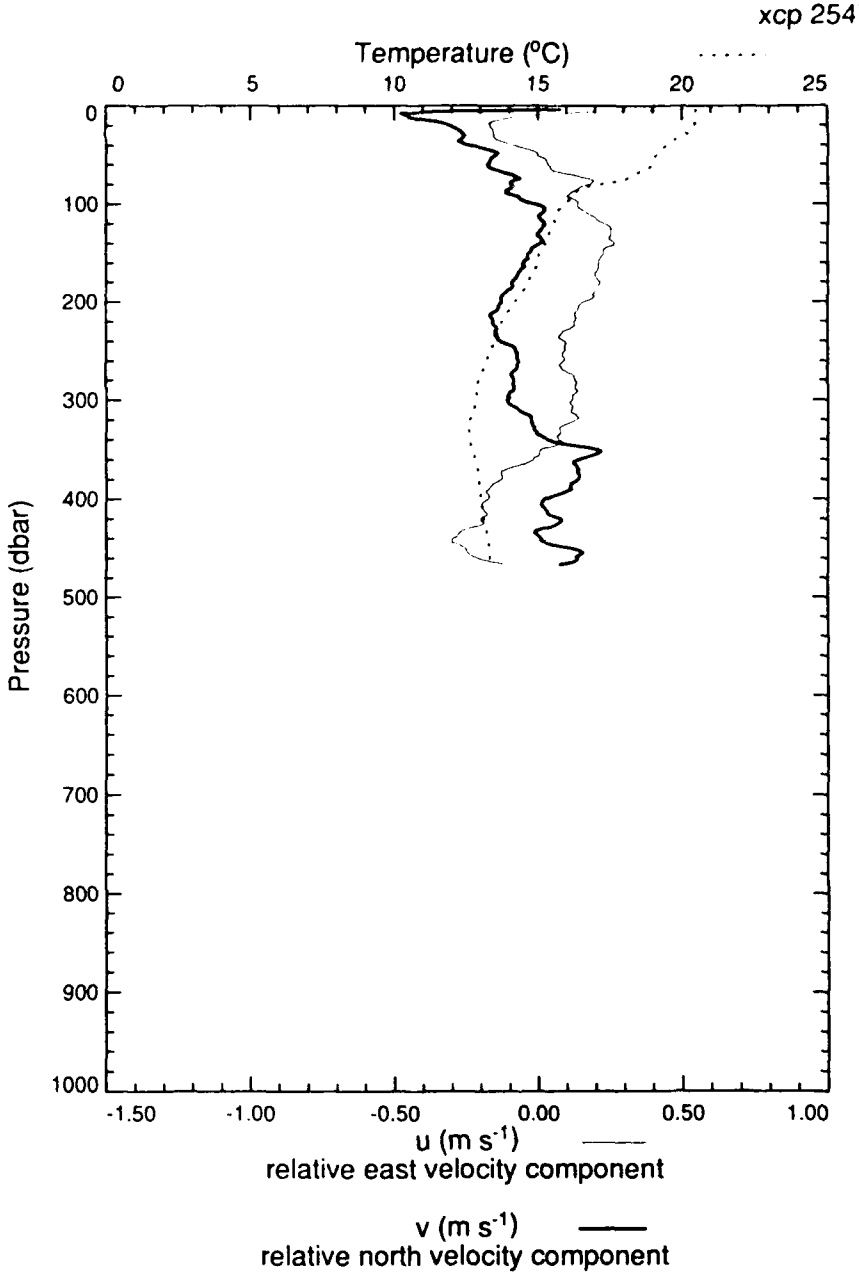
xcp 2547
Temperature (°C)
0
5
10
15
20
25
Pressure (dbar)
0
100
200
300
400
500
600
700
800
900
1000
-1.50
-1.00
-0.50
0.00
0.50
1.00
u (m s-1)
relative east velocity component
v (m s-1)
relative north velocity component

N70 TR 8925

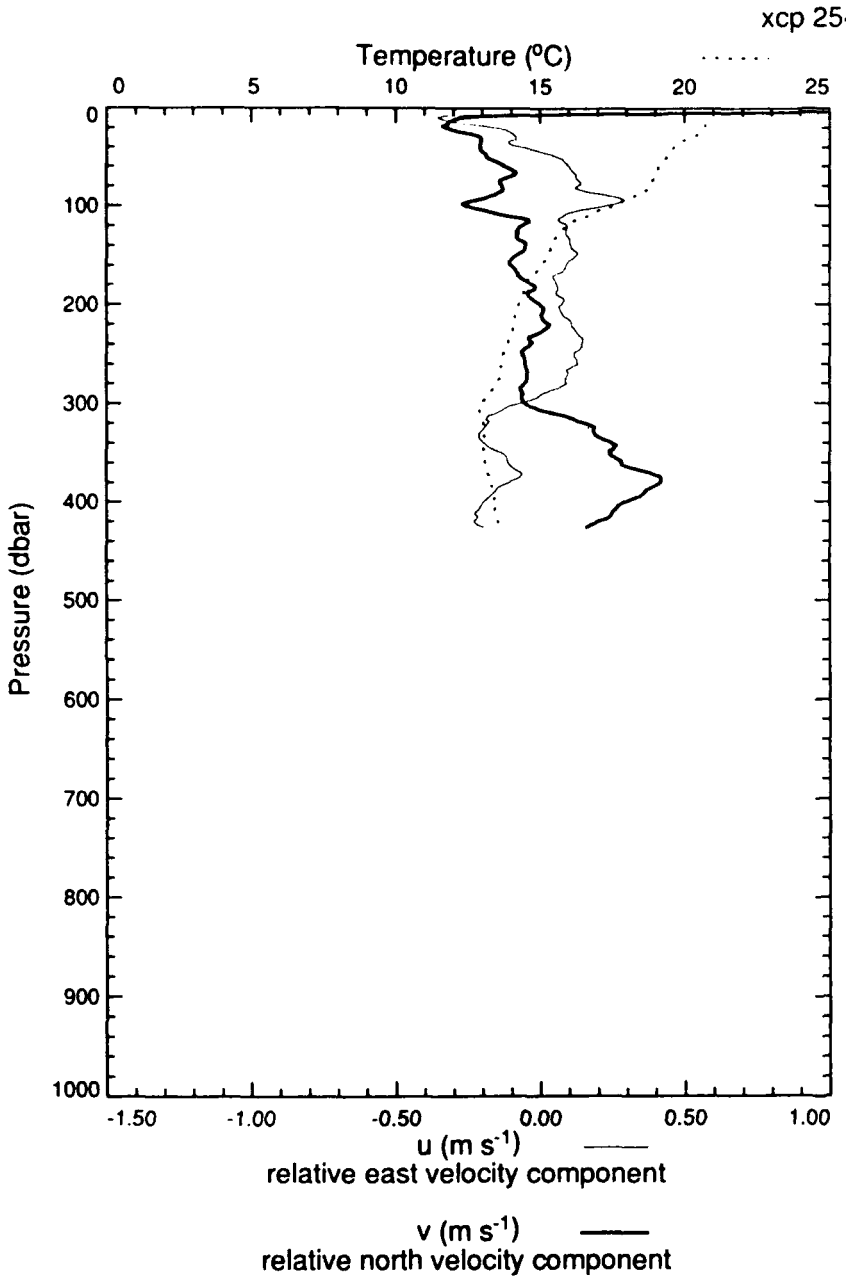
xcp 2548
Temperature (°C)
0
5
10
15
20
25
Pressure (dbar)
0
100
200
300
400
500
600
700
800
900
1000
-1.50
-1.00
-0.50
0.00
0.50
1.00
u (m s-1)
relative east velocity component
v (m s-1)
relative north velocity component

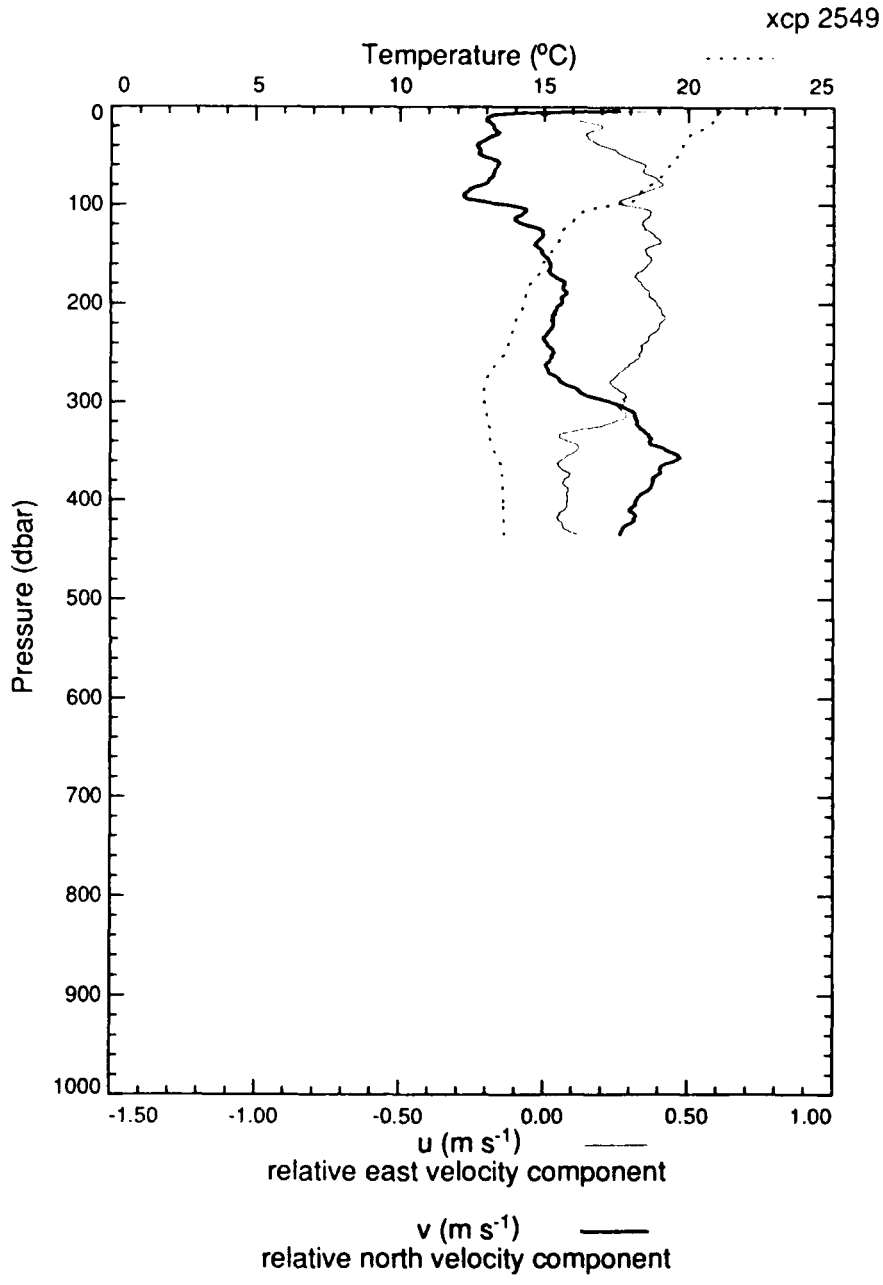
xcp 2549
Temperature (°C)
0
5
10
15
20
25
Pressure (dbar)
0
100
200
300
400
500
600
700
800
900
1000
-1.50
-1.00
-0.50
0.00
0.50
1.00
u (m s-1)
relative east velocity component
v (m s-1)
relative north velocity component

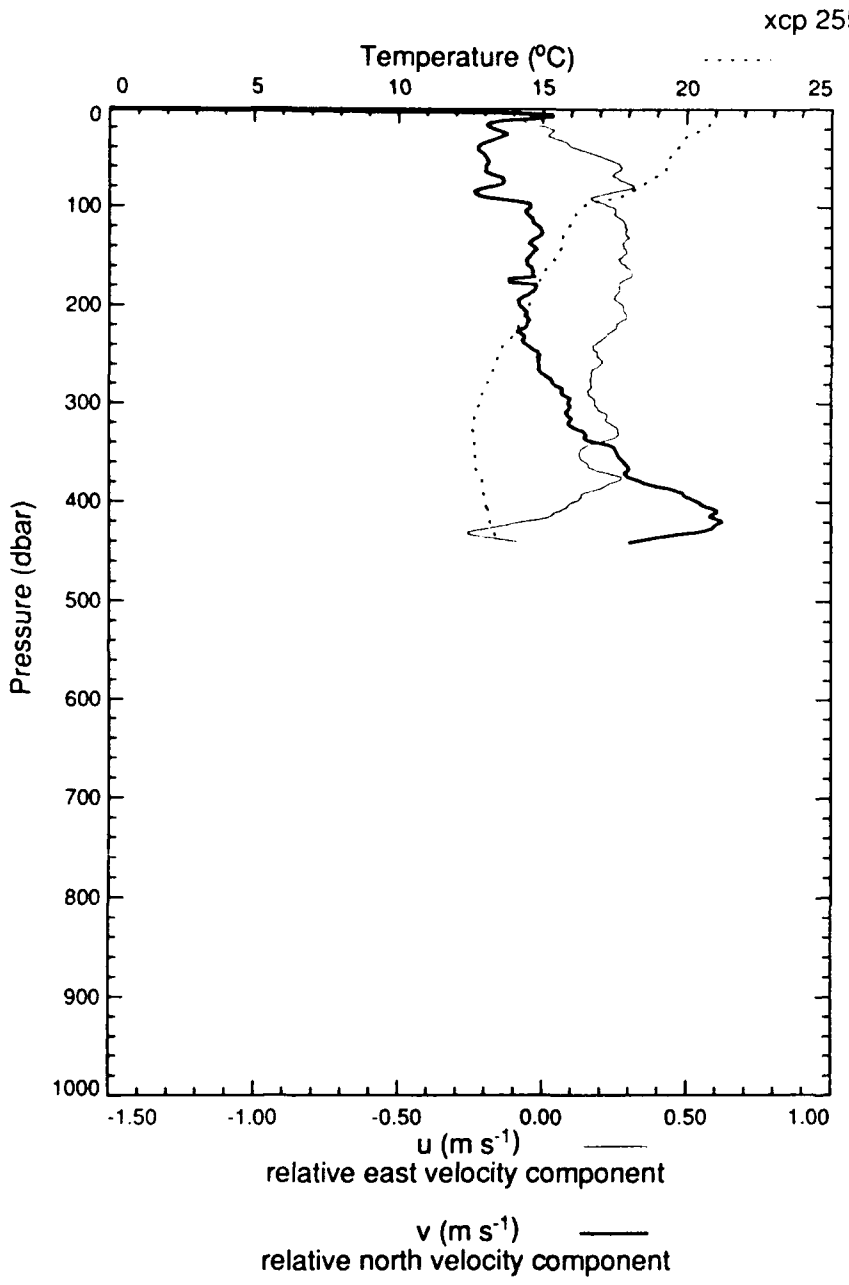
xcp 2550
Temperature (°C)
0
5
10
15
20
25
Pressure (dbar)
0
100
200
300
400
500
600
700
800
900
1000
-1.50
-1.00
-0.50
0.00
0.50
1.00
u (m s-1)
relative east velocity component
v (m s-1)
relative north velocity component

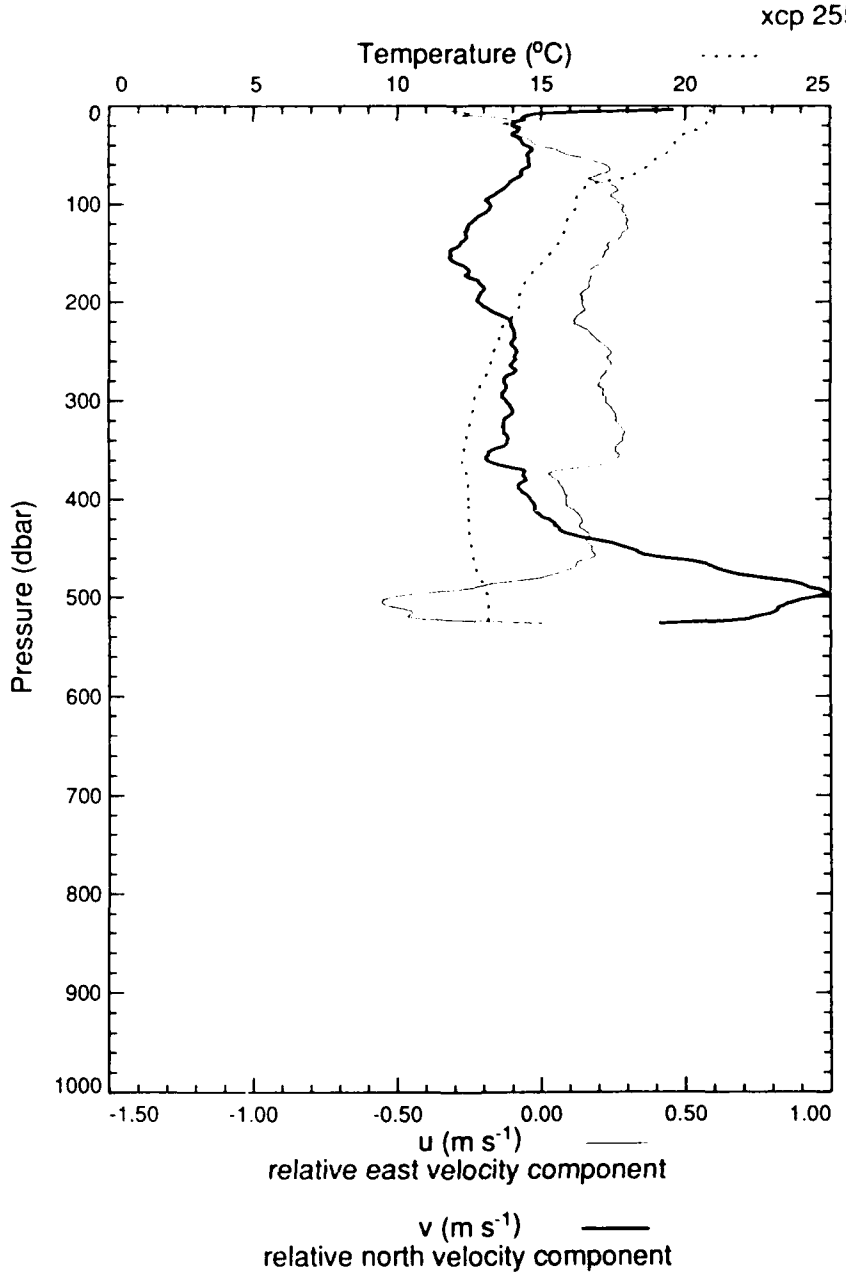
xcp 2551
Temperature (°C)
0
5
10
15
20
25
Pressure (dbar)
0
100
200
300
400
500
600
700
800
900
1000
-1.50
-1.00
-0.50
0.00
0.50
1.00
u (m s-1)
relative east velocity component
v (m s-1)
relative north velocity component

N72 TR 8925

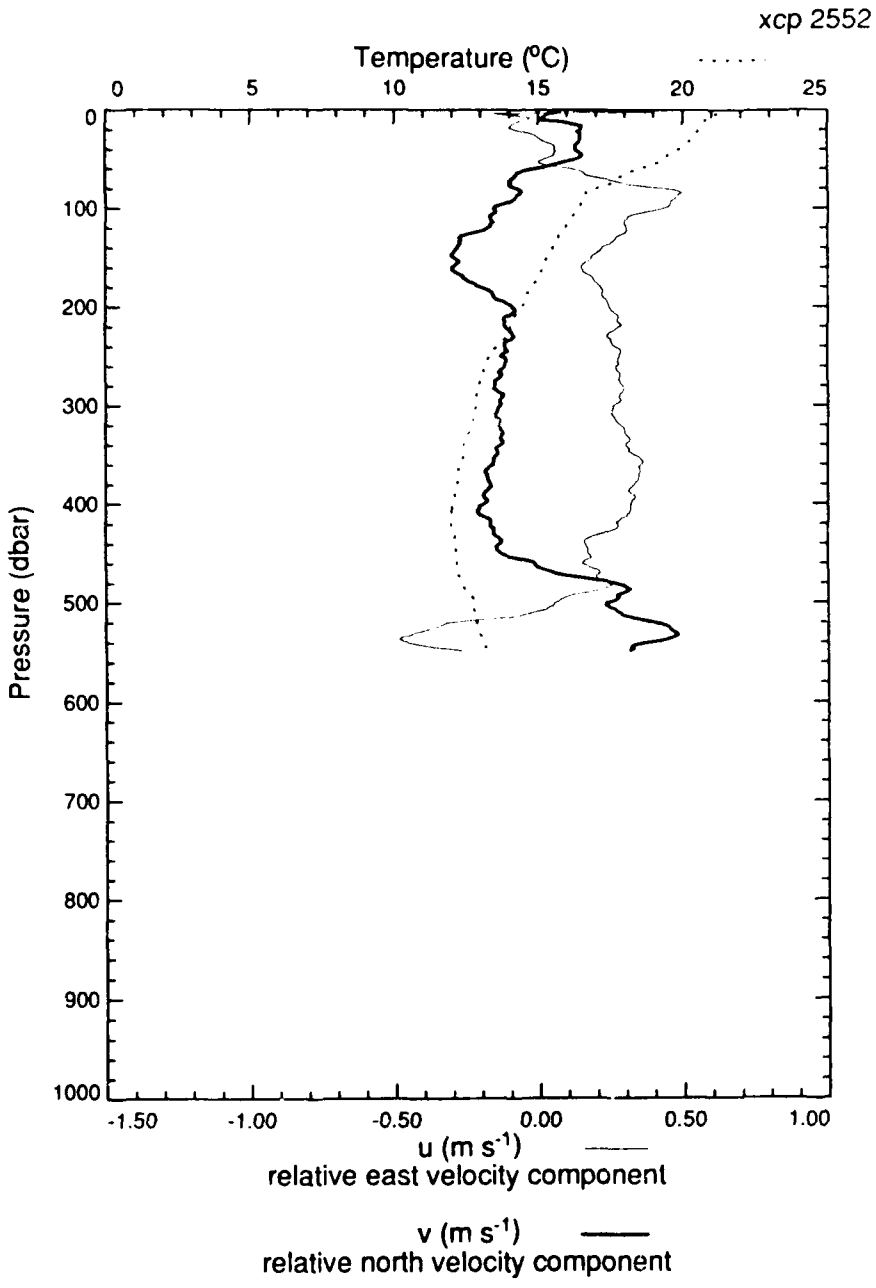
xcp 2552
Temperature (°C)
0
5
10
15
20
25
Pressure (dbar)
0
100
200
300
400
500
600
700
800
900
1000
-1.50
-1.00
-0.50
0.00
0.50
1.00
u (m s-1)
relative east velocity component
v (m s-1)
relative north velocity component

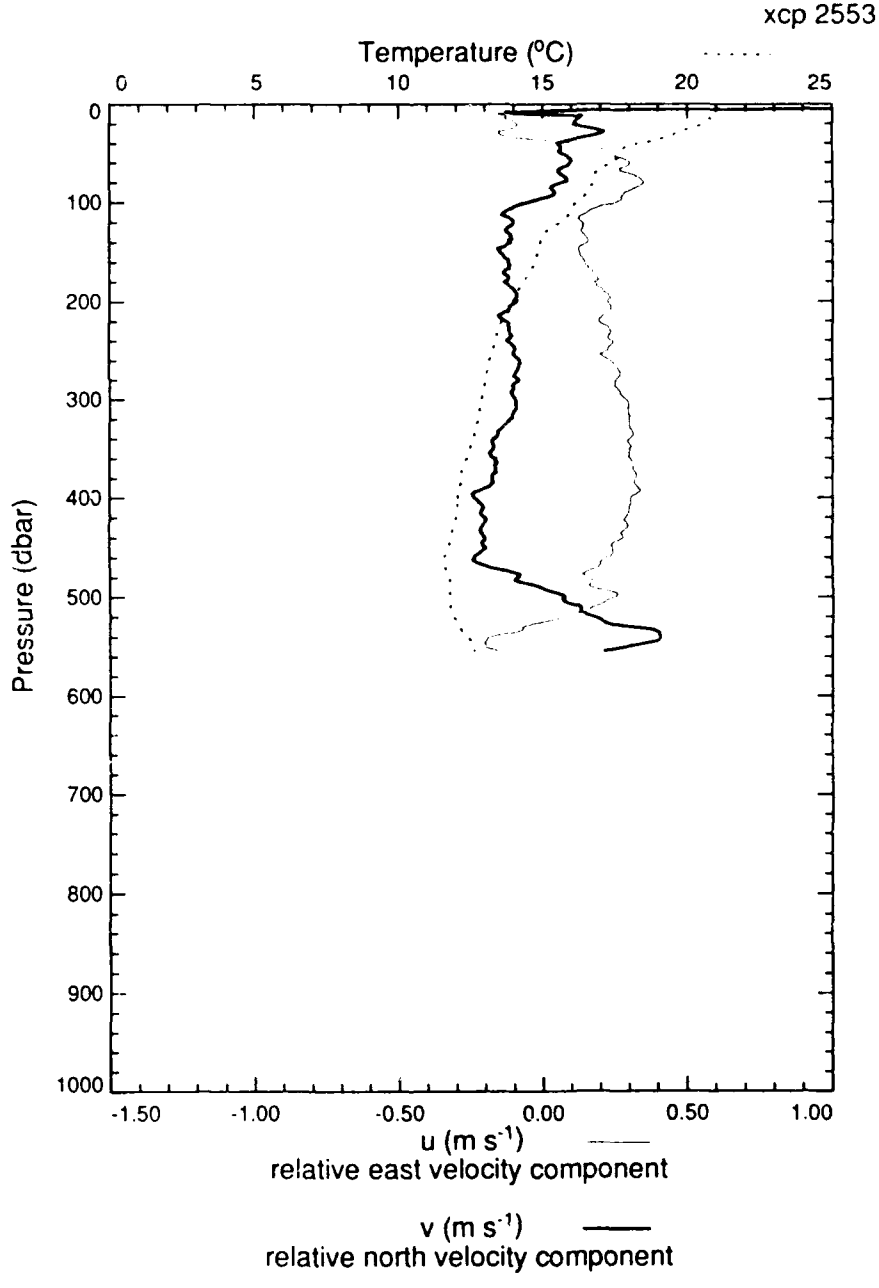
xcp 2553
Temperature (°C)
0
5
10
15
20
25
Pressure (dbar)
0
100
200
300
400
500
600
700
800
900
1000
-1.50
-1.00
-0.50
0.00
0.50
1.00
u (m s-1)
relative east velocity component
v (m s-1)
relative north velocity component

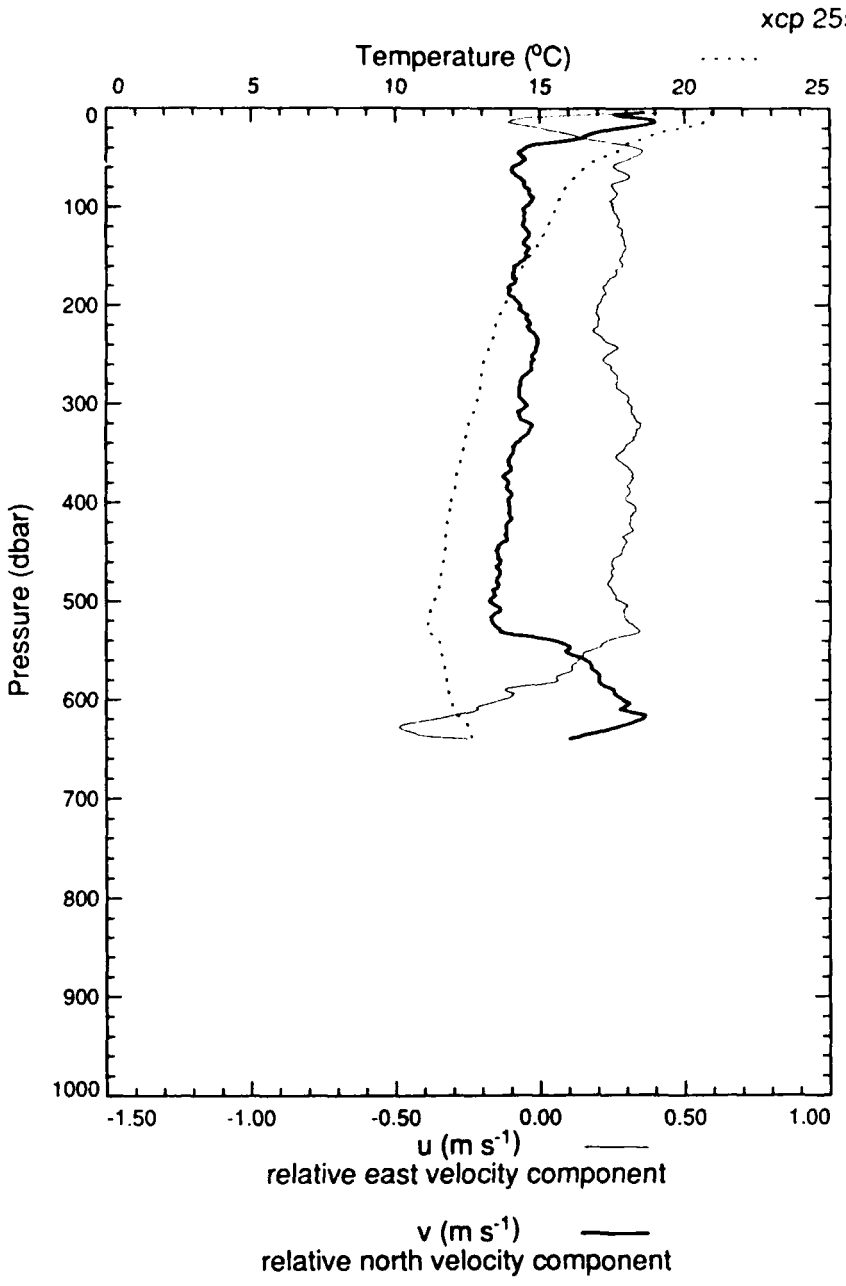
xcp 2554
Temperature (°C)
0
5
10
15
20
25
Pressure (dbar)
0
100
200
300
400
500
600
700
800
900
1000
-1.50
-1.00
-0.50
0.00
0.50
1.00
u (m s-1)
relative east velocity component
v (m s-1)
relative north velocity component

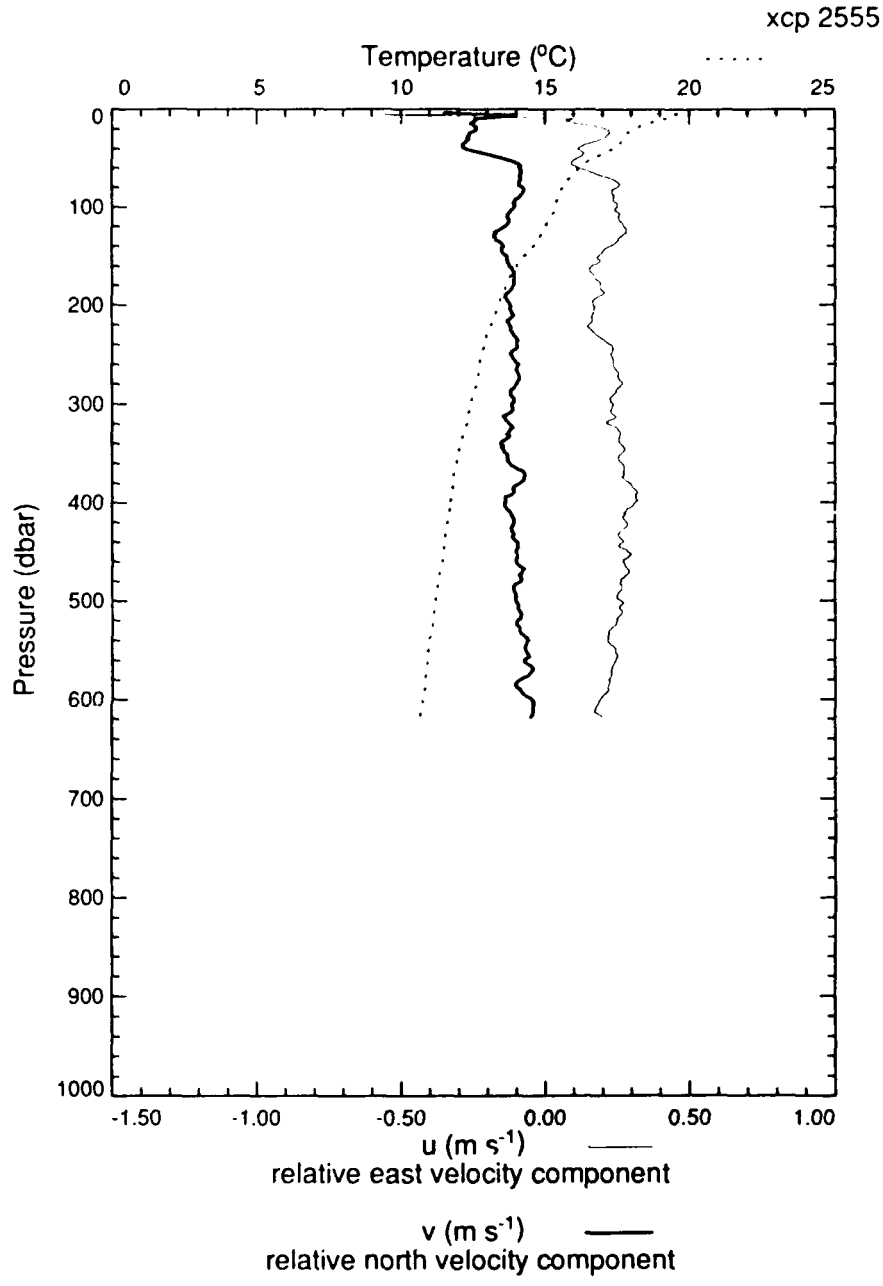
xcp 2555
Temperature (°C)
0
5
10
15
20
25
Pressure (dbar)
0
100
200
300
400
500
600
700
800
900
1000
-1.50
-1.00
-0.50
0.00
0.50
1.00
u (m s-1)
relative east velocity component
v (m s-1)
relative north velocity component

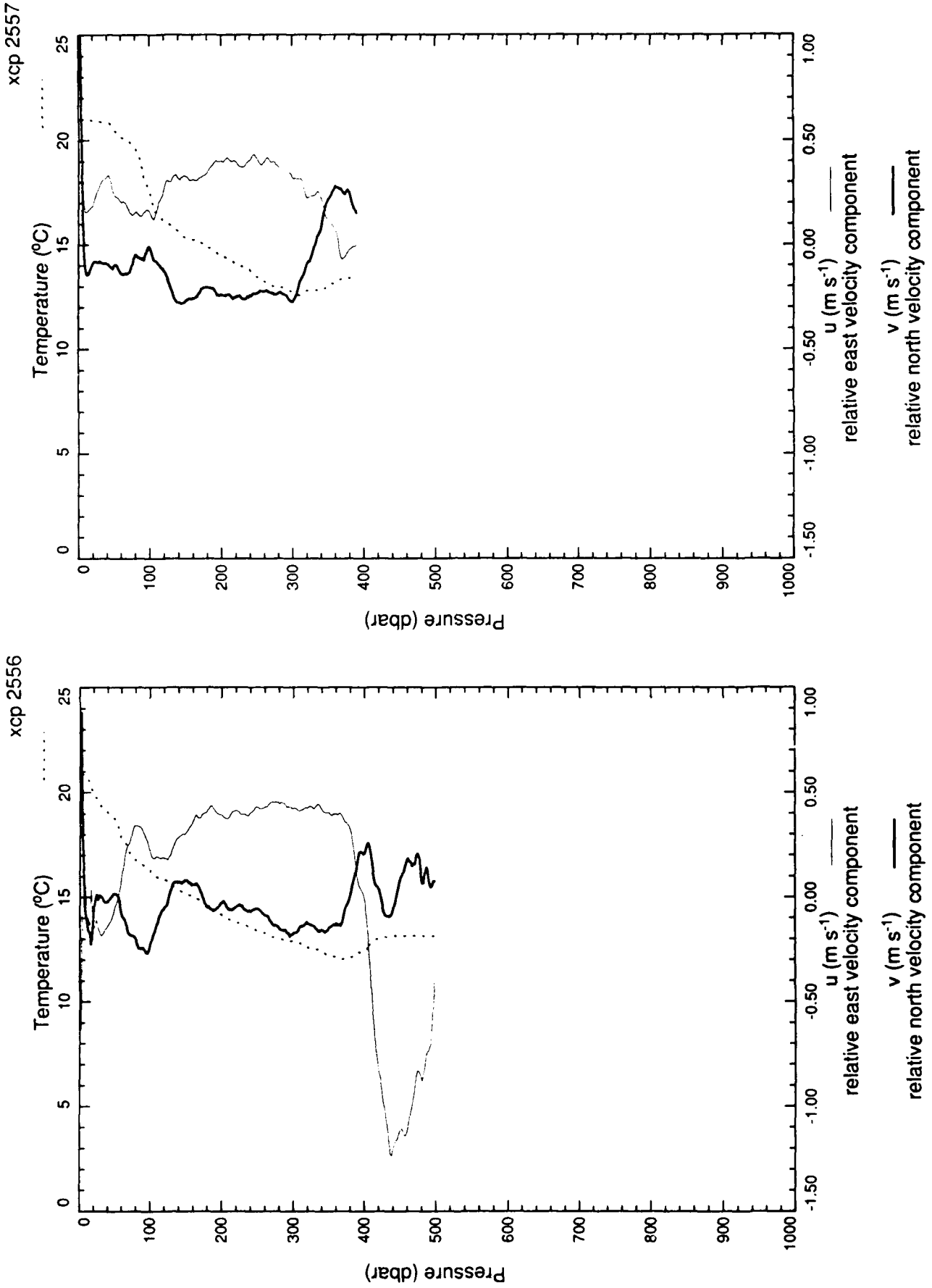
xcp 2557
Temperature (°C)
Pressure (dbar)
u (m s-1)
relative east velocity component
v (m s-1)
relative north velocity component
xcp 2556
Temperature (°C)
Pressure (dbar)
u (m s-1)
relative east velocity component
v (m s-1)
relative north velocity component

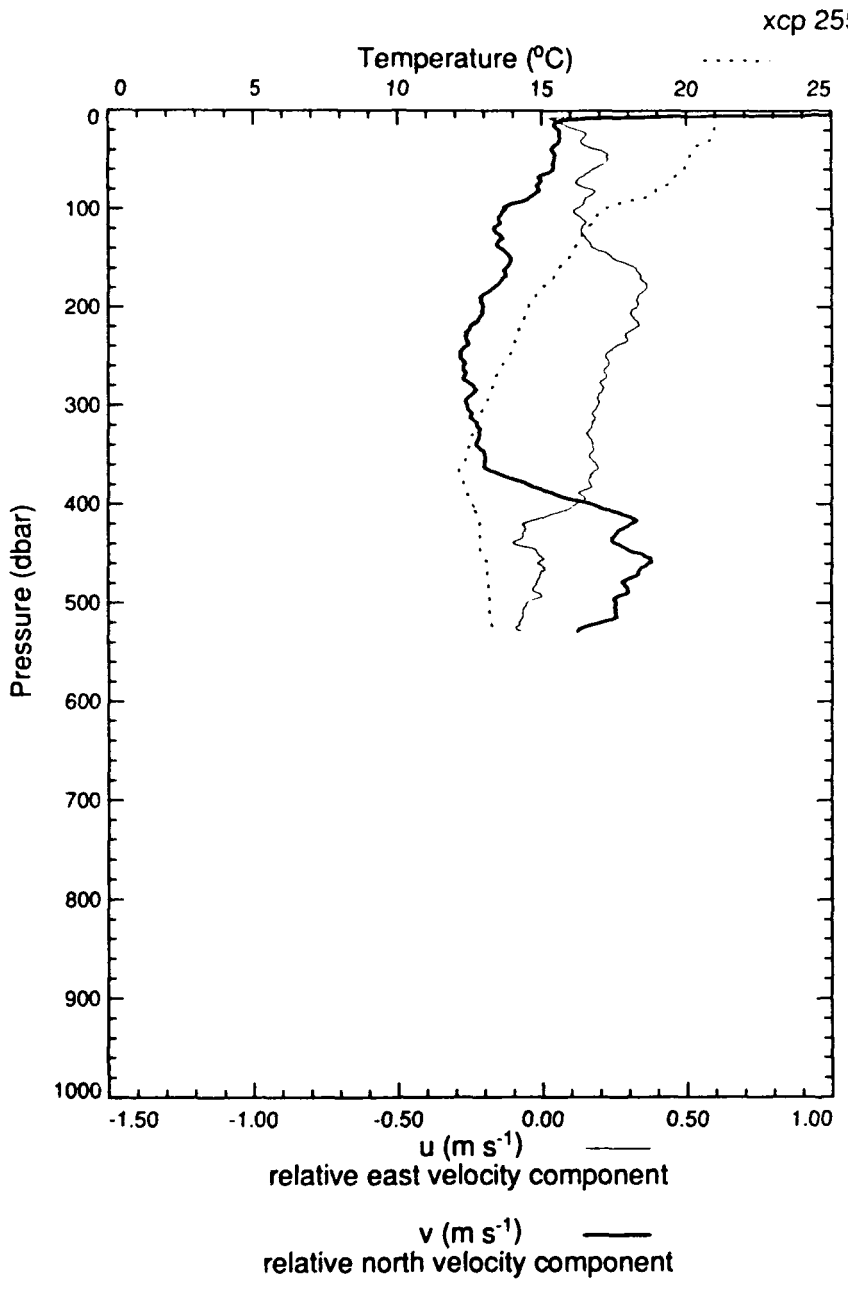
xcp 2558
Temperature (°C)
0
5
10
15
20
25
Pressure (dbar)
0
100
200
300
400
500
600
700
800
900
1000
-1.50
-1.00
-0.50
0.00
0.50
1.00
u (m s-1)
relative east velocity component
v (m s-1)
relative north velocity component

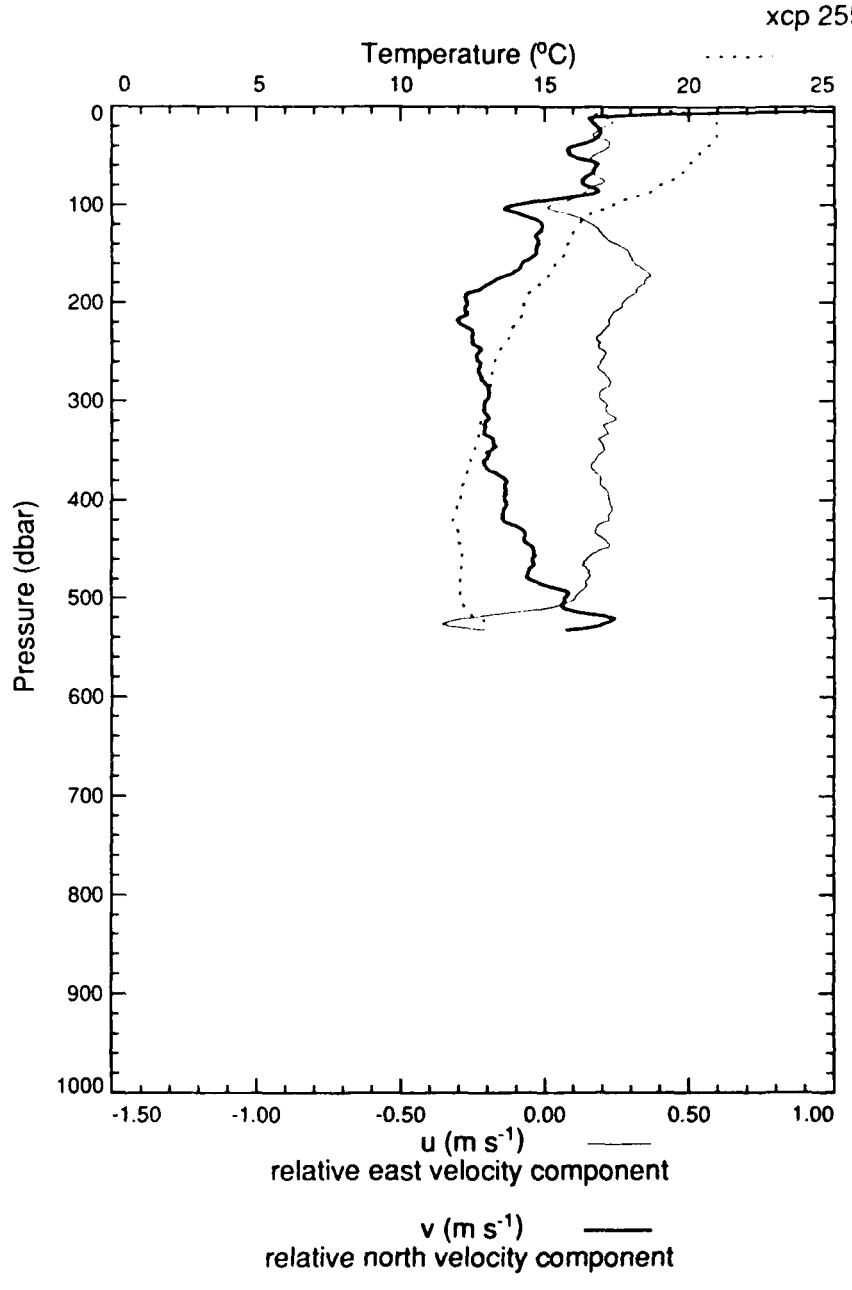
xcp 2559
Temperature (°C)
0
5
10
15
20
25
Pressure (dbar)
0
100
200
300
400
500
600
700
800
900
1000
-1.50
-1.00
-0.50
0.00
0.50
1.00
u (m s-1)
relative east velocity component
v (m s-1)
relative north velocity component

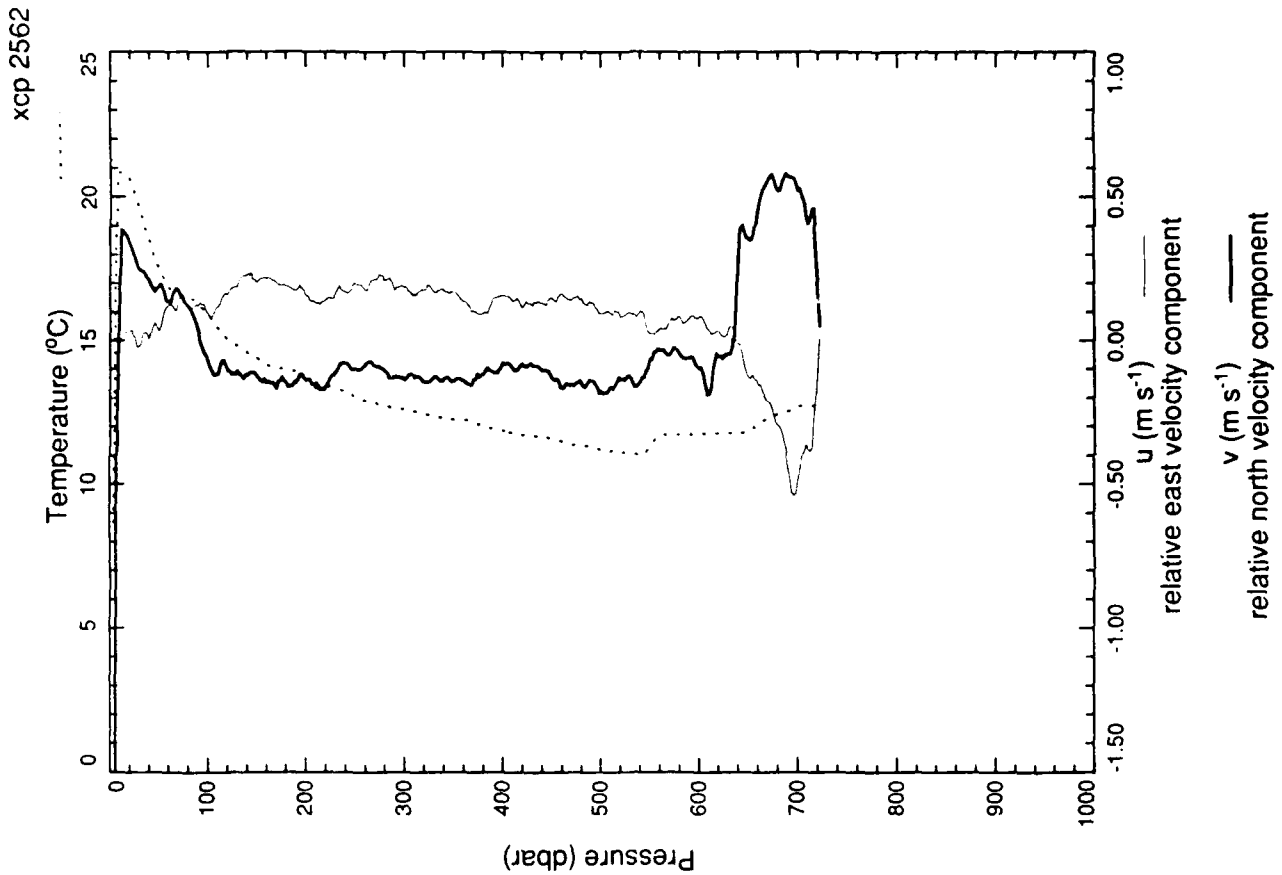
xcp 2562
Temperature (°C)
Pressure (dbar)
u (m s-1)
relative east velocity component
v (m s-1)
relative north velocity component

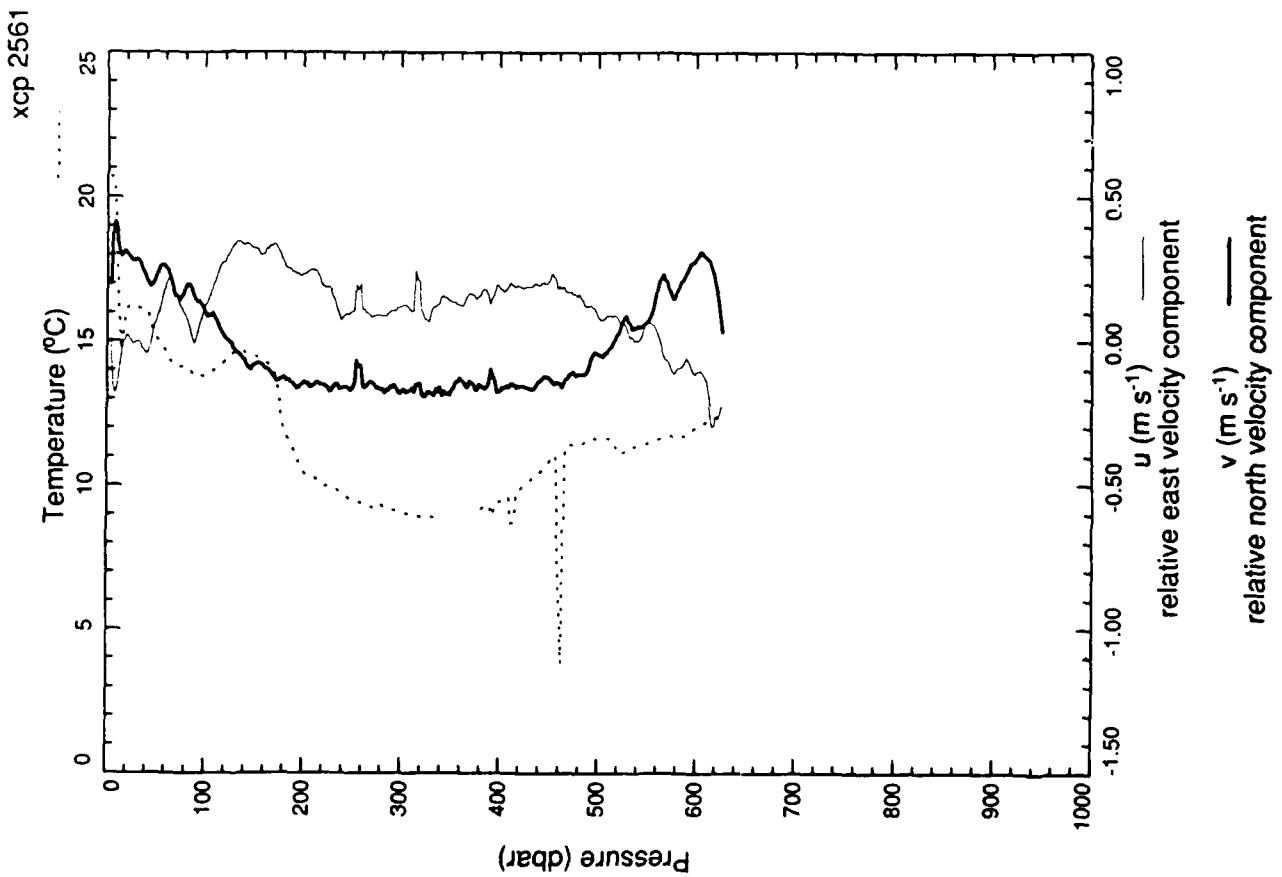
xcp 2561
Temperature (°C)
Pressure (dbar)
u (m s-1)
relative east velocity component
v (m s-1)
relative north velocity component

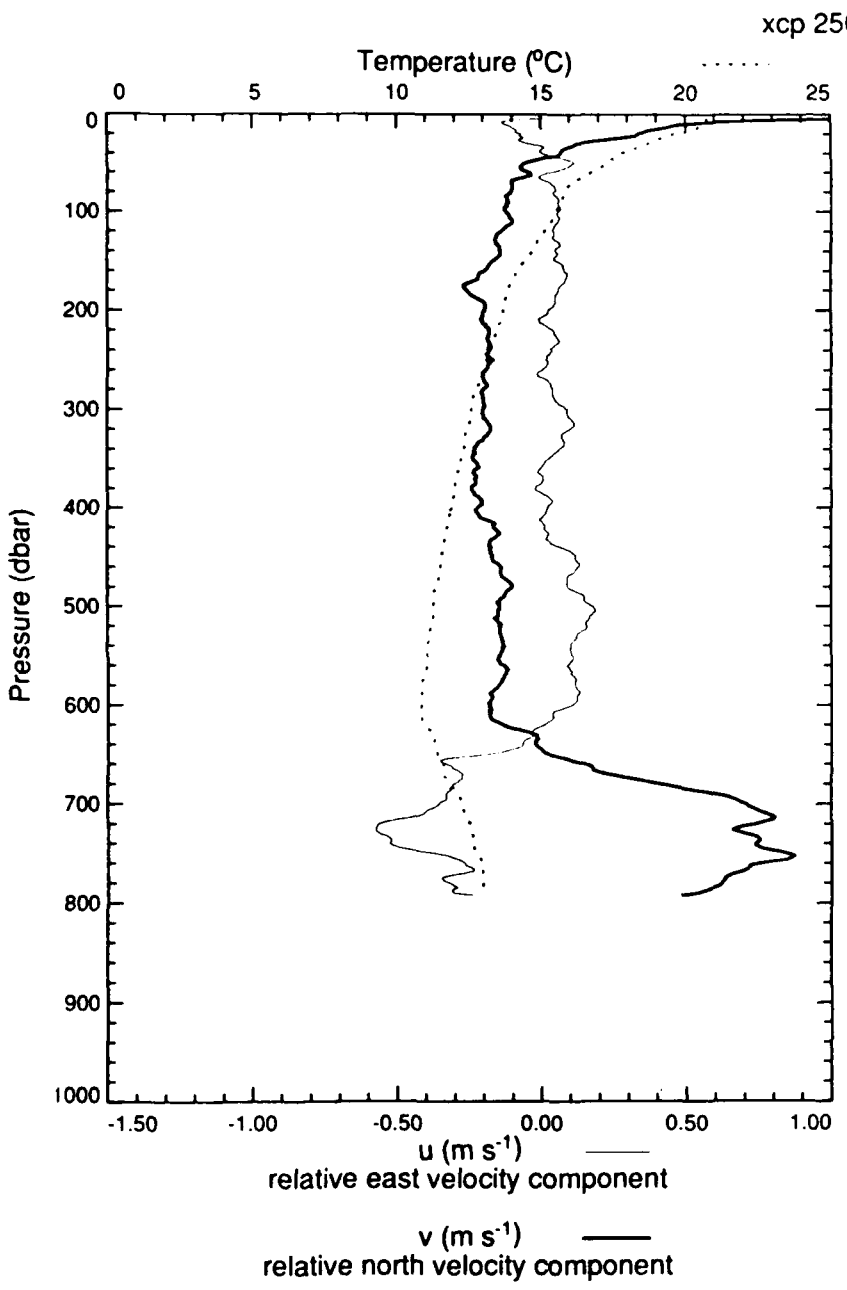
xcp 2563
Temperature (°C)
0
5
10
15
20
25
Pressure (dbar)
0
100
200
300
400
500
600
700
800
900
1000
-1.50
-1.00
-0.50
0.00
0.50
1.00
u (m s-1)
relative east velocity component
v (m s-1)
relative north velocity component

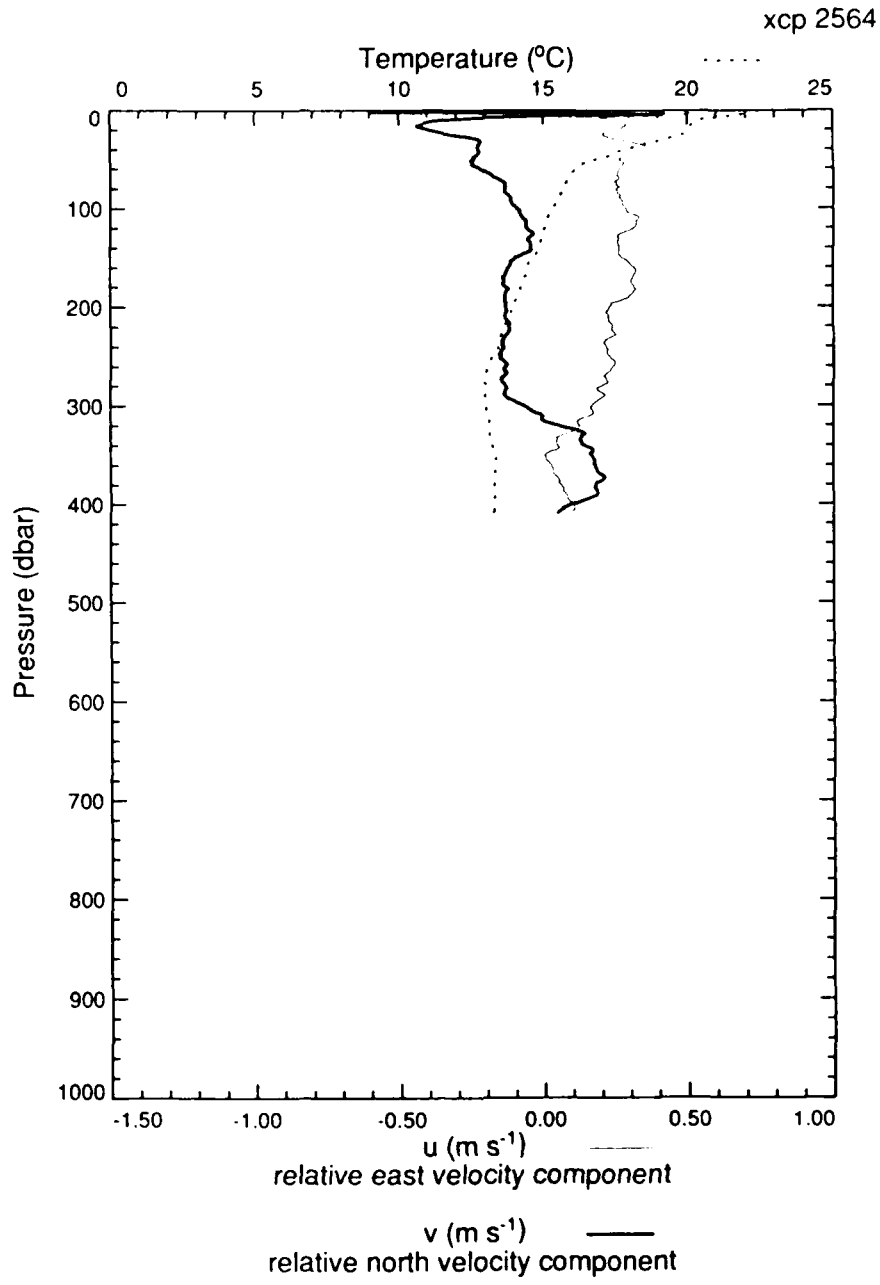
xcp 2564
Temperature (°C)
0
5
10
15
20
25
Pressure (dbar)
0
100
200
300
400
500
600
700
800
900
1000
-1.50
-1.00
-0.50
0.00
0.50
1.00
u (m s-1)
relative east velocity component
v (m s-1)
relative north velocity component

N78 TR 8925

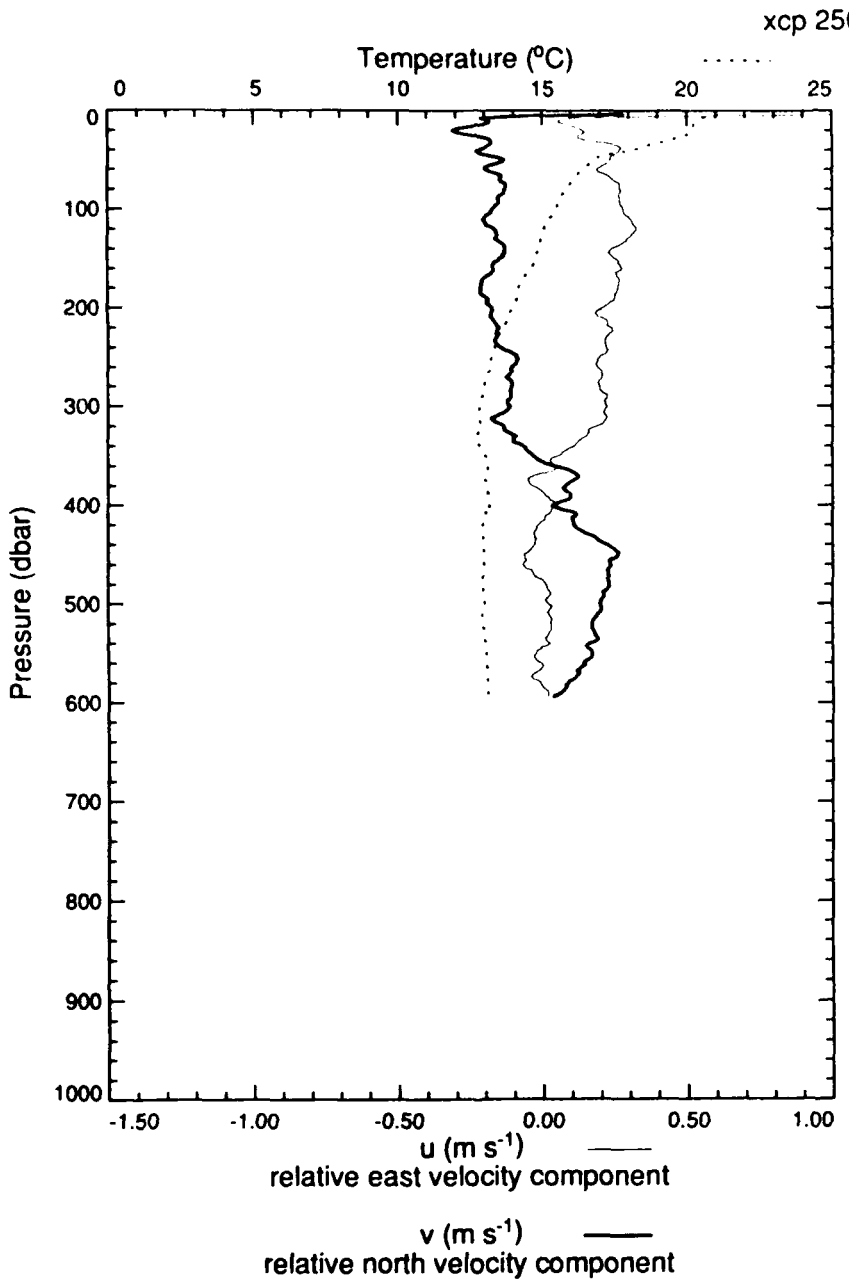
xcp 2565
Temperature (°C)
0
5
10
15
20
25
Pressure (dbar)
0
100
200
300
400
500
600
700
800
900
1000
-1.50
-1.00
-0.50
0.00
0.50
1.00
u (m s-1)
relative east velocity component
v (m s-1)
relative north velocity component

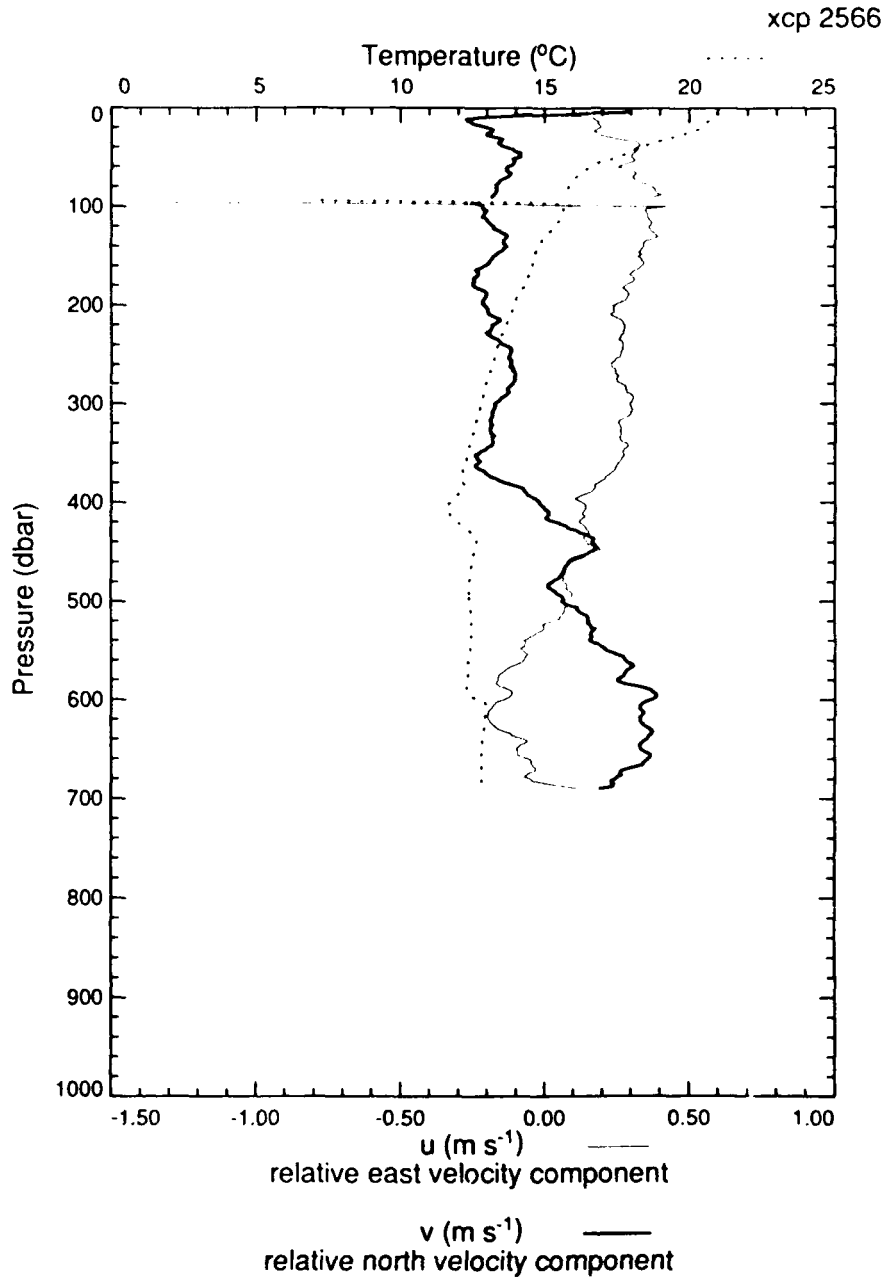
xcp 2566
Temperature (°C)
0
5
10
15
20
25
Pressure (dbar)
0
100
200
300
400
500
600
700
800
900
1000
-1.50
-1.00
-0.50
0.00
0.50
1.00
u (m s-1)
relative east velocity component
v (m s-1)
relative north velocity component

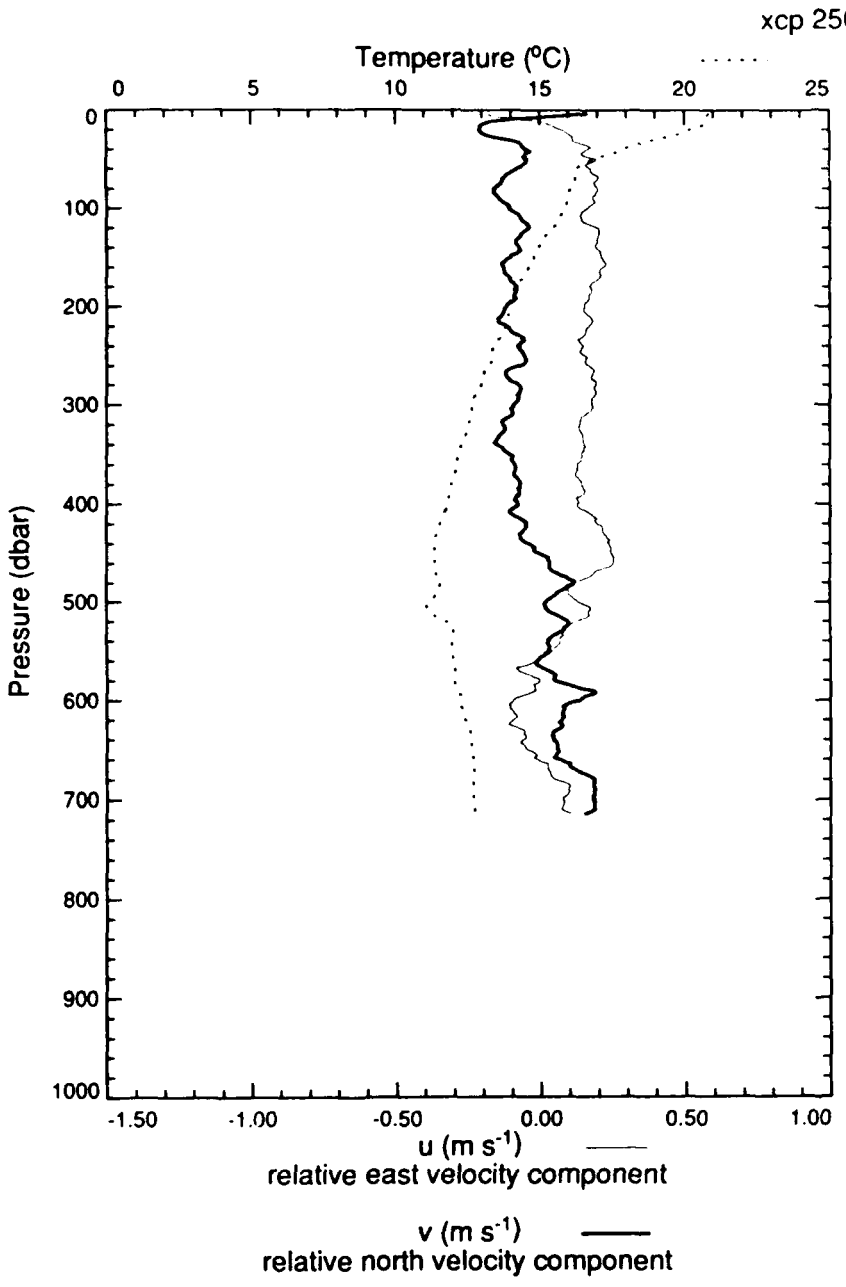
xcp 2567
Temperature (°C)
0
5
10
15
20
25
Pressure (dbar)
0
100
200
300
400
500
600
700
800
900
1000
-1.50
-1.00
-0.50
0.00
0.50
1.00
u (m s-1)
relative east velocity component
v (m s-1)
relative north velocity component

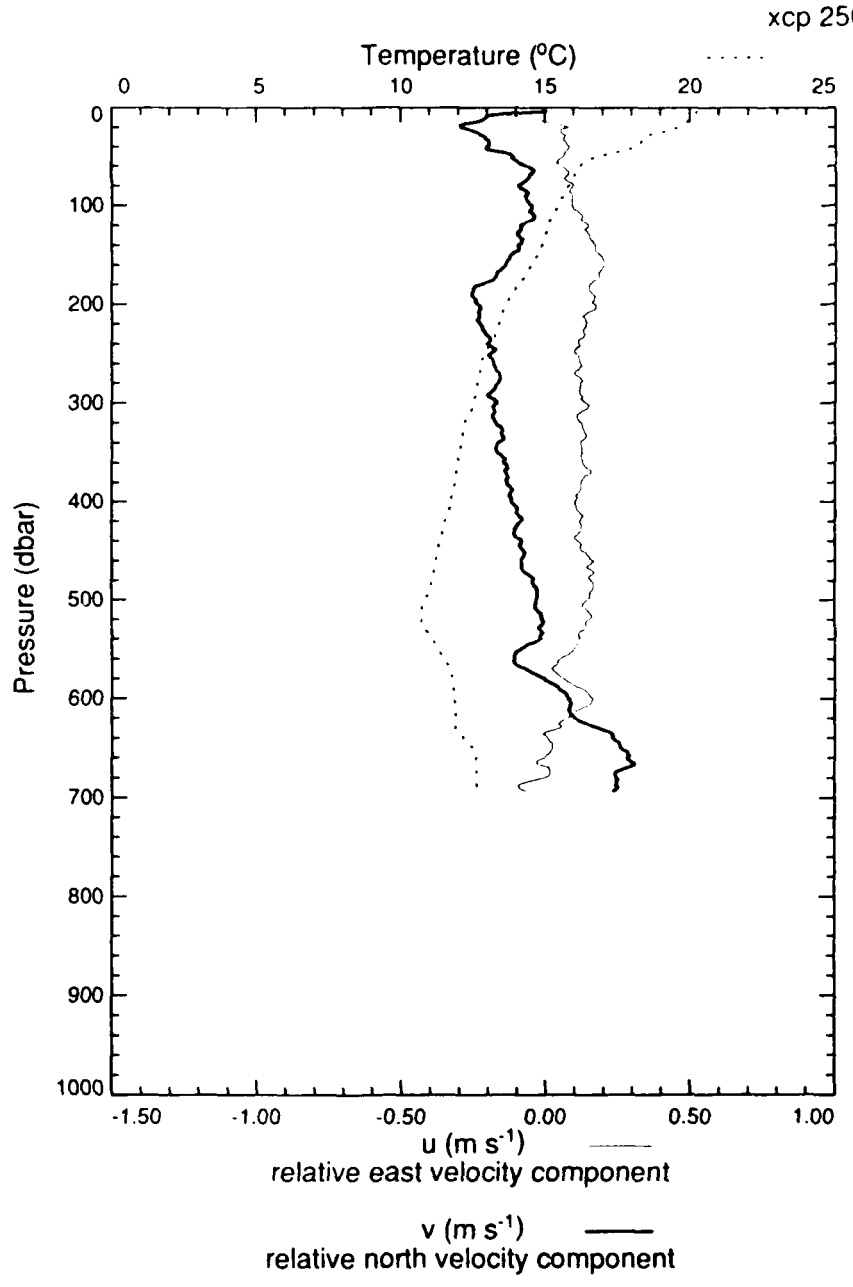
xcp 2568
Temperature (°C)
0
5
10
15
20
25
Pressure (dbar)
0
100
200
300
400
500
600
700
800
900
1000
-1.50
-1.00
-0.50
0.00
0.50
1.00
u (m s-1)
relative east velocity component
v (m s-1)
relative north velocity component

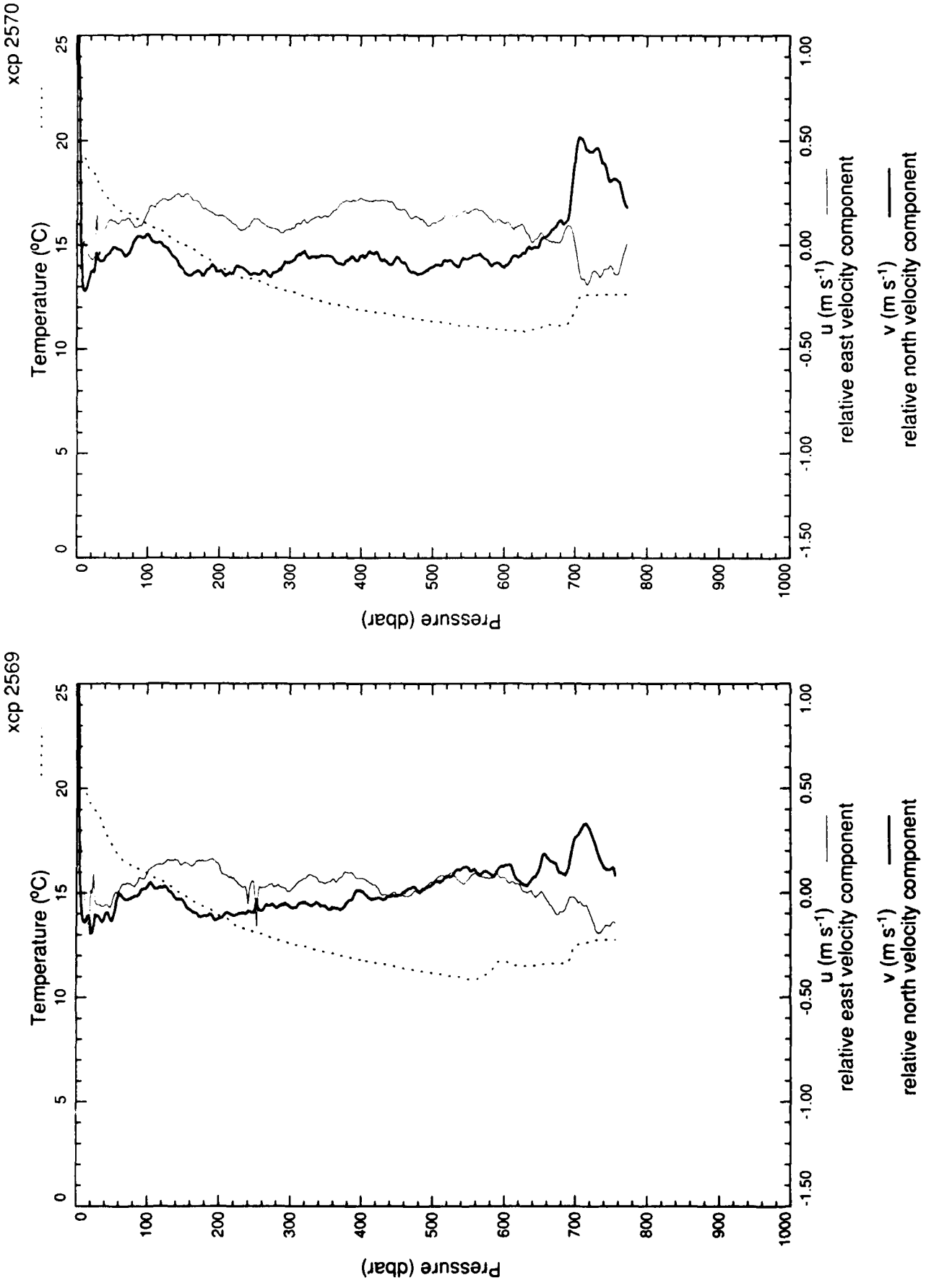
xcp 2570
Temperature (°C)
Pressure (dbar)
u (m s-1)
relative east velocity component
v (m s-1)
relative north velocity component
xcp 2569
Temperature (°C)
Pressure (dbar)
u (m s-1)
relative east velocity component
v (m s-1)
relative north velocity component

N80 TR 8925

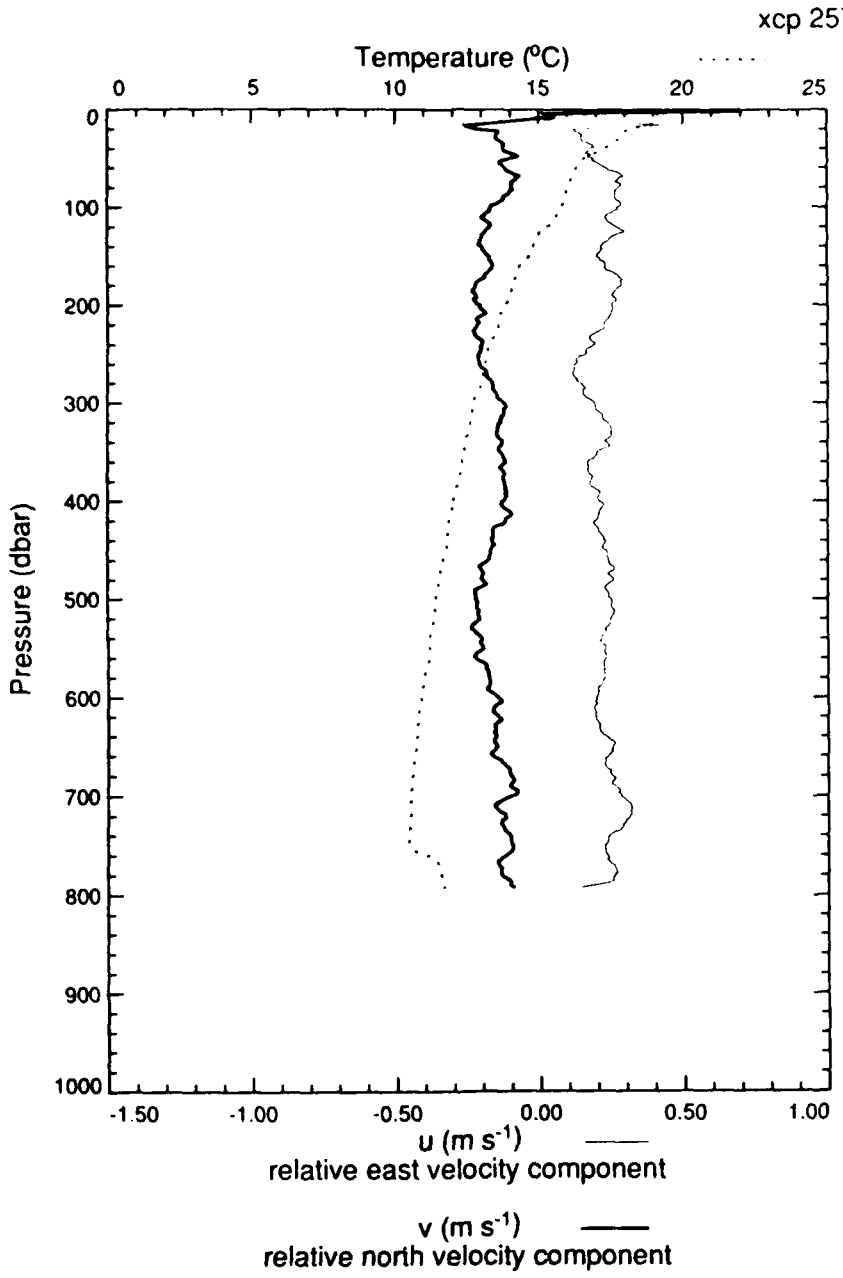
xcp 2571
Temperature (°C)
0
5
10
15
20
25
Pressure (dbar)
0
100
200
300
400
500
600
700
800
900
1000
-1.50
-1.00
-0.50
0.00
0.50
1.00
u (m s-1)
relative east velocity component
v (m s-1)
relative north velocity component

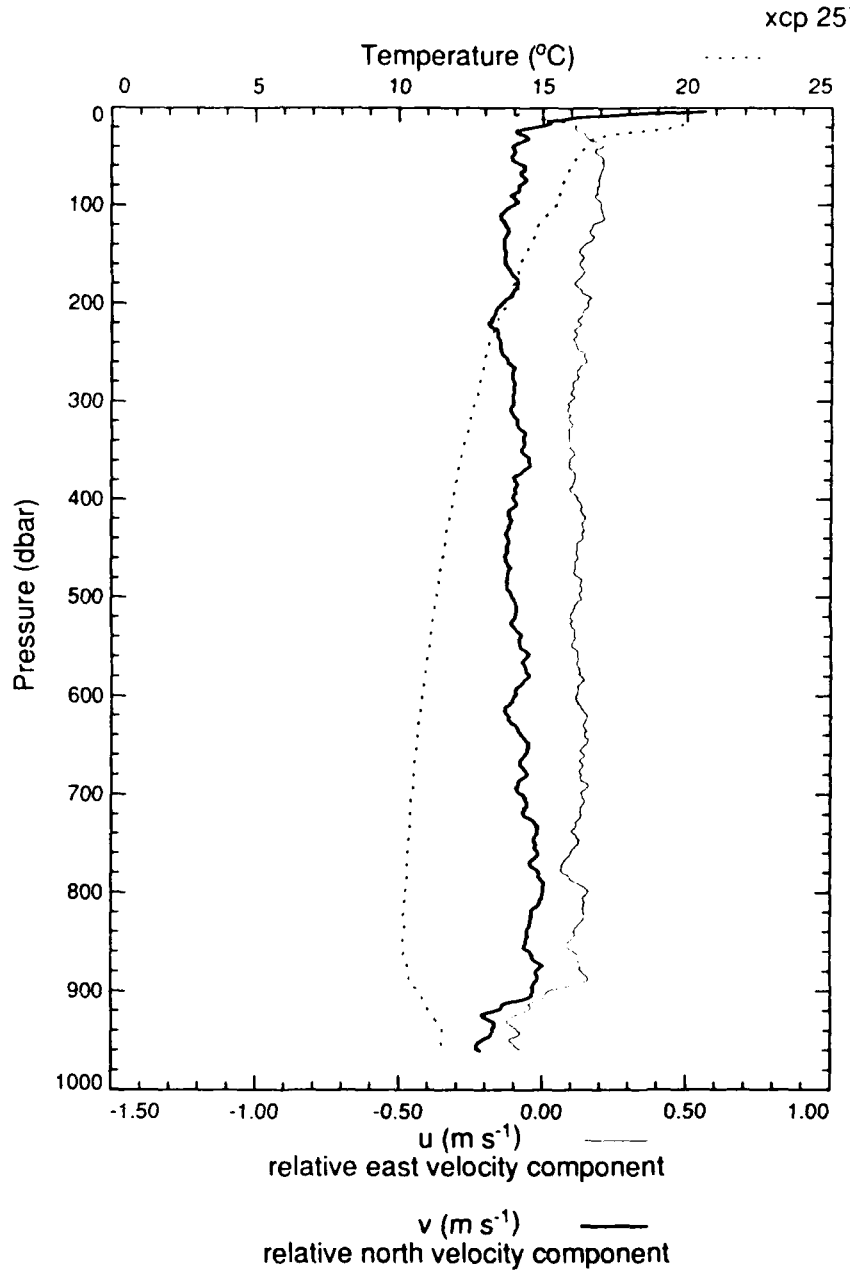
xcp 2572
Temperature (°C)
0
5
10
15
20
25
Pressure (dbar)
0
100
200
300
400
500
600
700
800
900
1000
-1.50
-1.00
-0.50
0.00
0.50
1.00
u (m s-1)
relative east velocity component
v (m s-1)
relative north velocity component

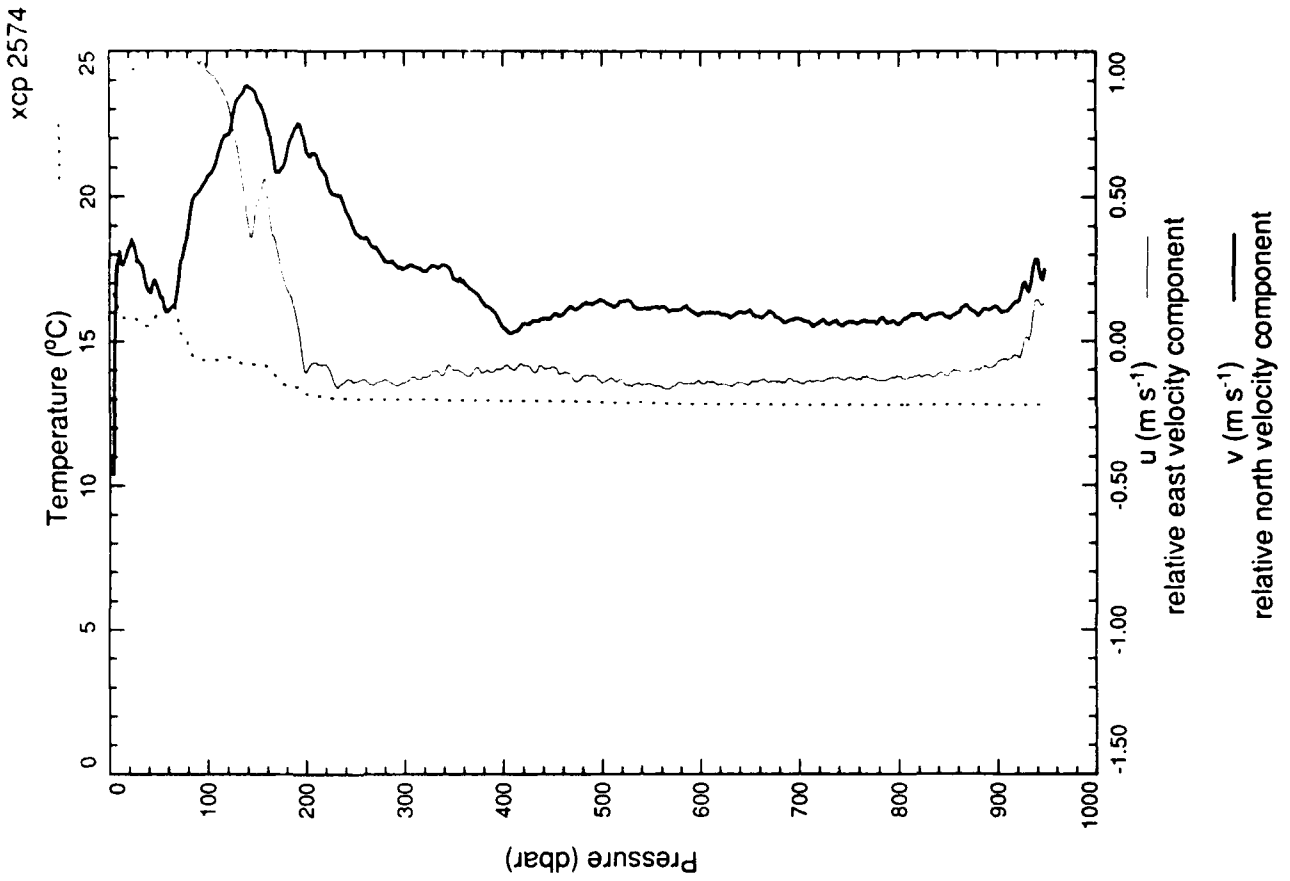
xcp 2574
Temperature (°C)
Pressure (dbar)
u (m s-1)
relative east velocity component
v (m s-1)
relative north velocity component

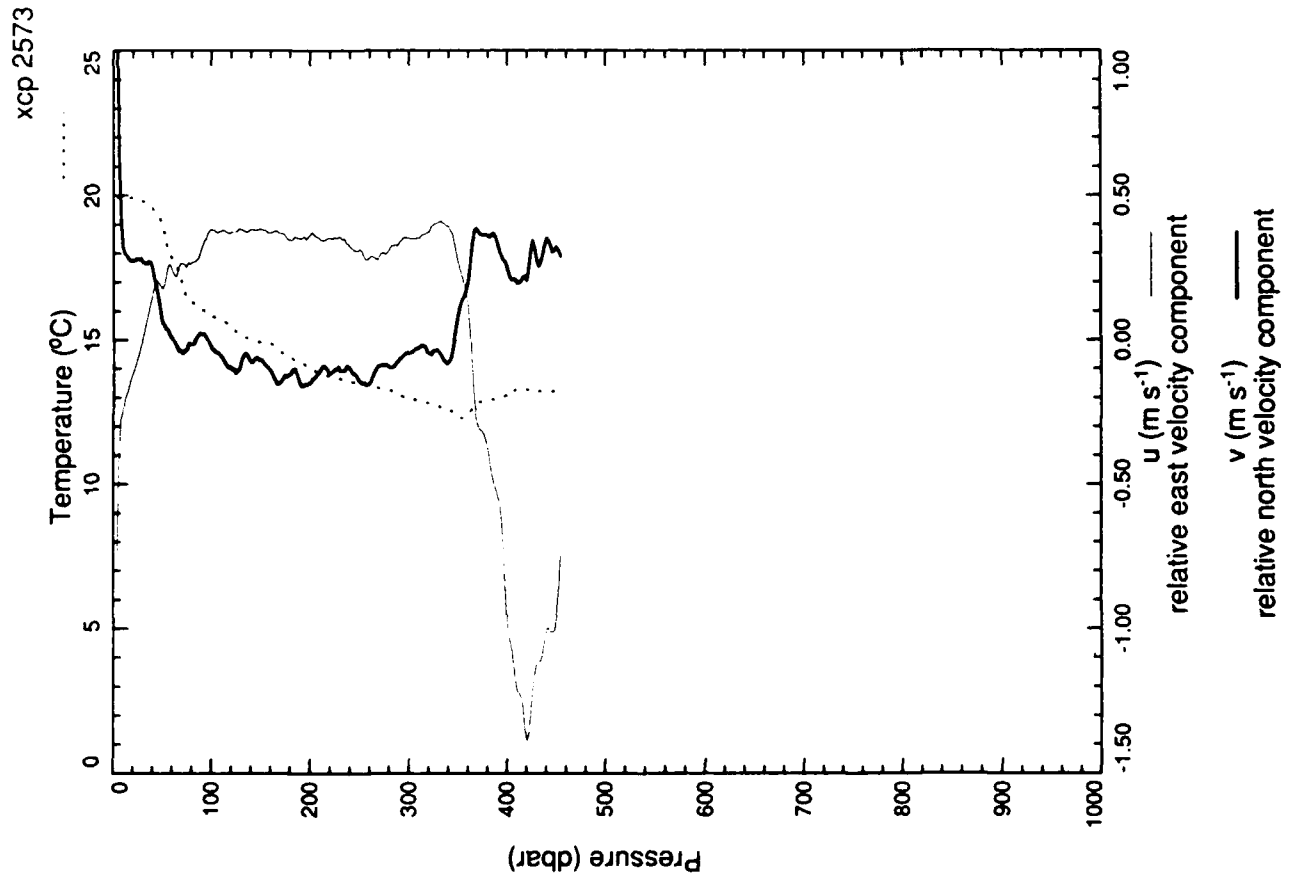
xcp 2573
Temperature (°C)
Pressure (dbar)
u (m s-1)
relative east velocity component
v (m s-1)
relative north velocity component

N82 TR 8925

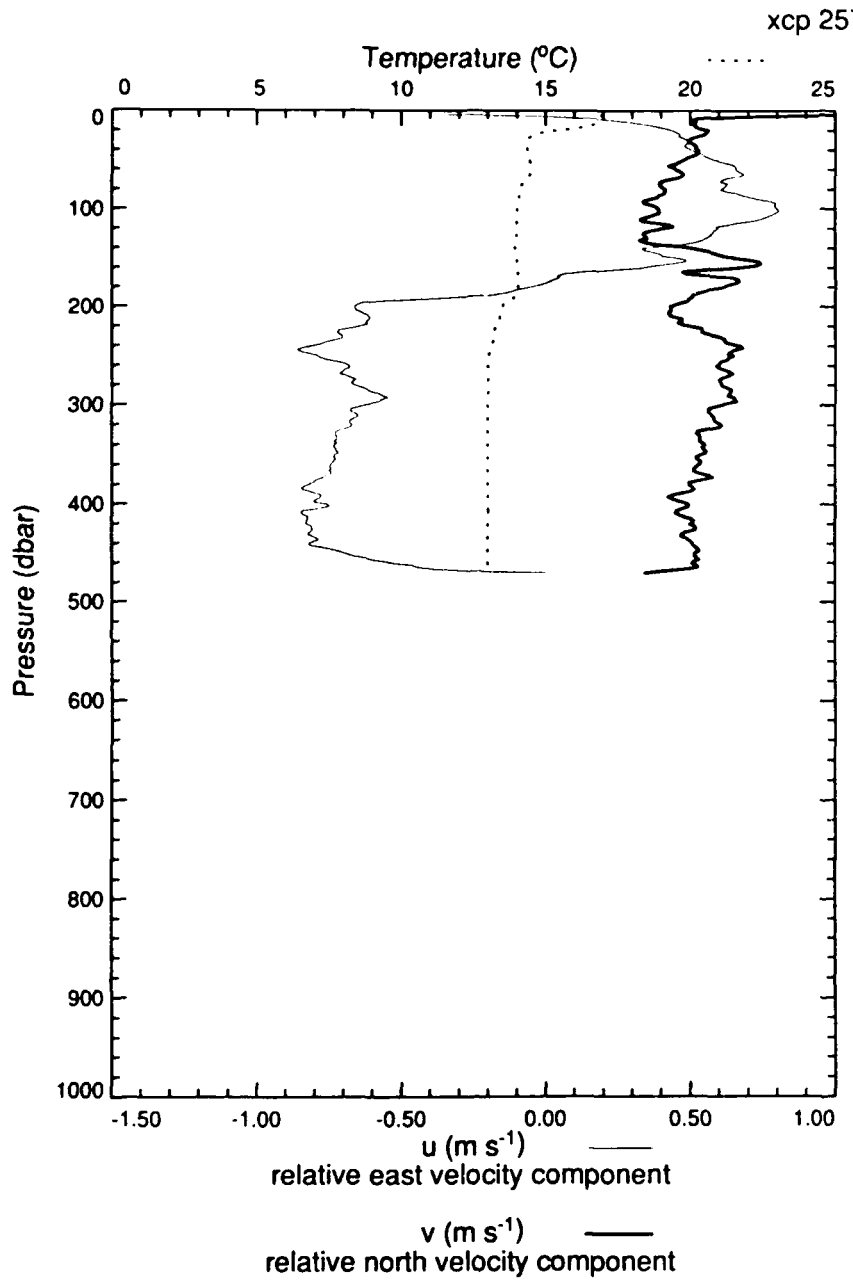
xcp 2575
Temperature (°C)
0
5
10
15
20
25
Pressure (dbar)
0
100
200
300
400
500
600
700
800
900
1000
-1.50
-1.00
-0.50
0.00
0.50
1.00
u (m s-1)
relative east velocity component
v (m s-1)
relative north velocity component

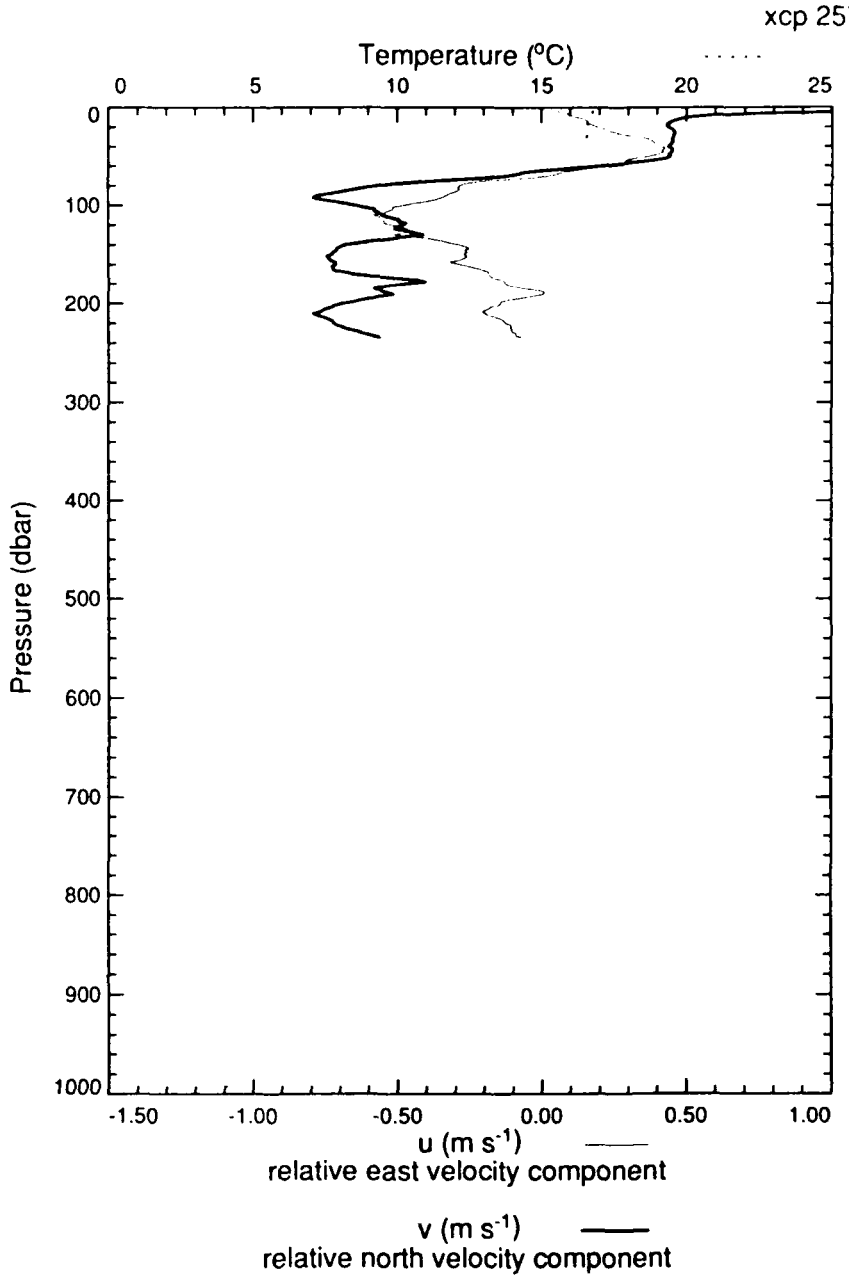
xcp 2576
Temperature (°C)
0
5
10
15
20
25
Pressure (dbar)
0
100
200
300
400
500
600
700
800
900
1000
-1.50
-1.00
-0.50
0.00
0.50
1.00
u (m s-1)
relative east velocity component
v (m s-1)
relative north velocity component

N84 TR 8925

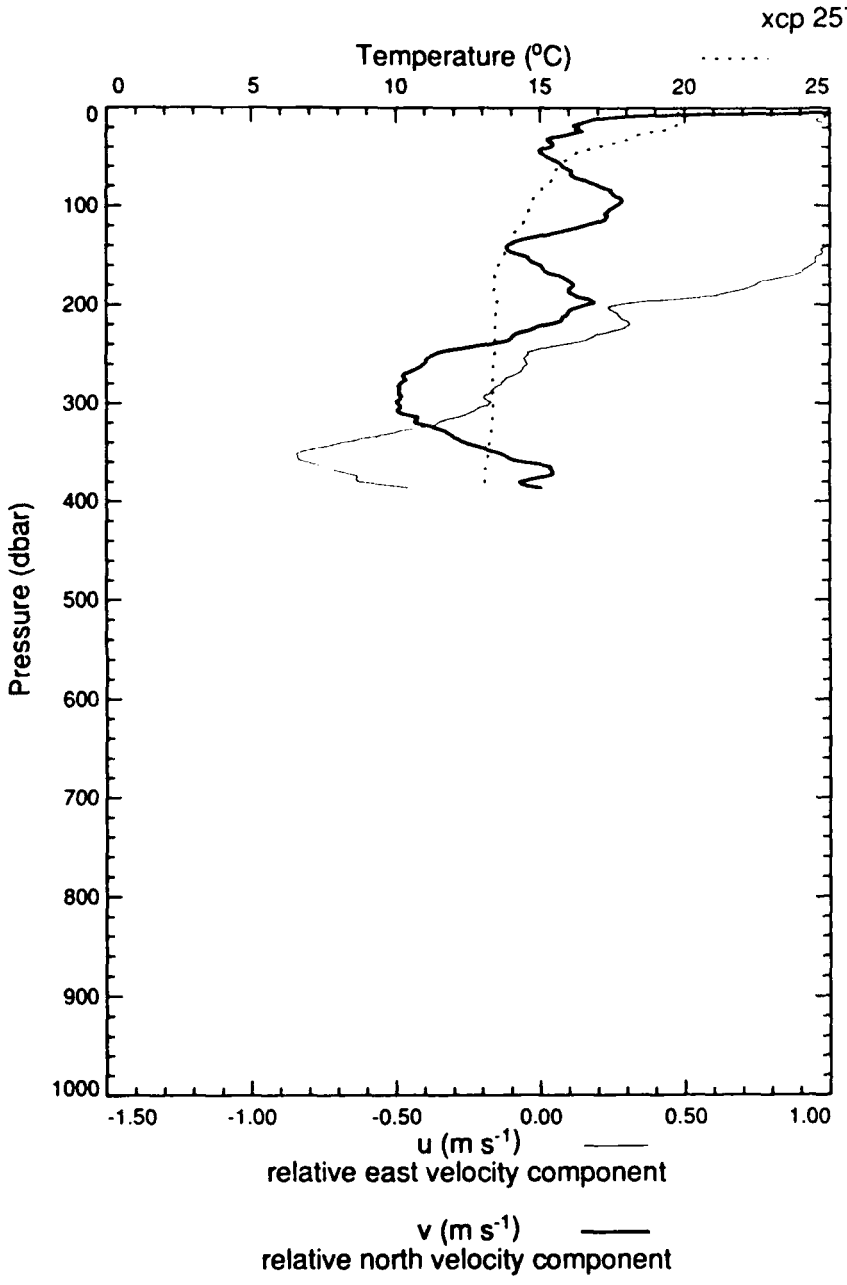
xcp 2577
Temperature (°C)
0
5
10
15
20
25
Pressure (dbar)
0
100
200
300
400
500
600
700
800
900
1000
-1.50
-1.00
-0.50
0.00
0.50
1.00
u (m s-1)
relative east velocity component
v (m s-1)
relative north velocity component

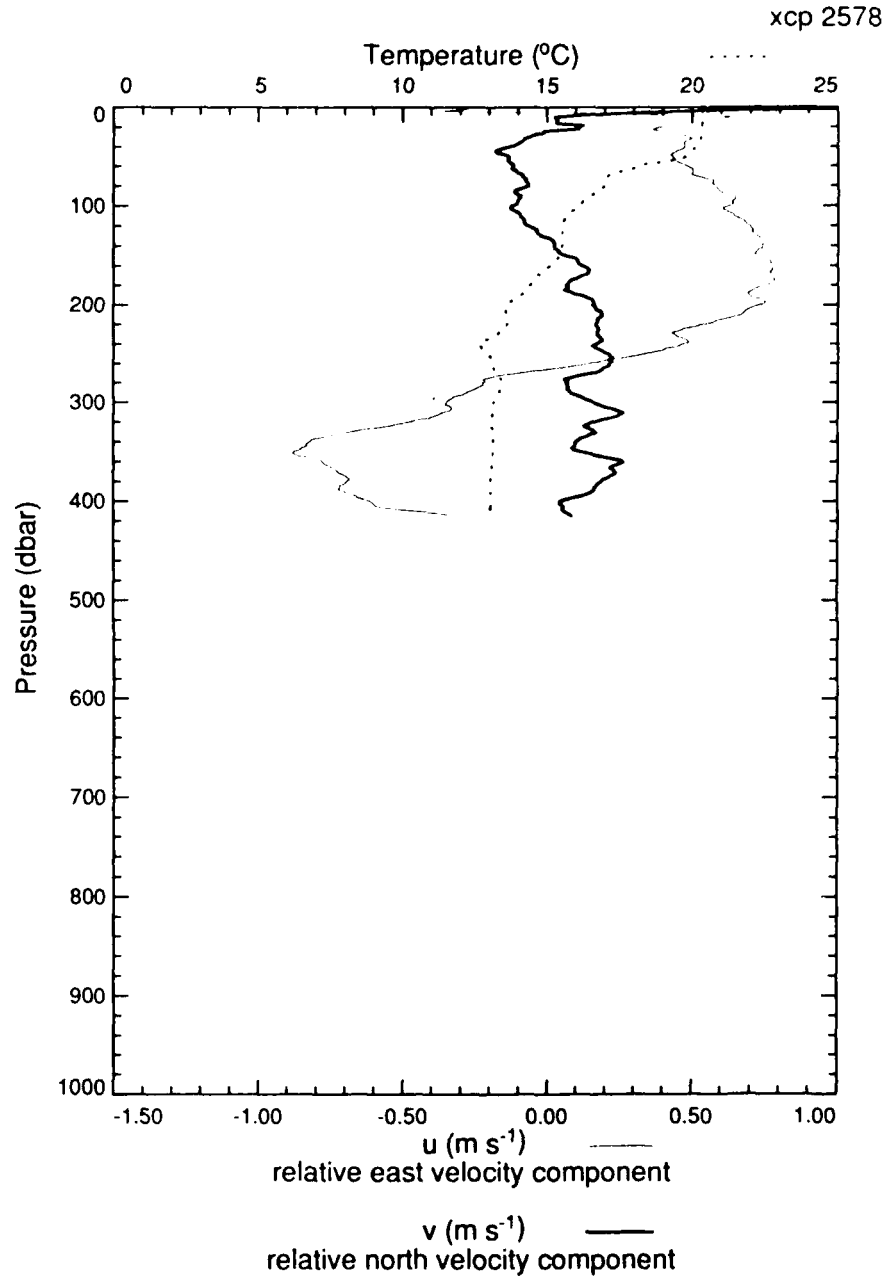
xcp 2578
Temperature (°C)
0
5
10
15
20
25
Pressure (dbar)
0
100
200
300
400
500
600
700
800
900
1000
-1.50
-1.00
-0.50
0.00
0.50
1.00
u (m s-1)
relative east velocity component
v (m s-1)
relative north velocity component

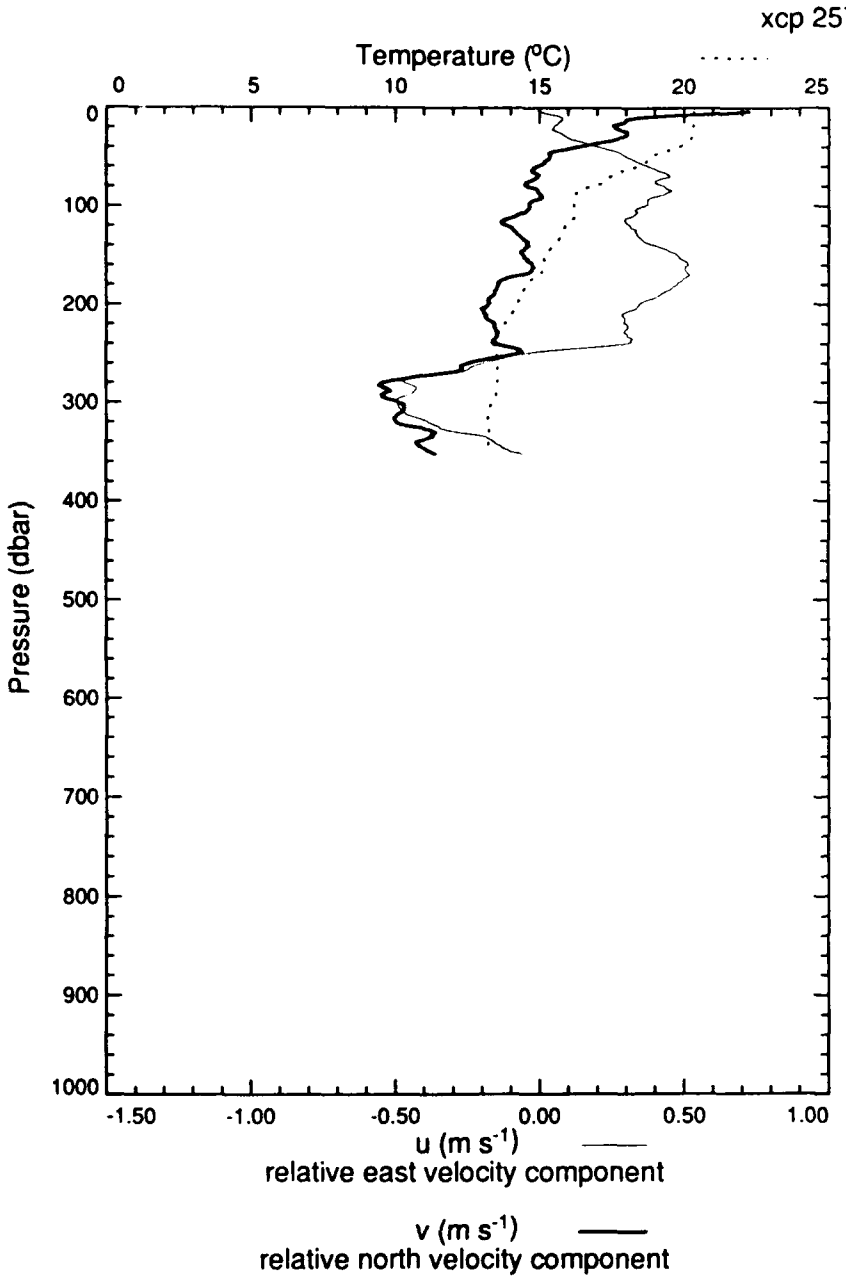
xcp 2579
Temperature (°C)
0
5
10
15
20
25
Pressure (dbar)
0
100
200
300
400
500
600
700
800
900
1000
-1.50
-1.00
-0.50
0.00
0.50
1.00
u (m s-1)
relative east velocity component
v (m s-1)
relative north velocity component

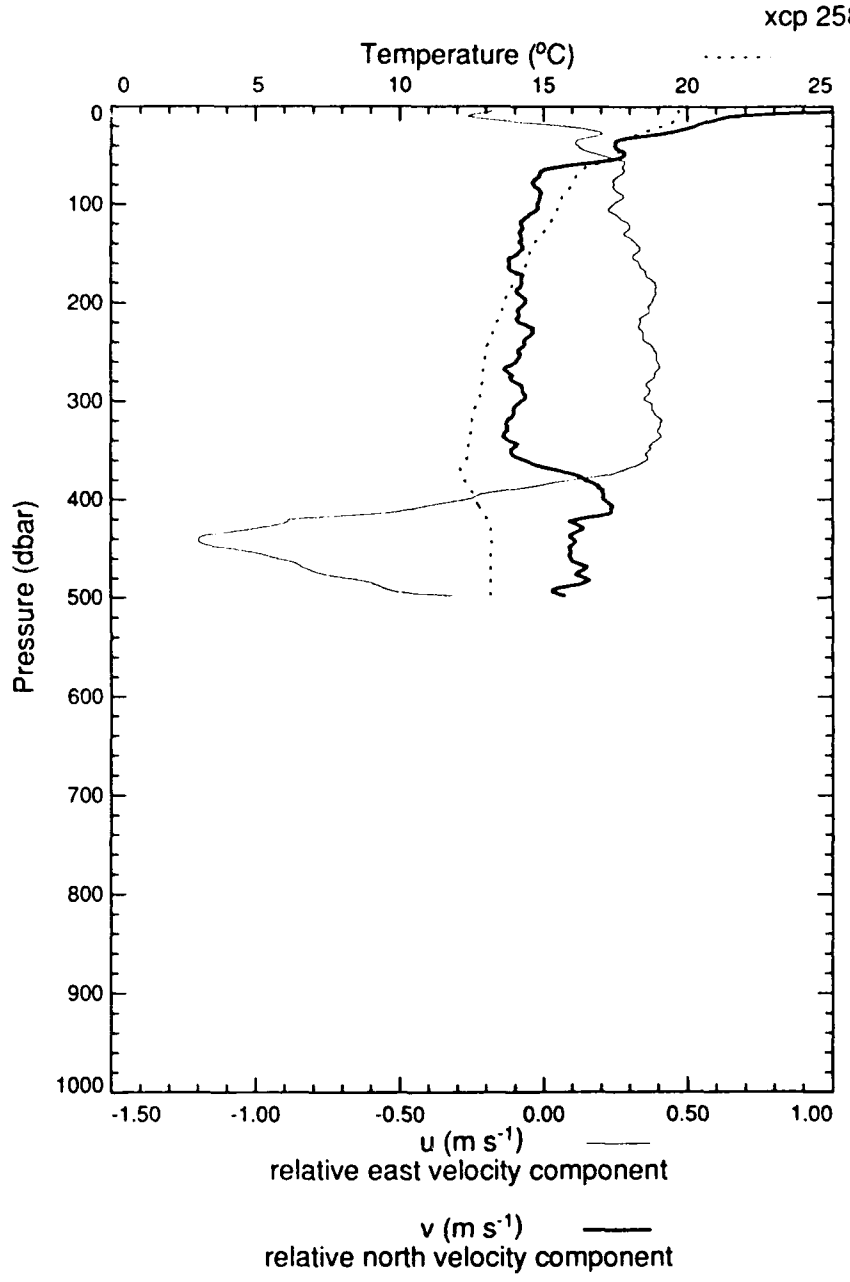
xcp 2580
Temperature (°C)
0
5
10
15
20
25
Pressure (dbar)
0
100
200
300
400
500
600
700
800
900
1000
-1.50
-1.00
-0.50
0.00
0.50
1.00
u (m s-1)
relative east velocity component
v (m s-1)
relative north velocity component

N86 TR 8925

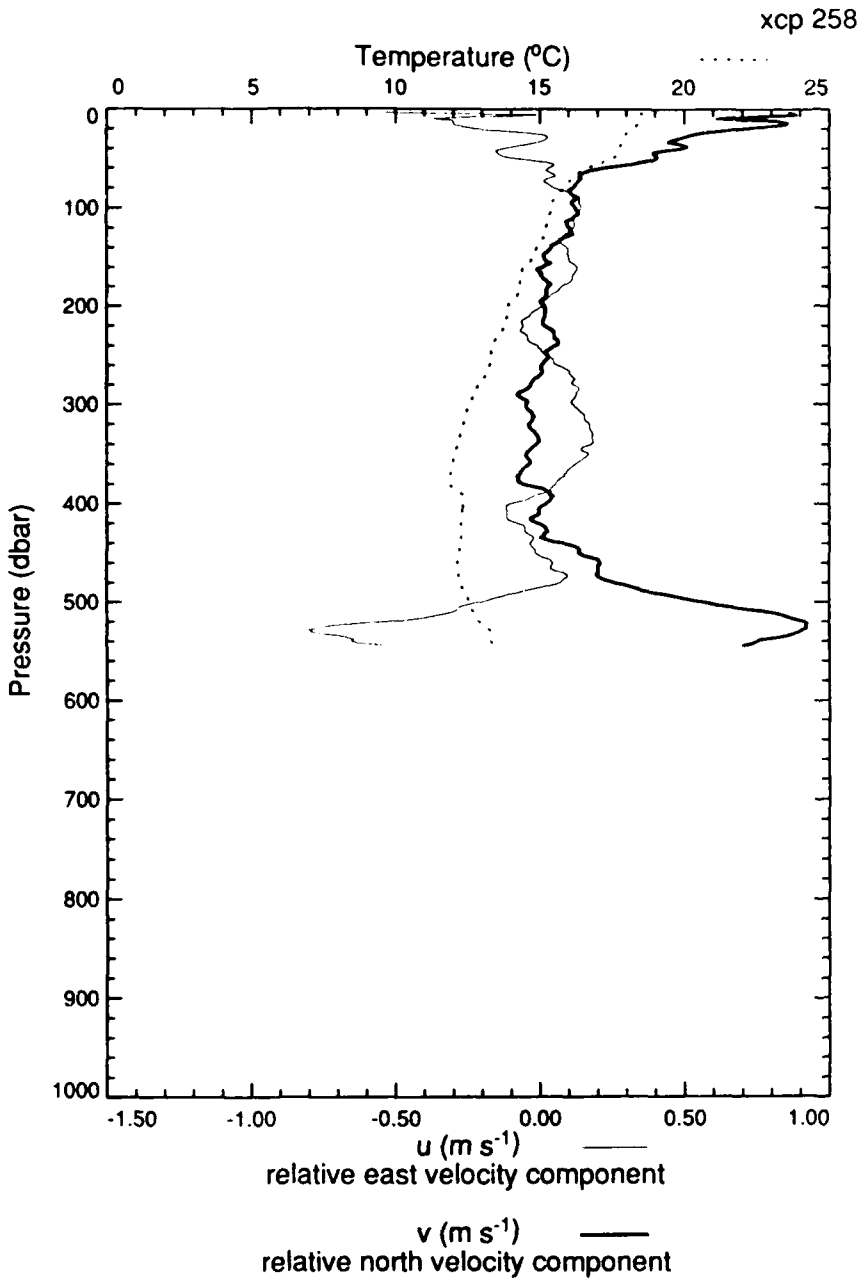
xcp 2581
Temperature (°C)
0
5
10
15
20
25
Pressure (dbar)
0
100
200
300
400
500
600
700
800
900
1000
-1.50
-1.00
-0.50
0.00
0.50
1.00
u (m s-1)
relative east velocity component
v (m s-1)
relative north velocity component

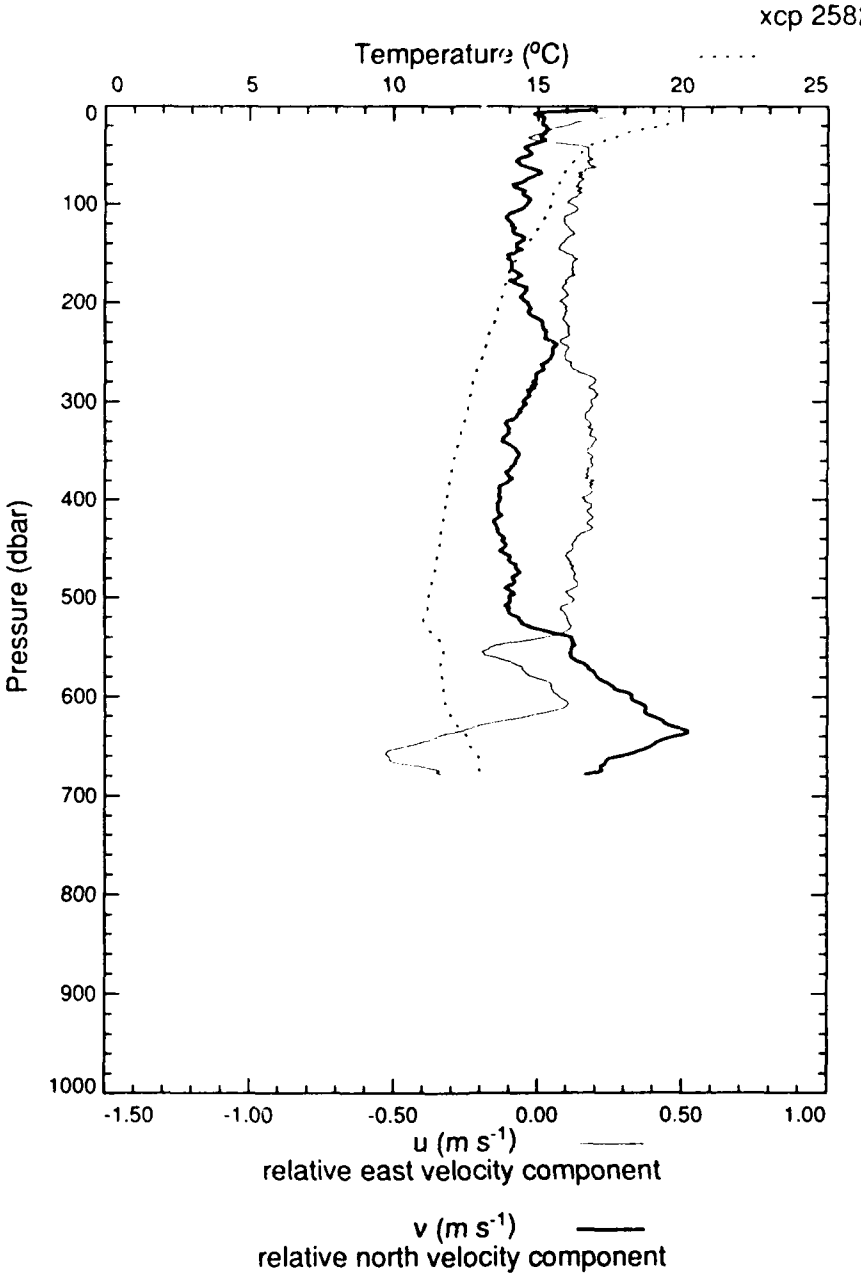
xcp 2582
Temperature (°C)
0
5
10
15
20
25
Pressure (dbar)
0
100
200
300
400
500
600
700
800
900
1000
-1.50
-1.00
-0.50
0.00
0.50
1.00
u (m s-1)
relative east velocity component
v (m s-1)
relative north velocity component

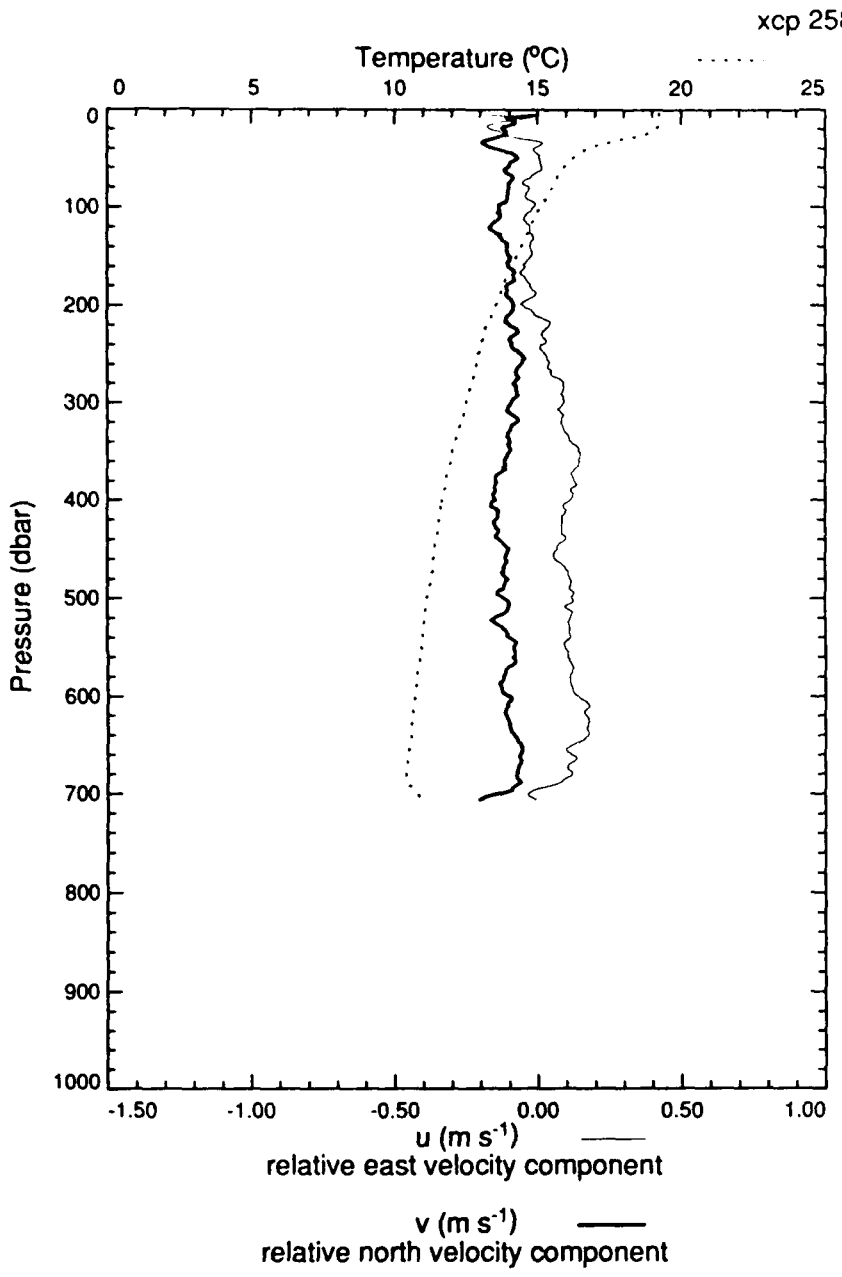
xcp 2583
Temperature (°C)
0
5
10
15
20
25
Pressure (dbar)
0
100
200
300
400
500
600
700
800
900
1000
-1.50
-1.00
-0.50
0.00
0.50
1.00
u (m s-1)
relative east velocity component
v (m s-1)
relative north velocity component

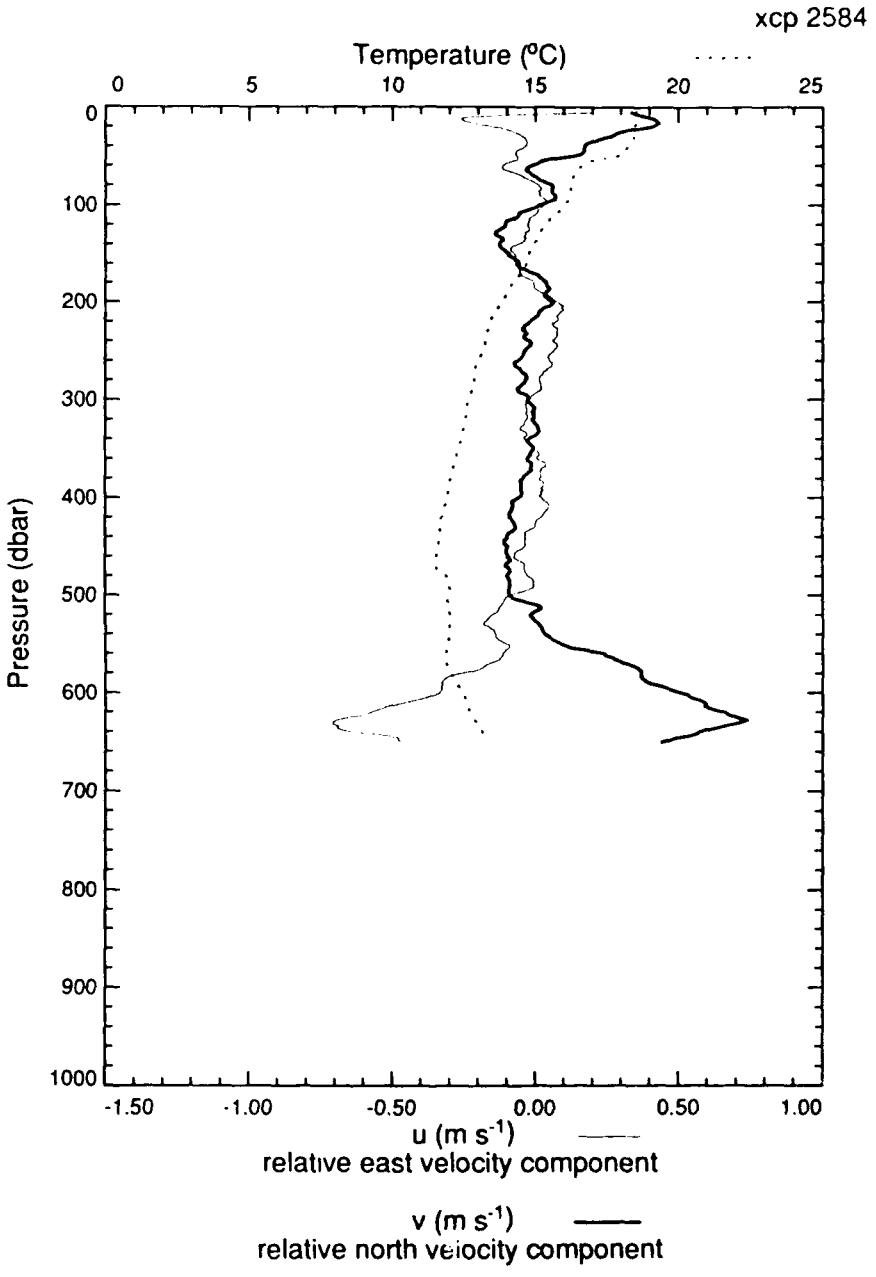
xcp 2584
Temperature (°C)
0
5
10
15
20
25
Pressure (dbar)
0
100
200
300
400
500
600
700
800
900
1000
-1.50
-1.00
-0.50
0.00
0.50
1.00
u (m s-1)
relative east velocity component
v (m s-1)
relative north velocity component

Unclassified

SECURITY CLASSIFICATION OF THIS PAGE

REPORT DOCUMENTATION PAGE

Form Approved
OMB No 0704-0188

1a REPORT SECURITY CLASSIFICATION	1b RESTRICTIVE MARKINGS
2a SECURITY CLASSIFICATION AUTHORITY	3 DISTRIBUTION/AVAILABILITY OF REPORT Distribution unlimited
2b DECLASSIFICATION/DOWNGRADING SCHEDULE	
4 PERFORMING ORGANIZATION REPORT NUMBER(S) APL-UW TR 8925	5 MONITORING ORGANIZATION REPORT NUMBER(S)
6a NAME OF PERFORMING ORGANIZATION Applied Physics Laboratory University of Washington 6b OFFICE SYMBOL (If applicable)	7a NAME OF MONITORING ORGANIZATION Office of Naval Research (Code 1122PO)
6c ADDRESS (City, State, and ZIP Code) 1013 N.E. 40th Street Seattle, WA 98105-6698	7b ADDRESS (City, State, and ZIP Code) 800 North Quincy Street Arlington, VA 22217-5000
8a NAME OF FUNDING/SPONSORING ORGANIZATION Office of Naval Research 8b OFFICE SYMBOL (If applicable)	9 PROCUREMENT INSTRUMENT IDENTIFICATION NUMBER N00014-87-K-0004
8c ADDRESS (City, State, and ZIP Code) 800 North Quincy Street Arlington, VA 22217-5000	10 SOURCE OF FUNDING NUMBERS PROGRAM ELEMENT NO: 422PO; PROJECT NO: --; TASK NO: --; WORK UNIT ACCESSION NO: 06

11 TITLE (Include Security Classification)

XCP Data from the Gulf of Cadiz Expedition: R/V Oceanus Cruise 202

12 PERSONAL AUTHOR(S)

Maureen A. Kennelly, Mark D. Prater, John H. Dunlap, Eric L. Kunze, Thomas B. Sanford

13a TYPE OF REPORT	13b TIME COVERED	14 DATE OF REPORT (Year, Month, Day)	15 PAGE COUNT
Data	FROM 9/4/88 TO 9/28/88	November 1989	206

16 SUPPLEMENTARY NOTATION

17 COSATI CODES			18 SUBJECT TERMS (Continue on reverse if necessary and identify by block number)
FIELD	GROUP	SUB-GROUP	Meddy; Cape St. Vincent, Portugal; Gulf of Cadiz; Ampere Seamount; XCP profiles
08	03		

19 ABSTRACT (Continue on reverse if necessary and identify by block number)

Velocity and temperature profiles from expendable current profilers (XCPs) were obtained during the Gulf of Cadiz Expedition, 4-28 September 1988, from R/V *Oceanus*. This report describes the instrumentation used, discusses data acquisition and processing methods, and presents the resulting velocity and temperature profiles.

20 DISTRIBUTION/AVAILABILITY OF ABSTRACT	21 ABSTRACT SECURITY CLASSIFICATION
☐ UNCLASSIFIED/UNLIMITED ☒ SAME AS RPT ☐ DTIC USERS	Unclassified
22a NAME OF RESPONSIBLE INDIVIDUAL David Evans and Alan Brandt	22b TELEPHONE (Include Area Code) (202) 696-4441 22c OFFICE SYMBOL

DD Form 1473, JUN 86 *Previous editions are obsolete*

S/N 0102-LF-014-6603

SECURITY CLASSIFICATION OF THIS PAGE

Unclassified